Boronic Acid & Nitrofuranyl Derivatives as Potential Therapeutics

Michaelmas 2021

Ashley L. Dey

Acidum Boronicum et Nitrofuran derivata sicut Potentiale Clinice

Supervisor: Prof Christopher Joseph Schofield

Ashley Laurence Dey

Doctor Philosophiae (DPhil)

Universitas Oxoniensis

Linacre Domus

Michaelmas 2021

Copyright © 2021, omnia jura reservata.







Dominus illuminatio mea

The Lard is my light

in memoriam

Ludwig Eduard Boltzmann

(1844 – 1906)

$$S = k_B \, Ln \, W$$

L. E. Boltzmann, 1877

Almost 150 years ago Ludwig E. Boltzmann pioneered the concepts of 'statistical mechanics' by inception of 'entropy' and during the last century or two, much development work has been carried out in this field and some acknowledgment of great help rendered to mankind by other pioneers in this field such as Erwin R. J. A. Schrodinger for inception of 'negentropy' in his 1944 book 'What is Life?', is long overdue; it is, by all means, no exaggeration to admit that they have materially assisted the advancement of science and more importantly humanity.

The pioneering work of such curious minds and advocates, has truly established and taught us the basis of 'life', and the stage is now set for us to build upon the scientific assets that have been left for us to shape the future of mankind; a future in which no one ever suffers from the pain and suffering of infectious diseases, which are all spontaneous by their very 'entropically favourable' nature.

As Arthur Schopenhauer beautifully put it: "the task is not so much to see what no one has seen yet, but to think what nobody has thought about that which everybody sees."

Pandemics, epidemics, progressive insidious suffering and deaths are all a corollary of tiny creatures that are knitted within us and taken for granted – bacteria!

Indolence and ignorance together with arrogance and incompetence of the so called 'elite' inflicts the pain and suffering of infectious diseases on many, and unless until mankind comes to terms with freeing themselves from bacteria, that pain and suffering will perpetuate...

In the absence of compelling evidence to the contrary, the probability of occurrence of a macrostate is very much dependent on its corresponding number of probable microstates; thus, it begs the question of whether, as a tiny voice amongst many, my meandering in wonderlands, just as that of Boltzmann in 1906, would prompt others far more important than me to get behind this and sort it out?!

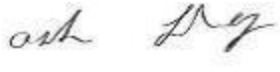

London, N1

December 2021

List of Abbreviations

Acetic acid	**AcOH**
Acetonitrile	**MeCN**
Acetylcholinesterase	**AChE**
N-Acetylglucosamine	**GlcNAc**
N-Acetylmuramic acid	**MurNAc**
2-Acetylphenylboronic acid	**2-APBA**
2-Acetylthiophen-3-ylboronic acid	**2-ATBA**
Active pharmaceutical ingredient	**API**
Adenosine triphosphate	**ATP**
Adsorption, distribution, metabolism and excretion	**ADME**
Allyloxycarbonyl	**Alloc**
Alzheimer's disease	**AD**
p-Aminobenzoic acid	**PABA**
Ampicillin resistant Class C	**AmpC**
Angiotensin II	**AT_1**
Antibacterial resistance gene	**ARG**
Antibody drug conjugate	**ADC**

Antimicrobial peptide	**AMP**
Aspartate	**Asp**
Barium hydroxide octahydrate	**$Ba(OH)_2$•8(H_2O)**
2-(1*H*-Benzotriazol-1-yl)-1,1,3,3-tetramethyluronium hexafluorophosphate	**HBTU**
Benzyl	**Bn**
Benzylpenicillin	**Penicillin G**
Binding efficiency index	**BEI**
1-[Bis(dimethylamino)methylene]-1*H*-1,2,3-triazolo[4,5-b]pyridinium-3-oxide hexafluorophosphate	**HATU**
1,3-Bis(diphenyphosphino)propane	**DPPP**
Boron trichloride	**BCl_3**
N-Bromosuccinimide	**NBS**
tert-Butoxycarbonyl	**Boc**
Caesium carbonate	**Cs_2CO_3**
Carbobenzyloxy	**Cbz**
K. pneumoniae carbapenemase	**KPC**
Cefotaxime	**CTX**
Central nervous system	**CNS**
Copper iodide	**CuI**
Deoxyribonucleic acid	**DNA**

Developmentally-regulated GTP-binding protein 1	**Drg-1**
2,3-Dichloro-5,6-dicyano-*p*-benzoquinone	**DDQ**
Dichloromethane	**CH_2Cl_2**
Dihydrofolic acid	**DHF**
Dimethylformamide	**DMF**
N,*N*'-Dimethylpropyleneurea	**DMPU**
Dimethylsulfoxide	**DMSO**
Direct repeat	**DR**
DNA Cross-Link Repair	**DCLRE**
Dopamine	**DA**
Drug metabolism and pharmacokinetics	**DMPK**
Dutch imipenemase	**DIM-1**
Dynamic combinatorial chemistry	**DCC**
Dynamic combinatorial library	**DCL**
Dynamic combinatorial mass spectrometry	**DCMS**
Ease of synthesis	**EoS**
Eigenvalue	$\boldsymbol{E}$
Eigenvector angular momentum	$\boldsymbol{\hat{L}^2}$

Electrospray ionisation	**ESI**
Endothelin-1	**ET_A**
Ethanol	**EtOH**
Ethyl acetate	**EtOAc**
Ethylenediaminetetraacetic acid	**EDTA**
Extended-spectrum β-lactamase	**ESBL**
Ferric chloride	**$FeCl_3$**
Florence imipenemase	**FIM-1**
Fluorenylmethoxycarbonyl	**Fmoc**
2-Formylphenylboronic acid	**2-FPBA**
3-Formylthiophen-2-yl boronic acid	**3-FTBA**
Fragment based drug design	**FBDD**
Functional group interconversion	**FGI**
Generating antibiotic incentives now	**GAIN**
Genomic island	**GEI**
German imipenemase	**GIM-1**
GlaxoSmithKline	**GSK**
G-protein-coupled receptor	**GPCR**
Guanosine triphosphate	**GTP**

Hamiltonian operator	$\widehat{\boldsymbol{H}}$
Heat shock factor 1	**HSF-1**
Heteronuclear single quantum coherence	**HSQC**
Highest occupied molecular orbital	**HOMO**
High-resolution mass spectrometry	**HRMS**
High-throughput screening	**HTS**
Histamine	**H**
D,L-Homocysteine thiolactone hydrochloride	**D,L-HCTL.HCl**
Horizontal gene transfer	**HGT**
Human ether-à-go-go-related gene	**hERG**
Imperial Chemical Industries	**Imp. Chem. Ind.**
Imipenemase	**IMP**
Indole carboxylate	**InC**
Insertion sequence	**IS**
Iodobenzene diacetate	**IPh(OAc)$_2$**
N-Iodosuccinimide	**NIS**
Kyorin Health Science MBL	**KHM-1**
Ligand efficiency	**LE**
Lipopolysaccharide	**LPS**
Liquid chromatography–mass spectrometry	**LC-MS**
Lithium hydroxide	**LiOH**

Lithium iodide	**LiI**
Lowest unoccupied molecular orbital	**LUMO**
Bacillus cereus MBL	**BcII**
S. marcescens MBL	**SMB-1**
Metallo-*β*-lactamase	**MBL**
Methanol	**MeOH**
Methicillin resistant *S. aureus*	**MRSA**
p-Methoxybenzyl	**PMB**
p-Methoxybenzyl carbonyl	**Moz**
β-Methoxyethoxymethyl	**MEM**
Methoxymethyl	**MOM**
Methylthiomethyl	**MTM**
Molecular weight	**MW**
2-(*N*-morpholino)ethanesulfonic acid	**Mes**
Multicomponent drug efflux pump system	***mex***
Multidrug resistant	**MDR**
Multiparameter optimisation	**MPO**
Native chemical ligation	**NCL**

New Delhi metallo-β-lactamase	**NDM**
Nitrofuranyl indole carboxylate	**NInC**
Noradrenaline	**NA**
Nuclear factor erythroid 2-related factor 2	**Nrf2**
Nuclear magnetic resonance	**NMR**
Nuclear overhauser effect	**NOE**
Outer membrane vesicle	**OMV**
Oxacillinase	**OXA**
2-Oxoglutarate	**2OG**
Palladium	**Pd**
Parity operator	$\hat{\boldsymbol{P}}$
Penicillin binding protein	**PBP**
Percentage efficiency index	**PEI**
Phenoxymethylpenicillin	**Penicillin V**
Phosphate-buffered saline	**PBS**
Pig liver esterase	**PLE**
Platelet activating factor	**PAF**
Polar surface area	**PSA**

Potassium trimethylsilanolate	**$KOSiMe_3$**
Potential energy	***V***
Preparative reversed phase high performance liquid chromatography	**RP-HPLC**
Protecting group	**PG**
Quantitative structure-activity relationship	**QSAR**
Ribonucleic acid	**RNA**
Rule of 3	**Ro3**
Sao Paulo MBL	**SPM-1**
Selective serotonin reuptake inhibitor	**SSRI**
Seoul imipenemase	**SIM-1**
Serine- β-lactamase	**SBL**
Serotonin	**5-HT**
Severe acute respiratory syndrome coronavirus 2	**SARS-CoV-2**
Sodium cyanoborohydride	**$NaCNBH_3$**
Sodium hydroxide	**NaOH**
Sodium methoxide	**NaOMe**
Sodium triacetoxyborohydride	**STAB**
Solid phase synthesis	**SPS**

Structure-activity relationship	**SAR**
Sulfhydryl variable	**SHV**
Surface efficiency index	**SEI**
Temoniera	**TEM**
TentaGel trityl	**TGT**
Tetrahydrofuran	**THF**
Tetrahydropyranyl	**THP**
Tetramethylsilane	**TMS**
Thiazolidine	**Thz**
Thin layer chromatography	**TLC**
Thromboxane A_2 receptor	**TxR**
Thromboxane A_2 synthase	**TxS**
Toll-like receptor 4	**TLR4**
Transfer RNA	**tRNA**
Tributylammonium fluoride	**TBAF**
Trifluoroacetic acid	**TFA**
Triethylamine	**Et_3N**
Trimethylsilylethoxymethyl	**SEM**

Trimethylsilyl trifluoromethanesulfonate	**Me_3SiOTf**
Trimethyltin hydroxide	**Me_3SnOH**
Tripoli MBL	**TMB-1**
Tris(2-carboxyethyl)phosphine hydrochloride	**TCEP·HCl**
Tris(hydroxymethyl)aminomethane	**Trizma**
Trityl	**Trt**
Tuberculosis	**TB**
United States of America	**US/USA**
Verona Integron-en-coded metallo-β-lactamases	**VIM**
World Health Organisation	**WHO**
Zinc chloride	**$ZnCl_2$**

Acknowledgements

I find this opportunity to thank Prof Christopher J. Schofield for taking me on as his advisee.

I am also indebted to Prof Mark G. Moloney for his advice and suggestions on the NOE experiments of boronate esters presented herein, without which their absolute configurations could not have been elucidated. With special gratitude, I acknowledge the specialist NMR contributions of Prof Timothy D. W. Claridge which greatly improved the quality of this text.

I would also like to acknowledge the kind assistance of Dr Jürgen Brem in our preliminary DCC experiments. In addition, I am grateful to Prof Akane Kawamura for liaising with our industry partners and am also indebted to Prof Vipul Patel and Dr Jacob Bush for supporting this work.

The assistance of Dr William D. Figg Jr in protein expressions has been invaluable which with a heavy heart had to be omitted from this text in virtue of the Covid-19 pandemic; I am also indebted to Will for being a genuine friend and ally. Special gratitude is due to Dr Victor Lee for pointing out errors and infelicities, and also making valuable suggestions on the manuscript which undoubtedly helped to improve the final text. I am also grateful to Mrs Zahn Gowar and Gwendoline Denning for arranging meetings and keeping us informed with important announcements, in particular, during the pandemic.

Special thanks are due to Janice French, Sue Henderson, and Helen Elliott for their generous hospitality during my commutes from London to Oxford occasioned by the outbreak of coronavirus pandemic and several national lockdowns. I also wish to express my gratitude to Callum D. Buchanan for making the hostile environment of my second job somewhat bearable, and also for fixing my old banger which otherwise would have rendered commuting to Oxford, especially, in the early hours of the mornings after 18–20 hours of flat-out lab work, improbable. I wish to thank Dr Jane Hoverd and Thea Teasdale for their assistance and support towards both the inter-departmental and financial affairs, and also thanks to Dr Lennart Brewitz for his day-to-day assistance around the lab.

Many thanks to Thomas Corner for courteously safeguarding the indispensable equipment of CABFLGL1A1 and pertinent contents thereof in LG1 from looting, in particular, in my absence.

As always, I am extremely grateful to Biotechnology and Biological Sciences Research Council & GlaxoSmithKline for funding this work, and am also indebted to the Royal Society of Chemistry Chemists' Community Fund for their generous donations, facilitated by Kim Sutton, without which this work would have not been completed; additionally, on a separate note, it leaves me only to thank Kim again for her kind counselling and consultations as well.

Preface

With the advent of novel medicines and a desire for longevity, synthetic chemistry has been at the frontiers of life sciences more than ever before. Despite rapid advances in technology and human modernisation, our knowledge of environmental and biological problems is still embryonic. As such, synthetic chemistry is an important key to overcoming global disease burdens such as antimicrobial, in particular, antibacterial resistance.

The burden of antibacterial resistance is currently one of the greatest threats to public health, and unless immediate action is taken globally, the infectious diseases are expected to become even a more serious and unmanageable problem worldwide. In addition, the clinically relevant resistant strains of bacteria responsible for nosocomial deaths are just a drop in the ocean. It has been reported that 99% of bacteria cannot be cultured, thus there is not a full account available for all the pathogenic bacteria to which we are exposed. Further, antibacterial resistance is much more complex than often perceived. There are many pathogenic bacteria making up the erroneously perceived '*natural flora/microbiome*' which cause chronic infections to which the body develops '*immunological tolerance*', and this effect leads to many more complications such as cancer, dementia, Alzheimer's disease, chronic fatigue syndromes, depression, to name but a few.

Not all bacterial infections lead to changes in the blood pressure, heart rate and body temperature, as well as changes in the inflammatory markers, such as erythrocyte sedimentation rate, C-reactive proteins and white blood cell count; and that this should be so is a corollary of immunological tolerance to these bacteria, such that they are no longer deemed '*exogenous*' by the body and would never be eradicated by the immune system.

Although, this immunological tolerance palliatively protects us from spontaneous death as well as detrimental effects of immune response ensuing an acute bacterial infection, these bacteria are able to alter the morphology and physiology of the body and impair its normal functioning which gradually leads to progressive and insidious suffering, and ultimately death.

As delineated above, the immune system does not always completely eradicate the invading pathogens; the immunological tolerance plays an important role in infectious disease management. In addition, the development of a dynamic endosymbiosis between the body and invading bacteria could result in many detrimental impacts on the host, and the host itself does not always benefit from this erroneously perceived '*mutualistic relationship*.'

Inarguably, the general public is becoming averse to antibiotics due to the media coverage on these topics, encouraging people not to take antibiotics, and rely on their own innate immune system to tackle the infections. This has led many, though by no means all, not to protect themselves from pathogens, in particular bacteria, to such an extent that they really believe pathogens are good for them, and personal hygiene together with antibiotics would weaken their immune system.

In the light of what has been said above, the primary aim of the work described herein is to introduce *inter alia* novel antibacterial agents of very varied type, in fight against the foregoing antibacterial resistance. Unfortunately, despite the author's heart's desire, a description of several novel anti-infectives which were developed during the course of this endeavor had to be curtailed due to the outbreak of Covid-19 pandemic, and will, hopefully, be the subject of future publications, should such there be.

To this end, Chapter 1 makes every endeavor to retain the comprehensive character of the literature on some aspects of this work which would be discussed further in subsequent chapters, and reference to the pertinent sections have been provided. The reader is strongly encouraged to familiarise themselves with the specialist topics to which reference has been made in the text.

Relative to other global disease burdens, there has been a general lack of interest in antibacterial research by large pharmaceutical companies due, in part, to financial returns.[*,†] However, recently, efforts have been made to encourage work in the field of tackling antibacterial resistance *e.g.* Longitude Prize, Generating Antibiotic Incentives Now Act *etc.*

It is hoped that the rise in mortality and morbidity of antibacterial resistance together with these pharmaceutical incentives will trigger copious research into different ways of tackling this global disease burden.

It is now nearly five years since this work was first undertaken in Oxford in the summer of 2017. Since that day the field of these studies has enormously grown, and the task of compiling this work has been rather daunting, and as such, has been stretched over more years than it would have been desired. Thus, I sincerely seek the reader's forbearance, should, on occasions, discussions on certain subjects fall short of or are not as detailed as they may wish.

Furthermore, I strongly encourage those who read and might end up using this work or even find it fruitful, to get in touch: be it a comment, error, or even expression of interest for future collaborations, I very much look forward to hearing from you.

[*] H. Kresse, M. J. Belsey and H. Rovini, *Nat. Rev. Drug Discovery*, 2007, **6**, 19.
[†] S. J. Projan and P. A. Bradford, *Curr. Opin. Microbiol.,* 2007, **10**, 441.

Table of Contents

1.1 Antibiotics History 4

1.1.1 Sulfonamide Antibacterials 5

1.1.2 Penicillin ß-Lactam Antibiotics 6

1.1.3 Aminoglycoside Antibiotics 8

1.1.4 Chloramphenicol Antibiotics 8

1.1.5 Tetracycline Antibiotics 9

1.1.6 Macrolide Antibiotics 10

1.1.7 Glycopeptide Antibiotics 11

1.1.8 Cephalosporin ß-Lactam Antibiotics 12

1.1.9 Quinolone & Fluoroquinolone Antibacterials 13

1.1.10 Carbapenem ß-Lactam Antibiotics 14

1.1.11 Nitrofuran Antibacterials 15

1.1.12 Oxazolidinone Antibacterials 16

1.2 Medicinal Chemistry & Drug Discovery 18

1.2.1 Drug & Its Principal Components 19

1.2.2 Target Identification & Validation 21

1.2.3 Hits & Leads 21

1.2.4 Concepts of Druglikeness 22

1.2.5 Lead Identification 28

1.2.5.1 Analogue Profiling Strategies 29

1.2.5.2 Systematic Screening Strategies 29

1.2.5.3 Biological Data Exploitation 30

1.2.5.4 Planned & Rational Research 30

1.2.6 Lead Optimization 30

1.3 Current Antibacterial Targets 34

1.4 Antimicrobial Peptides – a New Chasm 35

1.5 Antibacterial Resistance 41
1.6 Horizontal Gene Transfer 43
1.6.1 The Importance of HGT in Microbial Phylogenies 44
1.6.2 Mechanisms of HGT & Their Contribution to the Pool of Antibacterial Resistance Genes 45
1.6.2.1 Conjugation 45
1.6.2.2 Transformation 46
1.6.2.3 Transduction 47
1.6.2.4 HGT Facilitated by GEIs 47
1.6.2.5 HGT Mediated Through OMVs 49
1.6.3 HGT Beyond Prokaryotic Realm 50
1.7 Immunological Tolerance 51
2.1 Solid Phase Synthesis 55
2.1.1 Solid Supports in Solid Phase Synthesis 56
2.1.2 Linkers in Solid Phase Synthesis 57
2.1.3 The Scope of Solid Phase Synthesis 58
2.2 Compound Library Design Strategies 59
2.3 Parallel Synthesis 60
2.3.1 Microwave and Microfluidics in Parallel Synthesis 62
2.4 Combinatorial Chemistry 63
2.4.1 Combinatorial Synthesis Design 64
2.4.2 Dynamic Combinatorial Chemistry 65
2.4.2.1 A Brief History of Dynamic Combinatorial Chemistry 66
2.4.2.2 Reversible Covalent Dynamic Combinatorial Chemistry Reactions 67
2.4.2.3 Scope & Limitations of Dynamic Combinatorial Chemistry 71
2.5 ß-Lactamases 73
2.5.1 ß-Lactamase Classification 74
2.5.2 Class A – Serine Penicillinases & Carbapenemases 74
2.5.3 Class C Cephalosporinases 75
2.5.4 Class D Oxacillinases 76

2.5.5 Class B Metallo-ß-lactamases 76
2.6 Dynamic Combinatorial Chemistry of Benzodiazaborines & Boronate Esters 78
2.7 Polyfunctional DCC Support Ligands & the Expansion of our DCL 95
2.7.1 Synthesis of (*R*)-*N'*-(L-cysteinyl)-2-amino-3-mercaptopropanehydrazide 96
2.7.2 Synthesis of 2-amino-*N'*-homocysteinyl-4-mercaptobutanehydrazide 101
2.8 Dynamic Combinatorial Chemistry of Polyfunctional Ligands 111
2.8.1 Dynamic Combinatorial Chemistry of Polyfunctional Ligands with 2-FPBA 112
2.8.2 Dynamic Combinatorial Chemistry of Polyfunctional Ligands with Formaldehyde 114
3.1 Heterodimer & Dual Acting Drugs 135
3.1.1 Heterodimers & Dual Acting Drugs as Receptors Binders 135
3.1.2 Heterodimers & Dual Acting Drugs as Enzyme Inhibitors 137
3.1.3 Heterodimers & Dual Acting Drugs of Both Enzymes and Receptors 138
3.2 Pharmacodynamics of Nitrofuran Antibacterials 139
3.3 Design & Synthesis of Novel Nitrofuranyl Indole Carboxylate Heterodimers 142
3.3.1 Design & Synthesis of NInCs at C-3 of the Core InC 144
3.3.1.1 Synthesis of Nitrofuranyl Hydrazone & its Imine Counterpart 144
3.3.1.2 Reactivity of Polar Protic Solvents Towards 5-Nitrofurfural & its Derivatives 155
3.3.1.3 Conjugative Effects on Nitrofuranyl Hydrazone Colour 166
3.3.1.4 Synthesis of Sulfoximinyl & Sulfonyl Spacers 171
3.3.1.5 Synthesis of InCs & Their Borylation 178
3.3.1.6 Synthesis of NInC Esters via Buchwald Amination 183
3.3.2 Hydrolysis of NInC Esters 188
3.3.2.1 Acid & Base hydrolysis of NInC Ethyl Ester 188
3.3.2.2 Enzymatic Hydrolysis of NInC Ethyl Ester 192
3.3.2.3 Synthesis of NInC Methyl Ester 198
3.3.2.4 Alternative Methods for Hydrolysis of NInC Methyl Esters 208
3.3.3 Alternative Protecting Group Strategies for the Carboxyl Moiety of NInC Hybrids 214
3.3.3.1 p-Methoxybenzyl Ester Protecting Group Strategy 215
3.3.3.2 Trimethylsilylethoxymethyl Ether Protecting Group Strategy 216

3.3.3.3 No Carboxyl Protecting Group Strategy 219
3.3.4 Bypassing Carboxyl Protection in NInC Synthesis 219
3.3.5 Design & Synthesis of NInC Hybrids Featuring a Stable Cleavable Linker 224
3.3.6 Design & Synthesis of NInCs at C-7 of the Core InC 237
3.3.6.1 Synthesis of Ethyl 7-Acetyl-1-H-indole-2-carboxylate 238
3.3.6.2 Coupling of Nitrofuran Hydrazones to Ethyl 7-Acetyl-1-H-indole-2-carboxylate 239
3.3.6.3 Ester Hydrolysis of Ethyl 7-Acetyl-1-H-indole-2-carboxylate & its Corresponding NInC Esters 241
3.3.6.4 Synthesis of Stable NInC Hybrids 242
3.4 Biological Evaluation of NInC Hybrids 245
Reference 248
Experimental S1

Abstract

Chapter 1 commences with a brief panorama of antibacterial development from the very first modern antibacterial agent, namely Salvarsan® to the very last class of clinically significant antibacterials, namely oxazolidinones. It then goes on to briefly outline the practice of modern Drug Design under the heading '*Medicinal Chemistry & Drug Discovery*', before discussing molecular targets in bacteria and further reiterating that there are several '*conserved*' molecular targets in bacteria for which there are no antibacterial agents in clinical use as yet, under the heading '*Current Antibacterial Targets*.'

Whereas in the recent past drug development has often focussed on molecular structures with limited pharmacokinetic parameters *e.g.* '*Rule of 5*', there has been extensive research on lead-like compounds other than those in the realm of small molecule drug-likeness. With this borne in mind Chapter 1, Antimicrobial Peptides – a New Chasm, introduces the concept of protein-protein interactions (PPIs),[I] which could pave the way for development of promising therapeutic agents of various properties such as pacidamycin[II] and muraymycin[III] which are all peptide-based antibiotics that are concerned with PPIs.

The remainder of Chapter 1 discusses antibacterial resistance and invites the reader to consider other subtle but crucially important facets of antibacterial resistance *i.e.* Horizontal (Lateral) Gene Transfer & Immunological Tolerance, which are often not considered due to their inherent complexities.

[I] D. R. Spring, *Chemistry in Health Symposium: Towards New Therapeutics to Fight Disease*, Burlington House, London, 26 May 2015.
[II] M. T. Rodolis, A. Mihalyi, C. Ducho, K. Eitel, B. Gust, R. J. Goss and T. D. H. Bugg, *Chem. Commun.*, 2014, **50,** 13023.
[III] A. P. Spork, M. Bschleb, O. Ries, D. Wiegmann, S. Boettcher, A. Mihalyi, T. D. H. Bugg, and C. Ducho., *Chem. Eur. J.*, 2014, **20**, 15292.

Chapter 2 is devoted to a detailed discussion on Solid Phase Synthesis which serves as a gateway to descriptions of Combinatorial Chemistry, and subsequently Dynamic Combinatorial Chemistry (DCC). It is expected that the average reader would like to skip through the literature review of this chapter; however, at the risk of being forward and in the interests of completeness, a knowledge of its existence is thought desirable for the curious reader so that they may wish to utilise them when occasion demands.

The aforementioned relatively short introduction in Chapter 2 precedes the detailed preparations of the Dynamic Combinatorial Library of benzodiazaborines and boronate esters herein. Attention is particularly directed to the second half of Chapter 2 in which the Design & Synthesis of novel polyfunctional DCC ligands is thoroughly discussed with a fuller discussion on their DCC systems with 2-formylphenyl boronic acid & formaldehyde which led to identification of novel and intriguing heterocycles. Chapter 2 also features a new reaction for deprotection of the thiazolidine protecting group which is hoped to arm the synthetic chemist with an additional synthetic tool at their disposal. However, a mere perusal of this novel synthetic tool herein by those whose time for chemical synthesis is constrained may assist them to be impressed on the memory.

The tortuous path to novel Nitrofuranyl Indole Carboxylate (NInC) hybrids is delineated in Chapter 3 which opens with a brief review of drug conjugates and their linkers, in particular, cleavable linkers so as to precede fuller discussions on the Design, Synthesis & Modification of novel NInC hybrids herein. Considerable detail is given in parts of Chapter 3 which are concerned with the intrinsic colour of nitrofuranyl derivatives; in the author's opinion, the onus is upon the writer to lay a secure foundation of sound theory of observable phenomena in question for the outsider.

Chapter 3 by a large part is confined to ester hydrolysis of carboxyl ester protected NInCs. After numerous failed attempts, the synthesis of a deprotected carboxyl ester NInC was achieved. However, the desired NInC proved unstable and the studies on ester hydrolysis of these novel NInCs suggest that a suitable ester prodrug of these potential drug conjugates may be promising in a clinical setting.

Last but not least, it is hoped that a handful of these potentially novel therapeutics could further be developed into leads or drug candidates either in Oxford or elsewhere in an attempt to tackle the ever-increasing antibacterial resistance.

Chapter 1

A Literature Perspective

Introduction

"A wise man should consider that health is the greatest of human blessings and learn how by his own thought to derive benefit from his illnesses."

Hippocrates

Tinctures, infusions, poultices and soups of freshly ground extracts or dried herbs and livestock products might no longer be available in western pharmacies, but these were the basis of Hippocratic medicine upon which many of our ancestors of bygone eras relied, in order to balance the body's '*humors*' – sanguine, phlegmatic, choleric and melancholic.[1] The discipline of pharmacy emanated from ethnomedicine with roots in ancient medicine for which the concept of a medicine was confined to natural extracts and devoid of the chemical definition of today's drugs.

It was not until the 18th century when scientists such as Joseph Priestly and Scheele, who discovered oxygen and other chemical elements, that chemistry began to be connected with medicine. Antoine Laurent de Lavoisier is regarded as the founder of modern chemistry and his theory of oxygen combustion was important in the concept of mass conversion.[2] The discovery of oxygen combustion established distinctions between elements and compounds which was the foundation of modern chemistry. The work of many other scientists in the 18th century such as Louise Nicolas Vauquelin, Humphrey Davy, Jöns Jakob Berzelius and others, also introduced important new concepts in chemistry in a similar timeframe.[3]

The 19th century saw the greater availability of new therapeutic resources owing to the work of pioneers such as Justus Von Liebig and Gay-Lussac.[4] The pioneering works of Claude Bernard,[5] Rudolph Virchow[6] and Louise Pasteur[7] prompted 19th century scientists to realise the contribution that scientific disciplines such as physiology and microbiology could make to pharmacology.

The use of rational treatment was born from clinical achievements and the advances in chemistry that gave birth to synthetic chemistry laboratories. It was these advances that led to the first purified synthetic organic compounds suitable for use in therapeutic contexts. For example, chloroform was independently discovered by Eugene Soubeiran,[8] Justus Von Liebig[9] and Samuel Guthrie,[10] and was the first identified general anaesthetic with rather mild side effects.

The concept of chemical isomerism was first coined by Berzelius, following the discovery of cyanic and fulminic acid by Wöhler and Liebig in 1825; both possessing the same chemical composition, but different physical properties – Liebig's silver compound was explosive, whilst Wöhler's silver compound was not. This difference resulted in Berzelius's proposal that despite their apparently identical chemical disposition, the arrangement of their atoms within the molecules must be different. A famous early case of isomerism was Wöhler's precipitous urea; whilst he was attempting the synthesis of ammonium cyanate, he serendipitously synthesised organic urea from inorganic precursors.[11]

The road to modern medicinal chemistry was possibly first crossed by organic chemistry in 1856, when William Perkin serendipitously stumbled across mauveine in a failed synthesis attempt at quinine. This first synthetic dye was later developed into antimicrobials, which were the first modern therapeutics and used in the early 20th century.[12]

In 1848 Louis Pasteur in work on crystals of tartaric acid realised that tartaric acid derived from living entities rotated plane-polarised light; however, its synthetic counterpart lacked that property. This observation led him to conceive that since bacteria can affect organic compounds, they should be able to live on humans too. The renowned father of microbiology then hypothesised the germ theory of disease and argued in his papers – *Etudes sur le Vin* and *Etudes sur la Bière* – that microorganisms can infect humans and cause diseases,[13] the cause of which was previously thought to be demons.[14]

In addition to the advances in disease identification and rational disease treatments of the 19th century, in 1809 Charles Louis Cadet de Gassicourt proposed that complex therapeutic mixtures should be replaced by pure substances so as to assess the quality of treatments based on variations amongst patients than any differences in mixture preparations.[15] This idea gave birth to a new era in medicinal chemistry and ultimately led to the current classification of active pharmaceutical ingredients (APIs).

Throughout history the works of scientists and medicinal chemists have brought about numerous treatments to improve human (and animal) health and increase longevity. The vast history of drug discovery is beyond the scope of this short survey, which below focusses on antimicrobial history, in particular, that of antibacterials.

1.1 Antibiotics History

"One sometimes finds, what one is not looking for. When I woke up just after dawn on September 28, 1928, I certainly didn't plan to revolutionise all medicine by discovering the world's first antibiotic, or bacteria killer. But I suppose that was exactly what I did."

Alexander Fleming

The first milestone towards combating infectious diseases by chemotherapy, perhaps dates back to 1785 when chlorine gas was dissolved in water to remove stains on textiles.[16] Inspired by this and following the discovery of potassium hypochlorite (produced by reaction of chlorine with potassium hydroxide) by Berthollet in 1789,[17] Antoine Germain Labarraque moved away from potassium hydroxide in favour of cheaper sodium hydroxide and synthesised sodium hypochlorite, *i.e.* bleach in 1820.[18] As a result, in the 1820s Oliver Wendell Holmes was able to demonstrate a reduction in prevalence of puerperal fever if midwives washed their hands in dilute bleach.[19]

A few decades later in 1873, in light of germ theory of diseases by Louis Pasteur in the 1850s, Casimir Davaine was able to treat anthrax with iodine.[20] The discovery of phenol by Friedlieb Runge in 1834[21] revolutionised hygiene in hospitals; in 1865 Joseph Lister who generally is considered as the father of modern surgery,[22] pioneered the use of phenolic antiseptic dressings for wound treatment and surgery.[23] Lister with the help of Robert Koch was able to culture purified *Bacillus Lactis* in soil, and show that the spores of the bacterium can survive for a long time, thriving and replicating when the conditions are suitable (for this discovery they are regarded as the founders of medical microbiology).[24]

In 1881, Koch showed pure cultures of bacteria were killed by hypochlorite; later in 1894, Isidor Traube was able to purify and disinfect water with hypochlorite.[25] During World War I solutions of sodium hypochlorite and sodium chloride *e.g.* Milton® were extensively used for disinfecting open wounds.[26]

1.1.1 Sulfonamide Antibacterials

Whereas the discovery of many microbial infectious diseases was the hallmark of the 19th century disease aetiology, the treatment of infectious diseases such as syphilis, bubonic plague and tuberculosis (TB) remained a distant dream. Until the early 20th century the fight against microbial diseases was confined only to cuts and wounds disinfection, and drinking water sanitisation.

The dyestuff chemistry breakthrough in virtue of booming dye industry of the 19th century was to unexpectedly improve infectious disease treatments.[27] In the 1880s, Paul Ehrlich realised that living cells incorporated dyes in a different fashion to dead cells; he then envisaged that this process could alter their compartments.[28] As a result, Ehrlich and Sahachiro Hata analysed over 606 dyes to treat syphilis in animals and succeeded in treating all within three weeks with no fatalities.[29]

The outbreak of the flu pandemic (also referred to as Spanish Flu) in 1918–1920, which claimed approximately 50 million lives,[30] put the burden on scientists to be ever more determined in combating infectious diseases. In 1927 Gerhard Domagk at Bayer was focussed on design of a drug to treat streptococcal infections. He hypothesised that since diazo dyes were observed to bind tightly to the proteins in textiles, so as to dye the fabric; they could also bind to the bacterial proteins and bring about apoptosis or inhibit their cell growth. To this end, he synthesised sulfamidochrysoidine, naming it Prontosil® in 1932, which gave birth to a new era of chemotherapy.[31] Domagk received the 1939 Nobel Prize in Physiology or Medicine for his discovery of Prontosil®, although the prize was only given after World War II in 1947,[32] due to a veto on Germans receiving the prize.[33]

A team at the Pasteur Institute unravelled the mode of action of Prontosil® and discovered that reductases were needed to convert the Prontosil® prodrug to its active sulfonamide antibacterial.[34] In the late '30s and early '40s, almost 5000 sulfonamides were developed, some of which such as sulfathiazole, sulfadiazine and trimethoprim/sulfamethoxazole (co-trimoxazole) are still in clinical use.[35]

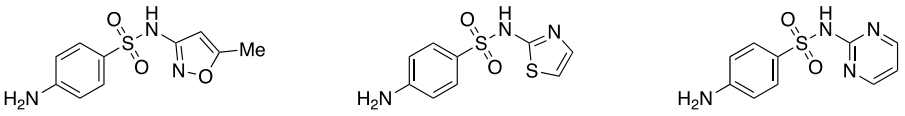

sulfamethoxazole sulfathiazole sulfadiazine

Figure 1.1 Representative examples of sulphonamide antibacterials in clinical use.

1.1.2 Penicillin ß-Lactam Antibiotics

With the advent of sulfonamides, the search for more systematic and internal antiseptics became particularly appealing. In pursuit of new antibiotics in the 1920s, Alexander Fleming discovered that human teardrops were able to kill bacteria and he named the active material lysozyme; however, this lysozyme was ineffective against known bacterial pathogens and considered not to have therapeutic potential.[36] Fleming did not give up and whilst in the process of growing *Staphylococci* cultures, he observed that the unexpected mould in one of the cultures was destroying the bacteria. After further experimentation and isolation of the mould extracts, Fleming introduced the activity of penicillin extracts to the world in 1928.[37]

The overwhelming number of casualties during World War II led Howard Florey and Boris Ernst Chain to utilise Fleming's penicillin, and their work was published in '*Lancet*' in 1940; however, unfortunately, the study did not attract much attention from the pharmaceutical industry.[38]

Nevertheless, the Oxford team developed a powdered form of penicillin and were able to treat their first patient with it in 1941, an achievement for which Fleming, Florey, and Chain shared the 1945 Nobel Prize in Physiology or Medicine.[39]

Unfortunately, Fleming's penicillin was likely a mixture of penicillins with polar side chains. Work in the US led to development of penicillins with hydrophobic side chains such as benzylpenicillin (penicillin G) and phenoxymethylpenicillin (penicillin V). In the early 1940s, Dorothy Crowfoot Hodgkin used X-ray crystallography to determine the molecular structure of penicillin G in Oxford, for which she was awarded the 1964 Nobel Prize in Chemistry.[40]

Once the structure of penicillin was revealed John Clark Sheehan was able to complete the first total chemical synthesis of penicillin G and some of its derivatives.[41] However, his synthesis was not cost-effective for mass production (as has been the case with subsequent penicillin syntheses); the lack of oral bioavailability of penicillin G and the orally bioavailable phenoxymethylpenicillin (penicillin V), directed research towards broad-spectrum orally bioavailable derivatives of penicillin. As a result, ampicillin was developed in 1960;[42] this was a major milestone in ß-lactam chemotherapy due to the broader spectrum of activity of ampicillin compared to both penicillin G and V.

ß-lactam resistant strains of *Staphylococcus aureus* were known as early as 1945.[43] With the aim of overcoming this resistance, Beecham and Bristol-Meyers Squibb developed methicillin, but it did not take long for methicillin resistant strains of *S. aureus* to appear. Extensive research further brought about ß-lactamase resistant penicillins such as flucloxacillin and oxacillin;[44] however, resistance to these newly developed penicillins has long been known. Thus, work focussed on discovering new types of the ß-lactam class of antibiotics, ultimately leading to development of the cephalosporins, carbapenems and monobactams (Fig. 1.7).

1.1.3 Aminoglycoside Antibiotics

Soil species have been the subject of thorough antibacterial research as early as 1914;[45] this work resulted in the discovery of *Streptomyces griseus* by one of Selman Abraham Waksman's graduate students *i.e.* Albert Schatz in 1940.[46] Actinomycin, the first *S. griseus* isolate proved too toxic for clinical studies, however Schatz *et al.*,[47] isolated streptomycin from *S. griseus*.

In 1942 an outbreak of TB troubled millions and claimed hundred thousands of lives globally; with *M. tuberculosis* being resistant to sulfonamides and penicillins, Merck & Co. was quick to initiate streptomycin manufacturing and on 20 November 1944, the first TB patient was treated with streptomycin,[48] which earned Selman the 1952 Nobel Prize in Physiology or Medicine. One of the major side effects of streptomycin which hampered its widespread clinical use was its ototoxicity particularly to the inner ear;[49] this resulted in the sequential development of an array of tuberculicids – isoniazid in 1952,[50] pyrazinamide in 1954,[51] ethambutol in 1962[52] and rifampicin in 1963[53] are a few to name.

1.1.4 Chloramphenicol Antibiotics

The numerous *Streptomyces* antibiotics inspired David Gottlieb to isolate chloramphenicol from *Streptomyces venezuelae*, which was found in a field near Caracas, Venezuela in 1947.[54] Chloramphenicol was the first antibiotic to be mass produced purely by synthesis.[55] Chloramphenicol contains two stereogenic centres, with only the (*R*,*R*)-stereoisomer being active (Fig. 1.2).

Chloramphenicol binds to the same molecular target as macrolides *i.e.* the 50S subunit of bacterial ribosome (Section 1.3), and its co-administration with macrolides is contraindicated. As illustrated in Fig. 1.2 chloramphenicol possesses an aryl nitro moiety, a known toxicity threat which should be treated with caution in drug design, and which induces hepatotoxicity.

As a result, similar to aminoglycosides, the toxicity of chloramphenicol coupled with availability of better alternatives reduced its popularity in the 1950s.[56] However, in the UK as elsewhere chloramphenicol is widely available on prescription and over the counter in various eye drop formulations.[57]

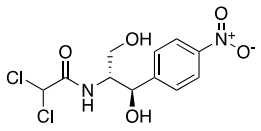

Chloramphenicol

Figure 1.2 The aryl nitro moiety of chloramphenicol is potentially toxic.

1.1.5 Tetracycline Antibiotics

One of the most widely prescribed antibiotics is the tetracycline class of antibiotics. The first of its kind to be discovered was chlortetracycline which was isolated from *Streptomyces aureofaciens* in Missouri in 1948.[58] Chlortetracycline was marketed as Aureomycin due to its golden colour, derived from the Latin *aurum*.[59]

Streptomyces aureofaciens was of interest to Lloyd Conover at Pfizer who was able to convert chlortetracycline to oxytetracycline by removal of the chloride substituent *via* palladium catalysed hydrogenolysis (Fig. 1.3).[60] This prompted medicinal chemists to pursue modification of other antibiotics to generate more effective analogues – the basis of a quite common lead optimisation process (Section 1.2.6). To date, doxycycline is the most commonly prescribed tetracycline antibiotics.

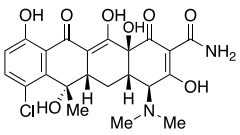

Chlortetracycline

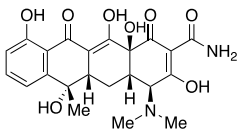

Oxytetracycline

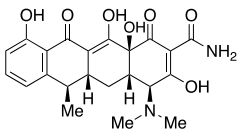

Doxycycline

Figure 1.3 Representative examples of marketed tetracycline antibiotics.

1.1.6 Macrolide Antibiotics

The mid-20th century saw the development of many penicillin antibiotics; however, some patients are penicillin intolerant and experience severe side effects, in particular, the life-threatening toxic epidermal necrosis. This problem was addressed when Abelardo Aguilar who was working for Eli Lilly sent a soil sample from Iloilo to the company in 1949. Eli Lilly was able to isolate erythromycin (a macrolide) from *Saccharopolyspora erythraea* and in 1952 launched Ilosone®; named in honour of Iloilo in Philippine where the soil sample was collected.[61] In essence, erythromycin is an effective antibiotic similar to penicillin with no severe side effects which was made available to many penicillin intolerant patients.

A team led by Robert Burns Woodward,[62] was able to complete the first asymmetric synthesis of erythromycin in 1981. The asymmetric synthesis helped researchers at Taisho Pharmaceutical to overcome the acid instability of erythromycin and develop clarithromycin,[63] and a few years later the world's popular antigonoccocal *i.e.* azithromycin (Fig. 1.4) was developed by Pliva in 1988.[64]

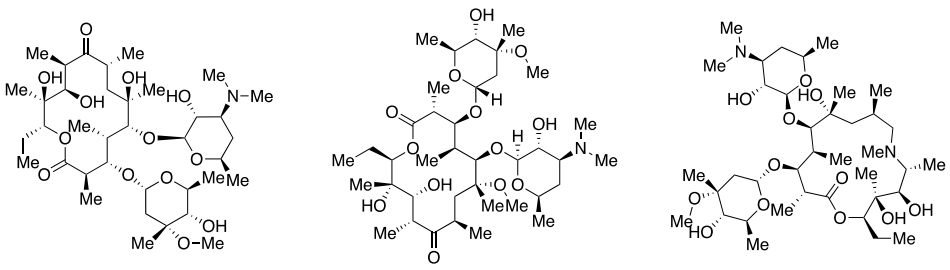

Erythromycin Clarithromycin Azithromycin

Figure 1.4 Representative examples of macrolide antibiotics in clinical use.

1.1.7 Glycopeptide Antibiotics

Streptomycetaceae produce almost half of the class of the antibiotics in current clinical use, the latest in the series of medicinally important compounds being glyco and lipopeptides. In 1953, Edmund Carl Kornfield – a medicinal chemist working at Eli Lilly – discovered an isolate from *Streptomyces orientalis*[65] which was referred to as '*compound 05865*' and active against most Gram-positive bacteria including

methicillin-resistant *S. aureus* (MRSA).[66] The initial purification method required the explosive picric acid; Kornfield then employed an alternative purification, which only gave an 82% pure compound with a distinctive brownish colour – this was dubbed '*Mississippi mud*'.

This concoction was first tried on a patient with a severe foot infection who was unresponsive to multiple antibiotics. His surgeons advised either amputation or the use of the new drug; he replied: "anything that might save my foot." He was then given high doses of the drug over five days, and was discharged from the hospital with a pristine foot two months later. Compound 05865 was subsequently launched as vancomycin, a name derived from '*vanquish*' in 1958.[67]

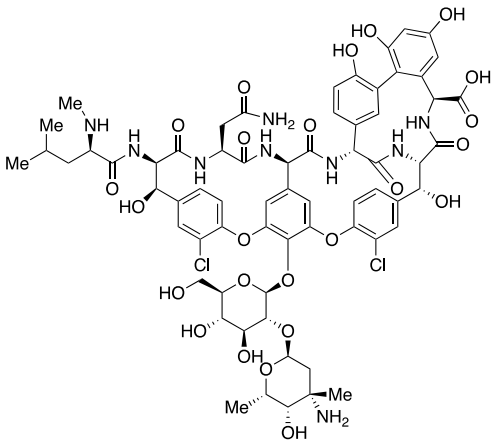

Figure 1.5 Vancomycin – the first marketed glycopeptide antibiotics still in clinical use.

1.1.8 Cephalosporin ß-Lactam Antibiotics

In 1948 Giuseppe Brotzu, an Italian pharmacologist and politician, isolated the cephalosporins from *Cephalosporium acremonium* which was obtained from a sewer in Sardinia. He realised that the fungal extracts had antibacterial activity against *Salmonella typhi* and could treat typhoid fever.[68] Subsequently, five generations of cephalosporin were developed:

- the first-generation cephalosporins *e.g.* cephalothin, cefalexin *etc.*, are broad spectrum with activity against both Gram-positive and Gram-negative bacteria.

- The second-generation *e.g.* cefaclor, cefuroxime, cephamycins *etc.*, have reduced activity against Gram-positive bacteria, but possess much better activity against Gram-negative bacteria with even broader spectrum of activity.

- The third-generation *e.g.* cefixime, ceftriaxone *etc.*, effectively target Gram-negative bacteria, but are mostly ineffective against Gram-positive bacterial pathogens; they are particularly useful in treating nosocomial bacterial infections.

- The fourth-generation *e.g.* cefiderocol, cefpirome *etc.*, are analogous to the first-generation cephalosporins *i.e.* having broader spectrum of activity with improved activity against Gram-negative bacteria, but no orally bioavailable cephalosporin of this class has been marketed.

- The fifth and last generation cephalosporins *e.g.* ceftaroline, according to the Washington Post[69] are highly effective antibiotics of the last resort.

1.1.9 Quinolone & Fluoroquinolone Antibacterials

The early 1960s witnessed the emergence of quinolones when George Lesher serendipitously stumbled across nalidixic acid as a side product when distilling products of the antimalarial chloroquine synthesis.[70] As a Gram-negative urinary tract antibacterial, nalidixic acid opened up research towards the development of more structurally diverse set of quinolone and fluroquinolone antibacterials. This gave rise to a second-generation fluoroquinolone *i.e.* ciprofloxacin, which is potent against Gram-negative bacteria; however, with only moderate activity against *S. aureus*, it manifested the rapid emergence of resistance.[71] The latter brought about a further third-generation of quinolones *e.g.* ofloxacin, moxifloxacin *etc.*, in the early 1990s.[72]

Ofloxacin is widely in clinical use and marketed as a racemate, with one enantiomer being completely inactive. Levofloxacin is the active enantiomer of ofloxacin and marketed as an antibacterial with twice the potency of that of ofloxacin.[73] Besifloxacin, a fourth-generation fluroquinolones, has improved activity against pneumococcal infections and was first marketed in 2009.[74]

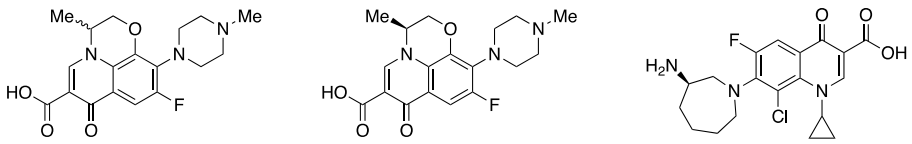

Figure 1.6 Representative examples of fluoroquinolones in clinical use.

1.1.10 Carbapenem ß-Lactam Antibiotics

The prolific development of other classes of ß-lactam antibiotics began in 1976 when fermented broths of the soil organism *Streptomyces cattleya* proved to inhibit the peptidoglycan bacterial cell-wall.[75] The extensive purification of the aforementioned broth resulted in the isolation of thienamycin in 1979,[76] which gave birth to a new class of ß-lactam antibiotics – the carbapenems. Thienamycin never reached clinical trials due to being unstable in water similar to many other novel antibacterials (Chapter 3), instead more stable derivatives such as imipenem and meropenem have been developed and marketed ever since.

The ß-lactam family of antibiotics was completed with the introduction of aztreonam in 1986[77] – the only monobactam class of ß-lactam antibiotics in clinical use, which is derived from *Chromobacterium violaceum*[78] (Fig. 1.7).

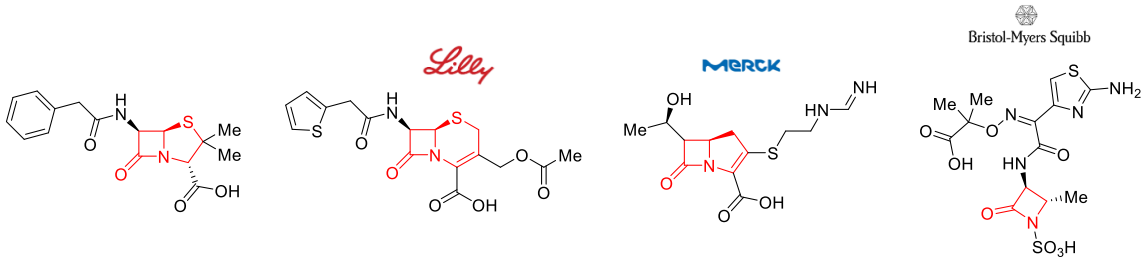

Figure 1.7 The first marketed antibiotic of each ß-lactam class. The core ß-lactam ring system of each class shown in red. Benzylpenicillin the first penicillin; Keflin® the first cephalosporin; Primaxin® the first carbapenem; and Azactam® the first and only marketed monobactam ß-lactam antibiotic in clinical use.

1.1.11 Nitrofuran Antibacterials

Whereas in the early 1940s the fight against microbial diseases was mostly focussed on the discovery and isolation of antibiotics from soil species, in particular, *Streptomycetaceae*, the advances in drug discovery enabled medicinal chemists to introduce purely synthetic classes of antibacterials, notably the nitrofuran class of antibacterials.

Nitrofurantoin, the first member of the nitrofuran class of antibacterials was launched in 1953,[79] though the exact mechanism of its action is not well understood, it is thought to undergo reduction in the bacterial cells and then generate radicals which damage their deoxyribonucleic acid (DNA).[80] This reduction reduces the concentration of nitrofurantoin inside the bacterial cell, generating a concentration gradient down which more nitrofurantoin in the extracellular environment enters the cell.

Nitrofurantoin is commonly administered orally for treatment of acute or recurring uncomplicated urinary tract infections and pyelitis.[81]

A closely related antibacterial to nitrofurantoin is furazolidone which was marketed as Furoxone by Robert Laboratories and used as a third-line of treatment for *Helicobacter pylori* infections; however, this indication is now unlicensed.[82] Nitrofurazone is another nitrofuran antibacterial which was marketed as Furacin for topical indications; however, it has now become obsolete by virtue of better alternatives.[83] Ranbezoild which was discovered by Ranbaxy is also a nitrofuran antibacterial and currently in clinical trials as an oxazolidinone type antibacterial.[84]

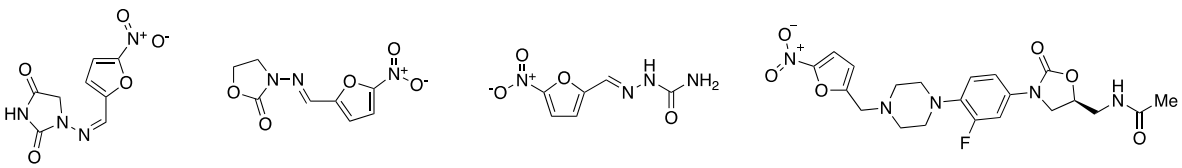

Figure 1.8 Representative examples of nitrofuran antibacterials.

1.1.12 Oxazolidinone Antibacterials

Further improvements in drug discovery especially target identification and drug screening, prompted researchers at DuPont to repurpose oxazolidinone monoamine oxidase inhibitors as antibacterials; a patent for oxazolidinone compounds as effective agents in treating bacterial and fungal plant diseases was filed in 1978;[85] followed by another patent concerning treatment of mammalian bacterial infections in 1984.[86] In 1987, DuPont successfully presented a detailed description of oxazolidinones as a new class of antibacterials with a novel mode of activity.[87]

In the 1990s, Pharmacia & Upjohn began oxazolidinone antibacterial research, and after a careful structure-activity relationship (SAR) study of several oxazolidinone derivatives, they introduced two drug candidates – eperezolid (PNU-100592) and linezolid (PNU-100766).[88] In Phase I clinical trials it was demonstrated that linezolid possessed better pharmacokinetics than eperezolid, and also required only twice daily dosage as opposed to three daily dosage regimen for eperezolid; linezolid proved superior to eperezolid and was marketed as Zyvox® on 18 April 2000.[89]

Cubist Pharmaceuticals which was later acquired by Merck & Co. developed tedizolid, a second-generation oxazolidinone, which was later marketed by Merck & Co. as Sivextro® in June 2014 (Fig. 1.9).[90]

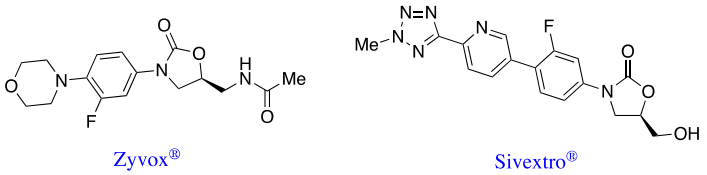

Figure 1.9 Representative examples of oxazolidinone antibacterials in clinical use.

Antibacterial discovery was a triumph hallmark of the 20th century science – all classes of antibiotics currently in clinical use were developed in the last century. Despite advances in medicinal chemistry, in particular, drug discovery, no new classes of antibiotics/antibacterials have been introduced since the late 1980s. Some new classes of antimicrobial peptides (AMPs) such as copsin[91] and teixobactin[92] were recently discovered, but none have yet found their way into the market. Ever-increasing antibacterial resistance together with the lack of new classes of antibacterials poses a huge threat to global public health. Many believe that once again we should turn to the ingenuity of chemists and other scientists to solve this global health burden.

As delineated above a serendipitous drug discovery by Alex Fleming which revolutionised the way in which we treat bacterial infections, now has been evolved to become a systematic, expensive and complex drug discovery platform, which arguably precludes serendipitous drug discovery. In this perspective, we will briefly visit stages of the drug discovery, so as to gain insight into how modern drug discovery takes place.

1.2 Medicinal Chemistry & Drug Discovery

> *"Medicinal chemistry remains a challenging science which requires profound satisfaction to its practitioners. It integrates those of us who like to solve problems posed by nature. It verges increasingly on biochemistry and on all the physical, genetic and chemical riddles in animal physiology which bear on medicine. Medicinal chemists have a chance to participate in the fundamentals of prevention, therapy and understanding of diseases and thereby to contribute to a healthier and happier life."*
>
> *Alfred Burger*[93]

Medicinal chemistry can be considered as a branch of pharmacy that is dynamically linked with the life sciences. The inherent multidisciplinary nature of medicinal chemistry necessitates inputs from various sections of chemistry including, but not limited to, organic, physical, computational, X-ray crystallography and process chemistry, as well as biological aspects of chemistry such as biochemistry, immunology, structural biology, pharmacology, genetics and toxicology.

The International Union of Pure and Applied Chemistry gives a specific definition for medicinal chemistry, which as follows:

> *"Medicinal chemistry concerns the discovery, the development, the identification and the interpretation of the mode of action of biologically active compounds at the molecular level. Emphasis is put on drugs, but the interest of the medicinal chemist is not restricted to drugs but include bioactive compounds in general. Medicinal chemistry is also concerned with the study, identification and synthesis of the metabolic products of these drugs and related compounds"*[94]

To date, the World Drug Index has registered almost 80,000 drugs and pharmaceutically active compounds, of which 1,357 are APIs;[95] the WHO list of essential medicines contained 433 drugs in 2017.[96]

A thorough analysis of marketed drugs published by Overington *et al.*[97] revealed 324 drug targets for the marketed drugs, linked with 1,204 small molecules and 166 biologics, of which 27% are G-protein-coupled receptor (GPCR) binders, 13% target intracellular nuclear receptors, and 13.4% bind to ion channels. On the other hand, Imming *et al.*[98] proposed that there are 66 biologics (mostly protein-based drugs) marketed for human enzymes, 20 for microorganism enzymes, 12 for intracellular nuclear receptors, and 10 ion channel binders. Thus, relative to the small molecule drugs, the biologics field of drug discovery appears to be a much unexplored territory, and the clinical potential of biologics has not been fully exploited (Section 1.4).

The drug discovery process delineates a very convoluted path which requires consideration of many variables such as compound potency, solubility, selectivity, bioavailability, cellular activity, metabolic stability and acceptable toxicity. The lengthy and strenuous drug discovery road has exquisitely been put in context by the Tufts Centre for the Study of Drug Development which estimates that on average it takes 12 to 15 years and costs $2.6 billion (*ca.* £2.1 billion) to get a drug from an initial discovery onto the shelves of pharmacies.[99]

1.2.1 Drug & Its Principal Components

In the context of pharmacology, a drug is a chemical substance that alters the function of one or more organs or the process of a disease.[100] Thus, drugs generally increase or decrease biological functions and do, normally, not confer new functions on them. However, from the medicinal chemist perspective, the API together with its excipients, forms a complete drug by virtue of appropriate formulation.

The multicomponent characteristics of a drug target renders '*druggability*' a dynamic term such that no universal descriptors are available to signify a molecular target, druggable. Nevertheless, in an ideal world a new drug might be considered to possess most, though by no means all, of following properties:

- Substantially advances disease treatment.
- Be a novel substance with a unique mode of action and patentability attributes.
- Be prepared by four or less process steps,[101] and if synthetic be prepared using sustainable chemistry with no heavy metal catalysts and toxic wastes, but with a purity of ≥99%.
- Be able to withstand high temperatures and be stable towards humidity and light *i.e.* have a long shelf-life.
- Be a crystalline substance which is not hygroscopic, and which integrates well with a tablet binder.
- Be readily water soluble to generate haematologically isotonic blood solutions *in vivo*.
- Manifest >90% oral bioavailability which is not influenced by individuals' genetic variations.
- Be highly potent so as to permit no more than a 5–10 mg daily dosage regimen.

Unfortunately, there is no ideal drug in the real world, and likely there is a compromise in all real drugs (Fig. 1.10).

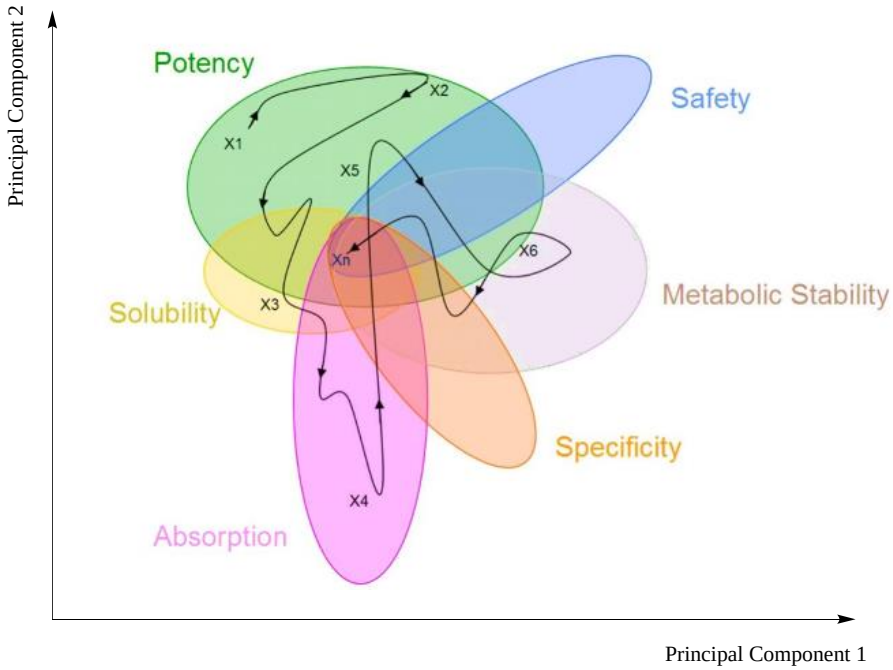

Figure 1.10 A hypothetical principal components analysis for selected drug properties.

1.2.2 Target Identification & Validation

It is now well-established that in order for a drug molecule to have an effect, it ought to interact with its '*target(s)*', which are most commonly proteins *i.e.* enzymes, ion channels and receptors. Some drugs have a physiochemical mode of action and some have unknown mechanisms.[102] Burgess *et al.*[103] identified nearly 8,000 human "*druggable*" targets in 2002, which is an infinitesimal figure compared to the theoretically available $>10^{60}$ small molecules of less than 500 molecular weight (MW) drug ligands.[104]

The current trends in medicinal chemistry reveal that, whereas historically the practising medicinal chemist used to elucidate the molecular target with which a natural product *e.g.* morphine just happened to interact, the stage is now set for identifying ligands which modulate '*orphan receptors*' / '*targets*' unknown to nature with the help of molecular biology and disciplines such as metabolomics and proteomics.[105]

Two major concerns about the rate of attrition of drugs in clinical trials are safety and efficacy, thus the identification and verification of appropriate targets is integral to further success of the clinical development, and ultimately approval and marketing of a potential drug molecule.

1.2.3 Hits & Leads

An area of drug discovery in which medicinal chemists play a huge part is lead identification and optimisation. In the lead identification phase, medicinal chemists aim to generate a starting point in the drug discovery programme for a given target, the latter chosen *via* various molecular biology techniques or the aetiology of the disease in question. They commonly do so by identifying one or several '*hits*'.

Generally speaking, all leads are hits, but not all hits are leads. The definition of a '*hit*' compound varies amongst researchers in different sectors; however, in the context of *in vitro* and *in silico* screening, a hit is a compound which exceeds a set threshold value for activity and binding affinity, respectively; the initial results can be confirmed upon resynthesis and retesting *i.e.* hit validation. From this onwards, a lead which could be one or more compounds possessing all the drug development prerequisites such as selectivity, desired activity, novelty, reproducibility *etc.*, will be developed.[106]

In most cases leads need to be optimised so as to meet the physiochemical criteria required in adsorption, distribution, metabolism and excretion (ADME) assessments to become a '*preclinical candidate*'. All being well, if no toxicity was observed in animal models the honour of '*clinical candidate*' will be granted, and the drug candidate will be submitted to the monopolistic clinical trials.[107]

1.2.4 Concepts of Druglikeness

Ever-increasing knowledge of the complexity of molecular targets, coupled with improvement in the resolution of disease aetiology, driven by the desire for high efficiency and speed of productivity, has resulted in major changes in pharmaceutical industry. Drug designers have consequently resorted to certain parameters to cherry pick the best selection of compounds for screening from the limitless chemical space defined by physiochemical parameters.

The endeavours of Lipinski *et al.*[108] *i.e.* Rule of 5, Ghose *et al.*,[109] Oprea *et al.*,[110] Veber *et al.*[111] have attempted to characterise compounds as '*druglike*' based on specific physiochemical parameters such as MW, lipophilicity *i.e.* $\log D_{5.5}$, electrostatic interactions *e.g.* number of hydrogen bond donors and acceptors, number of atoms and rings, molecular flexibility and polar surface area (PSA). However, none of these rules can predict oral bioavailability, which is a complex phenomenon, entailing dissolution rates, distribution and metabolism.[112]

Factors influencing the central nervous system (CNS) activity of a drug are even more sophisticated and harder to predict. To this end, Wager *et al.*[113] have devised a CNS multiparameter optimisation (MPO) calculator, which hitherto is the most accurate predictive tool for CNS druglikeness. This gives compounds a value from 0 to 6; compounds with high MPO values being more likely to exhibit CNS activity. Nonetheless, compounds that fall within the MPO druglikeness range, fail in clinical trials and thus druglikeness can be thought of the liabilities that make a compound fail in clinical trials.

A more fruitful strategy for avoiding these liabilities might be the use of '*privileged structures.*'[114] These can be classed as simplified structures (scaffolds) of currently marketed drugs that are likely to be converted to derivatives capable of binding with high affinity to (unclassified) molecular targets (Fig. 1.11).[115] However, privileged structures cannot guarantee oral bioavailability and non-toxicity; appropriate drug metabolism and pharmacokinetics (DMPK) must be kept in mind when designing libraries based on privileged structures.[116]

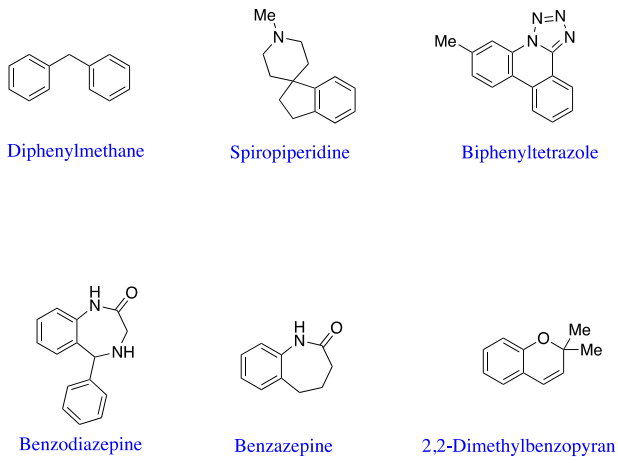

Figure 1.11 Representative set of privileged structures as identified by Evans *et al.*[114]

In 2002 an analysis of recently launched drugs by Proudfoot[117] revealed that many drug candidates submitted to the clinical trials resembled that of the original lead compounds. This introduced the concepts of '*leadlikeness*' which endows a druglike lead instead of uncertain compounds with many liabilities.

Several studies[118,119] have shown that lead optimisation processes generally result in compounds with lower solubility, greater complexity and lower bioavailability. Thus, so far as '*leadlikeness*' is concerned, high quality leads should be kept as small and hydrophilic as reasonably practicable, as Corwin Hansch noted: "*The principle is proposed that, without convincing evidence to the contrary, drugs should be made as hydrophilic as possible without loss of efficacy*."[120]

Another important parameter in defining leadlikeness is ligand efficiency (LE). The concept of LE was first coined by Andrews *et al.*[121] and later developed by Kuntz *et al.*,[122] which followed further by Hopkins *et al.*[123] and Abad-Zapatero *et al.*[124]

In its simplest form LE is defined as the free energy of binding per Dalton (Eq. 1.1) and can be the scoring function of choice for lead selection.[125] Displaying data in this manner leads to attribution of intermolecular interactions to the ligand only, and it is very useful, as the interactions between the ligand and target are not always known.[126]

Eq. 1.1 $$LE = \frac{\Delta G}{N} \qquad LE = 1.4\left[\frac{pIC_{50}}{N}\right]$$

Where ΔG is $-RTLnK_i$ and N is the number of heavy atoms; pIC_{50} is $-\log(IC_{50})$

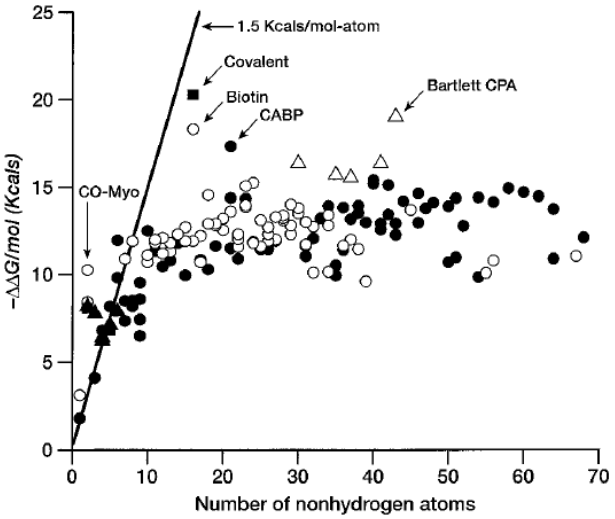

Figure 1.12 ΔG of binding (in kcal mol^{-1}) for ligands and enzyme inhibitors plotted as a function of the number of heavy atoms in the ligand. △ : metal ions or metalloenzymes; ▲ : small anions; ○: natural ligands; ● : enzyme inhibitors. (*Figure taken from Kuntz et al.*[122])

Fig. 1.12, clearly illustrates that the free energy of binding is directly proportional to the number of heavy atoms, with a starting slope of ≈ −1.5 kcal mol^{-1} per atom,[122] which implies that sub-nanomolar binding can, in theory, be feasible with ligands containing as little as 7–10 heavy atoms. In this context, interactions with metal ions, covalently bound compounds and a few interactions with small anions are outliers and should be disregarded.[127]

In practice, LE indices have demonstrated to be useful both in experimental and computational fragment-based drug design (FBDD) in virtue of their simplicity and ease of calculation,[128] and also their ability to help qualitatively describe the chemico-biological space under consideration for fragment optimisation.[129]

There are several arguments against validity of LE in the literature.[130,131] Nonetheless, LE appears to be a useful tool for selecting smaller drugs with better solubility, bioavailability and fewer metabolic liabilities.[132] The LE-based quantitative structure-activity relationship (QSAR) models are thought to have higher stability, predictive ability and robustness than the conventional models.

Eq. 1.2 $$PEI = \frac{\%\ inhibition\ at\ a\ given\ [compound]}{MW}$$

Eq. 1.3 $$BEI = \frac{pK_{i,}pK_{d}or\ pIC_{50}}{MW}$$

Eq. 1.4 $$SEI = \frac{pK_{i,}pK_{d}or\ pIC_{50}}{PSA}$$

Where pK_i & pK_d are $-\log(K_i)$ & $-\log(K_d)$ respectively; $K_{i,d}$ & IC_{50} are in mol dm^{-3}; MW is in g mol^{-1}

Over the last decade or two, the Percentage Efficiency Index (PEI) (Eq. 1.2), Binding Efficiency Index (BEI) (Eq. 1.3) and Surface Efficiency Index (SEI) (Eq. 1.4) have been introduced in order to reduce the number of variables by mixing potency with PSA and MW.

For instance, Abad-Zapatero *et al.*[124] were able to demonstrate that plotting the SEI-BEI plane which simultaneously considers three variables (potency, MW and PSA) in a 2-dimensional space is a fast and efficient technique for lead selection, and suggested that molecules with the highest probability of having favourable pharmacokinetics would have SEI–BEI pairwise values in the upper regions (lower PSA per MW <0.5 kDa) (Fig. 1.13).

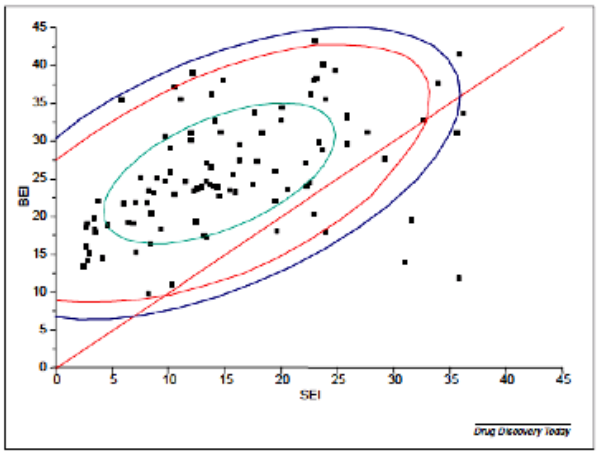

Figure 1.13 Mapping of the SEI and BEI for a sample of 92 marketed drugs; with values between 0 and 50 SEI–BEI have been plotted as well as the ellipsoids including 50% (green), 90% (red) and 95% (blue) of the sample. Most marketed oral drugs map close and above the diagonal line, which is a direct reflection of reasonable optimization of both BEI (MW) and SEI (PSA) (*Figure taken from Abad-Zaptero et al.*[124]).

Li *et al.*[133] carried out 2-dimensional multiple linear regression and 3-dimensional comparative molecular field analyses based on SEI and pIC_{50} metrics to investigate the SAR of a series of hydantoin derivatives as androgen receptor antagonists. It was shown that SEI-based models, though containing only three descriptors, outcompeted pIC_{50}-based models which require five descriptors. Their SEI data were not normalised, but the SEI approach outcompeted the normalised pIC_{50} model, showing that an SEI-based approach is capable of incarnating the relationship between biological activities and molecular structures somewhat better than a pIC_{50} model.

There are various other LE indices such as Ligand Lipophilicity Efficiency,[134] Group Efficiency, fit quality Scaled Ligand Efficiency and Size Independent Ligand Efficiency,[135] which are explained in the literature and accessible to those who wish to explore.

In recognition of the above, when screening for a premium small molecule druglike lead, it is worth paying attention to the following three golden principles:

- Selection of small and hydrophilic compounds with high LE values, if known. The Rule of 3 (Ro3),[136] which selects compounds with MW < 300 Da, ClogP, number of hydrogen bond acceptors and donors < 3 has been described as an excellent predictive tool.[137]
- Avoid known threats – Rishton[138] proposed many moieties which could be significantly detrimental to the success of a drug candidate in clinical trials, either by introducing toxicity due to their high reactivity or generating false positives in screening (Fig. 1.14). Another classical threat is '*frequent hitters*,'[139] these are promiscuous compounds with high protein binding propensity which could induce the human Ether-à-go-go-Related Gene (hERG) toxicity and also, could perturb the *in vitro* assays due to their intrinsic features such as fluorescence, *etc*.
- Ease of synthesis (EoS) and capability for analogue profiling.[140] This enables efficient mapping of chemico-biological space.

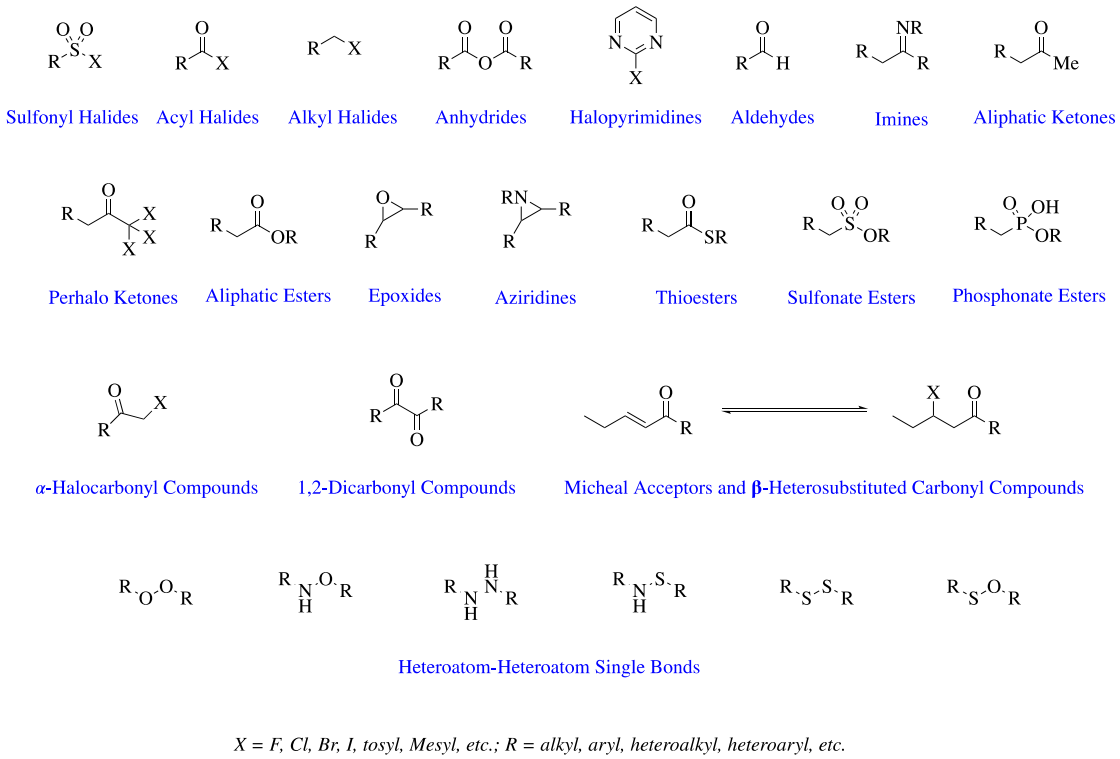

Figure 1.14 The prime example of known threats to druggability in the form of reactive functional groups (Rishton, 1997).[138]

1.2.5 Lead Identification

A second determinant of the fate of a successful drug discovery programme ensuing the initial target identification phase, is a well-informed lead identification process. Today, this is frequently performed *via* many state-of-the-art screening techniques, which gets more and more sophisticated with improved efficiency and prospects of automation. However, traditionally there are four major screening strategies which the practising medicinal chemist can utilise in their search for a '*magic bullet*.'

1.2.5.1 Analogue Profiling Strategies

The most common lead identification strategy is searching for analogues[141] of the existing drugs, also referred to as '*me-too drugs*' or '*follow-on drugs*'.[142] Although criticism has been directed at developing me-too drugs in terms of promoting imitation and reducing innovation.[143] Nevertheless, me-too drugs are often fruitful due to their improved potency, specificity, selectivity and better safety or formulation profiles, relative to the pioneering drugs.[144]

From a structural perspective, drug analogues can be divided into three categories:

- Analogues exhibiting similar chemical and pharmacophoric properties.[145]
- Analogues which are only chemically similar.[146]
- Analogues which are not chemically similar, but possess similar field effects with similar biological properties.[147]

1.2.5.2 Systematic Screening Strategies

There are many screening tools such as high-throughput,[148] virtual,[149] fragment-based,[150] ligand-based,[151] structure-based,[152] NMR,[153] X-ray crystallography[154] *etc.*, available for screening libraries of compounds in the lead identification phase. From a strategic perspective, screening can be carried out in either a directed[155] or random fashion.[156]

- Directed screening typically involves a small number of compounds with structures considered likely to elicit binding to or inhibition of their molecular target(s).
- Random screening involves a huge (typically hundreds of thousands) set of compounds for activity against a particular target.

1.2.5.3 Biological Data Exploitation

Mining biological information immensely contributes to the lead discovery. This could be in the form of physiological observations obtained as a result of substance interactions in cells from or studies on intact humans,[157] animals[158] or plants and microbial organisms.[159]

1.2.5.4 Planned & Rational Research

The lead identification strategies discussed above are either heavily dependent on chance *e.g.* high-throughput screening (HTS), or in the case of me-too drugs, an approach that lacks innovation. The most innovative and fruitful *de novo* strategy for a high quality druglike lead identification is rational research with a specific molecular target (if known). For example, Cushman *et al.*[160] were able to discover potent inhibitors of angiotensin converting enzyme using a *de novo* analysis of the enzyme's very own active site.

1.2.6 Lead Optimization

One of the most daunting tasks of the medicinal chemist is lead optimisation. The stringent clinical trials standard could lead to several rounds of lead optimisations for a drug candidate to finally get approved. The SAR studies around a lead compound could be envisaged as thousands of analogues, which would be immense and at times futile.

There are several approaches one can take, when it comes to considering molecular variations during lead optimisation. A disjunctive[161] approach *i.e.* dissection and removal of substituents, structural elements, rings, cycles *etc.*, is a method of choice when simplification of the lead is desired *e.g.* disjunctive optimisation of quinacrine furnished the antimalarial chloroquine.[162]

When the structural complexity of a lead is being examined, analogical[163] optimisation *i.e.* isosteric/bioisosteric and functional group interconversion (FGI) and inversion *etc.*, is frequently utilised *e.g.* analogical optimisation of imipramine gave amitriptyline.[164] On the other hand, approaches which result in greater complexity *i.e.* structural element additions, drug conjugations *etc.*, are considered to be conjunctive[161] (Chapter 3) *e.g.* impromidine was conjunctively designed from histamine (Fig. 1.15).[165]

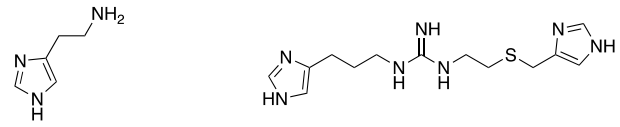

Histamine Impromidine

Figure 1.15 The selective H_2-histaminergic agonist impromidine was designed *via* a conjunctive optimisation of histamine.

Which lead optimisation strategy is going to be employed, will significantly depend on the information about the molecular target at hand. Knowledge of the molecular target structure would enable one to exercise any optimisation strategy *in silico* so as to investigate the SAR and validate the results *in vitro*. However, in the absence of knowledge about the target structure, similarities to the indigenous ligand or other related structures, if known, can direct the SAR towards analogue profiling and examination of the outcomes.

Cases in which the target is completely new and no prior knowledge is available, a way to progress would be to attempt as many syntheses as possible, so as to identify favourable molecular features and avoid the detrimental counterparts such that effectively establish the pharmacophore of the molecular target in question. Regardless of the method of optimisation there are a few key factors to which attention must be paid:

- Small structural changes can have a huge impact on biological activity (Section 2.6); for example, the insulin secretory imidazoline I_3 receptor can accommodate the saturated efaroxan as an agonist[166] and the unsaturated KU-14R as an antagonist (Fig. 1.16).[167]
- Any pertinent biological implementation should be applied as early as possible. This consideration can save a lot of time when dealing with toxicity and safety affairs.[168]
- Key structural features should be maintained *e.g.* charge distances, stereoelectronic configurations *etc.* The so-called receptor mapping which was first introduced by Marshall *et al.*[169] has proved effective in avoiding syntheses of inactive compounds.[170]
- The choice of correct substituents. The right substituent can have a profound impact on the number of test compounds required for the 3D space volume, this has been explicitly expressed by Craig[171] and Austel.[172] The Topliss scheme is a useful tool for selecting the right substituents with the highest potency.[173,174]
- EoS – the lead optimisation process entails synthesis of many compounds, which could in turn be costly and time consuming; therefore, the consideration of time and costs are imperative. Easy synthesis, in particular, heterocycles synthesis as opposed to their carbocycle counterparts is a facile way for generating large libraries of compounds.[175]
- Elimination of chiral centres – it is well established that a racemate together with its corresponding enantiomers can be considered as three separate pharmacological entities, requiring separate DMPK, toxicological and clinical research. As a result, removing the chirality whilst maintaining the potency could reduce these efforts to a third (Fig. 1.17).[175]

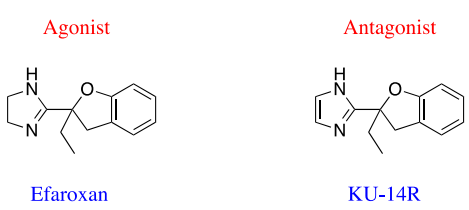

Figure 1.16 A simple desaturation of efaroxan was sufficient to convert it into an imidazoline I_3 antagonist.

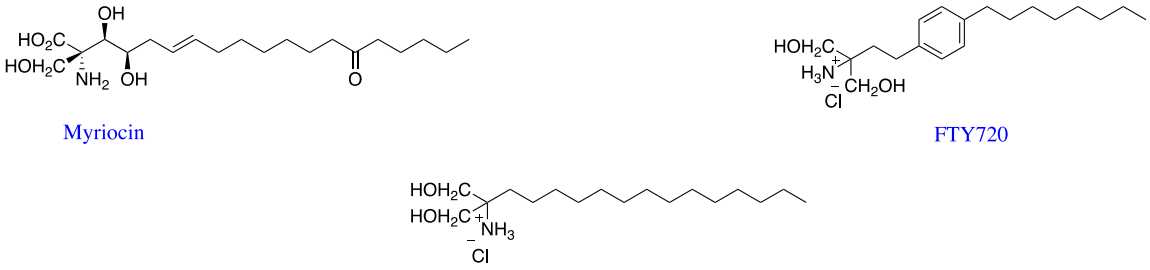

Figure 1.17 Effects of symmetry on chirality.[176]

The resulting preclinical candidate at the end of lead optimisation process will be handed to pharmacologists for preclinical assays and should it obtain the green light, the drug candidate will be put through the stringent clinical trials.

The clinical trials assess the safety and efficacy of the proposed drug candidate, whether the safety and efficacy will be demonstrated in humans is mostly beyond the medicinal chemist's control. Nevertheless, in most cases either the preclinical or drug candidate fails to meet one or more regulatory standards and will be sent back to the medicinal chemist for further optimisation; this merry-go-round will continue until the drug candidate gets approved or the drug developer decides the effort is not worthwhile, and the painstaking venture will be ceased.

This section aimed to highlight the role of medicinal chemists at the forefront of a drug discovery programme from innovation to clinical trials. In order for a drug to have an effect, it must interact with its molecular target(s). As we saw early on in this chapter (Section 1.1), there are currently several distinct classes of antibiotics/antibacterials in clinical use and most were discovered during a relatively short period of time, but do they all hit more or less the same molecular target(s) or their choice is varied? We are about to find out…

1.3 Current Antibacterial Targets

Mankind has immensely benefited from the first marketed antibacterial drug Salvarsan® in 1910[177] to the recently released tedizolid[90] and the discovery of penicillin gave birth to the modern age of antibacterial treatment.[178] Since the '*golden age*' of antibacterial discovery (from the '40s to the '60s),[179] in which most common antibacterial agents were discovered, antibacterial discovery has slowed dramatically with no new antibacterial scaffolds being introduced from 1962 until 2000.[180]

From 2000 onwards, only a couple of new antibiotics closely related to current classes of antibacterials have been introduced – these are lipopeptide daptomycin and streptogramins.[181,182] Current antibacterials either actively induce bacterial cell death *e.g.* by inhibiting bacterial cell-wall synthesis, *i.e.* bactericidals, or inhibit bacterial growth *e.g.* by inhibition of their protein synthesis *i.e.* bacteriostatics.

It is of interest to draw attention to the fact that bactericidal agents kill both quiescent and proliferating susceptible bacteria, but bacteriostatic agents are quite benign to the quiescent bacteria.[183,184] Antibacterials can also be classified as narrow- or broad-spectrum antibacterials, depending on whether they target a particular species' process or display activity against common processes across species, respectively.[183]

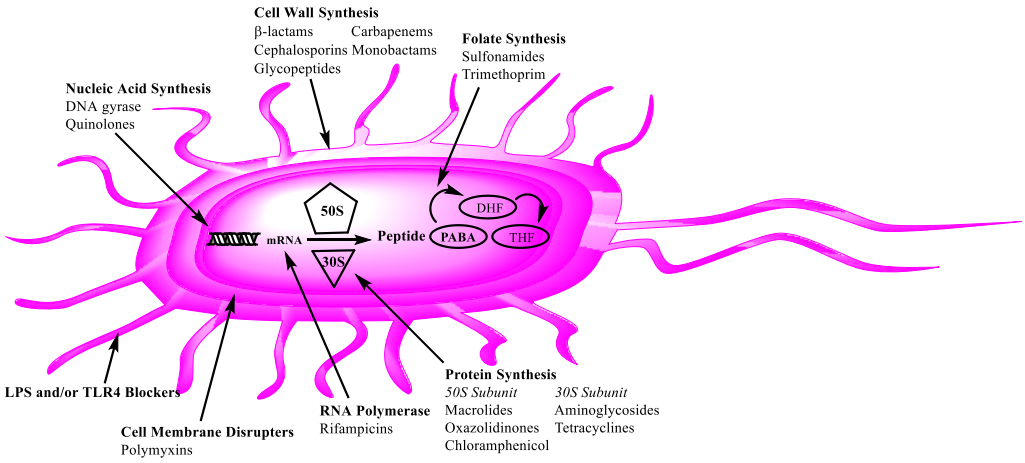

Figure 1.18 Molecular targets of current antibiotics on the market. Dihydrofolic acid (DHF); *p*-aminobenzoic acid (PABA); tetrahydrofolic acid (THF); toll-like receptor 4 (TLR4).

As illustrated in Fig. 1.18 antibacterials can target several parts of a bacterium including their cell-wall, cell membrane, lipopolysaccharide (LPS), DNA, metabolic pathways, ribosomes and a few other targets.[183]

There are also many other potentially druggable molecular targets in bacteria, including quorum sensing and transglycosylases – the latter are targets for phosphoglycolipid antibiotics which are widely used in animals *e.g.* moenomycins, and could be promising molecular targets for tackling antibacterial resistance in humans.

1.4 Antimicrobial Peptides – a New Chasm

"We are continually faced by great opportunities brilliantly disguised as insoluble problems."

Lee Iacocca

In pursuit of new antimicrobial agents, AMPs merit a prominent consideration. As we saw in Section 1.1 only a few of the many marketed antibiotics are peptidic; this implies that the clinical potential of peptide-based antibiotics has not been fully exploited.

Although the penicillins are derived from mono-substituted acetic acid, L-cysteine and D-valine residues, only those high molecular weight peptide-based antibiotics are considered here as peptidic.

To date, hundreds of peptide-based antibiotics have been discovered and as far as these natural peptides are concerned, they fit in two major classes: non-ribosomally and ribosomally biosynthesised peptide-based antibiotics.[185] The former, such as polymyxins and bacitracins are produced in bacteria, fungi and *Streptomycetaceae* and are made by a cascade of enzymes, in contrast, the latter which make up most of the AMPs such as bombinin[186] and melittin[187] are found in all animate species including bacteria, and made by ribosomes.[188]

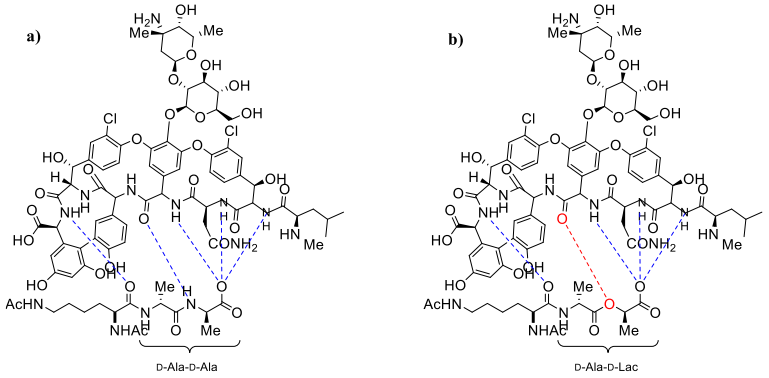

Figure 1.19 a) Hydrogen-bonding network of vancomycin with lipid II of a susceptible phenotype leading to inhibition of cell-wall assembly; b) Interaction of vancomycin with lipid II of a resistant phenotype; the strong electrostatic repulsion between the two partial negative charges shown in red.[192]

A well-established glycopeptide antibiotic still in clinical use is vancomycin, a non-ribosomal peptide isolated from *Amycolatopsis orientalis* in the '50s,[65] which has high activity against Gram-positive bacteria. It took 30 years for vancomycin resistance to emerge,[189] a potential sign of superiority of large peptidic antibiotics over their small molecule counterparts.

Similar to *β*-lactams and carbapenems, vancomycin and related antibiotics target the bacterial cell-wall, but instead of inhibiting enzymes, they bind to the L-Lys-D-Ala-D-Ala part of peptidoglycan *i.e.* lipid II [Fig. 1.19(a)], this binding in turn inhibits transpeptidation, and hence cell lysis. This unique mechanism is not subject to cellular modification and efflux pump clearance,[190,191] which may explain why resistance took so long to emerge.

Despite this unique activity, vancomycin resistance has, unfortunately, emerged by mutation of terminal D-Ala to D-Lac (D-lactic acid),[192] which removes a hydrogen bond from the complex [Fig. 1.19(b)], and confers almost thousand-fold decrease in binding affinity.[193,194]

Many attempts have been made to overcome vancomycin resistance and it has been shown that vancomycin dimerisation induces bioactive conformational constraints which greatly enhances hydrogen bonding interactions.[195,196] As a result, oritavancin which features a hydrophobic *p*-chlorobiphenylmethyl moiety in order to facilitate dimerisation, and hence activity against resistant strains has been developed.[197,198]

It is also postulated that increasing the lipophilic character of glycopeptides will result in a greater anchoring of the peptides to the cell membrane and improves binding to peptidoglycan. In recognition of this, Miller *et al.*[199] showed that site-selective lipidation and introduction of a decanoyl group markedly (up to 64-fold) improved the activity of vancomycin against resistant strains. Likewise, telavancin – a lipoglycopeptide antibiotic similar to vancomycin – is capable of binding to peptidoglycan as well as depolarising the cell membrane;[200] this dual mode of action makes telavancin very potent which shows how promiscuity can be a great advantage.

Some AMPs have multiple modes of binding. It is relatively difficult to predict the activity and structure of AMPs from their sequence alone.[201,202] There are many different structures for AMPs, which can include α- and β-secondary structures, CS$\alpha\beta$-type structures, and some do not have any defined structure until they come into contact with hydrophobic environments.[201,202]

Many AMPs, though by no means all, share three common features – small size (relative to proteins), a net positive charge, and amphiphilicity.[203] The bactericidal action of AMPs is extremely fast and hence difficult to study.[204] However, several membrane models such as the Monte Carlo,[205] barrel stave,[206] carpet-like[207] and toroidal[208] models have been used to study their bactericidal action.

Generally, activity is based on the following principle: the amphiphilic character of AMPs allows them to form initial electrostatic interactions with the net negative charge deposited on the bacterial cell membrane (this feature is absent in mammalian cells which makes AMPs relatively selective for bacteria), they are also highly charged and can displace native Ca^{2+} and Mg^{2+} charges on the LPS of particularly Gram-negative bacteria and permeabilise the outer membrane.[209] Thus, they aggregate on the bacteria and generate transient cracks which allow cellular uptake of the peptides.[210] Finally, these pores will be filled with the medium, and terminating the electric potential across the membrane; this ultimately leads to the observed cell lysis (Fig. 1.20). A benefit of targeting cell membrane is that target mutation for developing resistance is likely too costly for survival.[211]

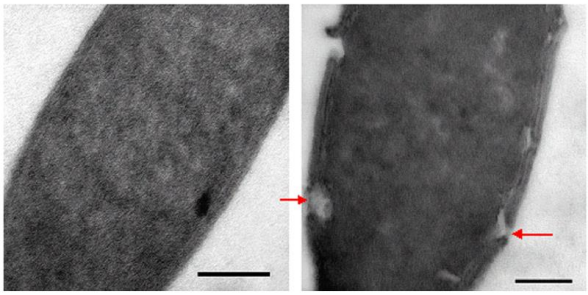

Figure 1.20 [LHS] *C. difficile* cell on its own. [RHS] *C. difficile* cell incubated with AMP HBD3; red arrows show where the pores have been formed. (Figure taken from Nuding *et al.*)[212]

AMPs also target intracellular processes such as protein folding, nucleic acids, specific protein sets and cell-wall synthesis. It is this promiscuous binding that is suggested to make AMPs such as pleurocidin[213] and indolicidin[214] superior to conventional antibiotics.

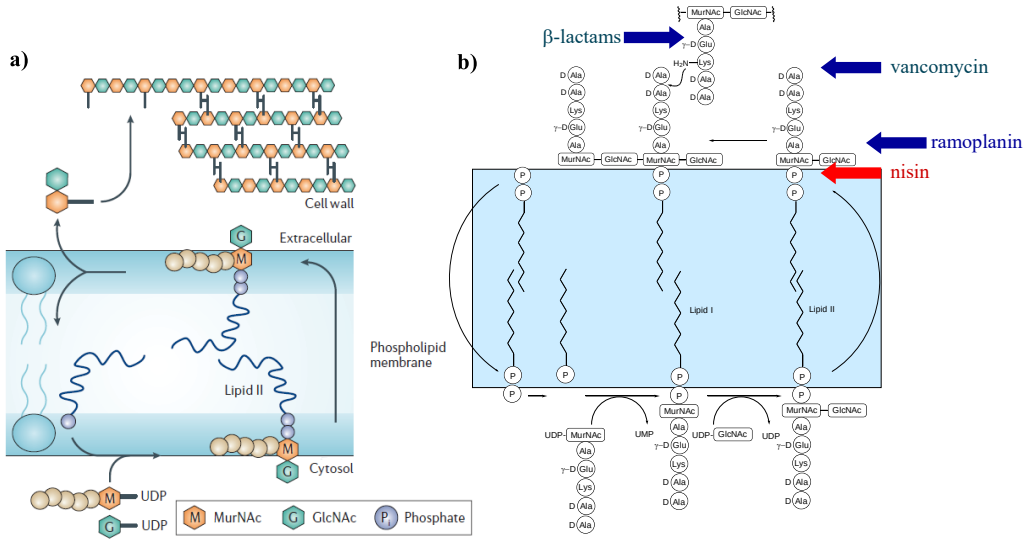

Figure 1.21 a) Biosynthesis of lipid II and its assembly in the peptidoglycan to form the basic structure of bacterial cell-wall.[215] b) Schematic view of bacterial membrane showing different parts of lipid II as a molecular target for different antibiotics.

On a similar note, some ribosomally synthesised peptides such as lantibiotics *e.g.* epidermin – the first discovered lantibiotic,[216] actagardine,[217] defensins including copsin[91] and teixobactin,[92] all bind to lipid II [Fig. 1.21(b)], and have shown excellent antibacterial properties *in vitro*.

The bacterial cell-wall is made up of alternating *N*-acetylglucosamine (GlcNAc) and *N*-acetylmuramic acid (MurNAc) amino sugar monomers, knitted into a polymer and are cross-linked with L-alanyl-γ-D-glutamyl-diaminopimelyl or L-lysyl-D-alanyl-D-alanine pentapeptides that are coupled to the MurNAc sugars *i.e.* lipid II, and scattered throughout the peptidoglycan polymer [Fig. 1.21(a)].

It is this lipid II cross-linking that makes the cell rigid and strong, and also protects it from the external environment.[215] It is worth mentioning that not only is lipid II highly conserved amongst bacteria, but also is it not readily susceptible to cellular modification and development of resistance.[218] Similar to telavancin, lantibiotic nisin also exhibits a dual mode of action – it tightly binds to lipid II and triggers pore formation, in addition to sequestering lipid II.[219]

In recognition of the above, most of the antibacterial agents in clinical use or under development focus on only a few of the many available bacterial molecular targets with a single or dual mode of action. With an increasing global prevalence of resistance to these antibacterials, there is every reason to expect that future antibacterial generations must have multiple modes of action and must be acting upon molecular targets which are preserved in the evolutionary process, and are less susceptible to mutation. Thus, if we are to develop the next generation of antibacterials with fewer tendencies for resistance, peptides are a must to consider.

Having said that, peptide-based antibacterials are subject to resistance, but there is some evidence that the pace of appearance of this resistance is by far slower than that of current marketed antibacterials. As a proof of concept, Zhang *et al*.[220] showed that resistance to AMPs in *P. aeruginosa* only increased by two to four-fold with sub-inhibitory concentrations after thirty generational transfers. Moreover, since many peptide-based antibiotics are likely promiscuous in character, then resistance to a single target should not confer resistance to their entire mode of action.

In addition, the highly conserved targets of these peptides (in particular precursors of bacterial cell membrane) indicate that cross-resistance may be less of a worry and not universal as many studies[221] suggest. AMPs, in particular, apart from having fewer tendencies to induce resistance, also possess anti-inflammatory, immunostimulatory and toxin neutralising properties which make them to stand out from other peptides in this category.[222] However, as outlined herein, peptide-based antibacterials are not perfect, there are particular difficulties associated with their production, optimisation, toxicity and formulation which with recent advances in this field are slowly being mitigated.

Antibacterial resistance has posed a major problem recently and if immediate action is not taken globally, its consequences may be dire. There is thus a strong incentive to develop the next generation of effective antibacterial agents with lower susceptibility to bacterial resistance. As a consequence, this field has had a renewed interest from both academia and industry. We shall now go on to briefly review this colossal global health burden.

1.5 Antibacterial Resistance

"To explain all nature is too difficult a task for any one man or even for any one age. 'T is much better to do a little with certainty and leave the rest for others that come after you, than to explain all things."

Sir Isaac Newton

It is unclear as to when the human antibiotic resistance era first started, but what is clear right now is a *de facto* entry to a post-antibiotic resistance era, in which minor surgeries can no longer be conducted and cuts and wounds will once again kill. This has been highlighted by the first global report of the WHO on fast development of resistance to antibacterial agents,[223] followed by announcing the first '*World Antibiotic Awareness Week*' which was held from 16 to 22 November 2015 worldwide.[224]

The reports on resistant strains of *Escherichia coli* to colistin[225] and *Neisseria gonorrhoeae* to azithromycin[226] are just a glimpse of the actual phenomenon. As depicted in Fig. 1.22, to emphasise the severity of this global health burden Jim O'Neill[227] issued a report in which he estimates the consequences of this problem from an economic standpoint.

As a result of these awareness raising activities, and incentives such as Longitude Prize,[228] Generating Antibiotic Incentives Now (GAIN) Act – featuring qualified infectious disease products, which enables pharma to benefit from priority review, eligibility for fast-track status and a five-year extension of Hatch-Waxman exclusivity for products once licensed,[229] – and also the consideration of innovative trial designs and alternative parameters for clinical effectiveness,[230] which could waive the need for demonstrating superiority, there has been copious research on different ways of tackling this disease burden.

Of particular importance are development of novel antibacterial agents and modification of the current obsolete antibiotics *e.g.* antibiotic resistance breakers,[231] or effective diagnostic tools and probes to better make use of the current very limited remnant of effective antibiotics. Moreover, alternatives such as vaccines[232,233] and β-lactamase inhibitors[234] have been developed (Chapter 3).

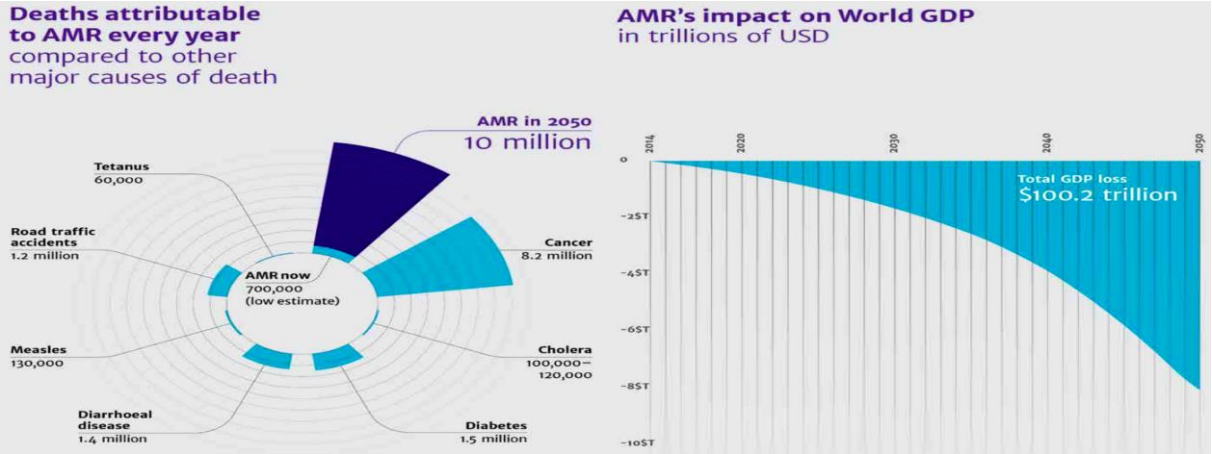

Figure 1.22 Number of deaths as a result of antimicrobial resistance by 2050 and its impact on global GDP. (Courtesy of Jim O'Neill)

The process of antibacterial resistance is a complex phenomenon, but it is deemed to be either *intrinsic* or *acquired*.[235] Generally Gram-negative bacteria are intrinsically resistant to those antibiotics to which Gram-positive bacteria are susceptible and *vice versa*; for instance, many Gram-negative bacteria, though by no means all, are susceptible to polymixins, but these will not work as well for Gram-positive bacteria.[235]

On the other hand, tigecycline is effective against both Gram-negative and -positive bacteria. However, there are no single antibacterial agents to which all bacteria are susceptible. In addition, since 99% of the bacteria cannot be cultured,[236] and given that the current standard diagnostic methods in most cases often do not identify the right pathogen, the bacterial infections are one of the greatest challenges that the prescribing physician is facing at the present time. In contrast to intrinsic resistance, acquired resistance arises when a bacterium that was susceptible to a given antibiotic suddenly becomes resistant in virtue of random mutations *e.g.* in the case of vancomycin mutation of terminal D-Ala to D-Lac (D-lactic acid)[192] [Fig. 1.19(a)], or through horizontal gene transfer (HGT) (Fig. 1.23).

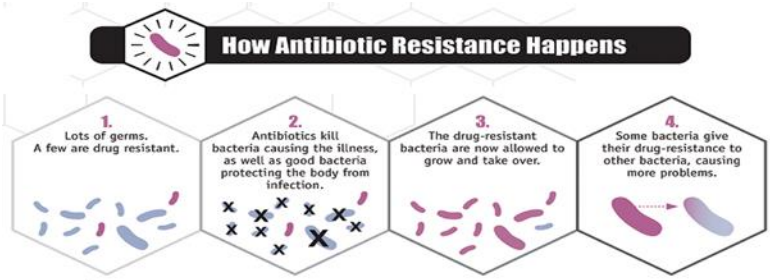

Figure 1.23 Acquired resistance in a population of bacteria.[237]

Antibacterial resistance is a tough challenge and our current understanding of these prokaryotic species does not permit a perpetual solution to the challenge of antibacterial resistance which, at least for now, is an ongoing battle, and we constantly need to develop novel antibacterials.

1.6 Horizontal Gene Transfer

"All truth passes through three stages. First, it is ridiculed. Second, it is violently opposed. Third, it is accepted as being self-evident."

Arthur Schopenhauer

At the outset, molecular phylogeny was used to construct phylogenetic relationships between species *via* molecular information.[238] To this end, categorising species by morphological, physiological and molecular markers led to the recognition of certain genes as phylogenetically incongruent, which in turn gave rise to conflictive phylogenies, particularly in the microbial realm.[239,240]

The mechanisms for transferring genetic materials amongst microorganisms were well-established[241,242] and potential for cross-species gene transfer was soon hypothesised.[243] As a result, in the early '90s the concept of '*horizontal*' or '*lateral'* gene transfer as opposed to vertical gene transfer was proposed to account for the aforementioned conflictive phylogenies.[244] HGT – the nongenealogical genetic material transmission from a donor to a recipient,[245] arming the recipient with the evolutionary novelties, which would otherwise be impossible.[246]

1.6.1 The Importance of HGT in Microbial Phylogenies

As discussed in the last section (Section 1.5), antibacterial resistance acquisition amongst previously susceptible bacteria is a corollary of either random mutations or HGT, and the latter seems to be the most preponderant factor.[247,248] It is postulated that between 1.6 and 32.6% of each and every single microbial genome has been shaped through HGT[249] and taking into account the cumulative impacts of these acquisitions through lineages, results in HGT forming 81 ± 15% of the entire microbial genomes.[250]

Given the incidence of HGT amongst prokaryotes, it was questioned whether it would be feasible to reconstruct an accurate phylogenetic tree of the microbial world at all.[251,252] It was suggested that some genes can be considered as core and non-transferable thereby assisting in maintaining a true phylogenetic signal through which the correct phylogenetic tree could be reconstructed.[253,254]

Others considered certain barriers that could render HGT negligible in reconstructing a microbial phylogenetic tree.[255,256] As a proxy for downplaying the importance of HGT by virtue of acceptance and incorporation barriers, Sorek *et al.*[257] searched all the genes that were proposed as non-transferable in *E. coli* and showed that there are no absolute barriers to HGT in virtue of the fact that all the erroneously perceived non-transferable genes could be cloned in *E. coli* from at least one of the genomes. As a result, Bapteste *et al.*[258] showed that less than 0.7% of the microbial genomes could be regarded as core genes, rendering the construction of a prokaryotic phylogenetic tree truly untenable and misleading!

1.6.2 Mechanisms of HGT & Their Contribution to the Pool of Antibacterial Resistance Genes

There are several known mechanisms by which microorganisms, in particular, bacteria laterally exchange genetic materials – conjugation, transformation, transduction, transfers facilitated by '*genomic islands*' (GEIs) and transfers mediated *via* outer membrane vesicles (OMVs). The most widely studied mechanism is conjugation;[259] however, recently the role of other mechanisms in HGT is being more frequently embraced.

1.6.2.1 Conjugation

Conjugative HGT is a cell-to-cell exchange of genetic materials and necessitates the microorganisms in question to be connected through self-spanning translocation channels either in the form of a pilus in Gram-negative bacteria or cell surface-associated adhesins in Gram-positive bacteria.[260]

Conjugation is governed by conjugative machinery which itself is transcribed either by autonomous plasmids or integrative conjugative entities in the chromosome.[261,262] Since most antibacterial resistance genes (ARGs) are affiliated with the conjugative entities *e.g.* plasmids or transposons, conjugation is regarded as the most likely mechanism for HGT in bacteria and archaea.

This can be explained by virtue of the fact that conjugation provides protection from the surrounding environment and would appear to be a more efficient mechanism for gene transfer than that of other HGT mechanisms. In comparison, although transduction could provide some environmental stability for the process, the transfer is not specifically directed, and is technically a side effect of bacteriophage invasion.[263]

Conjugative ARGs are present in many bacterial plasmids. The prime example is that of the *bla*$_{CTX-M}$ genes responsible for the extended-spectrum *β*-lactamases (ESBLs) in *Enterobacteriaceae* which are now ubiquitous in all kinds of life; be it pathogens,[264] humans,[265] animals and the environment.[266] It has been shown that *bla*$_{CTX-M}$ genes responsible for *ß*-lactam antibiotics resistance in many deadly pathogens were first developed in commensal *Kluyvera* bacteria, and then they have been transferred to many pathogenic species through HGT;[267] illustrating that a robust repertoire is present from which any organism can pool, irrespective of their speciation.

1.6.2.2 Transformation

As early as 1928, it was observed that different strains of *Streptococcus pneumoniae* were able to exchange virulence factors through extracellular media;[268] for them to do so three critical conditions should be satisfied:[269]

- Genetic material in the form of transposons, integrons, plasmids, gene cassettes *etc.* must be available in the extracellular media.
- The recipient must be '*competent*.'
- The new genetic material must be integrated either by incorporation into the recipient genome or by readmission.

Although, *Neisseria* spp. are inherently competent,[270] other species can develop a state of '*competence*' under certain circumstances for example in presence of some nutrients, peptides, autoinducers or several various stress factors.[271] Moreover, bacteria are prone to becoming competent when exposed to antibacterials, which can be conceded that under the antibacterial selection pressure, not only are the resistant strains selected, but also the advantageous resistance characteristics disseminate through transformative HGT.[272,273]

In recognition of the above, the patterns of transformative HGT have been observed for resistance to streptomycin, penicillins, rifampicin, erythromycin, nalidixic acid, and kanamycin (to mention a few) into *Streptococcus pneumoniae*,[274] *Neisseria gonorrhoeae*,[270] *Gallibacterium anatis*,[275] and *Bacillus* spp.[276] Intriguingly, transformative HGT has shown to be very common amongst genetically unrelated species.[277]

1.6.2.3 Transduction

One of the most ubiquitous and diverse species in the biosphere,[278] inadvertently, shapes a considerable portion of the bacterial and archaeal genomes. By the same token that an infected *Anopheles* mosquito inadvertently can act as a vector and transfers malarial *Plasmodium falciparum* to its victims,[279] bacteriophages ('*phages*', for short) also transfer genetic materials *via* HGT whenever they infect bacteria and archaea; this process is referred to as transduction.[280]

The genetic materials in transduction can vary in any form of chromosomal DNA fragments, plasmids, transposons and GEIs.[281] This feature, makes ARGs a very good cargo for such transfers; in fact, resistance genes for erythromycin and tetracyclines,[282] tetracyclines and gentamicin,[283] β-lactam and β-lactamase inhibitors and even multiple antibacterial resistance genes[284] have been transferred by phages through transduction amongst *S. pyogenes*,[285] enterococci,[283] *E. coli*,[286] *Salmonella* ssp.[287] and MRSA strains,[284] respectively. This widespread prevalence of transduction indicates that phages are acting as a significant repertoire for ARGs.

1.6.2.4 HGT Facilitated by GEIs

Some discrete DNA segments that can take part in transformation, conjugation, transduction or even actively determine their preferred method of transfer,[288] are known as GEIs.[289]

GEIs differ from the conventional genetic materials in HGT by virtue of the following:[290] (Fig. 1.24)

- Relatively large discrete DNA segments typically between 10 and 200 kb. Some smaller discrete DNA segments around 10 kb or smaller do also exist, which are referred to as '*islets*'.[291]
- The statistical nucleotides of GEIs are significantly different from the rest of the chromosome.
- The insertion of GEIs usually occurs at tRNAs.
- Start and end sequences of GEIs are 16–20 bp perfect or near perfect direct repeats (DRs). DRs acting as site-selective integration of GEIs into the target and are considered as recognition codons for enzymatic excision.[292]
- GEIs normally encompass functional and cryptic genes interpreting integrases or plasmid conjugation/transduction factors.
- GEIs often contain insertion sequences (IS) which mobilise or delete genetic material from the DNA.[293,294]
- GEIs often confer selective advantages on the recipient, and can be characterised as pathogenicity, symbiosis, metabolic, fitness or resistance GEIs.[289]

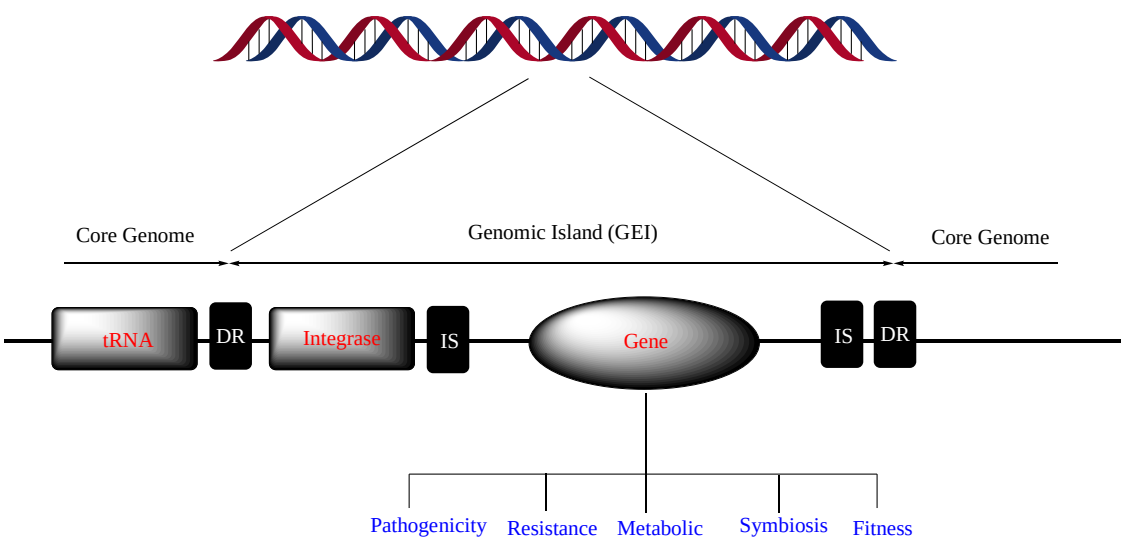

Figure 1.24 Typical characteristics of GEIs. GEIs are generally large discrete fragments of DNA whose nucleotide features differ from the rest of the genome. GEIs are inserted at tRNAs and flanked by DRs. GEIs often utilise genes encoding factors responsible for genetic mobility such as integrases, transposases and IS. GEIs can be identified as pathogenicity, resistance, metabolic, symbiosis and fitness islands.

1.6.2.5 HGT Mediated Through OMVs

Whilst classical HGT methods *i.e.* conjugation, transformation and transduction only transfer single-stranded DNA.[295,296] In recent years, the transfer of double-stranded DNA has also been observed in *E. coli*.[297,298] These findings suggest that other methods of HGT unknown to mankind do exist which makes controlling the spread of ARGs and the prevention of development of multi-drug resistant (MDR) bacteria extremely difficult.

It was once thought that *E. coli* is inherently not competent for transformation; however, the transformation of *E. coli*, on both nutrient-deficient and nutrient-rich agar plates has been achieved.[299,300] Moreover, the standard DNA uptake machinery for transformation is absent in transferring the double-stranded DNA in *E. coli*.[301] It was proposed that some conserved DNA uptake machinery is used to consume DNA as nutrient;[302,303] however, this was not observed in different independent laboratories and DNA as the sole source of carbon was not sufficient for cell growth and other sources of nutrients required in the culture.[271] Last but not least, adenosine triphosphate (ATP)-binding cassette transporters take part in transferring the double-stranded DNA in this non-canonical HGT, which are absent in the classical transformation.[304] This non-canonical HGT is referred to as HGT mediated via OMVs.[305]

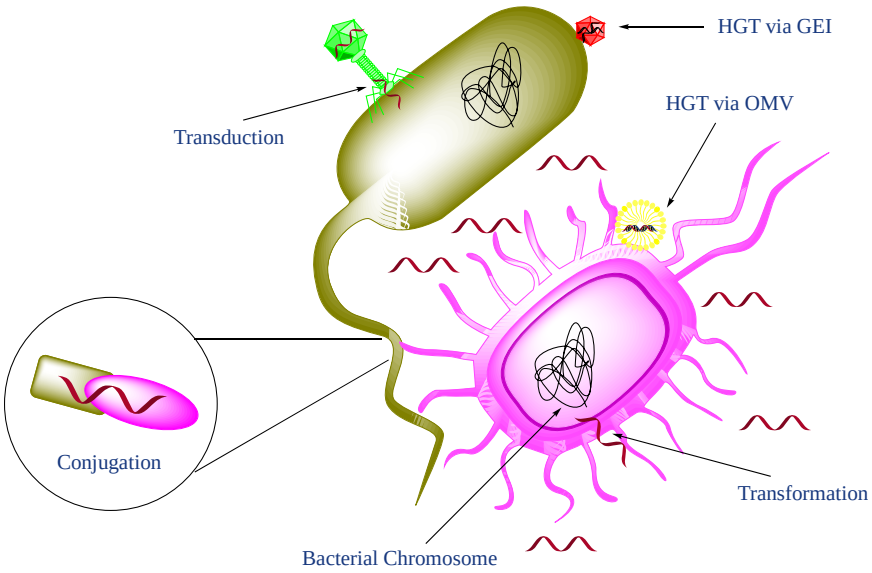

Figure 1.25 Schematic representation of the main mechanisms for HGT in bacteria (*not to scale*).

1.6.3 HGT Beyond Prokaryotic Realm

The emergence of HGT explained the incongruent phylogenies in prokaryotes, particularly in bacteria and archaea (Section 1.6.1); however, HGT is not confined to bacteria and archaea only and HGT in eukaryotes[306] has also been observed. In fact, HGT can occur across all domains of life and in all directions – from bacteria to archaea,[307] archaea to bacteria,[308] archaea to eukaryotes,[309] bacteria to eukaryotes,[310] eukaryotes to bacteria[311] and even amongst eukaryotes.[312]

The extensive research on HGT is gradually shedding light on detrimental impacts of bacteria on humans, it has been shown that HGT from bacteria to human genome can play a crucial role in development of carcinomas in humans.[313] On the other hand, it is becoming more apparent that there are far more '*carcinogenic bacteria*' than *Helicobacter pylori* which can cause cancer.[314]

Given the versatility of HGT in protecting bacteria from antibacterials and the ease with which all kinds of bacteria transfer their functional genes *e.g.* resistance, virulence, symbiosis *etc.*, it should not come as a surprise that a complete cure for cancer is as yet a distant dream. Thus, if we are to cure and prevent many diseases and overcome the antibacterial resistance burden, we should, in the first instance, stop HGT of ARGs in bacteria.

1.7 Immunological Tolerance

"(la) Amicus Plato — amicus Aristoteles — magis amica veritas

Plato is my friend; Aristotle is my friend, but my best friend is truth."

Sir Isaac Newton, 1664

It has long been known that the mammalian immune system inherits mechanisms to differentiate self from non-self in the foetus.[315] This concept was strengthened by Peter Medawar to introduce '*immunological tolerance*' for which Medawar and Burnet shared the 1960 Nobel Prize in Physiology or Medicine. In their seminal lecture, they defined immunological tolerance as *"a state of indifference or non-reactivity towards a substance that would normally be expected to excite an immunological response"*.[316] Neither should it be confused with '*immunological paralysis*' which is also a state of unresponsiveness due to a very high concentration of a given antigen, but where no antibodies form; however, a subsequent typical antigen exposure elicits a response;[317] nor should it be mistaken for '*immunopathological tolerance*,'[318,319] in which homeostasis and normal functioning of the affected tissues/organs are altered to reduce the host susceptibility to tissue damage. An immune response to a great deal of extent imposes costs on the host fitness.[320] For example, in the case of severe acute respiratory syndrome coronavirus 2 (SARS-CoV-2) infection, a phenomenon known as '*cytokine storm*'[321] – an excessive and often life-threatening inflammatory response – damages the lungs and also promotes multiple organ failure.[322]

The cumulative detrimental effects of immune response on host fitness are known as '*immunopathology*.'[323] This could range from vascular inflammatory which impedes epithelial respiration to complete destruction of infected cells by the white blood cells.[324] In the first instance, the body deploys certain mechanisms *e.g.* immunopathological tolerance to increase the threshold for cellular damage, allowing an effective response resists the invading pathogen. For example, fever and elevated body temperature upregulates the transcription factor, heat shock factor 1 (HSF-1), which in turn promotes expression of genes that manage protein folding, thereby counteracting proteotoxicity.[325]

On the other hand, increased activity of T-cells and oxidative stress as a result of immunopathological tolerance activates the transcription factor, nuclear factor erythroid 2-related factor 2 (Nrf2), leading to induction of genes for proteins that scavenge free radicals, eliminate metabolite oxidized membrane lipids and damaged proteins, and repair the damaged DNA.[326]

The degree to which the immunopathological tolerance is tolerated depends on the affected tissue(s), and is governed by factors such as damage susceptibility, repair capacity, functional autonomy of the cells *e.g.* homeostasis, and the consequences of the damage or impaired functions as a result of the resistance to the invading pathogen; generally, skin and soft tissues have much higher propensity to tolerance than neuronal and cerebral tissues.[327,328]

Immunopathological tolerance has downside; it is quite costly in its own right, even though it prevents damage to the tissue(s). Depending on the nature of the infection and tolerance capability of the affected tissue(s), there is a balance between resistance and tolerating malfunction.

Cases in which the infection becomes chronic, the body ceases to modulate the balance between resistance and cellular tolerance, and it undergoes a trade-off with the invading pathogen so as to switch off immune response mechanisms to the pathogen, thereby developing immunological tolerance to that specific pathogen. Upon this immunological tolerance the body may be considered evolving to recognise the pathogen as self. The immunological tolerance by no means unduly affects the virulence of the pathogen to which initially a rapid and thorough immune response was necessary.

Although the acquired immunological tolerance seeks to reduce tissue damage, conserve energy and promote commensalism, the pathogen is free to the cellular resources and the cells are vindictively exposed to direct damages of the pathogen *e.g.* toxins, digestion, metabolites *etc.*

Moreover, this symbiosis may enable the pathogen to freely disseminate its virulence factors to other commensal microorganisms or/and acquire drug resistance genes *via* HGT, as discussed in the last section (Section 1.6), and it becomes even more problematic,[329] in virtue of the fact that this type of immunological tolerance is individual specific and the nurtured pathogen which has acquired resistance genes through HGT in one individual could be transferred to another individual who could develop severe infections which do not respond to chemotherapy by virtue of HGT as observed in many infectious related mortalities.

In addition, the now erroneously commensal pathogen can easily evolve through HGT and become carcinogenic![330]

Chapter 2

Dynamic Combinatorial Chemistry of Benzodiazaborines & Their Therapeutic Potential

Introduction

"In theory, theory and practice are the same. In practice, they are not."

Lawrence Peter Berra

As described in the previous chapter (Section 1.2), contemporary drug discovery efforts aim to preclude fortuitous element by employing a combination of the best practice, innovation and technology. Thus, whereas in the past drugs were normally identified by screening for their physiological/biological mode of action(s), today with the help of molecular biology and state-of-the-art techniques, molecular targets are often identified first and further no matter how '*undruggable*' a molecular target is perceived, medicinal chemists will attempt to find an appropriate therapeutic for it.

During a typical drug discovery programme many synthetic compounds are explored, sometimes involving very large libraries of compounds. Although, some large pharmaceutical companies *e.g.* Pfizer, GSK, AstraZeneca *etc.* appear to be moving away from random screening of large libraries of compounds due to its inefficiency;[331] nevertheless, HTS is a mainstream lead identification method and has furnished several blockbuster drugs, such as sorafenib,[332] dasatinib,[333] sunitinib,[334] tipranavir,[335] maraviroc[336] and many others.

2.1 Solid Phase Synthesis

Solution chemistry can be time consuming and the purification of its products is often tedious and resource intensive. In comparison, solid phase synthesis (SPS) offers easier purification, as the products are attached to insoluble beads, with excess reagents and by-products being easily eliminated by washing and filtration. SPS can bring about high yields and shorter reaction time *e.g.* by using excess reagents.

Inasmuch as all the synthetic steps can be carried out in the same reaction vessel, and the manipulations are simple and fast (suitable for automation), SPS is thus a good approach for generation of large libraries of compounds than its solution phase counterpart. However, one of the limitations of SPS is the need for having a suitable reaction condition; after all, not all reactions can be done on a resin.

Since its inception by Robert Bruce Merrifield in 1963[337] for which he received the 1984 Nobel Prize in Chemistry, SPS has been extensively used in combinatorial[338] and parallel[339] synthesis so as to generate libraries of compounds for drug discovery endeavours.

2.1.1 Solid Supports in Solid Phase Synthesis

The first successful solid support developed for use in SPS was the Merrifield resin which consists of polystyrene beads partially crossed-linked with 2.0% divinylbenzene.[337] A problem with polystyrene beads is the tendency of peptide chain to '*curl*' up during long-chain peptide synthesis mainly in virtue of the polar nature of the growing peptide chain, which contrasts with the hydrophobic polystyrene resin, rendering peptide elongation inefficient.[340]

In an attempt to circumvent this problem Sheppard's polyamide resin was developed.[341] The more recent tentagel (NovaSynTGT alcohol) resin, which is made up of polyethylene glycol cross-linked polystyrenes, is superior for synthesis of long-chain peptides.[342] Resins are usually in the form of beads which require swelling in an organic solvent *e.g.* CH_2Cl_2 or dimethylformamide (DMF) prior to the synthesis, as the reactions are carried out inside the bead environment.

Other forms of resins such as pins have been developed, which can increase the accessible surface area for reactions.[343] Solid supports do not necessarily have to be organic polymers and functionalised glass surfaces have been developed as alternatives for oligonucleotide synthesis.[344]

2.1.2 Linkers in Solid Phase Synthesis

Solid support linkers are functionalised to enable connection of the desired chemical reagents to the solid support. The first Merrifield resin had a reactive chloromethyl group, which could be displaced by a nucleophile *e.g.* amino acid, yielding the starting material covalently linked to the resin. This linker must be cleaved at the end of the synthesis; in the case of Merrifield resin, the linker is an ester and is cleaved with a strong acid such as hydrofluoric acid.[337]

Due to the relatively harsh conditions for the Merrifield resin, alternatives such as the Wang resin, which features extensive conjugated linkers that are easily cleaved using TFA (Fig. 2.1) are commonly used.[345] However, the amino acid attached to the Wang resin may be prone to racemisation due to the strength of the acidic cleavage mixture; as a result, the Barlos resin which has a trityl (Trt) linker that is cleaved in dilute acetic acid was developed. Moreover, owing to the stability of the Trt cation even very mild nucleophiles such as alcohols can be attached to the Barlos resin.[346] The carboxyl starting material can be attached to the Rink resin, which following cleavage releases a primary amide product (Fig. 2.1).[347]

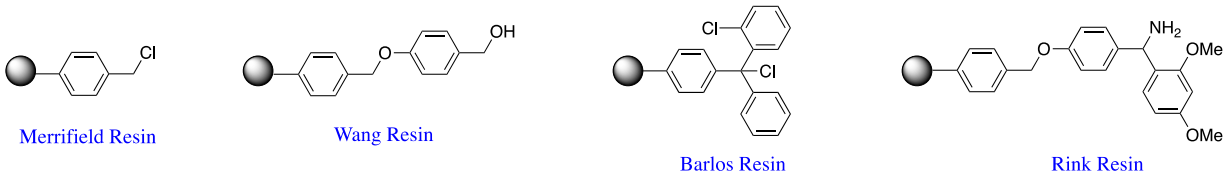

Figure 2.1 Representative examples of resins for SPS with their distinctive linkers.

2.1.3 The Scope of Solid Phase Synthesis

Peptide synthesis was the first synthetic application of SPS, but efforts were soon made to expand the scope of this versatile synthetic tool. The first approach was the modification of the peptides on the resin such as *N*-methylation of the *N*-termini.[348] Later, *N*-substituted glycines were used to synthesise peptoids on a resin; peptoids can have increased metabolic stability than peptides and some even exhibit antileishmanial properties.[349]

Unfortunately, most peptoids are linear, lack the tertiary structure of peptides (Section 1.4), and are not very suitable for drug development. A major breakthrough was the synthesis of heterocycles on a resin. 1,4-Benzodiazepines were successfully synthesised on the resin by addition of imines to the corresponding amino acid attached to a resin through a cyclo-release mechanism (Fig. 2.2).[350]

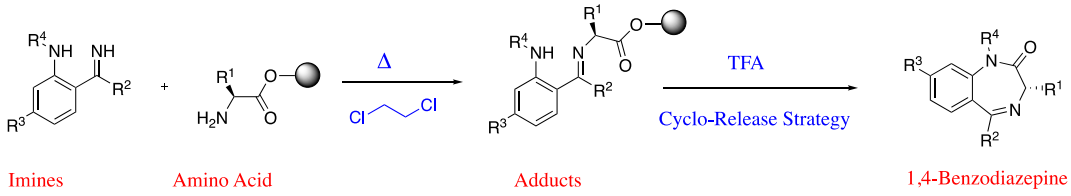

Figure 2.2 Synthesis of 1,4-benzodiazepines *i.e.* heterocycles on the resin.

Similar to benzodiazepines, hydantoins have been synthesised on resins *via* the cyclo-release strategy.[351] The solid phase synthesis of heterocycles led to development of other solution phase reactions on resins, such as aldol condensation, diisobutylaluminium hydride reductions, Wittig reactions, palladium catalysed couplings and others.

Multiple reactions can be carried out on the resin in an automated fashion, under an inert atmosphere, with either cooling or heating.

2.2 Compound Library Design Strategies

Compound libraries used in hit identification are often based on the molecular target for which a drug is being developed. Apart from other factors discussed previously (Section 1.2), it is normally considered important to have a selection of structurally diverse molecules *i.e.* focussed libraries.

To an extent, the design of compound libraries depends on availability of commercial building blocks; thus, there is a danger of repeating similar scaffolds. In order to maintain structural diversity, '*spider-like*' molecules are desired as opposed to '*tadpole-like*' molecules.

Spider-like scaffolds possess a centroid from which different arms *i.e.* substituents radiate. This strategy maximises the binding interactions with the molecular target in question.

On the other hand, in the case of tadpole-like molecules the desired substituents are concentrated on one side of the centroid, and the conformational space will not be fully accessed (Fig. 2.3).[352]

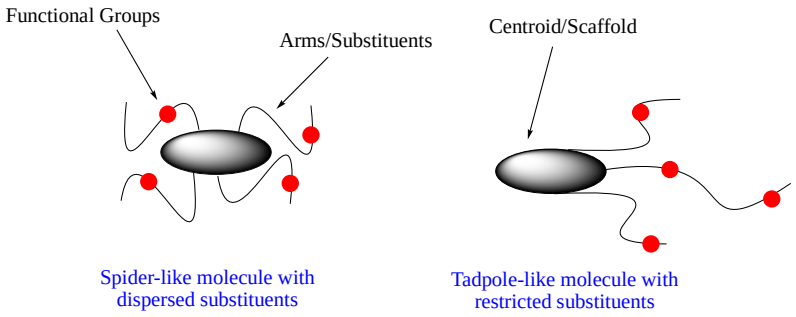

Figure 2.3 Spider-like and tadpole-like scaffolds.

2.3 Parallel Synthesis

In parallel synthesis a series of reactions is carried out such that each reaction vessel (ideally) contains one desired product; this contrasts with combinatorial synthesis (Section 2.4) in which each reaction vessel can contain dozens of the desired products. The parallel synthesis approach focusses on furnishing specific compounds *e.g.* for selective lead optimisation processes.

Most parallel syntheses are carried out using the classical solution phase organic chemistry; however, the need for fast and efficient syntheses for a versatile compound library necessitates the removal of nitty-gritty of organic synthesis, such as laborious workups, extractions and purifications.

For example, a simple amide synthesis from its corresponding carboxylic acid and amine starting materials and coupling reagents *e.g.* HBTU, HATU *etc.* typically requires several acid and base extractions, together with washings and filtrations, and finally purification by chromatography or recrystallisation, all could take several hours (at least) to complete. Instead, solid phase extraction columns which are also available in both acidic (SCX column) and basic (SAX column) forms, can be used to remove excess carboxylic acid and amine precursors, leaving essentially pure amide products in the eluent.[353,354]

Aqueous workups are sometimes inevitable; for example, following Grignard reactions or ortho-lithiation *etc.*; in such instances, the phase separation columns can be used through which a dense chlorinated solvent is filtered rapidly, but the less dense aqueous layer is retained on the hydrophobic frit.[355]

Another method for bypassing solution chemistry workups is the use of a resin. Reactions can be designed such that one reagent is used in excess to drive the reaction to completion; at the end of the reaction, a solid-supported scavenger is added to '*fish out*' the unreacted excess reagent and filtration gives the clean product (Fig. 2.4).

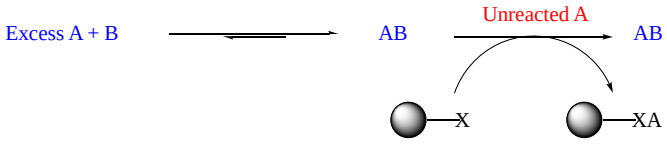

Figure 2.4 Scavenger resins can mop up excess reagents.

It is also possible to have the reagents attached to a resin; undesired side products formed during the course of the reaction remain on the resin and can be removed by filtration, thus side products can be avoided *via* a '*catch and release*' strategy.[356] For instance, in the amide synthesis below, the *N,N`*-dicyclohexylcarbodiimide coupling reagent can be attached to a resin, by doing so the urea side product after the coupling will be on the resin and can be removed by filtration (Fig. 2.5), which otherwise would be difficult using extraction techniques.

A variety of reagents attached to a resin are commercially available for different purposes; for example, a borohydride reducing agent on the resin can be used to reduce carbonyls to their corresponding alcohols.[357]

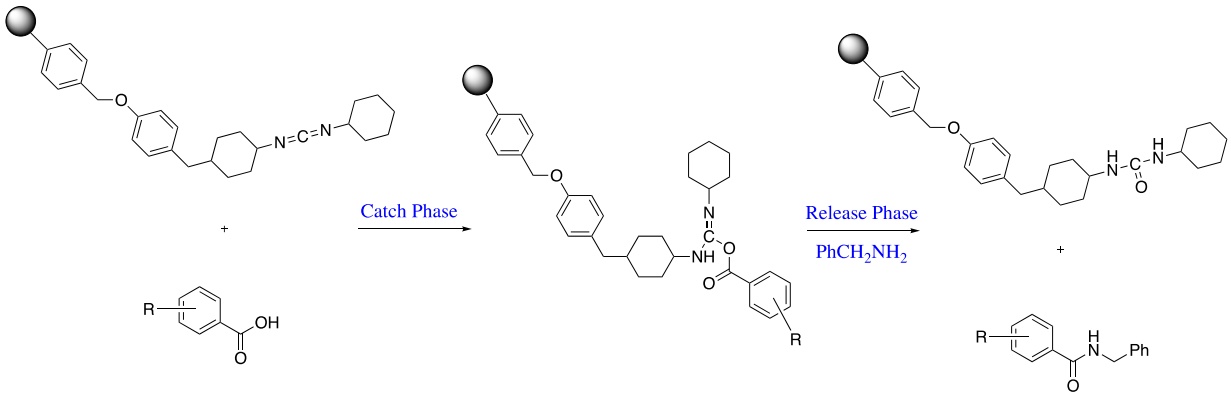

Figure 2.5 '*Catch and release*' strategy in amide synthesis.

2.3.1 Microwave and Microfluidics in Parallel Synthesis

Synthetic chemistry can be time consuming and some reactions *e.g.* palladium catalysed couplings can take a day or more to go to completion; to this end, microwave assisted synthesis can increase efficiency (Section 3.3.6.1).[358]

Energy transfer is more efficient using microwave technology, which enables reaction times to be significantly reduced.[359] For example, a conventional reduction of nitroquinoline to its corresponding aminoquinoline usually requires 24 h of reflux; however, it only takes 15 min to complete using microwave assisted heating (Fig. 2.6).[360]

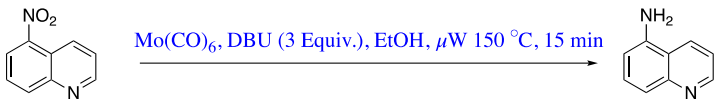

Figure 2.6 Microwave assisted reduction of 5-nitroquinoline.

The efficiency of parallel synthesis can be further enhanced using microfluidic devices. These microchips contain channels within which the reactants are mixed and reacted using flow chemistry to give the products. Microscale reactions can be completed simultaneously at a shorter reaction time and in higher yields.[361] Companies such as Dolomite Microfluidics can generate custom made microchips (Fig. 2.7) possessing the required number of channels suitable for a particular parallel synthesis.[362] Microfluidics technology can be coupled with microencapsulation technology *e.g.* pico-droplets for a faster and more efficient screening of the generated compounds using microfluidic devices.

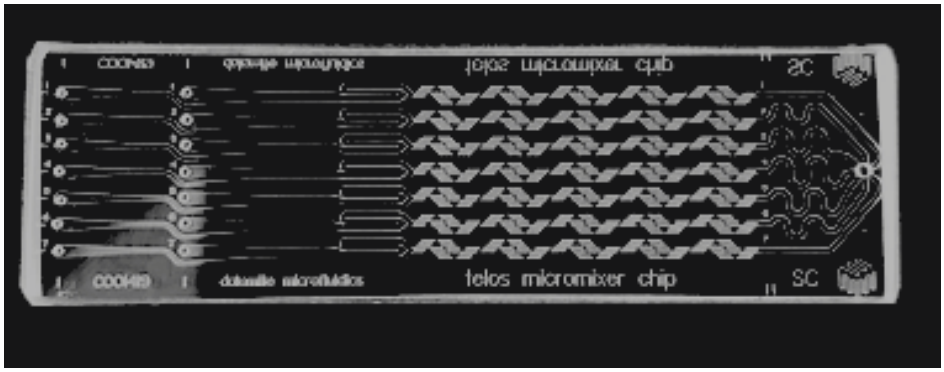

Figure 2.7 Telos® micromixer chip for rapid mixing of two fluid streams.

2.4 Combinatorial Chemistry

In marked contrast to parallel synthesis, combinatorial synthesis can generate thousands to millions of compounds in the time that would take to synthesise only a dozen of compounds using parallel synthesis. This combinatorial compound library generation obviates the need for isolation and purification of the synthesised compounds, and the thus obtained mixtures are tested for activity against a molecular target as a whole.[363]

Unfortunately, combinatorial chemistry is often not straightforward in practice, and there are significant caveats to which particular attention should be paid. Since several building blocks are mixed in the same reaction vessel and the resulting mixture is often later tested without purification, this method is very prone to yield false positives *e.g.* promiscuous inhibitors, frequent hitters *etc.* (Section 1.2.4).

Moreover, simply mixing several reagents in a vessel does not guarantee optimal and controlled conditions under which the classical organic synthesis operates, false negatives and potentially valuable lead compounds can be missed as the reagents might have not reacted to generate the predicted structures. Nonetheless, the benefit of not having to isolate and purify numerous compounds sometimes outcompetes the downsides.[364]

2.4.1 Combinatorial Synthesis Design

Combinatorial synthesis aims to generate a mixture of many compounds; however, mixing of conventional reagents in a reaction vessel can often produce a tarry mixture of polymers. To avoid this, one set of the desired reagents can be attached to a solid support *e.g.* a resin (Section 2.1); subsequent reactions give products attached to the resin. As a result, although several reactions may be occurring concurrently in the same reaction vessel, the solid support, in principle, provides a discrete reaction environment.[365] However, since several combinations are possible, designing a combinatorial library of compounds requires planning to minimise the effort and maximise the number of compounds in each mixture.

In the early '90s, three major methods for combinatorial chemistry emerged – mixed reactant, mix and split, and light-directed – for the rapid generation of new structures particularly for drug discovery.[366] Commonly a '*mix and split*' strategy is the method of choice.

In order to generate a library of all the possible dipeptides of valine, glycine, alanine, phenylalanine and serine, one needs to synthesise 25 dipeptides; there are five amino acids and since the *N*- and *C*-termini are different for each dipeptide a permutation of 5^2 requires a synthesis of 25 different dipeptides, which could take a considerable amount of time using classical solution chemistry. Instead, portions of each amino acid attached to solid supports can be equally mixed in each reaction vessel, resulting in five reaction vessels each containing equal amount of all five amino acids on the resin, and then adding each amino acid reagent separately to each reaction vessel to produce five different dipeptides in each vessel such that no two vessels possess the same dipeptides. In essence, a tedious overall 50 step synthesis of 25 dipeptides, will be reduced to only two steps *i.e.* Log_5 25 if carried out in parallel – parallel coupling and deprotection of the five reaction mixtures (Fig. 2.8).

The resulting mixtures of dipeptides can be tested for activity without purification; if activity is observed, the synthesis of discrete dipeptides will be carried out to validate the initial hits. If no activity is present the mixture can be stored for use against other potential molecular targets.

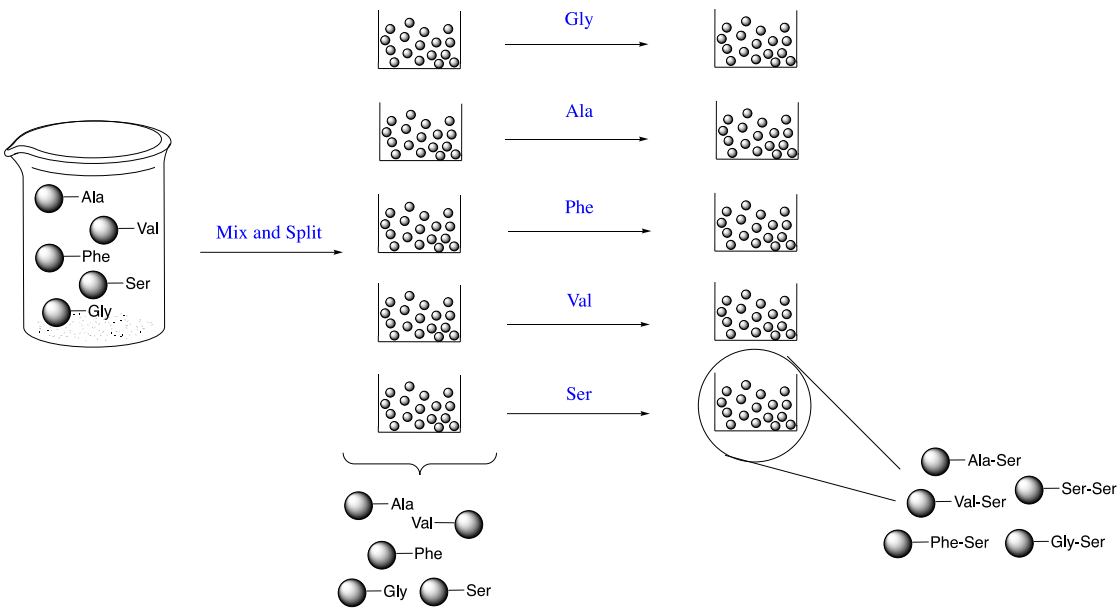

Figure 2.8 Mix and split strategy in combinatorial library generation. The coupling and deprotection of the dipeptides ensue the portioning-mixing to furnish mixtures of dipeptides for screening.

2.4.2 Dynamic Combinatorial Chemistry

A relatively recent development, alternative to classical combinatorial chemistry, is dynamic combinatorial chemistry (DCC). Unlike combinatorial chemistry in which the use of solid supports enables discrete reaction environments (Section 2.4.1), DCC uses reversible equilibria for which irreversible polymerisation is not much of a worry, and thus solid supports can be omitted. In its simplest form DCC is defined as combinatorial chemistry under thermodynamic control, thus all the constituents of a dynamic combinatorial library (DCL) are in constant equilibrium, and can be interconverted *via* both covalent and non-covalent interactions.[367]

2.4.2.1 A Brief History of Dynamic Combinatorial Chemistry

The concept of DCC and product selection under thermodynamic control can be traced back to the 19th century when Fischer[368] and Werner[369] extensively used thermodynamic control for reaction selectivity in their work on carbohydrates and coordination complexes, respectively; however, in modern times, it was substantially shaped by the pioneering work of Busch *et al.*[370] on metal ion '*templated*' synthesis in the '60s (Fig. 2.9); inspired by this, Jeremy Sanders of Cambridge coined the term DCC in 1992.[371]

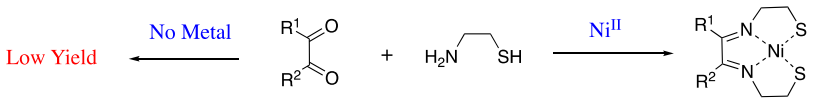

Figure 2.9 Busch's metal templating macrocycle synthesis.

Sanders and coworkers[372] reported their work on DCC in a publication titled '*living macrolactonisation*' in 1996. They generated a DCL from a reversible thermodynamically-controlled mixture of cholate-derived monomers/macrolactones, and since the cholate monomers were equipped with a chromophore at C-7 or/and C-12 the different ring sizes and constituents of macrolactones could be identified from on-line ultraviolet analysis of HPLC eluents.

They also suggested that a '*metal-ion-template*' could be used to select the thermodynamically most stable macrocycle from the DCL, as they reported in another publication titled '*metal ion templated living macrolactonisation*.'[373]

Although Sanders showed that unpredictable structures well-suited for drug discovery could potentially be discovered by stabilising the template in a DCL in a manner that would be difficult *via* conventional synthetic chemistry, DCC was not exploited in inhibitor drug discovery until the late 1990s, when Huc and Lehn used a protein (carbonic anhydrase II) as the '*template*' in their imine DCL to generate novel inhibitors of Zn^{II} metalloenzyme carbonic anhydrase II.[374]

Since their DCL was made up of imines in constant interconversion with their building blocks and were not very stable, they used a reducing agent *i.e.* sodium cyanoborohydride ($NaCNBH_3$) to convert the imine products to their corresponding irreversible amines, in essence '*freezing*' the equilibrium. The mixture was then purified by HPLC, such that the thermodynamically most stable inhibitor which was amplified by the protein template could be identified (Fig. 2.10).

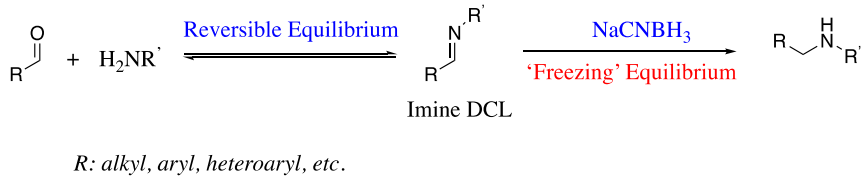

Figure 2.10 Stabilising the thermodynamically most stable product of a DCL by freezing the equilibrium.

2.4.2.2 Reversible Covalent Dynamic Combinatorial Chemistry Reactions

The interconversions between building blocks of a DCL can involve both covalent and non-covalent interactions. The non-covalent interactions heavily dominate inorganic DCC systems, mainly DCLs based on metal complexes. As a result, DCC systems solely based on non-covalent interactions *e.g.* metal-ligand coordination, hydrogen bonding *etc.* are not pertinent to this work, and this section focusses on reversible covalent interactions.

Much of the early DCC investigations revolved around transesterification and transallylesterification.[375] Sanders and coworkers[372] introduced DCC through '*living macrolactonisation*' based on transesterification of cholate derivatives (Section 2.4.2.1). The lactonisation of different families of carboxylic acids in presence of a lipase is the prime example of transesterification in DCC using a protein template.[376,377]

The preponderance of amide bonds in drug molecules has incentivised researchers to explore transamidation in DCC, even though the reversibility of amide DCLs could be kinetically very slow. For instance, the protein-directed synthesis of aspartame has been successfully achieved using the enzyme thermolysin in a DCL of Z-Asp-OH and phenylalanine methyl ester.[378] Intriguingly, thermolysin has been extensively used for transamidation in DCC.[379,380]

Thiol-thioester exchange is rapid in water and was identified as being reversible in the 1950s.[381] To this end, thioester exchange has been frequently used in native chemical ligation (NCL)[382] for total chemical synthesis of large peptides/proteins, and also could be a great means for generating DCLs. For instance, Ramström and coworkers[383] used protein-directed DCC of a mixture of thioesters and aliphatic thiol nucleophiles to study the effect of acetylcholinesterase on both kinetics and thermodynamics of their DCL, which reaches equilibrium within 2.0 h at 5.0 mM concentration.

Thiol-thioester exchange is not the only soft-soft thiol interaction used in DCC; Greaney and coworkers[384] used glutathione *S*-transferase as a protein template to find inhibitors for it from a DCL of thiols and Michael acceptors by means of thiol-enone exchange.

The DCC systems based on exchange reactions between carbonyls and nitrogen-based nucleophiles (amines, hydroxylamines, hydrazines, hydrazides *etc.*) have been of longstanding interest to chemists. Perhaps the most suitable C=N exchange so far as DCC is concerned, is formation of Schiff bases.[385]

Schiff base formation is reversible at physiological conditions and their DCC systems reach equilibrium relatively fast. Thus, the mesomeric effect of a heteroatom attached to the nitrogen nucleophile can significantly disturb the equilibrium.[386,387] As a result, hydrazone and oxime DCLs cannot form true DCC systems even though the DCC of such systems have been investigated.

Since imine DCLs are thermodynamically unstable, kinetic trapping *via* a reducing agent (sodium or tetrabutylammonium[388] cyanoborohydride) can be employed to identify the thermodynamically most stable product. However, a protein-directed DCC for inhibitors of glycosidase carried out by the Vogel laboratory brought home to us that the corresponding isolated amines did not possess the inhibitory effects of the imines selected by the protein template.[389]

The DCC of hydroxylamines with carbonyls is biased towards the adduct due to the mesomeric effect of the oxygen lone pair adjacent to the nitrogen which stabilises the oxime, and shifting the equilibrium towards the products. To this end, oxime DCC systems appear to have been developed by Eliseev's laboratory.[390] On the other hand, since nitrogen is mesomerically more electron donating than oxygen, the hydrazone adducts of hydrazines and carbonyl compounds are relatively stable in water, and even at low pH values.[391] Thus, without an acyl or electron withdrawing group adjacent to the hydrazone, they are not very useful in DCC systems. In recognition of this, Nguyen and Huc were able to generate hydrazone DCLs at a neutral pH, only when the hydrazine building blocks bear electron withdrawing substituents.[392] In addition, DCC systems based on acetal exchange have been explored,[393] though have yet to be applied to enzyme inhibitor discovery.

In other developments, DCC systems based on alkene metathesis have been reported. Although, all metathesis steps are in principle reversible, the metathesis catalyst *i.e.* the Grubbs' catalyst is very insoluble in water, and attempts to develop a water-soluble metathesis catalyst have not been fruitful.[394] Nonetheless, DCC systems based on alkene metathesis have been established in aqueous solutions using a biphasic system and phase transfer catalysis.[395] DCC systems based on alkyne metathesis do also exist.[396] However, such exotic DCC systems have remained in the realm of polymer chemistry.

The use of disulfide exchange reactions has been one of the most recent and widely used application in DCC,[397,398] particularly for enzyme inhibitor discovery (Section 2.6). As a result, Lehn and Ramsröm were able to find novel ligands for concanavalin A using a protein-directed DCC from a DCL of carbohydrates and disulfides.[399]

DCC systems based on disulfide exchange remained the latest DCC advances in drug discovery until 2011, when Schofield and coworkers[400] pioneered the use of boronic acids in DCC and discovered novel inhibitors for α-chymotrypsin; their protein-directed DCC used α-chymotrypsin as a protein template to generate a DCL of boronate esters from boronic acids and alcohols (Fig. 2.11). They were also able to discover potent boronate ester inhibitors using the earlier approach, but this time for an oxygenase, in particular, a 2-oxoglutarate (2OG) oxygenase.[401]

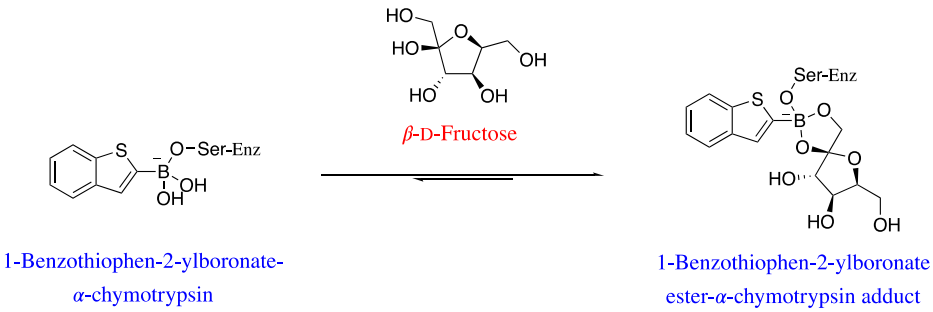

Figure 2.11 The addition of α-chymotrypsin disturbs the equilibrium towards formation of 1-benzothiophen-2-yl-ß-D-fructose boronate ester adduct.

2.4.2.3 Scope & Limitations of Dynamic Combinatorial Chemistry

Be it rotaxanes,[402] sensors,[403] molecular capsules[404,405] or even drug molecules, DCC has demonstrated its capability and versatility for discovery of novel molecules. Whilst DCC has eased some of the synthetic challenges, it has introduced analytical challenges. Notably, the identification of labile constituents of a DCL together with isolation of thermodynamic products of such DCLs has posed signification challenges. High-resolution NMR spectroscopy and X-ray crystallography can provide accurate detail about DCC systems, but these techniques can be costly and time consuming.[406]

Schofield and coworkers[407] have developed non-denaturing protein mass spectrometry to identify protein-ligand components of a protein-directed DCL. The so called dynamic-combinatorial mass spectrometry (DCMS) can also be coupled to HPLC to isolate the stable products for further analysis. However, without isolation of the DCL constituents, DCMS itself does not provide direct structural detail.

These complications have led others to bring about innovative analytical techniques; for example, Sanders and coworkers[408] used crown ethers to trap linear hydrazides of a DCL, which were in equilibrium with their corresponding peptides and aliphatic acyl hydrazides. Deconvolution processes such as knockout experiments are routinely employed in protein-directed DCC systems to identify the most stable products or best binders.[409,410]

DCC is a promising tool in drug discovery, even more so for molecular targets which their exact 3D structures are unknown or are highly substrate dependent. The niche reaction conditions for molecular targets as protein templates in DCC preclude the vast majority of exchange reactions applicable to DCC (Section 2.4.2.2). In this context, the most widely used exchange reaction to date is disulfide exchange,[411] mainly due to the demonstrated role of aqueous disulfide exchange in many biological applications,[412,413] followed by Schiff bases,[414] though Schiff bases are normally reduced to their corresponding amines for isolation and identification.

In contrast, hydrazone exchange reactions, though being chemoselective and tolerant of many solvents and functional groups, require acidic conditions which are incompatible with most molecular targets (Section 2.4.2.2). In addition, thioester[415] and peptidic[416] exchange reactions together with some aldol reactions[417,418] are all compatible with molecular targets.

The intrinsic feature of DCC is the reversibility of reactions in the system for which an equilibrium develops between the building blocks and products; thus, in a true DCC system these reactions must satisfy the following:

- The kinetics of the equilibration has to be on a reasonable timescale.
- The selection and equilibration processes must be compatible, as in principle, the selection and equilibration occur simultaneously. Moreover, the compatibility of building blocks bearing functional groups, the DCC template, solvent and pH (in particular, if protein-directed DCC employed) all must be considered.
- Mild reaction conditions are desirable, as slight changes in factors governing reaction conditions *e.g.* temperature, pressure, concentration *etc.* can significantly alter the position of equilibrium.
- Poor solubility of the building blocks can act as a kinetic trap, and insolubility of products *e.g.* salt formation can act as a thermodynamic trap; thus, solubility of all the constituents of a DCL at equilibrium must be guaranteed for a true DCC system.
- Ideally all members of a DCL should be isoenergetic so as to reach an impartial and unbiased equilibrium.

In view of the above, DCC is still an emerging synthetic tool and more work needs to be done for its optimisation. To this end, other variants of DCC such as pseudo-dynamic combinatorial chemistry[419] have been introduced and others may well be discovered in the future.

2.5 ß-Lactamases

ß-Lactam antibiotics (Section 1.1) account for almost 60% of antibacterials used by weight worldwide, and are the most widely used class of antibiotics in virtue of their safety, efficacy and the broader-spectrum of activity relative to other classes of antibacterials in clinical use.[420] However, bacteria have been highly efficient in developing resistance to ß-lactam antibiotics (Section 1.5), and can develop resistance to ß-lactam antibiotics *via* the following four primary mechanisms:

- The alteration of the active site of penicillin binding proteins (PBPs), which is either a result of random mutation due to the selection pressure or can be acquired through HGT (Section 1.6). Intriguingly, the latter is much more prevalent than the former; for example, penicillin resistance in *Streptococcus* spp. was developed after acquisition of PBP2b gene from *S. pneumoniae via* HGT.[421]
- PBPs are located on the inner membrane of bacterial cells and for ß-lactams to reach them, they have to either diffuse through the cell-wall or get passed through porin channels in the outer membrane of Gram-negative bacteria. Thus, some ß-lactam resistant Gram-negative bacteria, in particular, those which are resistant to carbapenems express modified or reduced porin channels which hamper the delivery of ß-lactams to PBPs, hence conferring resistance.[422]
- One way by which bacteria, especially Gram-negative bacteria protect themselves from exogenous toxins is the use of multicomponent drug efflux pump systems (*mex*). These pumps extrude many substances including ß-lactams to the surrounding environment and rendering them ineffective. For example, multidrug resistance in *P. aeruginosa* can be attributed to low permeability and *mex*A – *mex*B systems which make them invincible to all ß-lactam antibiotics, including carbapenems as well as fluoroquinolones, tetracyclines and chloramphenicol.[423]
- Last but not least, ß-lactamases are powerful arsenals at their disposal against ß-lactam antibiotics. ß-Lactamases hydrolyse the ß-lactam ring, rendering ß-lactam antibiotics completely ineffective. This method of protection is the most common resistance mechanism,[424] and will be the focus of this short review.

2.5.1 ß-Lactamase Classification

ß-Lactamases were first discovered in *Escherichia coli* before the therapeutic introduction of penicillin.[425] To date, almost 2,800 naturally occurring unique ß-lactamases have been described,[426] of which many are metallo-ß-lactamases (MBLs) such as Verona Integron-en-coded metallo-*β*-lactamases (VIM) and New Delhi metallo-*β*-lactamases (NDM) (Section 2.5.5).[427]

On the other hand, related MBLs such as DNA Cross-Link Repair (DCLRE) 1A and 1B,[428] are found in humans and are targets for oncology. There are two major classification schemes for ß-lactamases – the Ambler and Bush–Jacoby classifications, which are based on ß-lactamase amino acid sequence homology and functionality *i.e.* substrate hydrolysis profiles, respectively.

The Ambler classification divides ß-lactamases into four groups (Class A, B, C & D); Ambler Classes A, C and D are serine-ß-lactamases (SBLs), whereas Ambler Class B ß-lactamases are MBLs which hydrolyse ß-lactam antibiotics using a pair of divalent zinc ions in their active sites.[429]

The Bush–Jacoby classification divides ß-lactamases into three groups – Group 1 cephalosporinases which belong to Ambler Class C, Group 2 SBLs (Ambler Classes A & D), and Group 3 MBLs (Ambler Class B).[430,431] Although, classifications of ß-lactamases based on their affinity for a particular ligand have been reported,[432] these are relatively new and have not been widely accepted.

2.5.2 Class A – Serine Penicillinases & Carbapenemases

Ambler Class A ß-lactamases are usually plasmid-encoded and are easily transferred amongst bacteria through HGT (Section 1.6); however, chromosomally encoded Class A ß-lactamases do exist, though some of these might have been incorporated into the chromosome after acquisition of the plasmid. For instance, $bla_{\text{SHV-1}}$ is located on the chromosome of *Klebsiella pneumoniae*, but the same gene is also found on plasmids.[433]

Class A ß-lactamases are generally susceptible to established ß-lactamase inhibitors such as clavulanic acid, sulbactam, tazobactam, avibactam and the recently developed boron based ß-lactamase inhibitor, vaborbactam.[434] Clinically most important Class A ß-lactamases are TEM (Temoniera),[435] SHV (sulfhydryl variable: a biochemical property of this type of ß-lactamases),[436] and CTX-M (confers resistance to cefotaxime).[437] These ESBLs such as CTX-M-14 and CTX-M-15 are observed in many advanced cephalosporin resistant strains of *E. coli* worldwide.[438]

Some Class A ß-lactamases are also carbapenemases, most importantly *K. pneumoniae* carbapenemase (KPC).[439] KPC-type Class A effectively hydrolyses carbapenems and penicillins as well as cephalosporins and aztreonam. They are not inhibited by the established ß-lactamase inhibitors; however, avibactam inhibits KPC-type ß-lactamases, but is hydrolysed slowly.[440]

2.5.3 Class C Cephalosporinases

The ampicillin resistant Class C (AmpC) ß-lactamases are mostly encoded by *bla* genes which are found on both bacterial chromosomes and plasmids. As the name suggests, AmpC ß-lactamases are resistant to penicillins (penicillin G, ampicillin, amoxicillin *etc*.), most clinically relevant ß-lactamase inhibitors, and many cephalosporins including, but not limited to, cefoxitin, cefotetan, ceftriaxone and cefotaxime. They slowly hydrolyse cefepime, and are susceptible to carbapenems.[441]

Certain ß-lactamase inhibitors, in particular, clavulanic acid, not only have negligible inhibitory effect, but also are inducers of AmpC ß-lactamases. For example, the AmpC inducing effects of clavulanic acid in *P. aeruginosa* significantly hamper the antibacterial activity of ticarcillin.[442]

In addition, AmpC expression in Gram-negative bacteria, in particular, *Citrobactor* spp., *Solmonella* spp. and *Shigella* spp. are normally low; however, most ß-lactams, such as cefoxitin and imipenem, can induce AmpC expression.[443]

2.5.4 Class D Oxacillinases

Class A and C ß-lactamases hydrolyse oxacillin slowly; on the other hand, the SBLs which metabolise oxacillin at a rate nearly 50% that for penicillin G were named oxacillinases – Class D ß-lactamases. Thus, oxacillinase harbouring bacteria are generally resistant to penicillins, extended-spectrum cephalosporins (OXA-type ESBLs), and carbapenems (OXA-type carbapenemases).[444]

A wide range of bacteria harbour oxacillinases which are capable of hydrolysing both aminopenicillins (penicillin G, ampicillin, amoxicillin *etc.*) and carboxypenicillins (carbenicillin, ticarcillin *etc.*) and are generally not inhibited by common ß-lactamase inhibitors,[445] but are inhibited by sodium chloride *in vitro*.[446] However, some oxacillinases such as OXA-2 and OXA-32 are inhibited by tazobactam, but sulbactam and clavulanic acid are not active against them.[447]

2.5.5 Class B Metallo-ß-lactamases

Unlike SBLs which span across three major groups in the Ambler classification, MBLs belong to only one class of ß-lactamases in both the Ambler and Bush–Jacoby classification schemes. Though, they effectively carry out the same hydrolysis reaction as the SBLs *i.e.* breaking the amide bond in ß-lactams, they are structurally and mechanistically different to their serine counterparts.

MBL harbouring bacteria are generally resistant to penicillins, cephalosporins, carbapenems and clinically relevant ß-lactamase inhibitors. MBLs are encoded by *bla* genes, which are located on the bacterial chromosomes, integrons and plasmids.[448] The necessity of one or two divalent $zinc^{II}$ ions, making MBLs susceptible to metal chelators such as ethylenediaminetetraacetic acid (EDTA).[449] Nonetheless, there are currently no EDTA based ß-lactamase antibacterials found in clinical use, even though EDTA has long been used in chelation therapy to treat lead and mercury poisoning.[450]

Globally widespread MBLs such as NDM, VIM and imipenemase (IMP) are worrisome as the mortality rate for pathogens producing MBLs is between 18 to 67%.[451]

NDM-1 was first isolated in Sweden from a patient of Indian heritage in 2008.[452] NDM-1 shares nearly 32% sequence homology with VIM-1 and VIM-2, and is a 28 kDa MBL with high affinity for penicillins and cephalosporins, but relatively low affinity for carbapenems.[453] The NDM-1 binding mode of ß-lactams was first shown using ampicillin as a substrate; however, recent X-ray crystallographic studies have revealed insight into the binding modes for carbapenems.[454]

Convenient and affordable international travel has apparently led to a worldwide dissemination of NDM-1, which once was only endemic to the Indian subcontinent. Reported cases of Gram-negative bacilli expressing $bla_{\text{NDM-1}}$ worldwide suggest that $bla_{\text{NDM-1}}$ can be transferred horizontally amongst bacteria; concerns that the identified cases did not have any contact with the local healthcare systems or endemic areas, make this HGT an autochthonous acquisition.[455]

Before the worldwide dissemination of NDM-1, IMP and VIM ß-lactamases were much more prevalent than NDM-1 and the genes encoding for these MBLs are mostly located on integrons; it has been shown that incorporation of these integrons with transposons or plasmids results in a rapid transfer of these genes between bacteria through HGT.[456] In addition, VIM-type MBLs are presently becoming more prevalent than IMP; VIM-1 was first isolated from *P. aeruginosa* in Italy in 1997, which followed by discovery of VIM-2 in France using samples taken from a neutropenic patient in 1996.[456]

Other notably endemic MBLs are Sao Paulo MBL (SPM-1) in Brazil,[457] German imipenemase (GIM-1) found in Germany,[458] Seoul imipenemase (SIM-1) in Korea,[459] Kyorin Health Science MBL (KHM-1)[460] isolated from *C. freundii* and *S. marcescens* MBL (SMB-1)[461] both in Japan, Dutch imipenemase (DIM-1) isolated from *P. stutzeri* in Netherlands,[462] Tripoli MBL (TMB-1) from *A. xylosoxidans* in Libya,[463] and Florence imipenemase (FIM-1) which is found in Italy.[464]

2.6 Dynamic Combinatorial Chemistry of Benzodiazaborines & Boronate Esters

The DCC of disulfide complexes has been widely studied for enzyme inhibitor discovery (Section 2.4.2). For example, Schofield and coworkers[465] generated a DCC system of disulfides from which a potent inhibitor for *Bacillus cereus* MBL (BcII) – a clinically important subclass of MBLs (Section 2.5.5) – was designed (Fig. 2.12).

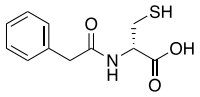

N-Benzoyl-*D*-cysteine

$IC_{50} = 0.74\ \mu M$

Figure 2.12 A potent inhibitor for BcII, designed based on a protein-directed DCC system of equilibrating thiols and disulfides.[465]

In their pioneering work they showed that a dithiol *i.e. meso*-2,3-dimer-captosuccinic acid can act as a '*support ligand*' and bind to a protein template *i.e.* BcII, using one of its thiol moieties, and then subsequently forming a disulfide bond through its other thiol with another thiol component of the DCC system *e.g.* phenyl mercaptan, which in turn could inhibit the protein template (Fig. 2.13).

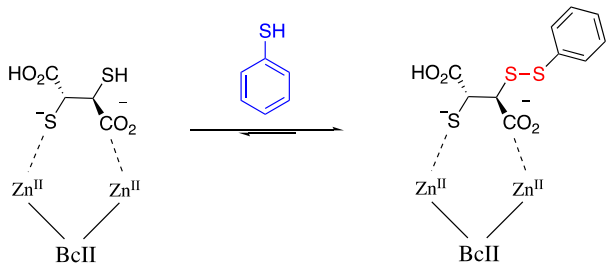

Figure 2.13 *meso*-2,3-Dimer-captosuccinic acid bound to BcII acts as a '*support ligand*'; this facilitates formation of a disulfide, which in turn inhibits BcII.

Inspired by the above tethering strategy in DCC, our group recently developed a protein-directed DCC system of cysteine derivatives and boronic acids (unpublished data), which generates novel cyclic boronate esters on the surface of OXA-10 *i.e.* the protein template (Fig. 2.14a), as evidenced by high throughput X-ray crystallography (Fig. 2.14b).

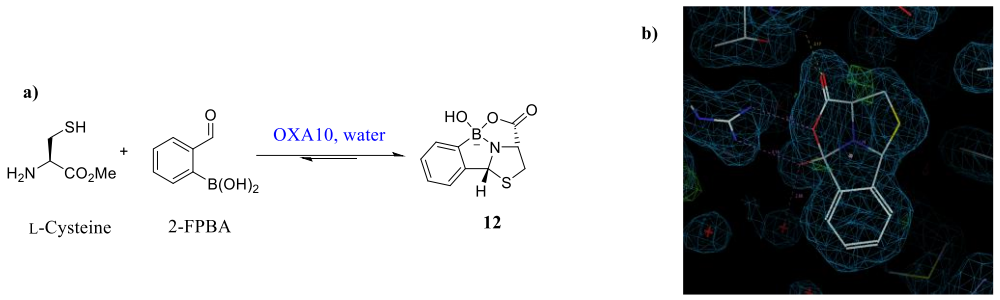

Figure 2.14 a) The DCC of L-cysteine methyl ester with 2-FPBA on the surface of OXA-10. b) X-ray crystal structure of the boronic ester 12 on OXA-10 (*courtesy of Dr Jürgen Brem*).

Gao and coworkers[466] have reported that on reacting 2-formylphenylboronic acid (2-FPBA) and 2-acetylphenylboronic acid (2-APBA) with D-cysteine in 0.10 M phosphate-buffered saline (PBS) buffer at physiological pH, bicyclic or tricyclic heterocycles form.

A DCC system of 2-FPBA/2-APBA with D-cysteine in 0.10 M PBS buffer at physiological pH was established, and its results indicated that under thermodynamic control, the most stable products are in fact tetracycles, as evidenced by LC-MS (Fig. 2.15a) and ^{1}H NMR (Fig. 2.15b).

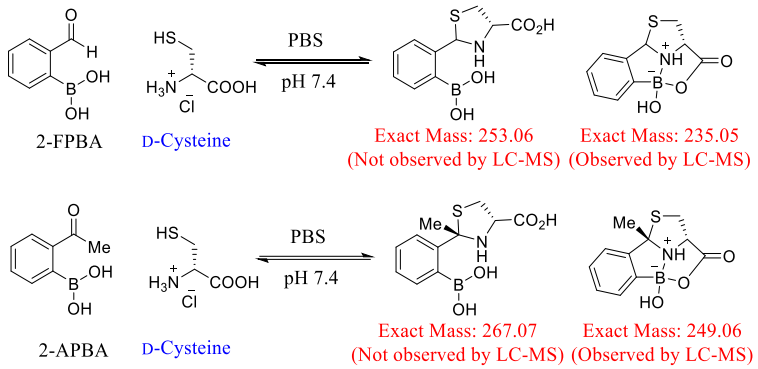

Figure 2.15a Observed products (by LC-MS) when equimolar amounts of 2-FPBA and 2-APBA were equilibrated with D-cysteine hydrochloride in 0.10 M PBS buffer at physiological pH.

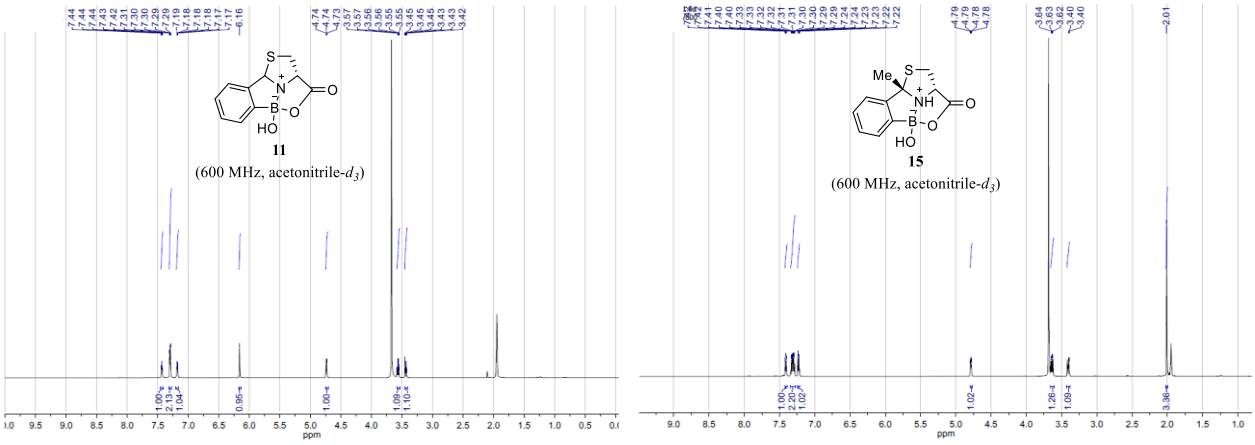

Figure 2.15b ^{1}H NMR spectra of products from the DCC of 2-FPBA and 2-APBA with D-cysteine hydrochloride in 0.10 M PBS buffer at physiological pH. The singlet from *δ*-C*H* in boronate ester 11 at δ 6.16 (left) is absent in the ^{1}H NMR spectrum of 15 (right).

In recognition of the above and the observed structures on the surface of OXA-10 from previous protein-directed DCC studies in Oxford, a series of DCC systems from a set of dielectrophiles and dinucleophiles (Fig. 2.16) were designed and developed.

Stable products were identified for *in vitro* screening against various clinically important MBLs *i.e.* VIM-1/2, IMP and NDM-1, and also *in vivo* screening against H37Rv, which is a clinically relevant strain of *M. tuberculosis*.

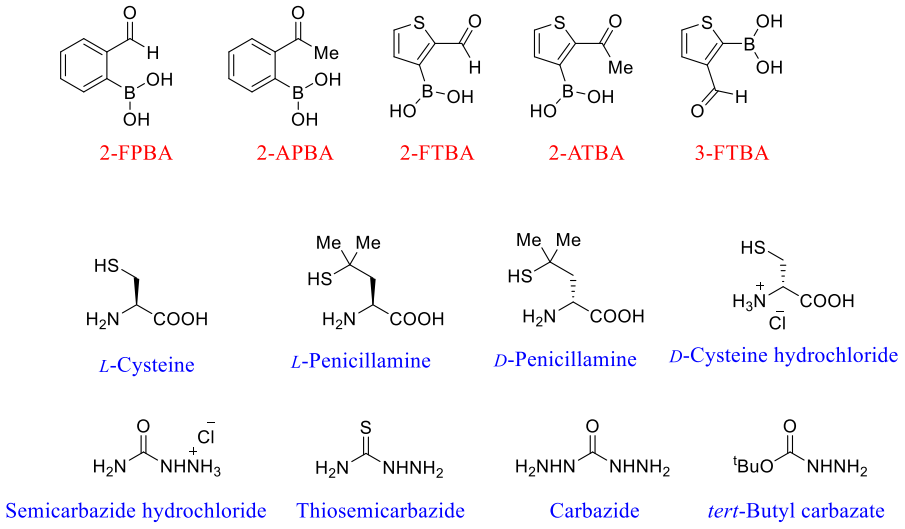

Figure 2.16 Dielectrophile (red) and dinucleophile (blue) building blocks for which various DCC systems were developed.

The DCC systems of 2-FPBA, 2-APBA, 2-formylthiophen-3-ylboronic acid (2-FTBA) and 2-acetylthiophen-3-ylboronic acid (2-ATBA) with semicarbazide in 0.10 M PBS buffer at physiological pH, resulted in a spontaneous precipitation. Thus, these systems are not true DCC systems as the precipitates act as a thermodynamic trap, perturbing the equilibrium in favour of the products (Section 2.4.2.3). The DCC system of 3-formylthiophen-2-ylboronic acid (3-FTBA) with semicarbazide in 0.10 M PBS buffer at physiological pH, also gave a precipitate. Analysis of the obtained solid revealed the deborylated diazaborine **8** (Fig. 2.17).

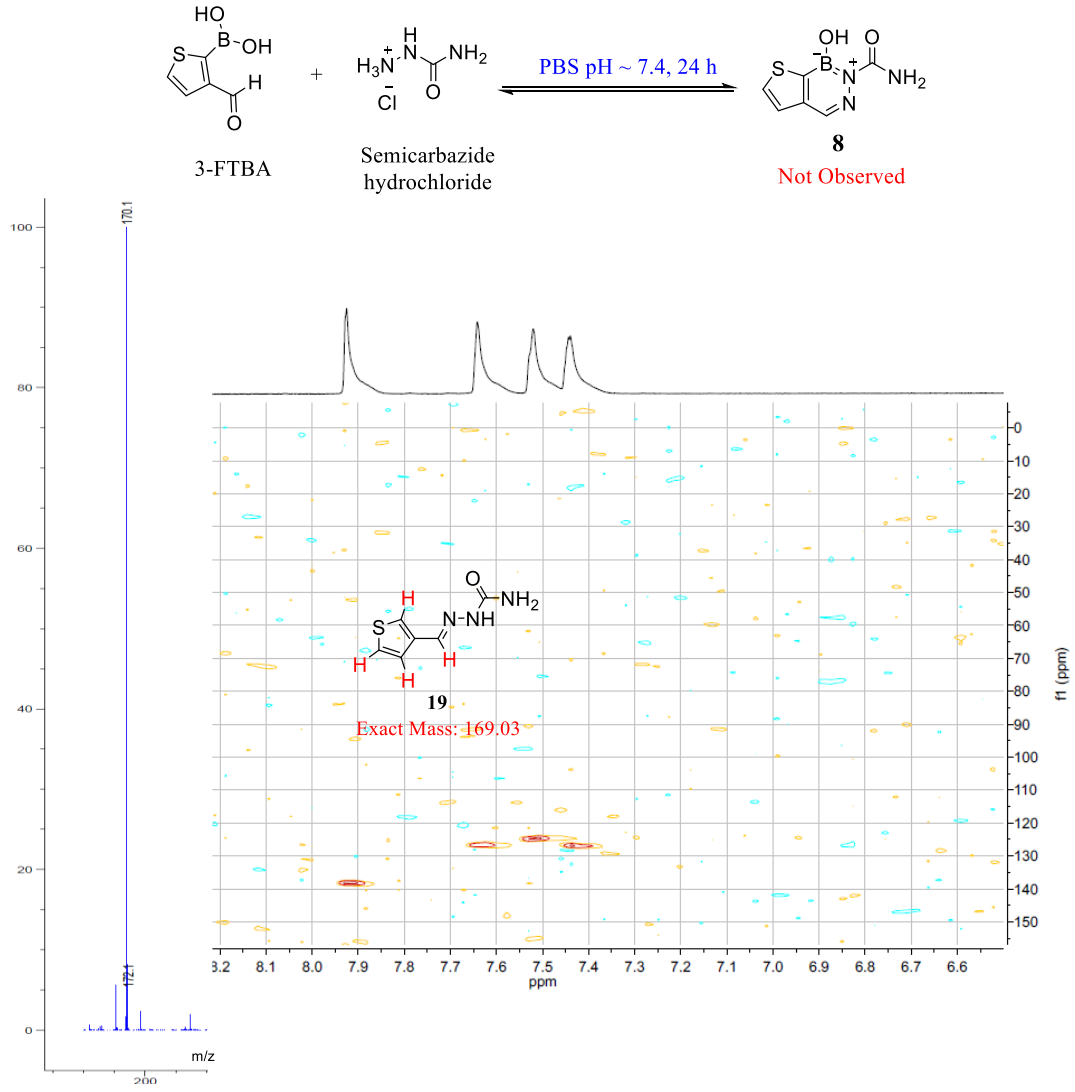

Figure 2.17 Mass chromatogram and HSQC NMR spectrum of compound 19 *i.e.* deborylated compound 8.

Since compound **8** is a structural isomer of compound **6** and could be useful for SAR studies of this set of diazaborines, it was eventually synthesised under anhydrous conditions (Fig. 2.18) as evidenced by IR, NMR (^{1}H, ^{13}C & ^{11}B), LC-MS and HRMS *cf.* Experimental p. S11.

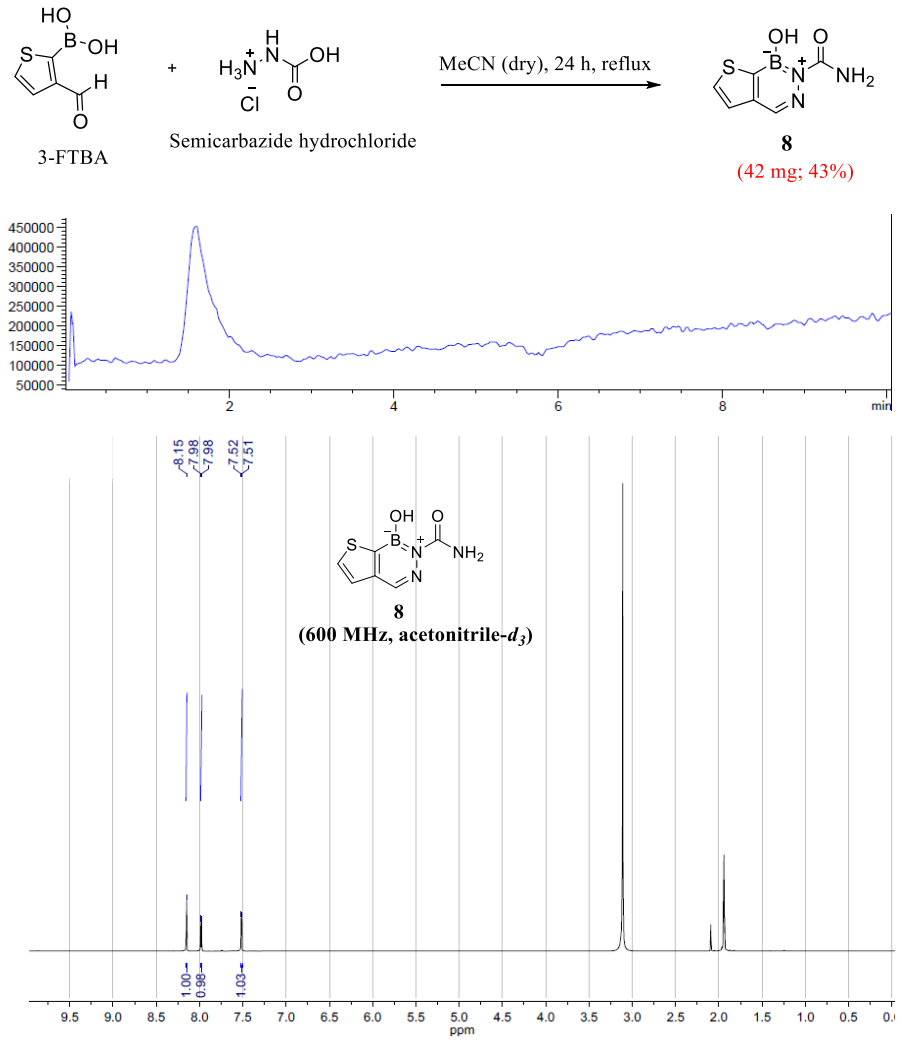

Figure 2.18 Synthesis of diazaborine 8 under anhydrous conditions. The signals at δ 7.98 & 7.52 in the ^{1}H NMR spectrum are from the thiophenyl protons, and the distinctive singlet from *γ*-C*H* on the diazaborine core ring resonates at the lowest field *i.e.* δ 8.15. For a detailed discussion on structural features of diazaborines, see Appendix I.

Upon isolation of the most stable products of the aforementioned DCC systems, the ^{1}H NMR spectrum of compound **6** revealed several unrelated peaks, indicating the existence of a side product which was unravelled to be the linear uncyclised diazaborine **6** (Fig. 2.19).

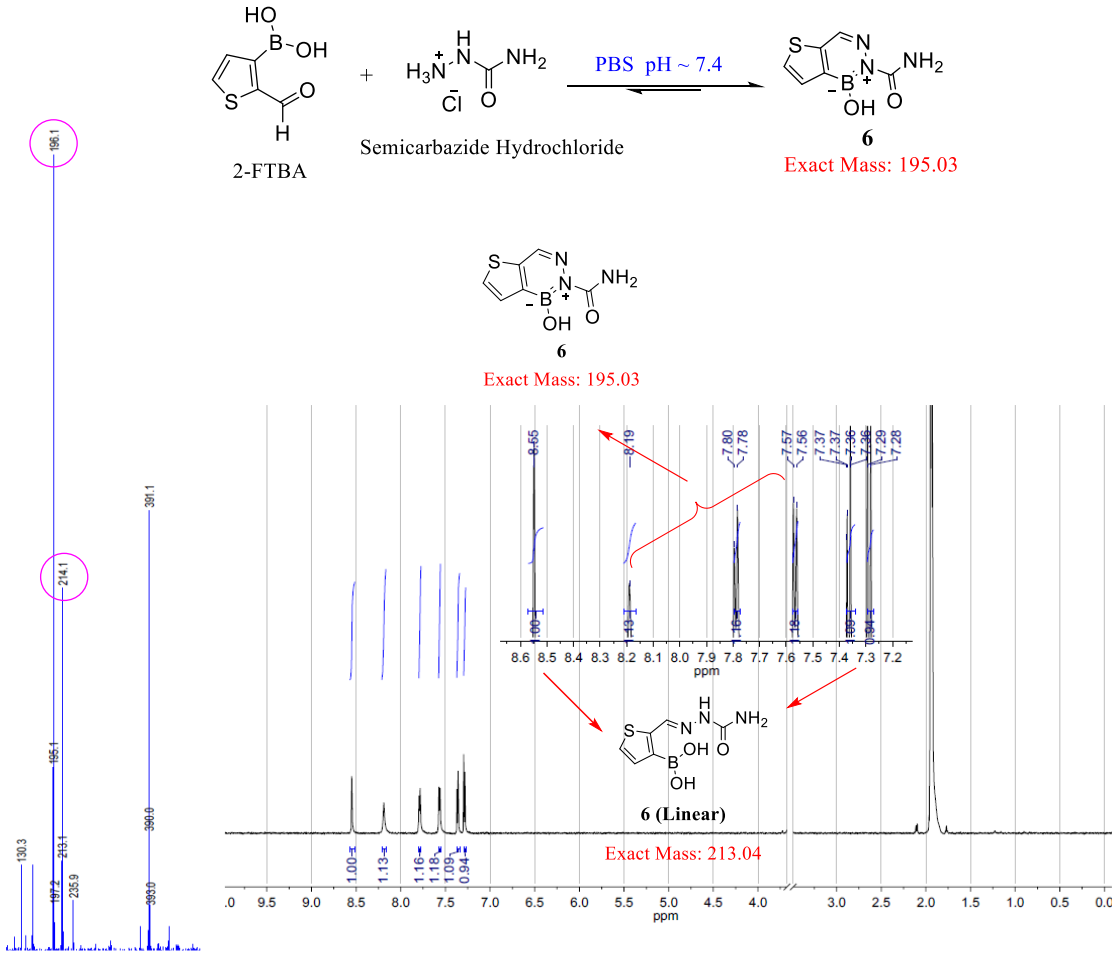

Figure 2.19 Mass chromatogram and ^{1}H NMR of a mixture of cyclised (desired) and uncyclised (linear) diazaborine 6. The uncyclised diazaborine 6 whose mass was detected by mass-spectrometry *i.e.* [M^{+} + H] *m/z* 214, can also complicate the ^{1}H NMR spectrum of diazaborine 6 (*vide infra*); *cf.* Experimental p. S9 for full characterisation of 6.

Attempts at separation of the above linear and cyclised diazaborine **6** with either sedimentation and filtration or preparative RP-HPLC were unsuccessful. As a result, DCC systems of 2-FTBA and semicarbazide hydrochloride both at low pH values *i.e.* 0.10 M 2-(*N*-morpholino)ethanesulfonic acid (Mes) buffer pH ~ 3.4, and high pH values *i.e.* 0.10 M tris(hydroxymethyl)aminomethane (Trizma®) buffer pH ~ 10.7, were established.

The results of the concerned DCC system at high pH values *i.e.* 0.10 M Trizma® buffer pH ~ 10.7 closely matched that of the PBS buffer *i.e.* physiological pH, again giving a mixture of both desired and undesired diazaborine **6**. However, the same DCC system at low pH values *i.e.* 0.10 M Mes buffer pH ~ 3.4, furnished the clean desired diazaborine **6** after purification by preparative RP-HPLC (Fig. 2.20).

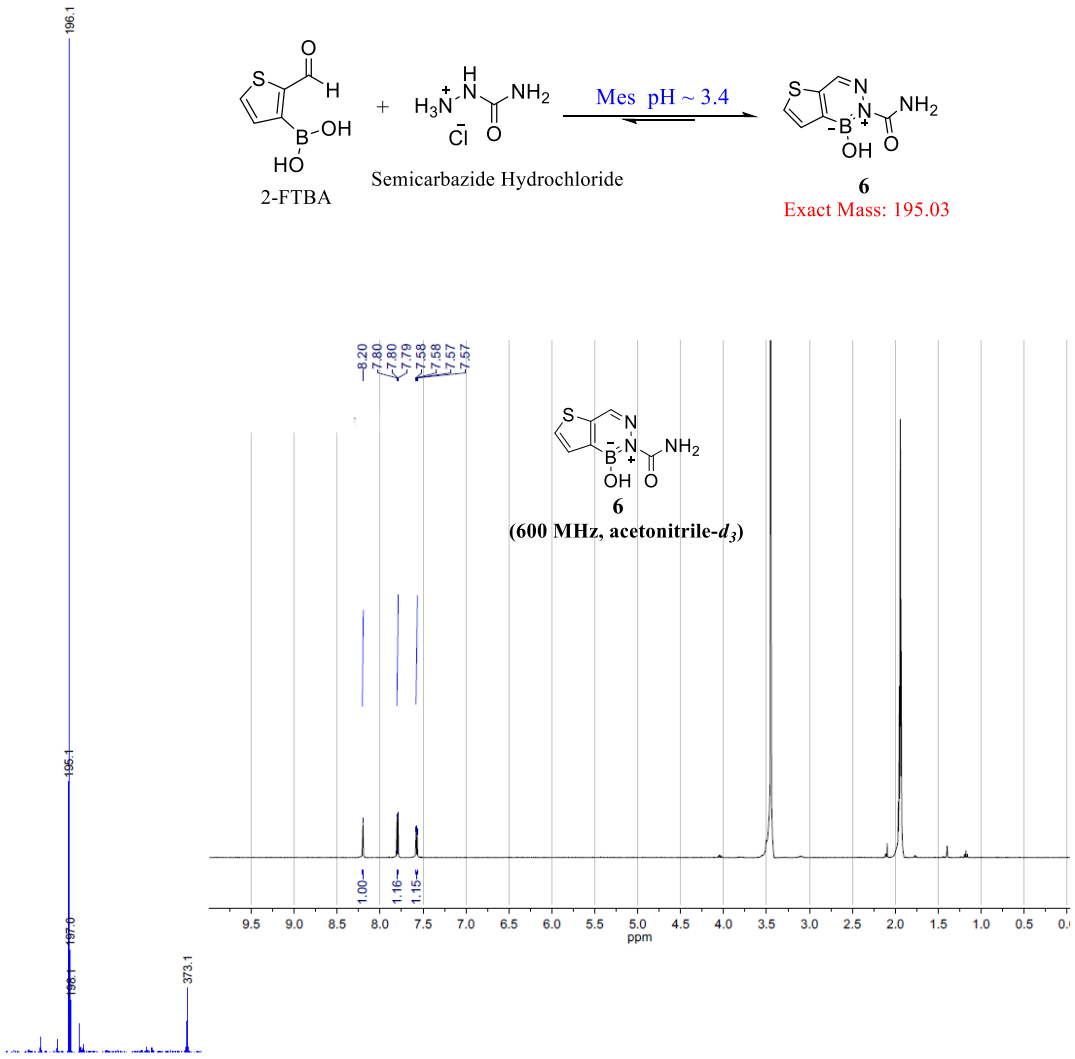

Figure 2.20 Mass chromatogram and ^{1}H NMR of diazaborine 6. The signals at δ 7.80 & 7.58 are from the thiophenyl protons, and the distinctive singlet from *γ*-C*H* in the diazaborine core resonates at the lowest field *i.e.* δ 8.20. For a detailed discussion on structural features of diazaborines, see Appendix I.

The DCC systems of 2-FPBA and 2-APBA with thiosemicarbazide and D-cysteine (but not L-cysteine) and 2-APBA alone with both D- and L-penicillamines in 0.10 M PBS buffer at physiological pH, initially gave a clear solution which after standing for 3.0 h became turbid. This observation, indicates that, though not spontaneous, during the course of equilibration, the formation of a precipitate perturbs the equilibrium, and hence these systems are not true DCC systems likewise.

On the other hand, the DCC systems of 2-FPBA and 2-APBA with *tert*-butyl carbazate, carbazide and L-cysteine (but not D-cysteine) and 2-FPBA alone with both D- and L-penicillamines in 0.10 M PBS buffer at physiological pH, gave a clear solution. Upon standing for 24 h no obvious precipitation was observed, indicating that a somewhat true DCC system was established.

It is worth reiterating that whereas the DCC systems of 2-APBA with both D- and L-penicillamines in 0.10 M PBS buffer at physiological pH did not form true DCC systems, the DCC system of 2-FPBA with both D- and L-penicillamines in 0.10 M PBS buffer at physiological pH, in point of fact, did form a reversibly reacting DCC system, and a relatively unbiased equilibrium might have been reached by virtue of no precipitation upon standing for 24 h. This observation highlights how very small changes in a DCC system *e.g.* 2-FPBA only lacks a methyl group relative to 2-APBA can have significant impacts on the entire system.

The most stable products of our DCC systems were identified and isolated *via* various purification techniques (sedimentation, filtration, RP-HPLC *etc.*); however, the DCC systems in which precipitates were formed, the filtration of precipitates did not provide clean products suitable for analytical structure elucidation and preparative RP-HPLC had to be recruited. As a result, a series of benzodiazaborines, diazaborines and boronate esters (Fig 2.21) were obtained from the aforementioned DCC systems.

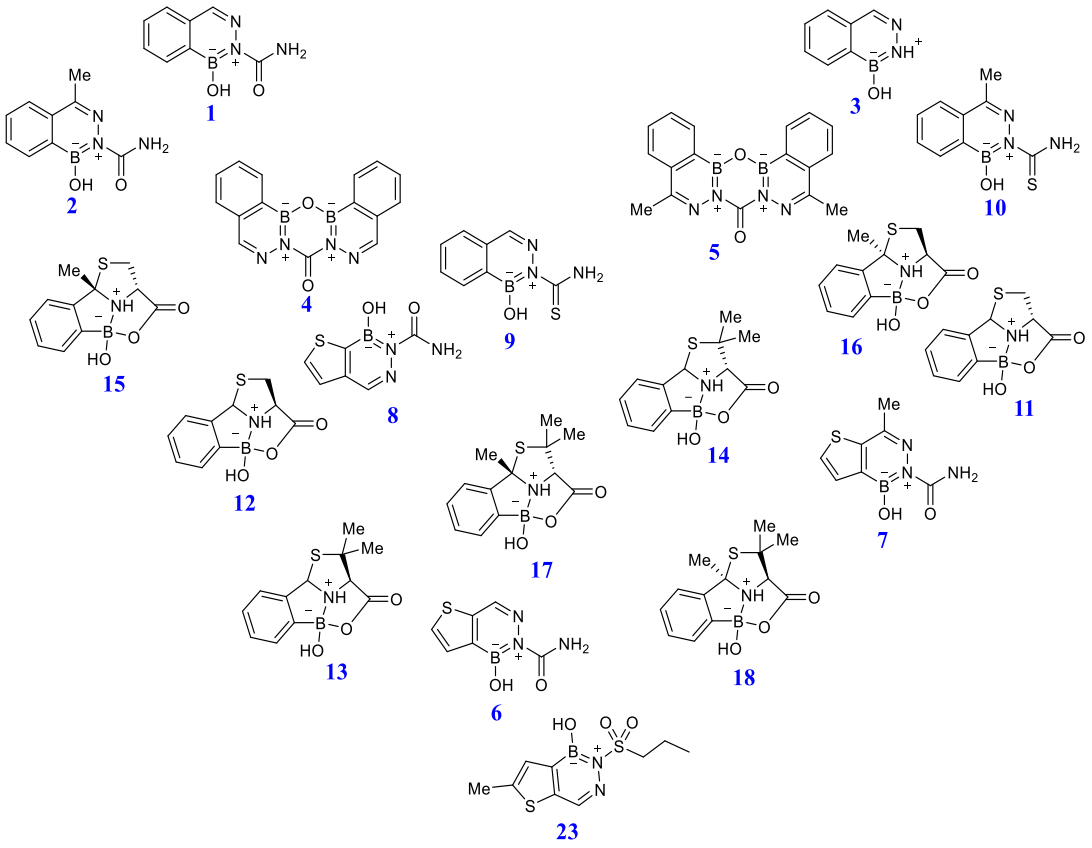

Figure 2.21 Our DCL of benzodiazaborines, diazaborines and boronate esters; for a detailed discussion on structural assignments and features of diazaborines & boronate esters, see Appendix I.

Synthesis of the above cyclic boronate esters *via* addition of D/L-penicillamines and D/L-cysteines to 2-FPBA/2-APBA, generates three new stereogenic centres (Fig 2.22). At first glance, it was likely that since all the steps are reversible and several mechanistic pathways could be involved, a racemate of diastereomers would be obtained.

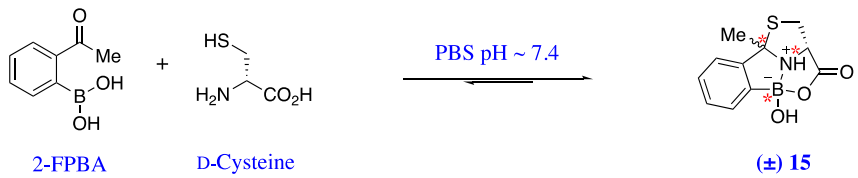

Figure 2.22 Synthesis of cyclic boronate ester 15. The new stereogenic centres are marked by red asterisks (*).

However, since both the α-amine and ß-thiol of D-cysteine are nucleophilic, the scenario is more complicated than a straightforward addition reaction. The pKa_H of the α-amine is around 10.3[467] and it is expected to be fully but reversibly protonated at physiological pH *i.e.* ~ 7.4; both boron and nitrogen are hard species, and hard—hard interactions are more favourable than hard—soft interactions *i.e.* boron—sulfur interaction, and since in this reaction the most electrophilic centre is the empty $2p_z$ orbital of the boron, it is conceivable that the α-amine first adds to the electrophilic boron to give a new boronate, thereafter, at least two scenarios are feasible (Scheme 2.1).

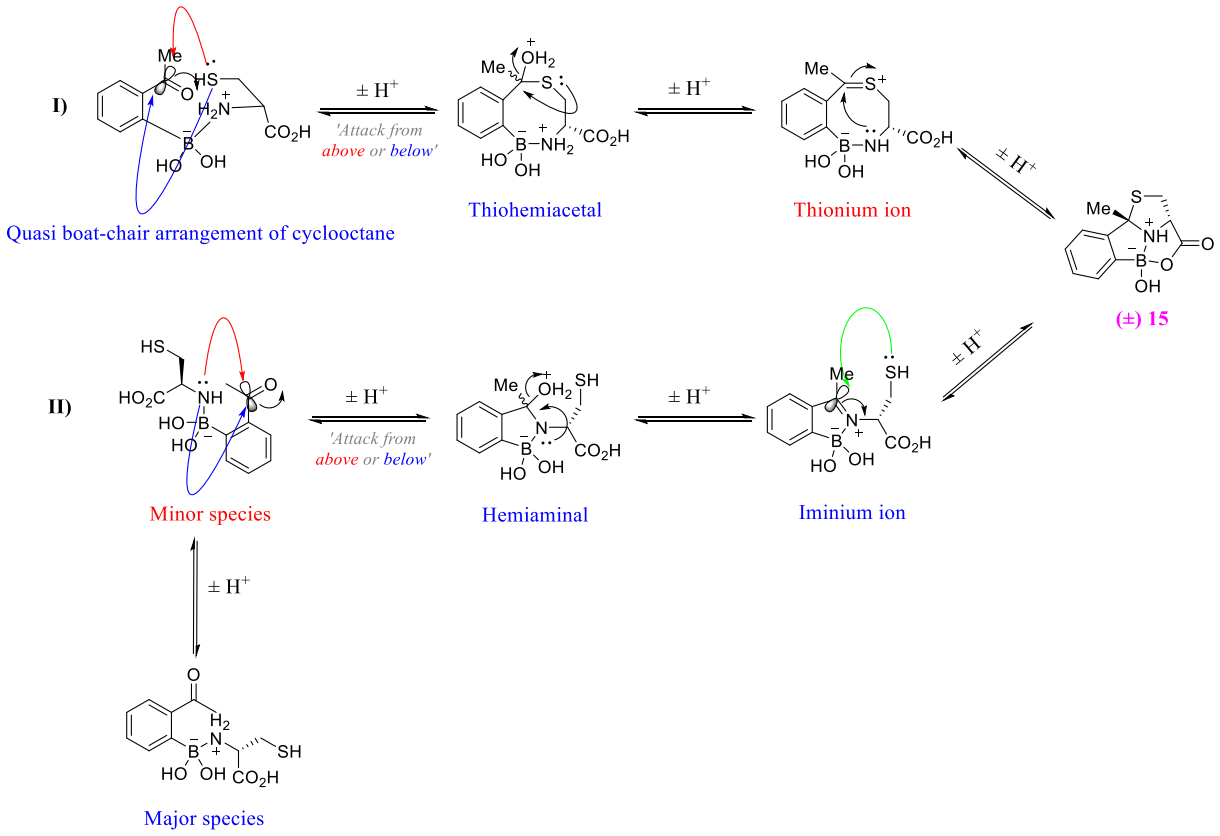

Scheme 2.1 Plausible mechanisms for synthesis of the cyclic boronate ester 15: I) The thionium ion is followed by *cis*-fused ring formation; II) Classical addition to a carbonyl.

Both the addition to boron and pH of the reaction significantly draws electron density from the α-amine and it would be very ambitious to think the rest of the mechanism proceeds solely by the addition of α-amine to the electrophilic carbonyl of 2-APBA (Scheme 2.1.II).

However, since the entire system is under thermodynamic control, at times the *α*-amine would possess a lone pair to add to the carbonyl. Although the addition ideally occurs from the least hindered side, the stereochemistry of the resulting hemiaminal is not retained by the subsequent iminium ion and it is the addition of the nucleophilic *ß*-thiol that determines the absolute stereochemistry of the final cyclic boronate ester **15**.

As depicted in Scheme 2.1.II (green arrow), the *ß*-thiol attacks from behind (as drawn) *i.e.* D-cysteine in a '*5-endo-trig*' cyclisation fashion; even though, this does not fully satisfy the required orbital overlap and the Bürgi-Dunitz angle of 107º for a nucleophilic attack to sp^2 hybridised electrophilic centres, as argued by Baldwin,[468] such cyclisations involving cations are somewhat treated similar to '*carbenium ions*' and the nucleophilic attack is perpendicular to the plane of the iminium ion, thus overcoming the geometrical restrictions. This cyclisation pushes the methyl group away from the plane of the newly formed stereogenic centre, resulting in a *cis*-fused ring.

On the other hand, since the *α*-amine after addition to 2-APBA is most likely to be protonated and '*non-nucleophilic*', it is feasible for the entire adduct to wrap into a '*quasi boat-chair or crown*' heterocyclooctane conformation (the energy difference between these two conformations is only 47.7 kJ mol^{-1}),[469] so as to promote the addition of the nucleophilic *ß*-thiol to the electrophilic carbonyl, and give a heterocyclooctane (Scheme 2.1.I).

As with the hemiaminal, the absolute stereochemistry of the thiohemiacetal is not retained following the formation of prochiral '*thionium ion,*' which will undergo an allowed '*5-exo-trig*' cyclisation to give a *cis*-fused ring. The nuclear overhauser effect (NOE) spectrum of the cyclic boronate ester **15** is in agreement with the proposed mechanisms (Fig. 2.23).

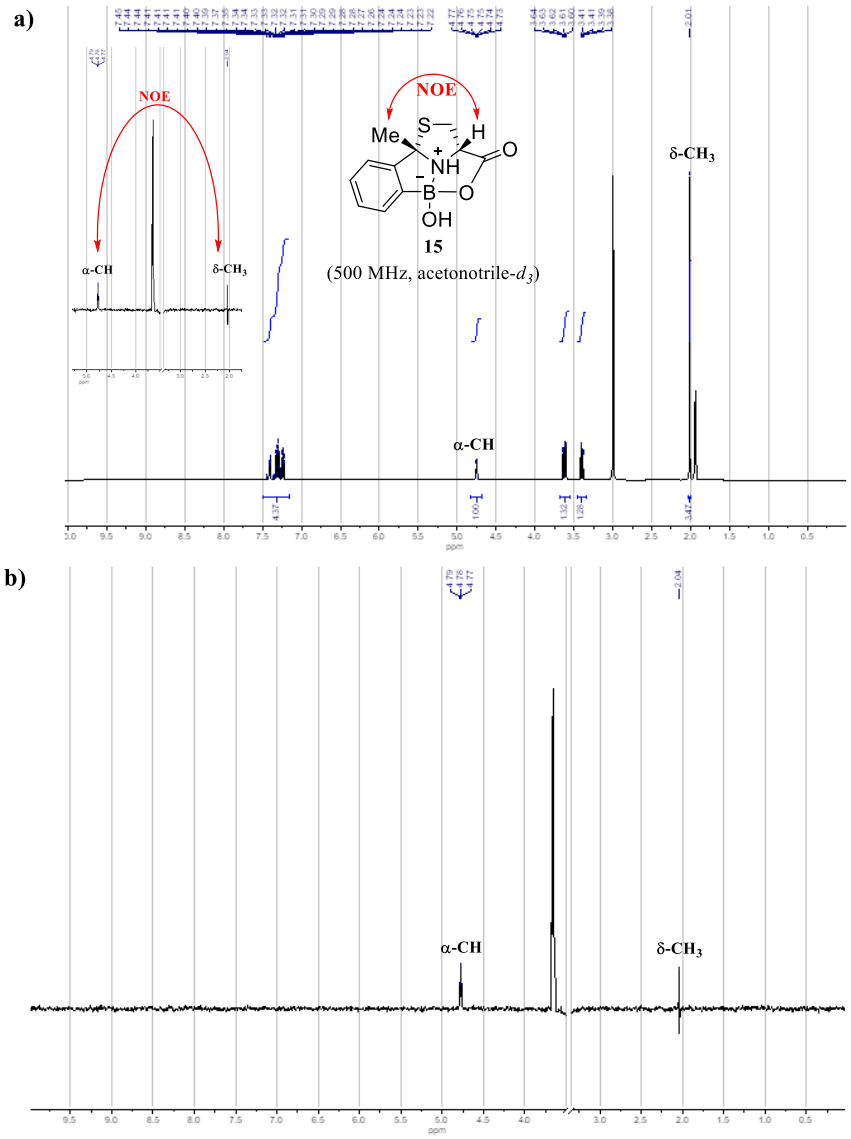

Figure 2.23 a) ^{1}H NMR of the boronate 15; b) NOE spectrum of the boronate 15 showing *α*-C*H* is close to the *δ*-CH_3.

It is evident from the NOE spectrum (Fig 2.23b) that the *δ*-CH_3 protons at δ 2.0 are close to the *α*-CH at δ 4.8 spatially; thus, they must be *cis* to one another which is in line with the proposed mechanisms.

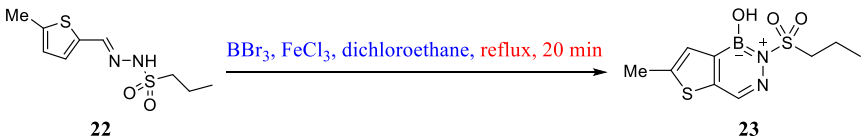

Figure 2.24 Reported synthesis of 6-methyl-2-(propylsulfonyl)thieno[3,2-*d*][1,2,3]diazaborinin-1(2*H*)-ol (23) by Grassberger *et al.*[471]

A literature precedent for the antibacterial properties of sulfonylthienodiazaborines against *E. coli*, *K. pneumoniae* and *N. gonorrhoea*,[470,471] prompted the synthesis of diazaborine **23** for our *in vitro* and *in vivo* screening studies using the method of Grassberger *et al.*[471] (Fig. 2.24), which required extensive optimisation.

Though they did not report how thiophene **22** was prepared, it was accomplished from commercially available *n*-propanesulfonyl chloride in two steps (Scheme 2.2).

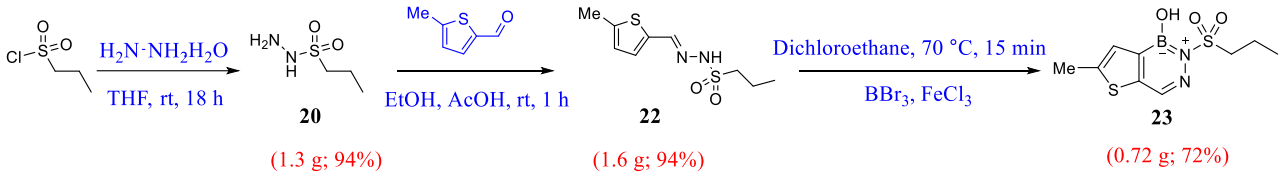

Scheme 2.2 Synthesis of 6-methyl-2-(propylsulfonyl)thieno[3,2-*d*][1,2,3]diazaborinin-1(2*H*)-ol (23) from commercially available *n*-propanesulfonyl chloride.

The last step, namely, the conversion of thiophene **22** to diazaborine **23** required a thorough optimisation. Grassberger *et al.*[471] reported that refluxing thiophene **22** with boron tribromide and ferric chloride (Lewis acid catalyst) in dichloroethane for 20 min (Fig. 2.24) gave the desired diazaborine **23** in 78% yield. However, under the proposed reaction condition by Grassberger, a complete decomposition of diazaborine **23** was observed.

Extensive optimisation borne out that under the proposed conditions the precursor **22** must not be stirred more than 15 min at 70 ºC (Fig 2.25) to give the desired diazaborine **23** in a moderate yield *i.e.* 72%, after flash column chromatography purification, as evidenced by its ^{1}H NMR spectrum (Fig. 2.26).

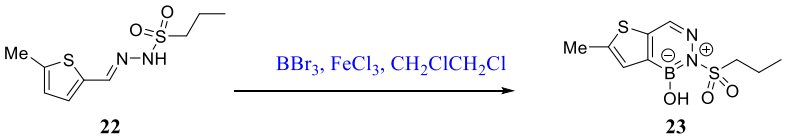

Entry	Catalyst	Temperature (˚C)	Time (min)	22:23:Dec (%)†
1	$FeCl_3$	28	60	100:0:0
2	$FeCl_3$	80	60	0:0:100
3	$FeCl_3$	80	30	0:2:98
4	$FeCl_3$	70	20	0:50:50
5	$FeCl_3$	70	15	5:90:5

Reagents and reaction conditions: **22** (3.7 mmol, 1.0 equiv.), BBr_3 (11 mmol, 3.0 equiv.), $FeCl_3$ (0.37 mmol, 0.10 equiv.), dichloroethane (70 ml). †; **22**: Starting Material; **23**: Desired Product *i.e.* Diazaborine **23**; **Dec**: Decomposed Diazaborine **23**; conversion ratios were determined by LC-MS analysis.

Figure 2.25 Reaction optimisation for synthesis of 6-methyl-2-(propylsulfonyl)thieno[3,2-*d*][1,2,3]diazaborinin-1(2*H*)-ol (23).

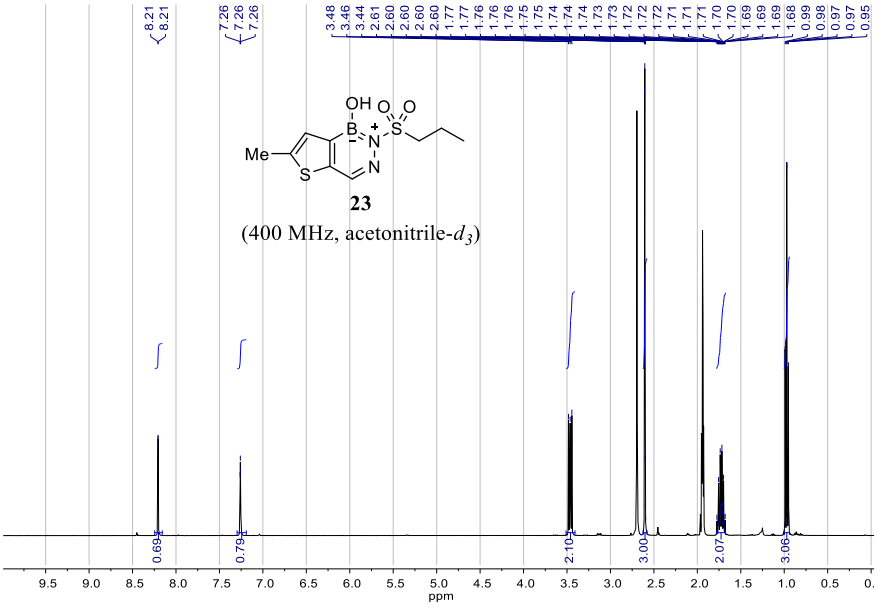

Figure 2.26 ^{1}H NMR spectrum of 6-methyl-2-(propylsulfonyl)thieno[3,2-*d*][1,2,3]diazaborinin-1(2*H*)-ol (23). The signals from *γ*-C*H* and CH_3 resonate at the lowest (8.21 ppm) and highest (0.97 ppm) fields in ^{1}H NMR spectrum of 23; *cf.* Experimental p. S26 for full characterisation.

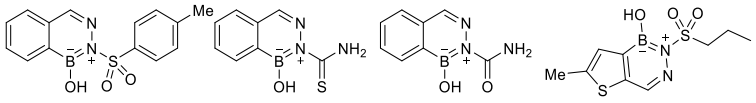

Compounds	MIC H37Rv (µM)
Drg-1	> 80
9	> 80
1	> 80
23	> 80

Figure 2.27 *in vivo* screening results of the selected benzodiazaborines against H37Rv (assays were carried out by GSK, Spain).

Diazaborine **23**, alongside a developmentally-regulated GTP-binding protein 1 (Drg-1) inhibitor (obtained commercially) and two more selected benzodiazaborines from our DCL were screened against H37Rv strain of *M. tuberculosis* by our collaborators (GSK, Spain). Unfortunately, no useful H37Rv inhibitions were observed (Fig. 2.27); however, cell-based assays of these set of compounds have yet to be carried out for other clinically relevant bacterial and fungal pathogens.

Furthermore, a series of 20 compounds obtained from our DCC systems were screened against VIM-1/2, NDM-1 and IMP-1. However, apparently almost all had lower or comparable activity to the positive control MBL inhibitor captopril (Fig. 2.28).

Given that diazaborine **23**,[470] benzodiazaborines **9** and **5**, have all been reported to have antibacterial properties,[472] the *in vivo* studies of this set of compounds merit a full consideration.

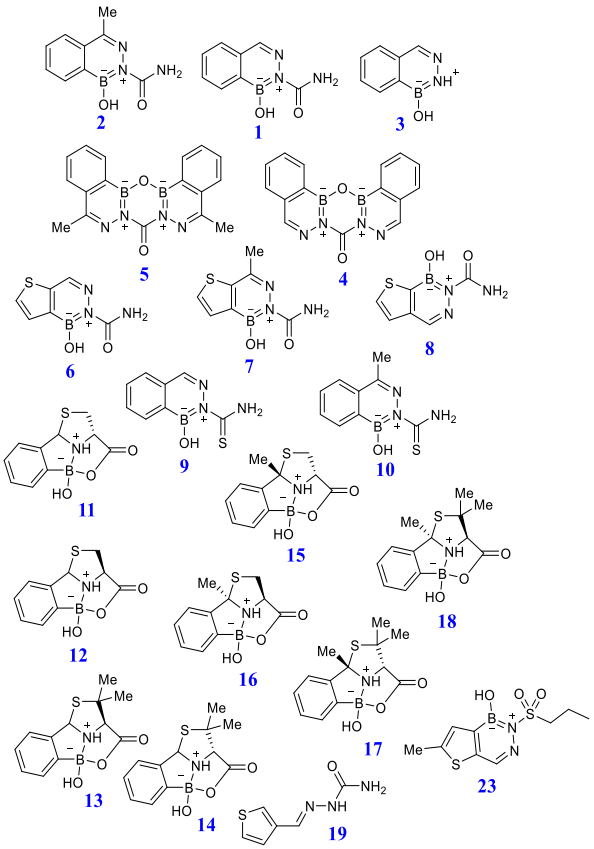

Compound No.	pIC$_{50}$			
	VIM-2	IMP-1	NDM-1	VIM-1
1	< 4.4	< 4.4	< 4.4	< 4.4
2	< 4.4	< 4.4	< 4.4	< 4.4
3	< 4.4	< 4.4	< 4.4	< 4.4
4	< 4.4	5.7	< 4.4	5.2
5	< 4.4	< 4.4	< 4.4	< 4.4
6	< 4.4	< 4.4	4.6	< 4.4
7	< 4.4	< 4.4	< 4.4	< 4.4
8	< 4.4	< 4.4	4.7	< 4.4
9	< 4.4	< 4.4	4.8	< 4.4
10	< 4.4	< 4.4	4.8	< 4.4
11	< 4.4	< 4.4	< 4.4	< 4.4
12	< 4.4	< 4.4	< 4.4	< 4.4
13	< 4.4	< 4.4	< 4.4	< 4.4
14	< 4.4	< 4.4	< 4.4	< 4.4
15	< 4.4	< 4.4	< 4.4	< 4.4
16	< 4.4	< 4.4	< 4.4	< 4.4
17	< 4.4	< 4.4	< 4.4	< 4.4
18	< 4.4	< 4.4	< 4.4	< 4.4
23	< 4.4	< 4.4	4.5	< 4.4
D-Captopril	5.7	5.2	5.0	~ 4.4
L-Captopril	5.5	5.3	4.9	~ 4.4

Figure 2.28 *in vitro* screening results of DCC products against VIM-1/2, IMP-1, and NDM-1.

Of particular interest are the pIC$_{50}$ values of benzodiazaborine **4** against IMP-1 and VIM-1, which were higher than that of the positive control *i.e.* captopril, thus being more potent.

Whilst the structurally related benzodiazaborine **5** showed virtually no activity against IMP-1 and VIM-1, it follows that the extra methyl substituents in benzodiazaborine **5** could bring about some steric clash in the active sites of these MBLs, explaining its low potency relative to that of benzodiazaborine **4** (Fig. 2.29).

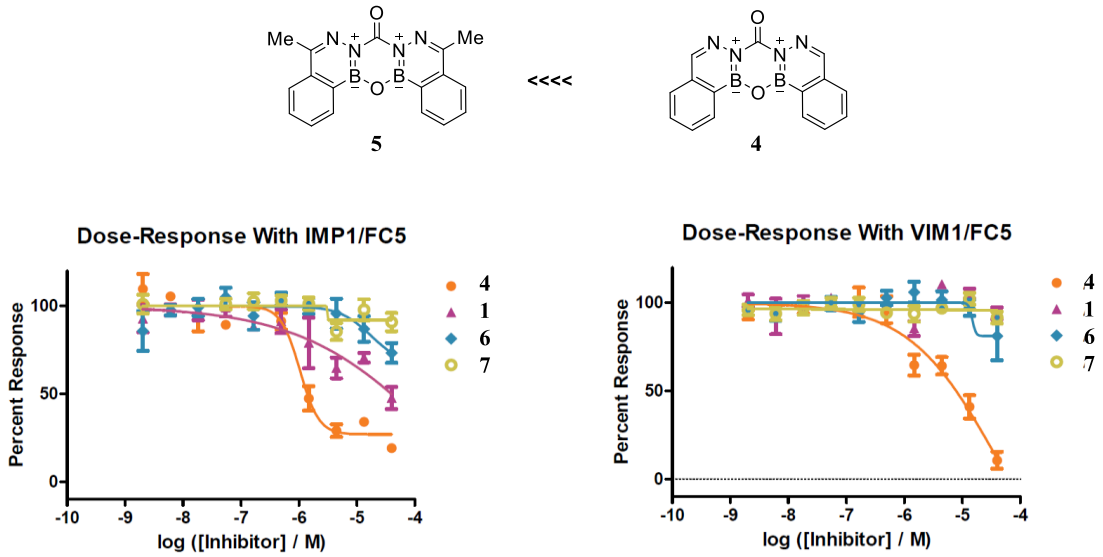

Figure 2.29 IMP-1 and VIM-1 inhibition dose-response curves for the benzodiazaborines 1, 4, 6, and 7.

2.7 Polyfunctional DCC Support Ligands & the Expansion of our DCL

Hitherto when used in a carefully designed protein-directed DCC system, dithiols can yield potent inhibitors. The work described here has shown that other bifunctional ligands can form unprecedented multicyclic structures in a DCC system (Section 2.6).

What would, however, happen if the functional groups on the ligands that took part in the aforementioned DCC systems were doubled? Would they continue to generate dynamic systems which furnish larger unprecedented cyclic structures or is there a limit to cyclic structures useful for DCC?

With that borne in mind, herein this work reports the synthesis of unprecedentedly novel polyfunctional ligands that can take part in DCC systems.

2.7.1 Synthesis of (*R*)-*N*′-(L-cysteinyl)-2-amino-3-mercaptopropanehydrazide

Cysteine readily equilibrates with 2-FPBA to give a tetracycle *e.g.* cyclic boronate ester **12** (Fig. 2.21). Equally, in principle, two cysteine molecules fused through their carboxyl groups could equilibrate with two 2-FPBA molecules to give novel multicyclic structures.

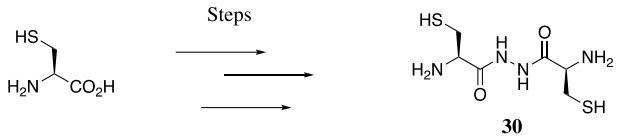

Figure 2.30 Structure of the dicysteinyl hydrazide 30.

In view of the above, the synthesis of dicysteinyl hydrazide **30** (Fig. 2.30) was tackled. Dicysteinyl hydrazide **30** as a '*pseudo-dipeptide*' with more heteroatoms than carbon atoms, could pose a significant synthetic challenge. Retrosynthetic analysis, suggests that the N–N bond of hydrazide ought not to be disconnected as this disconnection requires an '*umpolung*', thus this compound should be easily synthesised from hydrazine and L-cysteine.

However, the existence of many nucleophiles in this molecule compels resorting to protecting group (PG) strategies for a reliable synthesis. Nevertheless, PGs do not necessarily ease the synthetic burden, and in some cases can add to it.

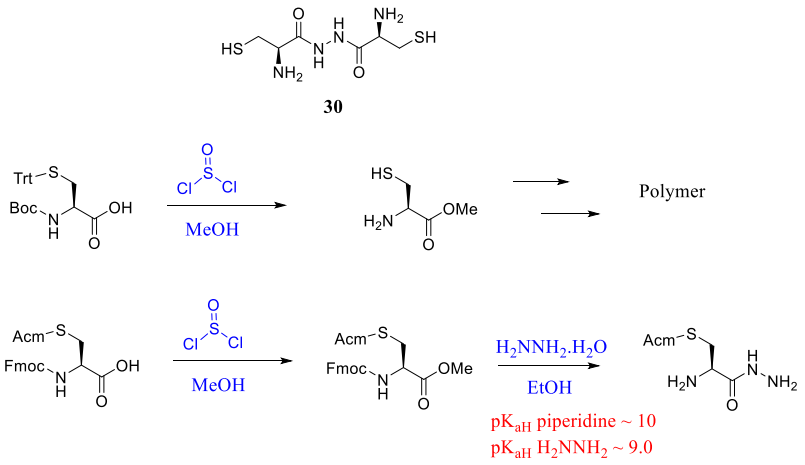

Figure 2.31 Standard peptide PGs are not suitable for the '*ideal*' synthesis of the dicysteinyl hydrazide 30.

Considering that PGs are designed to be introduced and removed easily under mild conditions, the harsh conditions for straightforward addition of hydrazine to two L-cysteine molecules in the '*ideal*' two-step synthesis could only be achieved by waving a magic wand. For example, both Trt and *tert*-butoxycarbonyl (Boc) PGs that are routinely used for protecting cysteine residues in peptides are not compatible with acidic conditions required for esterification of cysteine. On the other hand, hydrazine itself is sufficiently basic to remove fluorenylmethoxycarbonyl (Fmoc) PG that is stable in acidic conditions (Fig. 2.31).

Though quite challenging, the synthesis of dicysteinyl hydrazide **30** should be feasible (Scheme 2.3) *via* a PG strategy entailing many synthetic steps *i.e.* protection and deprotection steps, which makes the synthesis tedious, time consuming, low in atom economy, and more importantly far from '*ideal*'.

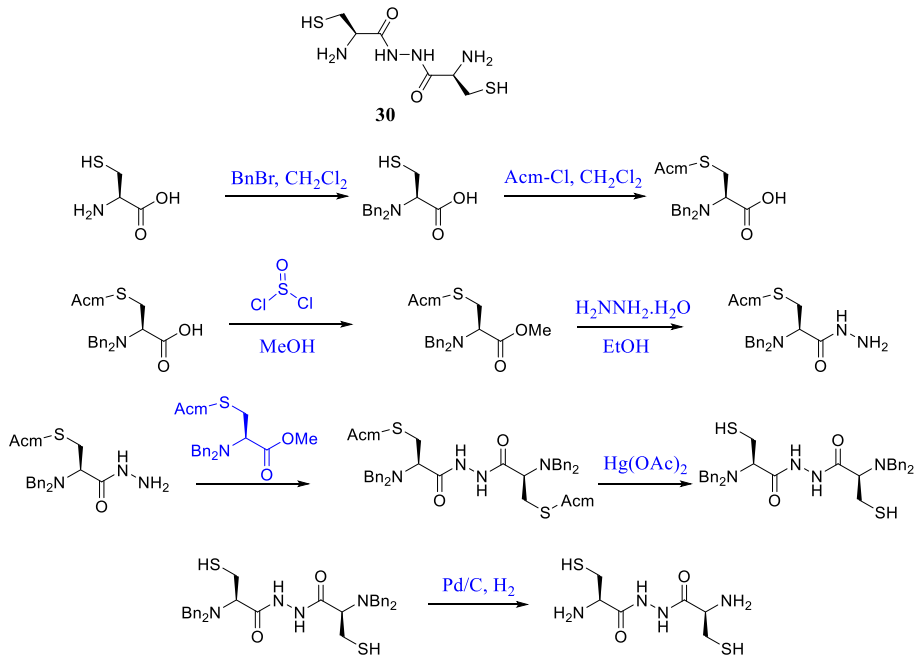

Scheme 2.3 A plausible multistep synthesis of the dicysteinyl hydrazide 30, involving several PG operations.

A closer look at dicysteinyl hydrazide **30** reveals that *α*-amine and *ß*-thiol of L-cysteine are not needed altogether throughout the synthesis, and that they could be capped until the bulk of the molecule has been synthesised. A useful PG for this purpose is 1,3-thiazolidine-4-carboxylic acid (Thz) PG, which is routinely used, in particular, in NCL to orthogonally protect *N*-terminal cysteine residues.[473]

The Thz PG is normally cleaved by phenylhydroxylamine or methoxylamine.[474,475] However, it was discovered that tris(2-carboxyethyl)phosphine hydrochloride (TCEP·HCl) can also efficiently remove this PG. A retrosynthetic analysis using Thz PG delineates a versatile four-step synthesis, as the shortest route to dicysteinyl hydrazide **30** (Scheme 2.4).

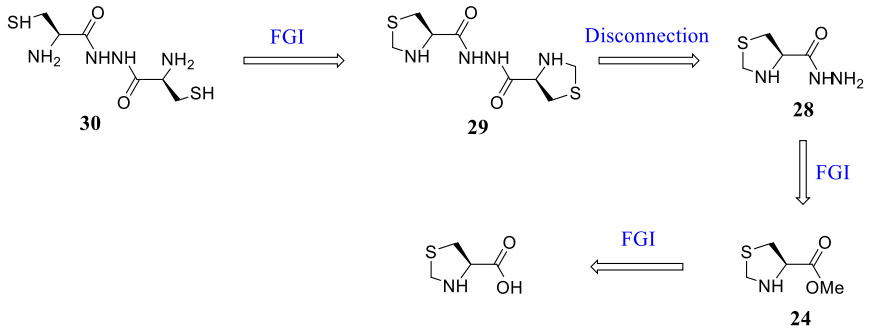

Scheme 2.4 A retrosynthetic analysis for synthesis of dicysteinyl hydrazide 30.

L-Thiaproline methyl ester was easily synthesised in excellent yields *i.e.* 90–95%, from L-cysteine methyl ester and formalin 39% *w/w*. However, conversion of the obtained ester **24** to its corresponding hydrazide **28** required a special treatment.

Firstly, the reaction appears not to proceed at ambient temperatures as reported elsewhere.[476] Moreover, the temperature at which the reaction is spontaneous *i.e.* $\Delta G < 0$, also significantly promotes its decomposition; thus, extensive optimisation was needed (Fig. 2.32).

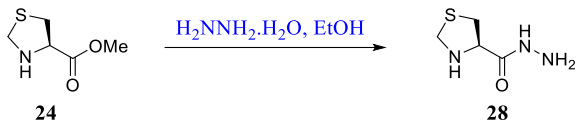

Entry	Hydrazine equiv.	Temperature (˚C)	Time (h)	Yield (%)†
1	10	25	24	0
2	3.0	85	24	0
3	9.0	85	5.0	15
4	9.0	85	6.0	5.0
5	3.0	85	3.0	20
6	1.0	85	3.0	8.0
7	6.0	85	1.3	35
8	6.0	85	1.5	54
9	4.0	85	1.0	54
10	4.0	85	0.67	29
11	9.0	85	0.27	83

Reagents and reaction conditions: **24** (2.0 mmol, 1.0 equiv.), ethanol (2.0 ml). †; Yields would significantly differ, should the reaction scale change. Yields are for the pure hydrazide **28**, after flash column chromatography purification.

Figure 2.32 Reaction optimisation for synthesis of hydrazide 28 from its corresponding ester 24.

With hydrazide **28** in hand, its coupling to L-thiaproline using a coupling agent *e.g.* HATU with a suitable base was studied. Unfortunately, the yields were not high as there are competing pathways for side products. The *α*-amine in hydrazide **28** is nucleophilic and the carbonyl group of the acyl hydrazide moiety withdraws electron density from the nucleophilic hydrazide, thus the success of this synthesis relies, in part, on differences in steric hindrance that these two nucleophiles experience during addition to the activated L-thiaproline ester (Fig. 2.33).

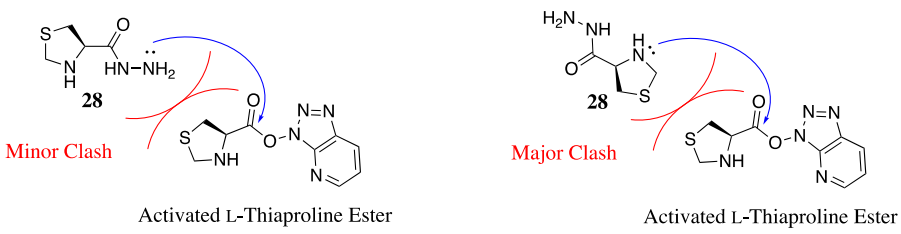

Figure 2.33 As a result of the relatively heightened steric clash for the nucleophilic attack of the *α*-amine relative to that of the hydrazide, more of the desired product will be formed.

Although such couplings are routinely carried out in DMF and an organic base *e.g.* Hünig's base by peptide chemists, those reactions are on a resin, thus DMF and organic bases can be easily removed; however, our reactions were in solution and from the synthetic chemist perspective, they are best to be avoided.

As a result, it was found that acetonitrile and potassium carbonate would be suitable substitutes for this purpose to furnish hydrazide **29** in a moderate yield *e.g.* 61%. In fact, the standard peptide reagents *i.e.* DMF and Hünig's base did not yield hydrazide **29**, possibly due to the difficulties in purification of the crude product (Scheme 2.5).

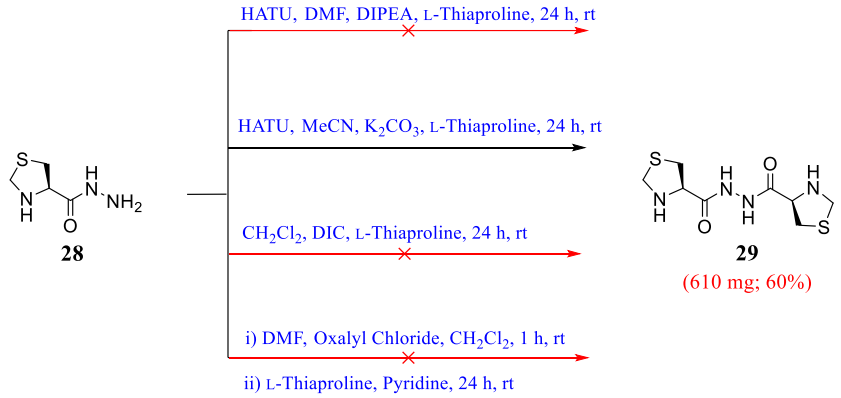

Scheme 2.5 Several attempted synthetic routes for synthesis of the hydrazide 29. In all cases 1.0 molar equiv. of both the hydrazide 28 and L-thiaproline was used.

Having successfully synthesised hydrazide **29**, the final step, namely, the removal of Thz PG (Scheme 2.6), was achieved *via* TCEP·HCl in water at 85 ºC in fair yields *i.e.* 30–35%. As low as 0.50 molar equiv. of TCEP·HCl with respect to hydrazide **29** *i.e.* the limiting reagent was sufficient to achieve this deprotection.

On the other hand, under the same reaction conditions **10 molar** equiv**.** of methoxylamine hydrochloride was needed to achieve similar results, which highlights the superiority TCEP·HCl for this reaction.

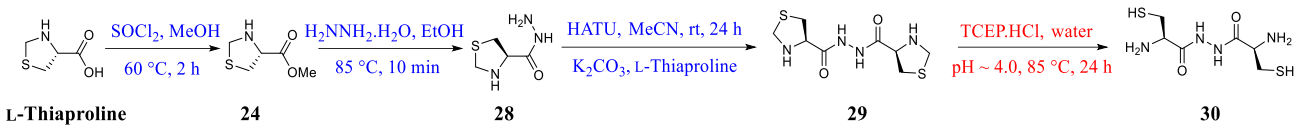

Scheme 2.6 A versatile four-step total chemical synthesis of (*R*)-*N′*-(L-cysteinyl)-2-amino-3-mercaptopropanehydrazide (30) from commercially available L-thiaproline, showcasing the removal of Thz PG by TCEP·HCl *i.e.* a new reaction.

Finally, a DCC system containing hydrazide **30** and 2-FPBA in 0.10 M PBS buffer was attempted. However, upon mixing 1.0 molar equiv. of hydrazide **30** with 2.0 molar equiv. of 2-FPBA in 0.10 M PBS buffer (pH ~ 7.4) a rapid precipitate was formed, which remained insoluble in most organic solvents (acetonitrile, methanol, DMF, DMSO *etc.*), even with prolonged sonication at elevated temperatures.

As a result, it was not feasible to analyse the obtained solid, and also since it was a very fine powder, its structure could not be resolved by X-ray crystallography.

2.7.2 Synthesis of 2-amino-*N′*-homocysteinyl-4-mercaptobutanehydrazide

In the face of the failure to establish a true DCC system for our novel polyfunctional ligand *i.e.* dicysteinyl hydrazide **30** with 2-FPBA, the synthesis of its sister dihomocysteinyl hydrazide **36** was considered.

Clearly the very rigid and thermodynamically stable multicyclic structures, if any, from the reaction of hydrazide **30** and 2-FPBA, could be a result of anisoenergetic equilibration (Section 2.4.2.3), hence hampering the DCC system. However, as discussed previously (Section 2.6) very small structural changes can have significant effects on the dynamics of a DCC system; as a result, it was envisaged that hydrazide **36** with extra methylenes relative to hydrazide **30**, would be more flexible and form six-membered cyclic structures *in lieu* of the five-membered rings of its sister hydrazide **30**, and hence generating somewhat less anisoenergetic DCL components.

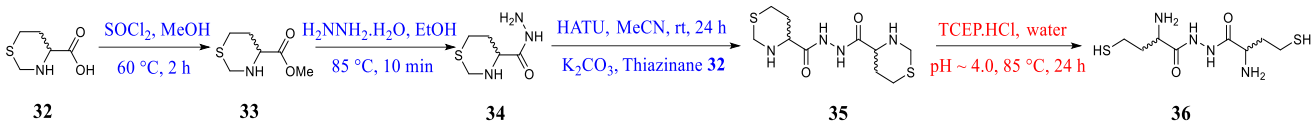

Scheme 2.7 A plausible four-step synthesis for 2-amino-*N′*-homocysteinyl-4-mercaptobutanehydrazide (36).

The structural similarity between hydrazide **30** and **36**, implies that they could potentially be synthesised *via* the same synthetic route (Scheme 2.7). Though, this might be feasible in theory; however, practical aspects of total chemical synthesis such as cost, render repeating the same synthetic route to hydrazide **30** for hydrazide **36** unviable.

Whereas 100 g of L-thiaproline typically costs around £40,[477] 30 mg of L-thiazinane **32** costs £45.[478] In other words, L-thiazinane **32** is typically 3750 times *w/w* more expensive *i.e.* 100 g of L-thiazinane **32** would cost £150,000.00, than L-thiaproline. A cheaper alternative was desired to enable affordable synthesis of hydrazide **36**. On the other hand, conversion of L-homocysteine to L-thiazinane **32** is also costly, as 10 mg of L-homocysteine costs ~ £35.[479] Therefore, the best commercially available starting material for this purpose ought to be D/L-homocysteine thiolactone hydrochloride (HCTL·HCl), a 100 g of which costs as little as £30.[480]

HCTL·HCl features a *γ*-thiolactone ring, which can be opened with a nucleophile such as methoxide to give homocysteine methyl ester, the obtained ester can be converted to the desired thiazinane ester **33** in formalin 39% *w/w* (Scheme 2.8).

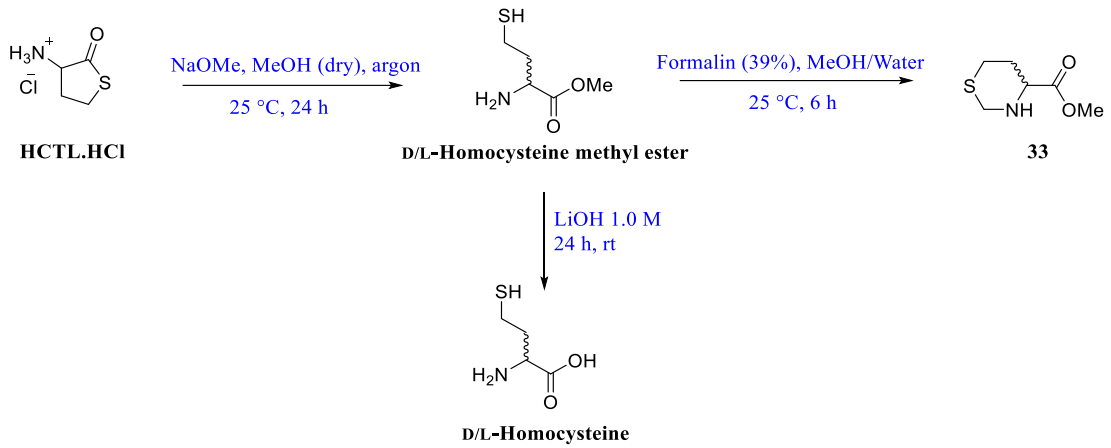

Scheme 2.8 Attempted synthesis of thiazinane methyl ester 33 from commercially available HCTL·HCl.

Kolenbrander[481] reported synthesis of homocysteine and methionine derivatives *via* a reductive ring opening of HCTL·HCl using dissolved sodium metal in methanol.[481] However, since sodium methoxide in methanol was deemed safer than dissolving pyrophoric sodium metal in methanol, the ring opening of HCTL·HCl with sodium methoxide salt in methanol was attempted so as to first synthesise homocysteine methyl ester *in situ* and then convert the obtained ester to thiazinane methyl ester **33** in formalin 39% *w/w* (Scheme 2.8).

It is noteworthy that Kolenbrander did not isolate the generated homocysteine methyl ester (possibly due to the difficulties in its purification); instead converting the homocysteine methyl ester to various homocysteine ester derivatives *in situ* by modification of the thiol side chain, and then hydrolysis of the modified esters with sodium hydroxide yielded homocysteine and methionine derivatives, which were later isolated and purified.

Thus far, attempts at synthesis of thiazinane methyl ester **33** *via* the above procedures have been unsuccessful. Although, a seemingly clean product was observed by LC-MS, the NMR spectrum of the isolated product was a mixture of several compounds (Fig. 2.34).

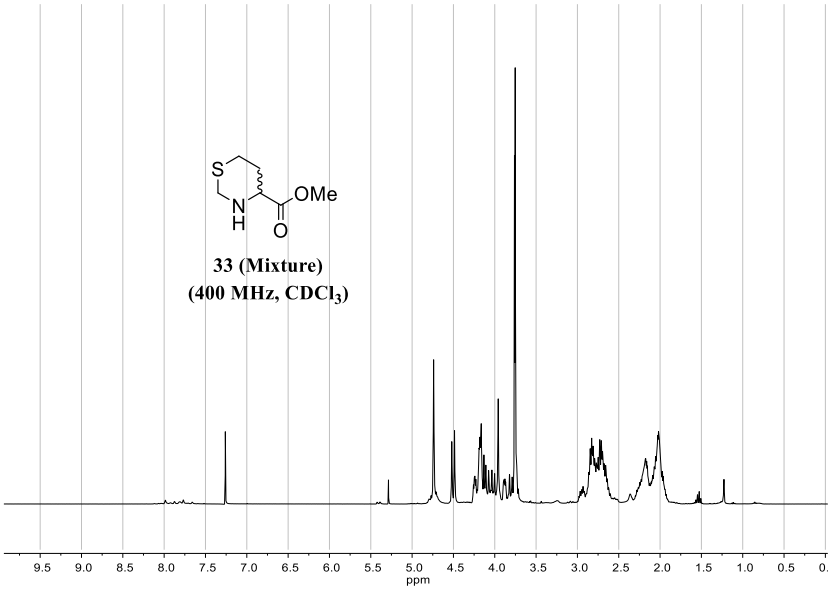

Figure 2.34 ^{1}H NMR spectrum of thiazinane ester 33 alongside by-products of the ring opening of HCTL·HCl by sodium methoxide in methanol.

One of the main hurdles in this synthesis is gel formation and aggregation of the reaction mixture.

As depicted in Fig. 2.35, less than one molar equiv. of sodium methoxide with respect to HCTL·HCl gives no product; consequently, the reaction mixture remains clear throughout the reaction.

On the other hand, one or more than one molar equiv. of sodium methoxide results in spontaneous precipitation.

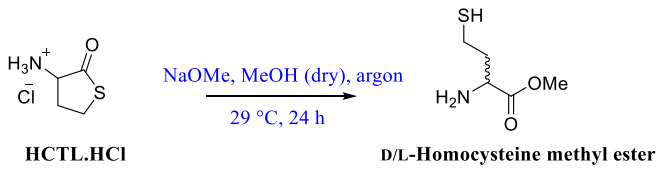

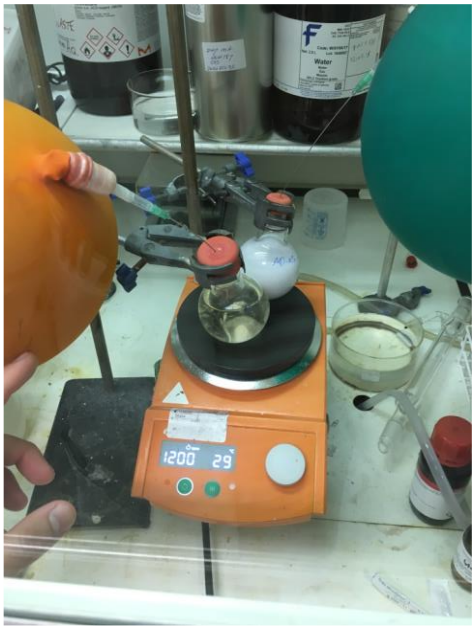

Figure 2.35 Gel formation and aggregation during ring opening of HCTL·HCl by sodium methoxide in methanol. The clear pale-yellow reaction mixture contains only 0.9 equiv. of sodium methoxide with respect to HCTL·HCl; the cloudy white reaction mixture contains 1.5 equiv. of sodium methoxide.

The observed gel formation and aggregation can be explained by nucleophilic addition of the *α*-amine of generated homocysteine methyl ester to the carbonyl group in another homocysteine methyl ester, this amide adduct can dimerise to give a diketopiperazine or add to another homocysteine methyl ester to give a trimer, which could in turn either cyclise or add to another ester and so forth (Fig. 2.36).

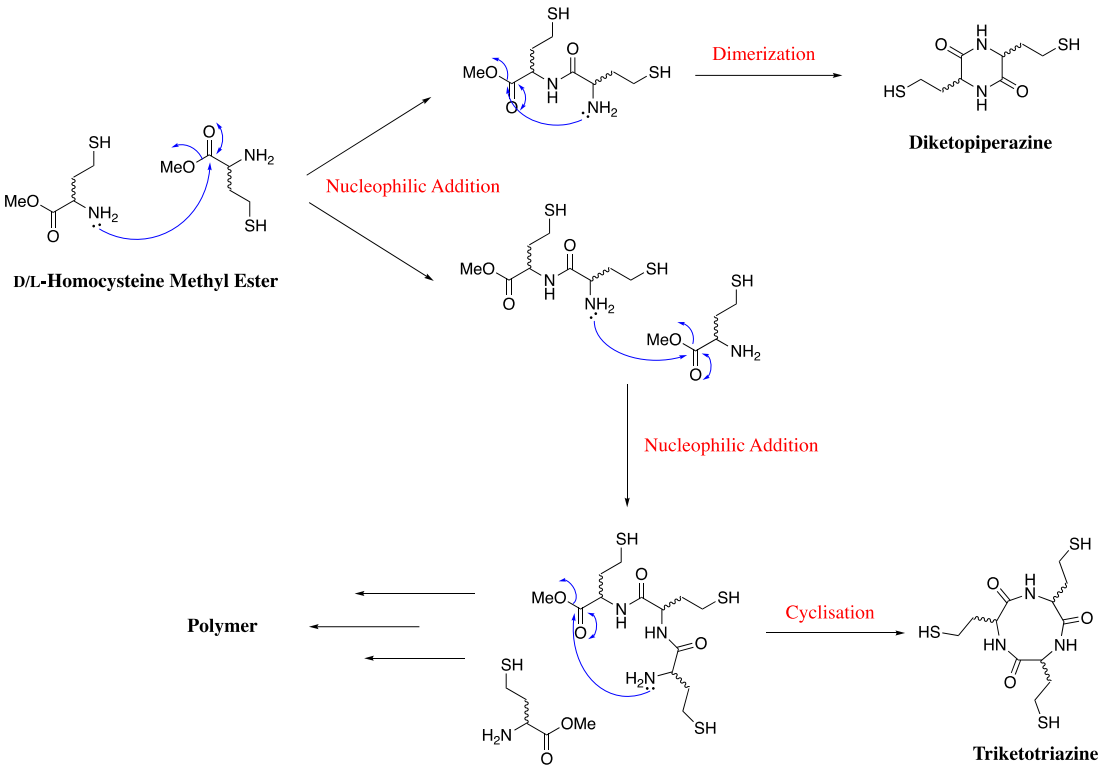

Figure 2.36 A series of possible dimers, trimers and polymers, following ring opening of HCTL·HCl with sodium methoxide in methanol.

In view of the irksome purification, and since Kolenbrander himself never isolated the *in situ* generated homocysteine methyl ester, the obtained ester was saponified *in situ* using lithium hydroxide. The thus obtained mixture was reacted with formalin (39% *w/w*) to give thiazinane **32** in acceptable yields *i.e.* 23–25%, after preparative RP-HPLC purification, as evidenced by its ^{1}H NMR spectrum (Fig. 2.37). Moreover, it was also feasible to isolate D/L-homocysteine in an excellent yield *i.e.* 97% from HCTL·HCl, after preparative RP-HPLC purification.

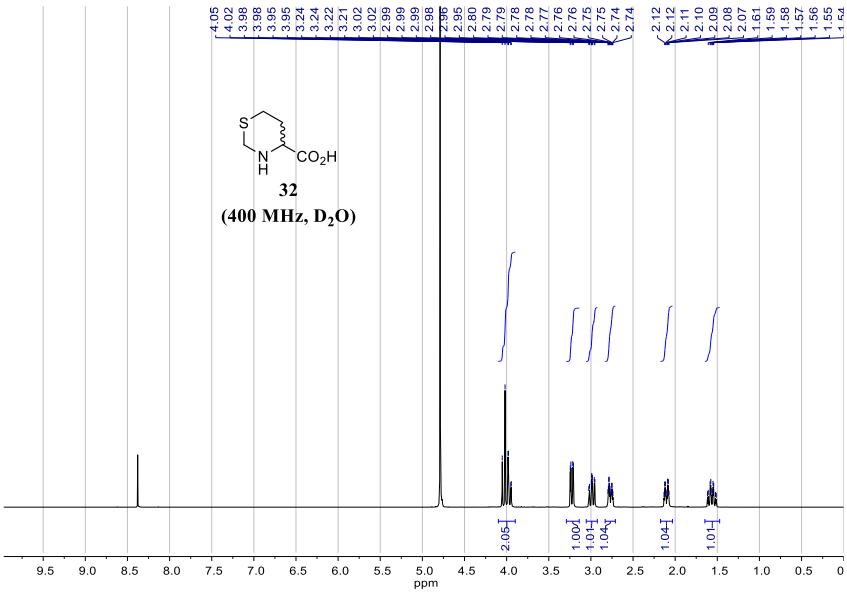

Figure 2.37 ^{1}H NMR spectrum of pure thiazinane 32. The AB quartet of γ-CH_2 at δ 2.99 & 2.77 is significantly perturbed by coupling to the neighbouring protons; for full characterisation and *J* values in Hz *cf.* Experimental p. S35.

It later became apparent that *in situ* conversion of thiazinane **32** to its corresponding methyl ester **33** in thionyl chloride would be much more fruitful than sequential isolation and conversion of thiazinane **32**; as a result, a one-pot synthesis of thiazinane methyl ester **33** from HCTL·HCl was devised to furnish the desired ester **33** in excellent yields (78% overall), giving a very clean product with minimal purification efforts.

In other words, whilst thiazinane **32** requires preparative RP-HPLC purification, which is very time consuming and resource intensive, a quick and easy flash column chromatography purification is all needed for a highly pure thiazinane methyl ester **33**, as evidenced by its ^{1}H NMR spectrum (Fig. 2.38).

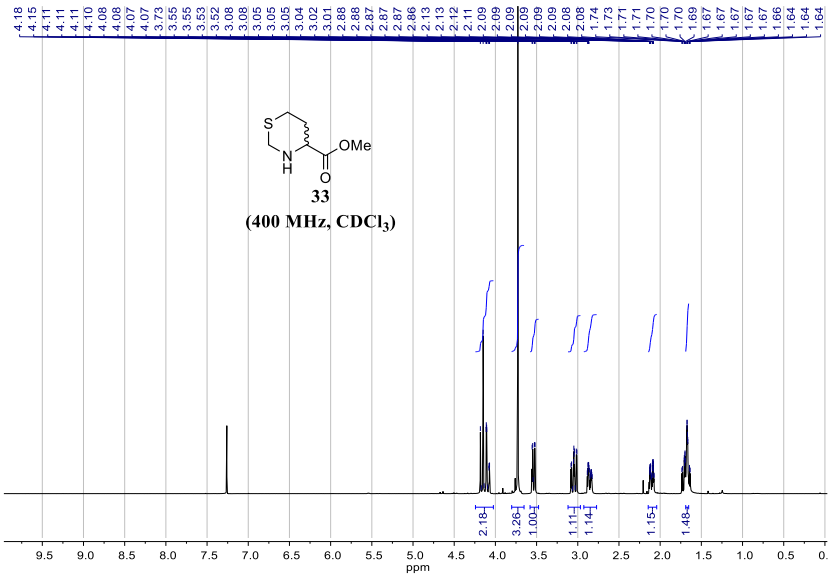

Figure 2.38 ^{1}H NMR spectrum of pure thiazinane methyl ester 33. The distinctive –OMe singlet of ester 33 resonates at δ 3.73; for full characterisation and *J* values in Hz *cf.* Experimental p. S36.

The next hurdle, namely, synthesis of hydrazide **34** from thiazinane methyl ester **33**, also proved challenging. Whereas, hydrazide **28** is tolerant of high hydrazine concentrations such that the nucleophilic substitution could take place as quickly as possible, so as to avoid the decomposition of the desired hydrazide **28** to its corresponding acid; hydrazide **34**, is not.

Strictly speaking, not only the temperatures at which the reaction is spontaneous *i.e.* $\Delta G < 0$ significantly promote its decomposition, but also high concentrations of hydrazine which previously used to drive the reaction towards completion and avoid the decomposition process, is detrimental to the desired hydrazide **34**. To this end, it was found that the least amount of hydrazine for the reaction to proceed with minimal decomposition, would be two molar equiv. of hydrazine hydrate with respect to thiazinane ester **33** *i.e.* the limiting reagent.

With hydrazide **34** in hand, its coupling to thiazinane **32** using a coupling agent *e.g.* HATU in acetonitrile and potassium carbonate was attempted.

This turned out to be the least troublesome step in this total chemical synthesis of hydrazide **36** from HCTL·HCl (Scheme 2.9). As a result, the desired hydrazide **35** was obtained in a moderate yield *i.e.* 56%; however, the same competing side reactions for synthesis of hydrazide **29** (Fig. 2.33) are also applicable to this synthesis, resulting in the observed relatively low yields.

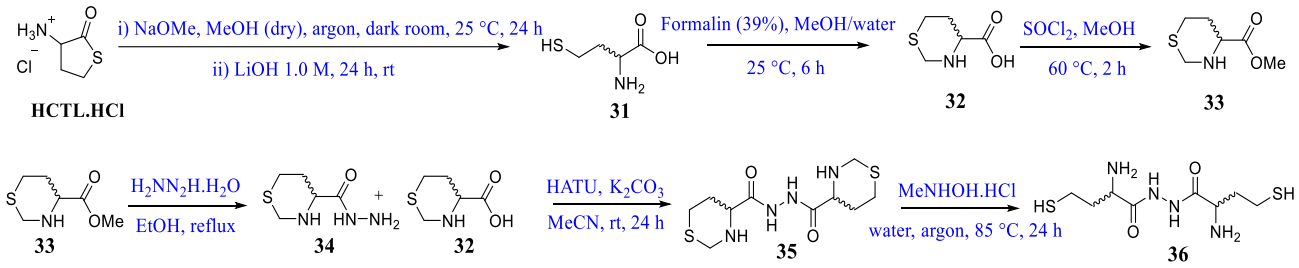

Scheme 2.9 A six-step synthesis of 2-amino-*N'*-homocysteinyl-4-mercaptobutanehydrazide (36) from commercially available HCTL·HCl.

The global deprotection step for conversion of hydrazide **35** to dihomocysteinyl hydrazide **36** can be achieved quite efficiently using the new deprotection method, *i.e.* TCEP·HCl; however, inasmuch as both dihomocysteinyl hydrazide **36** and TCEP have similar molar masses and polarities, it was not feasible to purify the crude material even when preparative RP-HPLC was recruited.

Dihomocysteinyl hydrazide **36** is extremely polar and readily elutes with water; moreover, it sticks to silica and flash column chromatography is also incapable of purifying this peculiar compound. Nevertheless, the new deprotection method in combination with SPS (Section 2.1) should be able to furnish highly pure dihomocysteinyl hydrazide **36** in excellent yields, as the excess TCEP·HCl can be removed with washing and filtration prior to cleavage of dihomocysteinyl hydrazide **36**, if any, from the resin (Fig. 2.39).

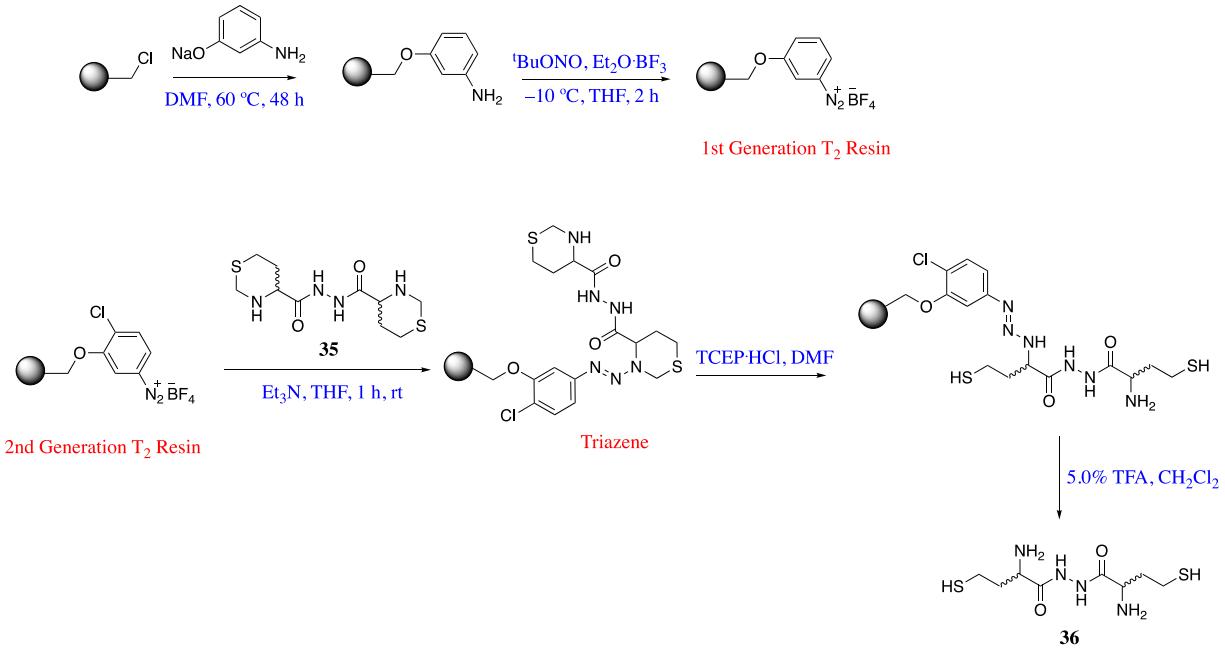

Figure 2.39 Circumventing purification difficulties by attaching hydrazide 35 to a solid support.

One of the most versatile solid supports for synthesis of cyclic amines on a resin is the T_2 diazonium resin, which was first introduced by Bräse *et al.*[482] in 1999. The first-generation resins were quite unstable and had to be stored at –10 ºC or used immediately once they were generated. However, Bräse and Dahmen were able to modify the resin by adding a chlorine substituent para to the diazonium salt, which made the resin stable at ambient temperatures (Fig. 2.39).[483] Ever since several variants of T_2 type resins have been developed, and have proved useful in SPS.[484]

Much to our delight, methoxylamine was able to remove the methylene bridge between the α-amine and γ-thiol in hydrazide **35** to furnish dihomocysteinyl hydrazide **36** in acceptable yields *i.e.* 25–27%, after preparative RP-HPLC purification as evidenced by its ^{1}H NMR spectrum (Fig. 2.40).

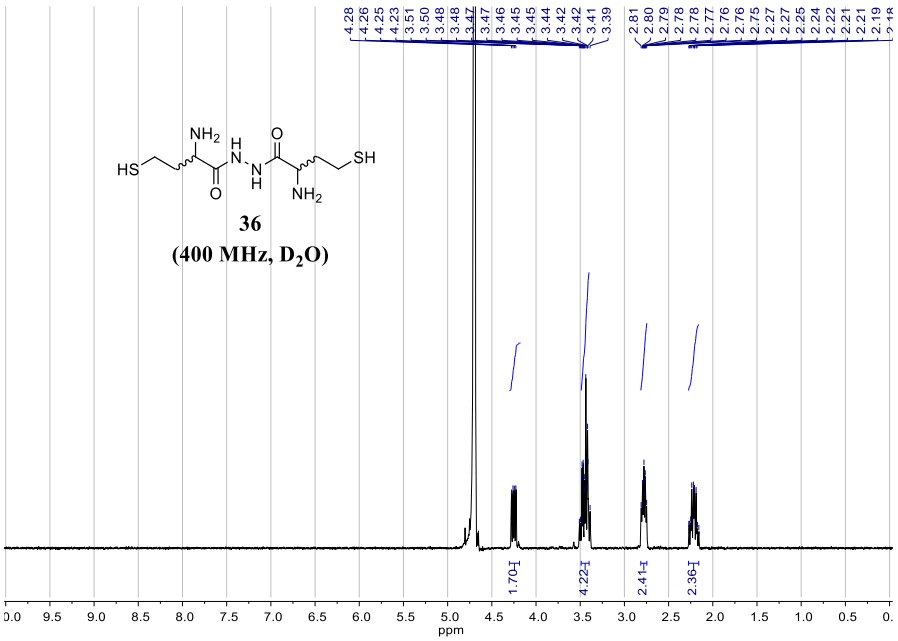

Figure 2.40 ^{1}H NMR spectrum of 2-amino-*N'*-homocysteinyl-4-mercaptobutanehydrazide (36); *puriss.* >99%. The AB quartet of *β*-C*H*$_2$ at δ 2.78 & 2.22 is almost indiscernible by coupling to the neighbouring protons in ^{1}H NMR spectrum of this novel four-carbon chain symmetrical dimer; for full characterisation and *J* values in Hz *cf.* Experimental p. S39.

2.8 Dynamic Combinatorial Chemistry of Polyfunctional Ligands

Inasmuch as, the first attempt at establishing a DCC system with our very first polyfunctional ligand *i.e.* dicysteinyl hydrazide **30** was not promising, it was conceivable that a slightly simpler system could establish a better DCC system. Thus, an electrophile with only one electrophilic centre *in lieu* of the previous dielectrophilic 2-FPBA would form better isoenergetic DCL components.

Formaldehyde was considered a good candidate for this purpose as it is singly electrophilic and highly reactive. This together with extra attempts at DCC systems of 2-FPBA with our novel polyfunctional ligands were explored.

2.8.1 Dynamic Combinatorial Chemistry of Polyfunctional Ligands with 2-FPBA

The first unsuccessful attempt at establishing a DCC system for dicysteinyl hydrazide **30** with 2-FPBA (Section 2.7.1), clearly illustrates that such systems, though by no means all, are not true DCC systems. As such, the DCL components are not isoenergetic and equilibration is biased by virtue of rapid precipitation.

In recognition of the above, a second attempt at the DCC of dicysteinyl hydrazide **30** with 2-FPBA was endeavoured; this time using time course NMR in order to observe the intrinsic features of this DCC system. A solution of dicysteinyl hydrazide **30** (8.0 μmol) dissolved in D_2O (0.50 ml) was locked on D_2O, tuned and shimmed as internal standard using a Bruker AVIII 700 equipped with a TCI H/C/N helium CryoProbe, and its ^1H NMR spectrum was recorded. 2-FPBA (3.0 equiv.) dissolved in D_2O (0.20 ml) was added to the same NMR tube containing dicysteinyl hydrazide **30**. The thus obtained clear solution was shaken for 1–2 sec, and its ^1H NMR spectrum was recorded immediately and every 30 sec thereafter, without further tuning and shimming of the probe.

As depicted in Fig. 2.41, several new peaks appeared upon mixing dicysteinyl hydrazide **30** with 2-FPBA; however, despite due diligence and the fact that the time lag between mixing the reagents and recording the initial spectrum *i.e.* t_0, was less than 10 sec, there appeared to be no significant changes in the system over the time that the mixture was monitored *i.e.* 30 min, and the solid precipitates were clearly visible at the outset. Attempts to isolate the DCL component of the mixture after filtration of the solid residues were futile, and only a negligible amount of the unreacted 2-FPBA was recovered.

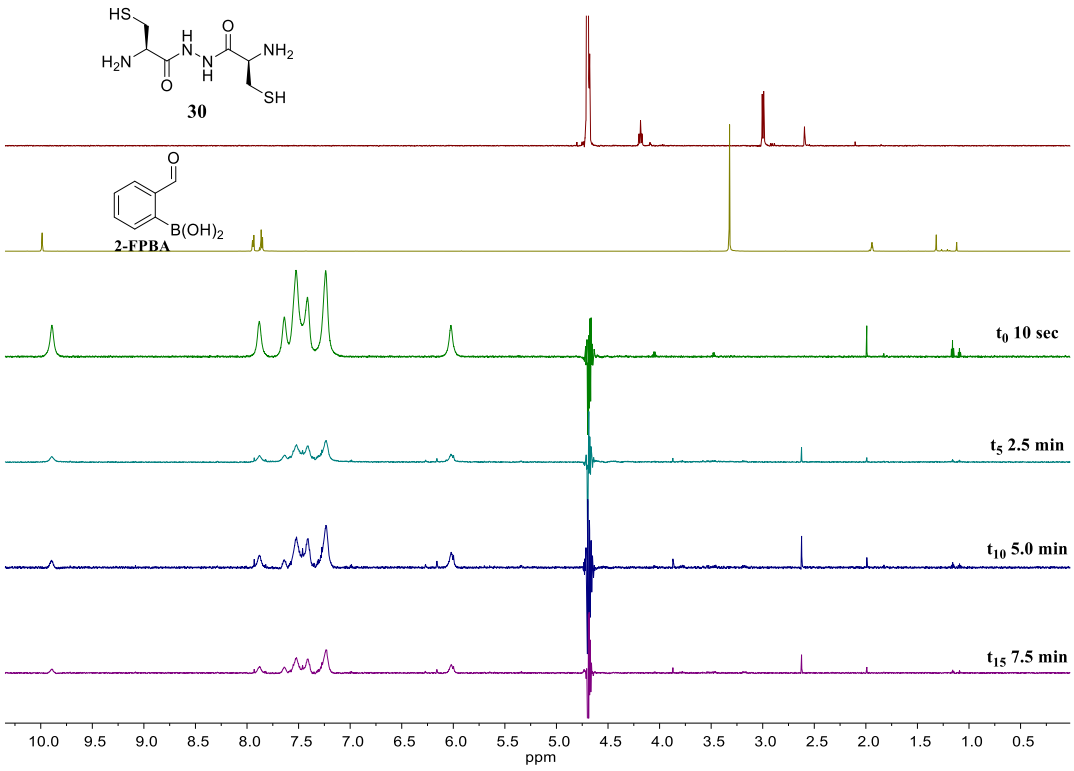

Figure 2.41 Time course ^{1}H NMR of DCC of the hydrazide 30 with 2-FPBA in D_2O; recorded on a Bruker AVIII 700 equipped with a TCI H/C/N helium CryoProbe at 700 MHz (298 K). The ^{1}H NMR spectrum of the DCC system remained intact at the very beginning (later runs not shown).

In light of the above disappointing results, we were inclined to attempt the DCC of dihomocysteinyl hydrazide **36** with 2-FPBA. A similar setup was arranged, and the aforementioned DCC system was monitored by time course ^{1}H NMR. To our delight, no precipitation was observed and the mixture remained clear throughout the experiment. However, it was not feasible to isolate the most stable DCL component, if any, and only a negligible amount of the unreacted 2-FPBA was recovered. The outcome was not so much discouraging; in point of fact, it seems as if the tortuous synthesis of dihomocysteinyl **36** in the end paid off by virtue of the following:

- No obvious precipitation.
- The ^{1}H NMR of the equilibrated DCC system clearly indicates the existence of several species (Fig. 2.42).
- The DCL components seem to be isoenergetic and equilibrate reversibly.

The kinetics of this DCC system is very fast and the initial changes in the system were not on a reasonable timescale to be observable by time course NMR at 298 K.

And also, we were unable to isolate and characterise the generated DCL components; however, this implies that templating this DCC system with a metal or protein template, could stabilise its most stable component(s) such that they could be isolated and characterised.

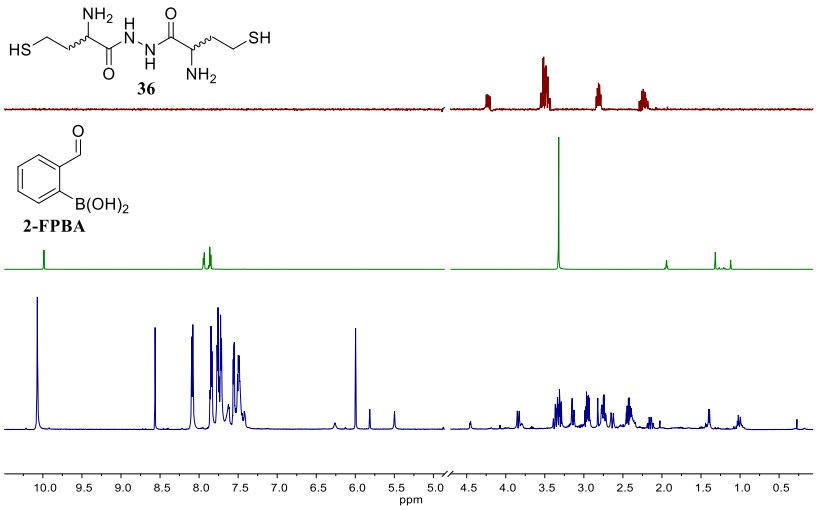

Figure 2.42 ^{1}H NMR spectra of dihomocysteinyl hydrazide 36 (red), 2-FPBA (green) and their DCC system (dark blue) in D_2O; recorded on a Bruker AVIII 700 equipped with a TCI H/C/N helium CryoProbe at 700 MHz (298 K).

2.8.2 Dynamic Combinatorial Chemistry of Polyfunctional Ligands with Formaldehyde

In this series of the DCC adventure, attention was turned to formaldehyde so as to make DCC systems of our novel polyfunctional ligands slightly less complex, and also learn a bit more about the utility of these novel ligands in DCC systems.

In light of the time-resolved NMR of the DCC of dicysteinyl hydrazide **30** with 2-FPBA, it was clearly palpable that by the same token, equilibration in DCC of our polyfunctional ligands with formaldehyde would not be a slow process.

As for the DCC of dicysteinyl hydrazide **30** with 2-FPBA, a solution of dicysteinyl hydrazide **30** (10 µmol) dissolved in D_2O (0.50 ml) was locked on D_2O, tuned and shimmed as internal standard using a Bruker AVIII 700 equipped with a TCI H/C/N helium CryoProbe, and its ^1H NMR spectrum was recorded. Paraformaldehyde (10 equiv.) cracked in D_2O (0.20 ml) was added to the same NMR tube containing dicysteinyl hydrazide **30**. Taking into account the rapid equilibration of this DCC system, the ^1H NMR spectrum of the thus obtained clear solution upon mixing was recorded immediately and every 10 sec thereafter for 5.0 min, without further tuning and shimming of the probe.

The mixture remained clear throughout the experiment and the kinetics of equilibration, though extremely fast, appeared to be on a reasonable timescale, as evidenced by time-resolved ^1H NMR (Fig. 2.43).

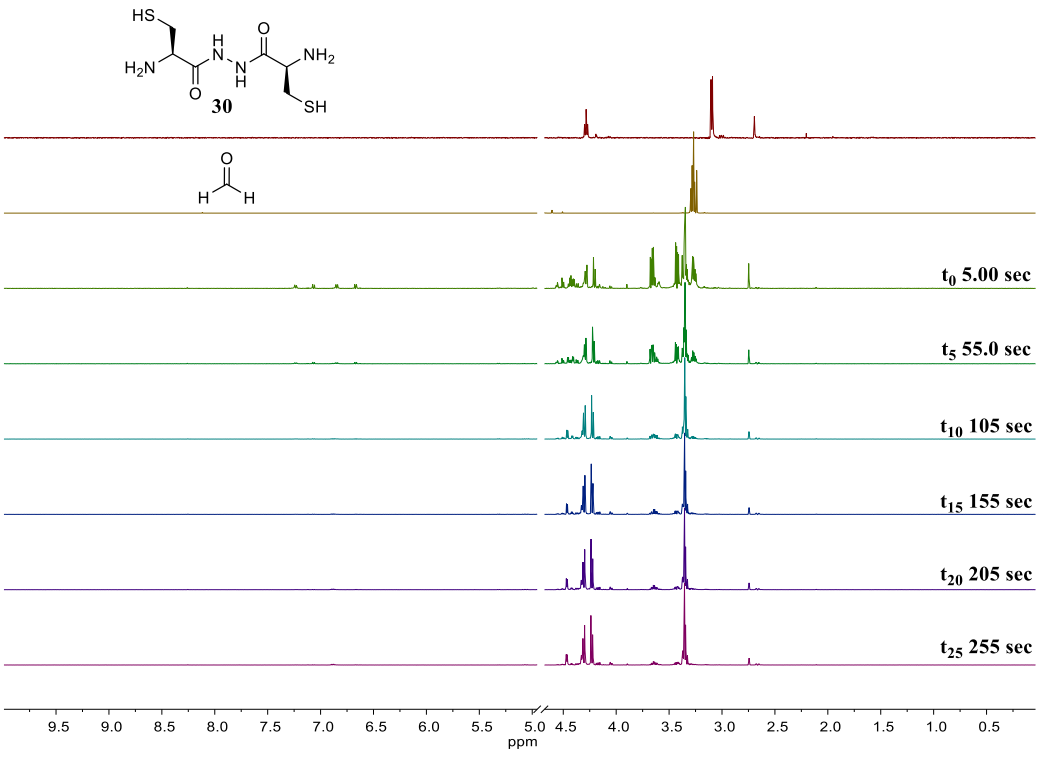

Figure 2.43 Time course ^1H NMR of DCC of System A in D_2O; recorded on a Bruker AVIII 700 equipped with a TCI H/C/N helium CryoProbe at 700 MHz (298 K). No significant changes to the ^1H NMR spectrum of the system after 2.0 min from the start of the reaction *i.e.* t_0 observed.

As depicted in Fig. 2.43, several new peaks appeared upon mixing dicysteinyl hydrazide **30** with formaldehyde (System **A**). The most noticeable changes were for the triplet and doublet of dicysteinyl hydrazide **30** at δ 4.27 and 3.09 respectively, which disappeared altogether spontaneously.

The peaks at *ca.* δ 7.14 to 6.57, with the exception of the peak at δ 6.75, also gradually disappeared during the equilibration.

Intriguingly, the peaks at δ 4.21 and 4.13 were increased in size; on the other hand, the peaks at δ 3.56 and 3.33 were decreased in size during the equilibration. The areas under the aforementioned peaks were compared to that of the peaks from dicysteinyl hydrazide **30**, as the standard, and used to calculate trends in concentrations of the DCL components (Fig. 2.44). However, this estimate is, by no means, accurate as there are several overlapping peaks, which cannot be assigned to different DCL components of this DCC system.

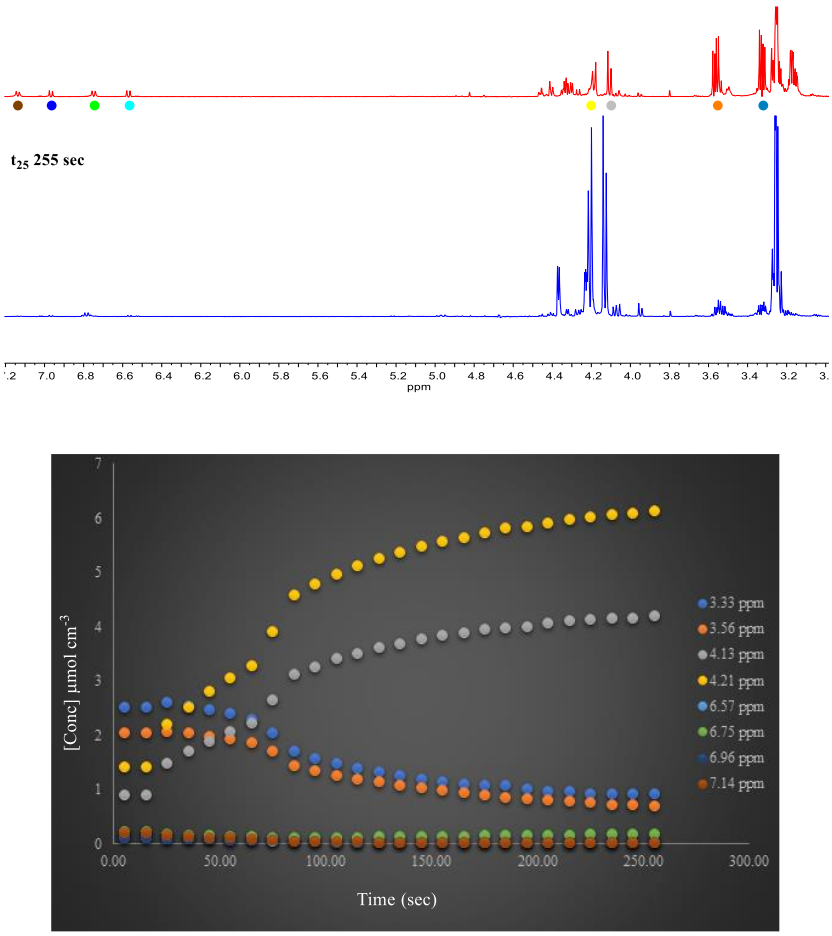

Figure 2.44 Changes in concentrations of the DCL components of System A: the peaks with most significant changes are colour coded. ^{1}H NMR spectrum of the DCL at t_0 (red), stacked over ^{1}H NMR spectrum of the DCL at t_{25} (blue) for comparison.

Unfortunately, it was not feasible to isolate any product from this DCC system, presumably due to the scale of the reaction. As a result, the same DCC system was repeated on a 50 µmol scale, and the system was monitored by LC-MS for 48 h. As for the previous attempt, no obvious precipitation was observed, even when the reaction scale was increased.

Aliquots of the mixture were periodically collected and analysed by LC-MS (2.0 – 98.0% formic acid (0.01% *v/v*) in acetonitrile/ formic acid (0.01% *v/v*) in water over 5.0 min, 1.5 ml min^{-1}, 40 °C). Initially more than 20 peaks were observed during elution with the predominant peak eluting at 4.5 min, which corresponds to a molecular ion at 287 *m/z* (Fig. 2.45a). Over time, the overall number of peaks increased and the peak eluting at 3.5 min, which corresponds to a molecular ion at 275 *m/z* (Fig. 2.45b) seemed to preponderate over others.

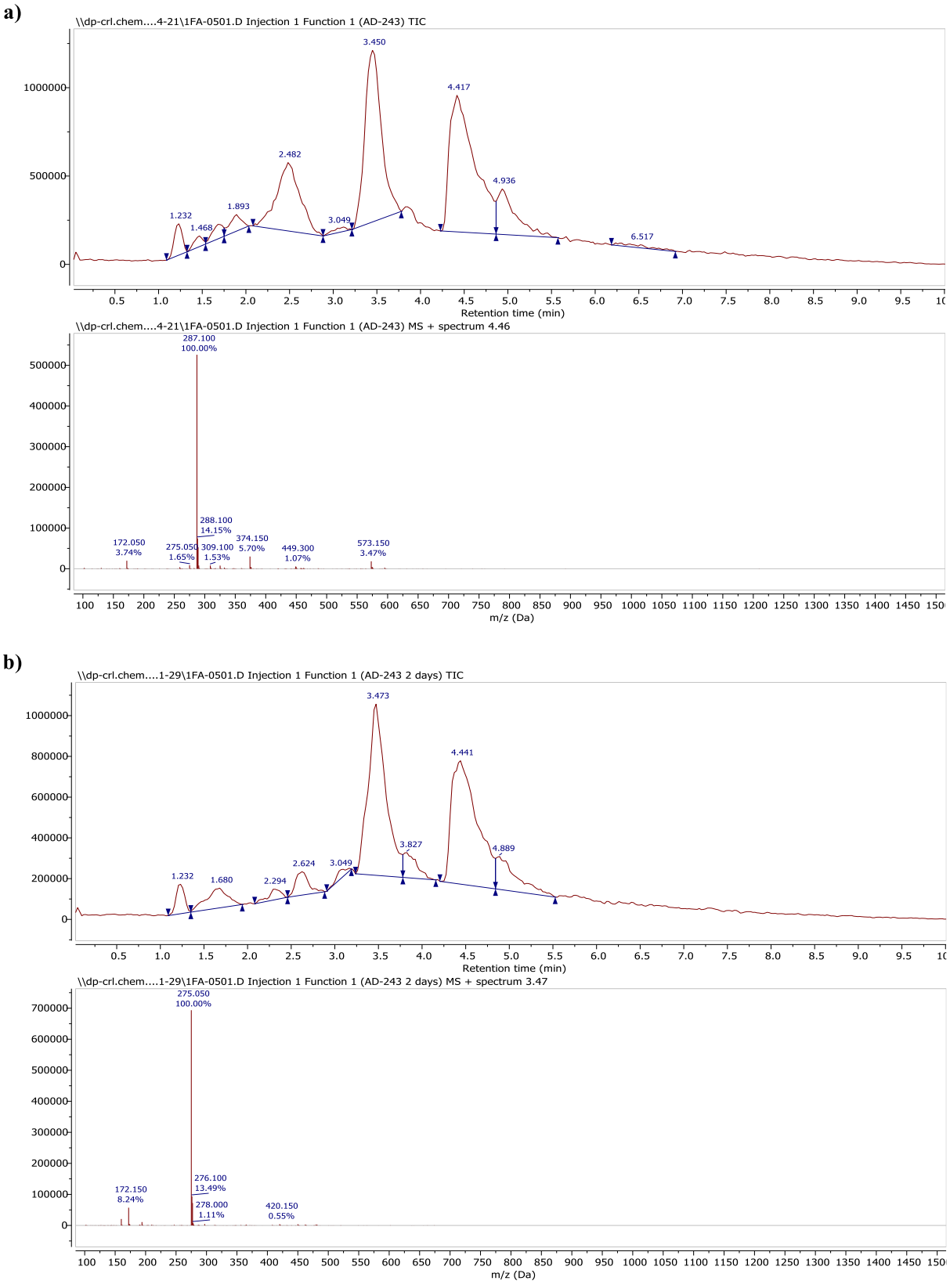

Figure 2.45 a) The molecular ion 287 *m/z* seems to preponderate over others; b) the molecular ion 275 *m/z* seems to preponderate over others.

Even though the parent dicysteinyl hydrazide **30** possesses two ionisable amines, a doubly charged molecular ion of dicysteinyl hydrazide **30** *i.e.* M^{2+} + 2H, was never observed on the mass-spec. This implies that the observed molecular ions on the LC-MS for System **A**, are also potentially singly charged *i.e.* M^{+} + H. Thus, the molecular ions at *m/z* 287 and 275 should correspond to compounds with molar masses of 286 and 274 g mol^{-1}, respectively.

Notably, hydrazide **29** lacks 24 Da in comparison with dicysteinyl hydrazide **30**, and since hydrazide **29** incorporates two thiazolidine rings in its structure, it follows that a 12 Da difference in this compound series corresponds to a *'methylene bridge*'. Thus, dicysteinyl hydrazide **30**, hydrazide **29**, **37**, and **43** with a *m/z* 275 (M^{+} + H, 100%) should have zero, two, four and three methylene bridges, respectively (Fig. 2.46).

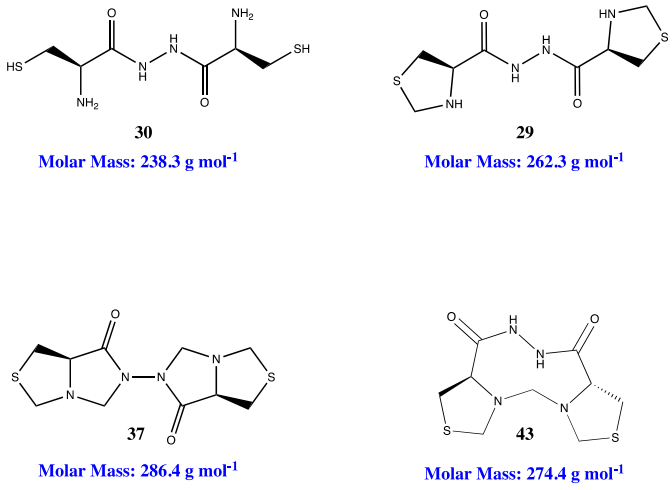

Figure 2.46 Methylene bridges of various dicysteinyl hydrazides with their corresponding molar masses.

In order to establish whether hydrazide **29** is a DCL component of System **A** or it plays any role in this DCC system at all, a separate DCC system of hydrazide **29** with formaldehyde (System **B**) on a relatively large scale (0.10 mmol) was set up and monitored by LC-MS for 6.0 days.

Initially, as for System **A**, two major peaks eluting at 4.1 and 3.2 min, corresponding to molecular ions at *m/z* 287 and 275 (M^+ + H) respectively, were observed; with the compound eluting at 4.1 min appeared to be the major product (Fig. 2.47a).

However, over time, quite opposite to System **A**, the main detectable product by LC-MS was the one eluting at 4.1 min with a molecular ion at *m/z* 287 (Fig. 2.47b). The clear mixture was purified using preparative RP-HPLC, and the main product was isolated.

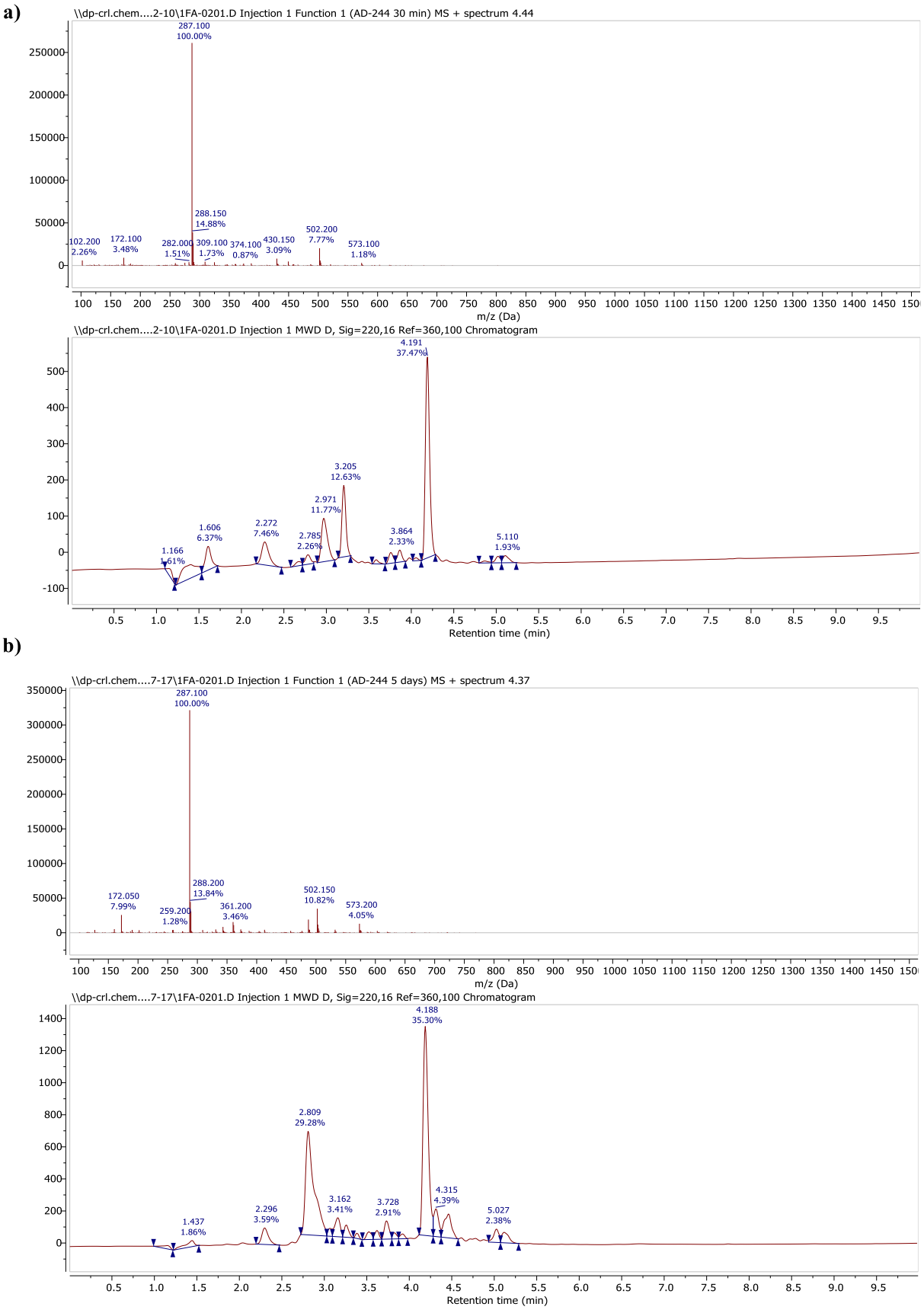

Figure 2.47 a) The peak eluting at 4.1 min seems to preponderate over others; b) After 5 days of equilibration, again, major product appears to be the one eluting at 4.1 min.

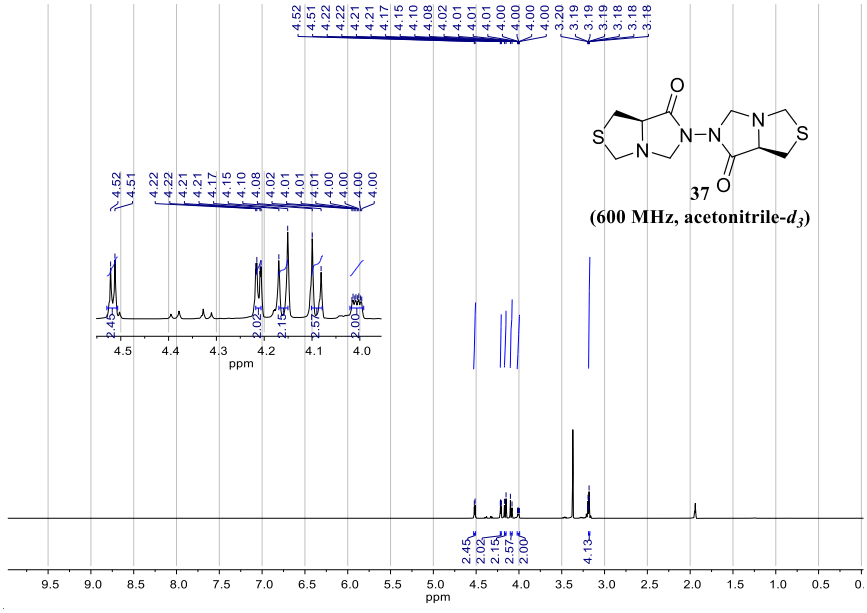

Figure 2.48 ^{1}H NMR spectrum of hydrazide 37. The '*roofing*' effects of the diastereotopic protons ζ-CH_2 (4.52 & 4.21 ppm) and δ-CH_2 (4.16 & 4.09 ppm) are clearly visible.

Formaldehyde reacts twice with hydrazide **29** to give a tetracycle as evidenced by its ^{1}H NMR spectrum (Fig 2.48); however, there are potentially two metamers that can arise from the addition of formaldehyde to hydrazide **29**.

The most nucleophilic centre of hydrazide **29** is, beyond reasonable doubt, its α-amine which adds to formaldehyde to bring about a highly reactive iminium ion; thenceforth, either the nitrogen in the hydrazide immediately adjacent to the carbonyl group would add to the ensuing iminium ion in a '*5-endo-trig*' cyclisation fashion or the other nitrogen next to the first one and further apart from the carbonyl group could attack the iminium ion in a '*6-endo-trig*' cyclisation manner. Since, the other half of the molecule is essentially identical, the same pattern repeats again to furnish two methylene bridges (Fig. 2.49).

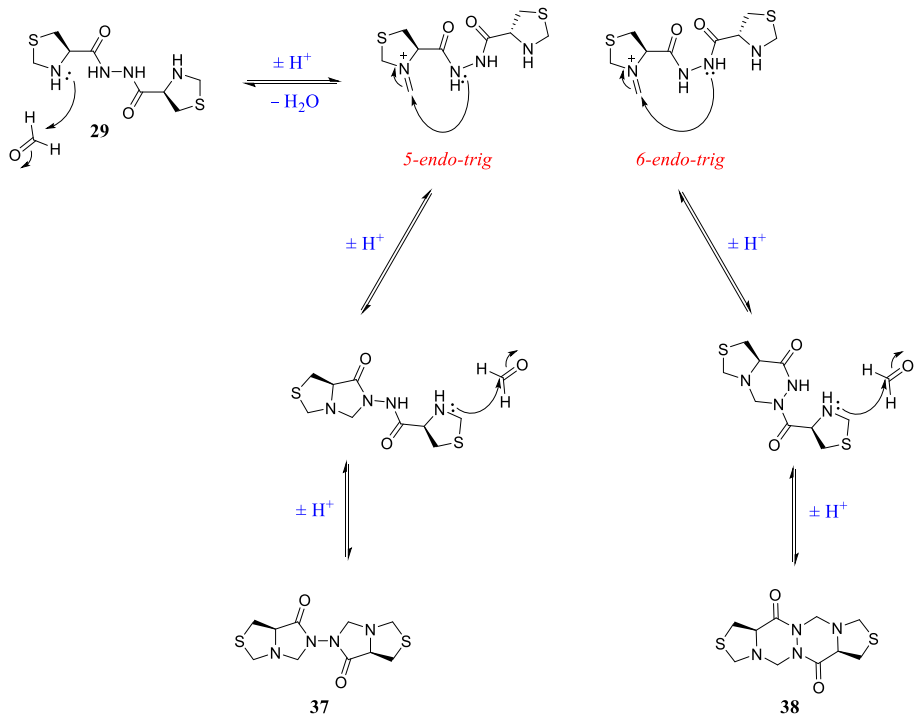

Figure 2.49 The most stable DCL components of System B and their plausible mechanistic pathways. The entire system is under thermodynamic control and the constituents are interconvertible.

Arguably, the '*6-endo-trig*' cyclisation is typically much more favourable in virtue of better orbital overlap, and in line with Baldwin's '*Rules for Ring Closure*',[485] a typical '*5-endo-trig*' cyclisation should be forbidden altogether, but this is permissible when cations are involved (Section 2.6).

One would envisage that as anticipated the '*6-endo-trig*' cyclisation route would preponderate and generate explicitly hydrazide **38** (Fig. 2.49). However, whilst hydrazide **28** would happily react with formaldehyde in a typical '*6-endo-trig*' cyclisation to give a triazinone (Fig. 2.50a), hydrazide **29** is peculiar and does the opposite.

A closer look at the molecules in 3D gives insight into preponderance of different species in the pot. Whereas, hydrazide **28** can form a *cis*-heterohydrindanone which is thermodynamically stable at room temperature (Fig. 2.50a), a similar type structure *i.e. cis*-heterodecalindione, as a result of action of hydrazide **29** on formaldehyde would be impossible, as the other half of the molecule would be pushed inside the other ring, causing a significant steric clash (Fig. 2.50b).

Similarly, the *trans*-heterodecalindione structure of hydrazide **38**, though not completely improbable, would put the outer five-membered ring in the thermodynamically unfavourable axial position (Fig. 2.50c).

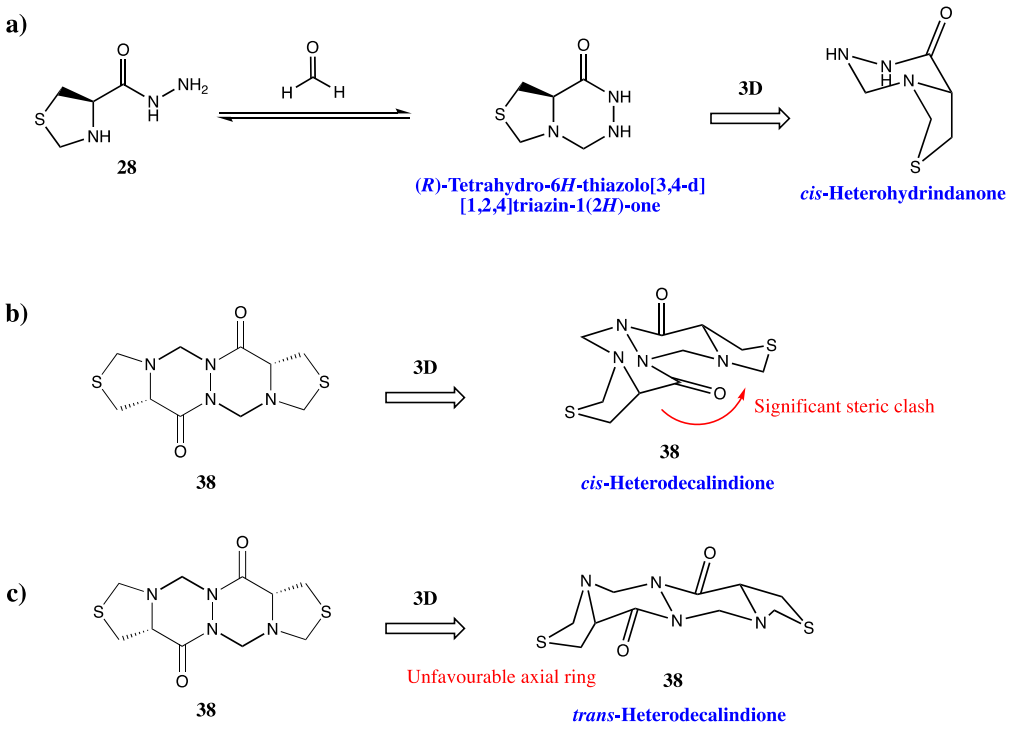

Figure 2.50 3D representation of a DCL component of system B; a) A *cis*-Heterohydrindanone should be stable at room temperature; b) *cis*-Heterodecalindione 38 is destabilised by its outer rings; c) *trans*-Heterodecalindione 38 is probable but unfavourable.

On the other hand, the '*5-endo-trig*' cyclisation route gives rise to two set of *cis*-fused rings *i.e.* bicyclo[**3.3.0**]octanes, resembling the thermodynamically stable '*boat-chair*' and '*crown*' structures of heterocyclooctanes (Fig. 2.51).

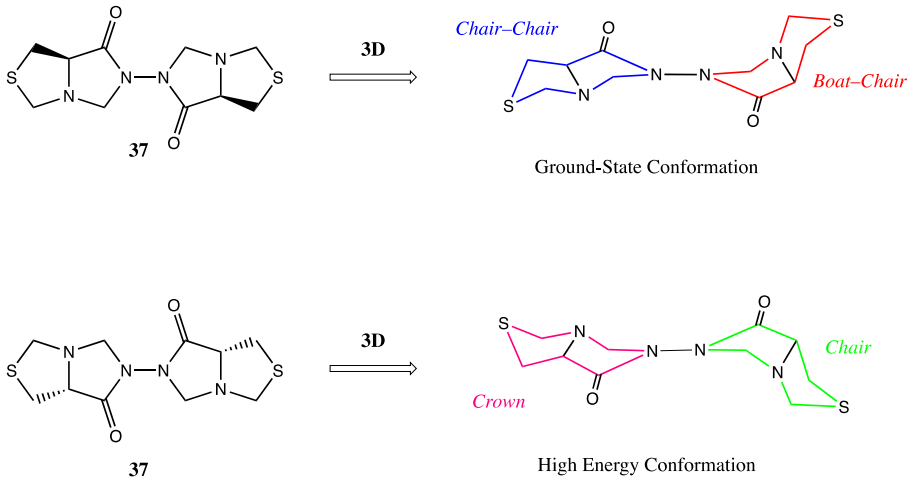

Figure 2.51 Ground-State and Global Maximum of hydrazide 37 conformations. A *Chair-Chair* and *Boat-Chair* combination sufficiently stabilises the molecule to outcompete hydrazide 38. A *Crown* and *Chair* combination represents its global maximum, and would be high in energy.

Inasmuch as the whole system is under thermodynamic control, it would be hard to delineate a precise mechanistic pathway for hydrazide **37**.

It could well be the case that hydrazide **38** was first generated as the kinetic product, and then fell apart in favour of the thermodynamically most stable hydrazide **37** *i.e.* the thermodynamic product. As an effect, traces of hydrazide **38** has been co-eluting with hydrazide **37** during the preparative RP-HPLC purification, and its traces is evident from both the ^{13}C and HSQC NMR spectra of the obtained product of System **B** (Fig. 2.52).

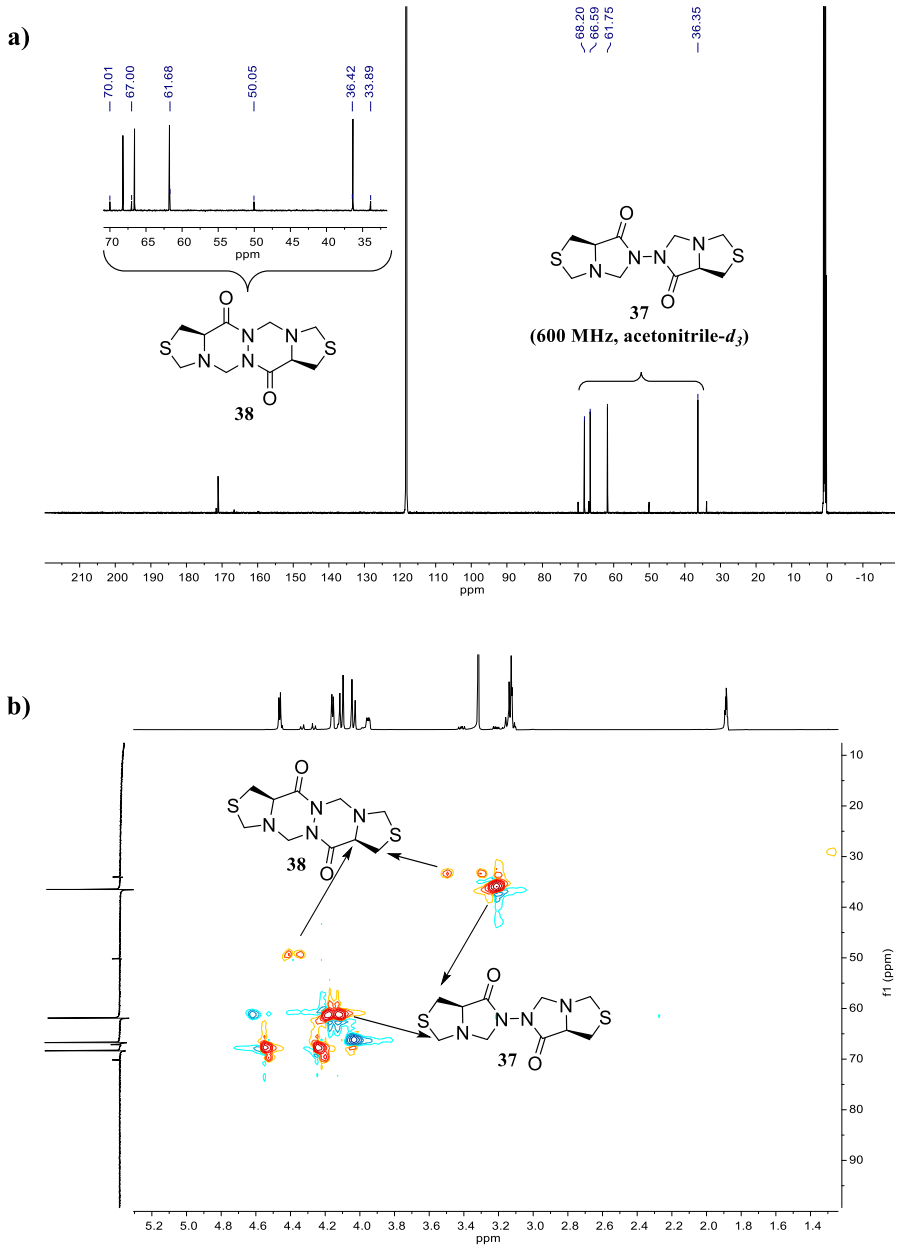

Figure 2.52 Detectable traces of the thermodynamically unfavourable hydrazide 38; a) downfield shift of hydrazide 38 ^{13}C NMR peaks compared to that of hydrazide 37, due to the electron deficient triazinone rings; b) traces of the ^{1}H–^{13}C coupled peaks for hydrazide 38 can vaguely be seen in the HSQC NMR spectrum of hydrazide 37.

The preparative RP-HPLC purified sample of hydrazide **37** still contains traces of the thermodynamically unfavourable hydrazide **38** which was concomitantly eluted with hydrazide **37**. Thus, the peaks at δ 33.9, 36.4, 50.1, 61.7, 67.0 and 70.0 in the ^{13}C NMR spectrum of hydrazide **37** (Fig. 2.52a) are indicative of hydrazide **38** with their distinctive downfield shift pattern due to the deshielding effect of the electron deficient triazinone rings.

Setting aside System **B**, we have not, however, yet established the thermodynamically stable DCL components of system **A**. System **B** clearly suggests that hydrazide **29** cannot be an intermediate in formation of the DCL components of System **A**, as System **B** pattern of reactivity was in a stark contrast to that of System **A**.

A salient determinant of this incongruity stems from the fact that whereas the nucleophilic amines in hydrazide **29** are enclosed within thiazolidine rings, which this significantly alters the reactivity of the amines, dicysteinyl hydrazide **30** enjoys the benefits of having free nucleophilic primary amines, and can approach formaldehyde at any angle, which would not be the case for hydrazide **29**.

Thus, it is conceivable that the highly reactive primary amines in dicysteinyl hydrazide **30** first add to one molecule of formaldehyde to afford a medium-sized ring, and then smaller adjacent rings would be formed, should the sterics permit (Fig. 2.53).

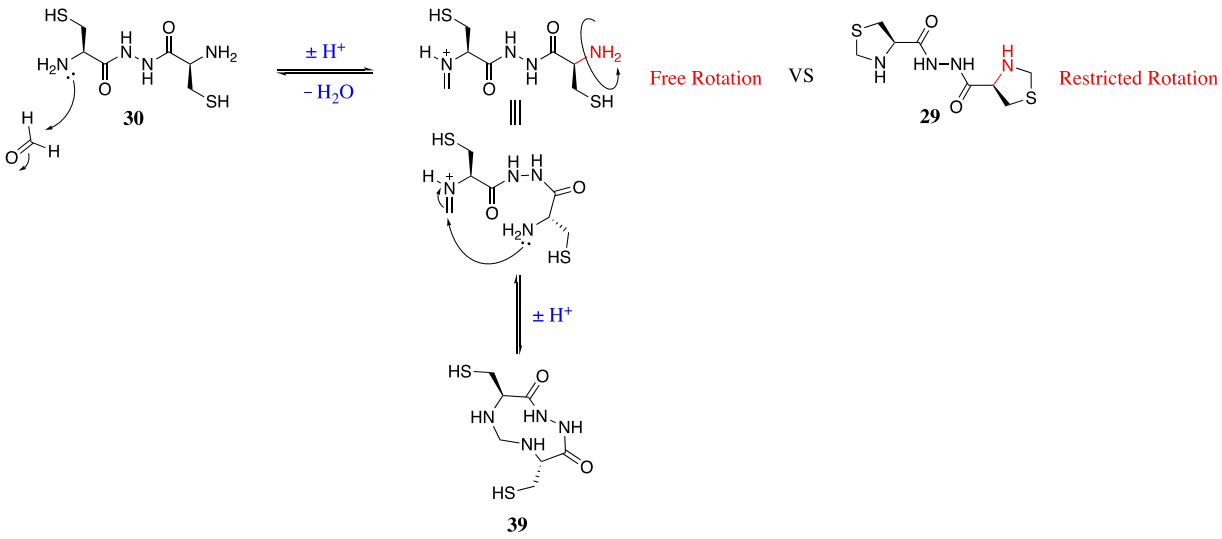

Figure 2.53 Conformational restrictions of hydrazide 29 compared to that for dicysteinyl hydrazide 30.

Since the predominant species detected by LC-MS in System **A** is deemed to have a molar mass of 274 g mol^{-1}; therefore, this hydrazide should have three methylene bridges.

As mentioned above, the nucleophilic primary amines in dicysteinyl hydrazide **30** must have been added to one molecule of formaldehyde to furnish heterocyclononanedione **39** wrapped in one medium-sized ring; this heterocycle can then add to two molecules of formaldehyde, yielding the bicyclic **40**, then a tricycle, and ultimately three metamers (Fig. 2.54).

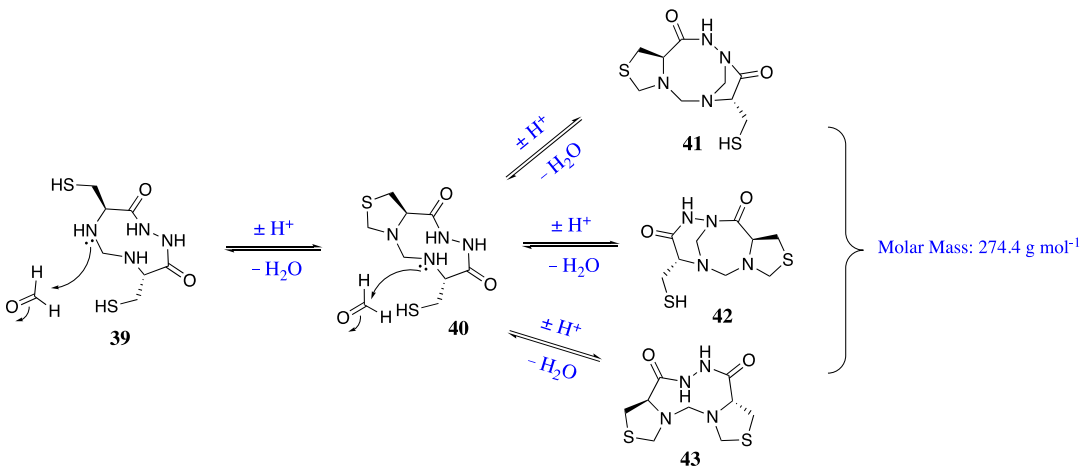

Figure 2.54 Putative metamers of System A.

Which one of the above metamers is the thermodynamic product or which mixtures would be stable under the reaction conditions, all merely depends on the entropy and stability of the ring systems, and hence 3D representations of these metamers can provide useful clues about their stability.

Starting from heterocyclononanedione **39**, one set of its *α*-amines and *ß*-thiols can form a thiazolidine ring with one molecule of formaldehyde to give the bicyclic heterocyclononanedione **40**, then the remaining secondary amine forms a methylene bridge across the ring with one of the hydrazide's nitrogen atoms to give the tricyclic metamer **41**. This metamer pushes the newly formed ring into the adjacent rings, which destabilises the whole molecule (Fig. 2.55a).

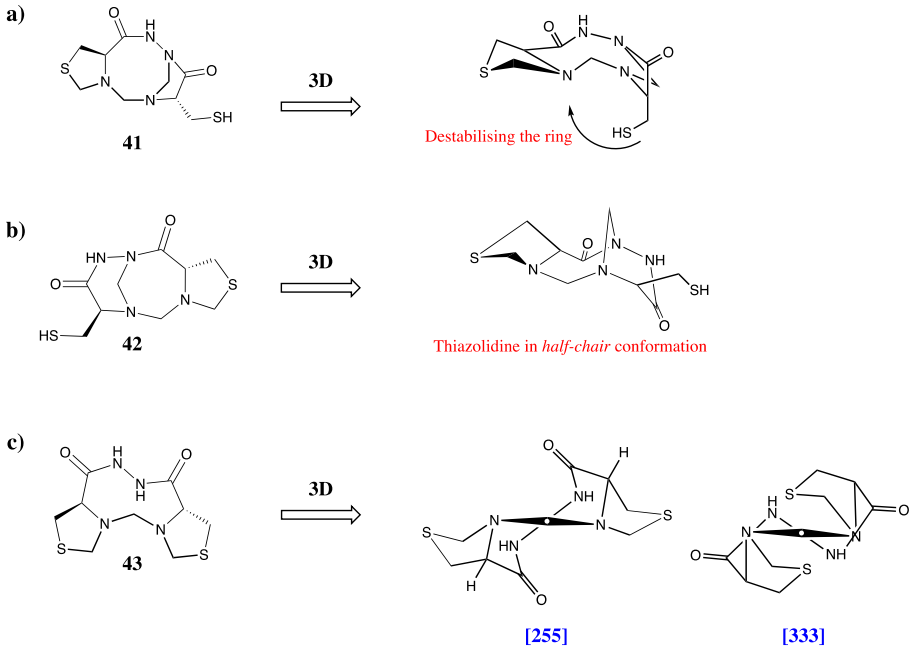

Figure 2.55 3D representations of putative metamers of System A: a) the puckered molecule is very unstable; b) thiazolidine *half-chair* conformation would be a high energy conformer; c) a mixture of thermodynamically stable [225] and [333] conformers of the tricyclic heterocyclononanedione 43.

The same bicyclic heterocyclononanedione **40** can similarly form another methylene bridge across the nine-membered ring to give the tricyclic metamer **42**. This metamer, though more stable than the former, still puts the thiazolidine ring in a high energy '*half-chair*' conformation which would not be ideal (Fig. 2.55b).

Finally, heterocyclononanedione **39** can form two side thiazolidine rings around the nine-membered ring to furnish the tricyclic metamer **43**. Calculations have shown that cyclononane, particularly at low temperatures, should mainly exist in its ground-state '*twist-boat-chair*' or [**333**] conformation.[486] However, detailed NMR investigation led to identification of two minor conformers *i.e.* [**225**] and [**144**] with higher entropy than that of [**333**] (Fig. 2.56). In point of fact, at room temperature it has been shown that cyclononane exists as a mixture of 40% of [**333**], 50% of [**225**] and 10% of [**144**].[487]

To this end, a combination of entropy and the steric effects of thiazolidine side chains should make the tricyclic metamer **43** more stable than the other two metamers such that it could exist in a mixture of [**333**] and [**225**] conformers; however, the [**225**] conformer might predominate as this conformation pushes the side thiazolidine rings away from the main ring, hence reducing any steric clash (Fig. 2.55c).

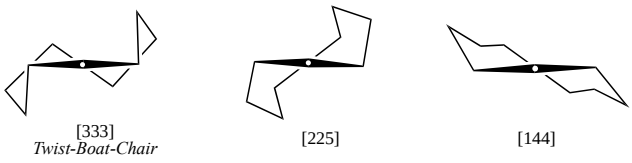

Figure 2.56 Low energy conformations of cyclononane at ambient temperatures.

Most synthetic compounds contain small four- to six-membered rings; nevertheless, medium to large-sized rings are ubiquitous amongst natural products and pharmacologically active compounds such as paclitaxel,[488] echinopines,[489] bielschowskysin,[490] cytosporolides[491] and many others (Fig. 2.57).

To this end, polyfunctional small molecules such as dicysteinyl hydrazide **30** can react with formaldehyde to furnish medium-sized rings, which could be a very useful tool in total chemical synthesis of natural products and pharmacologically active compounds.

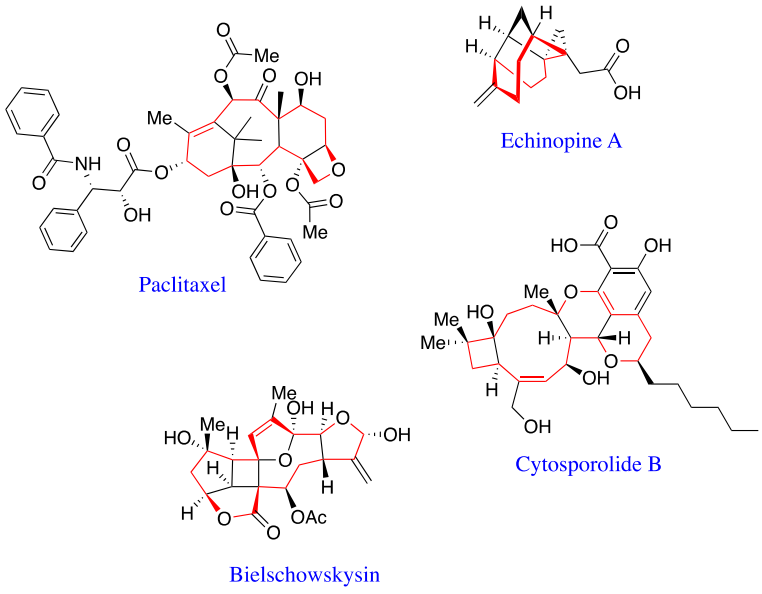

Figure 2.57 Representative examples of natural products containing large rings. The largest core ring shown in red.

The final DCC attempt was devoted to the somewhat peculiar dihomocysteinyl hydrazide **36** with formaldehyde (System **C**). This DCC system was set up as previous on a Bruker AVIII 700 equipped with a TCI H/C/N helium CryoProbe and the ^{1}H NMR spectrum of dihomocysteinly hydrazide **36** (10 µmol) in D_2O (0.50 ml) was recorded.

Upon addition of formaldehyde (10 equiv.) cracked in D_2O (0.20 ml) the ^{1}H NMR spectrum of thus obtained clear solution was recorded immediately and every 3.0 sec thereafter for 1.5 min, without further tuning and shimming of the probe.

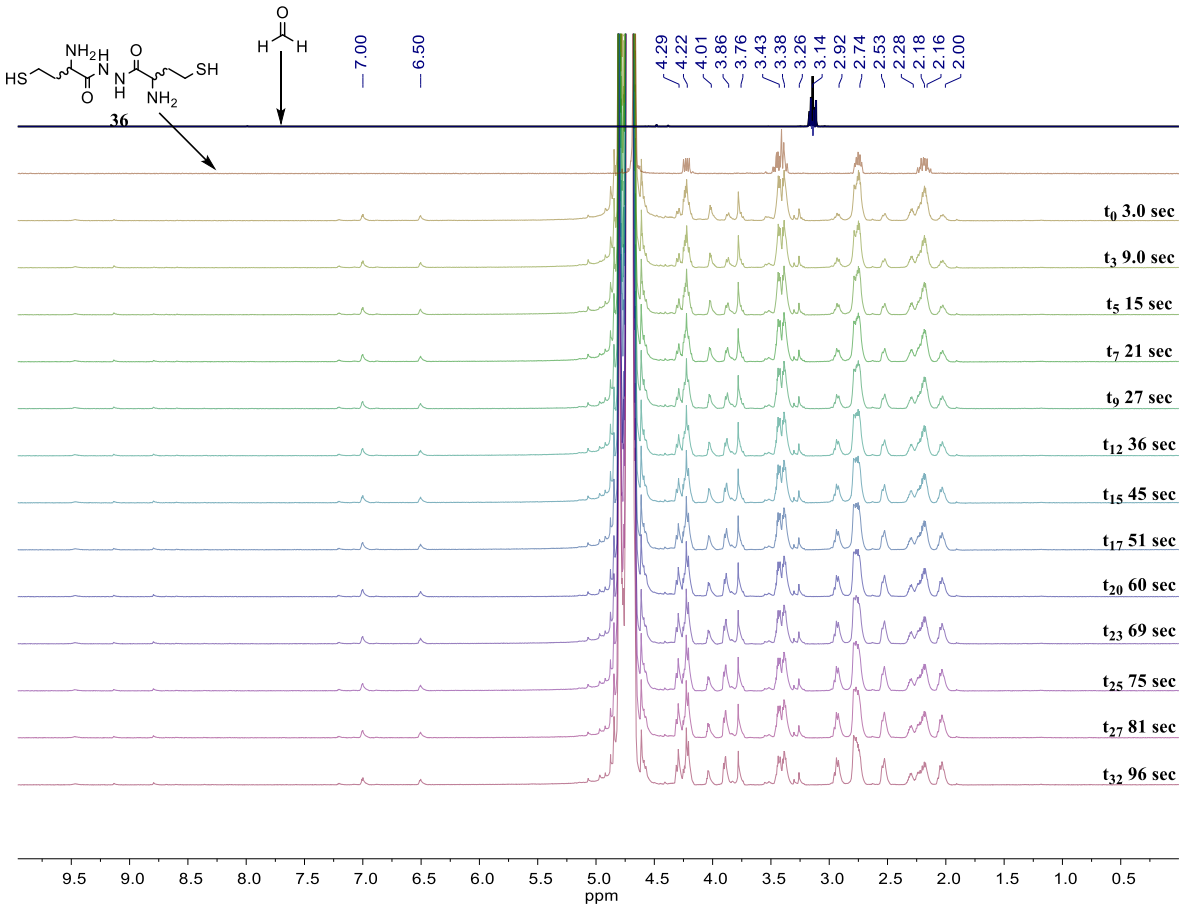

Figure 2.58 Time course ^{1}H NMR of System C in D_2O; recorded on a Bruker AVIII 700 equipped with a TCI H/C/N helium CryoProbe at 700 MHz (298 K). No significant changes to the ^{1}H NMR spectra after 2.0 min from the start of the reaction *i.e.* t_0 observed.

The speed with which the first measurement was taken, together with the frequency of measurements had a profound impact on the quality of the data extracted from System **C**. Even though, this DCC system appeared to be of the fastest kinetics out of all the DCC systems that were tried, owing to our fast and rapid measurement technique, a qualitative trend in DCL components of System **C** can be drawn from its time course ^{1}H NMR (Fig. 2.58).

First and foremost, the distinctive formaldehyde peak at δ 3.14, which was persistent in System **A**, completely vanished from the outset. Distinctive dihomocysteinyl hydrazide **36** signals at δ 4.22, 3.43, 3.38, 2.74 and 2.17 remained in place, but turned broad and lost their splitting patterns.

On the other hand, several distinctive peaks at δ 4.29, 4.01, 3.86, 3.76, 3.43, 3.26, 2.92, 2.53, 2.28 and 2.00 appeared and gradually grew in size. Finally, two peaks at δ 7.00 and 6.50 appeared at t_0 and remained unchanged throughout the equilibration; no significant changes were observed after 2.0 min from the start of the reaction.

Unfortunately, unlike System **A** it was not feasible to estimate the trends in concentrations of its DCL components due to many overlapping peaks. And also attempts at isolating the DCL components of system **C** using preparative RP-HPLC were unsuccessful; nonetheless, templating this DCC system with a metal ion or protein should, hopefully, bring about intriguing novel structures.

Chapter 3

Novel Nitrofuranyl Indole Carboxylate Heterodimers

Introduction

"Everything should be made as simple as possible, but not simpler."

Albert Einstein

Many clinically significant infectious diseases and cancer are prone to developing resistance to a single pharmacophoric therapeutic agent and hence combining two pharmacophoric molecular entities to give a single drug, not only improves formulation properties *i.e.* formulating one drug is easier than formulating two or more drugs, but can also hinder the resistance mechanisms.[492] Thus, covalently linking two therapeutics in a single drug molecule as a conjugate, is an appealing strategy in drug design.

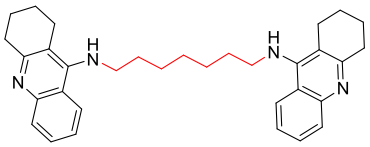

Figure 3.1 *Bis*-tacrine homodimer was achieved by linking two tacrine molecules using a polymethylenic linker shown in red.

Drug conjugates can be dimers of identical entities *i.e.* homodimers. For example, tacrine can be homodimerised by means of a polymethylenic linker to yield a potent cholinesterase inhibitor – *bis*-tacrine homodimer (Fig. 3.1), which is three times more potent than tacrine itself.[493]

Symbiotically dimerising two different pharmacophoric entities gives a conjugate heterodimer.[494] This is usually achieved associatively by covalently linking one pharmacophore with another, in which two different pharmacophores are readily discernible in the resulting heterodimeric conjugate (Fig. 3.2a); however, occasionally it is feasible to optimise a dual acting lead compound to furnish an inherently '*dual acting drug*' for which different pharmacophores are indiscernible in the thus obtained heterodimer (Fig. 3.2b).

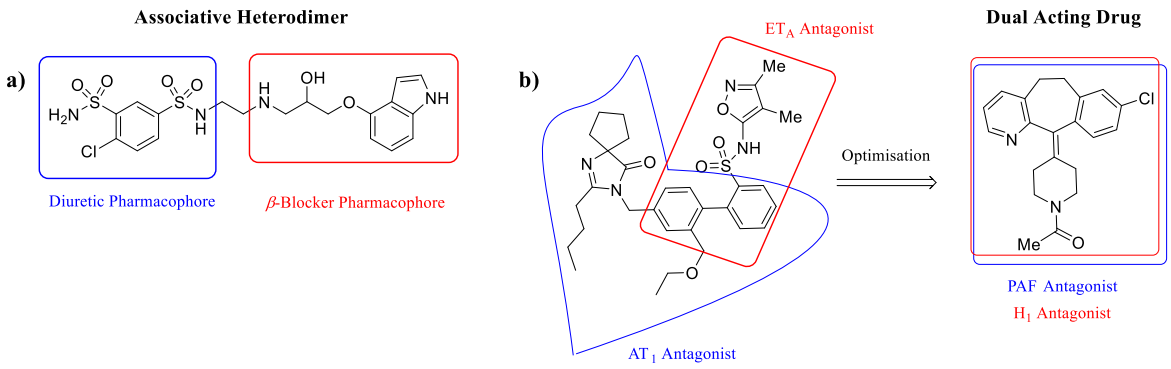

Figure 3.2 a) Symbiotically associative heterodimer of a diuretic and β-blocker;[495] b) the lead compound shares an angiotensin II (AT_1) and endothelin-1 (ET_A) antagonist.[496] Symbiotically optimisation of the lead gave an inherently dual acting histamine (H_1) and platelet activating factor (PAF) antagonist.[497] Note that the PAF and H_1 pharmacophores are virtually indistinguishable in the final drug molecule.

3.1 Heterodimer & Dual Acting Drugs

Associative heterodimers, and inherently dual acting drugs can be categorised into different groups depending on their molecular targets, which as follows:

- Heterodimers and dual acting drugs which bind to two different receptors, in particular, as exemplified by work on GPCRs and their receptor subtypes.
- Heterodimers and dual acting drugs as enzyme inhibitors.
- Heterodimers and dual acting drugs which possess a combination of both enzyme inhibition and receptor binding.

3.1.1 Heterodimers & Dual Acting Drugs as Receptors Binders

Structural and physiochemical properties of GPCRs render them lack selectivity towards monoamines (noradrenaline (NA)/norepinephrine, serotonin (5-HT), dopamine (DA)) and histamine (H), in virtue of the fact that they all share a similar pharmacophore, and selectivity merely depends on interactions with the conserved Asp residue in the 3rd transmembrane helix and secondary binding interactions. Thus, it is of particular interest to the practising medicinal chemist to develop heterodimers or dual acting drugs that can bind to GPCRs as antagonists, agonists or a mixture of both.

5-HT_2 antagonists *e.g.* ritanserin have shown promising therapeutic potential with minimal side effects in treating psychotic patients who experience hallucination and delusion; as a result, symbiotic optimisation of a γ-carboline derivative possessing potent 5-HT_2 and moderate D_2 antagonism has resulted in a potent dual acting 5-HT_2 and D_2 antagonist for treating schizophrenia (Fig. 3.3).[498]

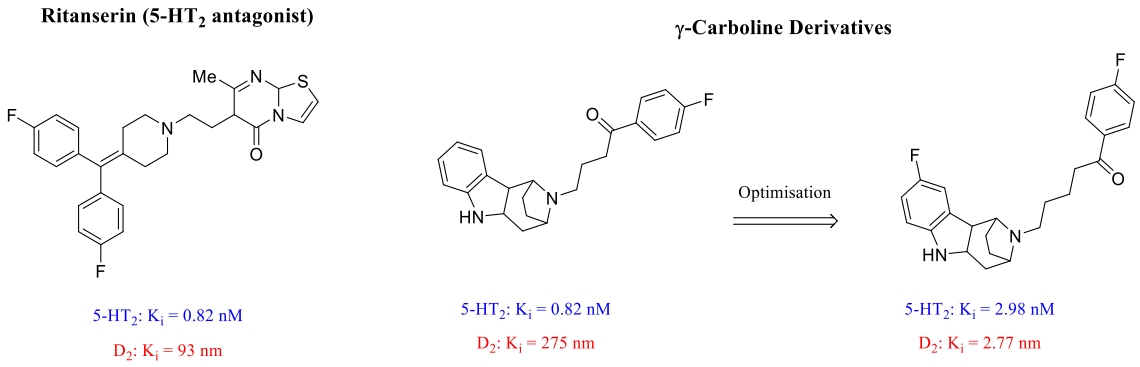

Figure 3.3 The γ-carboline derivative was symbiotically optimised to furnish a dual acting antipsychotic agent with an improved (100-fold increase) D_2 dopaminergic antagonism profile.

On the other hand, a weak histamine H_1 antagonist together with weak histamine H_2 agonist has been symbiotically coupled to give arpromidine associative heterodimer with a 100-fold increase in H_2 agonism, and 10-fold increase in H_1 antagonism profile of this positive ionotropic drug (Fig. 3.4). [499]

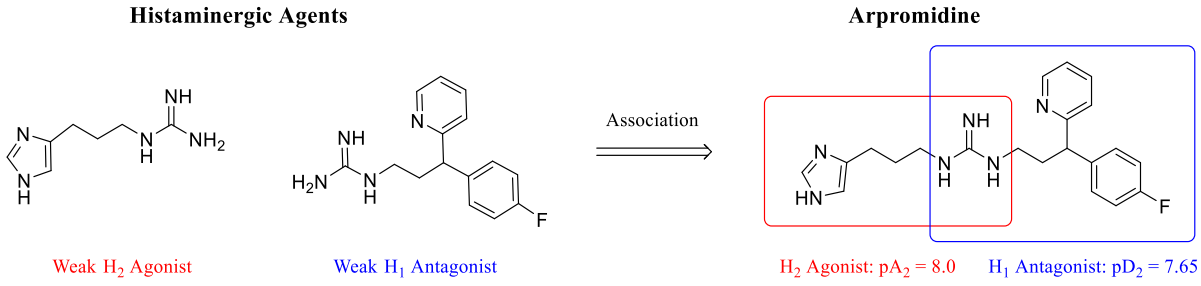

Figure 3.4 Arpromidine – a potent H_1 antagonist and H_2 agonist was achieved *via* associative heterodimerisation of both weak H_1 antagonist and H_2 agonist monomers.

3.1.2 Heterodimers & Dual Acting Drugs as Enzyme Inhibitors

Combining two inhibitors of different isoenzymes or inhibitors of different classes of enzymes to furnish a heterodimer pharmacophore is a promising approach in drug design. β-Lactamases can be categorised into four different Ambler classes (Class A–D), by virtue of their structures, sequences and activities (Section 2.5.1). Ambler Class A, C & D β-lactamases are SBLs; on the other hand, Ambler Class B β-lactamases are MBLs which can further be subdivided; to this end, combining different types of β-lactamase inhibitors can pave the way for protection of broad-spectrum antibacterials (Section 3.3) from β-lactamases.

Acetylcholinesterase (AChE) activity is reported to accelerate amyloid formation, and hence the onset of Alzheimer's disease (AD).[500] Since most AD patients also suffer from depression, Youdim and coworkers[501] developed a combined AChE and selective serotonin reuptake inhibitor (SSRI) heterodimer for a better therapeutic efficacy. Conjugation of rivastigmine with fluoxetine gave a moderately potent AChE and serotonin transporter inhibitor, respectively. Further modification of the heterodimer inhibitor furnished a potent dual acting SSRI and AChE inhibitor (Fig. 3.5).[502,503]

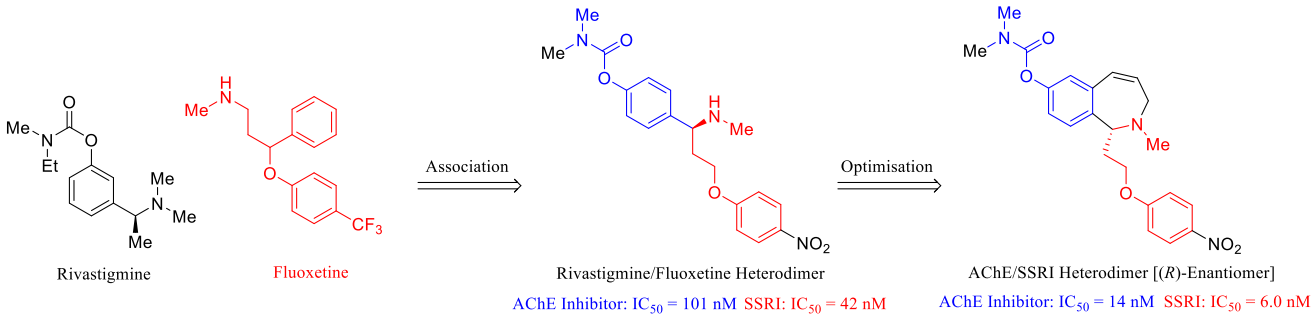

Figure 3.5 Associative heterodimer of rivastigmine and fluoxetine to give a potent AChE/SSRI heterodimer after SAR optimisation.

3.1.3 Heterodimers & Dual Acting Drugs of Both Enzymes and Receptors

Sometimes it is feasible to combine an enzyme inhibitor with a pharmacophoric molecular entity of a receptor to give a heterodimer for modulating the receptor activity and synergistically achieving enzyme inhibition; thus, achieving a better therapeutic effect.

To this end, isbogrel *i.e.* a thromboxane A_2 synthase (TxS) inhibitor was merged with daltroban *i.e.* a thromboxane A_2 receptor (TxR) antagonist, to yield samixogrel heterodimer as both an enzyme inhibitor of TxS (isbogrel), and antagonist of TxR (daltroban) for a complete synergistic alleviation of thromboxane A_2 effects on vasoconstriction and platelet aggregation to prevent cerebrocardiovascular diseases (Fig. 3.6).[504]

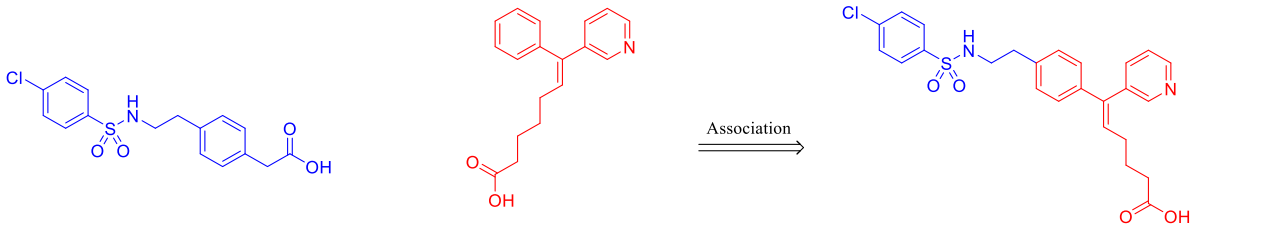

Daltroban (TxR Antagonist)
TxR Antagosim: IC_{50} = 150 nM
TxS Inhibition: IC_{50} > 100 μM

Isbogrel (TxS Inhibitor)
TxR Antagosim: IC_{50} = 2.7 μM
TxS Inhibition: IC_{50} = 3.0 nM

Samixogrel Heterodimer (TxR Antagonist & TxS Inhibitor)
TxR Antagosim: IC_{50} = 19 nM
TxS Inhibition: IC_{50} = 4.0 nM

Figure 3.6 Samixogrel – a potent TxR antagonist and TxS inhibitor.

Using the symbiotically associative drug design approach exemplified above, this chapter reports on work towards novel '*Nitrofuranyl Indole Carboxylate*' (NInC) heterodimers, which could exhibit potent antibacterial properties.

3.2 Pharmacodynamics of Nitrofuran Antibacterials

As previously discussed (Section 1.1.11), only three nitrofuran antibacterials have been marketed *i.e.* nitrofurantoin, furazolidone and nitrofurazone. Although the exact mode of antibacterial activity of nitrofurans is not well understood (Section 1.1.11), they all share a common pharmacophore (Fig. 3.7).

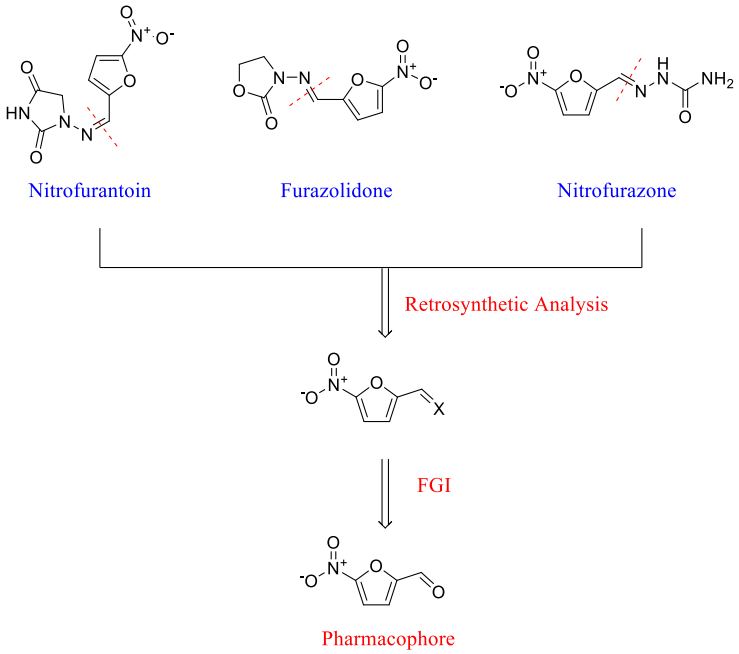

Figure 3.7 Retrosynthetic analysis reveals 5-nitrofurfural as the plausible pharmacophore.

Despite its toxicity, nitrofurantoin remains in clinical use, and similar but different to nitrofurazone and furazolidone, it also possesses a labile Schiff base, which could potentially be hydrolysed to give 5-nitrofurfural as the API (Fig. 3.7).[505]

It is proposed that nitroreductases reduce the nitro moiety of nitrofuran antibacterials to give a single-electron nitro radical anion species, which can react with cellular DNA and proteins, in particular, ribosomes; should this be its mode of action, it brings home to us the observed toxicity of nitrofurans as manifested by pulmonary toxicity,[506,507] hepatotoxicity[508] and neurotoxicity[509] *etc.*

The 5-nitrofurfural group's potential for reduction to generate reactive and unselective species that can damage bacterial and protozoal cells might be considered to render the pathogens less capable of developing resistance compared to other antibacterials. Unfortunately, worldwide resistance even to this class of promiscuous antibacterials has emerged, as it likely will for most, if not all, current and future novel and potent antibacterials under development in virtue of HGT (Section 1.6), which only reiterates the fact that it would be wholly and utterly futile to lock away newly marketed antibacterials at a time when needed most. Thus, until a major breakthrough in treatment of bacterial infections, the quickest and most fruitful, though not the most cost effective and profitable, remedy for this global disease burden is the '*levelling up*' and nothing but '*levelling up*' of novel antibacterials development, and more importantly their usage.

The main mode of resistance to nitrofuran antibacterials is lack of certain nitroreductases. Two classes of nitroreductases have been described for *E. coli* – oxygen sensitive and insensitive nitroreductases.[510]

Oxygen sensitive nitroreductases reduce nitroaryls such as nitrofurans to their corresponding single-electron nitro radical anions, which in the presence of oxygen, the ensuing radical anion can be recycled back to the parent nitrofuran with superoxide production.[511]

On the other hand, oxygen insensitive nitroreductases not only generate the radical anion, which can damage their DNA,[512] but also their further reductions lead to either the corresponding amine species (Fig. 3.8a) or a reactive cyano metabolite with nitrofuran ring opening (Fig. 3.8b).[513] Thus, the nitrofuran resistant *E. coli* lacks oxygen insensitive nitroreductases, which confer resistance to this class of antibacterial with multiple modes of action.

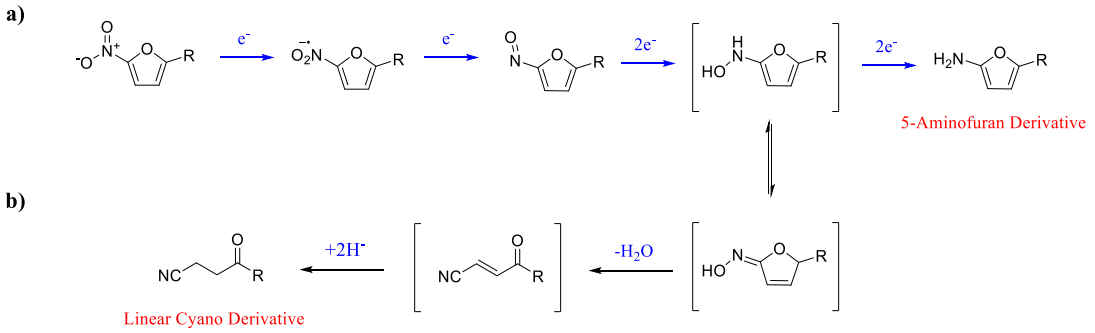

Figure 3.8 Reduction of 5-nitrofuran derivates with nitroreductases: a) reducing the nitrofuran to its corresponding amine; b) further reductions cleave the furan ring to give a linear cyano derivative.

In addition, the aldehyde or Schiff base at the C-2 position is also important for activity of nitrofuran antibacterials as replacement of this moiety with a carboxamide could render them essentially inactive (Fig. 3.9).[514]



Figure 3.9 The carboxamide analogue of the vinyl nitrofuran shows no antimicrobial properties.[514]

3.3 Design & Synthesis of Novel Nitrofuranyl Indole Carboxylate Heterodimers

"Ever tried. Ever failed. No matter. Try again. Fail again. Fail better."

Samuel Beckett

Recent developments in Oxford have led to identification of non-β-lactam indole carboxylates (InCs) as potent MBL inhibitors.[515] Inasmuch as these InCs are not antibacterial in their own right, and must be co-administered with a β-lactam antibiotic *e.g.* a penicillin, cephalosporin or carbapenems, it was of interest to partner the InC with an antibacterial agent *via* a cleavable linker so as to generate novel associative heterodimers, which could be co-administered with a β-lactam antibiotic for an improved therapeutic effect.

In view of the above, 5-nitrofurfural as potential pharmacophore of nitrofuran antibacterials[505] stood out as a promising candidate in virtue of its small size, simplicity, stability, EoS (Section 1.2.4) and multiple modes of action (Section 3.2).

Fragments of associative heterodimers are quite frequently linked to one another using methylene or polymethylenic linkers. However, heterodimers for which the constituting pharmacophoric agents act on molecular targets quite distinct in nature such as antibody drug conjugates (ADC),[516] the use of a cleavable linker is preferred over a non-cleavable methylenic linkers.

Of particular importance is the choice of linkers as they must be stable in systemic circulation in order to avoid unwanted side effects, systemic toxicity and reduction in therapeutic index,[516] and to be easily cleaved once inside the target cell for an efficient delivery of the drug(s).

Hydrazone linkers are by far the smallest and most versatile cleavable linkers that have been utilised in ADC and related applications. Hydrazone linkers owe their popularity to their stability under physiological conditions *i.e.* pH ~ 7.4 and 37 °C, and their lability inside the cells.[517] In other words, the blood is mildly alkaline *i.e.* pH 7.36 – 7.44,[518] which promotes stabilisation of the hydrazone in the systemic circulation; on the other hand, intracellular conditions, in particular, that of lysosomes and endosomes *i.e.* pH 6.5 – 4.5[519] promote hydrolytic hydrazone cleavage.

Although, hydrazone linkers have proved extremely effective in ADC design, their utilisation is more complex in the context of antimicrobials, in particular, antibacterial conjugate drugs, as the pertinent bacterial pH values can vary from very acidic *i.e.* acidophiles,[520] to highly basic alkaliphilic bacteria.[521]

It has, however, been shown that most pathogenic bacteria better thrive in moderately acidic conditions *i.e.* pH ~ 4.0 – 6.0,[522] under which the hydrazone linkers are unstable. To this end various antibacterial drug conjugates featuring hydrazone linkers have been explored,[523,524] in particular, for antitubercular agents.[525]

In recognition of the above, the design and synthesis of a series of novel NInC heterodimers featuring a hydrazone linker, as depicted in Fig 3.10 was pursued, in the fight against ever-increasing antibacterial resistance.

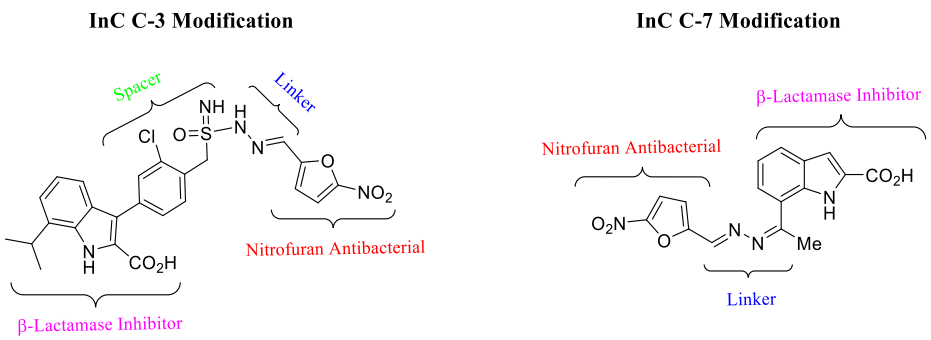

Figure 3.10 Novel NInC heterodimer hybrids.

3.3.1 Design & Synthesis of NInCs at C-3 of the Core InC

In order to achieve a degree of diversity for our conjugate analogues the '*spider-like*' approach was adopted (Section 2.2), as opposed to the more common '*tadpole-like*' approach, which has routinely been utilised for designing drug-conjugates. With the '*spider-like*' approach borne in mind, work to install a hydrazone linker on 5-nitrofurfural was initiated; moreover, in comparison to the hydrazone linker, the synthesis of a much more labile Schiff base *i.e.* imine linker was also attempted. Schiff bases have recently been utilised in a novel self-emulsifying drug delivery system.[526]

3.3.1.1 Synthesis of Nitrofuranyl Hydrazone & its Imine Counterpart

Although the existence of hydrazone **44** (Scheme 3.1) has been reported as early as 1959, as described in a patent by Imperial Chemical Industries Ltd (Imp. Chem. Ind.),[527] its full characterisation apart from a melting point of 164 °C (*dec.*),[527] which does not corroborate the phenomenologically observed melting point *i.e.* 153–154 °C (Experimental p. S41), had not been reported in the literature at the time of our nitrofuranyl hydrazone synthesis *i.e.* April 2018.

The Imp. Chem. Ind. patent reports use of a huge excess of 5-nitrofurfural (22 equiv.) with respect to hydrazine hydrate (65% *w/v* in methanol) for their purported synthesis of hydrazone **44** (Scheme 3.1), such that both 5-nitrofurfural in huge excess and the solvent would pave the way for polymerisation (Section 3.3.1.2), which casts doubt on the validity of the purported synthesis in the first place.

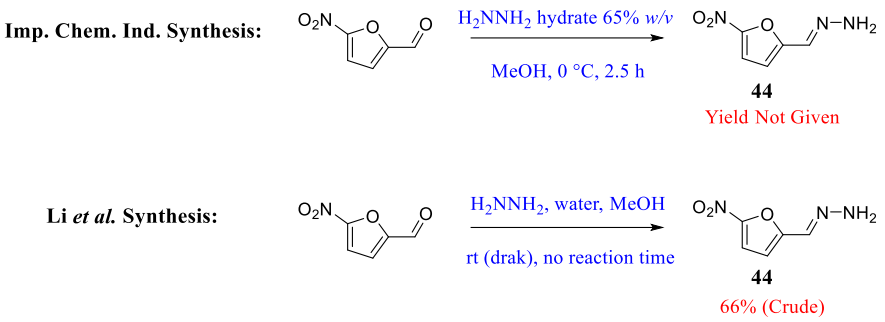

Scheme 3.1 The literature procedures for synthesis of hydrazone 44.

The use of a large excess of 5-nitrofurfural in synthesis of hydrazone **44** by Imp. Chem. Ind. violates the principles of '*ideal synthesis*'[101] to which all competent synthetic chemists should adhere (Section 1.2.1). However, unfortunately, only similar variations of the same synthesis have ever been reported in the literature by others,[528,529] with no reports on detailed characterisation of hydrazone **44** as yet.

Recently, Li *et al.*[530] have reported synthesis of hydrazone **44** using the above literature procedure with some modification (Scheme 3.1). Although the modification has not been disclosed, therein they have chronologically reported the ^{1}H NMR chemical shifts (δ, as ppm referenced to TMS) for hydrazone **44** in DMSO-d_6; however, neither have they interpreted the aforementioned quoted ^{1}H NMR chemical shifts in their publication, nor provided their supposedly obtained ^{1}H NMR spectrum for hydrazone **44** in or with their publication *e.g.* supplementary information.

In light of the highly impractical and far from ideal synthesis of hydrazone **44** in the literature, and also as a world-leading institution *i.e. Universitas Oxoniensis*, aiming to advance excellence in the chemical sciences; herein, this work reports the most practical and ideal synthesis of hydrazone **44** to date; notably, the first anhydrous/semi-anhydrous synthesis thereof (Scheme 3.2).

The condensation of 5-nitrofurfural with hydrazine generates water, and inasmuch as all the steps/intermediates in this process are in equilibrium with one another, the Le Châtelier's treatise[531] implies that removal of water should push the equilibrium towards the desired hydrazone **44**; thus, despite all reported procedures in the literature for synthesis of hydrazone **44** in water (*loc. cit.*), it appeared counterintuitive to use a mixture of water and methanol for this synthesis.

Anhydrous hydrazine itself is toxic and a powerful reducing agent capable of bringing about colossal explosions.[532] In point of fact, a mixture of methanol 57%, hydrazine 30% and water 13% *w/w*, which is similar to that of the literature procedure for synthesis of hydrazone **44** is also referred to as '*C-Stoff*' and was made use of by the Germans during World War II as a rocket fuel,[533] and by others elsewhere.[534]

Guiding principles the practising synthetic chemist encouraged thereunder, preclude the use of unsafe and risky practices, no matter how common they may be, as such a safer procedure for synthesis of hydrazone **44** was considered. A small-scale solubility test identified THF as a versatile solvent in which 5-nitrofurfural is readily soluble.

Given the aforementioned hazards associated with the use of anhydrous hydrazine, hydrazine monohydrate which is much safer to handle than anhydrous hydrazine in combination with a desiccant such as anhydrous sodium sulfate was deemed a suitable substitute for anhydrous hydrazine. Therefore, initially anhydrous sodium sulfate was placed in a flame-dried vessel; thereto was added 5-nitrofurfural, the vessel was sealed and degassed under a dry inert gas *e.g.* argon, nitrogen; thereafter, anhydrous THF was added until 5-nitrofurfural was completely dissolved, the thus obtained clear mixture was cooled in an ice-bath, hydrazine monohydrate (1.1 equiv.) was slowly added, and the mixture was stirred for 2.0 h.

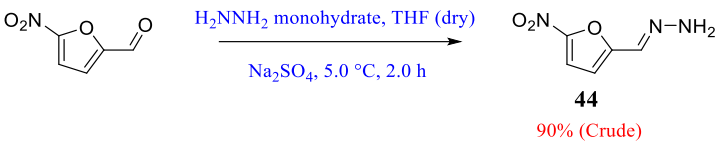

Scheme 3.2 The most practical and high yielding synthesis of hydrazone 44 under semi-anhydrous conditions.

The desiccant in the mixture was able to remove most of the water so as to provide a suitable anhydrous reaction condition under which the reaction proceeded to completion, and the desired crude hydrazone **44** was obtained in a pleasing 90% yield (Scheme 3.2).

The crude material was then purified using flash column chromatography (80% EtOAc in cyclohexane; R_f 0.25) to obtain hydrazone **44** (~ p.a. ≥99%), as an orange solid (Fig. 3.18) in 62% yield. It was later borne out that the desiccant on its own in an open vessel, and even reagent grade THF should give similar results to that from the stricter anhydrous conditions delineated above, such that the use of completely dry reaction vessels, and a dry inert gas, was not of an absolute necessity.

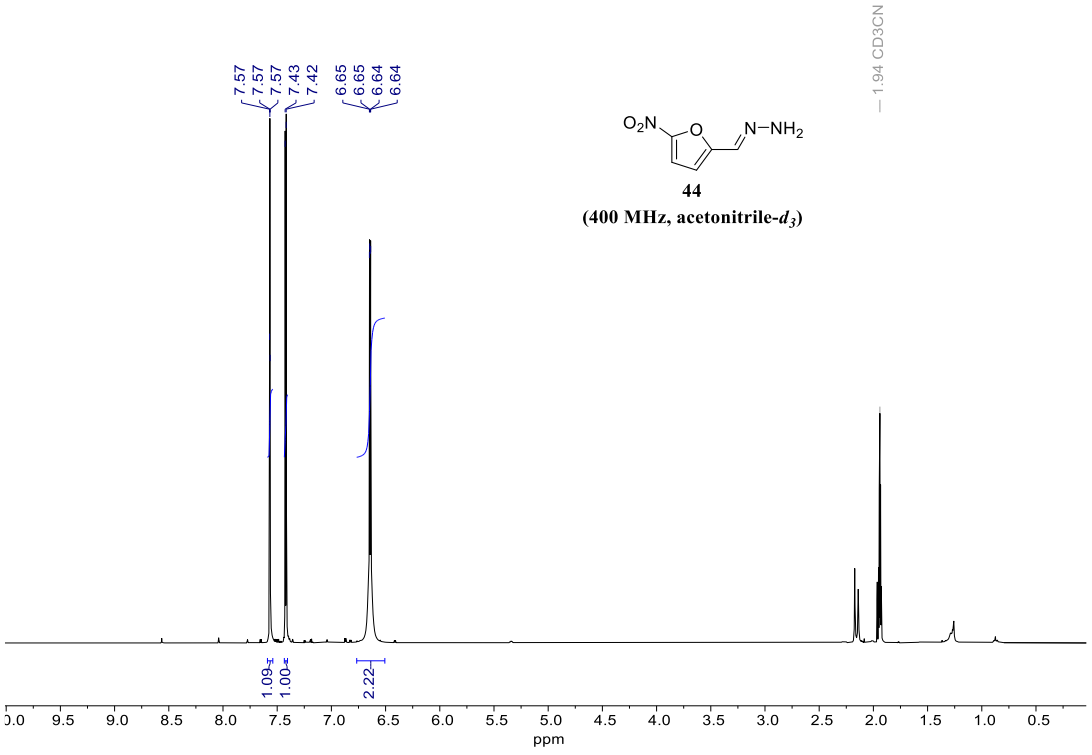

Figure 3.11 ^{1}H NMR spectrum of hydrazone 44. The signal from the exchangeable protons is masked by the aromatic signal at δ 6.65.

It should not come as a surprise that Li *et al.*[530] did not provide their obtained ^{1}H NMR spectrum for hydrazone **44**, in virtue of the fact that only the precipitated solid was collected, without recrystallisation or any other means of purification. It seems improbable that a precipitate of any reaction provides the desired product of acceptable purity for a reliable analytical chemical characterisation.

In addition, hydrazone **44** is peculiar in a sense that first and foremost, it does not dissolve well in the most commonly used NMR solvent *i.e.* $CDCl_3$ or less commonly used CD_2Cl_2. And also, it reacts with nucleophilic solvents, in particular, methanol (Section 3.3.1.2), and to a lesser extent water (Fig. 3.13); thus, methanol-d_4 and D_2O are not suitable deuterated NMR solvents for this compound.

Furthermore, hydrazone **44** is poorly soluble in benzene-d_6, and though it apparently is readily soluble in acetone, deuterated acetone cannot be employed for NMR spectroscopic purposes of this kind, for all the obvious reasons.

Other commercially available deuterated solvents are either equally reactive towards hydrazone **44** or not cost effective. This leaves us with either DMSO-d_6, which is very hygroscopic or acetonitrile-d_3; thus, acetonitrile-d_3 ought to be the solvent of choice for NMR analysis of hydrazone **44** (Fig. 3.11), in virtue of both its cost effectiveness and practicalities.

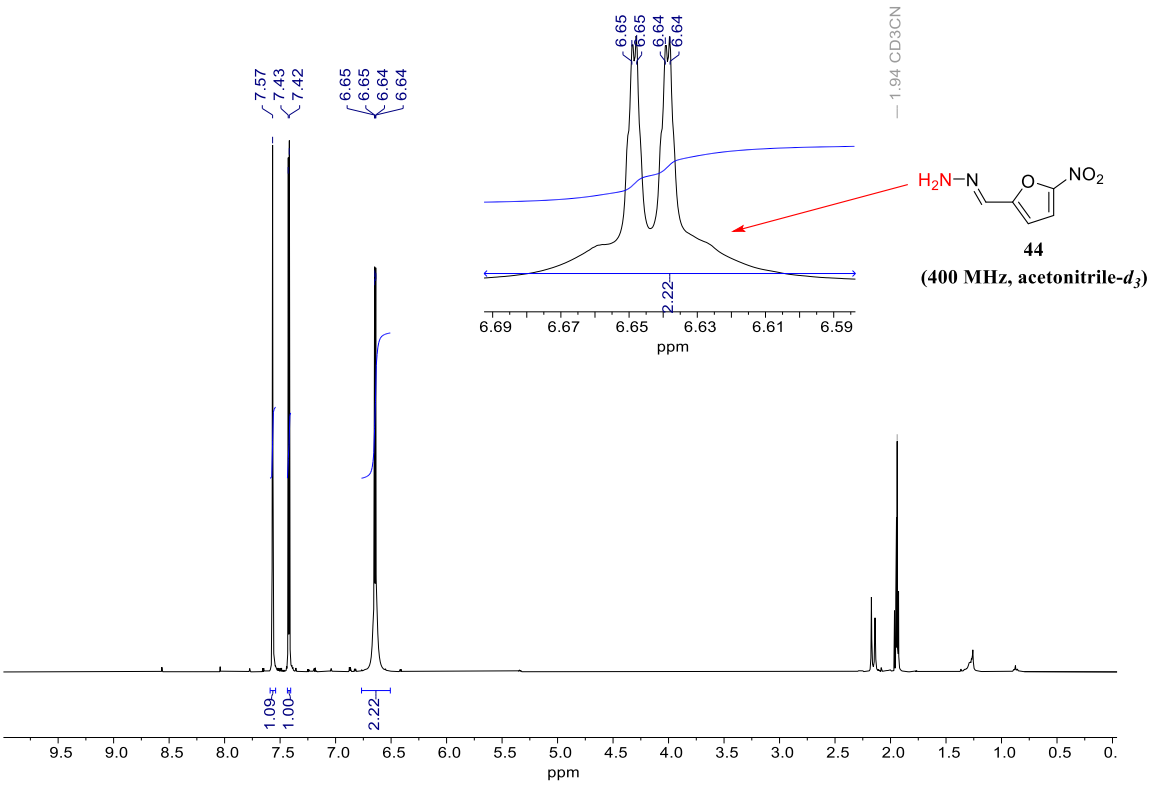

Figure 3.12 ^{1}H NMR spectrum of hydrazone 44 in CD_3CN (*nota bene*: signal from the exchangeable protons shown in red overlaps with that from furan ring in 44.

As depicted in Fig. 3.12, ^{1}H NMR spectrum of hydrazone **44** in acetonitrile-d_3 is complicated by virtue of the overlap of signals from exchangeable protons of the hydrazone moiety with that from protons on the furan ring at *ca.* δ 6.66–6.64.

As a result, the peak integrals in this particular case are not quantitative. This peculiarity was investigated by a '*D_2O shake*' *i.e.* addition of a small amount of D_2O ~ 1.0% to the NMR mixture in question, which requires further adjustments of the NMR probe, and repeat acquisitions. To our delight, the anticipated peak integrals for the non-exchangeable protons were observed in the obtained ^{1}H NMR spectrum of hydrazone **44** after the D_2O shake (Fig. 3.13).

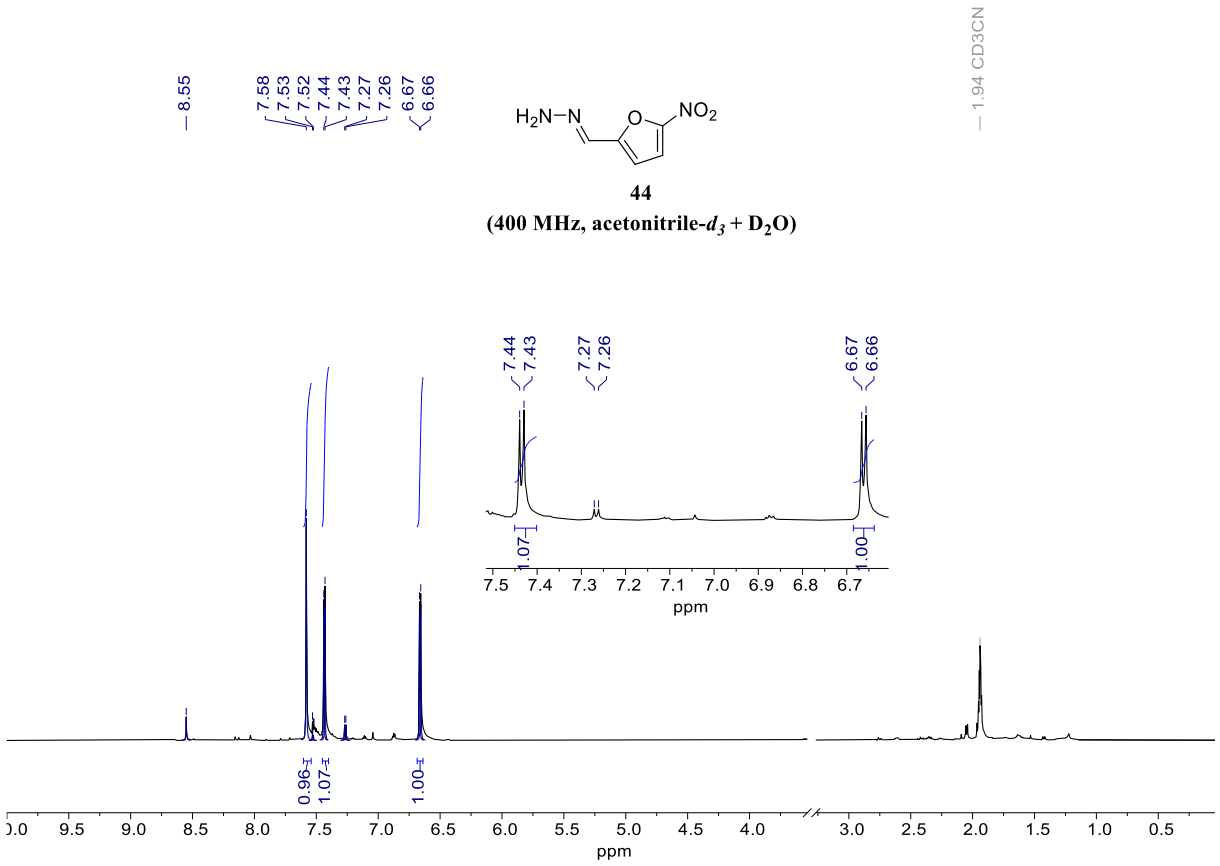

Figure 3.13 ^{1}H NMR spectrum of hydrazone 44 in acetonitrile-d_3 together with a drop of D_2O. The aromatic protons resonate at δ 7.44 & 6.67 almost at the same field as the singlet from the –N=C*H* in hydrazone 44 at δ 7.58; for full characterisation and *J* values in Hz *cf.* Experimental p. S41.

As illustrated above (Fig. 3.13), the D_2O shake restored overall peak integrals to add up to 3.0, corresponding to the sum of integrals 1.0, 1.0 and 1.0 due to each and only one proton at δ 7.58, 7.44 & 7.43 and lastly 6.67 & 6.66, respectively; as anticipated by replacing the exchangeable protons with deuterons, and hence brushing aside their corresponding problematic signal.

On the other hand, the exchangeable protons in the absence of deuterons, complicate the overall trace integration to be normalised to 4.0 (Fig. 3.12), which is made up of integrals 1.0, 1.0 and 2.0 by virtue of protons which give rise to the signals at δ 7.57, 7.43 & 7.42 and lastly 6.65–6.64, respectively, *i.e.* less than a total of 5.0 protons that is expected of hydrazone **44**. However, even though the trace integration problem was rectified in the above fashion, unfortunately, as previously mentioned the irksome residual water as a result of the D_2O shake reacts with hydrazone **44**, likely resulting in minor inexplicable new peaks at δ 8.55, 7.53, 7.52, 7.27 and 7.26 (Section 3.3.1.2).

Having successfully synthesised hydrazone **44**, the synthesis of its imine counterpart, namely, Schiff base **45** was attempted. Although, nitroaryl imines are ubiquitous in the literature,[535,536] neither was there any report on imine **45** in the literature at the time of the aforementioned Schiff base synthesis in May 2018, nor at the time of writing this text nearly three and a half years later.

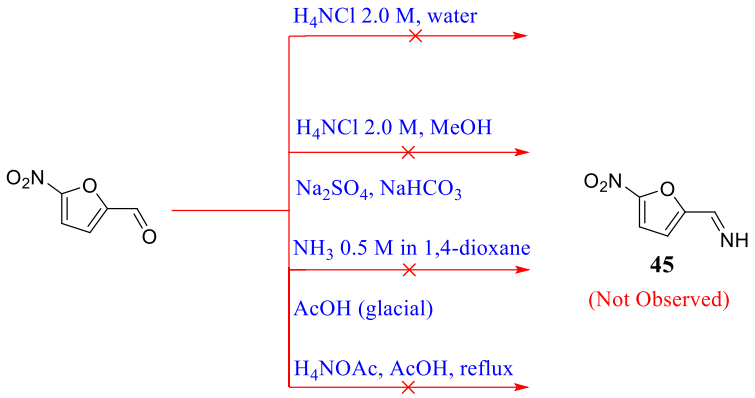

Scheme 3.3 Attempted synthesis of imine 45 under a variety of conditions.

Given that imine **45** is completely unprecedented in the literature, its introduction to the literature occurred to us as a splendid adventure. As with hydrazone **44**, all the steps/intermediates in formation of imine **45** from 5-nitrofurfural and potentially ammonia are likely in equilibrium; hence, removal of water should, by all means, favour the formation of imine **45**. Moreover, whereas hydrazones are often formed under neutral conditions, it is common to synthesise imines under mildly acidic conditions *i.e.* pH ~ 5.0 – 4.0.

Since ammonia is toxic, and dry ammonia gas is only available in pressurised cylinders, it is not worthwhile to use dry ammonia gas for micro-scale *i.e.* 1.0 mmol scale research laboratory endeavours. To this end, this Schiff base formation was first attempted using a buffered system *i.e.* $H_4NCl/NaHCO_3$ in the least, reasonably practicable, amount of water. However, unfortunately, to our regret imine **45** was not obtained using the aforementioned buffered system; its synthesis under various acidic and basic conditions was also attempted with no joy (Scheme 3.3).

Inasmuch as no desired imine **45** was isolated in each and every single attempt at its synthesis, a careful monitoring of the course of the reaction using LC-MS brought home to us that at times, imine **45**, in point of fact, was likely formed by virtue of a species with a mass corresponding to that of the plausible species **46** which was obtained under relatively anhydrous conditions (Fig. 3.14).

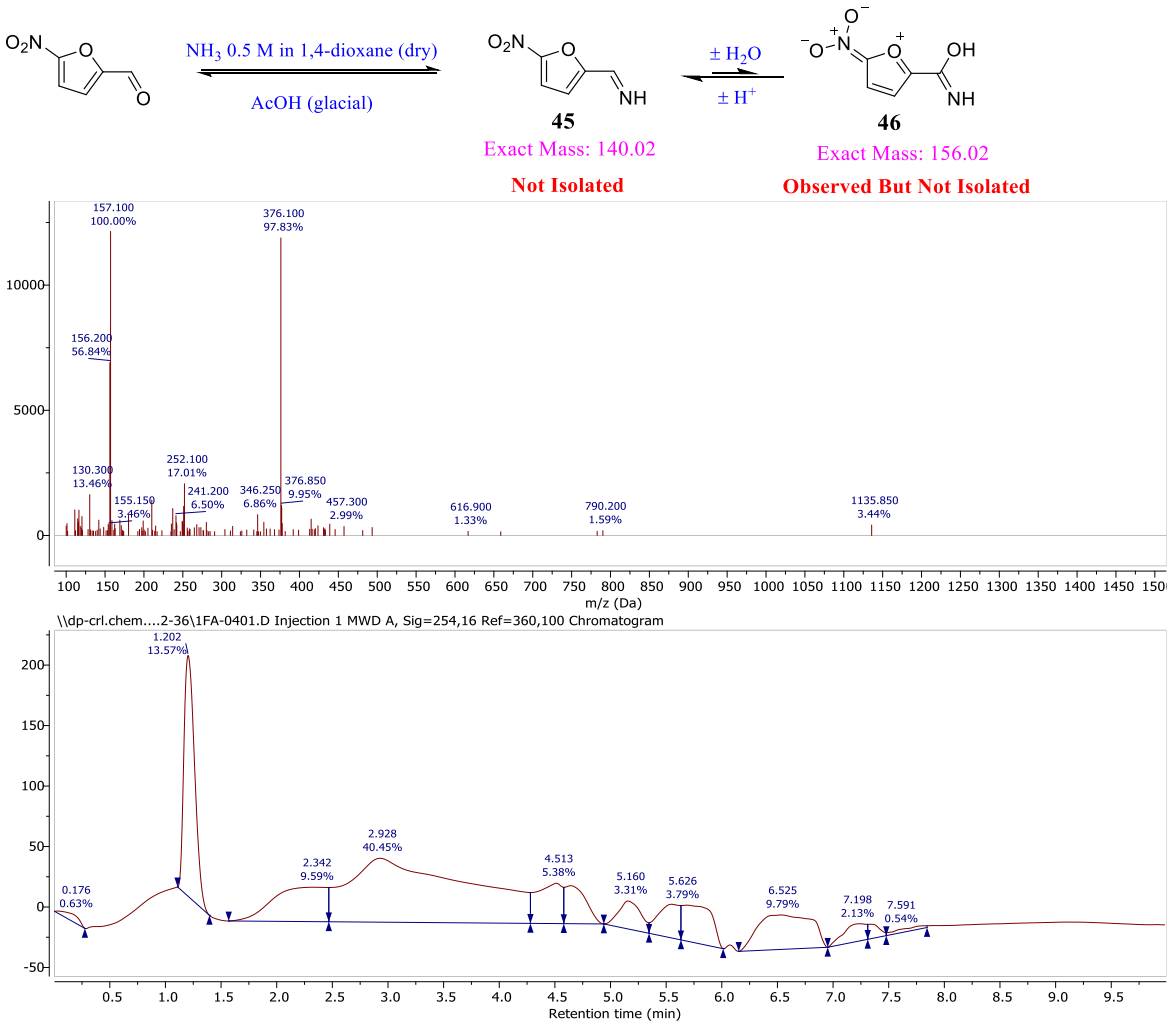

Figure 3.14 LC-MS trace of the tentative imine 45.

In the light of the above findings, it seems as if imine **45** might be either too short-lived under the stated reaction conditions or the reversal to 5-nitrofurfural starting material occurs on attempted isolation.

In order to validate this hypothesis that imine **45** does, in practice, exist, its *in situ* reduction to corresponding primary amine **47** under similar anhydrous conditions, which proved promising for imine **45**, but this time *via* sodium triacetoxyborohydride (STAB) as a reducing agent was also attempted. Gratifyingly, amine **47** was isolated as an orange oil in good yields *i.e.* 75–80% (Scheme 3.4), after flash column chromatography, and in excellent purity, as evidenced by both ^{1}H (Fig. 3.15), and ^{13}C NMR (Fig. 3.16).

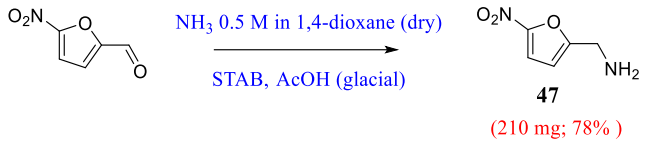

Scheme 3.4 Synthesis of 5-nitrofurfurylamine 47 under relatively anhydrous conditions.

As argued above, imine **45** or a species thereof, must have been formed somehow during the course of the reaction, as evidenced by its reduction to the corresponding amine **47** (Fig. 3.15).

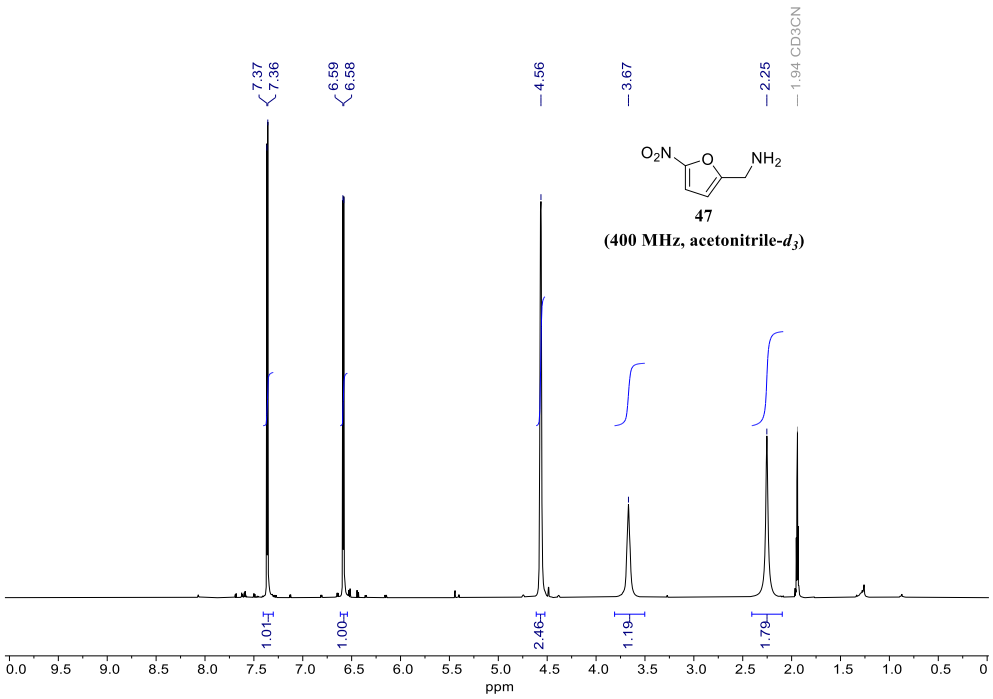

Figure 3.15 ^{1}H NMR spectrum of amine 47. The signal from the *T*$_d$ centre *i.e.* –C*H*$_2$NH$_3$ at δ 4.56 is atypical of a standard *T*$_d$ centre adjacent to amines (*vide infra*).

It is worth highlighting the huge shift of the methylene signal on the carbon adjacent to the primary amine group, which usually appears at ~ δ 2.70 for a normal T_d, sp^3 hybridised –C***H*₂**NH$_3$; however, it appears to have been significantly downshifted to δ 4.56. Such an unusual downfield shift may reflect conjugation as amine **47** itself is an orange oil, though its hydrochloride salt is apparently brown.[537]

Although impure compounds could sometimes appear coloured, but these nitro-heteroaromatic compounds have their own intrinsic colours due to their extended delocalised π systems to which particular attention must be paid (Section 3.3.1.2). Nevertheless, the ^{13}C NMR spectrum of amine **47** manifests a signal at δ 57.3 for carbon adjacent to the primary amine, as expected of a sp^3 hybridised carbon adjacent to an electronegative group. Thus, in the case of a conjugation no signals would be expected for this compound in the region δ 0 – 100 in its ^{13}C NMR spectrum, as a sp^2 hybridised carbon of C=C should appear at *ca.* δ 100 – 150, which is indeed the case for sp^2 hybridised carbons of the furan ring in amine **47** (Fig. 3.16).

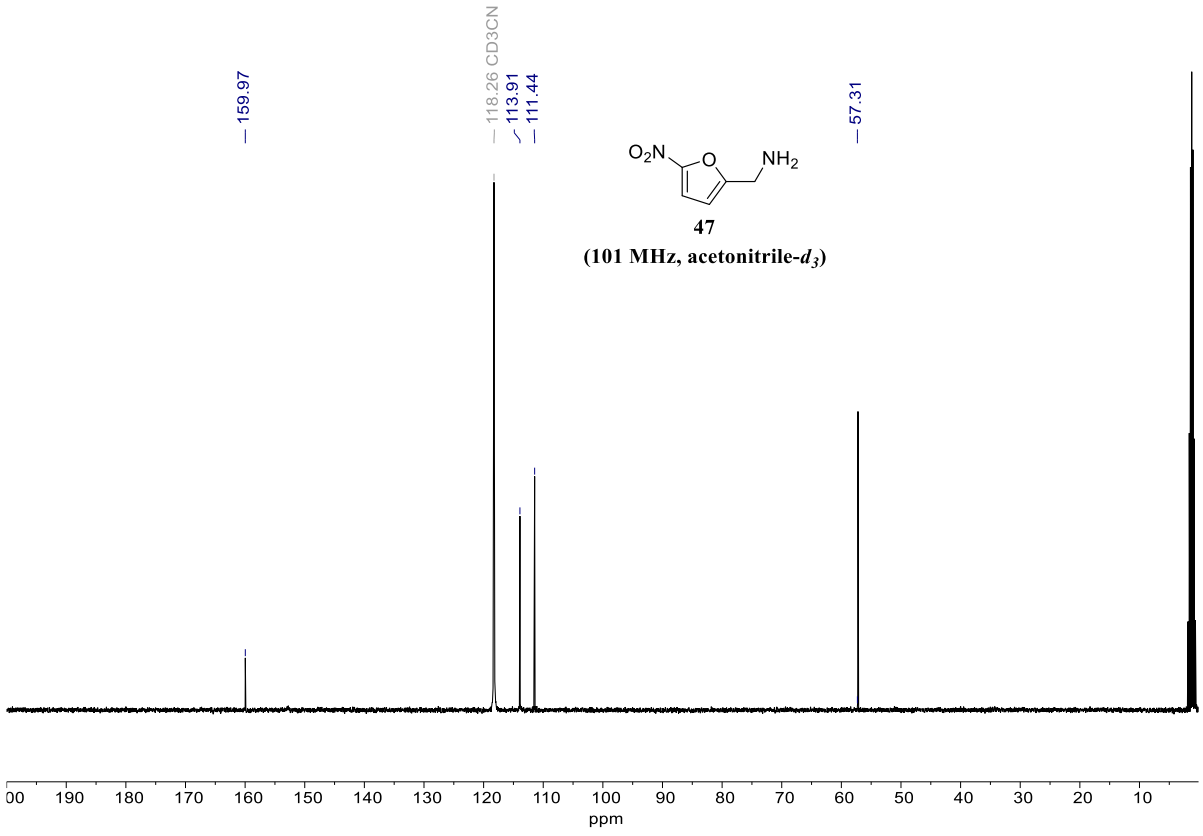

Figure 3.16 ^{13}C NMR spectrum of amine 47 in acetonitrile-d_3.

The establishment of whether the huge downfield shift of the signal from protons on the carbon adjacent to the primary amine moiety in ^{1}H NMR spectrum of amine **47** at δ 4.56 (Fig. 3.15) is due to any conjugative effect or not, unfortunately, is beyond the scope of this medicinally focussed endeavour.

3.3.1.2 Reactivity of Polar Protic Solvents Towards 5-Nitrofurfural & its Derivatives

The previously reported, somewhat predicted ^{1}H NMR of hydrazone **44** (*loc. cit.*), though not assigned, is in a stark contrast with that obtained phenomenologically. Although the predicted ^{1}H NMR spectrum of hydrazone **44** in the literature (*ibid.*) was recorded in DMSO-d_6 and that obtained phenomenologically was in acetonitrile-d_3, only ±0.3 ppm[538] should be expected for spectra of the same compound in a highly polar solvent such as DMSO-d_6, and signal patterns are usually more or less similar (Fig. 3.23). Inarguably, differences in the chemical shifts of exchangeable protons are permissible, but the reported data is nowhere near that of the empirical counterpart, irrespective of the different deuterated solvents in which the spectra were recorded.

Dismayed by the fact that all the empirical characterisation data for hydrazone **44** did not sit right with that of the literature *i.e.* melting point, colour and ^{1}H NMR; and also, in an attempt to be freed of the ensuing doubt that the wrong compound has been characterised herein, the authors *i.e.* Li *et al.*[530] of the only publication in which the ^{1}H NMR chemical shifts of hydrazone **44** have been reported were approached for sight of their obtained ^{1}H NMR spectrum of hydrazone **44** (Appendix II); intriguingly, it did not come as a surprise that they never replied.

In view of the above, ^{1}H NMR of hydrazone **44** in DMSO-d_6 was recorded, and compared with that obtained in acetonitrile-d_3 (Fig. 3.17).

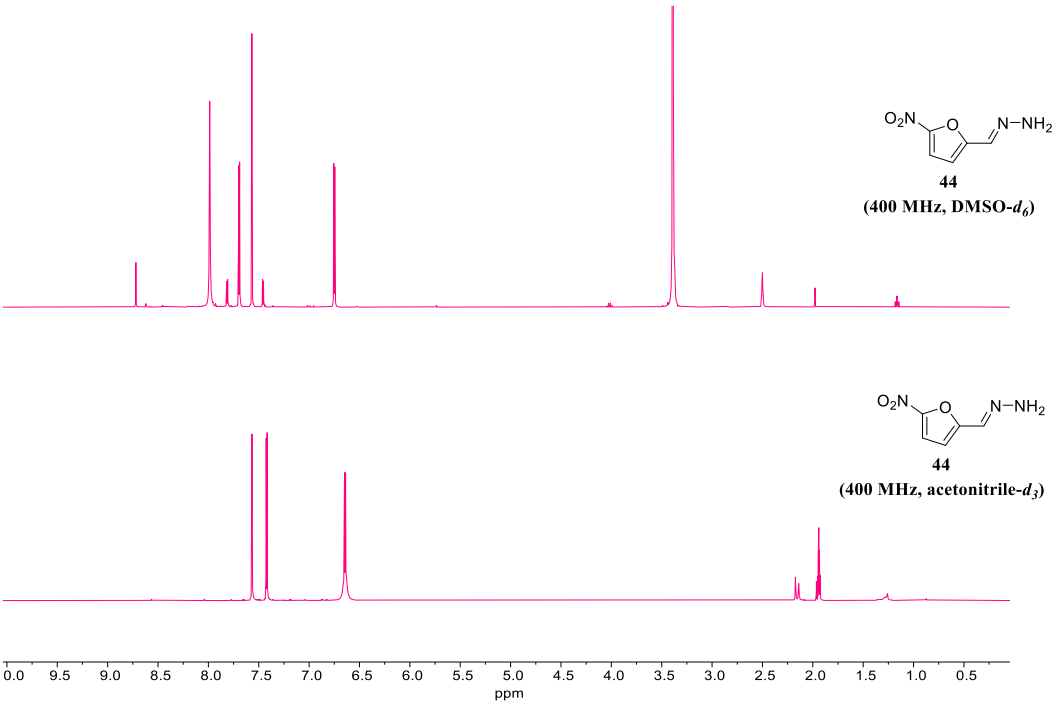

Figure 3.17 ^{1}H NMR spectra of hydrazone 44 recorded in DMSO-d_3 (top), and acetonitrile-d_3 (bottom).

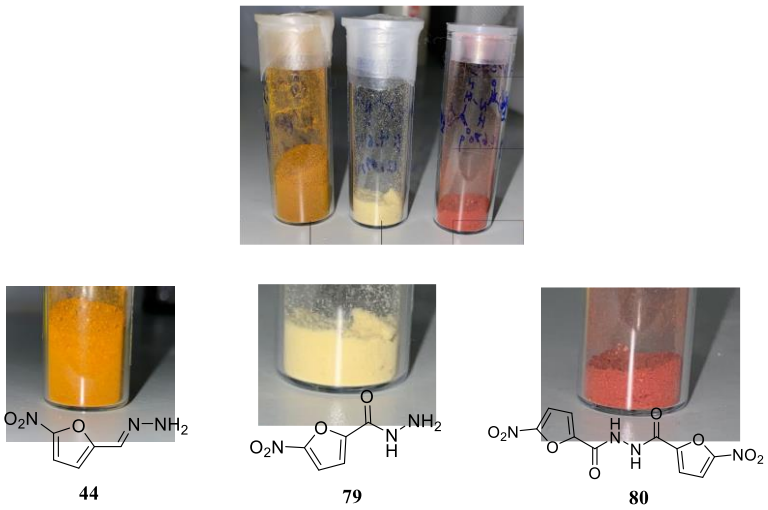

Figure 3.18 Images of nitrofuranyl derivatives 44, 79 & 80. Hydrazone 44 is, by all means, not yellow, whereas 79 is (*cf.* Fig. 3.69).

Li *et al.*[530] might have erroneously claimed that their compounds were of a purity >95%; though there is no proof of their claims, inductive inferential evidence unravelling such a false claim can be conceded from the reported intrinsic colour of hydrazone **44** which in this case is a good measure of its purity (Fig. 3.18).

Given that there is no indication of a source of Na^+ in any of their procedures for **44** synthesis and partial characterisation (*loc. cit.*), they managed to somehow arrive at HRMS (ESI) calcd. for $C_5H_5N_3O_3$ [M + **Na**]$^+$ *m/z* 178.0223, found 178.0225, such that as reported in their publication some numerical errors had to be factored in for the reported HMRS of the dimer, trimer, polymer *etc.* in their concoction to match that of hydrazone **44** by serendipitously swapping a proton for Na^+.

In marked contrast, the new inhouse synthesis of hydrazone **44** entails several sources of Na^+ *e.g.* Na_2SO_4, saturated $NaCl_{aq}$ *etc.*, and yet we were able to obtain the expected HMRS (ESI) calcd. for $C_5H_5N_3O_3$ [M + H]$^+$ *m/z* 156.0404, found 156.0403 (Fig. 3.19) with no errors and sodium ions. Had they synthesised hydrazone **44** in >95% purity, they would have definitely arrived at the same results; however, in reality their compound does not seem to represent hydrazone **44**.

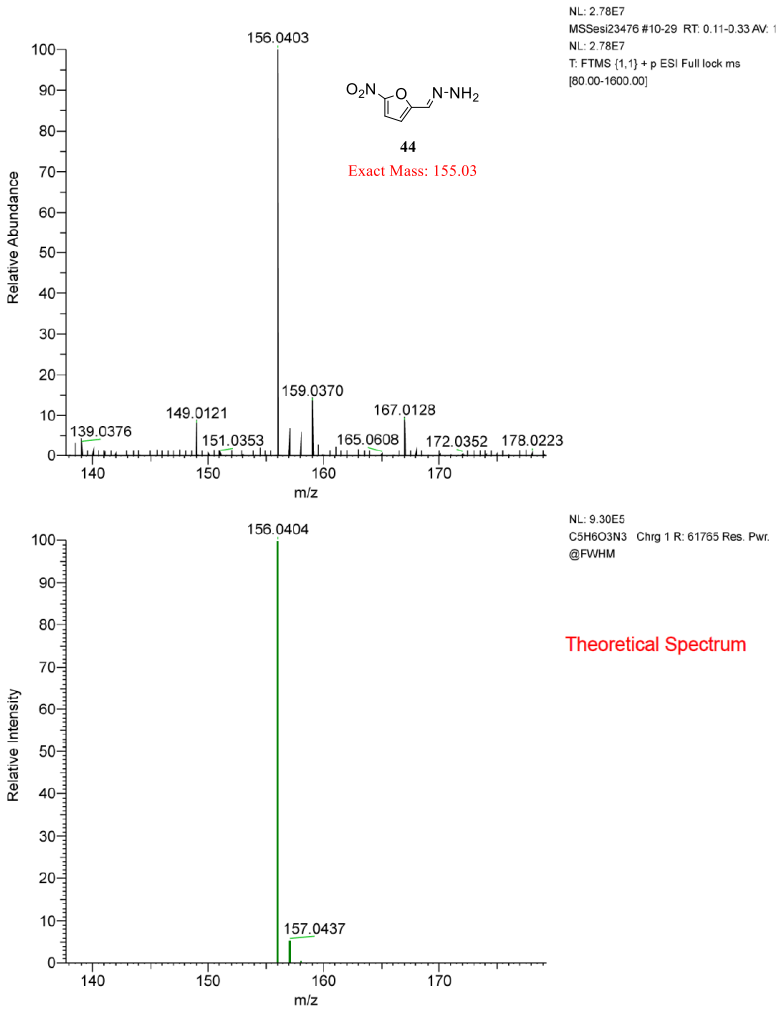

Figure 3.19 The obtained (top), and theoretical (bottom) HRMS spectra of 44.

As illustrated above (*cf.* Fig. 3.17) traces of water in DMSO-d_6 reacts with hydrazone **44**, and makes its ^{1}H NMR spectrum complex; thus, it was deduced that acetonitrile-d_3 ought to be the solvent of choice. Methanol-d_4 was also found not to be a suitable solvent for **44** (Section 3.3.1.1).

Given that almost exclusively all literature procedures (*loc. cit.*) used methanol as the solvent of choice for synthesis of **44**, upon its synthesis in Oxford, and in the face of its insolubility in dichloromethane and chloroform, its ^{1}H NMR was first recorded in methanol-d_4 (Fig. 3.20).

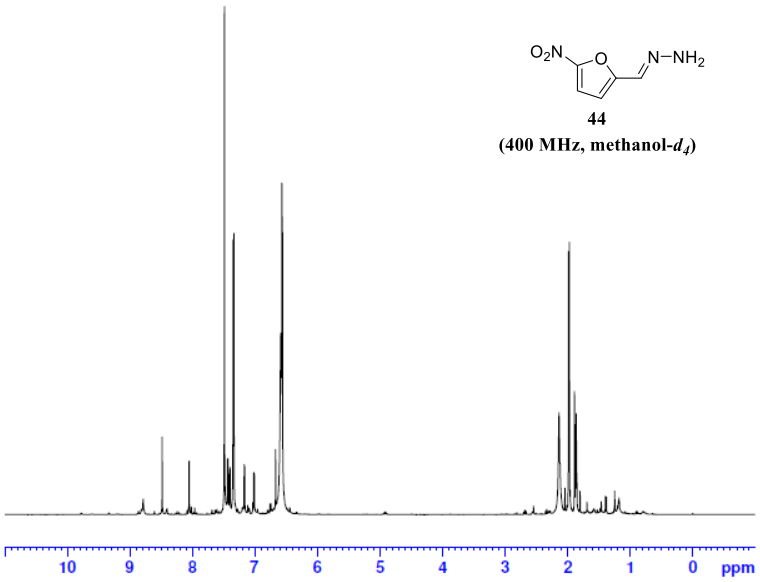

Figure 3.20 ^{1}H NMR spectrum of hydrazone 44 in methanol-d_4; *nota bene*: methanol reacts with 44 to give several undesired species (*vide infra*).

Unfortunately, despite our rigorous purification standards, and the fact that the purified hydrazone **44** appeared exclusively clean by TLC after flash column chromatography purification, its ^{1}H NMR spectrum in methanol-d_4 was a complete mess (Fig. 3.20). This anomaly led to a search for suitable deuterated solvent(s) for NMR studies of hydrazone **44**, which after trialling several deuterated solvents, acetonitrile-d_3 was deemed the most suitable solvent, and hydrazone **44** gave a clean ^{1}H NMR spectrum in acetonitrile-d_3 (Fig. 3.11).

The above findings clearly shed light on reactivity of methanol towards hydrazone **44**; thus, any synthesis of this compound in methanol could lead to impurities, and hence not a pure hydrazone **44**, in particular, should only the solid precipitates be collected without further purification. Knowing that methanol reacts with hydrazone **44**, it was then investigated as to whether methanol *in lieu* of the nucleophile would also react with the starting material, namely, 5-nitrofurfural, in this synthesis?!

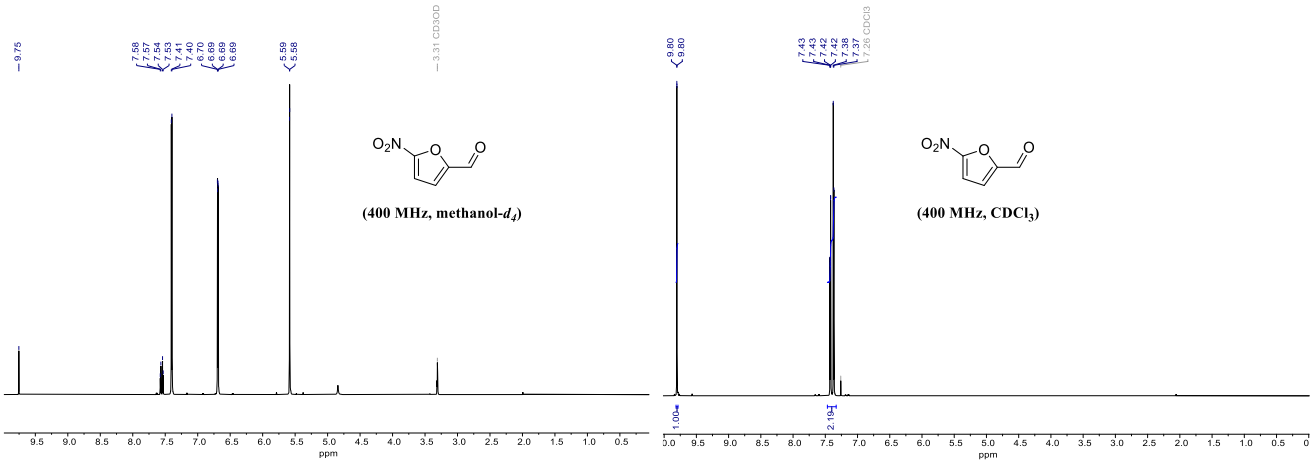

Figure 3.21 ^{1}H NMR spectra of 5-nitrofurfural in methanol-d_4 (left) and $CDCl_3$ (right). Methanol-d_4 reacts with 5-nitrofurfural to give a hemiacetal (left), as evidenced by the singlet at δ 5.59 from the methine adjacent to two oxygens in the thus obtained hemiacetal (*vide infra*).

Unlike hydrazone **44**, 5-nitrofurfural is sufficiently soluble in chloroform; to this end, its ^{1}H NMR spectrum in $CDCl_3$ was obtained and compared with that in methanol-d_4. It did not come as a surprise to discover that similar but different to hydrazone **44**, 5-nitrofurfural is equally susceptible to attack by methanol as its ^{1}H NMR spectrum in methanol-d_4 contains extra signals in the region δ 7.5 – 5.5, which were absent in its obtained spectrum in $CDCl_3$ (Fig. 3.21).

In an attempt to gain insight into the structural detail of product(s) of the 5-nitrofurfural reaction with methanol, 5-nitrofurfural in an acidified methanolic-d_x solution was subjected to further NMR analysis.

Reactions of 5-nitrofurfural with methanol-d_x could occur to form (Scheme 3.5):

- $-OCD_3$ substituted furan derivatives *via* S_EAr reaction.
- A deuterated hemiacetal/acetal or a species thereof *via* attack of methanol-d_x (*nota bene*: not methanolic-d_x acid) to the aldehyde moiety of 5-nitrofurfural.

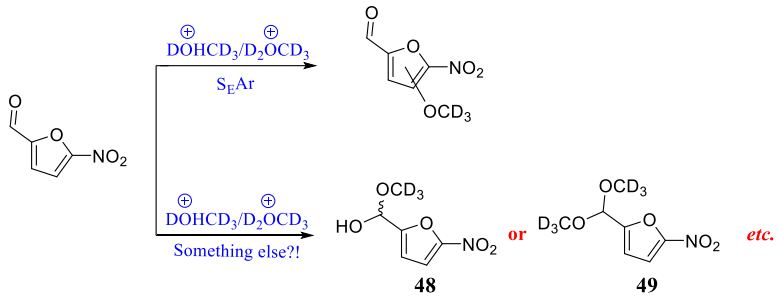

Scheme 3.5 Putative reactions of methanol with 5-nitrofurfural.

Analysis of the ^1H NMR spectrum of 5-nitrofurfural in methanol-d_4 (Fig. 3.21), on looking more closely, together with electron deficiency of the furan ring in 5-nitrofurfural despises any S_EAr reaction *i.e.* substitution of the furan ring, and suggests formation of hemiacetal **48** and/or acetal **49**.

It is unlikely for the reaction of methanol-d_x with 5-nitrofurfural to result in acetal **49**, such that even though the $-OCD_3$ moieties in acetal **49** are chemically equivalent, they are, in point of fact, anisochronous by virtue of the furan ring current (Fig. 3.28).

Thus, probably, almost certainly, two signals from the $-OCD_3$ moieties in acetal **49** should be observed in its ^{13}C NMR spectrum which is not the case, so it is very likely for the product to be hemiacetal **48** (Fig. 3.22).

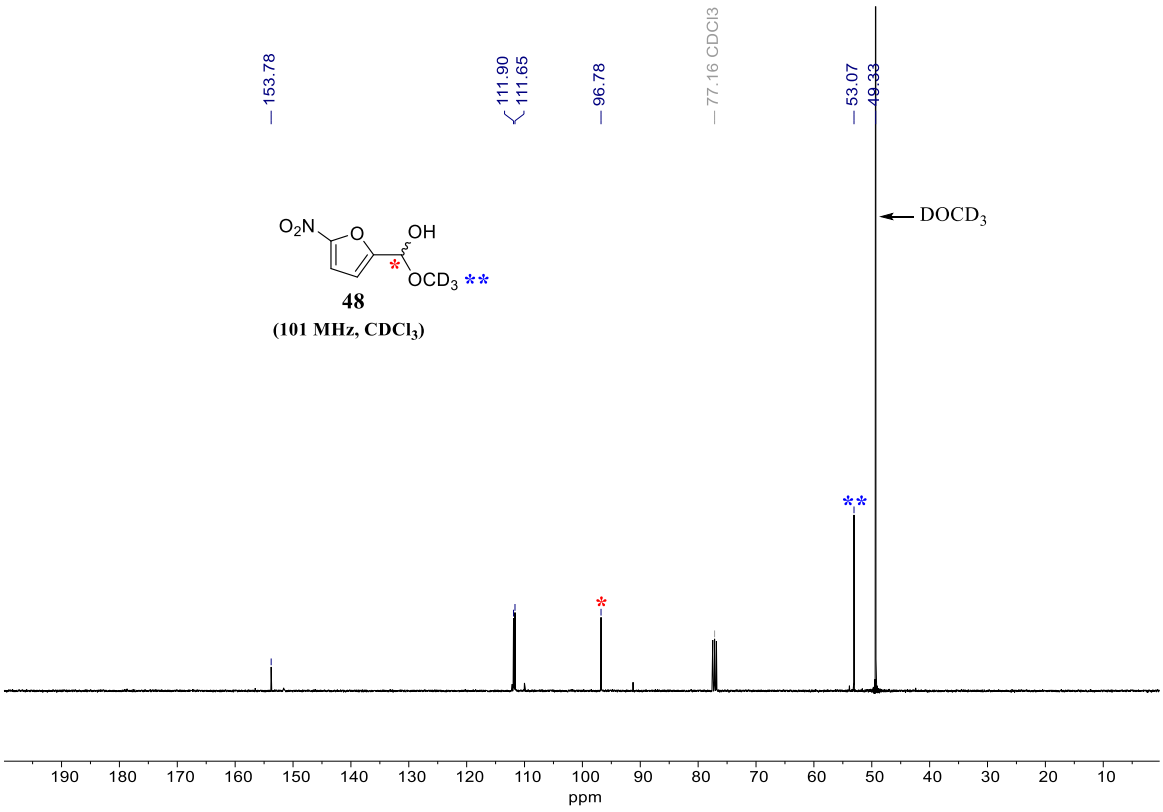

Figure 3.22 ^{13}C NMR spectrum of hemiacetal 48 plus acidified methanolic-d_x solution in $CDCl_3$.

As depicted in Fig 3.22, C-2 or C-5 gives rise to the signal at δ 153.8, C-3 and C-4 give rise to the signals at δ 111.9 and 111.7. The crucial signals are at δ 96.8 from the *ipso* carbon, and δ 53.1 from the –OCD_3 moiety.

Should we choose acetal **49**, two signals at *ca.* δ 53.0 would be expected; in point of fact, a much closer look at the spectrum reveals a very tiny signal to the left of the signal at δ 53.1, which should be from the other chemically equivalent but anisochronous –OCD_3 of acetal **49**; however, hemiacetal **48** preponderates over acetal **49**. Intriguingly, ^{1}H NMR spectra of 5-nitrofurfural in $CDCl_3$ and DMSO-d_6 did not differ much in terms of the overall pattern of signals (Fig. 3.23).

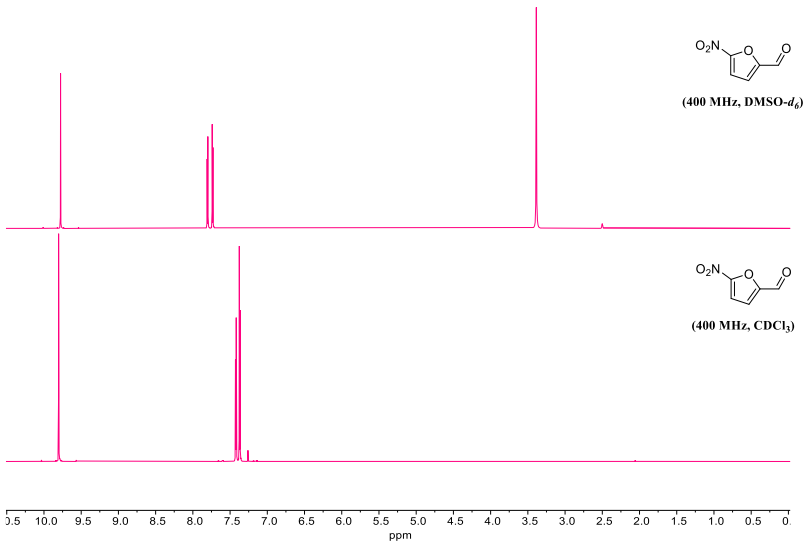

Figure 3.23 ^{1}H NMR spectra of 5-nitrofurfural in DMSO-d_6 (top), and $CDCl_3$ (bottom). The signal from the formyl moiety resonates at about δ 9.80 irrespective of the deuterated solvent in which the ^{1}H NMR spectra were recorded.

On the other hand, ^{1}H NMR signals at *ca.* δ 6.7 and 7.6 from protons on the furan ring in hydrazone **44** in DMSO-d_6 are wide apart *i.e.* ±1.0 ppm, this is not true for those from 5-nitrofurfural in DMSO-d_6, which are only *ca.* 0.1 ppm apart (Fig. 3.24).

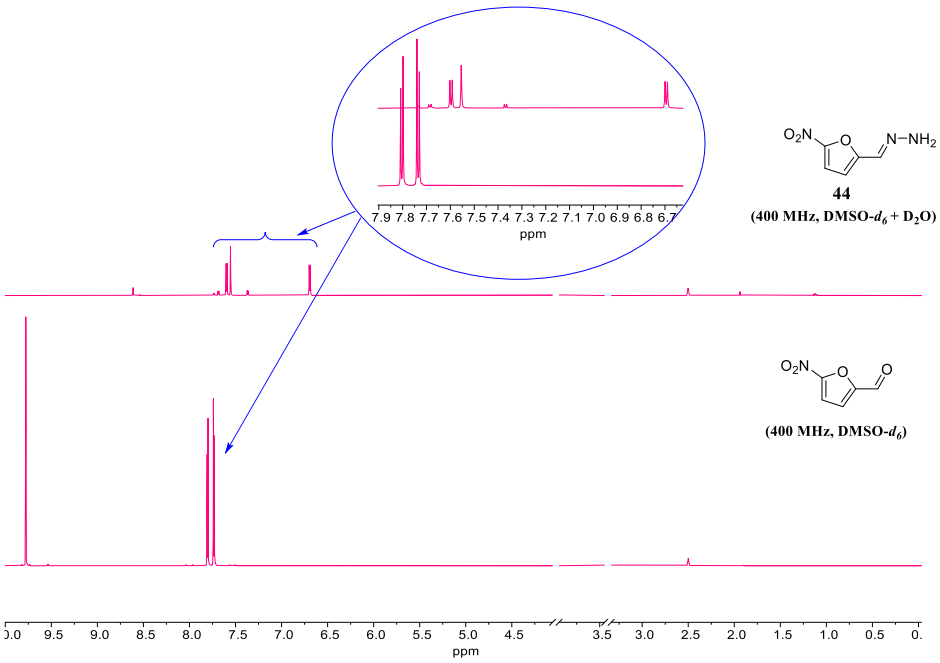

Figure 3.24 ^{1}H NMR spectrum of hydrazone 44 (top) stacked over that of 5-nitrofurfural (bottom) in DMSO-d_6; (*the pertinent section is magnified in the blue oval*).

It must be pointed out that the huge separation between signals (Fig. 3.17) from the furan protons in hydrazone **44** may be, at least in part, a result of conjugation, and the ensuing ring current stabilised by DMSO-d_6, which is not true for 5-nitrofurfural.

A regular 5-membered planar carbocyclic ring has an internal valence angle of 108°, though almost free of Baeyer strain, such a conformation creates a sizeable Pitzer strain (~ 42 kJ mol^{-1} in virtue of 10 pairs of eclipsing H–H) such that a regular cyclopentane becomes puckered, thereby reducing the sum of Pitzer and Baeyer strain to ~ 60% of that for a planar conformation.[539]

Thus, the most stable conformations of a regular cyclopentane are envelope and half-chair (Fig. 3.25), with the energy barrier between the two conformations being negligible *i.e.* 2.1 kJ mol^{-1},[540] a regular cyclopentane will not even pass the high energy planar conformation in a supposed '*conformational flux*'.

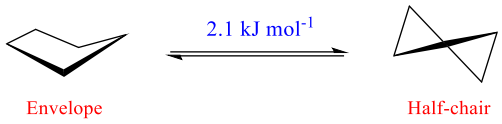

Figure 3.25 The most stable conformations of a regular cyclopentane.

Kilpatrick *et al.*[541] recognised that the envisaged '*conformational flux*' in a cyclopentane arises from oscillation of its carbons perpendicular to the plane of the ring, and thereupon imitating a rotating "bulge" (out-of-plane atom) around the ring, which has been referred to as '*pseudorotation*', even though, in point of fact, there is no movement in that direction.

To this end, for an asymmetric cyclopentane the aforementioned '*pseudorotation*' gives rise to a total of 20 unique energy minima (10 envelopes and 10 half-chairs), and an infinite number of quanta in between the aforementioned minima thereof.

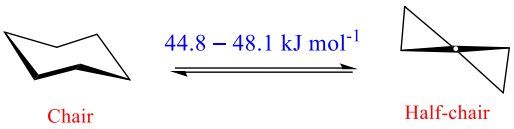

Figure 3.26 The global minimum (left), and maximum (right) conformations of cyclohexane.

Consequently, unlike cyclohexane for which its lowest energy minimum *i.e.* chair conformation is located in a deep energy valley, and with a conformational flux interconversion energy barrier of 44.8 – 48.1 kJ mol^{-1} (Fig. 3.26) between the chair *i.e.* global minimum and the half-chair *i.e.* global maximum conformations being nearly 20 times that of its cyclopentane counterpart,[542] the preferred conformation for a substituted cyclopentane is the one that minimises the sum of Pitzer and Baeyer strain in a manner that both interactions between the substituents on the ring and the substituents themselves with the ring are kept at the absolute minimum.

This phenomenon is also true for a regular cyclopentene,[543] and also cyclopentadiene even so with considerably less strain than both a regular cyclopentane and cyclopentene,[544,545] alongside most of their corresponding heterocyclic counterparts;[546] in point of fact, tetrahydrothiophene which is isoelectronic with THF, exists exclusively in its half-chair conformation with the thioether moiety in the least puckered middle region (Fig. 3.27). [547]



Figure 3.27 The most stable conformation of tetrahydrothiophene.

In recognition of the above, it is conceivable that the addition of hydrazine to 5-nitrofurfural renders a '*pseudoumpolung*' whereby the ensuing plausible conjugative effect pushes the furan ring into a nonplanar puckered heterocyclopentene conformation, facilitating a conjugated system (Fig. 3.28); in essence, setting up a weak induced '*ring current*' in an applied magnetic field, such that one of the protons on the furan ring falls inside the ring, and thence, is upshifted at *ca.* δ 6.7 in ^{1}H NMR spectrum of hydrazone **44**.

On the contrary, the other proton is pushed outside the ring current and downshifted at *ca.* δ 7.6, bringing about a huge shift, almost ±1.0 ppm between the signals from these two protons in ^{1}H NMR spectrum of hydrazone **44**, which are otherwise not chemically too different in say, 5-nitrofurfural (Fig. 3.24).

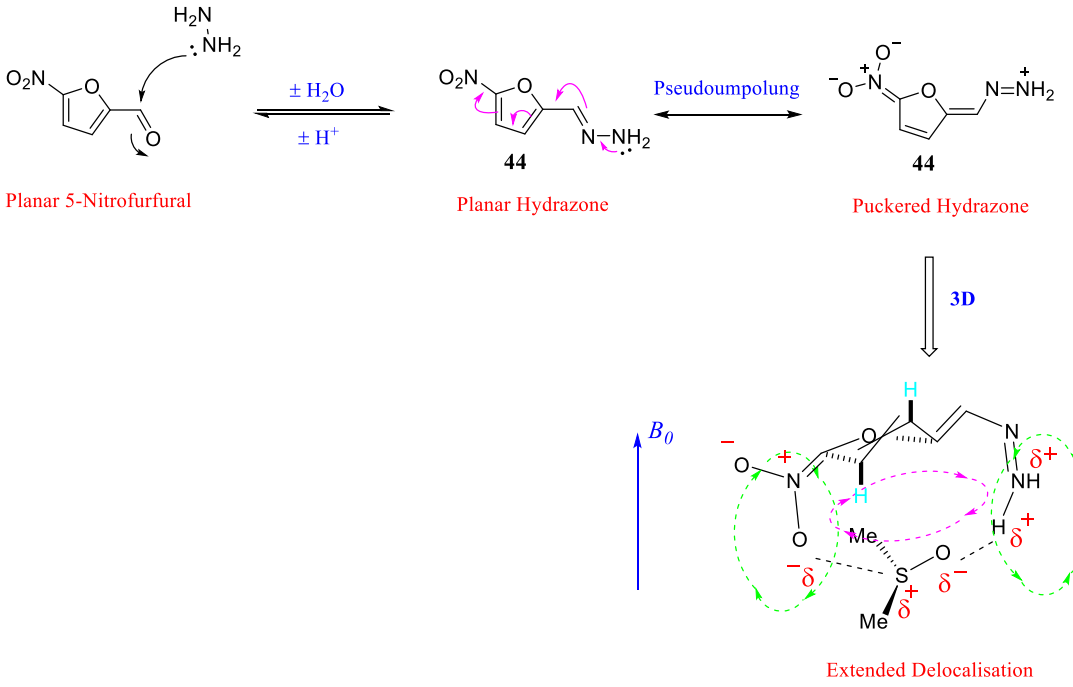

Figure 3.28 It can be hypothesised that the extended electron shuffle assisted by DMSO pushes the furan ring into a puckered conformation in virtue of the induced ring current (purple) in the applied magnetic field, resulting in ~ ±1.0ppm shift between the signals from protons (light blue) in ^{1}H NMR spectrum of hydrazone 44.

3.3.1.3 Conjugative Effects on Nitrofuranyl Hydrazone Colour

"One can no longer just mix things; sophistication in Physical Chemistry was the base from which all chemists – including the ORGANIC – must start"

Sir Christopher Kelk Ingold

Hitherto, all the literature precedents including that of Li *et al.*[530] have described hydrazone **44** as a yellow solid; however, this compound, in point of fact, is an orange solid (Fig. 3.18), and the intrinsic colour of this peculiar compound can be a good indication of its purity. As illustrated above, methanol can react with hydrazone **44** to yield unwanted by-products, which perturb its colour; in effect, solutions of hydrazone **44** in methanol have a yellow tinge.

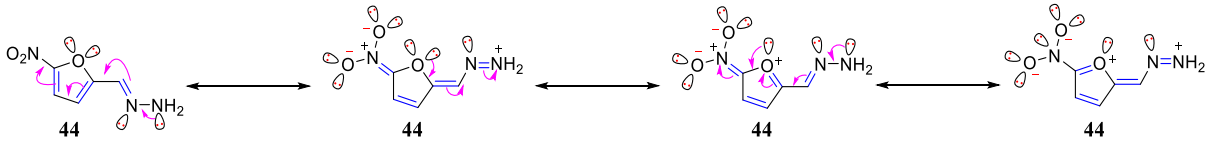

Figure 3.29 A set (*nota bene: there are more*) of canonical structures of hydrazone 44.

As depicted in Fig. 3.29, there are a total of eight delocalised π electrons in hydrazone **44** which set up a conjugated system, leading to π bonds elongation and lower energy gaps between the pertinent *ungeraden* and *geraden* molecular orbitals to such an extent that the 18 non-bonding electrons in this molecule can also participate in the delocalisation; as a result, the fundamental electronic excitation of hydrazone **44** absorbs greenish-blue light (λ_{max} ~ 480 – 490 nm),[548] and hence this compound appears as an orange solid. Henceforth, whereas energy is variant in all privileged frames of reference by all observers, the change in energy is invariant in all privileged frames of reference for the same observers. By the same token, the fundamental electronic excitation between the pertinent *ungeraden* and *geraden* molecular orbitals of inherently coloured organic compounds is invariant in a given polyene system in any privileged frame of reference, irrespective of variant energies of different molecules upon which the conjugated system is conferred, in that privileged frame of reference by all observers.

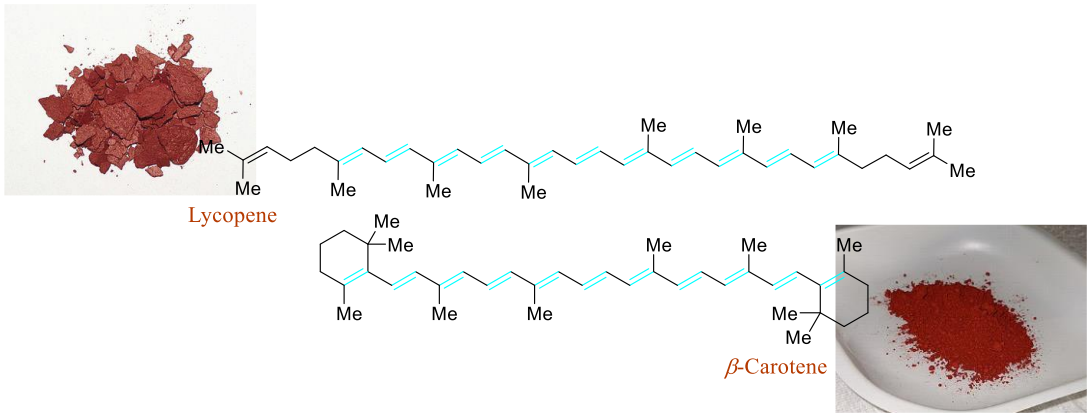

Figure 3.30 Thanks to their very similar conjugated systems, lycopene & *β*-carotene are of the same colour. [*Image Source: Wikipedia (Accessed September 2021)*]

For example, albeit lycopene and *β*-carotene are energetically variant in a privileged frame of reference, both exhibit the same characteristic colour to all observers in that frame of reference, in virtue of their pretty much identical conjugated systems (Fig. 3.30).

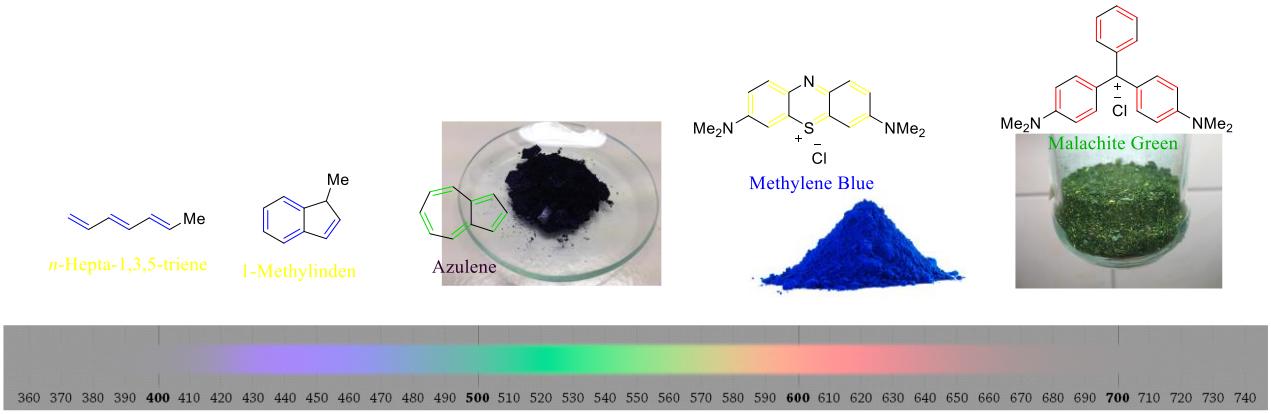

Figure 3.31 Increasing conjugation shifts the absorption spectrum towards a longer wavelength. [*Images Source: Wikipedia (Accessed September 2021)*]

It is well established that the more extended a conjugated polyene, the lower the energy gap between its $HOMO_u$ and $LUMO_g$.[549] Thus, as a rule of thumb, the more π electrons delocalise in a conjugated polyene system, the lower the energy gaps between its *ungeraden* and *geraden* molecular orbitals, which in turn this effect stabilises the system relative to that with equal but isolated π electrons.

It follows that increasing the length of conjugation leads to a bathochromic fundamental electronic excitation (Fig. 3.31). For this reason, *n*-hepta-1,3,5-triene with a six π electron conjugated system absorbs blue light, and appears as a deep-yellow solid.[550] On the other hand, azulene with ten delocalised π electrons in its conjugated system absorbs green light, and exhibits an intrinsic purplish[551] colour (Fig. 3.31).

Inasmuch as the fundamental electronic excitation is invariant in all privileged frames of reference by all observers, the number of delocalised π electrons in a conjugated system should in the absence of exceptions *e.g.* tunnelling[552] *etc.*, dictate the intrinsic colour of its corresponding polyene, provided that the conjugated system is not affected by other factors such as orbital interactions with adjacent non-bonding electrons *e.g.* auxochromic effects, Kuhn's[553] and Woodward's[554] rules *etc.*

To this end, empirically six to twelve delocalised π electrons in an uncomplicated linear conjugated polyene bring about a fundamental electronic excitation with $\lambda_{max} \sim 450 - 550$ nm, giving rise to coloured compounds from yellow such as *n*-hepta-1,3,5-triene to purplish-pink azulene that we have seen above, and so forth.

In view of the above, hydrazone **44** with eight delocalised π electrons (Fig. 3.29) similar to 1-methylinden should at a minimum, in theory, though not of necessity, absorb blue light ($\lambda_{max} \sim 430 - 480$ nm).[548] However, as reasoned above, the implied conjugative effect lowers the energy gaps between its *ungeraden* and *geraden* molecular orbitals such that the π orbitals would be in a much closer proximity to the non-bonding orbitals that accommodate more than twice as much electrons as that in the π bonding orbitals.

At this point, in practice, the fundamental electronic excitation of hydrazone **44** responsible for its orangish colour (λ_{max} ~ 480 – 490 nm)[548] must be probably, almost entirely due to one of the allowed $n_u \rightarrow \pi_g$ excitations with the highest transition probability, which would not be the case in the absence of its extended conjugation, and as purported in the literature (*loc. cit.*) would have been of a yellow colour.

The belief that the position of the absorption maximum is directly proportional to the length of the conjugated system implies that lycopene and *β*-carotene, both having 11 conjugated π bonds in which 22 π electrons shuffle (Fig. 3.30) ought to have a much longer λ_{max} than say, hydrazone **44** with only four conjugated π bonds (Fig. 3.29).

Brushing the effects of non-bonding orbitals in hydrazone **44** aside, the λ_{max} of lycopene/*β*-carotene seems to be close to that of hydrazone **44**, as all exhibit orangish-red colour.

This discrepancy stems from the fact that for a 1-dimensional observable '*particle in a box*',[555] its invariant symmetrical potential $V(x)$ with respect to space inversion is as follows:

Eq. 3.1 $$V(x) = V(-x)$$

The parity transformation ($\hat{P}$) of the above eigenfunction gives the following:[556]

Eq. 3.2 $$\hat{P}\, V(x) = V(-x)$$

Inasmuch as the potential energy (V) in Eq. 3.1 is centrosymmetric, then its Hamiltonian operator ($\hat{H}$) commutes with $\hat{P}$ to give the following relation:[557]

Eq. 3.3 $$[\hat{H}, \hat{P}] = 0$$

Thus, the following argument should be true for any eigenfunction of $\hat{H}$:

Eq. 3.4 $$\hat{H}|\psi_E(x)\rangle = E|\psi_E(x)\rangle = E\hat{P}|\psi_E(x)\rangle$$

Eq. 3.4 states that $\hat{P}|\psi_E(x)\rangle$ is an eigenfunction with the same eigenvalue (E), which implies that E would be a '*degenerate*' eigenvalue; however, that is not true in virtue of linear dependency of the eigenvectors $|\psi\rangle$ and $\hat{P}|\psi\rangle$.[558]

On the other hand, for the '*particle in an n-dimensional box*' *i.e.* '*Hilbert space*'[559] its centrosymmetric potential $V(r)$ is only dependent on the distance from the centre, and its eigenvector angular momentum $\hat{L}^2$ is as follows:[560]

$$|l, m\rangle$$

Where l is the total angular momentum, and m is its projection along a given axis. Since $\hat{L}^2$ is a unitary operator *i.e.* for different observables m can have the same l, and hence linearly independent, as such E_l is a '*degenerate eigenvalue*'.

In recognition of the above, even though both lycopene and β-carotene possess an 11 linear conjugated π bond system, but because they are centrosymmetric, half of their molecular orbitals '*degenerate*'. To this end, lycopene and β-carotene behave as if they only shuffle five or six conjugated π bonds, which is well in agreement with the empirical observations *i.e.* they appear as orangish-red pigments.

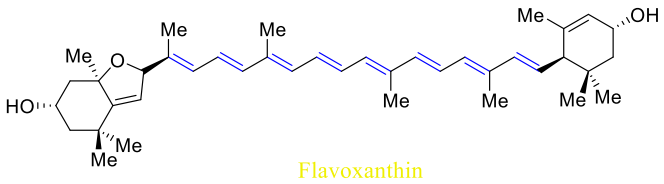

Flavoxanthin

Figure 3.32 Flavoxanthin with its eight linear conjugated π bond system shown in blue.

In contrast, a non-centrosymmetric polyene such as flavoxanthin with an eight linear conjugated π bond system (Fig. 3.32), appears exclusively as a bright yellow solid.[561]

This might seem a bit puzzling as the longer a conjugated system, the longer its λ_{max}. However, even though the gaps between the *ungeraden* and *geraden* molecular orbitals of flavoxanthin should be smaller than say, that of lycopene, but because the energy levels are getting much closer, then the fundamental electronic excitation is no longer $S_0 \rightarrow S_1$ and higher energy excitations will have a much higher transition probability to an extent that they preponderate over the lowest energy excitation, and hence flavoxanthin absorbs blue light, but lycopene absorbs the lower energy blue-green light.

Equally, whatever concoction was obtained by Li *et al.*[530] and their predecessors, all must have absorbed the higher energy blue light, hence the resulting yellow solid, as they described in their publication for hydrazone **44**.

Nevertheless, in contrast to the literature precedents, as delineated above, the true pure hydrazone **44** is an orangish solid (Fig. 3.18) in virtue of its unique conjugated π bond system.

3.3.1.4 Synthesis of Sulfoximinyl & Sulfonyl Spacers

The potentially preferred pharmacokinetics of sulfoximines[562,563] compelled attempting installation of this moiety *in lieu* of the previously reported sulfones.[515] Since the identification and characterisation of the first sulfoximine in 1949,[564] there have been rapid advances in its utility and scope in various chemical sectors such as catalysis,[565] late stage C–H functionalisation,[566] agrochemicals,[567] drug design[568] and beyond; all thanks to development of more feasible and facile synthetic strategies.[569,570]

Recently Bull and coworkers[571] have reported a direct and straightforward oxidation of sulfoxides to sulfoximines. Given that iodobenzene diacetate can oxidise thiols,[572,573] and inasmuch as no direct oxidation of benzylic thiols to their corresponding sulfoximines have been reported as yet, we bit the bullet and attempted oxidation of benzylic thiols to sulfonimidates, so as to be utilised in our potential NInC therapeutics (Scheme 3.6).

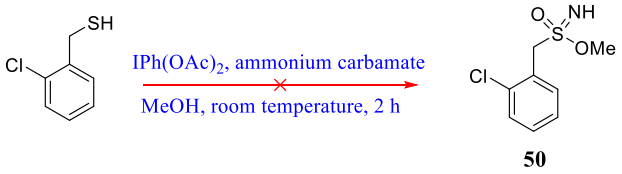

50

Scheme 3.6 Attempted synthesis of sulfonimidate 50 using iodobenzene diacetate and ammonium carbamate.

Rattanangkool *et al.*[574] have reported that in the presence of iodobenzene diacetate, thiols yield their corresponding disulfides; in point of fact, to our regret, and as was envisaged, the synthesis of sulfonimidate **50** using iodobenzene diacetate and ammonium carbamate according to the procedure of Bull and coworkers (*loc. cit.*) was not feasible, and disulfide **51** was isolated instead, as evidenced by its ^{1}H NMR and LC-MS spectra *m/z* (ESI) 359 (M^{+} + formate, 18%), 358 (100), 231 (10) (Fig. 3.33).

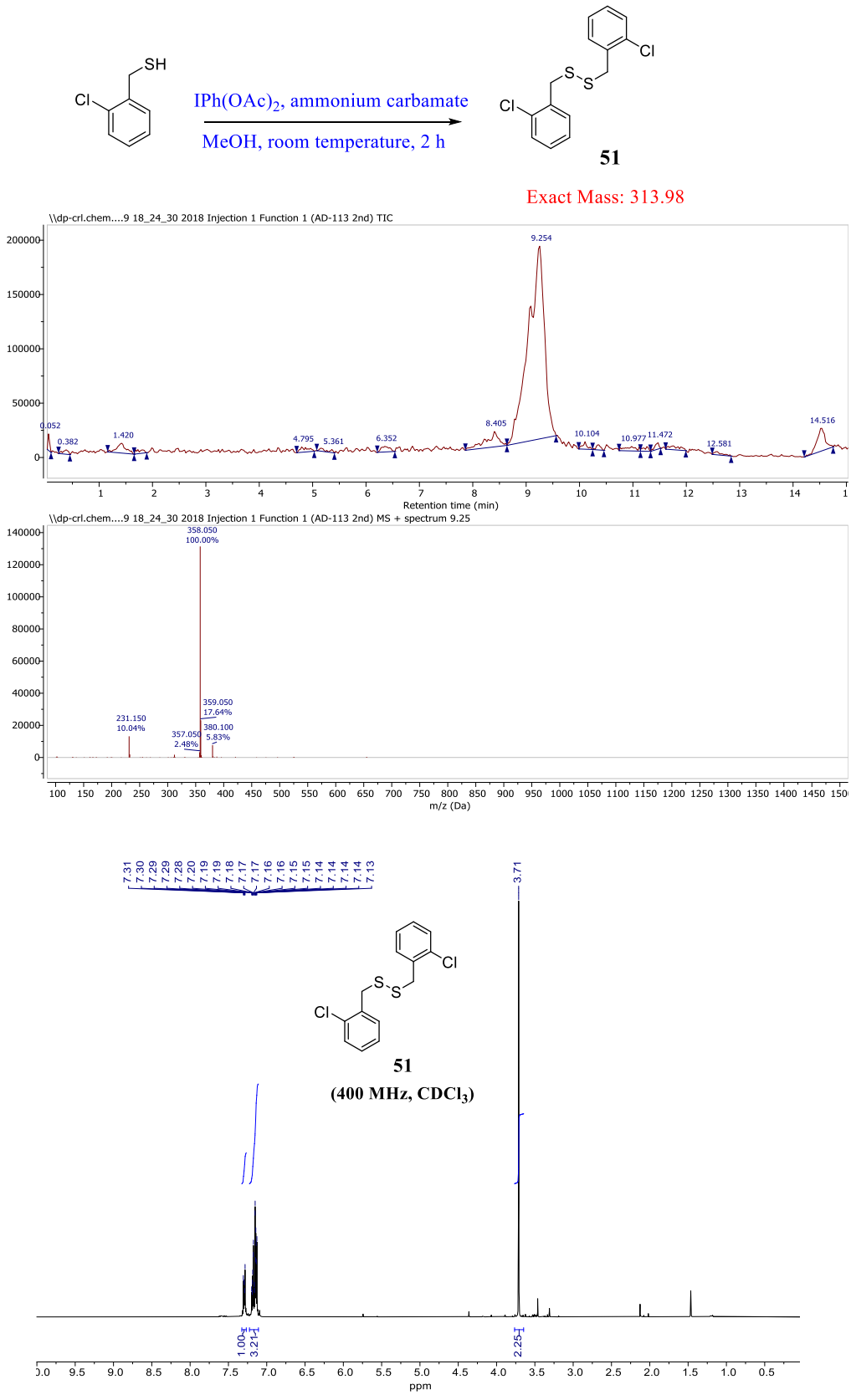

Figure 3.33 LC-MS and ^{1}H NMR spectra of disulfide 51. The singlet from the methylenes at δ 3.71 together with the mass at 359 *m/z* (M^{+} + formate, 18%) is indicative of dimer 51.

In the face of our unsuccessful attempt at synthesis of sulfonimidate **50**, and in order to verify and validate this synthetic methodology for our desired sulfonimidates, the synthesis of its phenyl counterpart, namely, sulfonimidate **52** was attempted (Scheme 3.7). Hardly surprisingly, in contrast to the literature precedents (*loc. cit.*) even this route to sulfonimidate **52** was unsuccessful, which casts doubt on the validity of this methodology to the previously reported sulfonimidates.

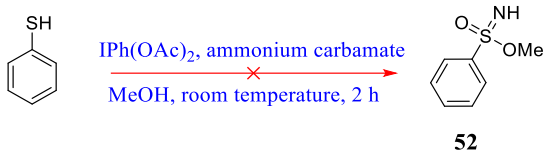

52

Scheme 3.7 Attempted synthesis of sulfonimidate 52 using iodobenzene diacetate and ammonium carbamate.

Intriguingly, the purified product of the reaction of phenyl mercaptan with iodobenzene diacetate and ammonium carbamate was further subjected to LC-MS analysis, which revealed sulfonimine **53** *in lieu* of sulfonimidate **52** (Fig. 3.34).

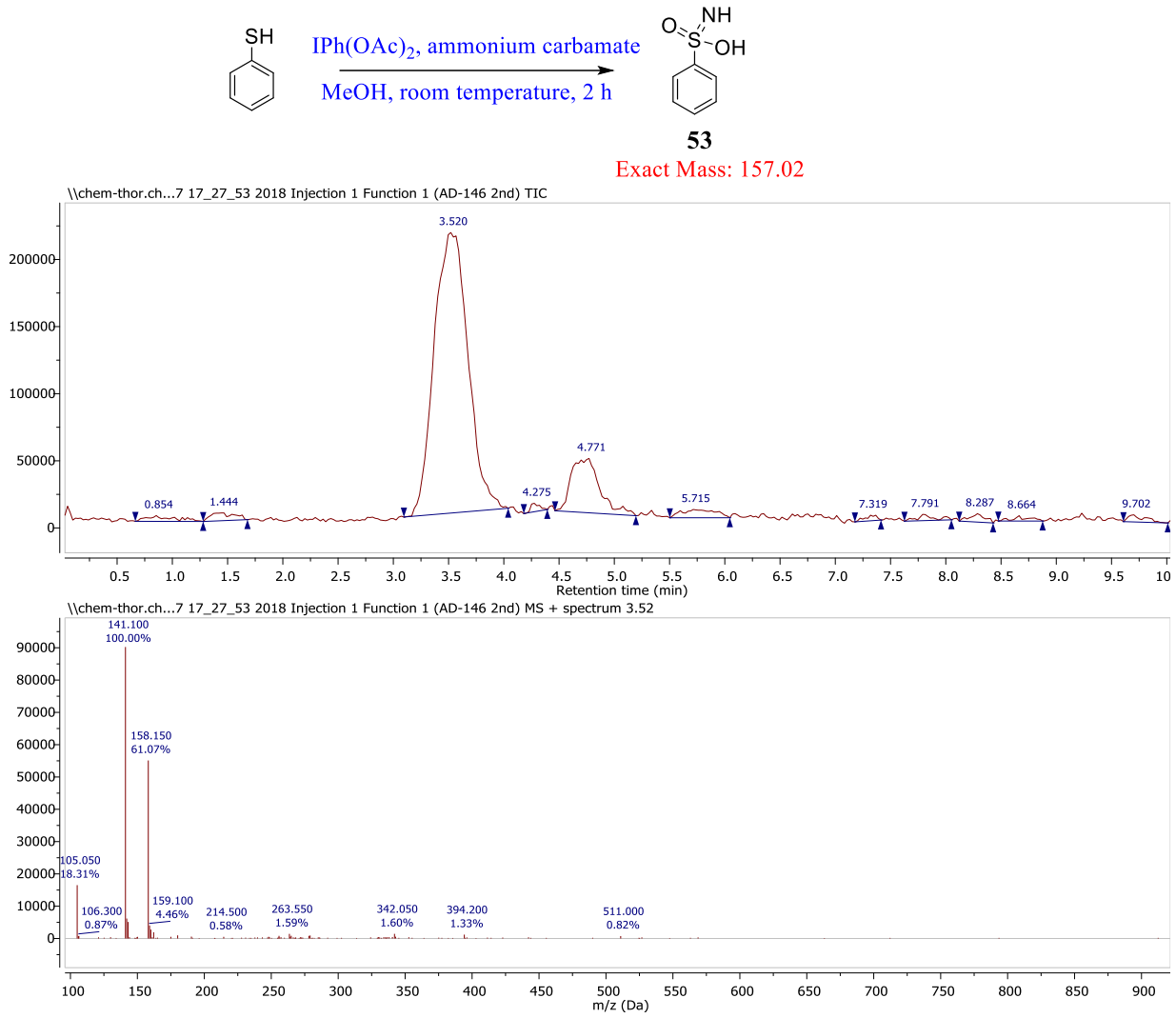

Figure 3.34 LC-MS spectra of the sulfonimine 53.

It was puzzling to stumble across sulfonimine **53** even though, the reaction was carried out in methanol, and it was conceivable that methanol should displace the hydroxyl group so as to furnish sulfonimidate **52**; however, it appeared not to be the case.

Suspicions arose that sulfonimidate **52** might well be the obtained product, but getting hydrolysed on the LC-MS. To this end, the aforementioned reaction was carefully monitored by LC-MS and despite the previously reported assumptions that sulfonimidate **52** is the thermodynamic product (*loc. cit.*), sulfonimidate **52**, in point of fact, exclusively formed at the outset, however though, overtime it was apparently converted to sulfonimine **53** (Fig. 3.35).

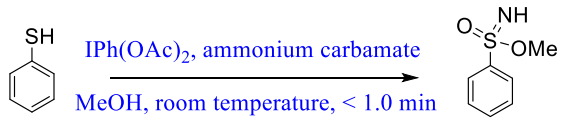

52

Exact Mass: 171.04

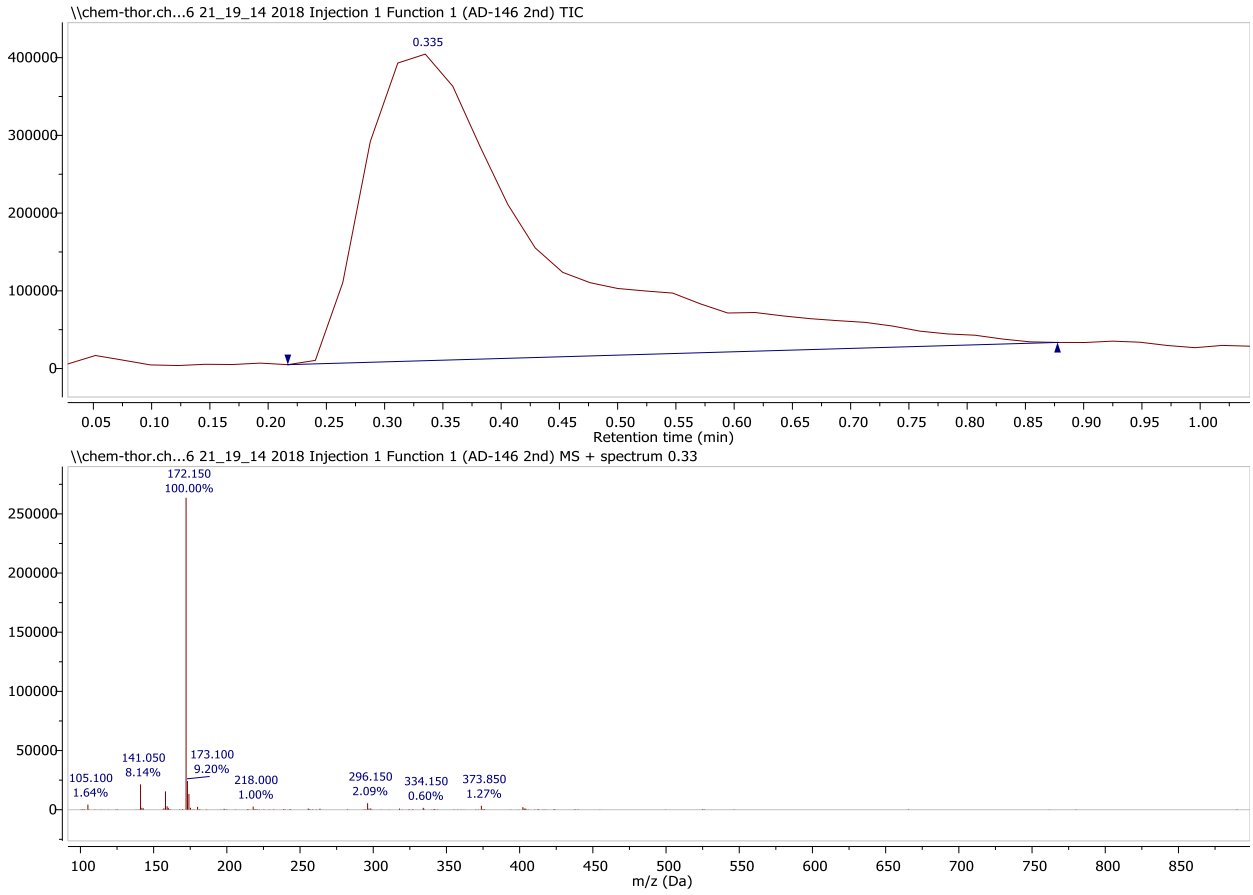

Figure 3.35 LC-MS spectra of sulfonimidate 52.

Given that sulfonimidate **52** was observed by LC-MS, its conversion to sulfonimine **53** cannot be due to the medium in which the LC-MS analysis was carried out, as sulfonimidate **52** was stable under such conditions.

Knowing that sulfonimidate **52** was rapidly formed at the very beginning of the reaction, the same might be true for its benzylic counterpart, and the fact that a direct oxidation of benzylic thiols to sulfoximines remains an insoluble phenomenon in the literature, extensive optimisation was carried out so as to achieve such a useful synthetic transformation (Fig. 3.36).

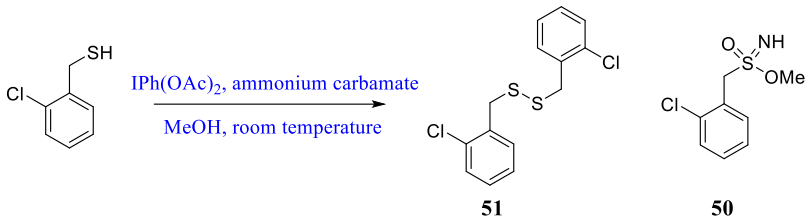

51 **50**

Entry	$IPh(OAc)_2$*	$NH_4[H_2NCO_2]$*	Argon/air	Time (h)	51:50 (%)†
1	4	4	air	2	100:0
2	4	4	argon	12	100:0
3	4	4	argon	96	100:0
4	2	2	argon	1.5	100:0
5	2	4	argon	2	100:0
6	6	4	argon	16	0:0
7	8	8	air	2	80:20
8	10	10	argon	2	90:10

Reagents and reaction conditions: 2-chlorobenzyl mercaptan (1.0 mmol, 1.0 equiv.). * Equivalent amounts with respect to 2-chlorobenzyl mercaptan; methanol (5.0 ml). † Determined by LC-MS after the specified time.

Figure 3.36 Optimisation data for oxidation of 2-chlorobenzyl mercaptan.

Unfortunately, however, despite numerous experiments carried out under a variety of conditions (Fig. 3.36), the desired oxidation, namely, the conversion of 2-chlorobenzyl mercaptan to sulfonimidate **50** was very poor and deemed futile; thus, this route to formation of sulfonimidate **50** had to be abandoned, and attention was directed to the use of sulfonamides.

In contrast to the unsuccessful sulfonimidation of 2-chlorobenzyl mercaptan, 4-bromobenzyl sulfonyl chloride easily reacted in presence of a nucleophilic catalyst *i.e.* pyridine, to give sulfonyl hydrazone **54** in a moderate yield *i.e.* 44% (Scheme 3.8).

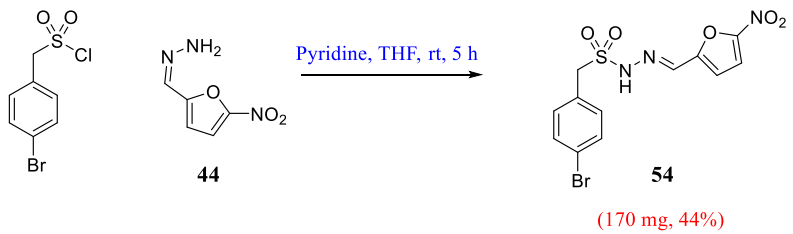

44 **54**

(170 mg, 44%)

Scheme 3.8 Synthesis of sulfonyl hydrazone 54.

However, in an alternating unfortunate manner, the borylation of thus obtained aryl bromide **54** turned out to be unsuccessful (Scheme 3.9).

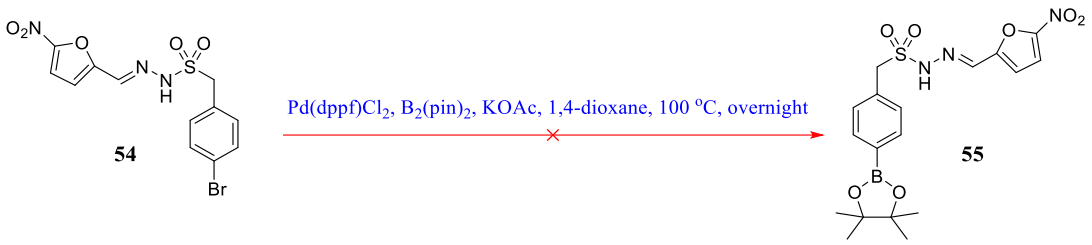

Scheme 3.9 Attempted borylation of aryl bromide 54.

3.3.1.5 Synthesis of InCs & Their Borylation

Boronate ester **55** could be coupled to iodo-InC **57** so as to furnish the desired NInC (Fig. 3.10); however, in the face of yet another unsuccessful operation, it was aimed to reverse the partners of this coupling reaction, and couple an InC boronic acid to the previously synthesised aryl halide **54** instead. InC **56** was successfully synthesised in good yields *i.e.* 64% using the reported procedures[515] in two steps (Scheme 3.10).

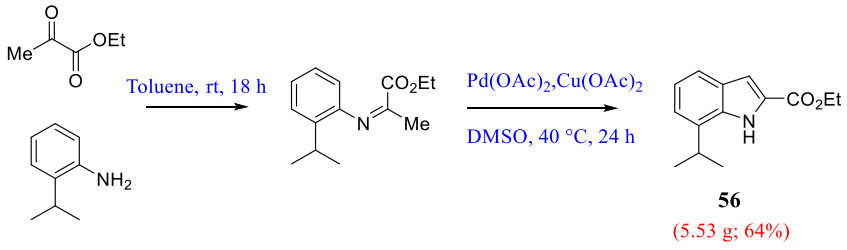

Scheme 3.10 Synthesis of InC 56 from readily available commercial reagents.

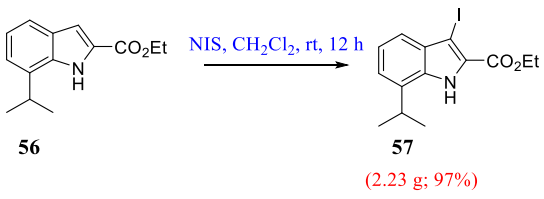

Scheme 3.11 Synthesis of iodo-InC 57.

It was well-established in Oxford that stirring InC **56** with NIS at ambient temperatures in an inert solvent *i.e.* dichloromethane overnight, would yield iodo-InC **57** (Scheme 3.11).

As anticipated, the above was indeed the case, and the desired iodo-InC **57** was synthesised in an astonishing yield (*i.e.* 97%) and purity, after flash column chromatography purification, as evidenced by ^{1}H NMR (Fig. 3.37).

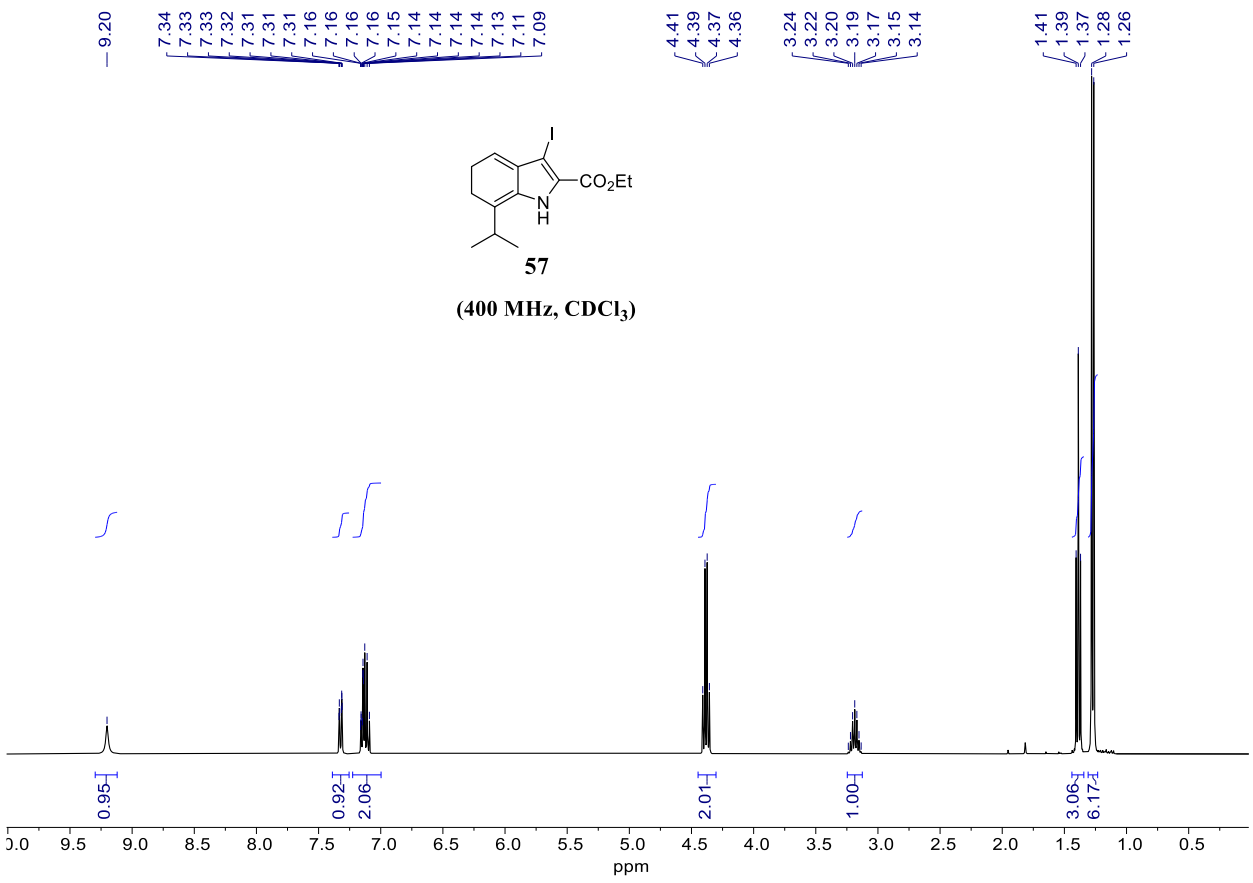

Figure 3.37 ^{1}H NMR spectrum of iodo-InC 57. The aromatic indole protons resonate at δ 7.32 & 7.23 – 7.00, that from the ethyl ester moiety at δ 4.38 & 1.39, and the isopropyl moiety at δ 3.19 & 1.27; for full characterisation and *J* values in Hz *cf.* Experimental p. S48.

To begin with, the next step in our journey towards the target NInC heterodimers, namely, borylation of the thus obtained iodo-InC **57** was also unsuccessful using the standard Miyaura borylation[575] conditions (Scheme 3.12).

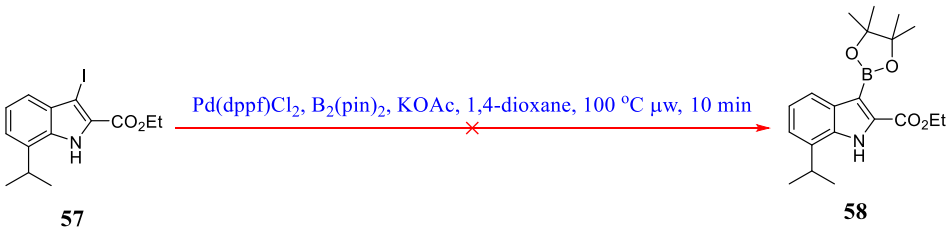

57 **58**

Scheme 3.12 Unsuccessful Miyaura Borylation of iodo-InC 57.

However, in an innovative and unprecedented fashion, combining the Buchwald amination reaction conditions and catalysts with that of Miyaura borylation, furnished the desired boronate ester **58** in acceptable yields *i.e.* ~ 30% (Scheme 3.13), and purity as evidenced by its ^{1}H and ^{11}B NMR spectra (Fig. 3.38).

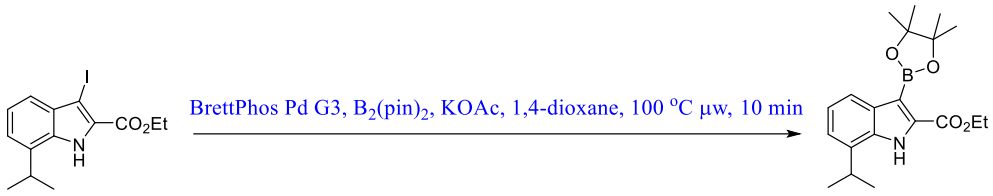

57 **58**

(50 mg; 30%)

Scheme 3.13 A novel Buchwald borylation.

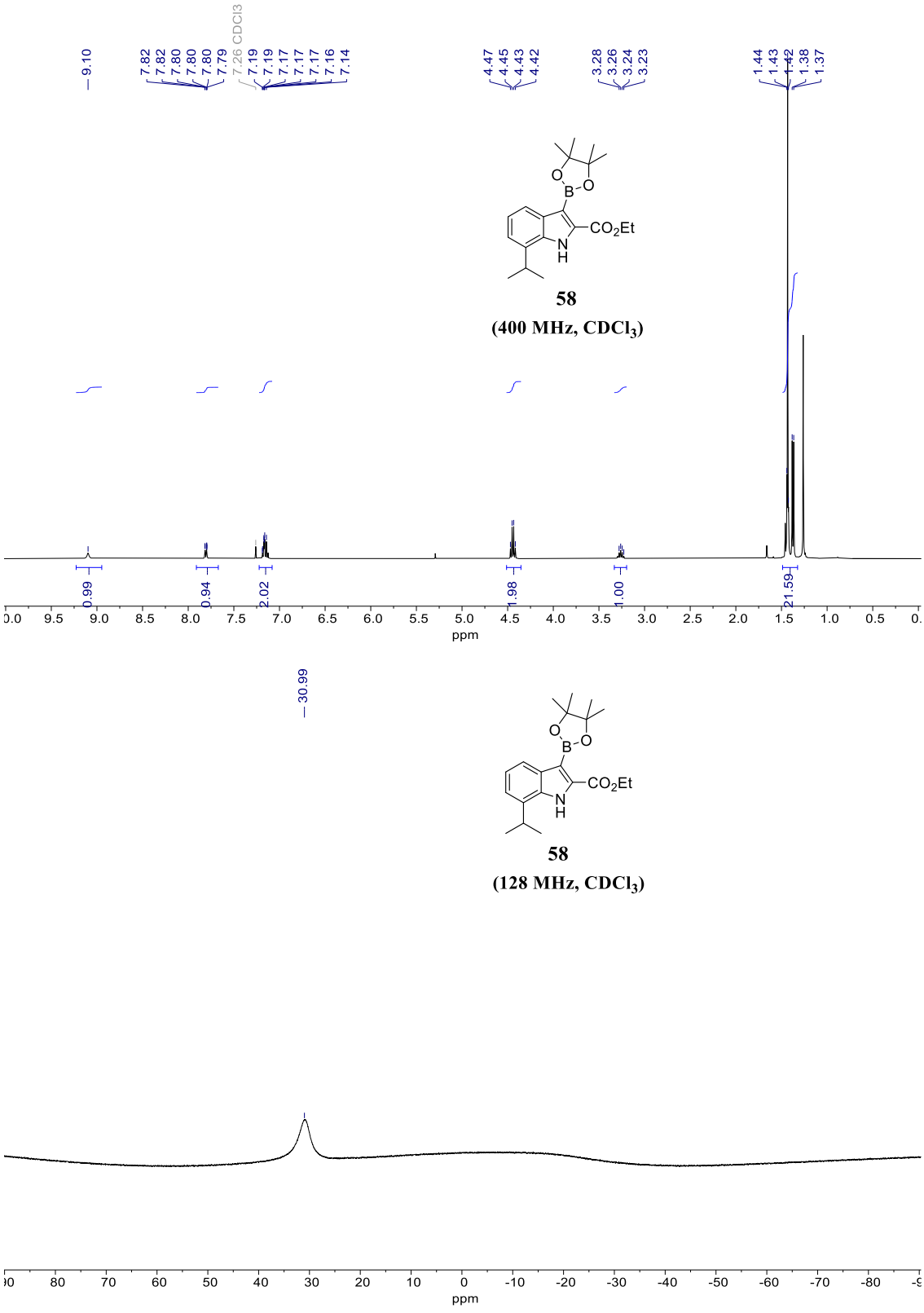

Figure 3.38 ^{1}H & ^{11}B NMR spectra of boronate ester 58. Intriguingly, the signal from boron in 58 resonates at about the same field as diazaborines (Appendix I) in the ^{11}B NMR spectrum of 58, in spite of being non-aromatic.

Despite the success of synthesising boronate ester **58**, unfortunately, however to our dismay, in the face of numerous experiments carried out under a variety of conditions (Scheme 3.14), the final step, namely, the coupling of boronate ester **58** to its haloaryl partner **54**, could not be accomplished, and hence this route to formation of our desired NInC heterodimer **59** was abandoned.

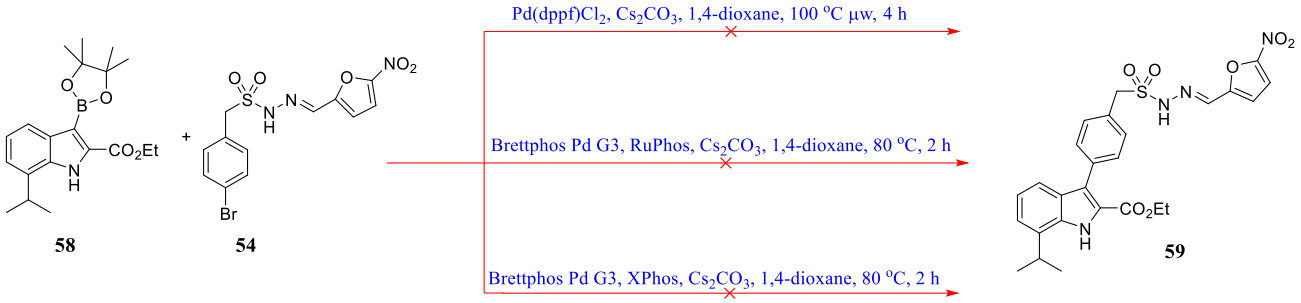

Scheme 3.14 Representative examples of failed attempts at synthesis of NInC 59.

The coupling of boronate ester **58** with bromoaryl **54** proved extremely difficult, in part by virtue of the fact that firstly, boronate **58** is highly unstable and undergoes protodeborylation.[576,577] Secondly, the same aforementioned phenomenon significantly reduces the yield of borylation of iodo-InC **57**, and in most cases as observed by others in Oxford (unpublished data) completely inhibits its formation in the first place. Moreover, boronate ester **58** appeared as a sticky wax which made its handling very problematic, in particular, on a small scale *i.e.* µmol quantities. Last but not least, the coupling reagents themselves, namely, both the hydrazone and indole are notoriously troublesome in the Suzuki coupling and poison the palladium catalyst.

Considering that 5-nitrofurfual is potentially the antibacterial agent in nitrofurantoin and its derivatives thereof (Section 3.2), it will be released upon hydrolytic cleavage of the hydrazone linker; then the other essential constituent of this associative heterodimer is mainly the InC fragment. To this end, it was deemed worthwhile to eliminate the problematic spacer from this series of prospective heterodimers in order to evaluate bioactivities of this two set of fragments, namely, hydrazones **54** and **60**, separately (Fig. 3.39).

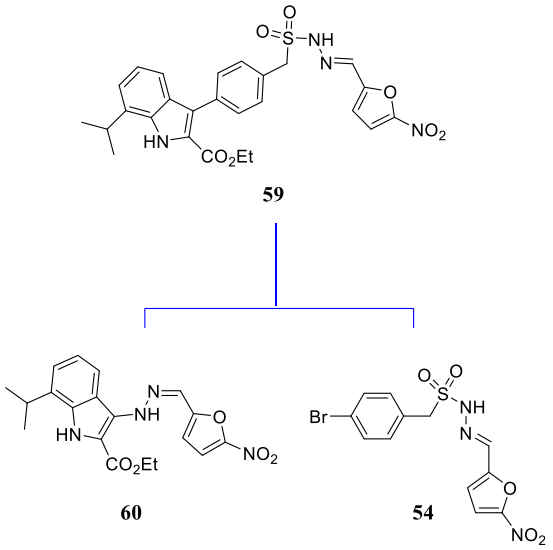

Figure 3.39 Fragments of the prospective NInC 59 suitable for *in vivo* studies.

3.3.1.6 Synthesis of NInC Esters via Buchwald Amination

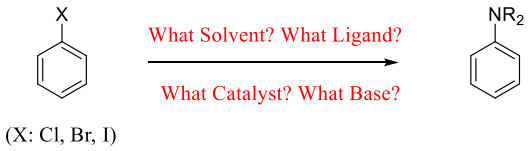

Figure 3.40 Governing factors in Buchwald amination.

There are essentially four factors by which the Buchwald amination is governed (Fig. 3.40), and are as follows:

- Solvent
- Ligand(s)
- Catalyst
- Base

In considering the above, and so far as Stephen L. Buchwald[578] himself is concerned, two key factors in this type of amination are the catalyst and base. The erstwhile is a phenomenon to which particular attention must be paid, in virtue of the fact that the Pd^{II} catalyst is air and moisture sensitive and that is what first prepared for storage and subsequent use; however, the catalytic cycle (Fig. 3.41) will not be triggered unless the Pd^{0} catalyst is formed, thus the choice of the latter is of paramount importance.

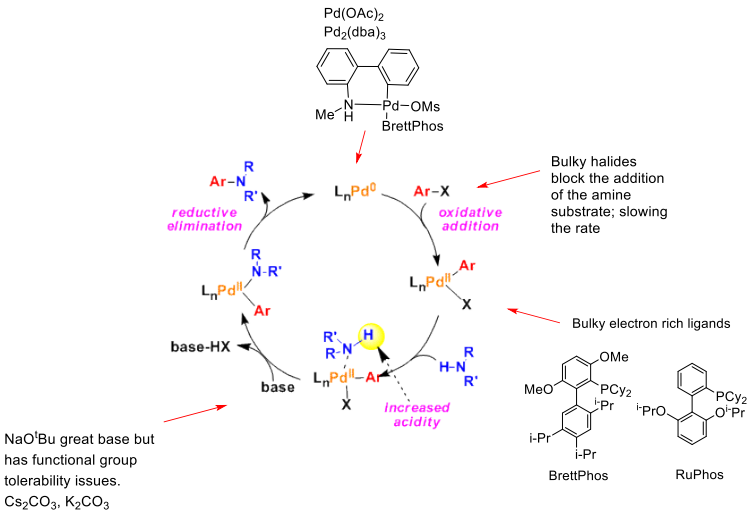

Figure 3.41 Buchwald amination catalytic cycle.

For reasons even unknown to Stephen L. Buchwald himself (*loc. cit.*), coupling of an amine to chloroaryls is much more facile than that of their bromo-counterparts and extremely torturous for iodoaryls. In agreement with this, the Buchwald coupling of hydrazone **44** with iodo-InC **57** was found not to be feasible.

A bottleneck in synthesis of NInC **60** was the formation of 3-bromo-InC **61**. Previous attempts in Oxford (unpublished data) for bromination of InC **56** under similar conditions used for iodo-InC **57** synthesis (Scheme 3.11) left our colleagues dismayed and dispirited.

Careful monitoring of the bromination of InC **56** revealed that two products, namely, 3-bromo-InC **61** *i.e.* the desired, and the unwanted, otherwise in preparative terms '*nuisance*' side-product *i.e.* 3,4-dibromo-InC **62**, are possible therein. Though, the erstwhile is the kinetic product and the latter the thermodynamic thereapart, it was found that under common iodination conditions, iodo-InC **57** is exclusively the sole product of the reaction; however, under the same reaction conditions for bromination of InC **56**, 3,4-dibromo-InC **62** would preponderate over its 3-bromo-InC **61** rival.

To this end, one might envisage that lowering the temperature and time of the reaction should favour the formation of 3-bromo-InC **61**. In theory, this indeed is the case; in practice, however, the desired product and nothing but the desired product is seldom observed, and the desired kinetic product *i.e.* 3-bromo-InC **61** is almost invariably accompanied by some degree of the '*nuisance*' side-product **62** (Scheme 3.15).

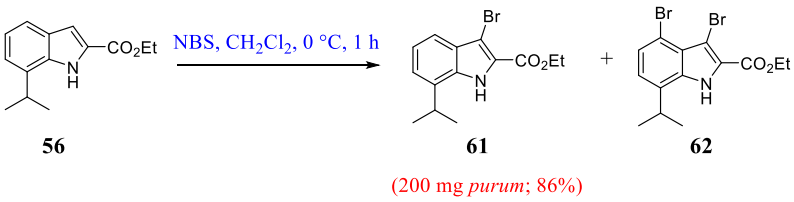

56 **61** **62**

(200 mg *purum*; 86%)

Scheme 3.15 Bromination of InC 56.

Hardly surprisingly, dibromo-InC **62** is very much akin to monobromo-InC **61** in polarity here as elsewhere,[579] and their separation even after three consecutive flash column chromatography purifications by a large part proved ineffective, as evidenced by ^{1}H NMR (Fig. 3.42).

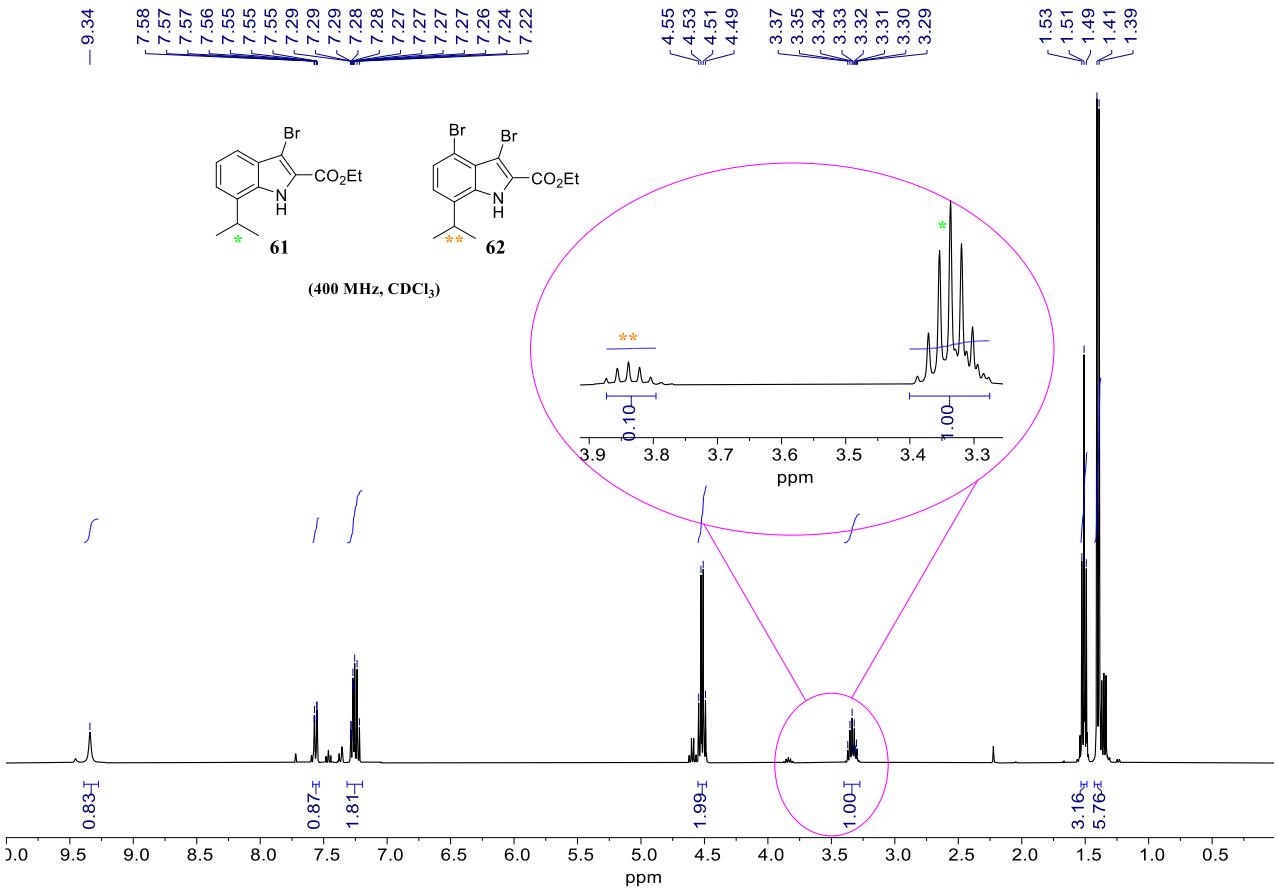

Figure 3.42 ^{1}H NMR spectrum of bromo-InC 61 (~ 90%); (*the pertinent section is magnified in the purple oval*).

Initially, Buchwald amination of the thus obtained bromo-InC **61** with hydrazone **44** using BrettPhos Pd G3 and equimolar amount of BrettPhos ligand in dry THF and Cs_2CO_3 as base (Scheme 3.16) gave poor yields of the desired NInC **60** *i.e.* ~ 20–25%. However, with some modification *i.e.* change of reagents and reaction conditions, the yields were almost doubled ~ 45–50% such that NInC **60** was accomplished in excellent purity after flash column chromatography purification, as evidenced by ^{1}H NMR (Fig. 3.43).

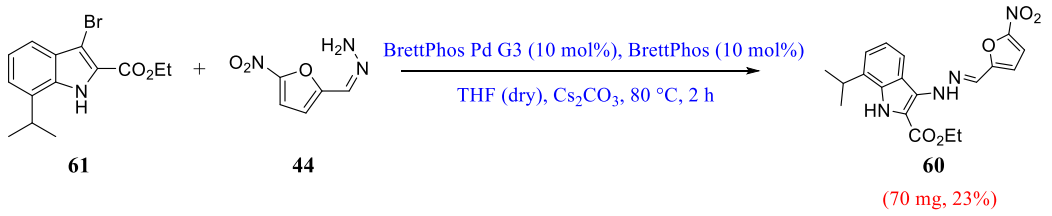

Scheme 3.16 Initial attempts at synthesis of NInC 60.

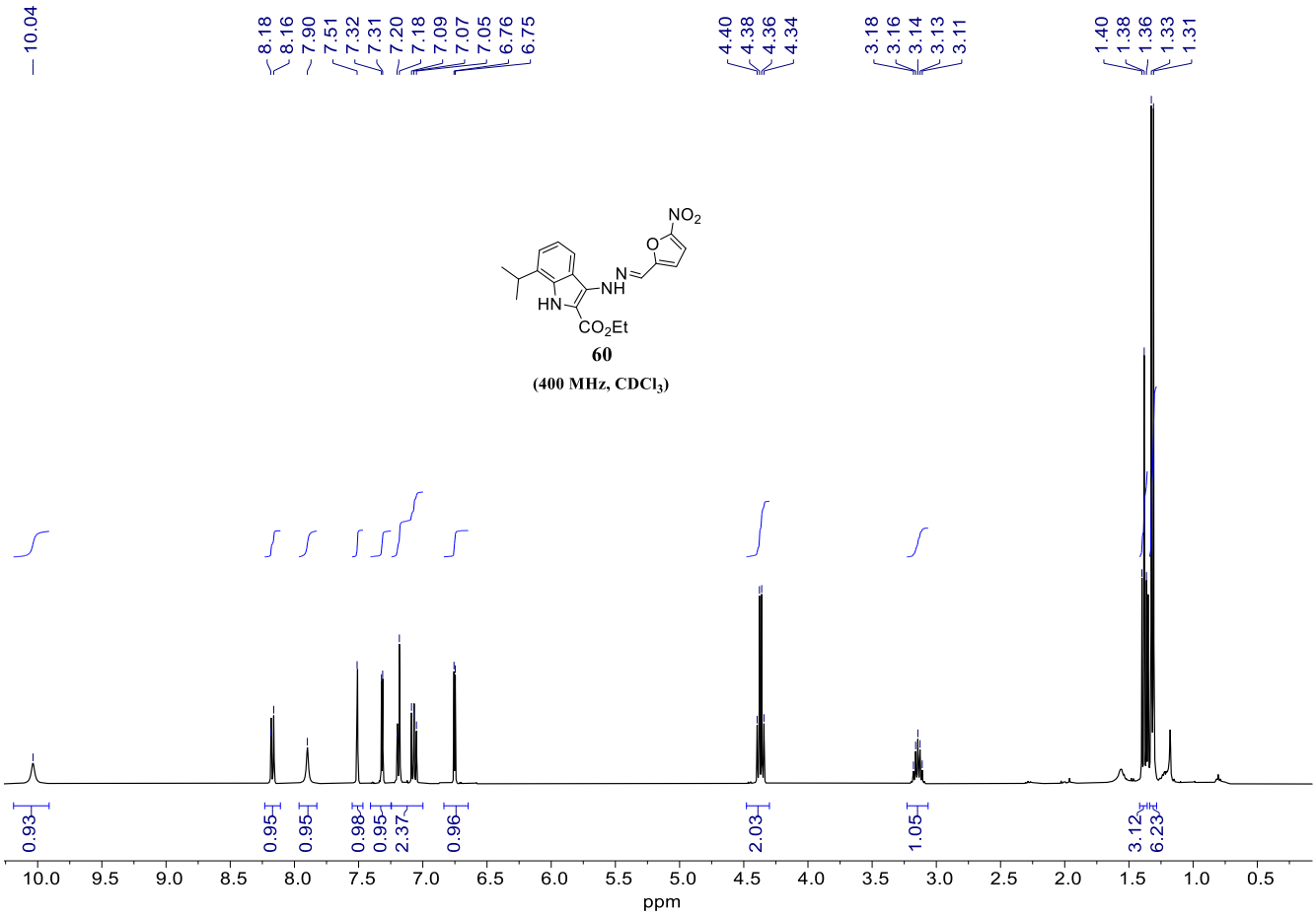

Figure 3.43 ^{1}H NMR spectrum of NInC ethyl ester 60. The carbon satellites of the signal from *α*-C*H*$_2$ at δ 4.37 clearly attest the purity of NInC ethyl ester 60; for full characterisation and *J* values in Hz *cf.* Experimental p. S51.

It is noteworthy to mention that even though bromo-InC **61** starting material was of a lower quality, the obtained NInC ethyl ester **60** was of high purity, and the negligible side-products arising from coupling of 3,4-dibromo-InC **62** to hydrazone **44** could easily be removed by flash column chromatography purification (Fig. 3.43).

3.3.2 Hydrolysis of NInC Esters

In this discussion of our NInC esters, painstaking efforts were made to hydrolyse various esters of this type NInC *e.g.* ethyl and methyl, but as yet this transformation proved, in practice, impractical.

In most cases, if the reaction conditions were sufficiently suitable for hydrolysis to take place, the hydrazone linker was also cleaved, with the exception of only one example for which difficulties in purification led to no or infinitesimal quantities of the desired product, and cases in which the reaction conditions were just too mild to hydrolyse anything, the intact NInC esters were recovered.

Thus, it is not necessarily safe to conclude that tinkering with kinetics can beat unfavourable thermodynamics. Some kinetic alterations manifest in thermodynamic allegiance better than do others, but the overall success of a transformation is demonstrated by the way in which thermodynamic soundness is evident, and hence the application of relatively rudimentary guiding principles can bring about light and order to bear on fundamentals of this very obvious phenomenon. We shall go on to review some representative examples of the aforementioned phenomenon.

3.3.2.1 Acid & Base hydrolysis of NInC Ethyl Ester

With NInC ethyl ester **60** in hand, first and foremost, the most obvious of all ester hydrolyses *i.e.* the LiOH hydrolysis, was attempted and unfortunately, to our regret, LiOH proved too harsh a reagent for hydrolysing this type of esters, and no matter what strength of $LiOH_{aq}$ solution *i.e.* molarity was used, the hydrazone linker was also cleaved *via* this method.

Ever after the unsuccessful attempts at hydrolysis of the aforementioned ester with LiOH, other bases such as NaOH, $Ba(OH)_2 \cdot 8H_2O$ to mention but a few, were all failed to furnish a clean or even partial hydrolysis of these NInC ethyl esters to yield carboxylic acid **63** without cleaving the hydrazone linker (Scheme 3.17).

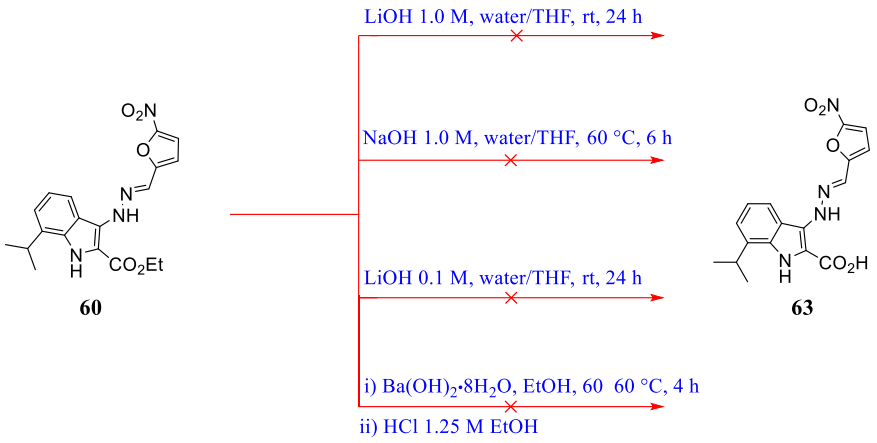

Scheme 3.17 Representative examples of attempts at base hydrolysis of NInC ethyl ester 60.

Although, a base hydrolysis is essentially irreversible, and in most cases far better than an acid hydrolysis, but given that we had no success with a base hydrolysis of NInC **60**, its acid hydrolysis was also attempted (Scheme 3.18).

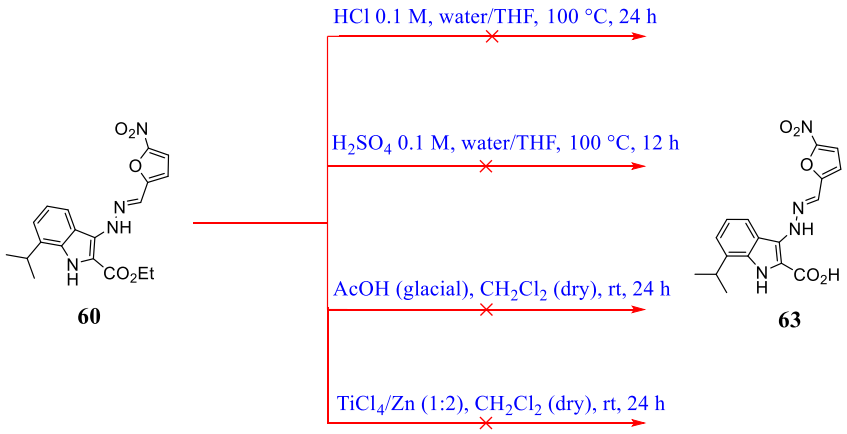

Scheme 3.18 Representative examples of attempts at acid hydrolysis of NInC ethyl ester 60.

The above failures turn essentially on the fact that either the chemistry was improbable by virtue of its unfavourable thermodynamics or the chemist was incompetent. The former again is a direct reflection of unbeatable thermodynamics; by analogy, at the very minimum, in a privileged frame of reference a '*perpetual machine*' is non-existence in virtue of its unfavourable thermodynamics.

Albeit, this thermodynamic phenomenology may, though it need not of necessity, explain the pertinent phenomenon in question, it should be remembered that phenomenology is not a fact in its own right, and this beautifully explains as to why the proposed thermodynamic phenomenology may well not be the phenomenon with which the phenomenology is concerned, as Edmund Husserl himself simply noted: "*phenomenology is just things back to themselves*."

Thus, as it was reiterated previously an unfavourable thermodynamics is unbeatable in a privileged frame of reference, and a different thermodynamically favourable chemistry must be sought in the same privileged frame of reference.

It is essential to remind ourselves that by Husserl's definition, phenomenology is '*the philosophical study of the structures of experience and consciousness'*.[580] To this end, phenomenology is integral to science and scientists in seeking an explanation for their scientific experiments, in point of fact, endeavour to reach their experiments' phenomenology; however, it might come as a surprise that many, though by no means all, do not even apply the concepts of phenomenology, and the reader is encouraged to ponder as to why this is the case?!

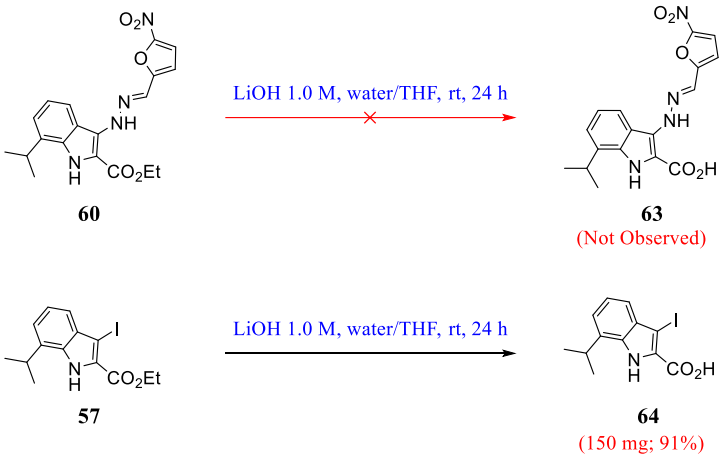

Scheme 3.19 Unsuccessful LiOH hydrolysis of NInC-OEt 60 (top) *vs* that of InC-OEt 57 (bottom).

Having said that, in an attempt to be freed of the ensuing doubt that the above failures were due to the incompetency of the chemist who attempted them, the standard LiOH hydrolysis of NInC ethyl ester **60** which left us dismayed, was also repeated by the chemist in question for InC ethyl ester **61** under exactly the same reaction conditions, and to the chemist's relief, it was unveiled that the aforementioned failure was due to the inherent improbable chemistry, and not the incompetency of the chemist such that indole carboxylic acid **64** was obtained in high yields (Scheme 3.19), and excellent purity, as evidenced by ^{1}H NMR (Fig. 3.44).

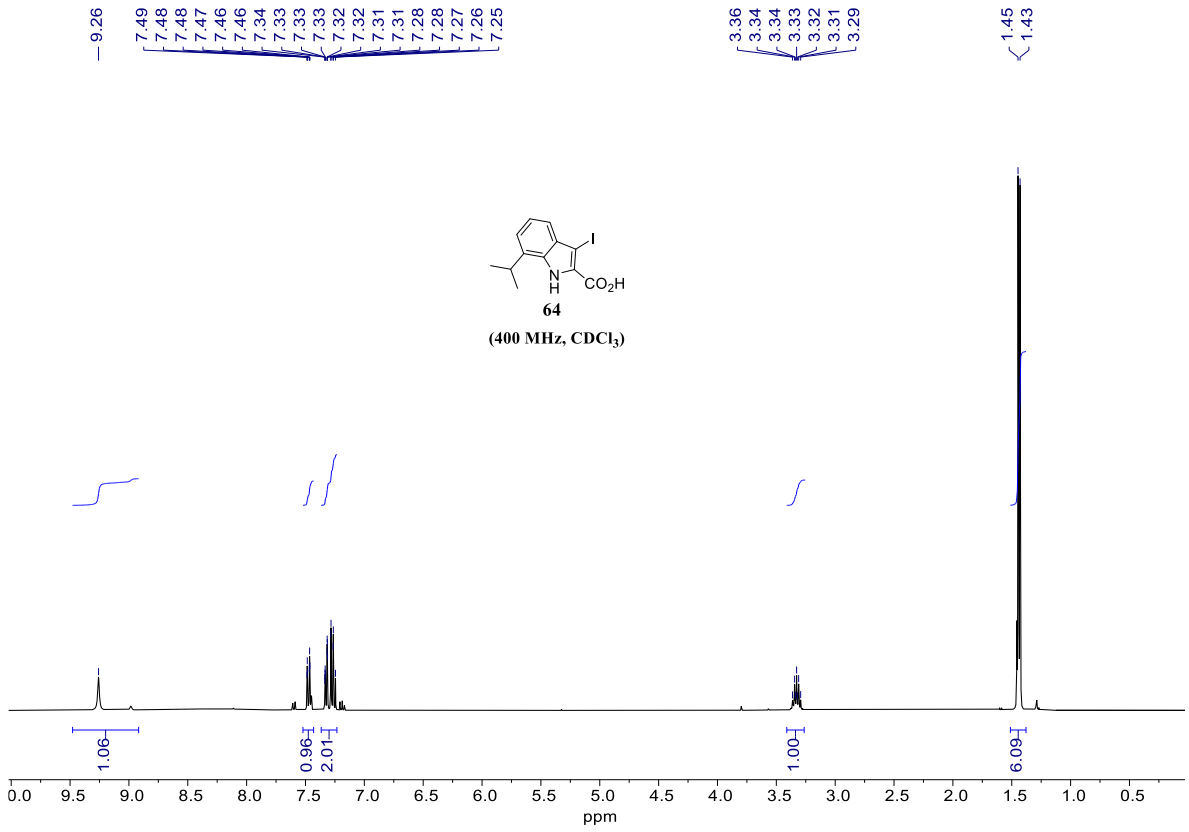

Figure 3.44 ^{1}H NMR spectrum of iodo-indole carboxylic acid 64. The carbon satellites of signals from the aromatic protons at δ 7.47 – 7.23 clearly attest the purity of iodo-indole carboxylic acid 64; for full characterisation and *J* values in Hz *cf.* Experimental p. S53.

As depicted in Scheme 3.17 and Scheme 3.18, both acid and base hydrolyses of NInC esters proved futile, at least in our laboratories. To this end, the use of much milder and chemoselective esterases was then explored *i.e.* nature's method of choice.

3.3.2.2 Enzymatic Hydrolysis of NInC Ethyl Ester

By definition enzymes are biological catalysts,[581] and without them life would not exist as we know it; however, inasmuch as enzymes mainly operate at physiological conditions, an element of which is water *i.e.* the least attractive reaction solvent to the synthetic chemist, no matter how efficient and chemoselective an enzyme may be, its hydrophilic deterrent nature is not for a moment in doubt. In other words, even a cat would probably, almost certainly think of water more than the synthetic chemist would do about running their reactions in water.

In the light of what has been said above, the most versatile esterase in chemical synthesis to date, however, is the classical pig liver esterase (PLE),[582] which has been extensively utilised in the literature for a variety of hard to achieve ester hydrolyses.[583]

Perhaps the most fundamental basis of a chemical reaction is that for it to take place, the participating molecules must collide with one another, and also such a collision must have sufficient energy to overcome the activation energy of the reaction: that this should be so is a corollary of Arrhenius hypothesis.[584]

Although, several organic co-solvents have been proposed for esterases,[585] of which acetone seems to be the most popular, broadly speaking any amount of the organic co-solvents greater than 10% could denature esterases, so that we end up, of necessity, wasting our endeavours. Knowing that ethyl ester **60** is essentially insoluble in water, no matter how good an organic co-solvent be at 10% concentration in water, this clearly sets limitations to which any esterase advanced for the hydrolysis will have to conform, and this debunks that prime tenet of esterases. It should, however, be reiterated, that in spite of the above limitations of esterases, PLE hydrolysis of ethyl ester **60** was carried out (Scheme 3.20), and the outcome was obviously that to which reference has already been made.

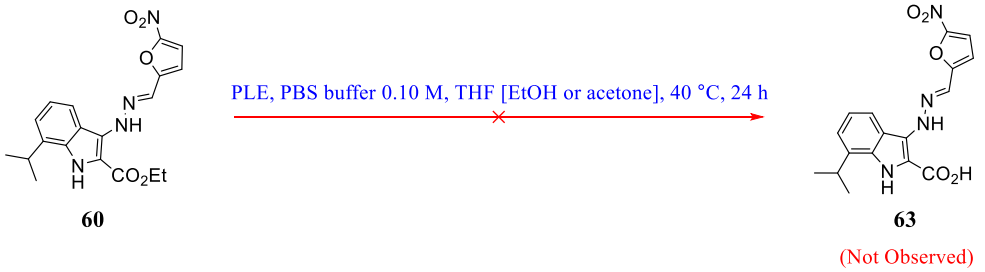

60 **63**

(Not Observed)

Scheme 3.20 Failed PLE hydrolysis of NInC-OEt 60 in a variety of organic co-solvents.

It will be seen from Scheme 3.20 that several common and versatile organic co-solvents *e.g.* acetone, THF *etc.*, failed to furnish the desired hydrolysis.

It is often a matter of some concern to establish whether a particular enzymatic reaction has, or has not been failed at a stage up to and including solvation.

Should you recall, we previously attributed the degree of success upon which a given chemical transformation is dependent, to either the chemist who carries out the reaction or nature of the transformation (Section 3.3.2.1).

However, similar, but different to this chemical synthesis principle, when we come to consider the degree of success of an enzymatic reaction, we must consider three variables as opposed to the aforementioned two variables, for though enzymes *e.g.* esterases are normally '*substrate specific*.'

Thus, it is not necessarily safe to conclude that the failure of the esterase hydrolysis was merely due to the chemist's incompetency or inherent infeasibility of its very own chemistry *i.e.* the hydrolysis; as though, it might just be the case that ethyl ester **60** is simply not a suitable substrate for PLE.

This esterase substrate specificity suspicion can easily be examined with malice aforethought of subjecting the esterase, in this case PLE, to another reagent, but with similar steric and electronic properties. Incidentally, ethyl indole carboxylate occurred to be just about the right substitute as such.

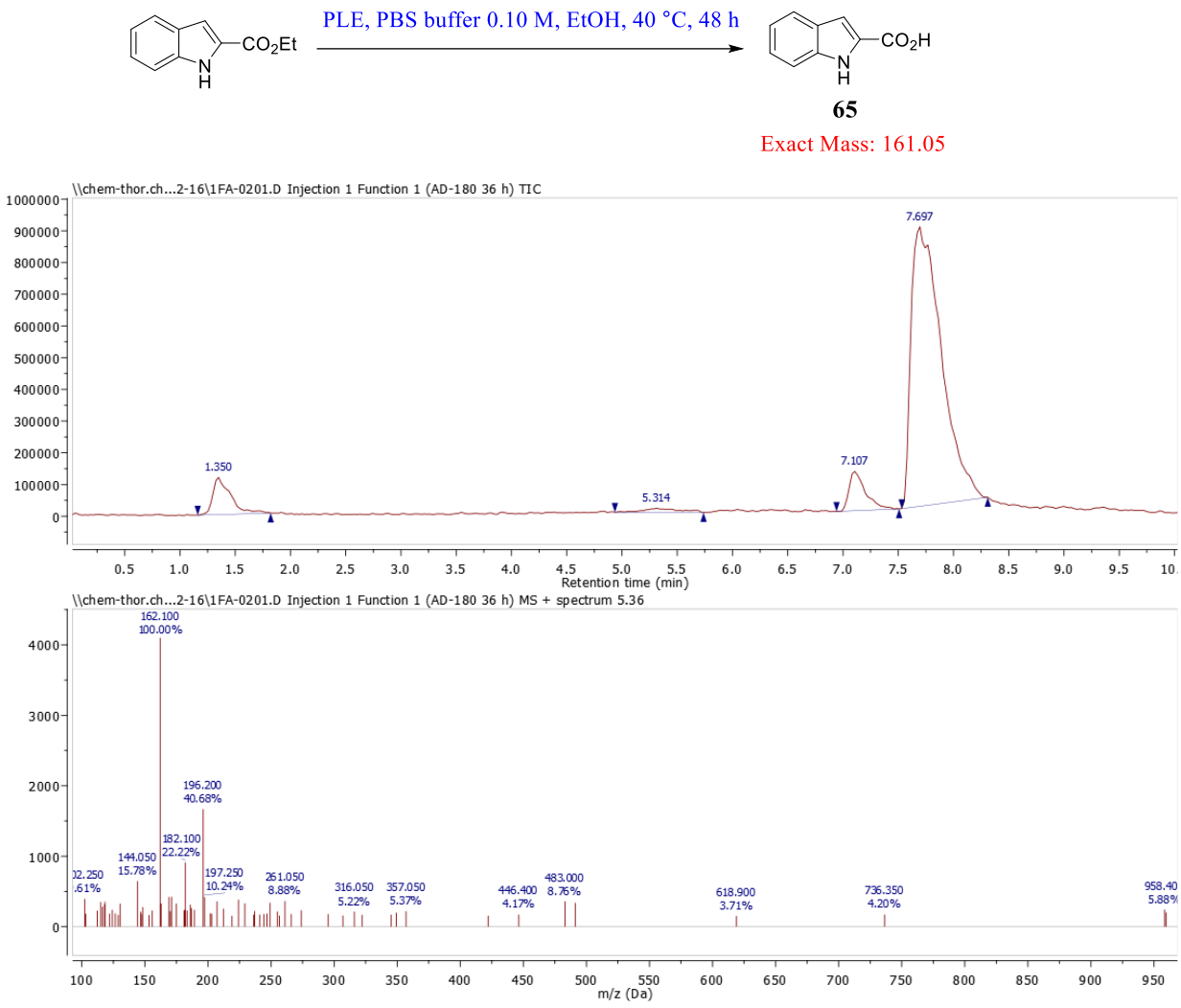

Figure 3.45 LC-MS trace of hydrolysis of ethyl indole carboxylate by PLE; full conversion achieved after 48 h.

Quite gratifyingly, PLE was able to hydrolyse ethyl indole carboxylate to yield its corresponding acid **65**, as was evident from LC-MS analysis of the reaction (Fig. 3.45), so as to give the lie to erroneous assumptions of both substrate incompatibility and more importantly, the chemist's incompetency.

Then again, with this NInC **60** the problem stems from the improbability of desired hydrolysis or inexplicitly, its unfavourable thermodynamics.

Mankind has been copying nature in drug discovery to such an extent that more than 70% of the marketed drugs have been derived from natural products.[586] Although, with advances in drug discovery this is slowly changing, but it is not uncommon to stumble across a synthetic molecule which had been in nature and unknown to mankind; bearing out yet again nature, in that beating us to it, the essence of which would have not been feasible, if not all, without enzymes.

Thus, esterases are not the only tools used by '*Mother Nature*' to hydrolyse esters, lipases can also equally do well, and have evolved for larger substrates such as triglycerides.

Triglycerides are essentially esters, made up of large fatty acids and glycerol, which are major components of the human skin, and the means by which the body stores energy *i.e.* adipose tissue.[587]

In this context, esterases that hydrolyse a triglyceride to its fatty acids and glycerol constituents have been called lipases;[588] thus, this esterase and lipase dichotomy can be looked upon as a special class of carboxyl ester hydrolases, such that the former is concerned with any ester, in particular, one which is not too large a substrate *e.g.* ethyl acetate, but the latter can be regarded as a subclass of the former, mainly directed towards larger substrates, typically triglycerides.

Given that we did not have much joy with esterases by the above definition, the more specialised lipases were recruited. Lipases are indeed commercially far cheaper and more cost effective than PLE, should they be able to perform the desired transformation. However, then again, the success of which by a large part relies on the substrate specificity factor.

It follows that inasmuch as PLE *i.e.* an esterase did hydrolyse ethyl indole carboxylate but not the relatively larger ethyl ester **60**, and the fact that lipases have a penchant for larger substrates than esterases, it was conceivable not to question substrate specificity of lipases for ethyl ester **60**.

In considering the unreliability of NInC esters as compatible substrates for esterases, and since ethyl indole carboxylate was hydrolysed by PLE but ethyl ester **60** was not, it appeared more practical to use a model system for the lipase hydrolysis first, before jumping into wasting more of the hard-earned ethyl ester **60**.

It should be remembered that most lipases prefer fatty esters, thus in order to strengthen our model system the synthesis of a full-blown long-chain ester should have not been overlooked. To this end, the previously synthesised carboxylic acid **65** was converted to its corresponding fatty *n*-heptyl ester **66** both in excellent yields *i.e.* ~ 73%, and purity (Fig. 3.46), the 15 *n*-heptyl protons of which giving rise to virtually indiscernible signals at *ca.* δ 1.80 – 0.90, clearly endorse its lipophilic nature.

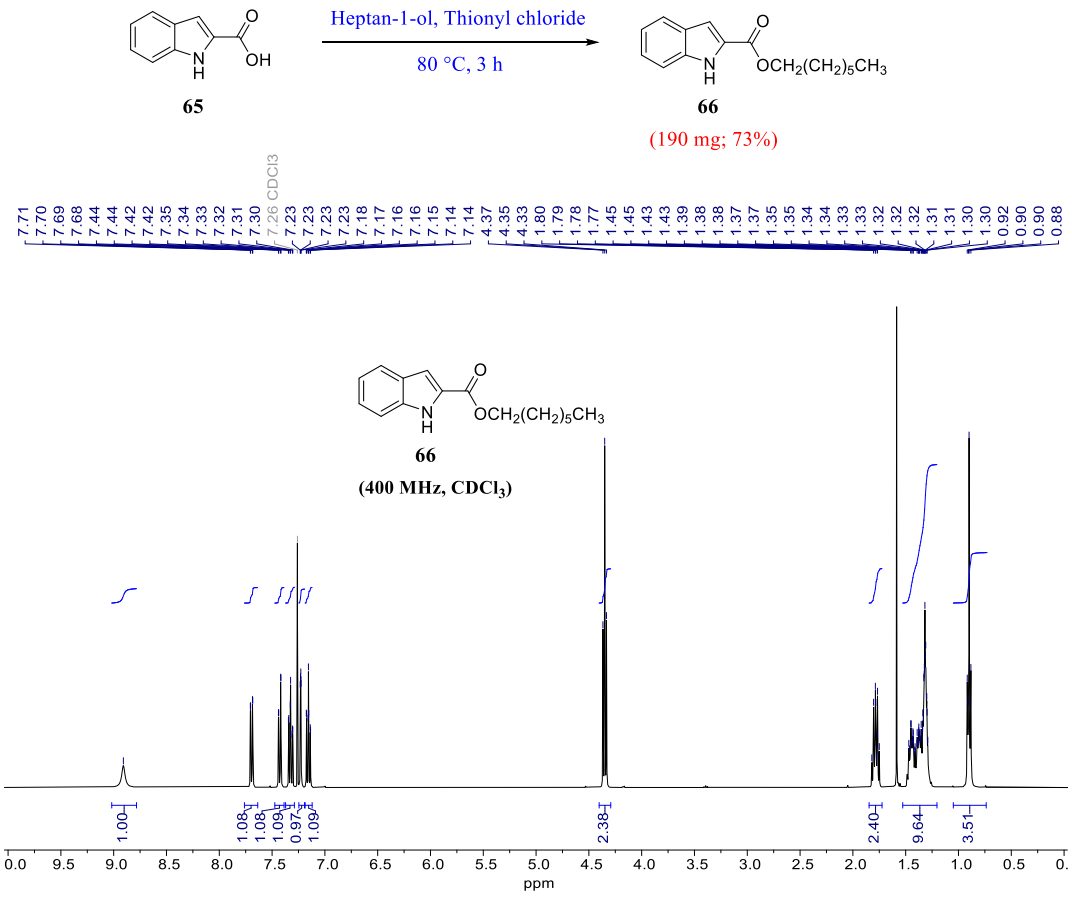

Figure 3.46 Synthesis and ^{1}H NMR spectrum of *n*-heptyl indole carboxylate 66.

In high hopes of winning out this ester hydrolysis *via* very much sophisticated lipases, it was utterly disappointing to be let down once again by not one, but all the lipases and reaction conditions with which it was pleaded (Scheme 3.21).

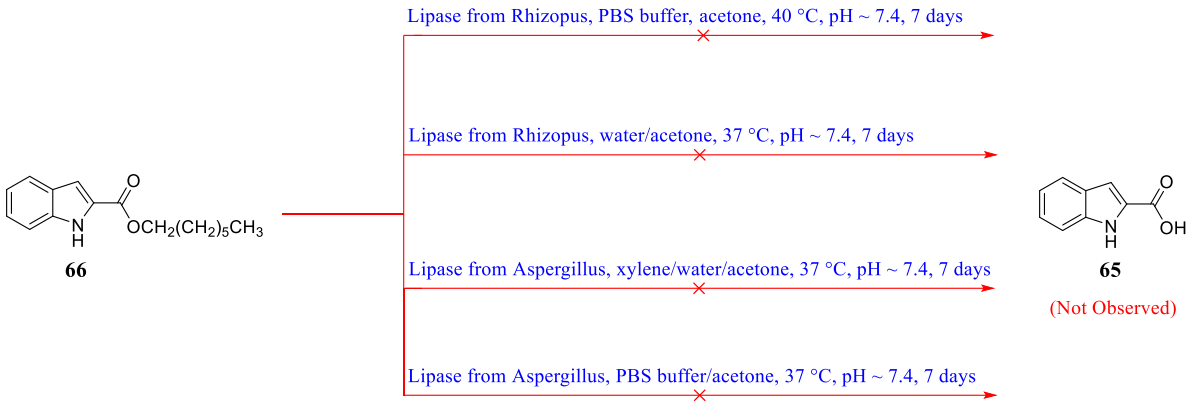

Scheme 3.21 Representative examples of failed attempts at lipase hydrolysis of *n*-heptyl indole carboxylate 66.

3.3.2.3 Synthesis of NInC Methyl Ester

The enormous increase in selectivity of modern synthetic methods has all but obliterated repetitive dull chemistry; nevertheless, many diverse and intriguingly chemistries have long remained a major problem, particularly, when modern chemists now strive for mapping the entire chemical space.

It is not much of a debate that hydrolysis of methyl esters is more facile than their ethyl counterparts. A type of reaction that has probably received more detailed study than the rest – largely due to the monumental work of Hans Finkelstein and his school[589] – is nucleophilic substitution at a saturated carbon atom: the classical displacement reaction exemplified by the conversion of an alkyl chloride or bromide into an alkyl iodide by the action of sodium iodide in acetone.[590]

Exactly the same discussion can be made over ester hydrolysis by lithium salts[591] in acetone as was made above for substitution of alkyl chlorides or bromides into alkyl iodides (*loc. cit.*), thus in an attempt to make the author's life more difficult, the synthesis of NInC methyl esters was also considered.

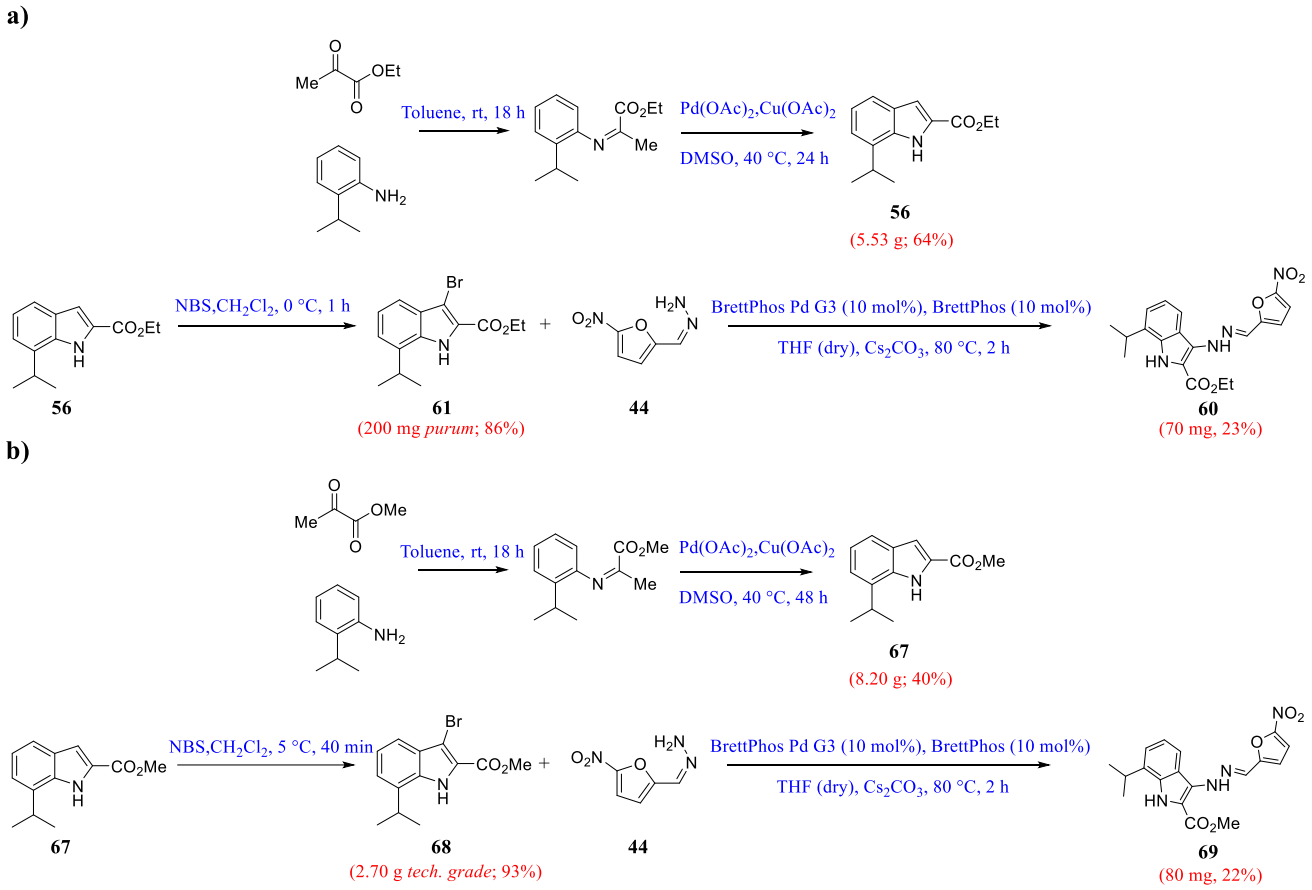

Scheme 3.22 a) Synthesis of NInC ethyl ester 60 *vs* b) synthesis of NInC methyl ester 69.

The synthesis of NInC methyl esters was more challenging than that of their NInC ethyl ester counterparts, challenging in that taking as an example ethyl ester **60** which was a somewhat fine powder, its analogous methyl ester **69** was a hygroscopic amorphous semi-solid species with high tendency for acquiring electrostatic charge so much of a nuisance, not least in its practicality and handling to mention but a few; never mind the difficulties in its synthesis, and subsequently lower yields in each and every single step of its synthesis relative to that of ethyl ester **60** (Scheme 3.22).

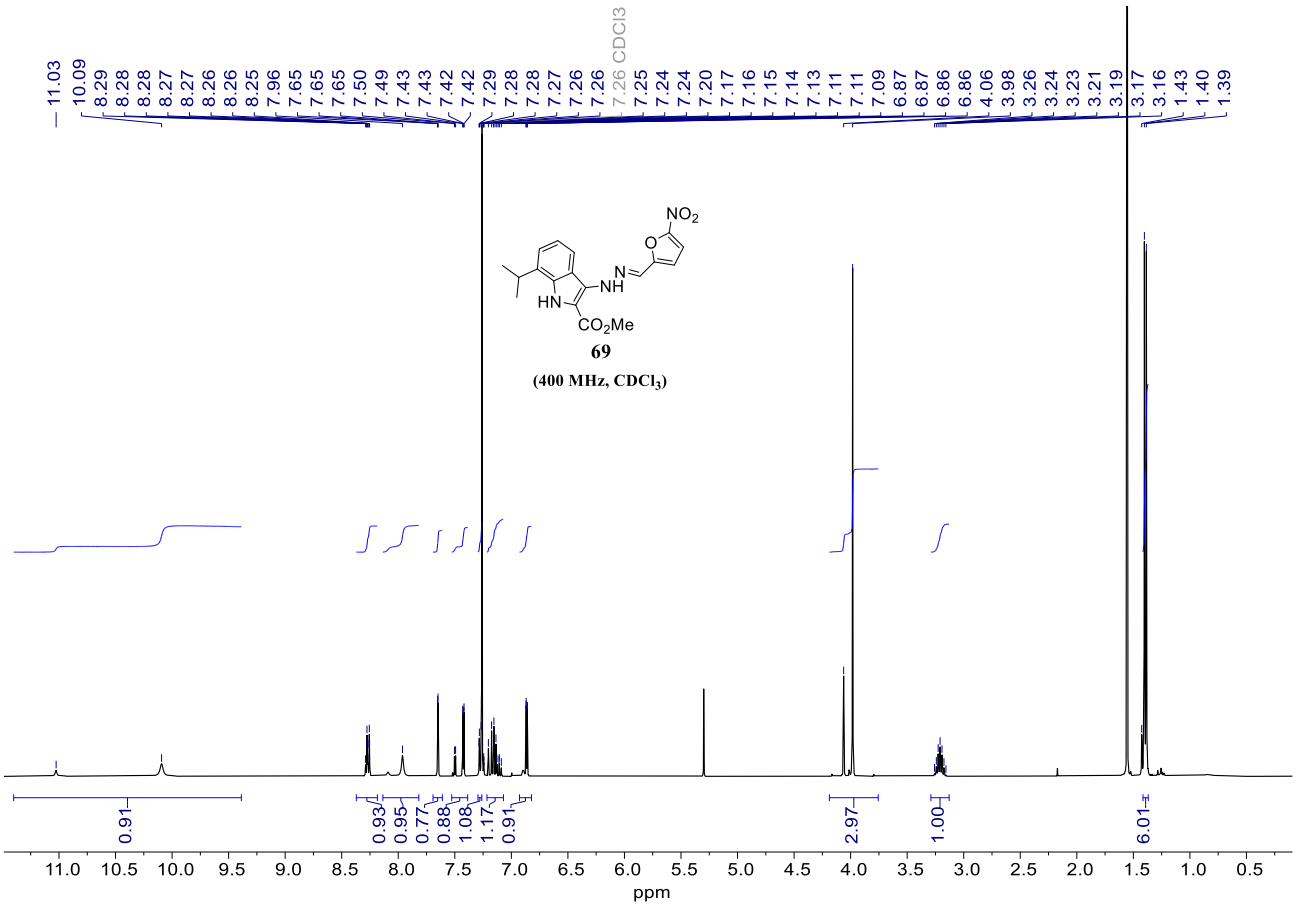

Figure 3.47 ^{1}H NMR spectrum of NInC methyl ester 69. The two singlets from –OMe moiety in 69 at δ 4.06 & 3.98 are rotameric in a similar but different fashion to Bamford tosylhydrazone rotamers.

Amongst the complications arising from this type of NInC methyl esters *e.g.* methyl ester **69** as the prime example, are the self-explanatory complications which are all evident from its ^{1}H NMR spectrum (Fig. 3.47) due to:

- Hygroscopicity
- Solid state solvent bridges and complexation possibilities
- Rotamers

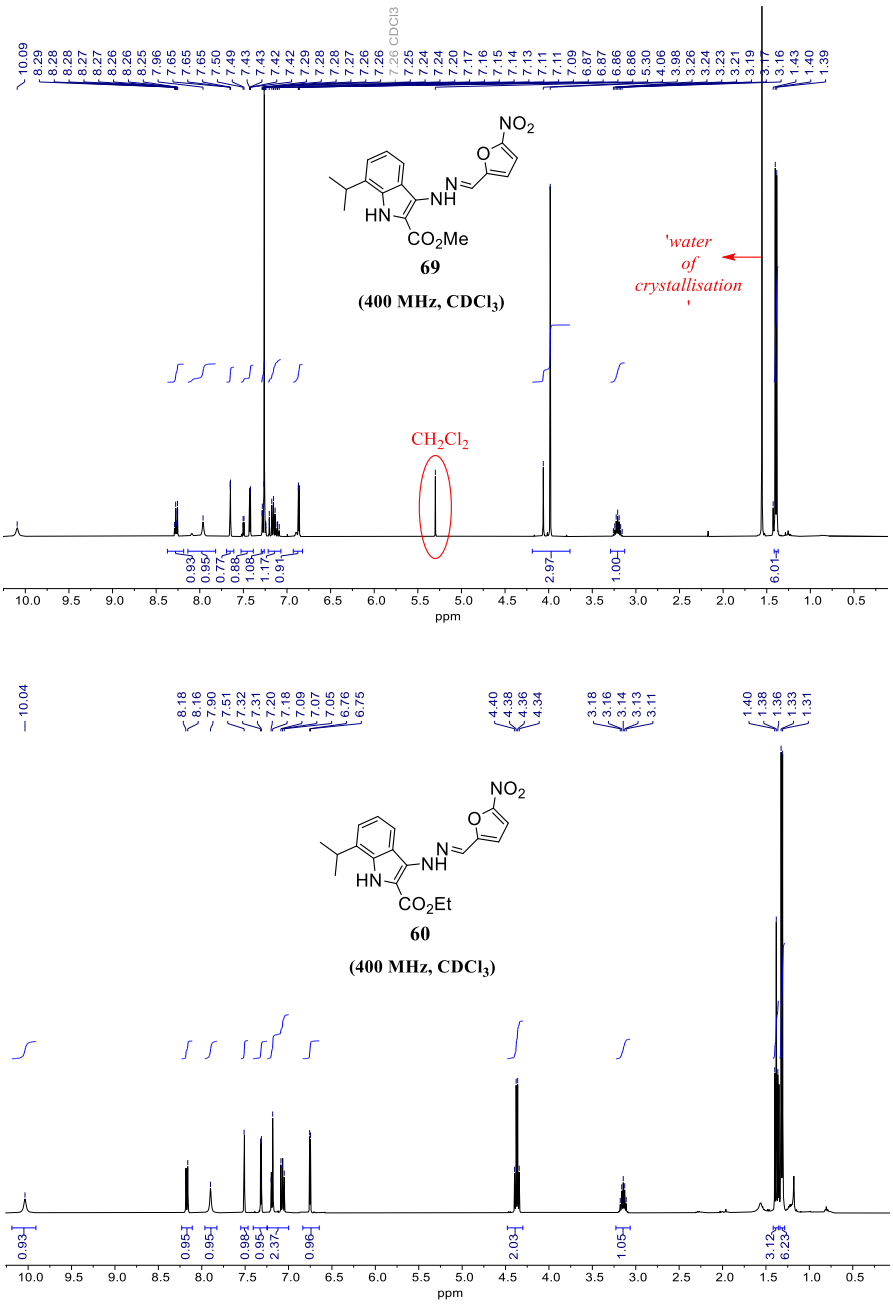

Figure 3.48 ^{1}H NMR spectrum of methyl ester 69 highlighting the propensity for complexation of solvents with 69, in particular, the presence of water of crystallisation (top); such complications not observed for its corresponding ethyl ester 60 (bottom).

Complications arising from solvent complexation with methyl ester **69** are reflected in the fact that after several days of drying ester **69** under high-vac, such that even though most of the remaining cyclohexane in the solid after flash column chromatography purification was removed, the amount of relatively much more volatile dichloromethane still preponderates over even notoriously hard to remove cyclohexane (Fig. 3.48).

This effect highlights the complexation of methyl ester **69** with dichloromethane in solid state (Fig. 3.48). By contrast, no such effects were, observed for the seemingly more chemist-friendly ethyl ester **60** (Fig. 3.43).

Thus, methyl ester **69** in the absence of organic solvent complexation complications and possibly more profoundly with water in solid state thereof, is otherwise of a very high quality *i.e.* purity >98%. However, much more important so far as its ^{1}H NMR is concerned, are the complications arising from methyl ester **69** rotamers by virtue of not fully restricted rotation around the α-bond of the hydrazone moiety in the aforementioned methyl ester **69**.

At first glance, the singlet signal at δ 4.06 in the ^{1}H NMR spectrum of methyl ester **69** (Fig. 3.47), looks nothing more than yet another solvent impurity trace. It is seldom, if ever, possible to directly link this signal with the much more pronounced singlet from the –OMe group in ester **69** at δ 3.98 in the same ^{1}H NMR spectrum (Fig. 3.47). However, in point of fact, both singlets are from the same –OMe group in ester **69**, but of different '*rotamers*.'

No clear distinction can necessarily be made between what constitutes a conformer and what a rotamer, for though rotamers are normally thought of as conformers, the rotamers could, at will, be either conformers or rotamers, when looked upon in a privileged frame of reference, for example, an inertial frame of reference. As such, support for the existence of stable rotamers of methyl ester **69** is provided by the complexity of the chemical shifts in its ^{1}H NMR spectrum.

In the light of what has been said above, the two singlets at δ 4.06 and 3.98 both belong to the chemical shifts from protons of –OMe moiety in methyl ester **69**, which otherwise would have been one clear uniform singlet in the absence of stable rotamers by virtue of their carbon '*satellites*' for the –OMe moiety at δ 4.16 and 3.80 (Fig. 3.49).

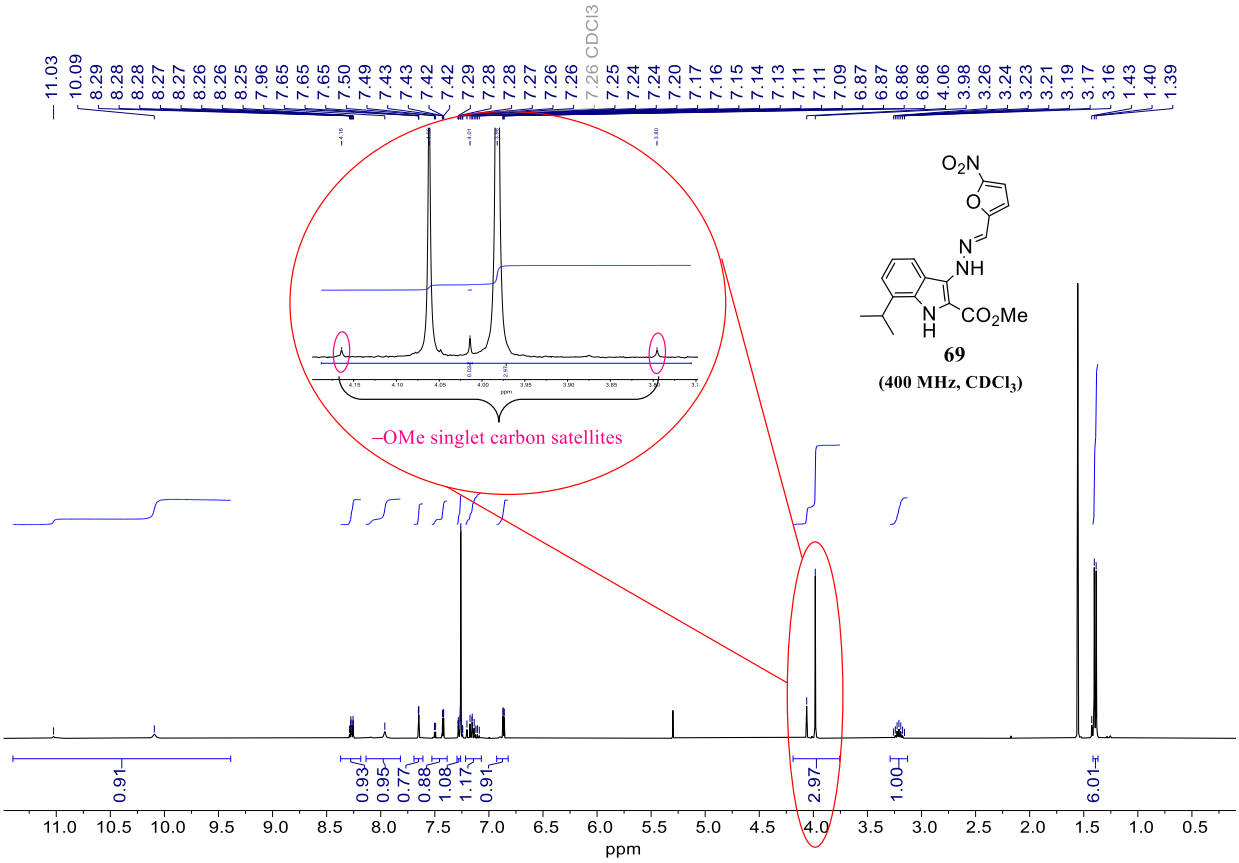

Figure 3.49 ^{1}H NMR spectrum of ester 69 highlighting the signals at δ 4.16 and 3.80 due to the carbon satellites of –OMe chemical shifts at δ 4.06 and 3.98, shedding light on existence of stable rotamers of ester 69 at room temperature NMR acquisitions; (*the pertinent section is magnified in the red oval*).

Another support for existence of stable rotamers of methyl ester **69** is provided by the fact that the signal integral of chemical shift from the main rotamer at δ 3.98 is only measured up to ~ 2.3 and would be too small for rounding that up to the anticipated integer 3.0 so as to account for the –OMe moiety.

However, by combining both singlet integrals of 0.6 and 2.3 due to the minor and major stable rotamers of ester **69** at δ 4.06 and 3.98, respectively; we will arrive at a signal integral of 2.9 (actual value from the spectrum measurement is ~ 2.97), which is easily permitted to be rounded up to the anticipated integer 3.0 for the 3.0 protons belonging to the –OMe moiety in ester **69** (Fig. 3.50).

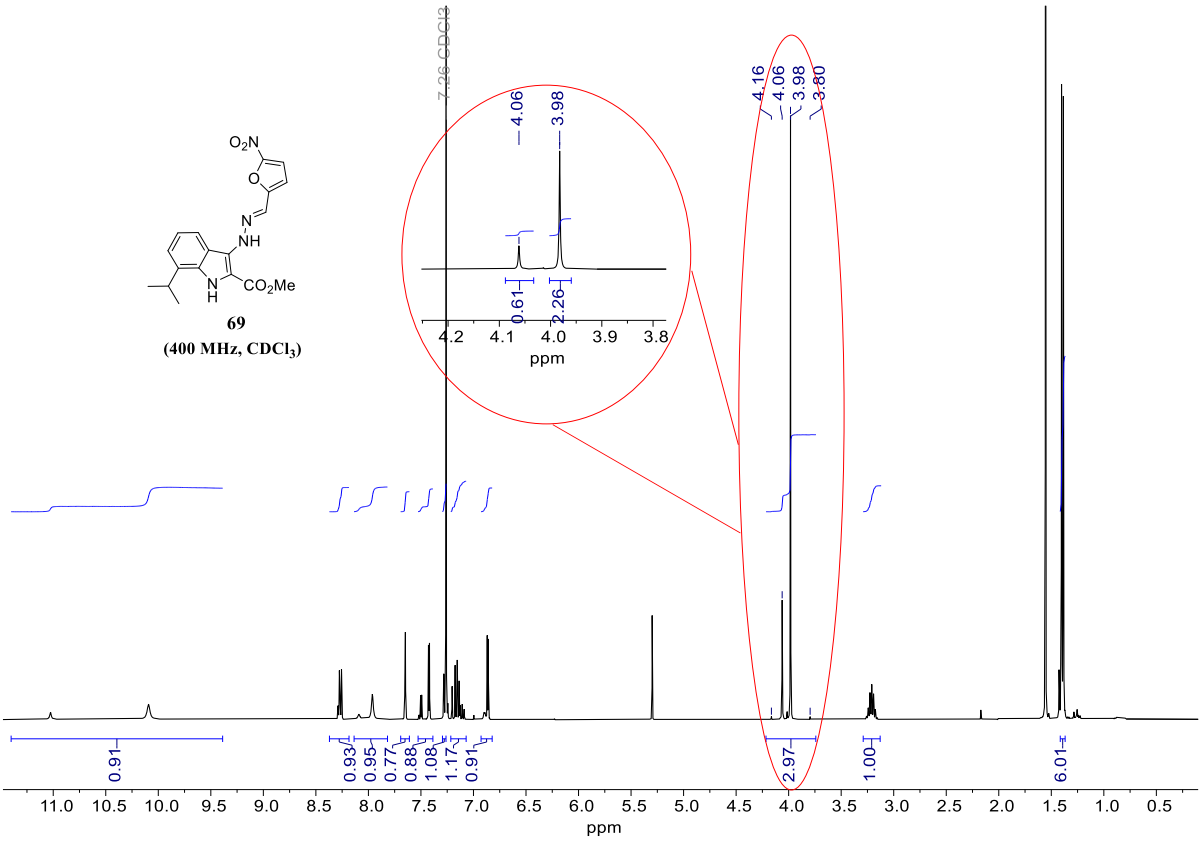

Figure 3.50 ^{1}H NMR spectrum of ester 69 highlighting the sum of signal integrals necessary for the 3.0 protons of the –OMe; (*the pertinent section is magnified in the red oval*).

Furthermore, this rotameric effect is very pronounced for the signals from exchangeable protons of hydrazone and indole moieties in ester **69** at *ca.* δ 11.0 – 10.0 and 8.0, respectively, strengthening the existence of stable rotamers of ester **69**; but the rotameric effect falls off sharply for the rest of the chemical shifts in the ^{1}H NMR spectrum of ester **69** (Fig. 3.51).

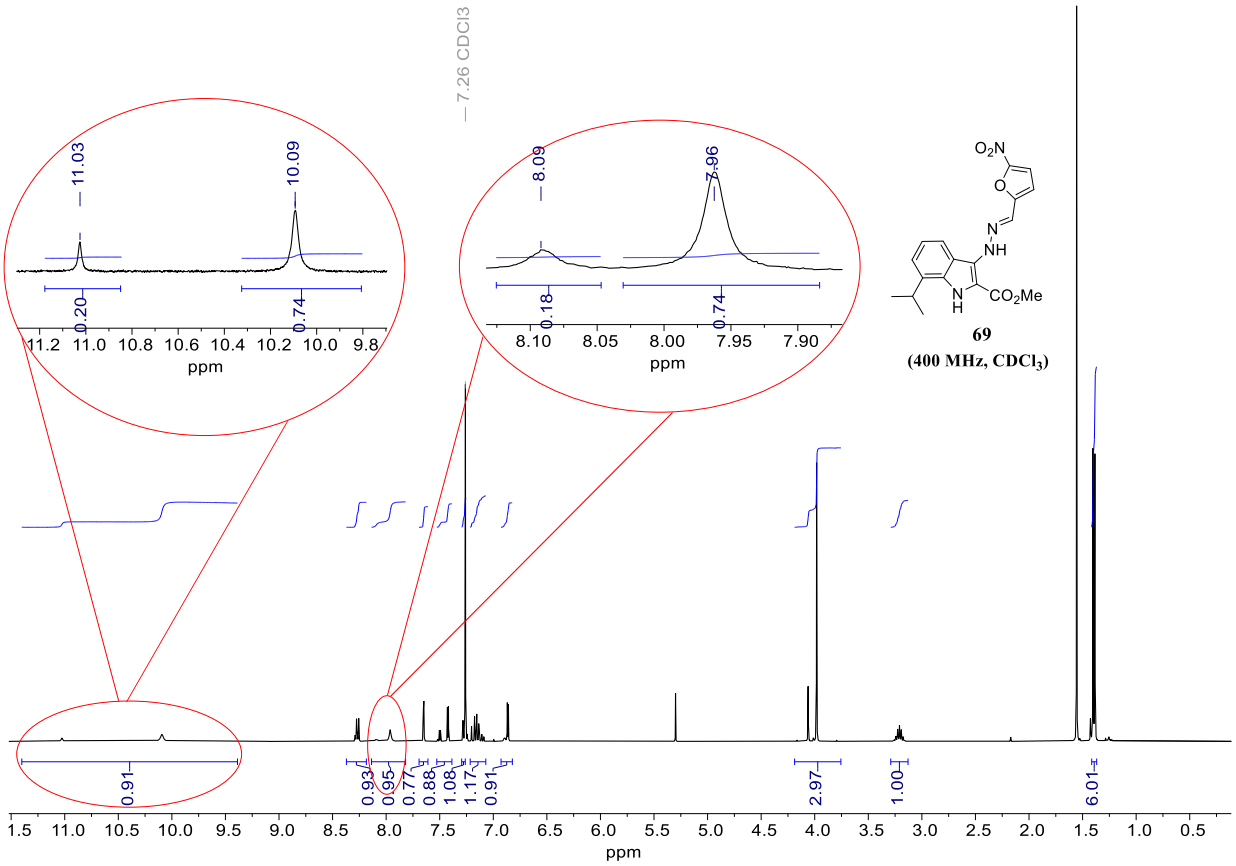

Figure 3.51 The rotameric effect on chemical shifts from exchangeable protons in ^{1}H NMR spectrum of ester 69; (*the pertinent sections are magnified in the red ovals*).

It will be found from the above ^{1}H NMR spectra of ester **69** so far, that it appears as though there are two overlapping spectra: one *i.e.* that of the major rotamer with chemical shift intensities of *ca.* 3 – 4 times greater than the other *i.e.* that of the minor rotamer somewhat imperceptibly shading into the erstwhile; hence, complicating the aforementioned ^{1}H NMR spectrum, and rendering it not as stunning as the other ^{1}H NMR spectra of the *puriss.* >98% grade compounds that have been scattered throughout this script.

A good deal of interest, and controversy, has centred on stability of DNA both in textbooks, and in the literature.[592] Nevertheless, unfortunately, despite the perceived high stability of DNA, yet proto-oncogenes can become oncogenes, and hence leading to all sorts of malignancies.[593]

This controversy of DNA stability can in part be explained by rotameric properties of the DNA backbone,[594] such that the pivotal feature of DNA stability, turns especially on its unique network of hydrogen-bonding, thereby attenuating the detrimental destabilising rotameric effect on the DNA; in point of fact, hydrogen-bonding has been utilised to separate planar rotamers.[595]

Generally, however, on a similar note, $Eu(dpm)_3$,[596] $Eu(fod)_3$,[597] and $Pr(fod)_3$[598] *i.e.* *β*-dicarbonyl lanthanide complexes are the commonest '*shift reagents*' which have been extensively used in chemistry for many applications such as competition experiments,[599] assignment of complex glycols' configurations,[600,601] expansion of NMR spectra to resolve overlapping signals,[602,603] and through space atomic distance measurements in NMR,[604] as assistive tools for *e.g.* NOE spectra *etc.*, to name but a few; as well as in biology for determination of shape and size of enzymes' '*active sites*' by replacing Ca^{2+} and Mg^{2+} ions bound to the enzyme whilst retaining biological activity,[605,606] attainment of coordinated conformations so as to validate protein X-ray crystallographic structures,[607] assignment of ^{13}C NMR spectra of AMP,[608] and many more.[609,610]

To this end, DMSO-d_6 *i.e.* a very closely related '*shift reagent*' even though not quite known as a '*shift reagent*' hardly surprisingly here as elsewhere (Section 3.3.1.2), was able to lock the main rotamer *i.e.* the '*global minimum*' in place so as to elucidate a much clearer picture, though quite distinct from that in $CDCl_3$ (Fig. 3.47), of ^1H NMR spectrum of methyl ester **69** (Fig. 3.52).

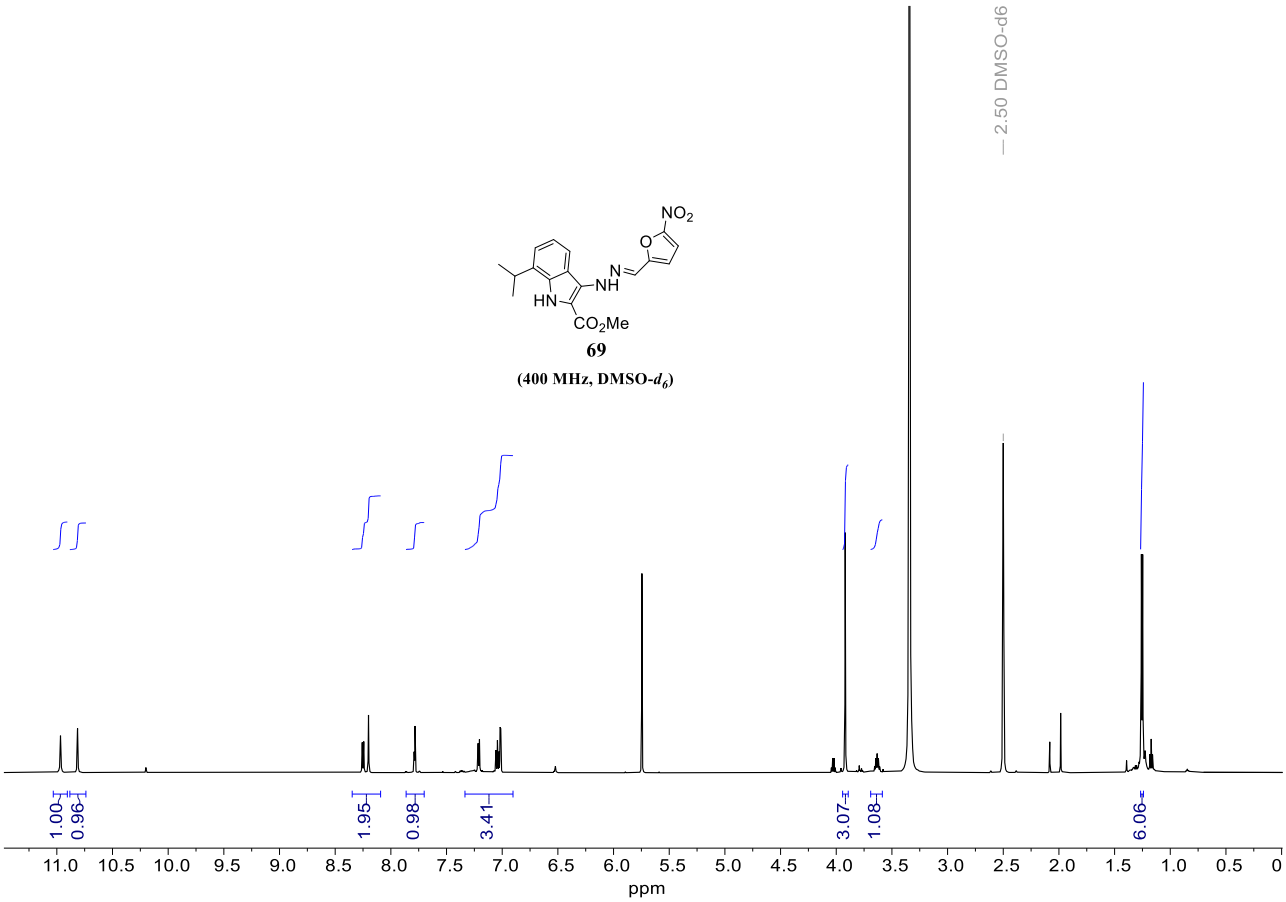

Figure 3.52 ^{1}H NMR spectrum of ester 69 in DMSO-d_6 representing the most stable rotamer *i.e.* the '*global minimum*' (*cf.* Fig. 3.47).

Intriguingly, stirring methyl ester **69** in BCl_3 1.0 M in dry dichloromethane, under an inert atmosphere *i.e.* N_2, Ar *etc.*, for a short period of time; and then quenching the thus obtained mixture with methanol at ambient temperature, exclusively furnished the major rotamer of ester **69** after preparative RP-HPLC purification, as evidenced by ^{1}H NMR (Fig. 3.53); however, some decomposition to give InC **67** was also observed, which seems to correspond to amount of the minor rotamer (Fig. 3.47).

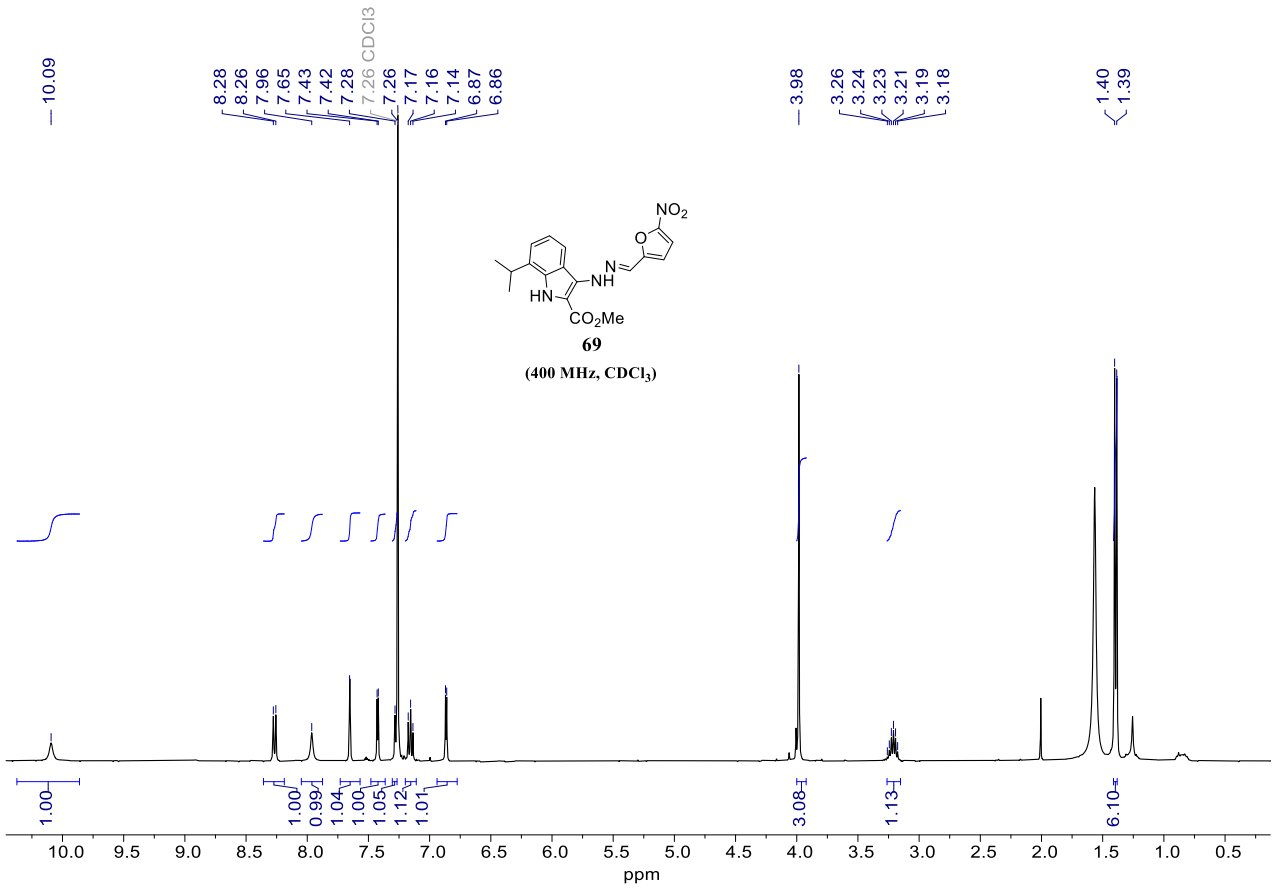

Figure 3.53 The cleanest ^{1}H NMR spectrum of the major rotamer of methyl ester 69 in $CDCl_3$ at ambient temperature, to date; for full characterisation and *J* values in Hz *cf.* Experimental p. S57.

3.3.2.4 Alternative Methods for Hydrolysis of NInC Methyl Esters

Having successfully synthesised methyl ester **69** in excellent purity *i.e.* >98% (*nota bene*: solvent complications aside *cf.* Fig. 3.48).

First and foremost, its hydrolysis using a modified procedure (Section 3.3.2.3) of Finkelstein reaction (*loc. cit.*) *via* the action of lithium iodide in pyridine on ester **69** was attempted, which turned out not to come to any fruition.

Thenceforth, several other, and perhaps some of the fanciest and most fable ester hydrolysis procedures of the literature were also attempted, and all were nothing but futile (Scheme 3.23).

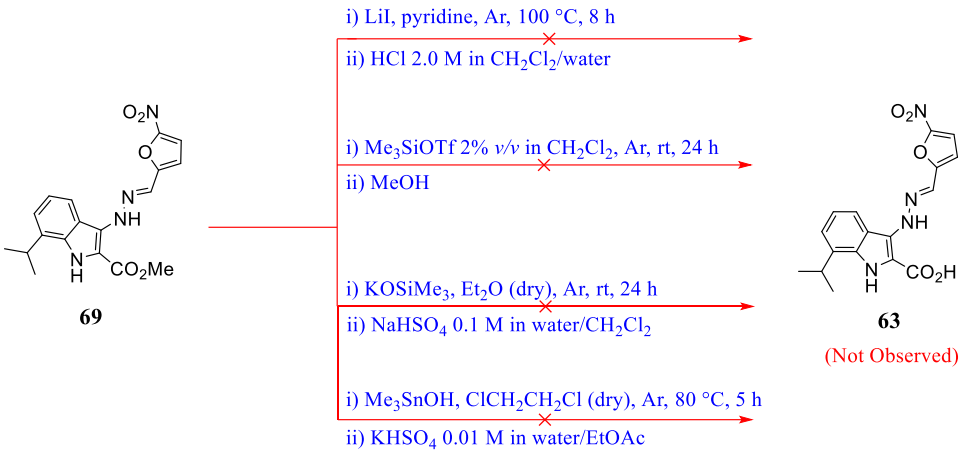

Scheme 3.23 Attempted hydrolysis of methyl ester 69 *via* a variety of different hydrolysis methods.

Perhaps the most referenced ester hydrolysis under anhydrous conditions in the literature is described by various silyl reagents such as potassium trimethylsilanolate,[611] and trimethylsilyl trifluoromethanesulfonate.[612] However, upon addition of such ester hydrolysing silyl reagents to carefully dried solutions of ester **69** in strictly anhydrous organic solvents, a spontaneous decomposition was observed on each and every single occasion, and the clear ruby in colour anhydrous mixtures of ester **69** all turned completely pitch-black upon addition of silyl reagents thereto.

Even trimethyltin hydroxide which has been hailed by Nicolaou *et al.*[613] as one of the mildest and most chemoselective methods for ester hydrolysis, also failed to furnish the desired outcome (Scheme 3.23).

P. S. Manchand[614] was first to report boron trichloride as a reagent for hydrolysis of esters, inspired by this a modified procedure for hydrolysis of the methyl ester moiety in ester **69** under strictly anhydrous conditions was devised (Scheme 3.24), which successfully hydrolysed some of the methyl ester moiety in ester **69**, leaving some of the hydrazone moiety in the thus obtained acid **63** intact.

However, some of the hydrazone moiety in acid **63** was also hydrolysed as well, the difficulty in achieving a satisfactory chemoselective ester hydrolysis *via* boron trichloride for ester **69** brings home to us the fact that the degree of success with which boron trichloride could or could not furnish a clean chemoselective ester hydrolysis for esters of this kind *e.g.* ester **69**, is determined solely by the following variables:

- Strength and amount of boron trichloride solution with respect to ester **69**
- Traces of water in the reaction mixture
- Temperature
- Reaction time

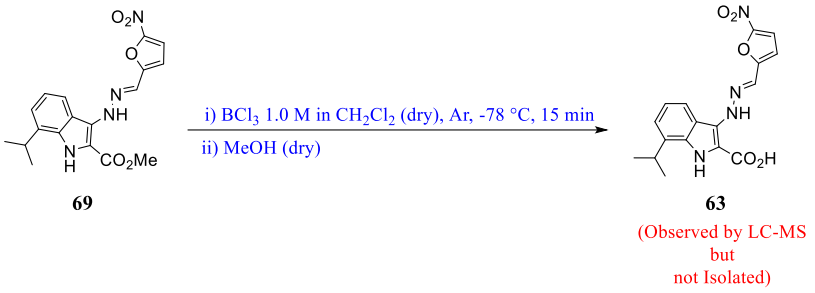

Scheme 3.24 A promising method for obtaining acid 63.

Initially, an anhydrous reaction condition was employed for the hydrolysis of ester **69**, in virtue of assumptions that boron trichloride activates the carboxyl moiety,[615] in a manner similar to A*cid*-catalysed, *alkyl*-oxygen cleavage, *unimolecular* ($A_{AL}1$) with a positive value of $\Delta S^{\ddagger}$ *i.e. dissociative*,[616] as opposed to commonly observed B*ase*-catalysed, *acyl*-oxygen cleavage, *bimolecular* ($B_{AC}2$) with a negative value of $\Delta S^{\ddagger}$ *i.e. associative*,[617] with nucleophiles of the general type $Nu^{\ominus}$ *e.g.* $HO^{\ominus}$ in saponification of uncomplicated esters.

Thus, the aforementioned ester cleavage with boron trichloride could, in theory, take place in the absence of water, even though by definition the carboxyl ester hydrolysis is not a hydrolysis without water.

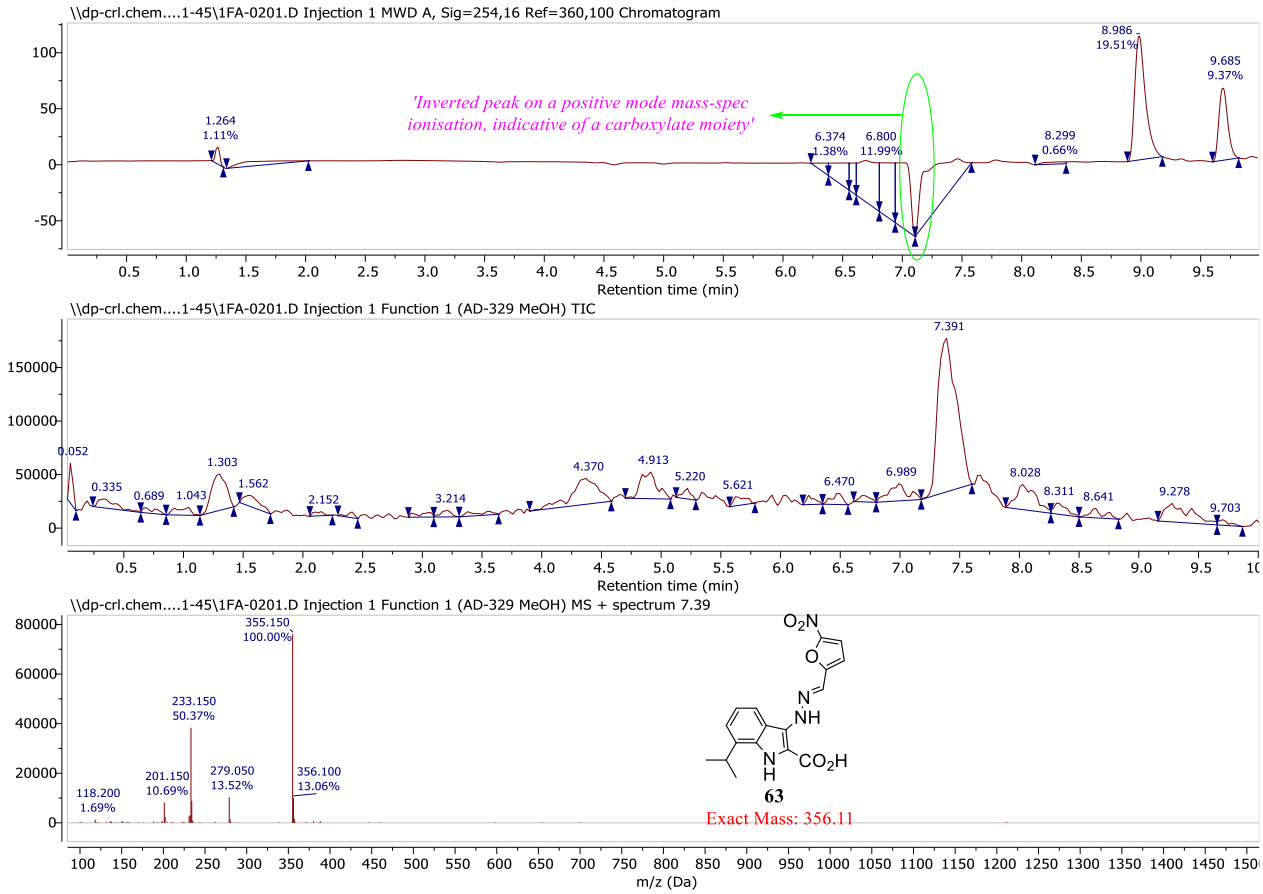

Figure 3.54 LC-MS evidence for formation of NInC 63; the inverted peak at *ca.* 7.15 min further establishes that the analyte was indeed a carboxylate species.

Support for the above view is provided by LC-MS analysis (Fig. 3.54), such that acid **63** was formed upon contact of the thus obtained crude species from the action of boron trichloride on ester **69** under anhydrous conditions with water under the LC-MS condition, which was not sufficient both in strength and time for the obtained acid **63** to completely fall apart, and crucial evidence for its existence was brought to light.

It should, however, be emphasised that the desired acid **63** is partially zwitterionic in character, and this full-blown charge distribution, by all means, not only renders its purification by flash column chromatography infeasible, but also portrays its flash column chromatography purification as being far from ambitious. Nevertheless, attempts at flash column chromatography purification of crude **63** all failed, and preparative RP-HPLC had to be recruited.

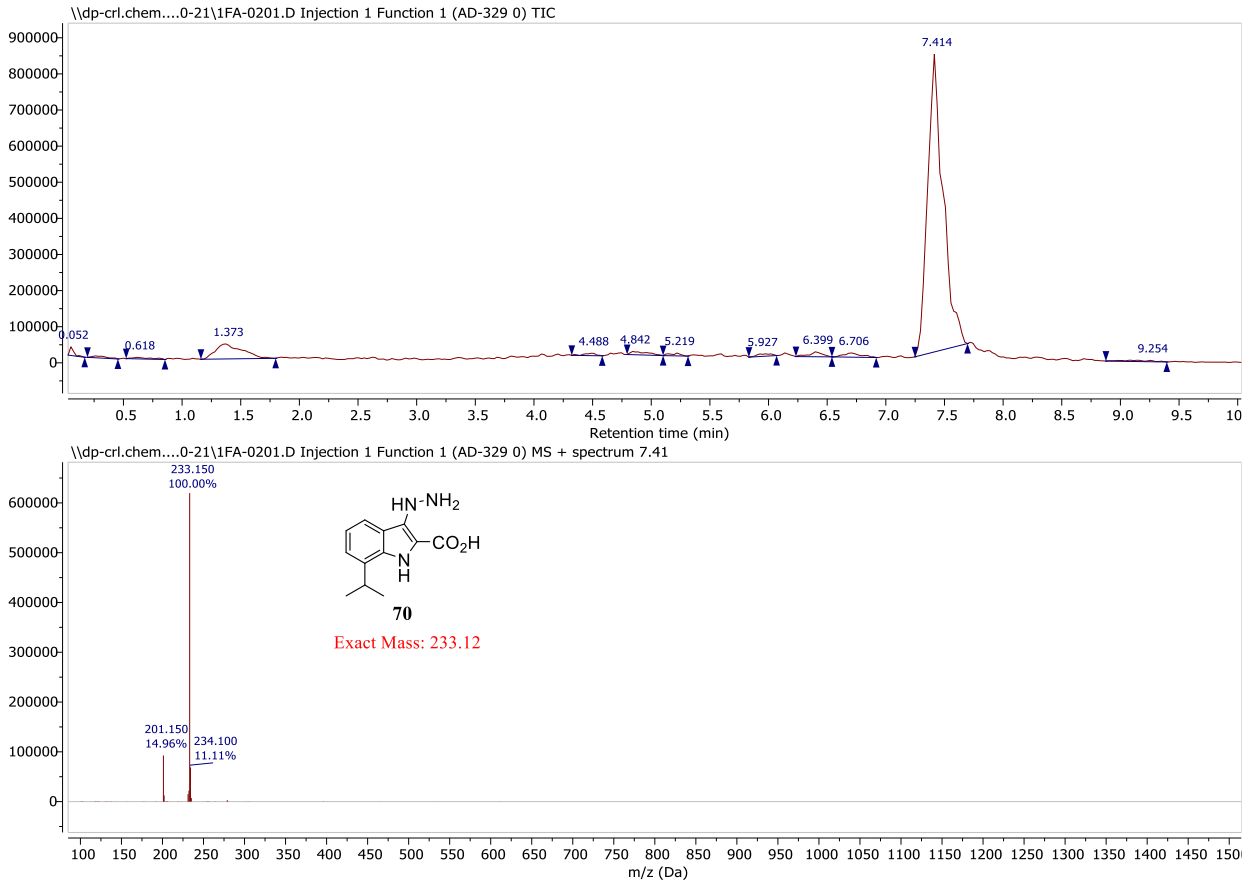

Figure 3.55 LC-MS trace of hydrazide 70 obtained from preparative RP-HPLC purification of crude acid 63.

It should not be overlooked that the desired acid **63** is still inherently unstable in water or polar solvents such as methanol *etc.*, and whilst the unreacted ester **69** was recovered in excellent purity by RP-HPLC purification (Fig. 3.53), the desired acid **63** was again hydrolysed this time to hydrazide **70**, as evidenced by both LC-MS (Fig. 3.55), and ^{1}H NMR (Fig. 3.56).

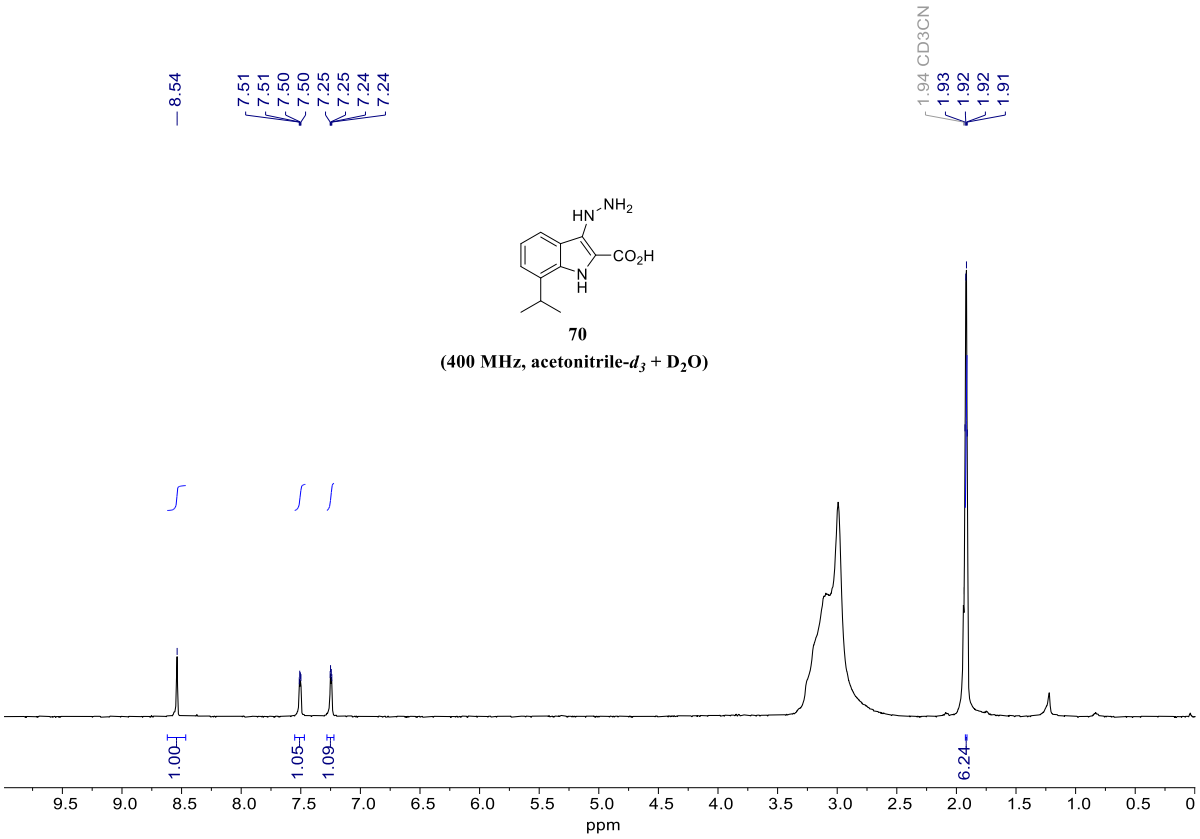

Figure 3.56 ^{1}H NMR spectrum of hydrazide 70. The singlets from the aromatic protons resonate at the lowest field *i.e.* δ 8.54, 7.51 & 7.25, whereas the methyls of isopropyl moiety resonate at the highest field *i.e.* δ l.92, with the broad H-bonding signal from the exchangeable protons at ~ δ 3.5 – 3.0 hovering over that from the methine.

The above findings are all valid reasons to suggest that both carboxyl ester and hydrazone moieties in NInC esters are thermodynamically similar in nature, and even though they, in point of fact, possess different kinetics *e.g.* as we saw above NInC **63** was the kinetic product and an intermediate in the course of hydrolytic decomposition of ester **69**, the activation barriers between acid **63** and its ensuing decomposed products are relatively insufficient to resist its further break down, in the face of unwanted thermodynamic products of potentially much lower energy than the desired acid **63**, in virtue of their entropic favourability thereof. Thus, the actual mechanism of the hydrolysis to which both the carboxyl ester and hydrazone are susceptible, could well have not changed on altering reagents and methods, so that we are not, of necessity, any the wiser about these hydrolysis methods such that rendering practical hydrolysis of the carboxyl ester moiety in presence of the hydrazone moiety virtually impossible, and a different PG for the carboxylate should ideally be explored.

3.3.3 Alternative Protecting Group Strategies for the Carboxyl Moiety of NInC Hybrids

Carboxylate esters that are otherwise difficult, or even impossible, to be directly hydrolysed to their corresponding carboxylic acids, may sometimes be accomplished by modification of the PG for the carboxyl group, often through the choice of a mild and inert PG, which could easily and chemoselectively be removed at will.

The prime example of such alternative PGs is benzyl (Bn) moiety, which could chemoselectively be removed by hydrogenolysis in presence of acid/base labile moieties – in this case, the hydrazone moiety. However, here again we have a clash of functional groups such that the essential nitrofuran moiety would also be reduced by hydrogenolysis; thus, the nitrofuran moiety in NInC hybrids precludes the use of Bn, carbobenzyloxy (Cbz), *p*-methoxybenzyl carbonyl (Moz), allyloxycarbonyl (alloc) PGs, to name but a few, for protection of the carboxylate moiety in the aforementioned NInC hybrids.

On the other hand, many other useful PGs for carboxylates including, but not limited to *β*-methoxyethoxymethyl ether (MEM), methoxymethyl ether (MOM), methylthiomethyl ether (MTM), tetrahydropyranyl (THP), Trt *etc.*, are equally removed by acids to which the hydrazone moiety in the NInC hybrids is very vulnerable (Section 3.3.2.1).

Thus, the salient functional group incompatibility arising from packing several characteristically similar functional groups, all in one molecule, leaves us with not many choices of PG strategies.

Nevertheless, in seeking a suitable alternative PG for the carboxyl group in NInC hybrids, a couple of too compelling not to miss, and potentially very chemoselective PGs strategies were also investigated.

3.3.3.1 p-Methoxybenzyl Ester Protecting Group Strategy

When we come to consider a PG strategy for complicated carboxylates of the type NInC hybrids, due credit must be paid to *p*-methoxybenzyl (PMB) PG, which can be cleaved in acids, by hydrogenolysis, and even more so intriguingly by oxidation with 2,3-dichloro-5,6-dicyano-*p*-benzoquinone (DDQ),[618] which are all valid deprotection methods so as to render PMB PG a very versatile tool at the synthetic chemist's disposal.

In view of the above, efforts were made to selectively PMB protect the carboxyl moiety in InC **71** (Scheme 3.25); however, unfortunately, even use of only one equiv. of PMB bromide with respect to InC **71** starting material yielded di-PMB protected InC **72**.

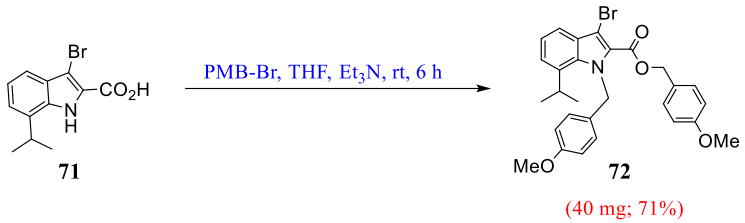

Scheme 3.25 Synthesis of unintended di-PMB protected InC 72.

With InC **72** in hand, its Buchwald coupling to hydrazone **44** was attempted, which to our dismay was unsuccessful, presumably due to steric limitations and/or unwanted PG deprotection during the aforementioned Buchwald coupling.

The above findings brought home to us the fact that it might be too ambitious trying to mono-protect the carboxylate moiety in the InC species in presence of the more nucleophilic nitrogen of the indole moiety in the same molecule.

By the same token that the pertinent indoles were synthesised with the carboxylate moiety already protected as an ester (Scheme 3.22), the corresponding alternatively protected carboxyl moiety should be synthesised first, and then using the thus obtained protected carboxyl building block, attempting the synthesis of the desired indole species (Scheme 3.26).

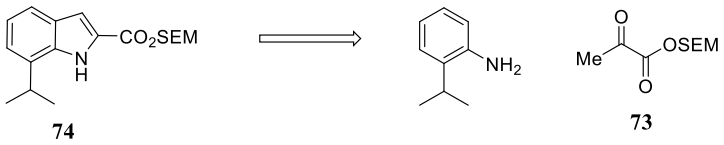

Scheme 3.26 Retrosynthetic analysis of SEM-protected InC 74.

3.3.3.2 Trimethylsilylethoxymethyl Ether Protecting Group Strategy

Inasmuch as PMB PG proved a bit risky in the aforementioned preliminary experiments, it appeared more practical to use a different PG for synthesis of the indole species from scratch.

Trimethylsilylethoxymethyl (SEM) PG has been extensively used in the literature for the protection of nucleophilic nitrogen and oxygen species,[619] and it has been purported that SEM PG is robust with excellent survival under bromination, saponification, oxidation and other harsh synthetic conditions,[620] not least it can chemoselectively and easily be removed in high yields *via* the action of magnesium bromide in nitromethane,[621] tributylammonium fluoride (TBAF) in THF and *N,N'*-dimethylpropyleneurea (DMPU)[622] *etc.*

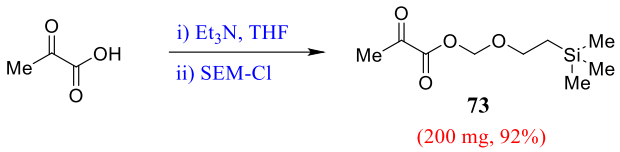

Scheme 3.27 Synthesis of SEM-protected pyruvate 73.

In the light of what has been said above, it was quite tempting to give SEM PG a chance, and synthesise SEM-protected pyruvate **73** by deprotonation of pyruvic acid using triethylamine in THF, and then addition of the thus obtained triethylammonium pyruvate *in situ*, to SEM chloride (Scheme 3.27).

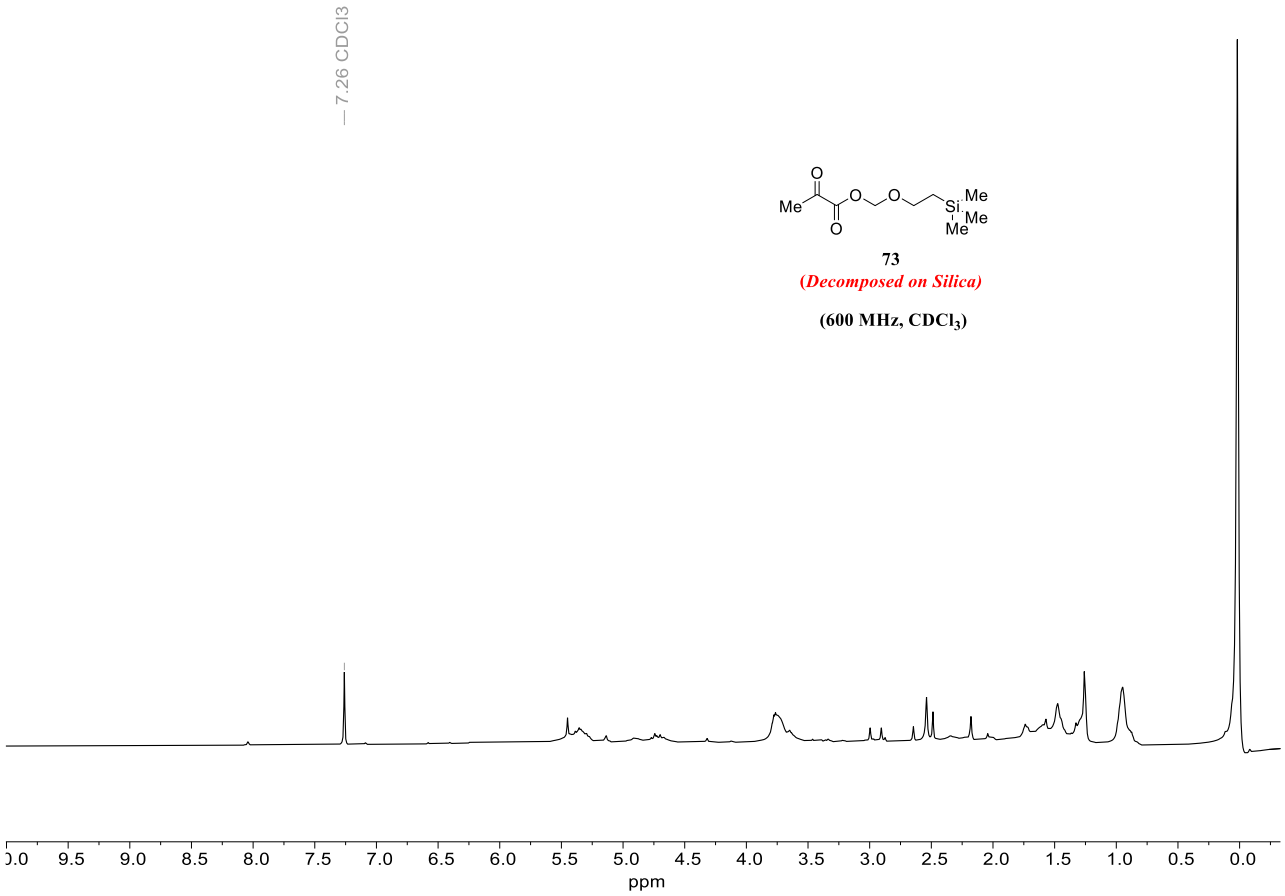

Figure 1.57 ^{1}H NMR spectrum of pyruvate 73 after flash column chromatography purification.

Some workers[623,624] have had better days than us for silica flash column chromatography purification of their crude SEM-protected intermediates.

It is seldom, if ever, possible to purify SEM-protected pyruvate **73** using silica flash column chromatography (Fig. 3.57); nevertheless, the obtained crude pyruvate **73** was of acceptable purity, as evidence by its ^{1}H NMR (Fig. 3.58), to be used in the next step *i.e.* indole synthesis, without further purification.

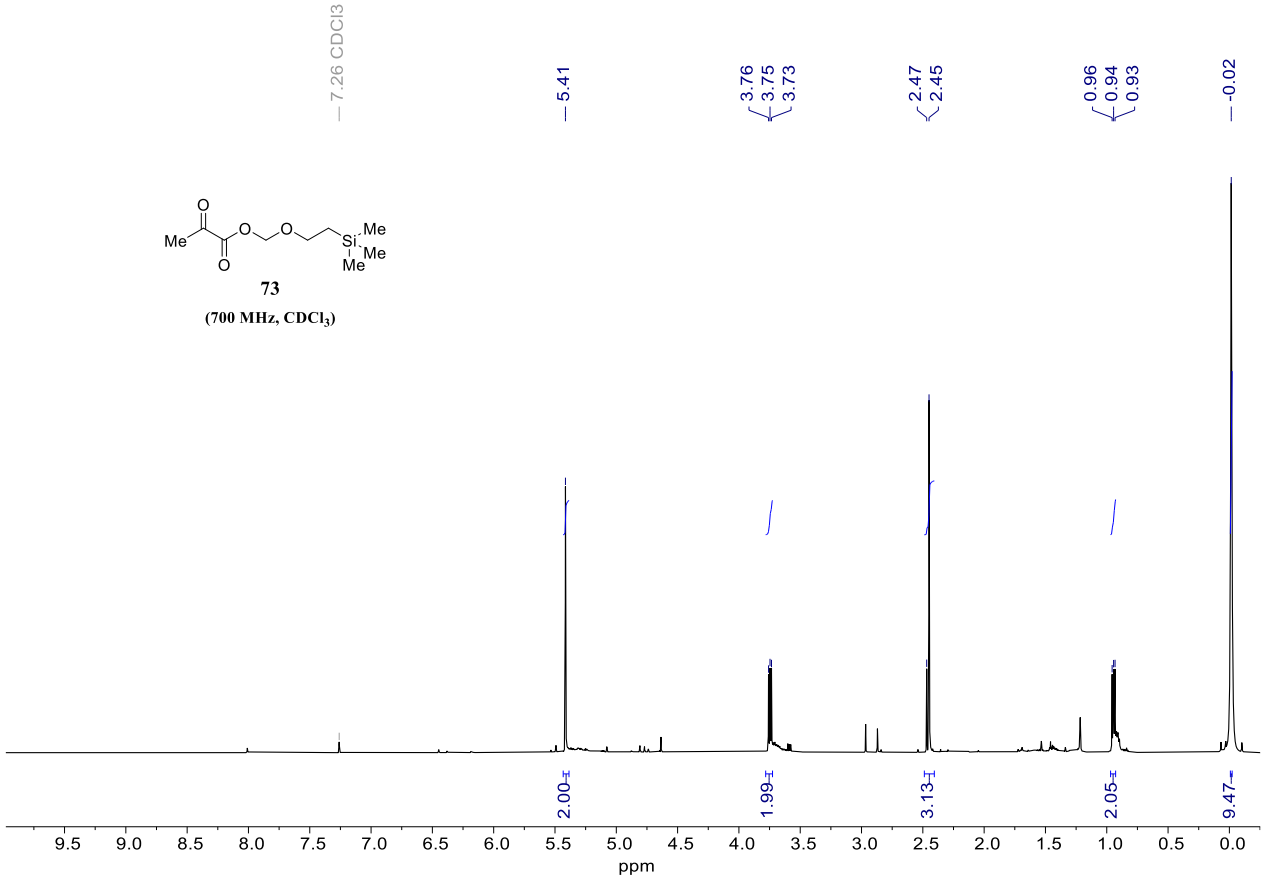

Figure 3.58 ^{1}H NMR spectrum of pyruvate 73 before flash column chromatography purification. The methylene ether flanked between the oxygens resonates at δ 5.41, followed by the successive methylenes away from the ether moiety at δ 3.75 & 0.94, respectively; the methyl of the dicarbonyl absorbs at δ 2.46, and last but not least the somewhat common internal standard *i.e.* TMS group appears at δ -0.02, as anticipated; for full characterisation *cf.* Experimental p. S63.

Having successfully synthesised pyruvate **73**, using the previous indole synthesis procedure (Scheme 3.22) by which methyl and ethyl pyruvates were recruited to synthesise InC esters **67** and **56**, respectively; the synthesis of InC **74** using pyruvate **73** was attempted, which then again, unfortunately, was futile (Scheme 3.28).

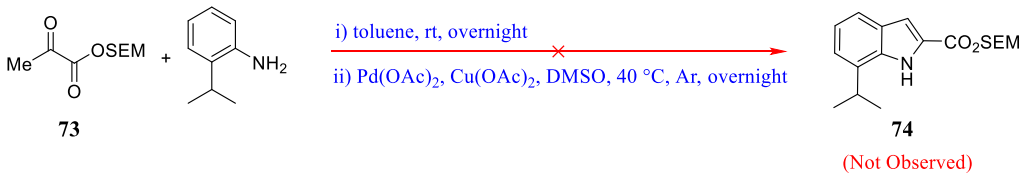

Scheme 3.28 Attempted synthesis of InC 74.

3.3.3.3 No Carboxyl Protecting Group Strategy

Finally, given that most, by no means all, attempts at converting the masked NInC hybrids to their corresponding carboxylic acid, namely, NInC **63** failed, a bold and ambitious move of coupling the zwitterionic InC **71** to hydrazone **44** without any type of carboxyl protection was also attempted, which did not come as a surprise that this approach also did not come to any fruition for synthesis of NInC **63** (Scheme 3.29).

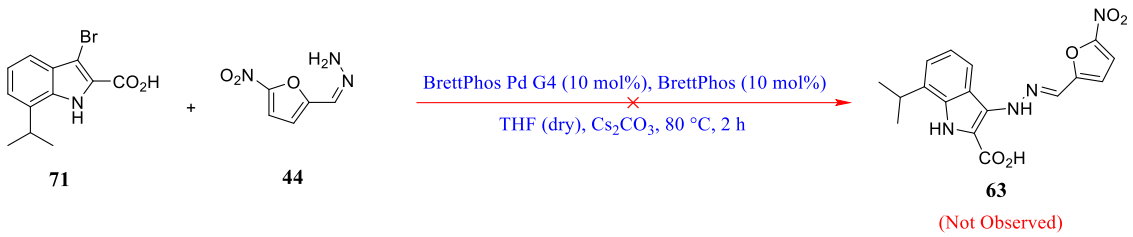

Scheme 3.29 Representative failed attempts at synthesis of NInC 63 from unprotected InC 71.

3.3.4 Bypassing Carboxyl Protection in NInC Synthesis

It cannot be too firmly emphasised, however, that the deprotection of protected carboxyl moiety of any kind is pretty much incompatible with the above NInC hybrids, and the difficulty in finding a compatible PG for the carboxyl moiety is somewhat dependent on incompatibility of the hydrazone linker with the former's deprotection conditions; as such, these difficulties prompted the possibility of bypassing protection of the carboxyl moiety with a PG altogether.

It should be remembered that once the desired NInC hybrid is inside the cell, the hydrazone linker would be cleaved to release the pertinent non-β-lactam β-lactamase inhibitor *i.e.* InC monomer and the nitrofuran warhead (Section 3.3).

Thus, it quickly becomes apparent that once again the inherent reversibility of carbonyl chemistry can be utilised to bypass the aforementioned difficulties in using PGs for the carboxyl moiety in NInC hybrids, by installing a masked benzaldehyde *i.e.* phenyl 1,3-dioxolane at C-3 of the InC species, which can be deprotected together with any of the pertinent carboxyl's PG to reveal the InC **77**, ready for the attack by nitrofuran **44** to yield the modified NInC hybrids.

Starting from *p*-bromobenzaldehyde and ethylene glycol in dry THF and catalytic amount of trifluoromethanesulfonic acid, the masked acetal **75** was accomplished in excellent yields, *i.e.* 85–90% (Scheme 3.30).

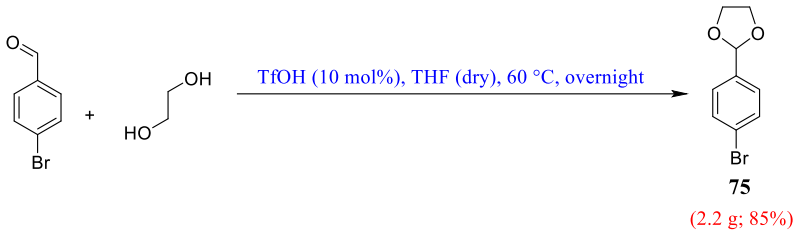

Scheme 3.30 Synthesis of acetal 75.

Once again, InC **58** (Section 3.3.1.5) came in handy, and was coupled to the above acetal **75** to furnish the protected InC ester **76** in good yields *i.e.* 65–70% (Scheme 3.31).

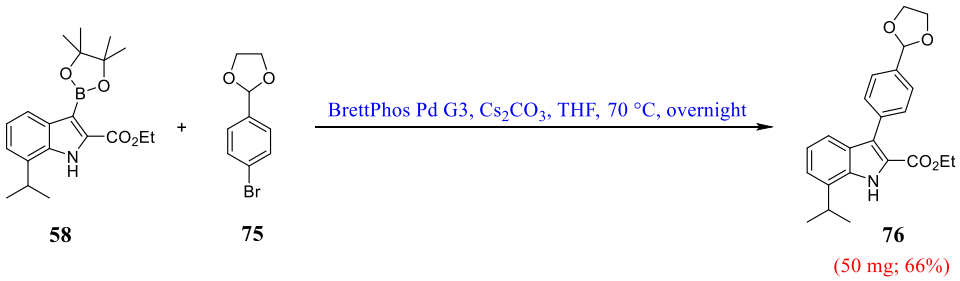

Scheme 3.31 Synthesis of InC ester 76.

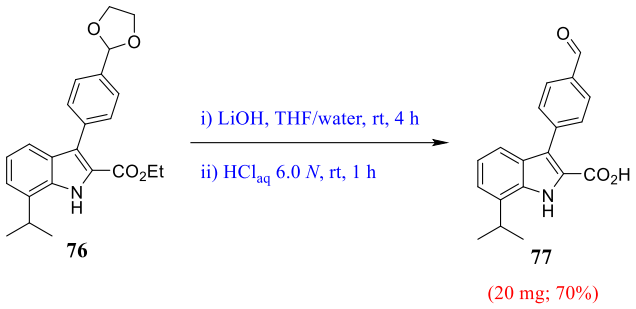

Scheme 3.32 Acid & base hydrolysis of InC ester 76.

Utilisation of acid/base dichotomy rendered telescoping both acetal and ester hydrolyses in one step (Scheme 3.32), so as to obtain InC **77** in good yields *i.e.* 67–70%, and as always, excellent purity, as evidenced by ^{1}H NMR (Fig. 3.59).

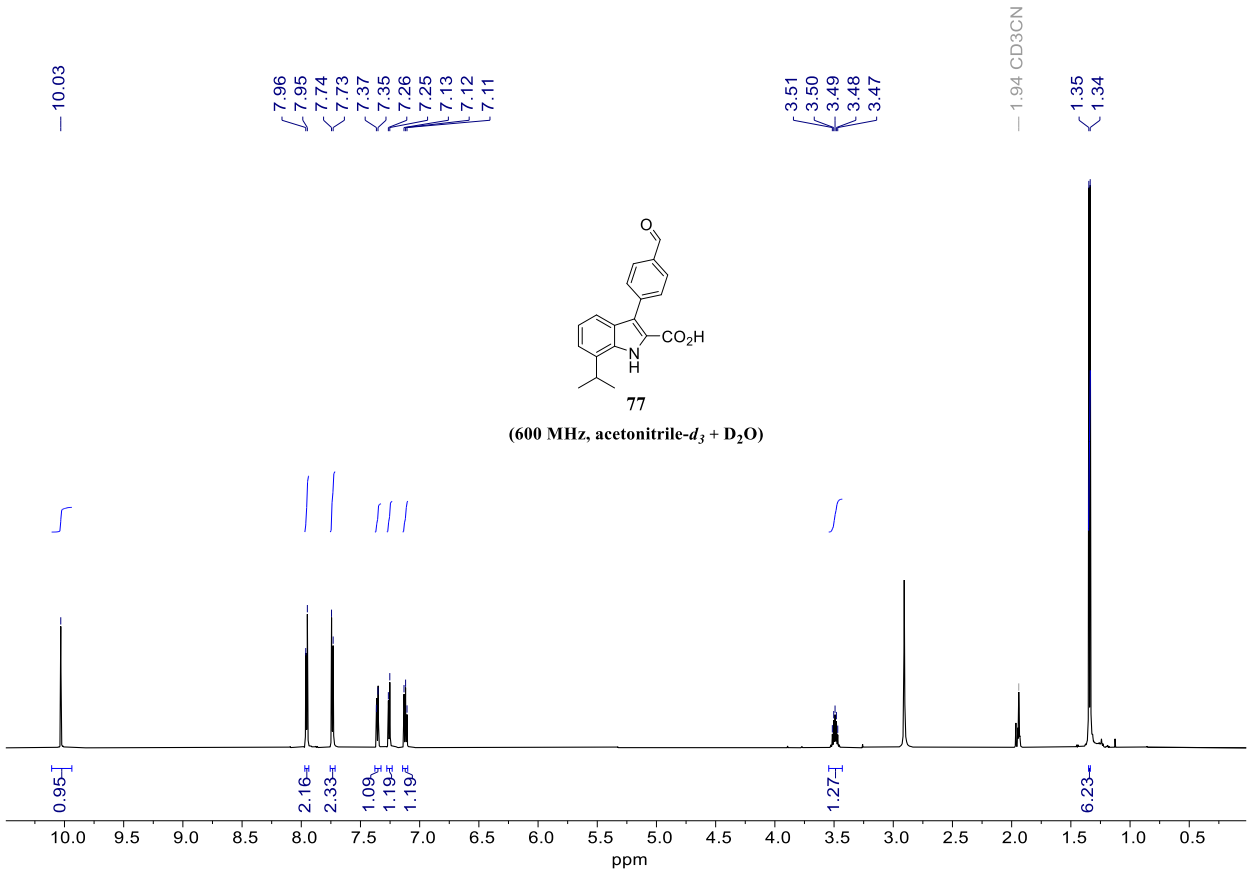

Figure 3.59 ^{1}H NMR spectrum of InC 77, illustrating its excellent purity. The formyl moiety resonates at the lowest field at δ 10.03, together with the aromatic protons at δ 7.96 – 7.12, and the isopropyl at δ 3.49 & 1.35; for full characterisation and *J* values in Hz *cf.* Experimental p. S63.

The importance of minimising overzealous use of PGs in synthesis is best delineated by the confusion that can result when PG strategy has been assumed, wrongly, as the synthetic chemist's go-to strategy, or established erroneously; this is so because the most practical and best total syntheses *i.e.* the '*ideal syntheses*' are those with no or, at the very best, minimal PG contribution.[625]

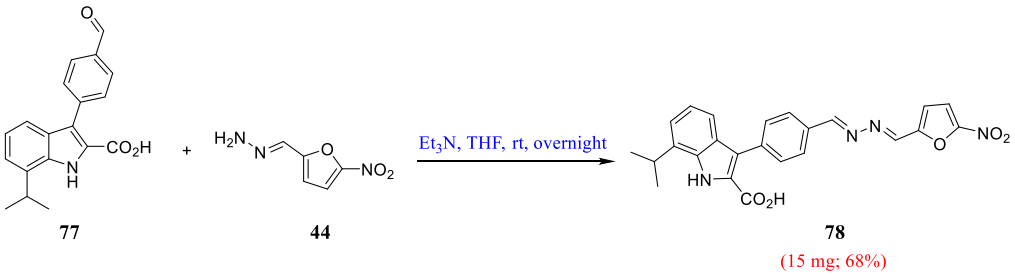

Scheme 3.33 Synthesis of NInC 78.

In the light of what has been said above, the elimination of various PG strategies from the aforementioned synthesis of NInC hybrids brought about the modified NInC **78** (Scheme 3.33), which in point of fact, exhibits better physical stability than its corresponding NInC **63**, such that it was, to some extent, feasible to purify the former using flash column chromatography on silica, which was otherwise impossible for the latter (Section 3.3.2.4).

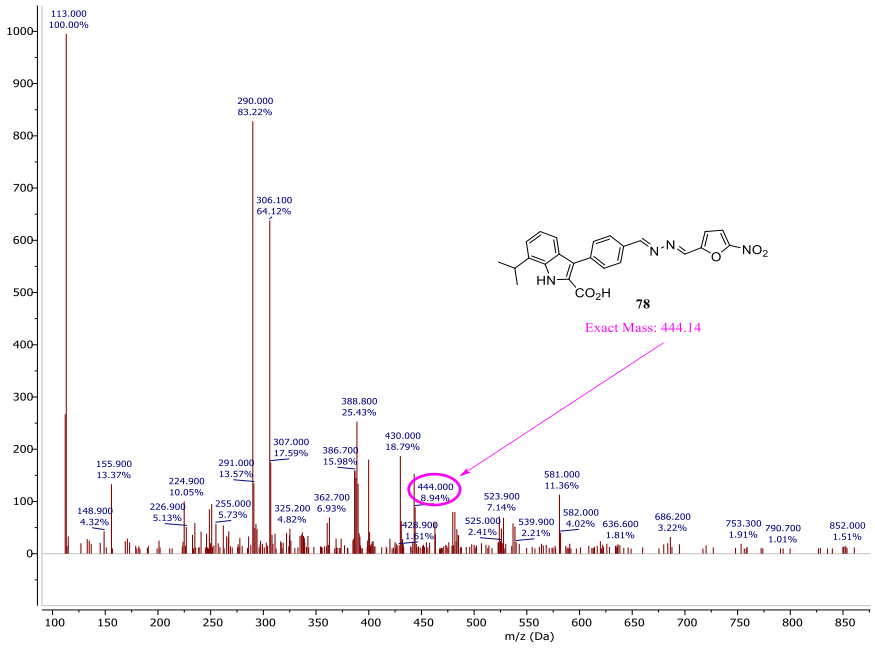

Figure 3.60 Mass-spec trace of NInC 78 on the negative ionisation mode (ESI).

Although, NInC **78** was solemnly detected on the negative mode ionisation (ESI) mass-spec (Fig. 3.60), its ^{1}H NMR spectrum indicated some contaminants, which were not resolved by flash column chromatography purification (Fig. 3.61). Nonetheless, the synthesis of **78** accomplished the objective of symbiotically associating InCs with nitrofurans in a single molecule of therapeutic potential.

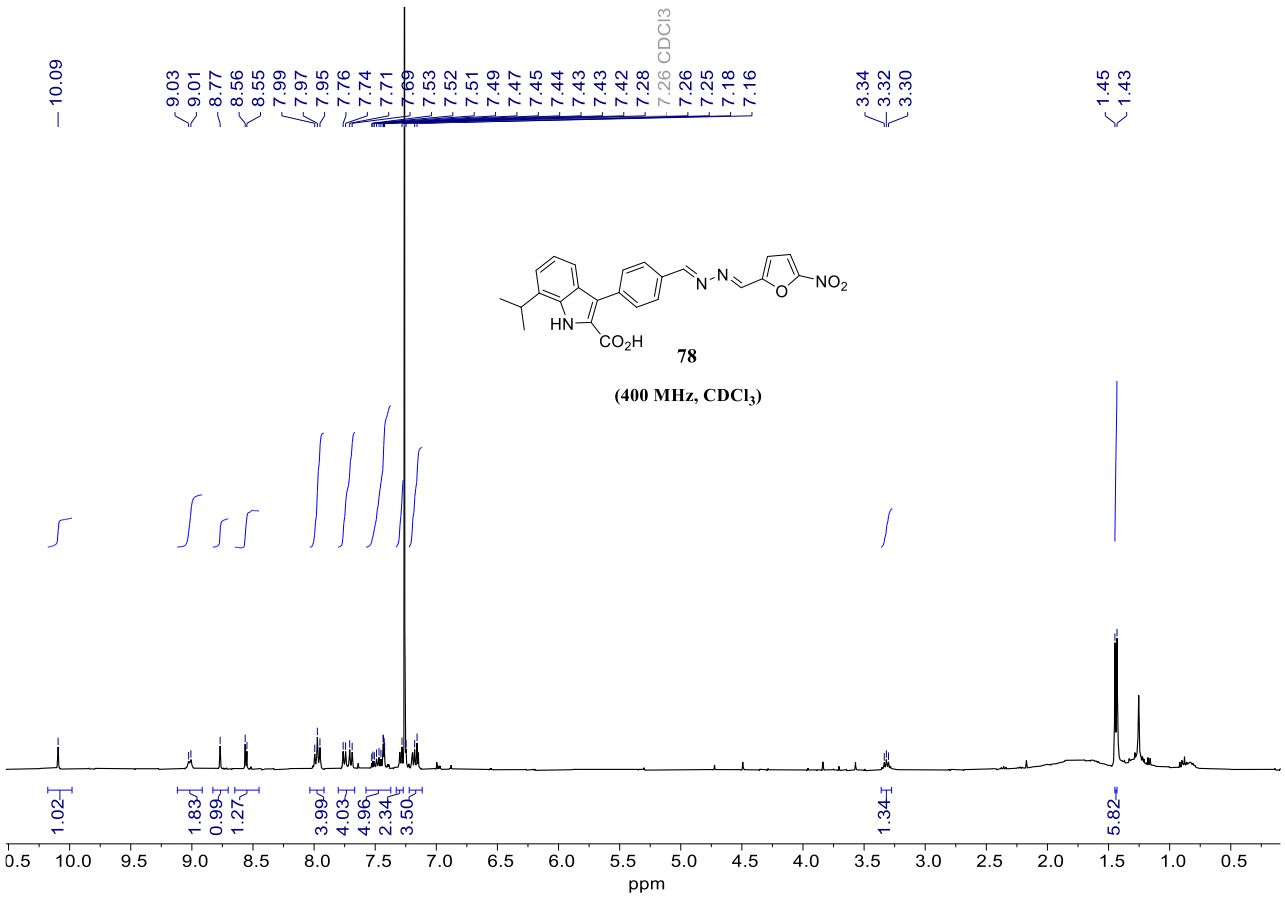

Figure 3.61 ^{1}H NMR spectrum of NInC 78. Apart from the singlet from the exchangeable proton of the indole ring at δ 10.09, the many aromatic protons in 78 resonate at ~ δ 8.77 – 7.17 with the methyls at the highest field *i.e.* δ 1.44; for full characterisation and *J* values in Hz *cf.* Experimental p. S67.

3.3.5 Design & Synthesis of NInC Hybrids Featuring a Stable Cleavable Linker

The hydrazone linker instability in drug conjugates here as elsewhere,[626] compelled resorting to a more stable cleavable linker than that used in the initial hydrazone linkers of the above NInC hybrids.

Inasmuch as Besponsa® *i.e.* inotuzumab ozogamicin conjugate owes its clinical success to its somewhat stable carbohydrazone linker in the systemic circulation,[627] this served as an inspiration for designing new NInC hybrids, featuring slightly more stable carbohydrazone linkers than the previously designed acid/base labile hydrazone linkers.

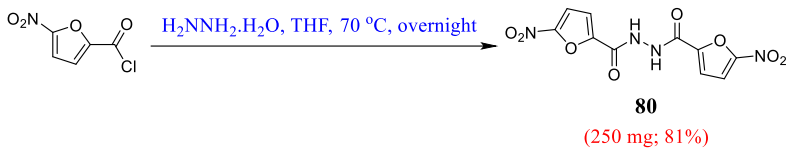

80
(250 mg; 81%)

Scheme 3.34 Serendipitous synthesis of nitrofuran dimer 80.

A requisite for the above initiative was the synthesis of nitrofuran **79** (Scheme 3.36); however, unlike the straightforward synthesis of nitrofuran **44** (Scheme 3.2), just mixing 5-nitro-2-furoyl chloride with hydrazine monohydrate did not furnish the desired nitrofuran **79**, instead the unexpected dimer **80** was serendipitously obtained in excellent yields (Scheme 3.34) as well as purity, as evidenced by ^{1}H NMR (Fig. 3.62).

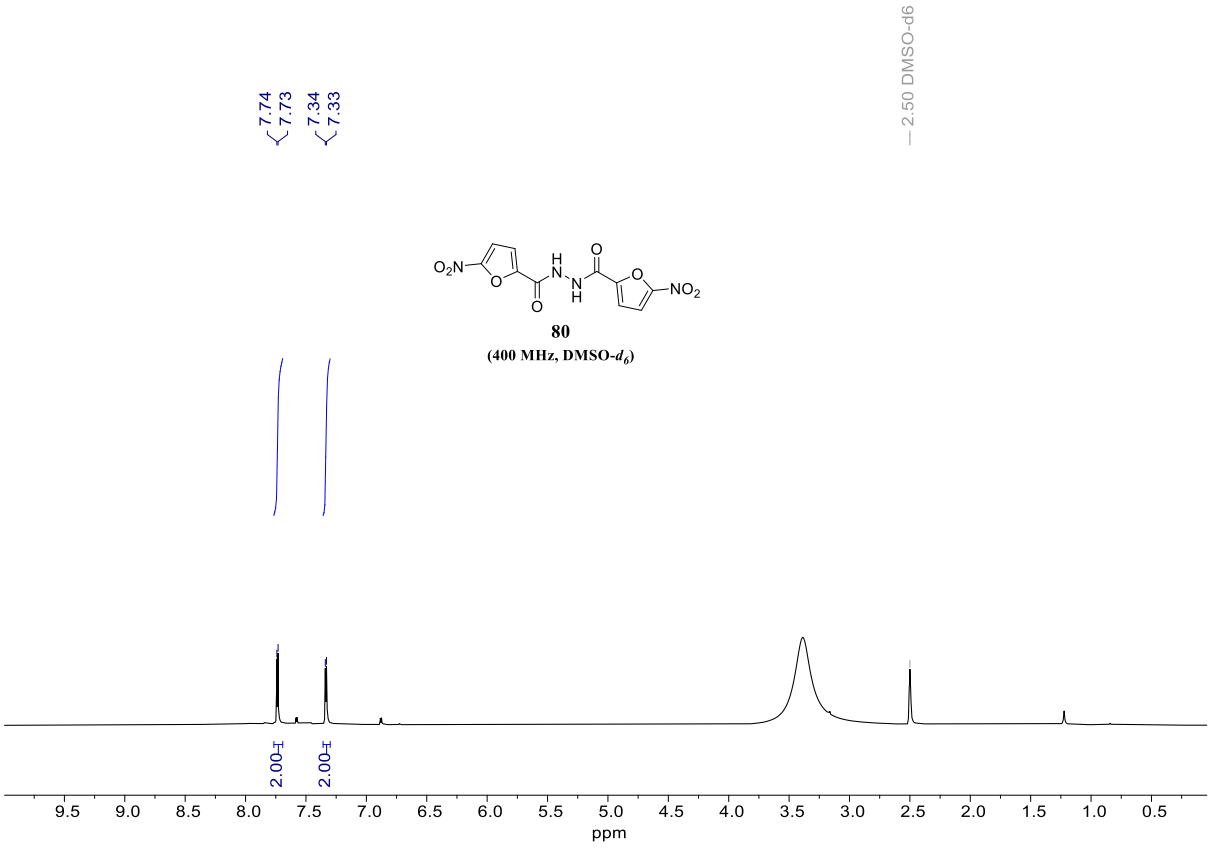

Figure 3.62 ^{1}H NMR spectrum of nitrofuran dimer 80. The aromatic protons of the furan ring give rise to the singlets at δ 7.74 & 7.34 in the thus obtained ^{1}H NMR spectrum of dimer 80.

The colour of nitrofuran dimer **80** is again of particular importance, and reference has already been made to the correlation between purity of conjugated nitrofuran compounds and their intrinsic colours (Section 3.3.1.3).

We previously saw that the delocalisation of eight π electrons in hydrazone **44** was responsible for its orangish colour. It also brought home to us that symmetry would influence the colour of conjugated molecules *cf.* lycopene and *β*-carotene; here again, dimer **80** is not fully conjugated, but indeed symmetric. On the other hand, dimer **80** possesses several nitrogen and oxygen auxochromes, which can donate their accessible lone pairs to the conjugated system so as to extend the electron delocalisation in the already established conjugated system. This effect together with the partial double bond character of semi-carbohydrazide in the dimer facilitates its tautomerisation to give a more stable fully conjugated dimer **81** with 16 delocalised π electrons in its conjugated system (Fig. 3.63).

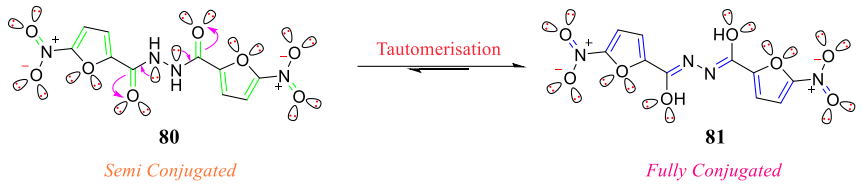

Figure 3.63 Tautomerisation of dimer 80 to 81 resulting in a fully conjugated system with 16 delocalised π electrons in the thus obtained more stable centrosymmetric molecule.

Although the thus obtained tautomer **81** is centrosymmetric, and in theory, its fundamental electronic excitation would be no different from that in hydrazone **44** with only eight π electrons in its conjugated system; however, in practice, it is unclear as to what extent this tautomerisation does take place in solid phase for dimer **80**; moreover, both dimer **80** and its tautomer **81** possess more auxochromic oxygens in their conjugated systems than that of hydrazone **44**, which should not be overlooked.

Thus, even though the above complications do add a certain element of confusion when we come to consider the fundamental electronic excitation for this type of conjugated nitrofuran species, but what matters is that the combined conjugative effect of dimer **80** together with its more stable tautomer **81** in solid phase gives its crystal lattice an intrinsic coral pink colour; otherwise, the pertinent dimer itself similar to hydrazone **44** would only exhibit a dark orangish colour, and that this should be so is a corollary of its centrosymmetric nature (Section 3.3.1.3).

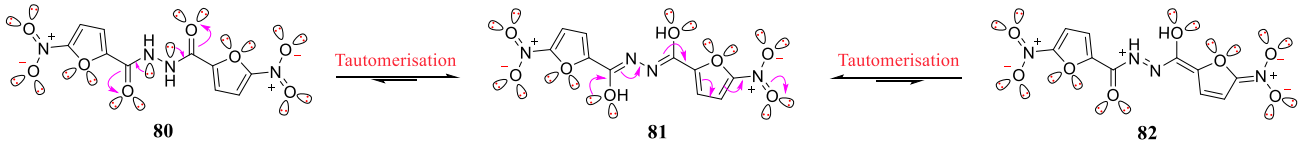

Figure 3.64 Further tautomerisation of homodimer 81 yields heterodimer 82.

It also appears as though in solution, especially in a DMSO medium ~ 5.0–10% of homodimer **81** tautomerises again to form heterodimer **82** (Fig. 3.64) by virtue of complexation with the polar solvent *i.e.* DMSO.

Support for the above phenomenon is provided by the observation that similar to hydrazone **44**, the enol part of heterodimer **82** now can push the furan ring into a puckered conformation so as to set up a weak induced ring current in an applied magnetic field by virtue of complexation with DMSO (Fig. 3.65).

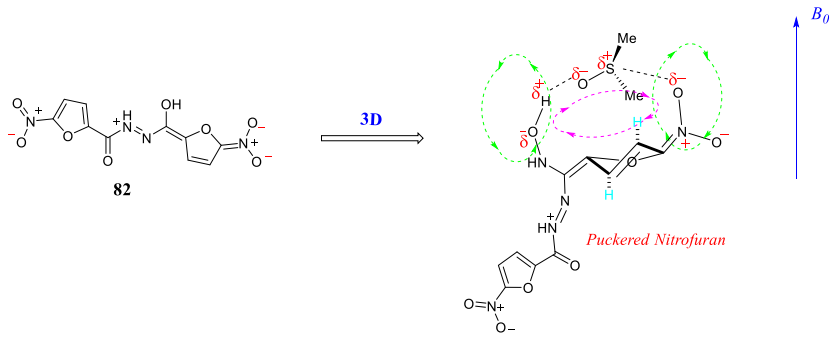

Figure 3.65 It can be hypothesised that dimer 82 sets up a weak induced ring current in an applied magnetic field by virtue of complexation with DMSO.

It will thus be apparent as to why the minor signals in the ^{1}H NMR spectrum of this nitrofuran at *ca.* δ 7.6 and 6.9 are exactly 0.7 ppm apart, nearly double of that observed for the major signals at *ca.* δ 7.7 and 7.3 (Fig. 3.66). This large shift between the minor signals can be explained by the aforementioned induced ring current (Fig. 3.65).

Unfortunately, this dimer is virtually insoluble in relatively less polar solvents such as chloroform, dichloromethane, diethyl ether *etc.*, so as to compare the solvent effects on the position of ^{1}H NMR signals from the protons of furan rings in the dimer, and validate the supposedly induced ring current.

Nevertheless, this effect has clearly been echoed by hydrazone **44** (Section 3.3.1.2), and it may, though it need not of necessity, be safe to conclude that in the light of its ^{1}H NMR spectrum in DMSO-d_6, this dimer also follows in footsteps of hydrazone **44**.

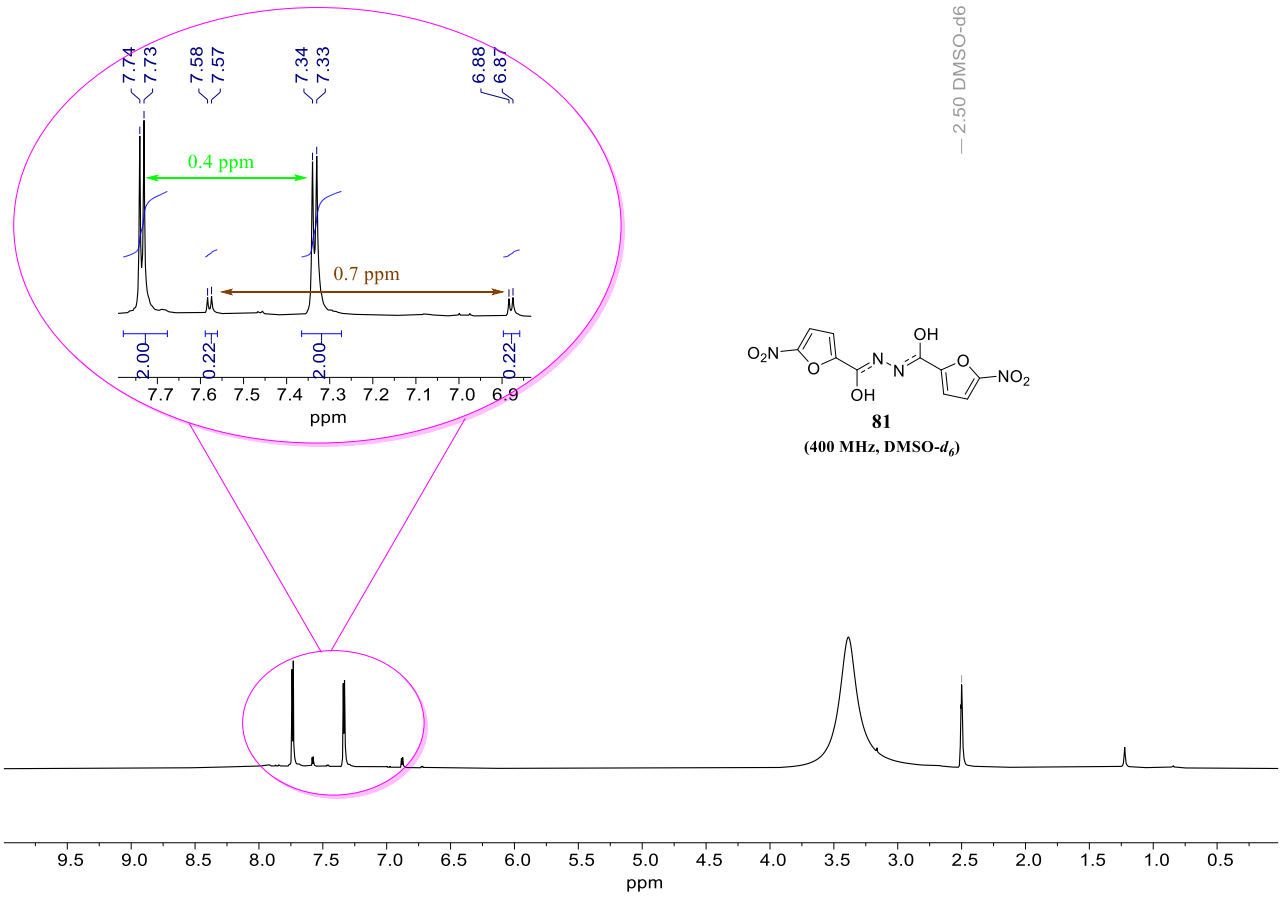

Figure 3.66 ^{1}H NMR spectrum of homodimer 81, illustrating a large shift *i.e.* 0.7 ppm between minor signals at δ 7.58 – 7.57 & 6.88 – 6.87, presumably due to complexation with DMSO-d_6 to set up a weak induced ring current in the applied magnetic field.

Away from induced ring currents and back to synthesis of stable NInC hybrids: the above findings proved 5-nitro-2-furoyl chloride too reactive to furnish nitrofuran **79**; as a result, 5-nitro-2-furoyl chloride was esterified in refluxing methanol to give the relatively less reactive ester **83** (Scheme 3.35), again in astonishing yields *i.e.* ~ 99%, and purity *i.e.* >99%, as evidenced by ^{1}H NMR (Fig. 3.67).

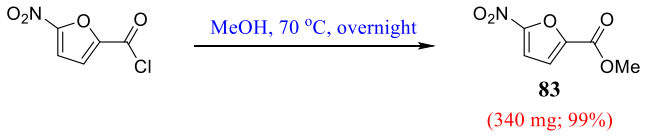

Scheme 3.35 Synthesis of ester 83 in excellent yields.

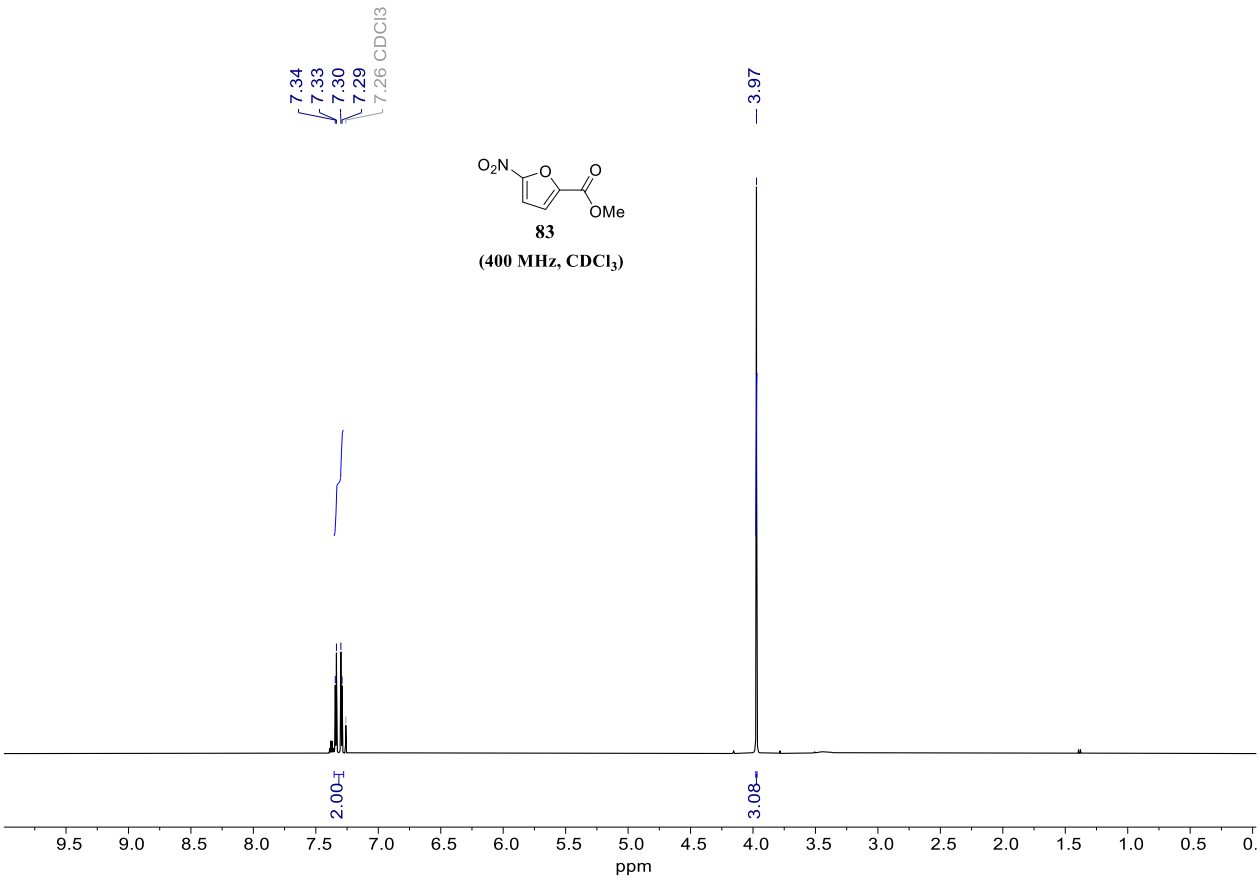

Figure 3.67 ^{1}H NMR spectrum of nitrofuran 83. The carbon satellites of the singlet from –OMe at δ 3.97 clearly attest the purity of nitrofuran 83; for full characterisation *cf.* Experimental p. S69.

With nitrofuran **83** in hand, its reactivity towards hydrazine monohydrate was put to test, and also as a precautionary measure, in contrast to the reaction of 5-nitro-2-furoyl chloride with hydrazine monohydrate at elevated temperatures, the reaction of nitrofuran **83** with hydrazine monohydrate was carried out at a relatively much lower temperature (Scheme 3.36).

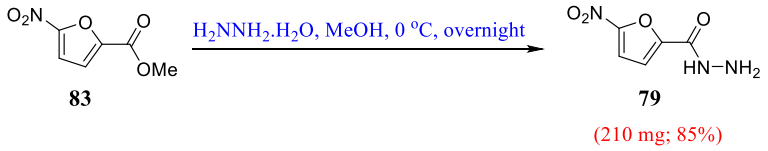

Scheme 3.36 Successful synthesis of nitrofuran 79.

Gratifyingly, the aforementioned reaction was able to smoothly proceed to completion in the literature's favourite solvent for this type of reaction *i.e.* methanol to finally furnish nitrofuran **79** as a yellow solid in excellent yields *i.e.* 85–90% after flash column chromatography, and ultra-high purity *i.e.* >99%, as evidenced by ^{1}H NMR (Fig. 3.68).

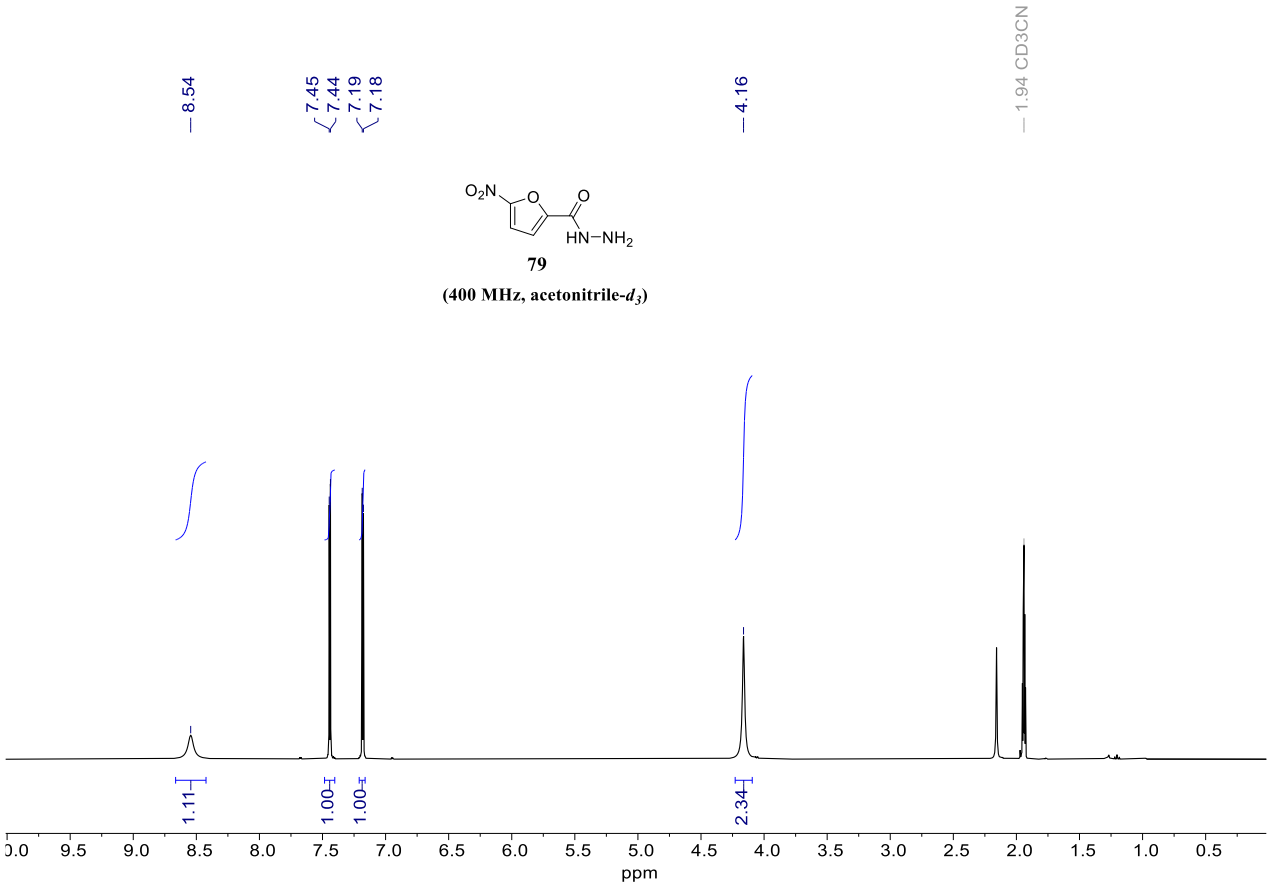

Figure 3.68 ^{1}H NMR spectrum of nitrofuran 79. The carbon satellites of the signals from aromatic protons at ~ δ 7.45 – 7.19 clearly endorse the purity of nitrofuran 79; for full characterisation and *J* values in Hz *cf.* Experimental p. S70.

It should, however, not be overlooked that in marked contrast to the ^{1}H NMR of hydrazone **44**, the signals at *ca.* δ 7.45 and 7.19 from protons on the furan ring in furan **79** (Fig. 3.68) are not unusually far apart, and that this should be so is a corollary of the fact that the furan ring itself in furan **79** is almost flat.

Moreover, similar but different to hydrazone **44** and dimer **81**, the semi-carbohydrazide moiety adjacent to the furan ring in furan **79** is unable to shuffle electrons towards the nitro moiety so as to push the furan ring into a '*puckered conformation.'*

On the other hand, the carbonyl group in the semi-carbohydrazide moiety is also in a '*trigonal planar'* geometry, and by all means, does not have the same properties as the π bond of the hydrazone moiety in hydrazone **44**, these geometrical restrictions clearly set limitations as to whether any polar solvent molecule could ever fully coordinate to furan **79**, and give the lie to that prime tenet of '*induced ring current*' in an applied magnetic field for hydrazone **79**, which is in good agreement with the aforementioned observation from its ^{1}H NMR *i.e.* the signals at *ca.* δ 7.45 and 7.19 from protons on the furan ring in furan **79** are not unusually far apart.

It must be pointed out that as was highlighted above, furan **79** exhibits a yellow colour, and inasmuch as this furan technically has only one extra auxochromic oxygen than say, hydrazone **44**; this auxochromic impact on the conjugated system of furan **79**, renders this molecule to fit into description of the concoction obtained by Li *et al.*[530], which seems to be very similar to furan **79** both in '*structure* & *colour*' (Fig. 3.69).

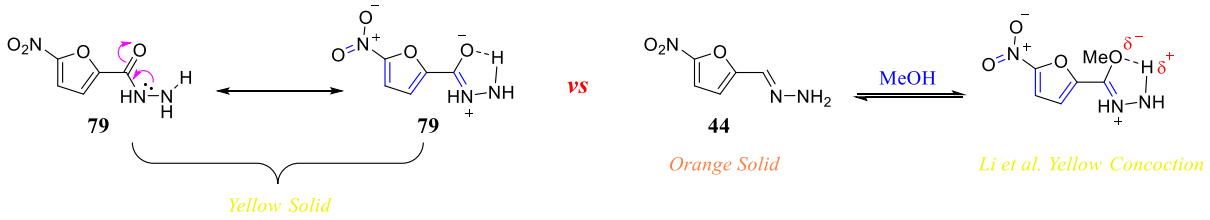

Figure 3.69 Nitrofuran 79 exhibits virtually the same colour as the compound obtained by Li *et al.*[530] (Section 3.3.1).

Unfortunately, however, despite numerous experiments carried out under a variety of conditions (Scheme 3.37), the Buchwald amination step, namely, the coupling of InC esters to nitrofuran **79**, could not be accomplished, and hence this route to formation of stable NInC hybrids had to be abandoned.

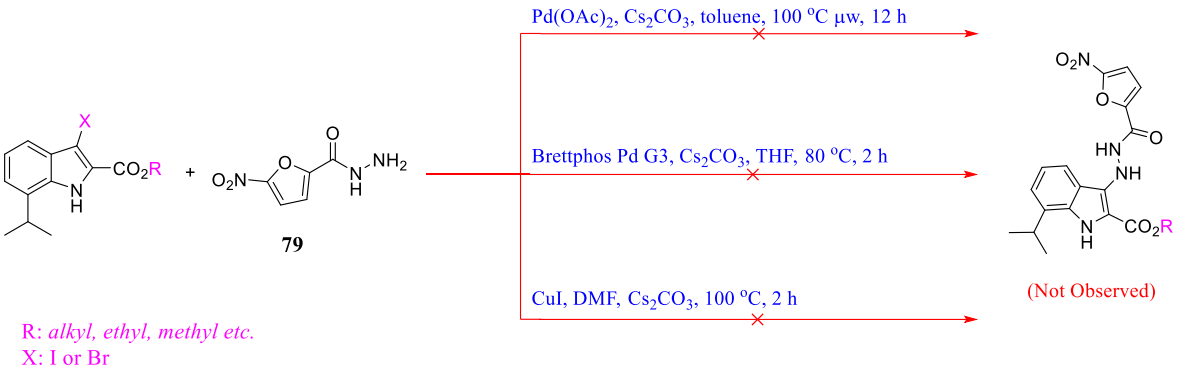

Scheme 3.37 Representative failed attempts at synthesis of stable NInC esters.

It cannot be too firmly emphasised, however, that the CuI coupling of InC esters with nitrofuran **79**, especially, that with InC ester **84**, exclusively gave dehalogenated InC ester **67** (Scheme 3.38).

This finding clearly borne out the formation of desired NInC esters in the decomposition process, such that the desired NInC esters must have been formed first for them to fall apart back to the dehalogenated starting material *i.e.* InC **67**.

This type of decomposition is not unprecedented, and has occasionally been observed during both Buchwald amination of InC esters, and ester hydrolysis of their corresponding NInC esters (Section 3.3.2.1).

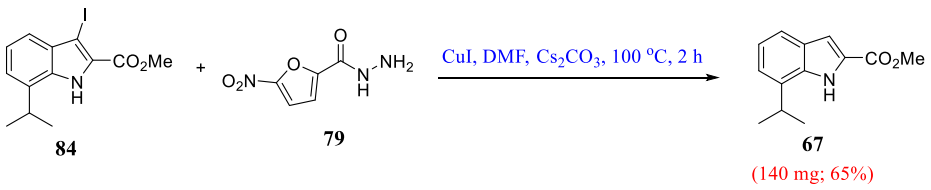

Scheme 3.38 Dehalogenation of InC ester 84.

Preliminarily experiments established that a phenyl spacer can improve the stability of NInC hybrids (Section 3.3.4), as such and together with recent work in Oxford which rendered pharmacodynamic improvement to InC *β*-lactamases by introducing an *o*-fluorophenylsulfonamide moiety at the C-3 position.[515]

And also given that 3-fluoro-4-formylphenyl boronic acid is commercially available, the palladium catalysed coupling of InC **68** to 3-fluoro-4-formylphenyl boronic acid was attempted: hardly surprisingly, InC **85** was accomplished in moderate yields (Scheme 3.39) after flash column chromatography purification. Although InC **85** was obtained as a sticky wax, it was of a high purity, which was verified by ^{1}H NMR (Fig. 3.70).

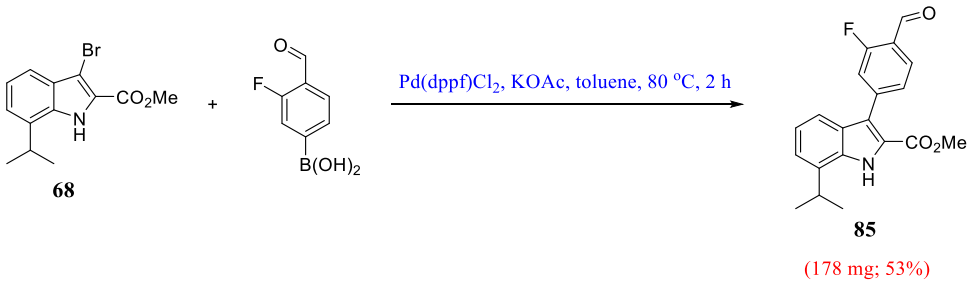

Scheme 3.39 Synthesis of InC ester 85.

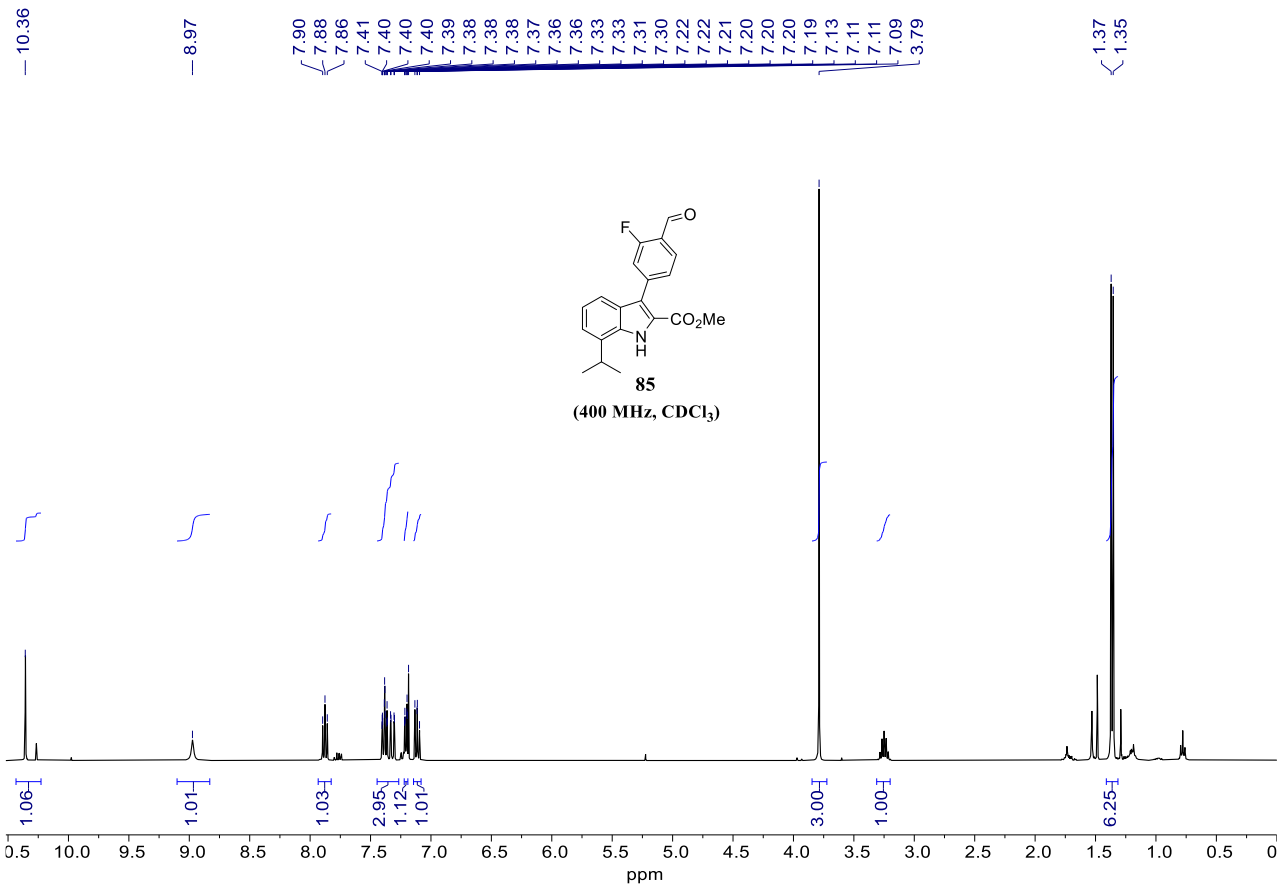

Figure 3.70 ^{1}H NMR spectrum of InC ester 85. The carbon satellites of the singlet from –OMe at δ 3.79 clearly attest the purity of InC ester 85. Moreover, the formyl group can marginally enolise which is evident from the small singlet adjacent to the singlet from the formyl moiety at δ 10.36; for full characterisation and *J* values in Hz *cf.* Experimental p. S72.

Surprisingly, InC ester **85** was neatly hydrolysed in an aqueous medium of LiOH to furnish InC **86**, however, in acceptable yields (Scheme 3.40) after flash column chromatography purification. Nevertheless, despite the relatively low yields, the purified InC **86** was of an excellent purity, as evidenced by ^{1}H NMR (Fig. 3.71).

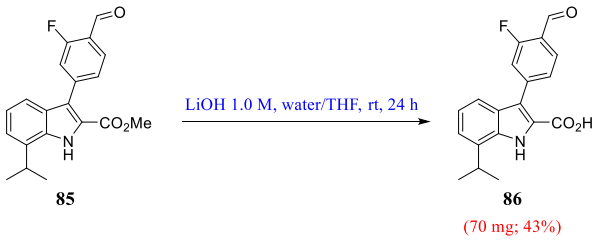

Scheme 3.40 Base hydrolysis of InC ester 85.

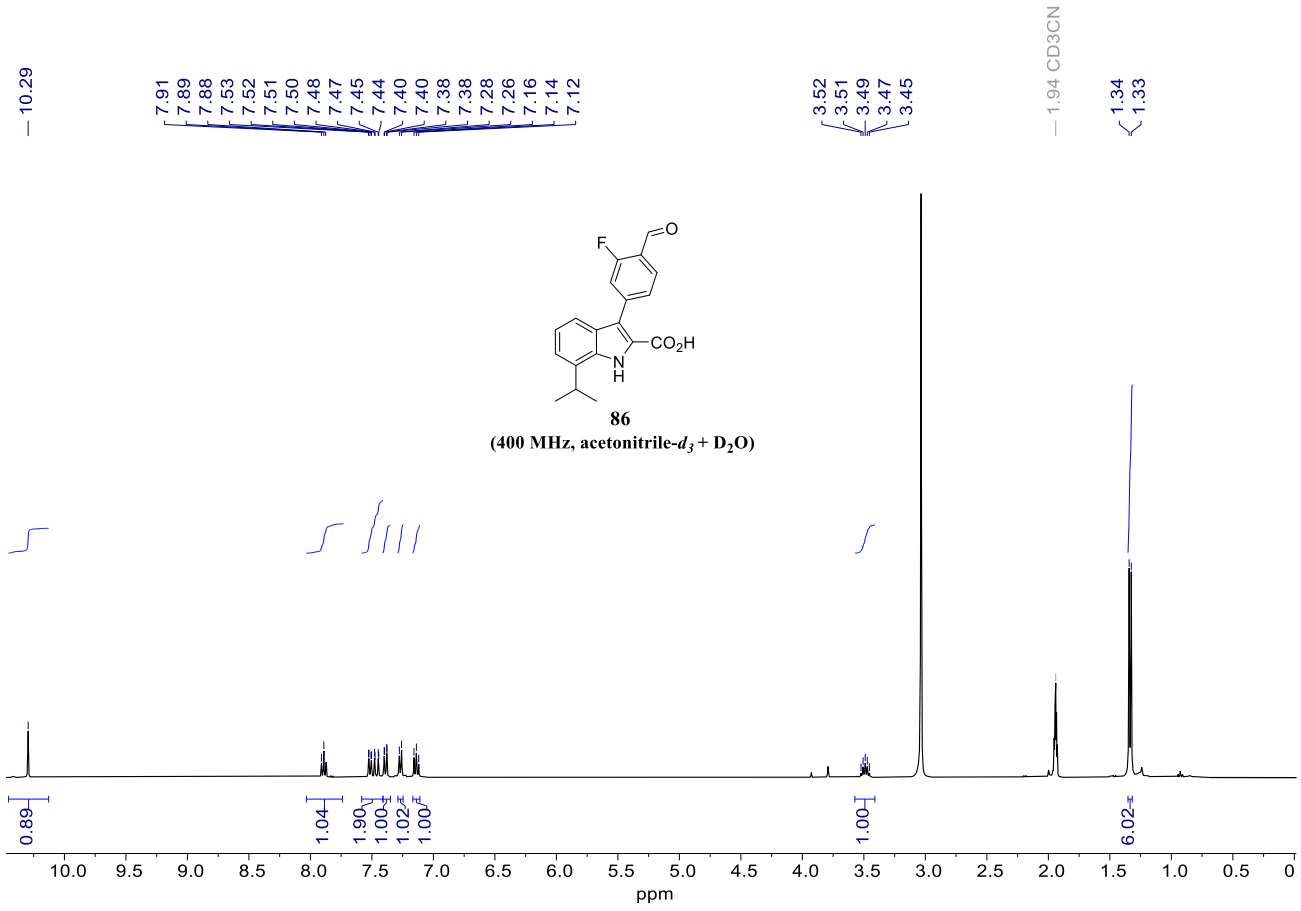

Figure 3.71 ^{1}H NMR spectrum of InC 86. Apart from the singlet from the C*H*O at δ 10.29, the many aromatic protons in 86 resonate at ~ δ 7.90 – 7.14 with the methyls at the highest field *i.e.* δ 1.34; for full characterisation and *J* values in Hz *cf.* Experimental p. S73.

Unfortunately, despite being of a very high purity, InC **86** similar, but different to InC **85**, was also obtained as a wax *i.e.* unlike InC **85** which was an orange wax, InC **86** was a pale-yellow wax.

There remains, however, the question of the remarked waxy nature of these compounds.

Part of this in no doubt arises from the very marginal solvent residues trapped in the solids, but a larger part could stem from the fact that these compounds must be low melting point solids, such that this effect together with the extended network of intermolecular hydrogen-bonding, in virtue of the indole carboxylate moiety, particularly, in InC **86**, paves the way for trapping solvent residues, should such there be.

Finally, as envisaged, and in a manner similar to InC **77** (Scheme 3.33), the thus obtained InC **86** was successfully linked to nitrofuran **79** *via* the stable *N*-acyl hydrazide linker, such that the crude product even survived flash column chromatography purification on silica to mark the first milestone towards synthesis of therapeutic NInC hybrids, and furnish NInC **87** in acceptable yields (Scheme 3.41), and high purity, as evidenced by ^{1}H NMR (Fig. 3.72).

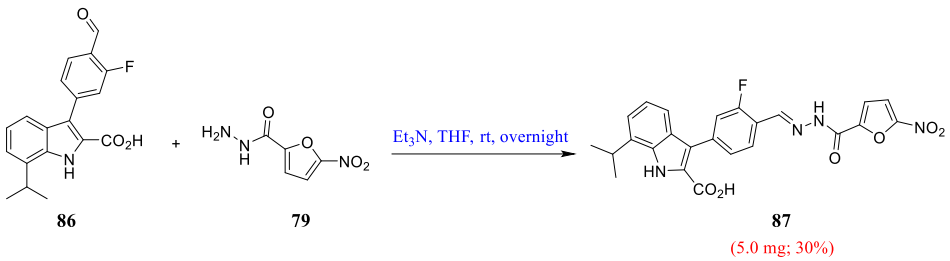

Scheme 3.41 Synthesis of NInC 87.

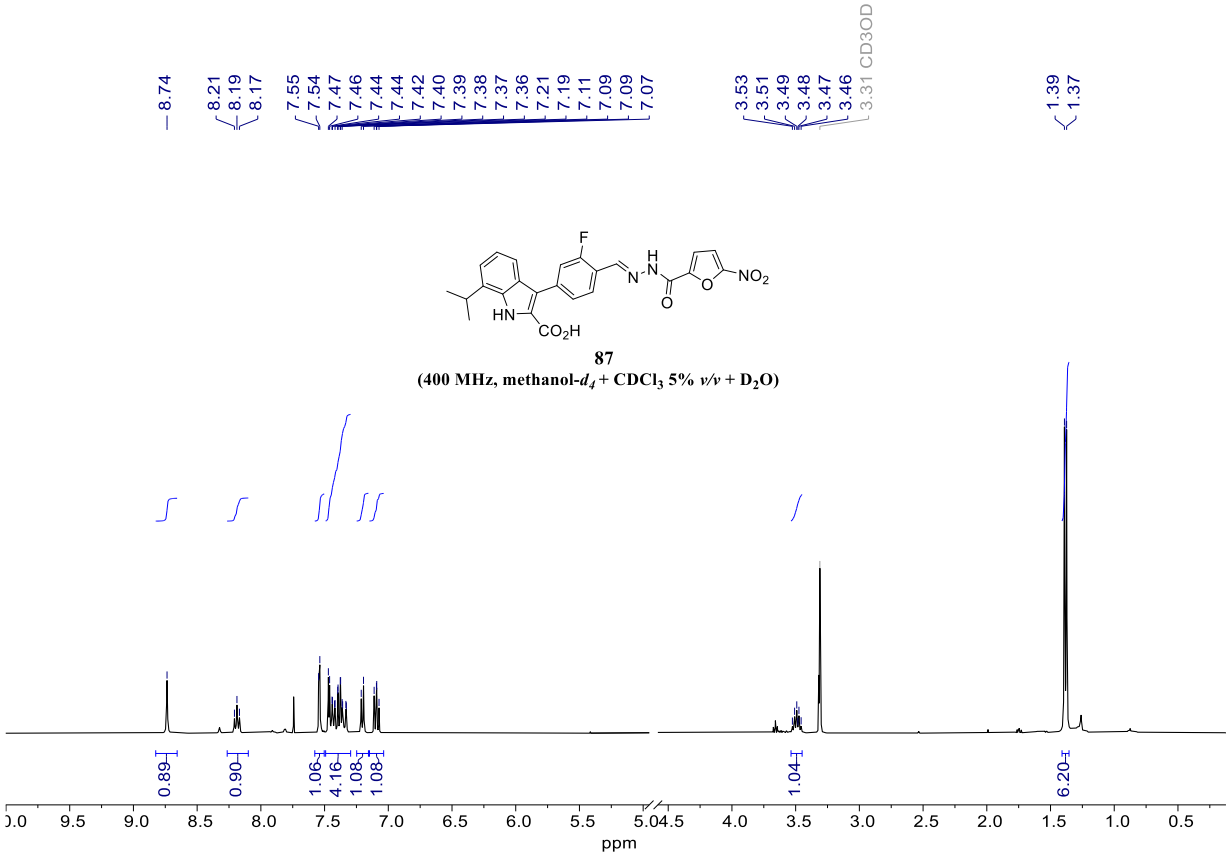

Figure 3.72 ^{1}H NMR spectrum of NInC 87. The multiplet from the methine of isopropyl moiety in 87 at δ 3.49 has a tiny corresponding counterpart adjacent to it such that it is unclear as to whether the corresponding signal is due to the rotamers or reactivity of methanol-d_4 with 87; for full characterisation and *J* values in Hz *cf.* Experimental p. S74.

3.3.6 Design & Synthesis of NInCs at C-7 of the Core InC

Traditionally, adding lipophilic side chains to a potential drug molecule usually increased potency.

Although for some time it was unclear as to why this phenomenon improved the potency of drug molecules; in 1958, Daniel E. Koshland proposed the '*induced-fit model*',[628] which served as a much better model for illustrating interactions between most drug molecules and proteins *i.e.* enzymes, receptors, channels *etc.*

Today, we know that protein pockets and cavities to which drug molecules bind are filled with water molecules, and binding affinity of a given drug molecule for its molecular target is very much dependent on the ability of the drug to compensate for '*keeping things in place*' *i.e.* loss of entropy.

Molecular recognition,[629] in virtue of hydrophobic interactions between drug molecules and their molecular targets, leads to dislodging water molecules to the surroundings and away from protein pockets and cavities, this phenomenon increases entropy, and hence, the more lipophilic a drug molecule, the higher increase in binding entropy, which in turn gives rise to a higher potency. Thus, potency to a great extent is governed by entropy, as is everything else, from expansion of the Universe to our very own life and death.

With the above borne in mind, the previous modifications at C-3 of the InCs increased hydrophilicity of InCs starting material, which could in part account for high instability of NInC hybrids such as NInC **63**. This can be conceded by virtue of the fact that the more lipophilic NInC **78** is more stable than the less lipophilic NInC **63** (Section 3.3.4). To this end, modifications at C-7 of the core InC were undertaken, in the hopes of achieving better stability for NInC hybrids.

3.3.6.1 Synthesis of Ethyl 7-Acetyl-1-H-indole-2-carboxylate

The introductory isopropyl group at C-7 of the core InC is relatively unreactive, and a functional group transformation is, of necessity, for it to serve as a handle for attachment of further building blocks to the core InC, and hence synthesis of NInC hybrids.

Perhaps one of the oldest, and first example of palladium catalysed couplings, all of which have now dominated the entire field of synthetic chemistry, is the well-known '*Heck reaction*',[630] for which Richard F. Heck shared the 2010 Nobel Prize in Chemistry with Ei-ichi Negishi and Akira Suzuki.[631]

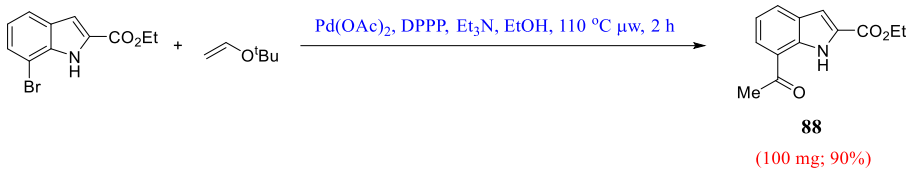

Scheme 3.42 Synthesis of InC ethyl ester 88 *via* microwave assisted Heck reaction.

Using the well-established Heck reaction, recent work in Oxford brought about a microwave assisted Heck reaction *via* which InC ethyl ester **88** was easily obtained from commercially available ^{t}butoxyethylene and ethyl 7-bromo-1-*H*-indole-2-carboxylate, in high yields and purity (Scheme 3.42) after flash column chromatography purification, as evidenced by ^{1}H NMR (Fig. 3.73).

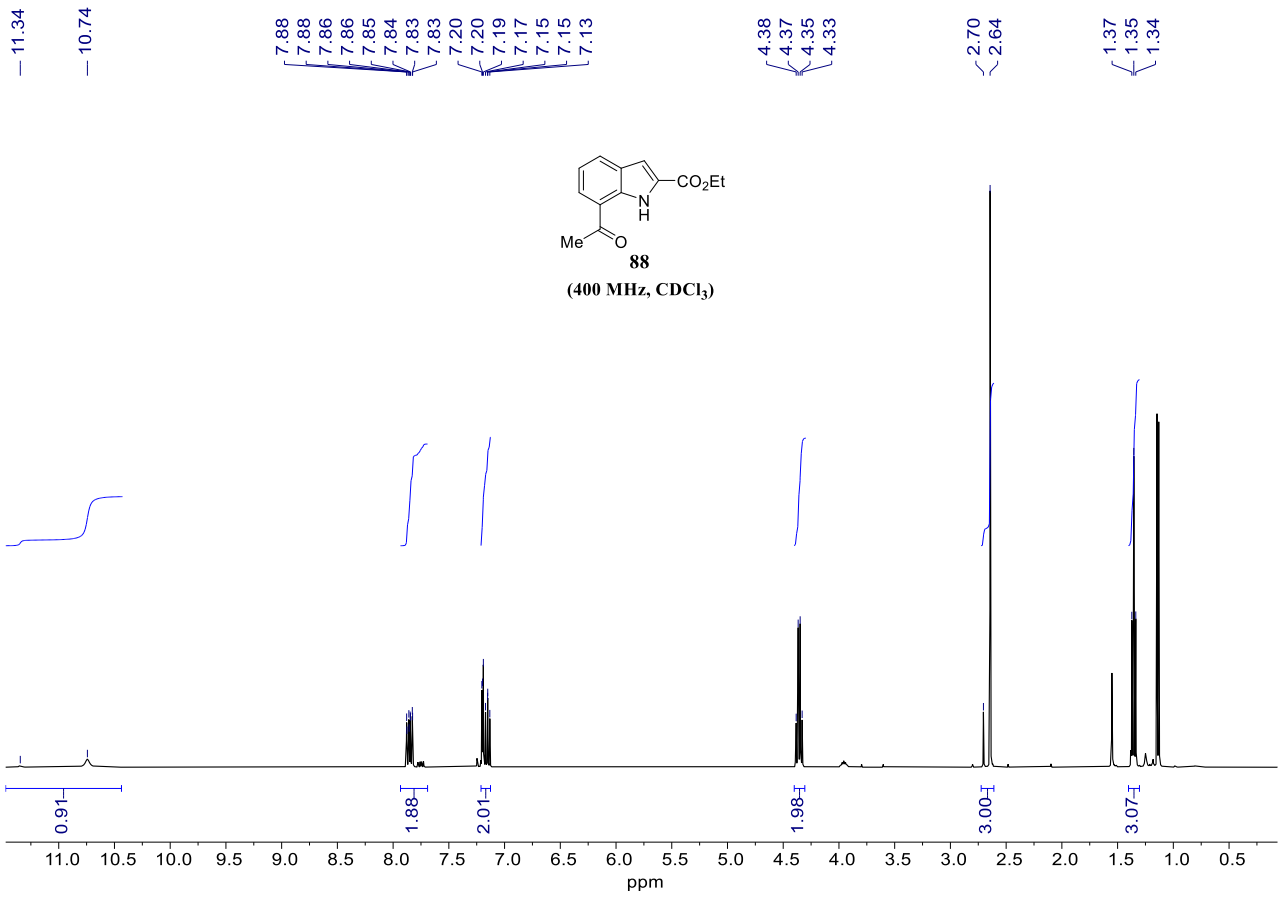

Figure 3.73 ^{1}H NMR spectrum of InC ester 88. The tiny singlet at δ 2.70 adjacent to the main singlet at δ 2.64 from the methyl of acyl moiety in 88 could be a result of rotameric effect; for full characterisation and *J* values in Hz *cf.* Experimental p. S75.

3.3.6.2 Coupling of Nitrofuran Hydrazones to Ethyl 7-Acetyl-1-H-indole-2-carboxylate

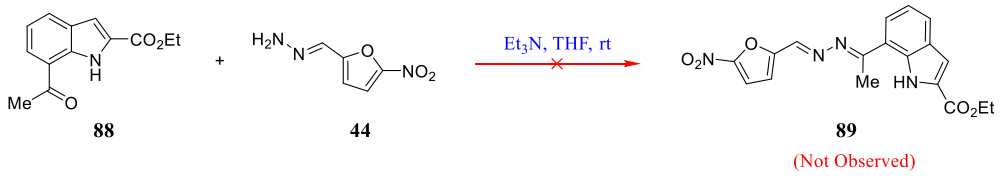

Scheme 3.43 It was not feasible to synthesise NInC ester 89 in basic and neutral media.

In marked contrast to InC **77**, stirring InC **88** with or without triethylamine in dry THF under anhydrous conditions, did not furnish the desired NInC **89** (Scheme 3.43).

In view of the above, the action of hydrazone **44** on InC **88** was then subjected to further LC-MS analysis; during the course of several days' reaction time with multiple attempts under variety of conditions and extensive LC-MS monitoring, it was revealed that both triethylamine and even the hydrazone starting material itself – even though was only present in the reaction mixture in slight excess *i.e.* 1.2 equiv. with respect to InC **88** – were detrimental to formation of NInC **89**. To this end, the aforementioned reaction was repeated; however, this time in presence of catalytic amount of a Lewis acid *i.e.* zinc chloride.

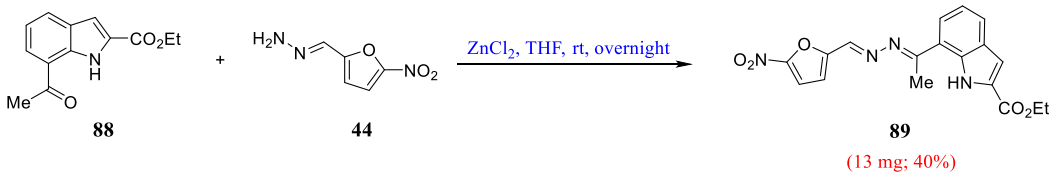

Scheme 3.44 Successful synthesis of NInC ester 89 under mildly acidic conditions.

Gratifyingly, zinc chloride was able to catalyse the coupling of hydrazone **44** to InC ester **88** to give ethyl ester protected NInC **89**, though in moderate yields (Scheme 3.44) after flash column chromatography purification, but in relatively good purity *i.e.* >90%, as verified by ^{1}H NMR (Fig. 3.74).

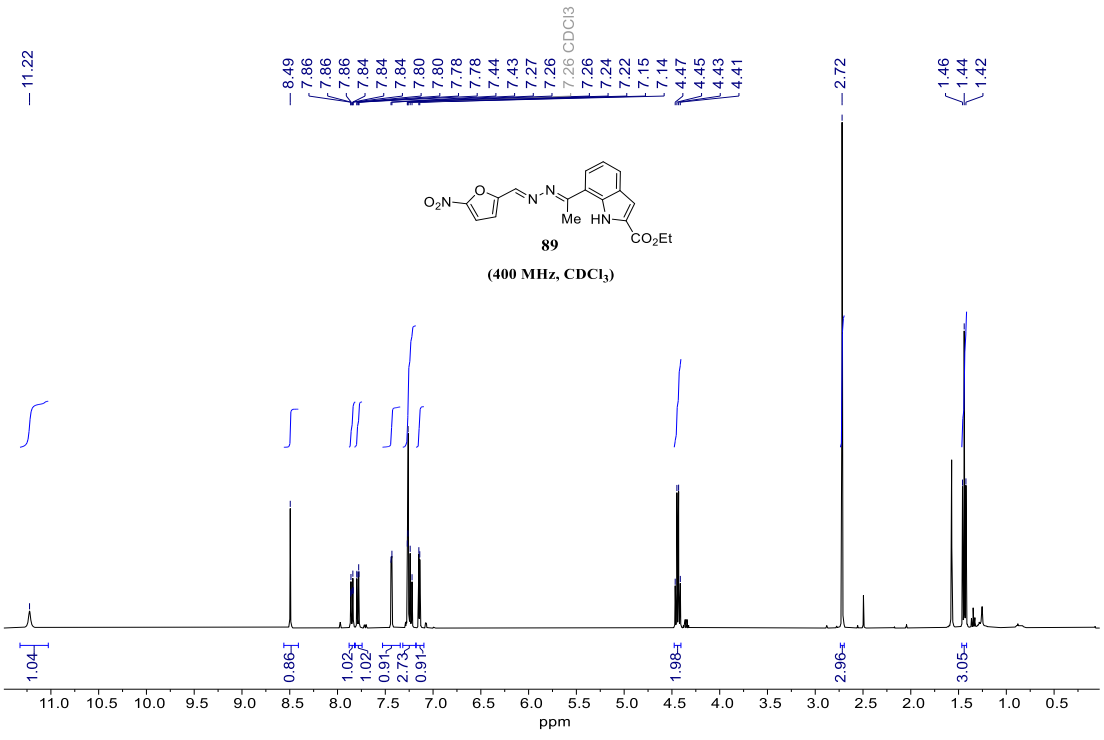

Figure 3.74 ^{1}H NMR spectrum of NInC ester 89.

3.3.6.3 Ester Hydrolysis of Ethyl 7-Acetyl-1-H-indole-2-carboxylate & its Corresponding NInC Esters

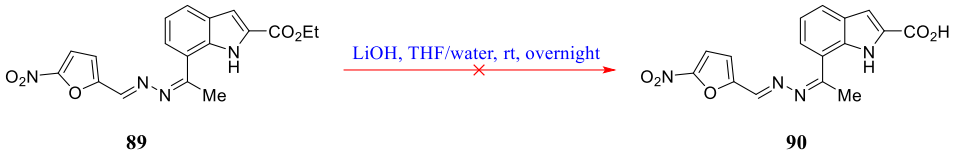

89 **90**

(Not Observed)

Scheme 3.45 As envisaged, NInC ethyl ester 89 was not suitably hydrolysed to its corresponding carboxylate 90.

It did not come as a surprise, as always, to find out that the ester hydrolysis of NInC ethyl ester **89** (Scheme 3.45) was not productive; however, to our delight the ester hydrolysis of its parent InC ethyl ester **88** was smoothly accomplished in excellent yields *i.e.* ≥99% (Scheme 3.46), and more importantly purity *i.e.* >99%, as evidenced by ^{1}H NMR (Fig. 3.75).

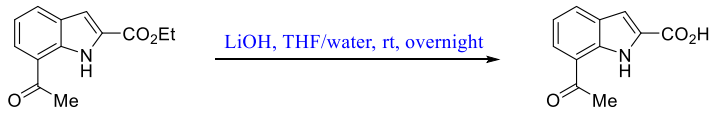

88 **91**

(80 mg; ≥99%)

Scheme 3.46 Ester hydrolysis of InC ester 88 to its corresponding carboxylate 91 in excellent yields.

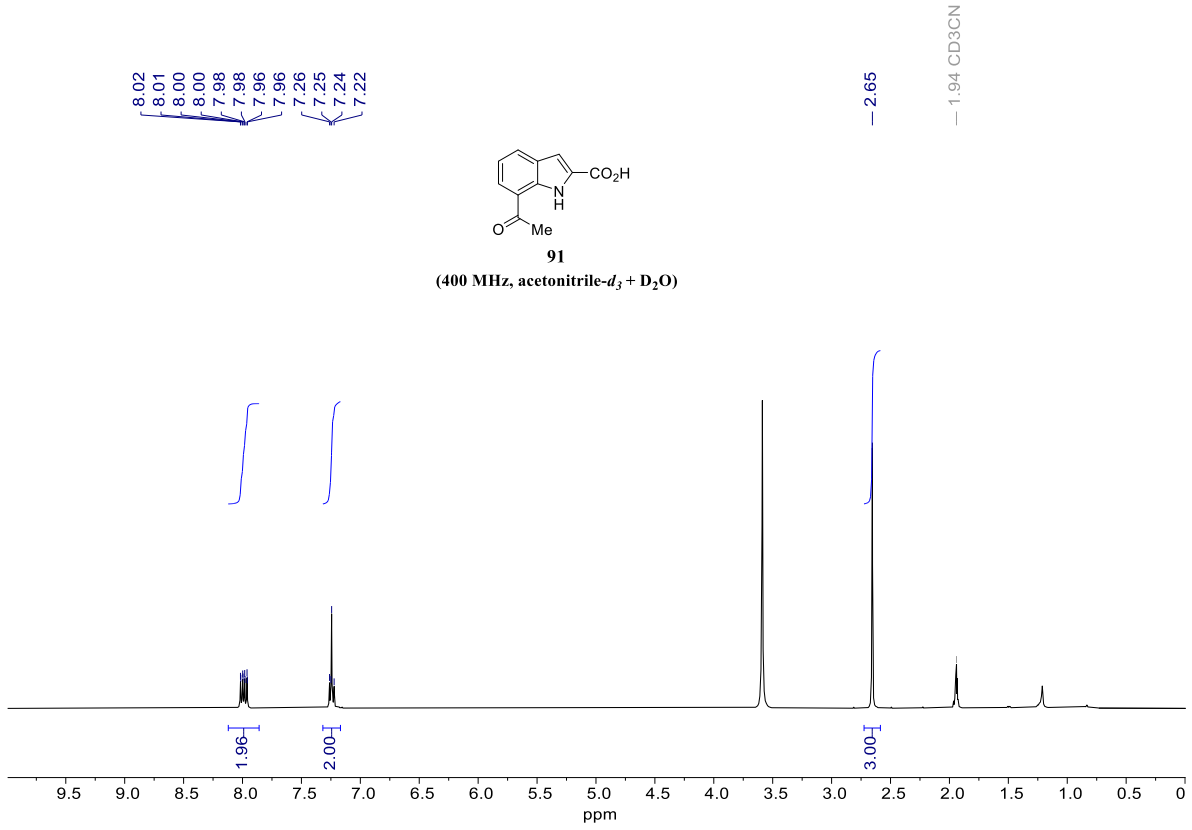

Figure 3.75 ^{1}H NMR spectrum of InC 91. The signals at δ 7.98 & 7.24 are from the aromatic indole protons, and the singlet at δ 2.65 is from the methyl of acyl moiety in 91; *nota bene*: The hydrolysis of ethyl ester removes the singlet at δ 2.70 in ^{1}H NMR spectrum of 88, providing support for its stable rotamers *cf.* Fig. 73.

3.3.6.4 Synthesis of Stable NInC Hybrids

Preliminary studies on modification of the core InC at C-3 position (Section 3.3.2 & 3.3.3), brought home to us that the most effective and efficient strategy for installation of the nitrofuran warhead should, at all costs, preclude the use of PGs, in particular, the troublesome carboxyl ester PGs (Section 3.3.4). This effect was again reflected here in modification of the core InC at C-7 position, and inasmuch as the ester hydrolysis of NInC ethyl ester **88** was also failed, without further ado, inarguably, no PGs for the carboxylate moiety, is indeed the best strategy. As a result, the thus obtained unprotected InC **91** was reacted with hydrazone **44** in a manner similar to that for InC **86** (Scheme 3.41); however, similar to InC **88**, the desired NInC **92** was not observed in basic and neutral media (Scheme 3.43). To this end, the coupling of InC **91** to hydrazone **44** was attempted in a mildly acidic medium featuring zinc chloride as a Lewis acid catalyst.

Unfortunately, it was disappointing to see that even zinc chloride was incapable of accomplishing the desired NInC **92**, as once it did for InC **88** in the previous successful attempts at synthesis of NInC **89** (Scheme 3.44).

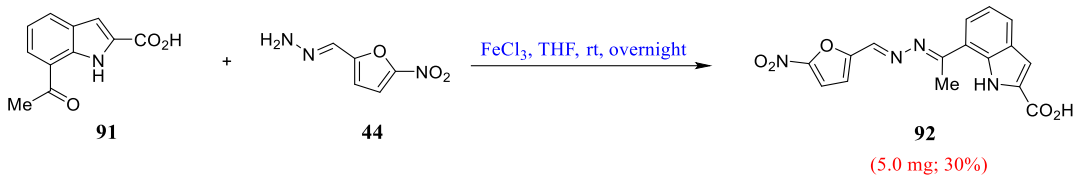

Scheme 3.47 Successful synthesis of NInC 92 *via* catalytic amount of ferric chloride.

Reference has already been made to '*soft & hard*' interactions in synthesis (Section 2.6; *cf.* p. 88), and one of the salient divisive factors amongst Lewis acid catalysts, in point of fact, is their inherent softness and hardness. Although, zinc possesses a larger metallic radius than iron, zinc is a d^{X} metal, but iron is a d^{VIII}, and hence iron is a transition metal, but zinc is not. Thus, even though iron possesses a smaller metallic radius than zinc and could be erroneously assumed harder than zinc; as a transition metal, iron forms complexes, in particular, with relatively low field ligands such as chloride ions, that are in point of fact more polarisable than analogous zinc complexes.

Whilst, zinc chloride is linear and somewhat covalent in character, ferric chloride as a d^{V} metal in its solid state exhibits an octahedral metal complex with a penchant for '*spin crossover*' *i.e.* high-spin and low-spin exchange. As such, ferric chloride is highly soluble in organic solvents, but zinc chloride is only slightly soluble in the same organic solvents. Thus, solvation and dissolution factors must also be factored in, when it comes to choosing the best Lewis acid/base catalyst for a given synthesis.

In the light of what has been said above, there are no particular hard and fast rules for choosing the best Lewis acid/base catalysts for a given synthetic transformation, and what sometimes works best for one reaction, turns out to be completely futile for another, even for seemingly similar reactions as we saw above.

However, experience and/or occasionally trial and error are the only solutions. To this end, ferric chloride *in lieu* of zinc chloride was able to catalyse the reaction of InC **91** with hydrazone **44** to furnish the monumental NInC **92** in moderate yields (Scheme 3.47) after flash column chromatography purification, and acceptable purity, as evidenced by ^{1}H NMR (Fig. 3.76), which otherwise, would have been virtually impossible using any established PG strategy.

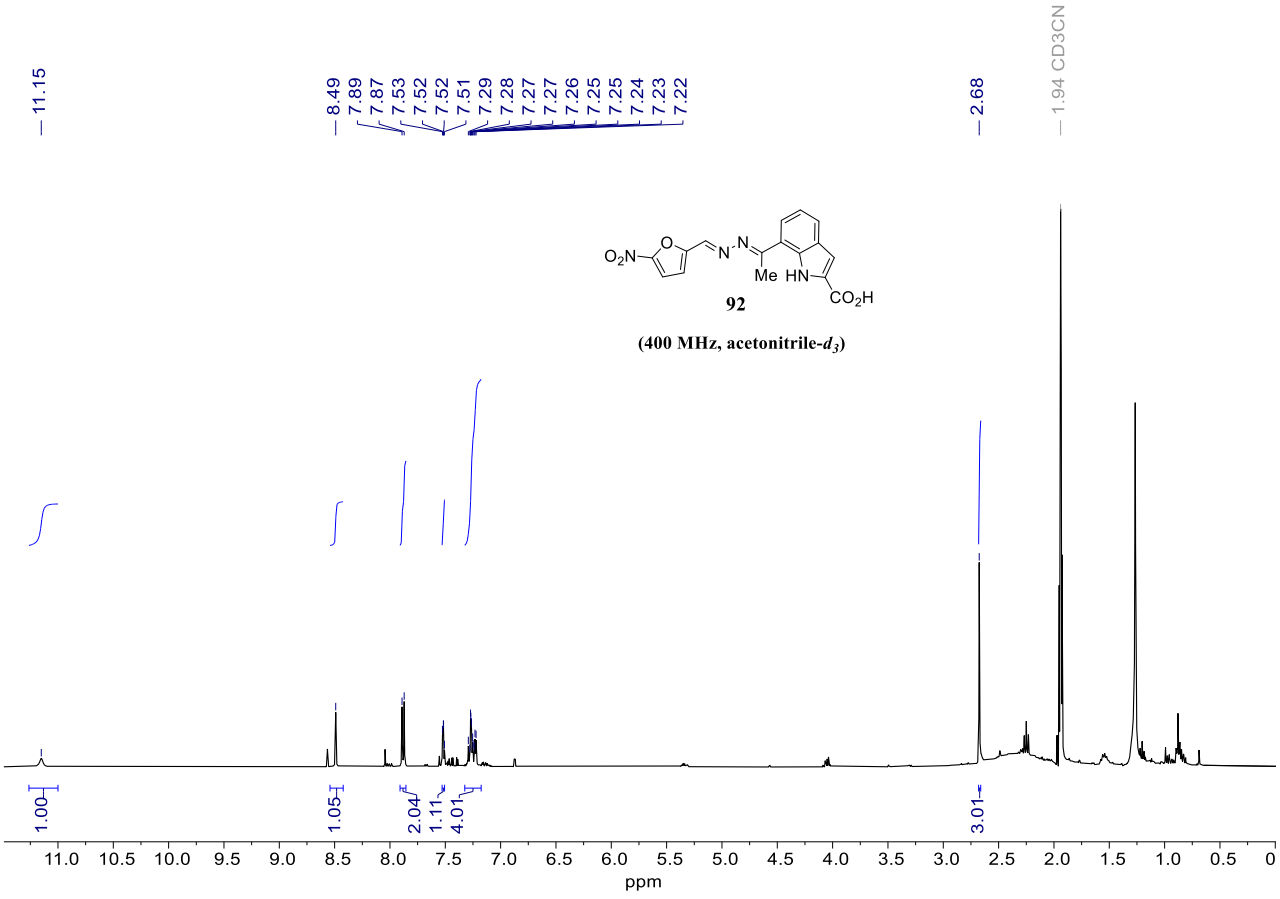

Figure 3.76 ^{1}H NMR spectrum of NInC hybrid 92. Whilst water was avoided at all costs, the instability of 92 is evident from its decomposition on silica after flash column chromatography, and hence the slightly less clean ^{1}H NMR spectrum of 92 relative to its precursors; for synthesis & full characterisation including *J* values in Hz *cf.* Experimental p. S78.

3.4 Biological Evaluation of NInC Hybrids

Although the exact mode of activity of nitrofuran antibacterials is not well understood, they are thought to undergo one or more reductions in the bacterial cells, and then generate radicals and subsequent reactive amines and cyano species (Fig. 3.8), which damage their DNA (Section 3.2).

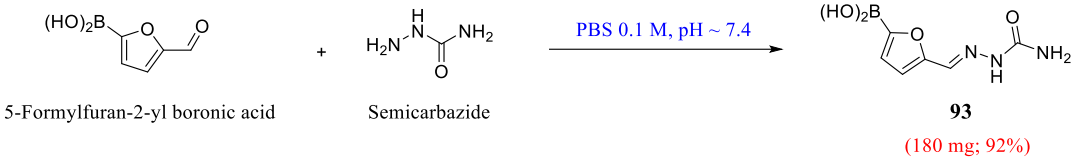

Scheme 3.48 Synthesis of heteroaryl boronic acid analogue of nitrofurazone.

Inspired by this hypothesis, and given that a simple boronic acid moiety has a vacant $2p_z$ orbital to which nucleophilic amino acid residues such as serine, cysteine *etc.* in bacterial proteins, and nucleophilic purine and pyrimidine bases of bacterial DNA can bind so as to interfere with metabolic activities of pathogens and cause bacterial cell death, the nitro warhead in nitrofurazone antibacterial was successfully replaced with a boronic acid by just one synthetic transformation (Scheme 3.48) to give heteroaryl boronic acid **93** in excellent yields *i.e.* 90–95%, and purity as evidenced by ^{1}H NMR (Fig. 3.77).

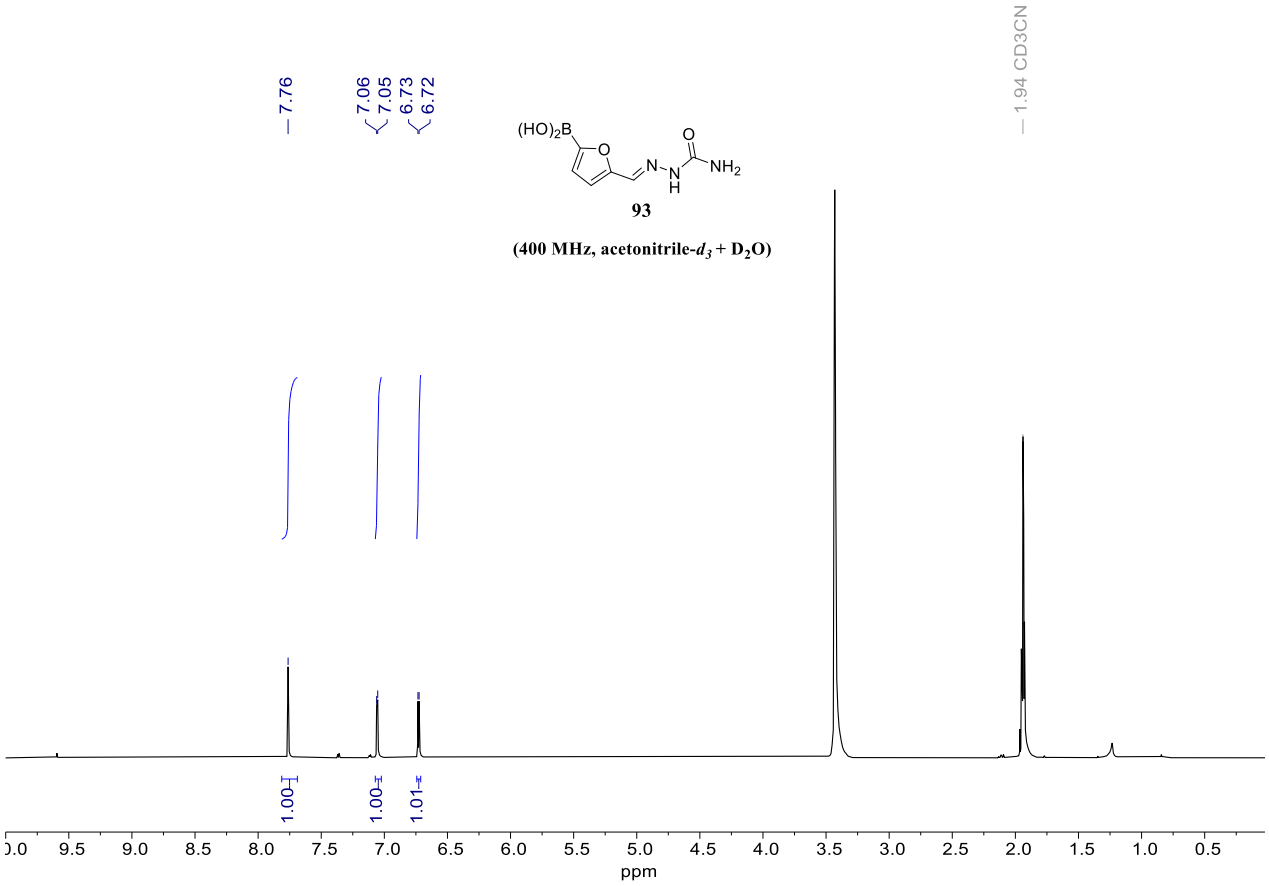

Figure 3.77 ^{1}H NMR spectrum of heteroaryl boronic acid 93. The signals at δ 7.06 & 6.73 are from the furan ring, and the distinctive unsaturated proton of –N=C*H* resonates at δ 7.76; for full characterisation and *J* values in Hz *cf.* Experimental p. S79.

With the boronic acid analogue of nitrofurazone, namely, boronic acid **93**, in hand; a sample of nitrofurantoin, nitrofurazone, furazolidone and boronic acid **93** were given to a microbiologist who pledged to evaluate them for their *in vivo* antibacterial activity; however, at the time of writing this text the results are still awaited. To this end, the *in vivo* antibacterial evaluation of boronic acid **93** against a range of Gram-positive and Gram-negative pathogenic bacteria merits a full consideration.

On the other hand, the same microbiologist, apparently tested, though it was never verified, NInC ethyl ester **60**, the relatively more stable NInC **87**, and NInC **92** for their *in vitro* enzymatic inhibition.

Inasmuch as, the InC moiety of these hybrids is, in point of fact, a potent *β*-lactamase inhibitor[515] (Section 3.3), and the cleavable linkers are extremely labile particularly in aqueous media, it did come as a surprise that all of which according to the aforementioned microbiologist showed no *in vitro* enzymatic inhibition whatsoever.

In the light of compelling evidence which gives us every reason to suspect the reliability of quoted biological data for this set of novel NInC hybrids, the *in vivo* antibacterial assays of these novel NInC hybrids together with their corresponding fragments and carboxylate ester analogues, on the basis of these studies, all merit a full consideration.

Reference

[1] W. A. Jackson, *Trends Pharmacol. Sci.*, 2001, **22**, 487.
[2] R. C. Olby, N. G. Cantor, J. R. R. Christie and M. J. S. Hodge, *Companion to the History of Modern Science*, Routledge, London, 1990.
[3] F. Aftalion, *Histoire de la Chimie*, Masson, Paris, 1988.
[4] B. Bensaude-Vincent and I. Stengers, *Histoire de la Chimie*, La Découverte, Paris, 1993.
[5] C. Bernard, *Leçons de physiologie expérimentale appliquée à la medicine*, J.B. Baillière, Paris, 1855.
[6] L. R. Virchow, *Die Cellularpathologie in ihrer Begründung auf physiologische und pathologische Gewebelehre*, A. Hirschwald, Berlin, 1858.
[7] L. Pasteur, *Euvres complètes réunies par Pasteur Vallery-Radot*, Masson, Paris, 1922.
[8] E. Soubeiran, *Ann. Chim.*, 1831, **48**, 113.
[9] J. Von Liebig, *Ann. Pharm.*, 1832, **1**, 182.
[10] S. Guthrie, *Am. J. Sci. Arts.*, 1832, **21**, 64.
[11] F. Wöhler, *Poggendorfs Ann. Phys. Chem.*, 1828, Leipzig.
[12] K. J. Williams, *J. R. Soc. Med.*, 2009, **102**, 343.
[13] K. Thiel, *the Germ Theory of Disease*, Cavendish Square, New York, 2018.
[14] The Plague of Justinian, *History Magazine*, 2009, **11**, 9.
[15] C. L. Cadet de Gassicourt, *Bull. Pharm.* 1809, **1**, 5.
[16] C. Aspin, *the Cotton Industry*, Shire Publications Ltd., Aylesbury, 1981.
[17] H. Vogt, J. Balej, J. E. Bennett, P. Wintzer, S. A. Sheikh and P. Gallone, *Ullmann's Encyclopedia of Industrial Chemistry*, Wiley, 2007.
[18] A. G. Labarraque, *Nouvelle Biographie Générale*, 1859, **28**, 323.
[19] P. M. Dunn, *Arch. Dis. Child Fetal Neonatal.*, 2007, **92**, 325.
[20] G. E. Abraham, *the Original Internist*, 2004, **3**, 17.
[21] F. F. Runge, *Ann. Phys. Chem.*, 1834, **31**, 65.
[22] D. Pitt and J. M. Aubin, *Can. J. Surg*., 2012, **55**, 8.
[23] J. Lister, *Br. Med. J.*, 1868, **2**, 53.
[24] S. W. Newsom, *J. Hosp. Infect.*, 2003, **55**, 246.
[25] J. T. Edsall, *Proc. Am. Philos. Soc.*, 1985, **129**, 371.
[26] *Our History*, milton-tm.com. https://www.milton-tm.com/en/consumer/our-history (accessed 21/04/20)
[27] F. Chast, *Rev. Hist. Pharm.*, 2005, **348**, 487.
[28] P. Ehrlich, *Arch. Mikr. Anat.*, 1877, **13**, 263.
[29] P. Ehrlich, *Chem. Ztg.*, 1912, **36**, 637.
[30] N. P. Johnson and J. Mueller, *B. Hist. Med.*, 2002, **76**, 105.
[31] H. Otten, *J. Antimicrob. Chemother.*, 1986, **17**, 689.
[32] T. Chorba, *Emerg. Infect. Dis.*, 2018, **24**, 611.
[33] S. Henrik, R. Sohlman, A. Österling, G. Liljestrand, A. Westgren, M. Siegbahn, A. Schou and N. K. Ståhle, *Nobel – The Man and His Prizes*, Klara Civiltryckeri, Stockholm, 1950.
[34] J. T. Tréfouël, F. Nitti and D. Bovet, *C. R. Soc. Biol.*, 1935, **120**, 756.
[35] *Co-trimoxazole (Apsen)*, medicines.org.uk https://www.medicines.org.uk/emc/search?q=%22Co-trimoxazole%22 (accessed 22/04/20)
[36] A. Fleming, *Proc. R. Soc. B.*, **93**, 306.
[37] A. Fleming, *Br. J. Exp. Pathol.*, 1929, **10**, 226.
[38] E. Chain, H. W. Florey, A. D. Gardener, N. G. Heatley, M. A. Jennings, J. O. Ewing and A. G. Sanders, *Lancet*, 1940, **2**, 226.
[39] M. Wainwright, *Miracle Cure – the Story of Penicillin and the Golden Age of Antibiotics*, Basil Blackwell, Oxford, 1990.
[40] *The Nobel Prize in Chemistry 1964*, nobelprize.org https://www.nobelprize.org/prizes/chemistry/1964/summary/ (accessed 22/04/20)

[41] J. C. Sheehan, *The Enchanted Ring – The Untold Story of Penicillin*, MIT Press, Massachusetts, Cambridge, 1982.
[42] F. P. Doyle, J. H. Nayler, H. Smith and E. R. Stove, *Nature*, 1961, **191**, 1091.
[43] S. B. Levy, *The Antibiotics Paradox*, Plenum Press, New York, 1992.
[44] J. C. Sheehan, *Ann. N. Y. Acad. Sci.*, 1967, **145**, 216.
[45] F. Ryan, *The Forgotten Plague – How The Battle Against Tuberculosis Was Won—and Lost*, Little, Brown and Company, London, 1993.
[46] P. Pringle, *Notebooks Shed Light on a Discovery, and a Mentor's Betrayal*, The New York Times, June 2012.
[47] A. Schatz, E. Bugie and S. A. Waksman, *Proc. Soc. Exp. Biol. Med.*, 1944, **55**, 66.
[48] S. Ainsworth, *Pharm. J.*, 2006, **276**, 237.
[49] E. Selimoglu, *Curr. Pharm. Des.*, 2007, **13**, 119.
[50] *History*, www.rocheusa.com. Roche USA https://web.archive.org/web/20071212082842/http://www.rocheusa.com/about/history.html (accessed 22/04/20)
[51] W. McDermott, L. Ormond, C. Muschenheim, K. Deuscfile, R. M. McCune Jr. and R. Tompsett, *Am. Rev. Tuberc.*, 1954, **69**, 319.
[52] S. Chakraborty and K. Y. Rhee, *Cold Spring Harb. Perspect. Med.*, 2015, **5**, a021147.
[53] T. D. McHugh, *Tuberculosis – Diagnosis and Treatment*, CAB International, Oxfordshire, Wallingford, 2011.
[54] M. C. Rebstock, H. M. Crooks, J. Controulis and Q. R. Bartz, *J. Am. Chem. Soc.*, 1949, **71**, 2458.
[55] W. P. O'Neill, R. F. Nystrom, K. I. Rinehart and D. Gottlieb Jr., *Biochemistry*, 1973, **12**, 4775.
[56] M. I. Rich, R. J. Ritterhoff and R. J. Hoffmann, *Ann. Intern. Med.*, 1950, **33**, 1459.
[57] *Chloramphenicol formulations*, medicines.org.uk https://www.medicines.org.uk/emc/search?q=%22Chloramphenicol%22 (accessed 07/05/20).
[58] T. H. Jukes, *Rev. Infect. Dis.*, 1985, **7**, 702.
[59] *Chlortetracycline*, pubchem.ncbi.nlm.nih.gov https://pubchem.ncbi.nlm.nih.gov/compound/54675777#section=Top (accessed 07/05/20).
[60] M. Schach von Wittenau, R. K. Blackwood, L. H. Conover, R. H. Glauert and R. B. Woodward, *J. Am. Chem. Soc.*, 1965, **87**, 134.
[61] *Erythromycin History*, en.wikipedia.org https://en.wikipedia.org/wiki/Erythromycin#cite_note-40 (accessed 24/04/20)
[62] R. B. Woodward, E. Logusch, K. P. Nambiar, K. Sakan, D. E. Ward, B. W. Au-Yeung, P. Balaram, L. J. Browne, P. J. Card and C. H. Chen, J. *Am. Chem. Soc.*, 1981, **103**, 3215.
[63] S. Morimoto, Y. Takahashi, Y. Watanabe and S. Omura, *A. J. Antibiot.*, 1984, **37**, 187.
[64] D. Greenwood, *Antimicrobial Drugs – Chronicle of a Twentieth Century Medical Triumph*, Oxford University Press, Oxford, 2008.
[65] K. C. Nicolaou, C. N. C. Boddy, S. Brase and N. Winssinger, *Angew. Chem. Int. Ed.*, 1999, **38**, 2096.
[66] R. C. G. R. Anderson, H. M. Higgins and C. D. Pettinga, *Cincinnati J. Med.*, 1961, **42**, 49.
[67] D. P. Levine, *Clin. Infect. Dis.*, 2006, **42**, S5.
[68] *Giuseppe Brotzu*, en.wikipedia.org https://en.wikipedia.org/wiki/Giuseppe_Brotzu#cite_note-1 (accessed 24/04/20)
[69] R. Weiss, *FDA Rules Override Warnings About Drugs*, the Washington Post, March 2007.
[70] G. Y. Lesher, E. D. Froelich, M. D. Gruet, J. H. Bailey and R. P. Brundage, *J. Med. Pharm. Chem.*, 1962, **5**, 1063.
[71] P. Ball, in *The Quinolones*, ed. V. T. Andriole, Academic Press, London, 3rd edn, 2000, ch. 1, pp. 1–31.
[72] J. Fischer and C. R. Ganellin, *Analogue-based Drug Discovery*, John Wiley & Sons, Weinheim, 2006.
[73] I. Morrissey, K. Hoshino, K. Sato, A. Yoshida, I. Hayakawa, M. G. Bures and L. L. Shen, *Antimicrob. Agents Chemother.*, **40**, 1775.
[74] *Bausch & Lomb Receives FDA Approval of Besivance, New Topical Ophthalmic Antibacterial for the Treatment of Bacterial Conjunctivitis ("Pink Eye")*, Bausch & Lomb, May 2009. https://web.archive.org/web/20090601075545/http://www.bausch.com/en_US/corporate/corpcomm/news/besivance_approval.aspx (accessed 24/04/20)
[75] J. S. Bradley, J. Garau, H. Lode, K. V. Rolston, S. E. Wilson and J. P. Quinn, *Int. J. Antimicrob. Agents.*, 1999, **11**, 93.

[76] J. S. Kahan, F. M. Kahan, R. Goegelman, S. A. Currie, M. Jackson, E. O. Stapley *et al.*, 1979, *J. Antibiot.*, **32**, 1.
[77] R. B. Sykes, J. S. Wells, W. L. Parker, W. H. Koster and C. M. Cimarusti, *N. J. Med.*, 1986, Spec No: 8-15.
[78] S. J. Yaffe and J. V. Aranda, *Neonatal and Pediatric Pharmacology – Therapeutic Principles in Practice*, Lippincott Williams & Wilkins, London, 2010.
[79] B. Blass, *Basic Principles of Drug Discovery and Development.*, Elsevier, London, 2015.
[80] Y. Tu and D. R. McCalla, *Biochim. Biophys. Acta.*, 1975, **402**, 142.
[81] *Macrobid Capsules 100mg B.P* medicines.org.uk https://www.medicines.org.uk/emc/product/429/smpc (accessed 07/05/20).
[82] *Helicobacter Pylori Infection*, bnf.nice.org.uk https://bnf.nice.org.uk/treatment-summary/helicobacter-pylori-infection.html (accessed 07/05/20).
[83] *Furacin Topical Cream*, drugs.com https://www.drugs.com/mmx/furacin-topical-cream.html (accessed 07/05/20).
[84] L. M. Ednie, A. Rattan, M. R. Jacobs, and P. C. Appelbaum, *Antimicrob. Agents Chemother.*, 2003, **47**, 1143.
[85] S. J. Brickner, *Curr. Pharm. Des.*, 1996, **2**, 175.
[86] R. C. Moellering, *Ann. Intern. Med.*, 2003, **138**, 135.
[87] A. M. Slee, M. A. Wuonola, R. J. McRipley, I. Zajac, M. J. Zawada, P. T. Bartholomew, W. A. Gregory and M. Forbes, *Antimicrob. Agents Chemother.*, 1987, **31**, 1791.
[88] M. R. Barbachyn and C. W. Ford, *Angew. Chem. Int. Ed. Engl.*, 2003, **42**, 2010.
[89] *Zyvox*®, U.S. Food and Drug Administration, April 2000. https://web.archive.org/web/20080110042651/https://www.fda.gov/cder/foi/nda/2000/21130_Zyvox.htm (accessed 24/04/20).
[90] *Approval Package for Application No. 205436Orig1s000*, Centre for Drug Evaluation and Research, June 2014. https://www.accessdata.fda.gov/drugsatfda_docs/nda/2014/205436orig1s000approv.pdf (accessed 24/04/20).
[91] A. Essig, D. Hofmann, D. Münch, S. Gayathri, M. Künzler, P. T. Kallio, et al., *J. Biol. Chem.*, 2014, **289**, 34953.
[92] L. L. Ling, T. Schneider, A. J. Peoples, A. L. Spoering, I. Engels, B. P. Conlon *et al.*, *Nature*, 2015, **517**, 455.
[93] A. Burger, *Comprehensive Medicinal Chemistry*, Pergamon Press, Oxford, 1990.
[94] C. G. Wermuth, C. R. Ganellin, P. Lindberg and L. A. Mitscher, *Pure Appl. Chem.*, 1998, **70**, 1129.
[95] *World Drug Index*, daylight.com https://www.daylight.com/products/wdi.html (accessed 25/04/20).
[96] World Health Organization, *WHO model list of essential medicines – 20th list*, Geneva, March 2017 (amended August 2017).
[97] J. P. Overington, B. Al-Lazikani and A. L. Hopkins, *Nat. Rev. Drug Discov.*, 2006, **5**, 993.
[98] P. Imming, C. Sinning and A. Meyer, *Nat. Rev. Drug Discov.*, 2006, **5**, 821.
[99] J. A. DiMasia, H. G. Grabowskib and R. W. Hansen, *J. Health Econ.*, 2016, **47**, 20.
[100] The British Medical Association, *Medical Dictionary*, Dorling Kindersley, London, 2008.
[101] T. Gaich and P. S. Baran, *J. Org. Chem.*, 2010, **75**, 4657.
[102] H. P. Rang, M. M. Dale, J. M. Ritter, R. J. Flower and G Henderson, *Rang and Dale's Pharmacology*, Churchill Livingstone, Edinburgh, 2012.
[103] J. Burgess and J. Golden, *Cracking the Druggable Genome*, bio-itworld.com http://www.bio-itworld.com/archive/100902/firstbase.html (accessed: 27/04/20).
[104] R. S. Bohacek, C. McMartin and W. C. Guida, *Med. Res. Rev.*, 1996, **16**, 3.
[105] B. Krumm and B. L. Roth, *Nature*, 2020, **579**, 35.
[106] C. S. Ramesha, *Drug Discov. Today*, 2000, **5**, 43.
[107] S. Fox, S. Farr-Jones, L. Sopchak, A. Boggs, H. W. Nicely, R. Khoury and M. Biros, *J. Biomol. Screen.*, 2006, **11**, 864.
[108] C. A. Lipinski, F. Lombardo, B. W. Dominty and P. J. Feeney, *Adv. Drug Deliv. Rev.*, 1997, **23**, 3.
[109] A. K. Ghose, V. N. Viswanadhan and J. J. Wendoloski, *J. Combin. Chem.*, 1999, **1**, 55.
[110] T. I. Oprea, *J. Comput. Aided Mol. Des.*, 2000, **14**, 251.
[111] D. F. Veber, S. R. Johnson, H. Y. Cheng, B. R. Smith, K. W. Ward and K. D. Kopple, *J. Med. Chem.*, 2002, **45**, 2615.

[112] L. Lin and H. Wong, *Pharmaceutics.*, 2017, **9**, 41.
[113] T. T. Wager, X. Hou, P. R. Verhoest and A. Villalobos, *ACS Chem. Neurosci.*, 2010, **1**, 435.
[114] B. E. Evans, K. E. Rittle, M. G. Bock, R. M. DiPardo, R. M. Freidinger, W. L. Whitter *et al.*, *J. Med. Chem.*, 1988, **31**, 2235.
[115] J. S. Mason, I. Morize, P. R. Menard, D. L. Cheney, C. Hulme and R. F. Labaudiniere, *J. Med. Chem.*, 1999, **42**, 3251.
[116] R. W. DeSimone, K. S. Currie, S. A. Mitchell, J. W. Darrow and D. A. Pippin, *Comb. Chem. High Throughput Screen.*, 2004, **7**, 473.
[117] J. R. Proudfoot, *Bioorg. Med. Chem. Lett.*, 2002, **12**, 1647.
[118] T. I. Oprea, T. K. Allu, D. C. Fara, R. F. Rad, L. Ostopovichi and C. G. Bologa, *J. Comput. Aided Mol. Des.*, 2007, **21**, 113.
[119] T. Sakaeda, N. Okamura, S. Nagata, T. Yagami, M. Horinouhi, K. Okumura *et al.*, *Biol. Pharm. Bull.*, 2001, **24**, 935.
[120] C. Hansch, J. P. Björkroth and A. Leo, *J. Pharm. Sci.*, 1987, **76**, 663.
[121] P. R. Andrews, D. J. Craik and J. L. Martin, *J. Med. Chem.*, 1984, **27**, 1648.
[122] I. D. Kuntz, K. Chen, K. A. Sharp and P. A. Kollman, *Proc. Natl. Acad. Sci. USA*, 1999, **96**, 9997.
[123] A. L. Hopkins, C. R. Groom and A. Alex, *Drug Discov. Today*, 2004, **9**, 430.
[124] C. Abad-Zapatero and J. T. Metz, *Drug Discov. Today*, 2005, **10**, 464.
[125] D. C. Rees, M. Congreve, C. W. Murray and R. Carr, *Nat. Rev. Drug Discov.*, 2004, **3**, 660.
[126] R. DeWitte and E. Shakhnovich, *J. Am. Chem. Soc.*, 1996, **118**, 11733.
[127] B. A. Katz, J. M. Clark, J. S. Finer-Moore, T. E. Jenkins, C. R. Johnson, M. J. Ross, C. Luong W. K. Moore and R.M. Stroud, *Nature*, 1998, **391**, 608.
[128] S. D. Bembenek, B. A. Tounge and C. H. Reynolds, *Drug Discov. Today*, 2009, **14**, 278.
[129] C. Abad-Zapatero and D. Blasi, *Mol. Inform.*, 2011, **30**, 122.
[130] P. Kenny, A. Leitão and C. Montanari, *J. Comput. Aided Mol. Des.*, 2014, **28**, 699.
[131] M. D. Shultz, *ACS Med. Chem. Lett.*, 2013, **5**, 2.
[132] C. H. Reynolds, *Future Med. Chem.*, 2015, **7**, 1363.
[133] J. Li, F. Bai, H. Liu and P. Gramatica, *Chem. Biol. Drug Des.*, 2015, **86**, 1501.
[134] A. T. Garcia-Sosa, C. Hetenyi and U. Maran, *J. Comput. Chem.*, 2010, **31**, 174.
[135] M. D. Shultz, *Bioorg. Med. Chem. Lett.*, 2013, **23**, 5980.
[136] M. Congreve, R. Carr, C. W. Murray and H. Jhoti, *Drug Discov. Today*, 2003, **8**, 876.
[137] H. Jhoti, G. Williams, D. C. Rees and C. W. Murray, *Nat. Rev. Drug Discov.*, 2013, **12**, 644.
[138] G. M. Rishton, *Drug Discov. Today*, 1997, **2**, 382.
[139] O. Roche, P. Schneider, J. Zuegge, W. Guba, M. Kansy, A. Alanine *et al.*, *J. Med. Chem.*, 2002, **45**, 137.
[140] Y. Takaoka, Y. Endo, S. Yamanobe, H. Kakinuma, T. Okubo, Y. Shimazaki *et al.*, *J. Chem. Inf. Comput. Sci.*, 2003, **43**, 1269.
[141] K. R. Freter, *Pharmaceut. Res.*, 1988, **5**, 397.
[142] J. E. Calfee, *Prices, Markets, and the Pharmaceutical Revolution*, American Enterprise Institute Press, Washington DC, 2000.
[143] M. Angell, *The Truth About the Drug Companies – How They Deceive us and What to do About it*, Random House, New York, 2004.
[144] S. Garattini, *J. Nephrol.*, 1997, **10**, 283.
[145] J. H. van Drie, *Internet Electron. J. Mol. Des.*, 2007, **6**, 271.
[146] Y. C. Martin, J. L. Kofron and L. M. Traphagen, *J. Med. Chem.*, 2002, **45**, 4350.
[147] G. A. Showell, J. S. Mills, *Drug Discov. Today*, 2003, **8**, 551.
[148] P. Gribbon and A. Sewing, *Drug Discov. Today*, 2005, **10**, 17.
[149] F. Brown, *Annu. Rep. Med. Chem.*, 1998, **33**, 375.
[150] C. W. Murray and D. C. Rees, *Nat. Chem.*, 2009, **1**, 187.
[151] J. Sadowski, M. Wagener and J. Gasteiger, *Angew. Chem. Int. Ed. Engl.*, 1995, **24**, 2674.
[152] M. Krier, J. X. de Araujo-Junior, M. Schmitt, J. Duranton, H. Justiano-Basaran, C. Lugnier *et al.*, *J. Med. Chem.*, 2005, **48**, 3816.
[153] S. B. Shuker, P. J. Hajduk, R. P. Meadows and S. W. Fesik, *Science*, 1996, **274**, 1531.

[154] V. L. Nienaber, P. L. Richardson, V. Koighofer, J. J. Bouska, V. L. Giranda and J. Greer, *Nat. Biotechnol.*, 2000, **18**, 1105.
[155] L. H. Sternbach, *J. Med. Chem.*, 1979, **22**, 1.
[156] A. Smith, *Nature*, 2002, **418**, 453.
[157] N. K. Terret, A. S. Bell, D. Brown and P. Ellis, *Bioorg. Med. Chem. Lett.*, 1996, **6**, 1819.
[158] R. L. Noble, C. T. Beer and J. H. Cutts, *Ann. N. Y. Acad. Sci.*, 1958, **76**, 882.
[159] T. Y. Shen, *Angew. Chem. Int. Edit.*, 1972, **11**, 460.
[160] D. W. Cushman, H. S. Cheung, E. F. Sabo and M. A. Ondetti, *Biochemistry*, 1977, **16**, 5485.
[161] F. W. Schueller, *Chemobiodynamics and Drug Design*, McGrawHill, New York, 1960.
[162] K. Krafts, E. Hempelmann and A. Skórska-Stania, *Parasitol. Res.*, 2012, **111**, 1.
[163] R. Gomńez-Bombarelli, J. N. Wei, D. Duvenaud, J. M. Hernańdez-Lobato, B. Sańchez-Lengeling, D. Sheberla *et al.*, *ACS Cent. Sci.*, 2018, **4**, 268.
[164] R. D. Hoffsommer, D. Taub and N. L. Wendler, *J. Org. Chem.*, 1963, **28**, 1751.
[165] G. J. Durant, W. A. M. Duncan, C. R. Ganellin, M. E. Parsons, R. C. Blakemore and A. C. Rasmussen, *Nature*, 1978, **276**, 403.
[166] S. L. Chan, A. L. Pallett and N. G. Morgan, *Naunyn-Schmiedebergs Arch. Pharmacol.*, 1997, **356**, 763.
[167] S. L. Chan, D. Atlas, R. F. James and N. G. Morgan, *Br. J. Pharmacol.*, 1997, **120**, 926.
[168] J. A. Bristol, *Annual Reports in Medicinal Chemistry*, Vol. 26, Academic Press, London, 1991.
[169] G. R. Marshall, C. D. Barry, H. E. Bosshard, R. A. Dammkoehler and D. A. Dunn, *Computer-Assisted Drug Design*, American Chemical Society, Washington DC, 1979.
[170] G. R. Marshall and D. R. Cramer, *Trends Pharmacol. Sci.*, 1988, **9**, 285.
[171] P. N. Craig, *the Basis of Medicinal Chemistry*, Wiley-Interscience, New York, 1980.
[172] V. Austel, *Steric Effects in Drug Design*, Lange & Springer, Berlin, 1984.
[173] J. G. Topliss, *J. Med. Chem.*, 1972, **15**, 1006.
[174] Y. C. Martin and W. J. Dunn, *J. Med. Chem.*, 1973, **16**, 578.
[175] W. Soudijn, *Stereochemistry and Biological Activity of Drugs*, Blackwell Scientific Publications, Oxford, 1983.
[176] M. Kiuchi, K. Adachi, T. Kohara, M. Minoguchi, T. Hanano, Y. Aoki *et al.*, *J. Med. Chem.*, 2000, **43**, 2946.
[177] A. Yarnell, *Chemical & Engineering News*, June 2005 http://pubsapp.acs.org/cen/coverstory/83/8325/8325salvarsan.html (accessed 10/05/20).
[178] N. C. Lloyd, H. W. Morgan, B. K. Nicholson and R. S. Ronimus, *Angew. Chem. Int. Ed.*, 2005, **44**, 941.
[179] J. Davies, *Can. J. Infect. Dis. Med. Microbiol.*, 2006, **17**, 287.
[180] C. Walsh, *Nat. Rev. Microbiol.*, 2003, **1**, 65.
[181] R. E. Hancock and R. Lehrer, *Trends Biotechnol.*, 1998**,** **16**, 82.
[182] H. G. Boman, *Annu. Rev. Immunol.*, 1995, **13**, 61.
[183] M. A. Kohanski, D. J. Dwyer and J. J. Collins, *Nat. Rev. Microbiol.*, 2010, **8**, 423.
[184] H. Neu, *Science*, 1992, **257**, 1064.
[185] H. Kleinkauf and H. von Dohren, *Crit. Rev. Biotechnol.*, 1988, **8**, 1.
[186] A. Csordas and H. Michl, *Monatsh. Chem.*, 1970, **101**, 182.
[187] E. Habermann, Science, 1972, **177**, 314.
[188] D. Perlman and M. Bodansky, *Annu. Rev. Biochem.*, 1971, **40**, 449.
[189] P. Courvalin, *Clin. Infect. Dis.*, 2006, **42**, S25.
[190] D. H. Williams and B. Bardsley, *Angew. Chem. Int. Ed.*, 1999, **38**, 1172.
[191] D. Kahne, C. Leimkuhler, W. Lu and C. Walsh, *Chem. Rev.*, 2005, **105**, 425.
[192] B. Perichon and P. Courvalin, *Antimicrob. Agents Chemother.*, 2009, **53**, 4580.
[193] C. C. McComas, B. M. Crowley and D. L. Boger, *J. Am. Chem. Soc.*, 2003, **125**, 9314.
[194] T. D. H. Bugg, G. D. Wright, S. Dutka-Malen, M. Arthur, P. Courvalin and C.T. Walsh, *Biochemistry*, 1991, **30**, 10408.
[195] J. P. Mackay, U. Gerhard, D. A. Beauregard, D. H. Williams, M. S. Westwell and M. S. Searle, *J. Am. Chem. Soc.*, 1994, **116**, 4581.
[196] D. H. Williams, A. J. Maguire, W. Tsuzuki and M. S. Westwell, *Science*, 1998, **280**, 711.

[197] T. I. Nicas, D. L. Mullen, J. E. Flokowitsch, D. A. Preston, N. J. Snyder, R. E. Stratford and R. D. G. Cooper, *Antimicrob. Agents Chemother.*, 1995, **39**, 2585.
[198] M. E. Rupp, P. D. Fey and G. M. Longo, *J. Antimicrob. Chemother.*, 2001, **47**, 705.
[199] S. Yoganathan and S. J. Miller, *J. Med. Chem.*, 2015, **58**, 2367.
[200] C. S. Lunde, S. R. Hartouni, J. W. Janc, M. Mammen, P. P. Humphrey and B. M. Benton, *Antimicrob. Agents Chemother.*, 2009, **53**, 3375.
[201] J. Bello, H. R. Bello and E. Granados., *Biochemistry*, 1982, **21**, 461.
[202] T. J. Falla, D. N. Karunaratne and R. E. W. Hancock, *J. Biol. Chem.*, 1996, **271**, 19298.
[203] J. P. S. Powers and R. E. W. Hancock, *Peptides*, 2003, **24**, 1681.
[204] M. Wu and R. E. W. Hancock, *J. Biol. Chem.*, 1999, **274**, 29.
[205] M. Milik and J. Skolnick, *Proc. Natl. Acad. Sci. USA*, 1982, **89**, 9391.
[206] S. J. Ludtke, K. He and H. Huang, *Biochemistry*, 1995, **34**, 16764.
[207] Z. Oren and Y. Shai, *Biopolymers*, 1998, **47**, 451.
[208] S. J. Ludtke, K. He, W. T. Heller, T. A. Harroun, L. Yang and H. W. Huang, *Biochemistry*, 1996, **35**, 13723.
[209] R. E. W. Hancock, *Lancet*, 1997, **349,** 418.
[210] B. L. Kagan, M. E. Selsted, T. Ganz and R. I. Lehrer, *Proc. Natl. Acad. Sci. USA*, 1990, **87**, 210.
[211] A. T. Y. Yeung, S. L. Gellatly and R. E. W. Hancock, *Cell. Mol. Life Sci.*, 2011, **68**, 2161.
[212] S. Nuding, T. Frasch, M. Schaller, E. F. Stange and L. T. Zabel, *Antimicrob. Agents Chemother.*, 2014, **58**, 5719.
[213] A. Patrzykat, C. L. Friedrich, L. J. Zhang, V. Mendoza and R. E. W. Hancock, *Antimicrob. Agents Chemother.*, 2002, **46**, 605.
[214] C. Subbalakshmi and N. Sitaram, *FEMS Microbiol. Lett.*, 1998, **160**, 91.
[215] E. Breukink and B. de Kruijff, *Nat. Rev. Drug Discov.*, 2006, **5**, 321.
[216] N. Schnell, K. D. Entian, U. Schneider, F. Gotz, H. Zahner, R. Kellner and G. Jung, *Nature*, 1988, **333**, 276.
[217] Y. Shi, A. Bueno and W. A. van der Donk, *Chem. Commun.*, 2012, **48**, 10966.
[218] B. de Kruijff, V. van Dam and E. Breukink, *Prostaglandins Leukot. Essent. Fatty Acids*, 2008, **79**, 117.
[219] A. B. Tabor, *Org. Biomol. Chem.*, 2011, **9**, 7606.
[220] L. J. Zhang, J. Parente, S. A. Harris, D. E. Woods, R. E. W. Hancock and T. J. Fallal, *Antimicrob. Agents Chemother.*, 2005, **49**, 2921.
[221] Ø. Samuelsen, H. H. Haukland, H. Jenssen, M. Kramer, K. Sandvik, H. Ulvatne and L. H. Vorland, *FEBS Lett.*, 2005, **579**, 3421.

[222] M. Upton, P. Cotter and J. Tagg, *Int. J. Microbiol.*, 2012, **2012**, 326503 (doi: 10.1155/2012/326503).
[223] World Health Organisation, *WHO's first global report on antibiotic resistance*, Geneva, April 2014 http://www.who.int/mediacentre/news/releases/2014/amr-report/en/ (accessed 25/05/20).
[224] World Health Organisation, *World Antibiotic Awareness Week* http://www.who.int/drugresistance/en/ (accessed 25/05/20).
[225] The U.S. Military HIV Research Program, *First discovery in United States of colistin resistance in a human E. coli infection*, May 2016 https://www.sciencedaily.com/releases/2016/05/160526152033.htm (accessed 25/05/20).
[226] The Guardian, *Doctors fear spread of 'super-gonorrhoea' across Britain*, April 2016 https://www.theguardian.com/society/2016/apr/17/gonorrhoea-will-spread-across-uk-doctors-fear (accessed 25/05/20).
[227] J. O'Neill, *Review on Antimicrobial Resistance: Tackling Drug-Resistant Infections Globally*, Feb. 2016 https://amr-review.org (accessed 25/05/20).
[228] Longitude Prize. https://longitudeprize.org/ (accessed 25/05/20).
[229] J. L. Fox, *Nat. Biotechnol.*, 2012, **30**, 733.
[230] Antibacterial Drug Development Task Force http://www.fda.gov/Drugs/DevelopmentApprovalProcess/DevelopmentResources/ucm317207.htm (accessed 26/05/20).
[231] D. Brown, *DNDi: Global Antibiotic R&D (GARD) Partnership Scientific Consultation*, Institut Pasteur, Paris, 29 Feb. 2016 http://www.dndi.org/wp-content/uploads/2016/03/David_Brown_ANTRUK_Antib_Resistance.pdf (accessed 26/05/20).

[232] R. P. Mishra, E. Oviedo-Orta, P. Prachi, R. Rappuoli and F. Bagnoli, *Curr. Opin. Microbiol.*, 2012, **15**, 596.
[233] R. Rappuoli, C. W. Mandl, S. Black and E. De Gregorio, *Nat. Rev. Immunol.*, 2011, **11**, 865.
[234] O. Eidam, C. Romagnoli, E. Caselli, K. Babaoglu, D. T. Pohlhaus, J. Karpiak, R. Bonnet, B. K. Shoichet and F. Prati, *J. Med. Chem.*, 2010, **53**, 7852.
[235] B. L. Hollenbeck and L. B. Rice, *Virulence*, 2012, **3**, 421.
[236] L. L. Ling, T. Schneider, A. J. Peoples, A. L. Spoering, I. Engels, B. P. Conlon *et al.*, *Nature*, 2015, **517**, 455.
[237] Centers for Disease Control and Prevention: Antibiotic/Antibacterial Resistance. http://www.cdc.gov/drugresistance/about.html (accessed 27/05/20).
[238] E. Zuckerkandl and L. Pauling, *J. Theor. Biol.*, 1965, **8**, 357.
[239] G. B. Golding and R. S. Gupta, *Mol. Biol. Evol.*, 1995, **12**, 1.
[240] R. S. Gupta and B. Singh, *Curr. Biol.*, 1994, **4**, 1104.
[241] J. Lederberg and E. L. Tatum, *Nature*, 1946, **158**, 558.
[242] N. D. Zinder and J. Lederberg, *J. Bacteriol.*, 1952, **64**, 679.
[243] M. Syvanen, *J. Theor. Biol.*, 1985, **112**, 333.
[244] E. Hilario and J. P. Gogarten, *BioSystems*, 1993, **31**, 111.
[245] N. Goldenfeld and C. Woese, *Nature*, 2007, **445**, 369.
[246] G. P. Fournier and J. P. Gogarten, *J. Bacteriol.*, 2008, **190**, 1124.
[247] C. Gyles and P. Boerlin, *Vet. Pathol.*, 2014, **51**, 328.
[248] E. Kay, T. M. Vogel, F. Bertolla, R. Nalin and P. Simonet, *Appl. Environ. Microbiol.*, 2002, **68**, 3345.
[249] E. V. Koonin, A. S. Makarova and L Aravind, *Annu. Rev. Microbiol.*, 2001, **55**, 709.
[250] T. Dagan, Y. Artzy-Randrup and W. Martin, *Proc. Natl Acad. Sci.*, 2008, **105**, 10039.
[251] W. F. Doolittle, *Science*, 1999, **284**, 2124.
[252] W. F. Doolittle and E. Bapteste, *Proc. Natl Acad. Sci.*, 2007, **104**, 2043.
[253] Y. I. Wolf, I. B. Rogozin, N. V. Grishin and E. V. Koonin, *Trends Genet.*, 2002, **18**, 472.
[254] J. Brown, *Nat. Rev. Genet.*, 2003, **4**, 121.
[255] C. G. Kurland, B. Canback and O. B. Berg, *Proc. Natl Acad. Sci. USA*, 2003, **100**, 9658.
[256] C. G. Kurland, *Bioessays*, 2005, **27**, 741.
[257] R. Sorek, Y. Zhu, C. J. Creevey, M. P. Francino, P. Bork and E. M. Rubin, *Science*, 2007, **318**, 1449.
[258] E. Bapteste, E. Susko, J. Leigh, I. Ruiz-Trillo, J. Bucknam and W. F. Doolittle, *Mol. Biol. Evol.*, 2008, **25**, 83.
[259] J. Guglielmini, F. de la Cruz and E. P. Rocha, *Mol. Biol. Evol.*, 2013, **30**, 315.
[260] I. Chen, P. J. Christie and D. Dubnau, *Science*, 2005, **310**, 1456.
[261] C. Smillie, M. P. Garcillan-Barcia, M. V. Francia, E. P. Rocha and F. de la Cruz, *Microbiol. Mol. Biol. Rev.*, 2010, **74**, 434.
[262] R. A. Wozniak and M. K. Waldor, *Nat. Rev. Microbiol.*, 2010, **8**, 552.
[263] A. Norman, L. H. Hansen, and S. J. Sorensen, *Philos. Trans. R. Soc. Lond. B Biol. Sci.*, 2009, **364**, 2275.
[264] R. Canton, J. M. Gonzalez-Alba and J. C. Galan, *Front. Microbiol.*, 2012, **3**, 110.
[265] P. L. Woerther, C. Burdet, E. Chachaty and A. Andremont, *Clin. Microbiol. Rev.*, 2013, **26**, 744.
[266] A. Hartmann, A. Locatelli, L. Amoureux, G. Depret, C. Jolivet, E. Gueneau *et al.*, *Front. Microbiol.*, 2012, **3,** 83.
[267] R. Canton and T. M. Coque, *Curr. Opin. Microbiol.*, 2006, **9**, 466.
[268] F. Griffith, *J. Hyg. (Lond.)*, 1928, **27**, 113.
[269] C. M. Thomas and K. M. Nielsen, *Nat. Rev. Microbiol.*, 2005, **3**, 711.
[270] P. F. Sparling, *J. Bacteriol.*, 1966, **92**, 1364.
[271] C. Johnston, B. Martin, G. Fichant, P. Polard and J. P. Claverys, *Nat. Rev. Microbiol.*, 2014, **12**, 181.
[272] X. Charpentier, E. Kay, D. Schneider and H. A. Shuman, *J. Bacteriol.*, 2011, **193**, 1114.
[273] X. Charpentier, P. Polard and J. P. Claverys, *Curr. Opin. Microbiol.*, 2012, **15**, 570.
[274] M. Prudhomme, L. Attaiech, G. Sanchez, B. Martin and J. P. Claverys, *Science*, 2006, **313**, 89.
[275] B. M. Kristensen, S. Sinha, J. D. Boyce, A. M. Bojesen, J. C. Mell and R. J. Redfield, *Appl. Environ. Microbiol.*, 2012, **78**, 4914.
[276] N. Harford and M. Mergeay, *Mol. Gen. Genet.*, 1973, **120**, 151.
[277] S. Domingues, K. Harms, W. F. Fricke, P. J. Johnsen, G. J. da Silva and K. M. Nielsen, *PLoS Pathog.*, 2012, **8,** e1002837.

[278] K. E. Wommack and R. R. Colwell, *Microbiol. Mol. Biol. Rev.*, 2000, **64**, 69.
[279] H. Caraballo, *Emerg. Med. Pract.*, 2014, **16**, 1.
[280] S. R. Modi, H. H. Lee, C. S. Spina and J. Collins, *Nature*, 2013, **499**, 219.
[281] M. Brown-Jaque, W. Calero-Caceres and M. Muniesa, *Plasmid*, 2015, **79**, 1.
[282] S. L. Hyder and M. M. Streitfeld, *J. Infect. Dis.*, 1978, **138**, 281.
[283] R. Mazaheri Nezhad Fard, M. D. Barton and M. W. Heuzenroeder, *Lett. Appl. Microbiol.*, 2011, **52**, 559.
[284] M. Varga, L. Kuntova, R. Pantucek, I. Maslanova, V. Ruzickova and J. Doskar, *FEMS Microbiol. Lett.*, 2012, **332**, 146.
[285] K. Ubukata, M. Konno and R. Fujii, *J. Antibiot.*, 1975, **28**, 681.
[286] T. Billard-Pomares, S. Fouteau, M. E. Jacquet, D. Roche, V. Barbe, M. Castellanos *et al.*, *Antimicrob. Agents Chemother.*, 2014, **58**, 6550.
[287] H. Schmieger and P. Schicklmaier, *FEMS Microbiol. Lett.*, 1999, **170**, 251.
[288] R. Jain, M. C. Rivera, J. E. Moore and J. A. Lake, *Theor. Popul. Biol.*, 2002, **61**, 489.
[289] U. Dobrindt, B. Hochhut, U. Hentschel and J. Hacker, *Nat. Rev. Microbiol.*, 2004, **2**, 414.
[290] G. S. Vernikos and J. Parkhill, *Genome Res.*, 2008, **18**, 331.
[291] J. Hacker and J. B. Kaper, *Annu. Rev. Microbiol.*, 2000, **54**, 641.
[292] H. Schmidt and M. Hensel, *Clin. Microbiol. Rev.*, 2004, **17**, 14.
[293] C. Buchrieser, M. Prentice and E. Carniel, *J. Bacteriol.*, 1998, **180**, 2321.
[294] O. Gal-Mor and B. B. Finlay, *Cell Microbiol.*, 2006, **8**, 1707.
[295] E. Cabezon, J. Ripoll-Rozada, A. Pena, F. de la Cruz, and I. Arechaga, *FEMS Microbiol. Rev.*, 2015, **39**, 81.
[296] A. Ilangovan, S. Connery and G. Waksman, *Trends Microbiol.*, 2015, **23**, 301.
[297] D. Sun, B. Wang, L. Zhu, M. Chen and L. Zhan, *PLoS One*, 2013, **8**, e59019.
[298] Y. Zhang, C. Shi, J. Yu, J. Ren and D. Sun, *PLoS One*, 2012, **7**, e33514.
[299] S. D. Tsen, S. S. Fang, M. J. Chen, J. Y. Chien, C. C. Lee and D. H. Tsen, *J. Biomed. Sci.*, 2002, **9**, 246.
[300] D. Sun, Y. Zhang, Y. Mei, H. Jiang, Z. Xie, H. Liu, *et al.*, *FEMS Microbiol. Lett.*, 2006, **265**, 249.
[301] D. Sun, X. Zhang, L. Wang, M. Prudhomme, Z. Xie, B. Martin *et al.*, *J. Bacteriol.*, 2009, **191**, 713.
[302] S. E. Finkel and R. Kolter, *J. Bacteriol.*, 2009, **183**, 6288.
[303] V. Palchevskiy and S. E. Finkel, *J. Bacteriol.*, 2006, **188**, 3902.
[304] D. Sun, *Biochem. Biophys. Res. Commun.*, 2016, **471**, 213.
[305] C. García-Aljaro, E. Ballesté and M. Muniesa, Curr. Opin. Microbiol., 2017, **38**, 95.
[306] J. O. Andersson, *Cell. Mol. Life Sci.*, 2005, **62**, 1182.
[307] J. S. Rest and D. P. Mindell, *Mol. Biol. Evol.*, 2003, **20**, 1134.
[308] U. Gophna, R. L. Charlebois and W. F. Doolittle, *Trends Microbiol.*, 2004, **12**, 213.
[309] J. O. Andersson, Å. M. Sjögren, L. A. M. Davis, T. M. Embley and A. J. Roger, *Curr. Biol.*, 2003, **13**, 94.
[310] R. F. Watkins and M. W. Gray, *J. Mol. Evol.*, 2006, **63**, 801.
[311] A. Guljamow, H. Jenke-Kodama, H. Saumweber, P. Quillardet, L. Frangeul, A. M. Castets *et al.*, *Curr. Biol.*, 2007, **17**, R757.
[312] A. M. Nedelcu, I. H. Miles, A. M. Fagir and K. Karol, *J. Evol. Biol.*, 2008, **21**, 1852.
[313] D. R. Riley, K. B. Sieber, K. M. Robinson, J. R. White, A. Ganesan *et al.*, *PLoS Comput. Biol.*, 2013, **9**, e1003107.
[314] F. Boccellato and T. F. Meyer, *Cell Host Microbe*, 2015, **17**, 728.
[315] E. Christ and A. I. Tauber, Biol. Philos., 1999, **15**, 509.
[316] P. Medawar, *Immunological Tolerance*, Nobel Lecture, December 1960 https://www.nobelprize.org/prizes/medicine/1960/medawar/lecture/ (accessed 01/06/20).
[317] J. Šterzl, *Nature*, 1966, **209**, 416.
[318] L. Råberg, A. L. Graham and A. F. Read, *Philos. Trans. R. Soc. Lond. B. Biol. Sci.*, 2009, **364**, 37.
[319] D. S. Schneider and J. S. Ayres, *Nat. Rev. Immunol.*, 2008, **8**, 889.
[320] P. Schmid-Hempel, *Evolutionary Parasitology*, Oxford University Press, Oxford, 2011.
[321] J. S. Peiris, K. P. Hui and H. L. Yen, *Curr. Opin. Immunol.*, 2010, **22**, 475.
[322] F. Coperchini, L. Chiovato, L. Croce, F. Magri and M. Rotondi, *Cytokine Growth Factor Rev.*, 2020, (in press) https://doi.org/10.1016/j.cytogfr.2020.05.003 (accessed 01/06/20).
[323] A. L. Graham, J. E. Allen and A. F. Read, *Ann. Rev. Ecol. Evol. Syst.*, 2005, **36**, 373.

[324] G. Majno and I. Joris, *Cells Tissues and Disease – Principles of General Pathology*, Oxford University Press, Oxford, 2004.
[325] W. E. Balch, R. I. Morimoto, A. Dillin and J. W. Kelly, *Science*, 2008, **319**, 916.
[326] T. W. Kensler, N. Wakabayashi and S. Biswal, *Ann. Rev. Pharmacol. Toxicol.*, 2007, **47**, 89.
[327] D. Bente, J. Gren, J. E. Strong and H. Feldmann, *Dis. Models Mech.*, 2009, **2**, 12.
[328] P. Matzinger and T. Kamala, *Nat. Rev. Immunol.*, 2011, **11**, 221.
[329] M. A. Curotto de Lafaille and J. J. Lafaillle, *Immunity*, 2009, **30**, 626.
[330] D. L. Mager, *J. Transl. Med.*, 2006, **4**, 14.
[331] K. H. Bleicher, H. -J. Böhm, K. Müller and A. I. Alanine, *Nat. Rev. Drug Discov.*, 2003, **2**, 369.
[332] R. A. Smith, J. Barbosa, C. L. Blum, M. A. Bobko, Y. V. Caringal, R. Dally *et al.*, *Bioorg. Med. Chem. Lett.*, 2001, **11**, 2775.
[333] L. J. Lombardo, F. Y. Lee, P. Chen, D. Norris, J. C. Barrish, K. Behnia, *et al.*, *J. Med. Chem.*, 2004, **47**, 6658.
[334] L. Sun, N. Tran, F. Tang, H. App, P. Hirth, G. McMahon and C. Tang, *J. Med. Chem.*, 1998, **41**, 2588.
[335] H. I. Skulnick, P. D. Johnson, W. J. Howe, P. K. Tomich, K. -T. Chong, K. D. Watenpaugh *et al.*, *J. Med. Chem.*, 1995, **38**, 4968.
[336] A. Wood and D. Armour, *Progr. Med. Chem.*, 2005, **43**, 239.
[337] R. B. Merrifield, *J. Am. Chem. Soc.*, 1963, **85**, 2149.
[338] G. A. Truran, K. S. Aiken, T. R. Fleming, P. J. Webb and J. H. Markgraf, *J. Chem. Educ.*, 2002, **79**, 85.
[339] T. Lee and Y. -D. Gong, *Molecules*, 2012, **17**, 5467.
[340] M. Stawikowski and G. B. Fields, *Curr. Protoc. Protein Sci.*, 2002, **18**, 1.
[341] E. Atherton, M. J. Gait, R. C. Sheppard and B. J. Williams, *Bioorg. Chem.*, 1979, **8**, 351.
[342] E. Boll, H. Drobecq, N. Ollivier, L. Raibaut, R. Desmet, J. Vicogne and O. Melnyk, *Chem. Sci.*, 2014, **5**, 2017.
[343] B. Yan, *Acc. Chem. Res.*, 1998, **31**, 621.
[344] R. T. Pon, N. Usman and K. K. Ogilvie, *Biotechniques*, 1988, **6**, 768.
[345] P. H. Hermkens, H. C. Ottenheijm and D. C. Rees, *Tetrahedron*, 1997, **53**, 5643.
[346] K. Barlos, O. Chatzi, D. Gatos and G. Stavropoulos, *Int. J. Pept. Protein Res.*, 1991, **37**, 513.
[347] E. Atherton, D. L. J. Clive and R. C. Sheppard, *J. Am. Chem. Soc.*, 1975, **97**, 6584.
[348] S. C. Miller and T. S. Scanlan, *J. Am. Chem. Soc.*, 1997, **119**, 2301.
[349] G. A. Eggimann, H. L. Bolt, P. W. Denny and S. L. Cobb, *ChemMedChem*, 2015, **10**, 233.
[350] S. Hobbs DeWitt, J. S. Kiely, C. J. Stankovic, M. C. Schroeder, D. M. Reynolds Cody and M. R. Pavia, *Proc. Natl. Acad. Sci. USA*, 1993, **90**, 6909.
[351] W. Karnbrocka, M. Deegb, J. Gerhardtc and W. Rapp, *Mol. Divers.*, 1998, **4**, 165.
[352] G. L. Patrick, *An Introduction to Drug Synthesis*, Oxford University Press, Oxford, 2015.
[353] M. -C. Hennion, *J. Chromatogr. A.*, 1999, **856**, 3.
[354] F. Augusto, L. W. Hantao, N. G. S. Mogollón and S. C. G. N. Braga, *Trends Anal. Chem.*, 2013, **43**, 14.
[355] Phase Separators, *www.biotage.com* https://www.biotage.com/product-page/phase-separators (accessed 27/06/20).
[356] O. Reimann, O. Seitz, D. Sarma and R. Zitterbart, *J. Pep. Sci.*, 2019, **25**, e3136.
[357] Biotage® MP-Borohydride, *www.biotage.com* https://www.biotage.com/product-page/biotage-mp-borohydride (accessed 27/06/20).
[358] C. O. Kappe, *Angew. Chem. Int. Ed.*, 2004, **43**, 6250.
[359] F. Mavandadi and Å. Pilotti, *Drug Discov. Today*, 2006, **11**, 165.
[360] J. Spencer, R. P. Rathnam, H. Patel and N. Anjum, *Tetrahedron*, 2008, **64**, 10195.
[361] Y. Liu and X. Jiang, *Lab Chip*, 2017, **17**, 3960.
[362] Custom Microfluidics devices, *www.dolomite-microfluidics.com* https://www.dolomite-microfluidics.com/products/custom-microfluidic-devices (accessed: 07/07/20)
[363] H. M. Geysen, F. Schoenen, D. Wanger and R. Wanger, *Nat. Rev. Drug Discov.*, 2003, **2**, 222.
[364] R. E. Dolle, *J. Comb. Chem.*, 2002, **5**, 693.
[365] A. Beck-Sickinger and P. Weber, *Combinatorial Strategies in Biology and Chemistry*, John Wiley & Sons, New Jersey, 2002.
[366] Á. Furka, *Drug Dev. Res.*, 1995, **36**, 1.

[367] S. J. Rowan, S. J. Cantrill, G. R. L. Cousins, J. K. M. Sanders and J. F. Stoddart, *Angew. Chem. Int. Ed.*, 2002, **41**, 898.
[368] H. Kunz, *Angew. Chem. Int. Ed.*, 2002, **41**, 4439.
[369] E. C. Constable and C. E. Housecroft, *Chem. Soc. Rev.*, 2013, **42**, 1429.
[370] M. C. Thompson and D. H. Busch, *J. Am. Chem. Soc.*, 1962, **84**, 1762.
[371] C. J. Walter, H. L. Anderson and J. K. M. Sanders, *J. Chem. Soc. Chem. Commun.*, 1993, 458.
[372] P. A. Brady, R. P. Bonar-Law, S. J. Rowan, C. J. Suckling and J. K. M. Sanders, *Chem. Commun.*, 1996, 319.
[373] P. A. Brady and J. K. M. Sanders, *J. Chem. Soc. Perkin Trans. 1*, 1997, 3237.
[374] I. Huc and J. -M. Lehn, *Proc. Natl. Acad. Sci. USA*, 1997, **94**, 2106.
[375] G. Kaiser and J. K. M. Sanders, *Chem. Commun.*, 2000, 1763.
[376] A. Makita, T. Nihira and Y. Yamada, *Tetrahedron Lett.*, 1987, **28**, 805.
[377] Z. W. Guo and C. J. Sih, *J. Am. Chem. Soc.*, 1988, **110**, 1999.
[378] Y. Isowa, M. Ohmori, T. Ichikawa, K. Mori, Y. Nonaka, K. Kihara *et al.*, *Tetrahedron Lett.*, 1979, **20**, 2611.
[379] R. V. Ulijn, L. De Martin, L. Gardossi and P. J. Halling, *Curr. Org. Chem.*, 2003, **7**, 1333.
[380] S. Toledano, R. J. Williams, V. Jayawarna and R. V. Ulijn, *J. Am. Chem. Soc.*, 2006, **128**, 1070.
[381] W. W. Kielly and L. B. Bradley, *J. Biol. Chem.*, 1954, **206**, 327.
[382] V. Agouridas, O. El Mahdi, V. Diemer, M. Cargoët, J. M. Monbaliu and O. Melnyk, *Chem. Rev.*, 2019, **119**, 7328.
[383] R. Larsson, Z. C. Pei and O. Ramström, *Angew. Chem. Int. Ed.*, 2004, **43**, 3716.
[384] B. Shi, R. Stevenson, D. J. Campopiano and M. F. Greaney, *J. Am. Chem. Soc.*, 2006, **128**, 8459.
[385] H. Schiff, *Ann. Chem. Pharm.*, 1864, **131**, 118.
[386] J. B. Conant and P. D. Barret, *J. Am. Chem. Soc.*, 1932, **54**, 2881.
[387] E. G. Sander and W. P. Jencks, *J. Am. Chem. Soc.*, 1968, **90**, 6154.
[388] M. Hochgurtel, H. Kroth, D. Piecha, M. W. Hofmann, C. Nicolau, S. Krause *et al.*, *Proc. Natl. Acad. Sci. USA*, 2002, **99**, 3382.
[389] S. Gerber-Lemaire, F. Popowycz, E. Rodriguez-Garcia, A. T. C. Asenjo, I. Robina and P. Vogel, *ChemBioChem.*, 2002, **3**, 466.
[390] V. A. Polyakov, M. I. Nelen, N. Nazarpack-Kandlousy, A. D. Ryabov and A. V. Eliseev, *J. Phys. Org. Chem.*, 1999, **12**, 357.
[391] F. A. Carey and R. J. Sundberg, *Advanced Organic Chemistry Part A*, Plenum Press, New York, 1990.
[392] R. Nguyen and I. Huc, *Chem. Commun.*, 2003, 942.
[393] R. Cacciapaglia, S. Di Stefano and L. Mandolini, *J. Am. Chem. Soc.*, 2005, **127**, 13666.
[394] B. Mohr, D. M. Lynn and R. H. Grubbs, *Organometallics*, 1996, **15**, 4317.
[395] K. C. Nicolaou, R. Hughes, S. Y. Cho, N. Winssinger, C. Smethurst, H. Labischinski and R. Endermann, *Angew. Chem. Int. Ed.*, 2000, **39**, 3823.
[396] W. Zhang and J. S. Moore, *J. Am. Chem. Soc.*, 2005, **127**, 11863.
[397] D. A. Erlanson, A. C. Braisted, D. R. Raphael, M. Randal, R. M. Stroud, E. M. Gordon and J. A. Wells, *Proc. Natl. Acad. Sci. USA.*, 2000, **97**, 9367.
[398] D. A. Erlanson and S. K. Hansen, *Curr. Opin. Chem. Biol.*, 2004, **8**, 399.
[399] O. Ramström and J. -M. Lehn, *ChemBioChem.*, 2000, **1**, 41.
[400] I. K. H. Leung, T. Brown Jr, C. J. Schofield and T. D. W. Claridge, *Med. Chem. Commun.*, 2011, **2**, 390.
[401] M. Demetriades, I. K. H. Leung, R. Chowdhury, M. C. Chan, M. A. McDonough, K. K. Yeoh *et al.*, *Angew. Chem. Int. Ed.*, 2012, **51**, 6672.
[402] B. Fuchs, A. Nelson, A. Star, J. F. Stoddart and S. B. Vidal, *Angew. Chem. Int. Ed.*, 2003, **42**, 4220.
[403] A. Buryak and K. Severin, *Angew. Chem. Int. Ed.*, 2005, **44**, 7935.
[404] S. W. Tam-Chang, J. S. Stehouwer and J. S. Hao, *J. Org. Chem.*, 1999, **64**, 334.
[405] K. R. West, K. D. Bake and S. Otto, *Org. Lett.*, 2005, **7**, 2615.
[406] S. A. Poulsen, *J. Am. Soc. Mass Spectrom.*, 2006, **17**, 1074.
[407] E. C. Y. Woon, M. Demetriades, E. A. L. Bagg, W. Aik, S. M. Krylova, J. H. Y. Ma *et al.*, *J. Med. Chem.*, 2012, **55**, 2173.
[408] R. L. E. Furlan, G. R. L. Cousins and J. K. M. Sanders, *Chem. Commun.*, 2000, 1761.

[409] T. Bunyapaiboonsri, O. Ramström, S. Lohmann, J. -M. Lehn, L. Peng and M. Goeldner, ChemBioChem., 2001, **2**, 438.
[410] T. Bunyapaiboonsri, H. Ramström, O. Ramström, J. Haiech and J. -M. Lehn, *J. Med. Chem.*, 2003, **46**, 5803.
[411] K. C. Nicolaou, R. Hughes, S. Y. Cho, N. Winssinger, H. Labischin-ski and R. Endermann, *Chem. Eur. J.*, 2001, **7**, 3824.
[412] H. F. Gilbert, *J. Biol. Chem.*, 1997, **272**, 29399.
[413] H. F. Gilbert, *Methods Enzymol.*, 1995, **251**, 8.
[414] S. Zameo, B. Vauzeilles and J. -M. Beau, *Angew. Chem. Int. Ed.*, 2005, **44**, 965.
[415] M. G. Woll and S. H. Gellman, *J. Am. Chem. Soc.*, 2004, **126**, 11172.
[416] P. G. Swann, R. A. Casanova, A. Desai, M. M. Frauenhoff, M. Urbancic, U. Slomczynska *et al.*, *Biopolymers*, 1996, **40**, 617.
[417] R. J. Lins, S. L. Flitsch, N. J. Turner, E. Irving and S. A. Brown, *Angew. Chem. Int. Ed.*, 2002, **41**, 3405.
[418] R. J. Lins, S. L. Flitsch, N. J. Turner, E. Irving and S. A. Brown, *Tetrahedron*, 2004, **60**, 771.
[419] J. D. Cheeseman, A. D. Corbett, R. Shu, J. Croteau, J. L. Gleason and R. J. Kazlauskas, *J. Am. Chem. Soc.*, 2002, **124**, 5692.
[420] D. M. Livermore and N. Woodford, *Trends Microbiol.*, 2006, **14**, 413.
[421] S. M. Drawz and R. A. Bonomo, *Clin. Microbiol. Rev.*, 2010, **23**, 160.
[422] I. Massova and S. Mobashery, *Antimicrob. Agents Chemother.*, 1998, **42**, 1.
[423] K. M. Papp-Wallace, A. Endimiani, M. A. Taracila and R. A. Bonomo, *Antimicrob. Agents Chemother.*, 2011, **55**, 4943.
[424] J. F. Fisher, S. O. Meroueh and S. Mobashery, *Chem. Rev.*, 2005, **105**, 395.
[425] E. P. Abraham and E. Chain, *Rev. Infect. Dis.*, 1988, **10**, 677.
[426] K. Bush, *Antimicrob. Agents Chemother.*, 2018, **62**, e01076-18.
[427] C. Bebrone, Biochem. Pharmacol., 2007, **74**, 1686.
[428] I. Demuth and M. Digweed, *Mutat. Res.*, 1998, **409**, 11.
[429] R. P. Ambler, *Phil. Trans. R. Soc. Lond. B*, 1980, **289**, 321.
[430] K. Bush, G. A. Jacoby and A. A. Medeiros, *Antimicrob. Agents Chemother.*, 1995, **39**, 1211.
[431] K. Bush and G. A. Jacoby, *Antimicrob. Agents Chemother.*, 2010, **54**, 969.
[432] M. A. Yildirim, K. I. Goh, M. E. Cusick, A. L. Barabasi and M. Vidal, *Nat. Biotechnol.*, 2007, **25**, 1119.
[433] K. M. Papp-Wallace, S. A. Becka, M. A. Taracila, M. L. Winkler, J. A. Gatta, D. A. Rholl *et al.*, *Antimicrob. Agents Chemother.*, 2015, **60**, 777.
[434] S. J. Hecker, K. R. Reddy, M. Totrov, G. C. Hirst, O. Lomovskaya, D. C. Griffith *et al.*, *J. Med. Chem.*, 2015, **58**, 3682.
[435] J. Ruiz, *Emerg. Infect. Dis.*, 2018, **24**, 709.
[436] J. Heritage, F. H. M'Zali, D. Gascoyne-Binzi and P. M. Hawkey, *J. Antimicrob. Chemother.*, 1999, **44**, 309.
[437] F. Perez, A. Endimiani, K. M. Hujer and R. A. Bonomo, *Curr. Opin. Pharmacol.*, 2007, **7**, 459.
[438] D. L. Paterson and R. A. Bonomo, *Clin. Microbiol. Rev.*, 2005, **18**, 657.
[439] K. Bush, *Curr. Opin. Microbiol.*, 2010, **13**, 558.
[440] N. Q. Nguyen, N. P. Krishnan, L. J. Rojas, F. Prati, E. Caselli, C. Romagnoli *et al.*, *Antimicrob. Agents Chemother.*, 2016, **60**, 1760.
[441] F. Perez, N. G. El Chakhtoura, K. M. Papp-Wallace, B. M. Wilson and R. A. Bonomo, *Expert Opin. Pharmacother.*, 2016, **17**, 761.
[442] K. M. Papp-Wallace, M. L. Winkler, J. A. Gatta, M. A. Taracila, S. Chilakala, Y. Xu *et al.*, *Antimicrob. Agents Chemother.*, 2014, **58**, 4290.
[443] R. A. Bonomo and M. E. Tolmasky, *Enzyme-Mediated Resistance to Antibiotics – Mechanisms, Dissemination and Prospects for Inhibition*, ASM Press, Washington D.C., 2007.
[444] D. A. Leonard, R. A. Bonomo and R. A. Powers, *Acc. Chem. Res.*, 2013, **46**, 2407.
[445] D. Girlich, T. Naas and P. Nordmann, *Antimicrob. Agents Chemother.*, 2004, **48**, 4217.
[446] V. Stojanoski, D. -C. Chow, B. Fryszczyn, L. Hu, P. Nordmann, L. Poirel *et al.*, *Biochemistry*, 2015, **54**, 3370.
[447] L. Poirel, P. Gerome, C. De Champs, J. Stephanazzi, T. Naas and P. Nordmann, *Antimicrob. Agents Chemother.*, 2002, **46**, 566.
[448] T. R. Walsh, J. Weeks, D. M. Livermore and M. A. Toleman, *Lancet Infect. Dis.*, 2011, **11**, 355.

[449] M. M. Sfeir, J. A. Hayden, K. A. Fauntleroy, C. Mazur, J. K. Johnson, P. J. Simner *et al.*, *J. Clin. Microbiol.*, 2019, **57**, e01757-18.
[450] S. J. S. Flora and V. Pachauri, *Int. J. Environ. Res. Public Health*, 2010, **7**, 2745.
[451] M. A. Adam and W. I. Elhag, *BMC Infect. Dis.*, 2018, **18**, 668.
[452] K. K. Kumarasamy, M. A. Toleman, T. R. Walsh, J. Bagaria, F. Butt, R. Balakrishnan *et al.*, *Lancet Infect. Dis.*, 2010, **10**, 597.
[453] D. Yong, M. A. Toleman, C. G. Giske, H. S. Cho, K. Sundman, K. Lee and T. R. Walsh, *Antimicrob. Agents Chemother.*, 2009, **53**, 5046.
[454] D. T. King, L. J. Worrall, R. Gruninger and N. C. Strynadka, *J. Am. Chem. Soc.*, 2012, **134**, 11362.
[455] P. Nordmann, L. Poirel, T. R. Walsh and D. M. Livermore, *Trends Microbiol.*, 2011, **19**, 588.
[456] M. F. Mojica, R. A. Bonomo and W. Fast, *Curr. Drug Targets*, 2015, **17**, 1029.
[457] F. M. Silva, M. S. Carmo, S. Silbert and A. C. Gales, *Microb. Drug Resist.*, 2011, **17**, 215.
[458] A. F. Wendel, S. Meyer, R. Deenen, K. Köhrer, S. Kolbe-Busch, K. Pfeffer *et al.*, *Microb. Drug Resist.*, 2018, **24**, 1305.
[459] K. Lee, J. H. Yum, D. Yong, H. M. Lee, H. D. Kim, J. -D. Docquier *et al.*, *Antimicrob. Agents Chemother.*, 2005, **49**, 4485.
[460] J. I. Sekiguchi, K. Morita, T. Kitao, N. Watanabe, M. Okazaki, T. Miyoshi-Akiyama *et al.*, *Antimicrob. Agents Chemother.*, 2008, **52**, 4194.
[461] J. -i. Wachino, H. Yoshida, K. Yamane, S. Suzuki, M. Matsui, T. Yamagishi *et al.*, *Antimicrob. Agents Chemother.*, 2011, **55**, 5143.
[462] L. Poirel, J. -M. Rodríguez-Martínez, N. Al Naiemi, Y. J. Debets-Ossenkopp and P. Nordmann, *Antimicrob. Agents Chemother.*, 2010, **54**, 2420.
[463] A. El Salabi, P. Saradhi Borra, M. A. Toleman, Ø. Samuelsen and T. R. Walsh, *Antimicrob. Agents Chemother.*, 2012, **56**, 2241.
[464] S. Pollini, S. Maradei, P. Pecile, G. Olivo, F. Luzzaro, J. -D. Docquier and G. M. Rossolini, *Antimicrob. Agents Chemother.*, 2013, **57**, 410.
[465] B. M. R. Liénard, R. Hüting, P. Lassaux, M. Galleni, J. -M. Frère and C. J. Schofield, *J. Med. Chem.*, 2008, **51**, 684.
[466] A. Bandyopadhyay, S. Cambray and J. Gao, *Chem. Sci.*, 2016, **7**, 4589.
[467] D. R. Lide, *Handbook of Chemistry and Physics*, CRC Press, Boca Raton, Florida, 1991.
[468] J. Baldwin, *Rules for Ring Closure*, Ciba Foundation Symposium 53, *Further Perspectives in Organic Chemistry*, Elsevier, New York, 1978.
[469] F. A. L. Anet, *Top. Curr. Chem.*, 1974, **45**, 169.
[470] Sandoz - DE2750878, *Chem. Abstr.*, 1978, **89**, 109937.
[471] M. A. Grassberger, F. Turnowsky and J. Hildebrandt, *J. Med. Chem.*, 1984, **27**, 947.
[472] D. Kanichar, L. Roppiyakuda, E. Kosmowska, M. A. Faust, K. P. Tran, F. Chow *et al.*, *Chem. Biodivers.*, 2014, **11**, 1381.
[473] Y. Sohma, B. L. Pentelute, J. Whittaker, Q. -X. Hua, L. J. Whittaker, M. A. Weiss and S. B. H. Kent, *Angew. Chem. Int. Ed.*, 2008, **47**, 1102.
[474] D. Bang and S. B. H. Kent, *Angew. Chem. Int. Ed.*, 2004, **43**, 2534.
[475] P. Thapa, R. Zhang, V. Menon and J. P. Bingham, *Molecules*, 2014, **19**, 14461.
[476] R. Nurdinov, É. É. Liepin'sh, I. B. Mazheika, I. Ya. Kalvin'sh, *Chem. Heterocycl. Compd.*, 1993, **29**, 1093.
[477] *L-Thiaproline*, fluorochem.co.uk http://www.fluorochem.co.uk/Products/Product?code=036413 (accessed: 06/09/20).
[478] *(S)-1,3-Thiazinane-4-carboxylic acid*, reaxys.emolecules.com https://reaxys.emolecules.com/cgi-bin/rene/show_hitlist.cgi?h=533806405 (accessed: 06/09/20).
[479] *L-Homocysteine*, sigmaaldrich.com https://www.sigmaaldrich.com/catalog/product/sigma/69453?lang=en&region=GB (accessed: 06/09/20).
[480] *D/L-Homocysteine thiolactone hydrochloride*, fluorochem.co.uk http://www.fluorochem.co.uk/Products/Product?code=242934 (accessed: 06/09/20).
[481] H. M. Kolenbrander, *Can. J. Chem.*, 1969, **47**, 3271.
[482] S. Bräse, J. Köbberling, D. Enders, R. Lazny and M. Wang, *Tetrahedron Lett.*, 1999, **40**, 2105.

[483] S. Dahmen and S. Bräse, *Angew. Chem. Int. Ed.*, 2000, **39**, 3681.
[484] P. J. H. Scott, *Linker Strategies in Solid-Phase Organic Synthesis*, John Wiley & Sons, Weinheim, 2009.
[485] J. E. Baldwin, *J. Chem. Soc. Chem. Commun.*, 1976, 734.
[486] F. A. L. Anet and J. J. Wagner, *J. Am. Chem. Soc.*, 1971, **93**, 5266.
[487] F. A. L. Anet and J. Krane, *Isr. J. Chem.* 1980, **20**, 72.
[488] R. A. Holton, C. Somoza, H. Baik Kim, F. Liang, R. J. Biediger, P. D. Boatman *et al.*, *J. Am. Chem. Soc.*, 1994, **116**, 1597.
[489] M. Dong, B. Cong, S. -H. Yu, F. Sauriol, C. -H. Huo, Q. -W. Shi *et al.*, *Org. Lett.*, 2008, **10**, 701.
[490] J. Marrero, A. D. Rodríguez, P. Baran, R. G. Raptis, J. A. Sánchez, E. Ortega-Barria and T. L. Capson, *Org. Lett.*, 2004, **6**, 1661.
[491] J. T. J. Spence and J. H. George, *Org. Lett.*, 2011, **13**, 5318.
[492] R. Morphy and Z. Rankovic, *J. Med. Chem.*, 2005, **48**, 6523.
[493] M. -K. Hu, L. -J. Wu, G. Hsiao and M. -H. Yen, *J. Med. Chem.*, 2002, **45**, 2277.
[494] J. J. Baldwin, W. C. Lumma, G. F. Lundell, G. S. Ponticello, A. W. Raab, E. L. Engelhardt *et al.*, *J. Med. Chem.*, 1979, **22**, 1284.
[495] V. Cecchetti, A. Fravolini, F. Schiaffella, O. Tabarrini, G. Bruni and G. Segre, *J. Med. Chem.*, 1993, **36**, 157.
[496] N. Murugesan, Z. Gu, L. Fandis, J. E. Tellew, R. A. Baska, Y. Yang *et al.*, *J. Med. Chem.*, 2005, **48**, 171.
[497] J. J. Piwinski, J. K. Wong, M. J. Green, A. K. Ganguly, M. M. Billah, R. E. West *et al.*, *J. Med. Chem.*, 1991, **34**, 457.
[498] R. E. Mewshaw, L. S. Silverman, R. M. Mathew, C. Kaiser, R. G. Sherrill, M. Cheng *et al.*, *J. Med. Chem.*, 1993, **36**, 1488.
[499] A. Buschauer, *J. Med. Chem.*, 1989, **32**, 1963.
[500] N. C. Inestrosa, A. Alvarez, C. A. Pérez, R. D. Moreno, M. Vicente, C. Linker *et al.*, *Neuron*, 1996, **16**, 881.
[501] C. J. Van der Schyf, W. J. Geldenhuys and M. B. H. Youdim, *J. Neurochem.*, 2006, **99**, 1033.
[502] H. Kogen, N. Toda, K. Tago, S. Marumoto, K. Takami, M. Ori *et al.*, *Org. Lett.*, 2002, **4**, 3359.
[503] N. Toda, K. Tago, S. Marumoto, K. Takami, M. Ori, N. Yamada *et al.*, *Bioorg. Med. Chem.*, 2003, **11**, 1935.
[504] R. Soyka, A. Heckel, J. Nickl, W. Eisert, T. H. Muller and H. Weisenberger, *J. Med. Chem.*, 1994, **37**, 26.
[505] Q. Wang, X. -F. Wang, Y. -Y. Jiang, Z. -G. Li, N. Cai, W. -Q. Guan *et al.*, *Sci. Rep.*, 2019, **9**: 19243.
[506] N. N. T. Goemaere, K. Grijm, P. T. W. van Hal and M. A. den Bakker, *J. Med. Case Rep.*, 2008, **2**, 169.
[507] A. Huttner, E. M. Verhaegh, S. Harbarth, A. E. Muller, U. Theuretzbacher and J. W. Mouton, *J. Antimicrob. Chemother.*, 2015, **70**, 2456.
[508] B. H. C. Stricker, A. P. R. Blok, F. H. J. Claas, G. E. van Parys and V. J. Desmet, *Hepatology*, 1988, **8**, 599.
[509] I. L. Tan, M. J. Polydefkis, G. J. Ebenezer, P. Hauer and J. C. McArthur, *Arch. Neurol.*, 2012, **69**, 265.
[510] D. W. Bryant, D. R. McCalla, M. Leeksma and P. Laneuville, *Can. J. Microbiol.*, 1981, **27**, 81.
[511] E. Perez-Reyes, B. Kalyanaraman and R. P. Mason, *Mol. Pharmacol.*, 1980, **17**, 239.
[512] D. I. Edwards, *J. Antimicrob. Chemother.*, 1993, **31**, 9.
[513] F. J. Peterson, R. P. Mason, J. Hovsepian and J. L. Holtzman, *J. Biol. Chem.*, 1979, **254**, 4009.
[514] D. W. Henry, V. H. Brown, M. Cory and J. G. Johansson, *J. Med. Chem.*, 1973, **16**, 1287.
[515] J. Brem, T. Panduwawala, J. Ulf Hanse, J. Hewitt, E. Liepins, P. Donets *et al.*, *Nat. Chem.*, 2022, **14**, 15.
[516] B. C. Laguzza, C. L. Nichols, S. L. Briggs, G. J. Cullinan, D. A. Johnson, J. J. Starling *et al*, *J. Med. Chem.*, 1989, **32**, 548.
[517] P. R. Hamann, L. M. Hinman, I. Hollander, C. F. Beyer, D. Lindh, R. Holcomb *et al*., *Bioconjugate Chem.*, 2002, **13**, 47.
[518] L. L. Hamm, N. Nakhoul and K. S. Hering-Smith, *Clin. J. Am. Soc. Nephrol.*, 2015, **10**, 2232.
[519] G. H. Diering and M. Numata, *Front. Physiol.*, 2013, **4**, 412.
[520] A. Sharma, Y. Kawarabayasi and T. Satyanarayana, *Extremophiles*, 2012, **16**, 1.
[521] L. Preiss, D. B. Hicks, S. Suzuki, T. Meier and T. A. Krulwich, *Front. Bioeng. Biotechnol.*, 2015, **3**:75.
[522] P. Lund, A. Tramonti and D. De Biase, *FEMS Microbiol. Rev.*, 2015, **38**, 1091.
[523] J. D. Kendall, G. W. Rewcastle, R. Frederic, C. Mawson, W. A. Denny, E. S. Marshall *et al.*, *Bioorg. Med. Chem.*, 2007, **15**, 7677.
[524] H. A. Abdel-Aziz and A. A. Mekawey, *Eur. J. Med. Chem.*, 2009, **44**, 4985.

[525] A. Kamal, S. K. Ahmed, K. S. Reddy, M. N. Khan, R. V. Shetty, B. Siddhardha *et al.*, *Bioorg. Med. Chem. Lett.*, 2007, **17**, 5419.
[526] A. Dizdarević, N. A. Efiana, T. N. Q. Phan, B. Matuszczak and A. Bernkop-Schnürch, *Eur. J. Pharm. Biopharm.*, 2019, **142**, 92.
[527] R. Hull, *GB816886 (A)*, Imp. Chem. Ind., Imp. Chem. House, Millbank, London, SW1, 1959.
[528] W Guerra, A. P. S. Fontes, M. V. D. Almeida and H. Silva, *Quim. Nova*, 2005, **28**, 809.
[529] V. G. Dudarev, O. M. Tikhomirova and A. A. Iozep, *Pharm. Chem. J.*, 2013, **47**, 31.
[530] H. Li, Z. Zhang, X. Yang, X. Mao, Y. Wang, J. Wang *et al.*, *Chem. Res. Toxicol.*, 2019, **32**, 681.
[531] H. L. Le Châtelier, *Ann. Mines*, 1888, **13**, 157.
[532] H. N. Nguyen, J. A. Chenoweth, V. S. Bebarta, T. E. Albertson and C. D. Nowadly, *Mil. Med.*, 2021, **186**, e319.
[533] J. D. Clark, *Ignition! An Informal History of Liquid Rocket Propellants*, Rutgers University Press, New Brunswick, New Jersey, 1972.
[534] https://www.heart.co.uk/london/news/local/chemical-spill-ucl/ (assessed 31/08/21).
[535] S. Wu, W. Sun, J. Chen, J. Zhao, Q. Cao, W. Fang and Q. Zhao, *J. Catal.*, 2019, **377**, 110.
[536] L. Han, P. Xing and B. Jiang, *Org. Lett.*, 2014, **16**, 3428.
[537] *(5-nitrofuran-2-yl)methanamine hydrochloride*, https://www.enaminestore.com/catalog/EN300-64528 (accessed 09/09/21).
[538] A. E. Derome, *Modern NMR Techniques*, Pergamon, Oxford, 1987.
[539] J. G. Aston, S. C. Schumann, H. L. Fink and P. M. Doty, *J. Am. Chem. Soc.*, 1941, **63**, 2029.
[540] K. S. Pitzer and W. E. Donath, *J. Am. Chem. Soc.*, 1959, **81**, 3213.
[541] J. E. Kilpatrick, K. S. Pitzer and R. Spitzer, *J. Am. Chem. Soc.*, 1947, **69**, 2483.
[542] G. M. Kellie and F. G. Riddell, *Top. Stereochem.*, 1974, **8**, 225.
[543] J. D. Cox and G. Pilcher, *Thermochemistry of Organic and Organometallic Compounds*, Academic, New York, 1970.
[544] K. B. Wiberg, G. Bonneville and R. Dempsey, *Isr. J. Chem.*, 1983, **23**, 85.
[545] K. B. Wiberg, F. H. Walker, W. E. Pratt and J. Michl, *J. Am. Chem. Soc.*, 1983, **105**, 3638.
[546] B. Fuchs, *Top. Stereochem.*, 1978, **10**, 1.
[547] F. G. Riddell, *The Conformational Analysis of Heterocyclic Compounds*, Academic, New York, 1980.
[548] R. W. Pridmore, *Col. Res. Appl.*, 2009, **34**, 233.
[549] P. Nayler and M. C. Whiting, *J. Chem. Soc.*, 1955, 3037.
[550] A. Capperucci, A. Degl'Innocenti, P. Dondoli, T. Nocentini, G. Reginato and A. Ricci, *Tetrahedron*, 2001, **57**, 6267.
[551] *Bicyclo[5.3.0]decapentaene*, Merck Specification Sheet https://www.sigmaaldrich.com/GB/en/specification-sheet/ALDRICH/A97203 (accessed 20/09/21).
[552] J. F. Pfanstiel and D. W. Pratt, *J. Phys. Chem. A*, 1999, **103**, 2337.
[553] R. Kuhn and C. Grundmann., *Ber. Dtsch. Chem. Ges.*, 1938, **71**, 442.
[554] R. B. Woodward, *J. Am. Chem. Soc.*, 1942, **64**, 72.
[555] D. J. Griffiths and D. F. Schroeter, *Introduction to Quantum Mechanics*, Cambridge University Press, Cambridge, 2018.
[556] M. Sozzi, *Discrete Symmetries and CP Violation – From Experiment to Theory*, Oxford University Press, Oxford, 2012.
[557] R. M. Wilcox, *J. Math. Phys.*, 1967, **8**, 962.
[558] P. W. Atkins and R. Friedman, *Molecular Quantum Mechanics*, Oxford University Press, Oxford, 2011.
[559] G. Cassinelli and P. Lahti, *Phil. Trans. R. Soc. A*, 2017, **375**: 20160393.
[560] H. A. Buchdahl, *Am. J. Phys.*, 1962, **30**, 829.
[561] Flavoxanthin, *Merck Index Online*, 11th Edition, **4032**.
[562] M. Frings, C. Bolm, A. Blum and C. Gnamm, *Eur. J. Med. Chem.*, 2017, **126**, 225.
[563] J. A. Sirvent and U. Lücking, *Chem. Med. Chem.*, 2017, **12**, 487.
[564] H. R. Bentley, E. E. McDermott, J. Pace, J. K. Whitehead and T. Moran, *Nature*, 1949, **163**, 675.
[565] M. Langner and C. Bolm, *Angew. Chem. Int. Ed.*, 2004, **43**, 5984.
[566] Y. Cheng, W. Dong, K. Parthasarathy and C. Bolm, *Org. Lett.*, 2017, **19**, 726.

[567] C. Gnamm, A. Jeanguenat, A. C. Dutton, C. Grimm, D. P. Kloer and A. Crossthwaite, *J. Bioorg. Med. Chem. Lett.*, 2012, **22**, 3800.
[568] U. Lücking, *Angew. Chem. Int. Ed.*, 2013, **52**, 9399.
[569] V. Bizet, C. M. M. Hendriks and C. Bolm, *Chem. Soc. Rev.*, 2015, **44**, 3378.
[570] J. A. Sirvent, D. Bierer, R. Webster and U. Lücking, *Synthesis*, 2017, **49**, 1024.
[571] M. Zenzola, R. Doran, L. Degennaro, R. Luisi and J. A. Bull, *Angew. Chem. Int. Ed.*, 2016, **55**, 7203.
[572] A. Yoshimura and V. V. Zhdankin, *Chem. Rev.*, 2016, **116**, 3328.
[573] A. H. Sandtorv and D. R. Stuart, *Angew. Chem. Int. Ed.*, 2016, **55**, 15812.
[574] E. Rattanangkool, W. Krailat, T. Vilaivan, P. Phuwapraisirisan, M. Sukwattanasinitt and S. Wacharasindhu, *Eur. J. Org. Chem.*, 2014, 4795.
[575] T. Ishiyama, M. Murata and N. Miyaura, *J. Org. Chem.*, 1995, **60**, 7508.
[576] P. A. Cox, A. G. Leach, A. D. Campbell and G. C. Lloyd-Jones, *J. Am. Chem. Soc.*, 2016, **138**, 9145.
[577] P. A. Cox, M. Reid, A. G. Leach, A. D. Campbell, E. J. King and G. C. Lloyd-Jones, *J. Am. Chem. Soc.*, 2017, **139**, 13156.
[578] S. L. Buchwald, *Oxford Synthesis Summer Conference*, Dyson Perrins Laboratory, England, June 2018.
[579] D. Prasannan, D. Raghav, S. Sujatha, H. H. kumar, K. Rathinasamy and C. Arunkumar, *RSC Adv.*, 2016, **6**, 80808.
[580] D. Zahavi, *Husserl's Phenomenology*, Stanford University Press, Stanford, 2003.
[581] J. M. Berg, J. L. Tymoczko, L. Stryer and G. J. Gatto Jr., *Biochemistry*, W. H. Freeman & Company, Basinstoke, England, 2012.
[582] C. Wong, *Science*, 1989, **244**, 1145.
[583] L. Zhu and M. C. Tedford, *Tetrahedron*, 1990, **46**, 6587.
[584] S. A. Arrhenius, *Z. Phys. Chem.*, 1889, **4**, 96.
[585] M. Ohno and M. Otsuka, *Org. React.*, 1989, **37**, 1.
[586] D. J. Newman and G. M. Cragg, *J. Nat. Prod.*, 2016, **79**, 629.
[587] M. A. Lampe, A. L. Burlingame, J. Whitney, M. L. Williams, B. E. Brown, E. Roitman and M. Elias, *J. Lipid Res.*, 1983, **24**, 120.
[588] Y. B. Ali, R. Verger and A. Abousalham, *Methods Mol. Biol.*, 2012, **861**, 31.
[589] W. Baker and J. F. W. McOmie, *Chem. Ber.*, 1959, **92**, XXXVII.
[590] H. Finkelstein, *Ber. Dtsch. Chem. Ges.*, 1910, **43**, 1528.
[591] S. Mattsson, M. Dahlström and S. Karlsson, *Tetrahedron Lett.*, 2007, **48**, 2497.
[592] K. Matange, J. M. Tuck and A. J. Keung, *Nat. Commun.*, 2021, **12**, 1358.
[593] C. M. Croce, *N. Engl. J. Med.*, 2008, **358**, 502.
[594] U. Weininger, K. Modig, H. Ishida, H. J. Vogel and M. Akke, *J. Phys. Chem. B*, 2019, **123**, 9742.
[595] L. Čechová, E. Procházková, I. Císařová, M. Dračínský and Z. Janeba, *Chem. Commun.*, 2014, **50**, 14892.
[596] F. F.-L. Ho, *J. Polym. Sci. B*, 1971, **9**, 491.
[597] C. C. Hinckley, *Nature*, 1972, **240**, 385.
[598] R. von Ammon and R. D. Fischer, *Angew. Chem. Int. Ed.*, 1972, **11**, 675.
[599] J. K. M. Sanders and D. H. Williams, *Chem. Commun.*, 1972, 436.
[600] K. Nakanishi and J. Dillon, *J. Am. Chem. Soc.*, 1971, **93**, 4058.
[601] K. Nakanishi, D. A. Schooley, M. Koreeda and J. Dillon, *Chem. Commun.*, 1971, 1235.
[602] C. P. Case and C. R. Cyr, *J. Am. Chem. Soc.*, 1971, **93**, 1280.
[603] E. Vedejs and M. F. Salomon, *J. Am. Chern. Soc.*, 1970, **92**, 6965.
[604] J. L. Greene and P. B. Shevlin, *Chem. Commun.*, 1971, 1092.
[605] R. J. P. Williams, *Quart. Rev.*, 1970, **24**, 331.
[606] G. E. Smolka, E. R. Birnbaum and D. W. Darnall, *Biochemistry*, 1971, **10**, 4556.
[607] C. D. Barry, A. C. T. North, J. A. Glasel, R. J. P. Williams and A. V. Xavier, *Nature*, 1971, **232**, 236.
[608] B. Birdsall, J. Feeney, J. A. Glasel, R. J. P. Williams and A. V. Xavier, Chem. Commun., 1971, 1473.
[609] V. F. Bystrov, N. I. Dubrovina, L. I. Barsukov and L. D. Bergelsor, *Chem. Phys. Lipids*, 1971, **6**, 343.
[610] A. S. Mildvan and M. Cohn, *Adv. Enzymol.*, 1970, **33**, 1.
[611] J. Dziemidowicz, D. Witt, M. Sliwka-Kaszynska and J. Rachon, *Synthesis*, 2005, **4**, 569.
[612] M. Nishizawa, H. Yamamoto, K. Seo, H. Imagawa and T. Sugihara, *Org. Lett.*, 2002, **4**, 1947.

[613] K. C. Nicolaou, A. A. Estrada, M. Zak, S. H. Lee and B. S. Safina, *Angew. Chem. Int. Ed.*, 2005, **44**, 1378.
[614] P. S. Manchand, *J. Chem. Soc. D*, 1971, 667.
[615] W. Gerrard and M. F. Lappert, *Chem. Rev.*, 1958, **58**, 1081.
[616] R. Gomez-Bombarelli, E. Calle and J. Casado, *J. Org. Chem.*, 2013, **78**, 6880.
[617] Z. Wang and H. Ma, *Molecules*, 2021, **26**, 3519.
[618] K. Ikeuchi, K. Murasawa, K. Ohara and H. Yamada, *Org. Lett.*, 2019, **21**, 6638.
[619] B. H. Lipshutz and J. J. Pegram, *Tetrahedron Lett.*, 1980, **21**, 3343.
[620] S. J. Kim, C. Lester and T. P. Begley, *J. Org. Chem.*, 1995, **60**, 6256.
[621] A. Vakalopoulos and H. M. R. Hoffmann, *Org. Lett.*, 2000, **2**, 1447.
[622] S. P. Govek and L. E. Overman, *J. Am. Chem. Soc.*, 2001, **123**, 9468.
[623] K. W. Knouse and W. M. Wuest, *J. Antibiot.*, 2016, **69**, 337.
[624] R. N. Nair and T. D. Bannister, *Org. Process Res. Dev.*, 2016, **20**, 1370.
[625] J. B. Hendrickson, *J. Am. Chem. Soc.*, 1975, **97**, 5784.
[626] M. Othus, F. R. Appelbaum, S. H. Petersdorf, K. J. Kopecky, M. Slovak, T. Nevill *et al.*, *Biol. Blood Marrow Transplant*, 2015, **21**, 559.
[627] Y. N. Lamb, *Drugs*, 2017, **77**, 1603.
[628] D. E. Koshland, *Proc. Natl. Acad. Sci. U.S.A.*, 1958, **44**, 98.
[629] C. Bissantz, B. Kuhn and M. Stahl, *J. Med. Chem.*, 2010, **53**, 5061.
[630] R. F. Heck, *J. Am. Chem. Soc.*, 1968, **90**, 5526.
[631] *The Nobel Prize in Chemistry 2010*, nobelprize.org https://www.nobelprize.org/prizes/chemistry/2010/summary/ (accessed 04/12/21)

Table of Contents

Materials and Instruments S1

General Procedure for Synthesis of Boronic Acid & Ester Heterocycles S3

1-Hydroxybenzo[*d*][1,2,3]diazaborinine-2(1*H*)-carboxamide (1) S4

1-Hydroxy-4-methylbenzo[*d*][1,2,3]diazaborinine-2(1*H*)-carboxamide (2) S5

Benzo[*d*][1,2,3]diazaborinin-1(*2H*)-ol (3) S6

8*H*-benzo[4,5][1,2,3]diazaborinino[3,2-*b*]benzo[4,5][1,2,3]diazaborinino[2,3-e][1,3,5,2,6]oxadiazadiborinin-8-one (4) S7

5,11-Dimethyl-8*H*-benzo[4,5][1,2,3]diazaborinino[3,2-*b*]benzo[4,5][1,2,3]diazaborinino[2,3-e][1,3,5,2,6]oxadiazadiborinin-8-one (5) S8

1-Hydroxythieno[3,2-*d*][1,2,3]diazaborinine-2(1*H*)-carboxamide (6) S9

1-Hydroxy-4-methylthieno[3,2-*d*][1,2,3]diazaborinine-2(1*H*)-carboxamide (7) S10

1-Hydroxythieno[2,3-*d*][1,2,3]diazaborinine-2(1*H*)-carboxamide (8) S11

1-Hydroxybenzo[*d*][1,2,3]diazaborinine-2(1*H*)-carbothioamide (9) S12

1-Hydroxy-4-methylbenzo[*d*][1,2,3]diazaborinine-2(1*H*)-carbothioamide (10) S13

(2a*S*)-4a-Hydroxy-2,2a,4a,8b-tetrahydro-3*H*-4-oxa-1-thia-2a^1-aza-4aλ^4-borapentaleno[1,6-*ab*]inden-3-one (11) S14

(2a*R*)-4a-Hydroxy-2,2a,4a,8b-tetrahydro-3*H*-4-oxa-1-thia-2a^1-aza-4aλ^4-borapentaleno[1,6-*ab*]inden-3-one(12) S15

(2a*R*)-4a-Hydroxy-2,2-dimethyl-2,2a,4a,8b-tetrahydro-3*H*-4-oxa-1-thia-2a^1-aza-4aλ^4-borapentaleno[1,6-*ab*]inden-3-one (13) S16

(2aS)-4a-Hydroxy-2,2-dimethyl-2,2a,4a,8b-tetrahydro-3H-4-oxa-1-thia-2a^1-aza-4aλ^4-borapentaleno[1,6-*ab*]inden-3-one (14) S17

(2a*S*)-4a-Hydroxy-8b-methyl-2,2a,4a,8b-tetrahydro-3*H*-4-oxa-1-thia-2a^1-aza-4aλ^4-borapentaleno[1,6-*ab*]inden-3-one (15) S18

(2a*R*)-4a-Hydroxy-8b-methyl-2,2a,4a,8b-tetrahydro-3*H*-4-oxa-1-thia-2a^1-aza-4aλ^4-borapentaleno[1,6-*ab*]inden-3-one (16) S19

(2a*S*)-4a-Hydroxy-2,2,8b-trimethyl-2,2a,4a,8b-tetrahydro-3*H*-4-oxa-1-thia-2a^1-aza-4aλ^4-borapentaleno[1,6-*ab*]inden-3-one (17) S20

(2a*R*)-4a-Hydroxy-2,2,8b-trimethyl-2,2a,4a,8b-tetrahydro-3*H*-4-oxa-1-thia-2a^{1}-aza-4aλ^{4}-borapentaleno[1,6-*ab*]inden-3-one (18) S21

(*E*)-2-(Thiophen-3-ylmethylene)hydrazine-1-carboxamide (19) S22

Propane-1-sulfonohydrazide (20) S23

6-Methylthieno[3,2-*d*][1,2,3]diazaborinin-1(2*H*)-ol (21) S24

(*E*)-*N*′-((5-Methylthiophen-2-yl)methylene)propane-1-sulfonohydrazide (22) S25

6-Methyl-2-(propylsulfonyl)thieno[3,2-*d*][1,2,3]diazaborinin-1(2*H*)-ol (23) S26

Methyl (*R*)-thiazolidine-4-carboxylate (24) S27

(*S*)-Thiazolidine-4-carboxylic acid (25) S28

Methyl (*S*)-thiazolidine-4-carboxylate (26) S29

L-Cysteine (27) S30

(*R*)-Thiazolidine-4-carbohydrazide (28) S31

(*R*)-*N*′-[(*R*)-Thiazolidine-4-carbonyl]thiazolidine-4-carbohydrazide (29) S32

(*R*)-*N*′-(L-Cysteinyl)-2-amino-3-mercaptopropanehydrazide (30) S33

D,L-Homocysteine (31) S34

1,3-Thiazinane-4-carboxylic acid (32) S35

Methyl-1,3-thiazinane-4-carboxylate (33) S36

1,3-Thiazinane-4-carbohydrazide (34) S37

N′-(1,3-Thiazinane-4-carbonyl)-1,3-thiazinane-4-carbohydrazide (35) S38

2-Amino-*N*′-homocysteinyl-4-mercaptobutanehydrazide (36) S39

(7a*R*,7'a*R*)-Tetrahydro-3*H*,3'*H*,5*H*,5'*H*,7*H*,7'*H*-[6,6'-biimidazo[1,5-*c*]thiazole]-7,7'-dione (37) S40

(*E*)-(5-Nitrofuran-2-yl)methylene hydrazine (44) S41

5-Nitrofuran-2-yl methanamine (47) S42

Methyl (2-chlorophenyl)methanesulfonimidate (50) S43

1,2-Bis(2-chlorobenzyl)disulfane (51) S44

Benzenesulfonimidic acid (53) S45

(*E*)-1-(4-Bromophenyl)-*N*′-5-nitrofuran-2-yl methylene methanesulfonohydrazide (54) S46

Ethyl 7-isopropyl-1*H*-indole-2-carboxylate (56) S47

Ethyl 3-bromo-7-isopropyl-1*H*-indole-2-carboxylate (61) S50

Ethyl (*E*)-7-isopropyl-3-[2-((5-nitrofuran-2-yl)methylene)hydrazineyl]-1*H*-indole-2-carboxylate (60) S51

3-Iodo-7-isopropyl-1*H*-indole-2-carboxylic acid (64) S53

Heptyl 1*H*-indole-2-carboxylate (66) S54

Methyl 7-isopropyl-1*H*-indole-2-carboxylate (67) S55

Methyl 3-bromo-7-isopropyl-1*H*-indole-2-carboxylate (68) S56

Methyl (*E*)-7-isopropyl-3-[2-((5-nitrofuran-2-yl)methylene)hydrazineyl]-1*H*-indole-2-carboxylate (69) S57

(*E*)-7-Isopropyl-3-[2-((5-nitrofuran-2-yl)methylene]hydrazineyl)-1*H*-indole-2-carboxylic acid (63) S58

3-Hydrazineyl-7-isopropyl-1*H*-indole-2-carboxylic acid (70) S60

3-Bromo-7-isopropyl-1*H*-indole-2-carboxylic acid (71) S61

4-Methoxybenzyl 3-bromo-7-isopropyl-1-(4-methoxybenzyl)-1*H*-indole-2-carboxylate (72) S62

[2-(Trimethylsilyl)ethoxy]methyl 2-oxopropanoate (73) S63

2-(4-Bromophenyl)-1,3-dioxolane (75) S64

Ethyl 3-[4-(1,3-dioxolan-2-yl)phenyl]-7-isopropyl-1*H*-indole-2-carboxylate (76) S65

3-(4-Formylphenyl)-7-isopropyl-1*H*-indole-2-carboxylic acid (77) S66

7-Isopropyl-3-[4-((*E*)-(((*E*)-(5-nitrofuran-2-yl)methylene)hydrazineylidene)methyl)phenyl]-1*H*-indole-2-carboxylic acid (78) S67

5-Nitro-*N'*-(5-nitrofuran-2-carbonyl)furan-2-carbohydrazide (80), (81) & (82) S68

Methyl 5-nitrofuran-2-carboxylate (83) S69

5-Nitrofuran-2-carbohydrazide (79) S70

Methyl 3-iodo-7-isopropyl-1*H*-indole-2-carboxylate (84) S71

Methyl 3-(3-fluoro-4-formylphenyl)-7-isopropyl-1*H*-indole-2-carboxylate (85) S72

3-(3-Fluoro-4-formylphenyl)-7-isopropyl-1*H*-indole-2-carboxylic acid (86) S73

(*E*)-3-(3-Fluoro-4-[(2-(5-nitrofuran-2-carbonyl)hydrazineylidene)methyl)phenyl]-7-isopropyl-1*H*-indole-2-carboxylic acid (87) S74

Ethyl 7-acetyl-1*H*-indole-2-carboxylate (88) S75

Ethyl 7-[(*E*)-1-(((*E*)-(5-nitrofuran-2-yl)methylene)hydrazineylidene)ethyl]-1*H*-indole-2-carboxylate (89) ... S76

7-Acetyl-1*H*-indole-2-carboxylic acid (91) S77

7-[(*E*)-1-(((*E*)-(5-nitrofuran-2-yl)methylene)hydrazineylidene)ethyl]-1*H*-indole-2-carboxylic acid (92) S78

(*E*)-[5-((2-carbamoylhydrazineylidene)methyl)furan-2-yl]boronic acid (93) S79

Experimental

Materials and Instruments

All reagents and solvents used in the experiments were of reagent grade quality. They were obtained from commercial sources and used without further purification, unless otherwise stated. Diethyl ether herein is referred to as ether.

2-FBPA, 2-APBA (purity: *ca.* 95.0+%) and sodium phosphate monobasic (*purum* p.a., anhydrous, >99.0%) were purchased from Sigma-Aldrich® Chemical Co. Semicarbazide hydrochloride (purity: *ca.* 99.0%) was purchased from *A*lfa *A*esar®. TCEP·HCl (purity: *ca.* 98.0%) was purchased from ACROS ORGANICS. HATU was purchased from **Nova**biochem®. Deionised water was obtained from Millipede Milli-Q EDM Water Purification A10 or used straight from Winchester bottles containing HPLC-grade water.

High performance liquid chromatography – mass spectrometry (LC-MS) analyses were performed using an Agilent UPLC SQD instrument equipped with a Chromolith®, C_{18}, 2.1 × 50 mm column. The eluent was made up of a mobile phase of 0.1% formic acid (*v/v*) in water (solvent A)/ acetonitrile (solvent B) over a 5–95% acetonitrile gradient, and were monitored at 214 nm over 10 min. Preparative reversed phase high performance liquid chromatography (RP-HPLC) was performed using a Shimadzu SPD-20A equipped with a Waters Sunfire, C_{18}, 250 × 21.2 mm column. The eluent was made up of a mobile phase of 0.1% TFA (*v/v*) in H_2O (solvent A) and 0.1% TFA (*v/v*) in MeCN (solvent B) over various MeCN gradients and flow rates as indicated and were monitored at wavelengths 214 or 254 nm. Electrospray ionisation mass spectra were recorded using an Agilent single quadrupole unit with CTC-PAL and high-resolution electrospray mass spectra were recorded using a Waters LCT Premier XE spectrometer.

The melting points of the compounds were determined using a Gallenkamp MFG 595 010 melting point apparatus or a Reichert Austria hot stage microscope.

The ^{1}H, ^{13}C and ^{11}B NMR spectra were recorded using Bruker AVIII HD 400, Bruker AVIIIHD 600 with prodigy N_2 broadband CryoProbe and Bruker AVIII 700 with TCI H/C/N helium CryoProbe unity spectrometers operating at 700, 600, 400 MHz, 193, 151, 101 MHz, 225, 193 and 128 MHz respectively, using $CDCl_3$, D_2O, methanol-d_4, acetonitrile-d_3 or dimethyl-d_6 sulfoxide (DMSO-d_6) as solvents. Chemical shifts (δ) are given in parts per million (ppm) relative to the internal tetramethylsilane (TMS). Coupling constants are given in Hz. The abbreviations s, d, t, td, dd, dt, dq, ddd, ddt, dtd, dddd and m are abbreviations for singlet, doublet, triplet, triplet of doublets, doublet of doublets, doublet of triplets, doublet of quartets, doublet of doublet of doublets, doublet of doublet of triplets, doublet of triplet of doublets, doublet of doublet of doublet of doublets and multiplet, respectively. IR spectra were recorded using a Bruker Tensor 27 Fourier Transform Infrared Spectrometer; the abbreviations br, w, m, s, vs stand for broad, weak, medium, sharp and very sharp respectively and provisional assignments are given; $[\alpha]_D$ values are given in 10^{-1} deg cm^2 g^{-1} at the specified temperature.

Reaction products were identified by their NMR and IR spectra or otherwise by LC-MS analyses.

General Procedure for Synthesis of Boronic Acid & Ester Heterocycles

The benzodiazaborines and boronate esters were generally synthesised according to the literature procedure[i] with some modification which as follows: the boronic acid (50 mM) and the nucleophile (50mM) in 0.10 M PBS buffer (pH ~ 7.4) were nutated for 2.0 min at ambient temperature. If a solid residue was precipitated, the slurry was centrifuged for 20 min at 4.0 °C and washed with water twice, followed by lyophilisation to furnish the desired semi-pure product. In cases where the product did not precipitate, it was purified using preparative RP-HPLC – 0.1% TFA (*v/v*) in H_2O (solvent A)/ 0.1% TFA (*v/v*) MeCN (solvent B) over a 5–50% MeCN gradient, and were monitored at 124 nm over 40 min at 40 °C. Samples of the semi-pure products from the aforementioned sedimentation process were also purified using the above preparative RP-HPLC for analytical characterisation purposes.

[i] A. Bandyopadhyay, S. Cambray and J. Gao, *J. Am. Chem. Soc.*, 2017, **139**, 871.

1-Hydroxybenzo-[*d*][1,2,3]-diazaborinine-2(1*H*)-carboxamide (1)[i]

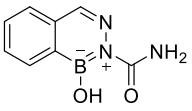

1

The diazaborine **1** was synthesised according to the general procedure, the precipitated powder was collected and purified using RP-HPLC (retention time: 12.2 – 12.5 min) (5.0 – 50% TFA (0.1% *v/v*) in MeCN/ TFA (0.1% *v/v*) in H_2O over 40 min; 3.0 ml min^{-1}, 40 °C) to furnish the desired compound **1** as a white fluffy powder (76 mg; 80%); mp 197 – 200 °C (dec.) (lit.[ii] 295 – 299 °C dec.); ν_{max}/cm^{-1} (ATR) 3418w (N–H asymmetric stretch), 3140br (N–H symmetric stretch), 2925w (C_{sp3}–H stretch), 1673s (C=O stretch), 1297m (C–N stretch), 1219m (C–B stretch); δ_H (600 MHz, acetonitrile-d_3) 8.15 (1 H, m, C*H*-Ar), 8.08 (1 H, s, *γ*-C*H*), 7.79 (2 H, m, 2 × C*H*-Ar), 7.70 (1 H, td, *J* 7.0 & 1.5, C*H*-Ar); δ_C (151 MHz; acetonitrile-d_3) 129.0 – 135.8 (4 × *C*H-Ar & 2 × *C*-Ar), 142.7 (*γ*-*C*H), 164.1 (*C*=O); δ_B (193 MHz, acetonitrile-d_3) 29.8; LC-MS (retention time: 5.6 – 5.9 min) *m/z* (ESI) 190 (M^+ + H, 100%); HRMS (ESI) calcd. for $C_8H_8BN_3O_2$ $[M+H]^+$ *m/z* = 190.0782, found: 190.0784.

[ii] P. Tschampel and H.R. Snyder, *J. Org. Chem.*, 1964, **29**, 2168.

1-Hydroxy-4-methylbenzo[*d*][1,2,3]-diazaborinine-2(1*H*)-carboxamide (2)

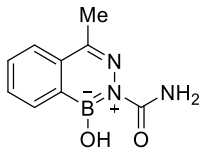

2

The diazaborine **2** was synthesised according to the general procedure, the precipitated powder was collected and purified using RP-HPLC (retention time: 12.7 – 13.0 min) (5.0 – 50% TFA (0.1% *v/v*) in MeCN/ TFA (0.1% *v/v*) in H_2O over 40 min; 3.0 ml min^{-1}, 40 °C) to furnish the desired compound **2** as a white fluffy powder (71 mg; 70%); mp 203 °C (dec.); ν_{max}/cm^{-1} (ATR) 3389w (N–H asymmetric stretch), 3205br (N–H symmetric stretch), 1687s (C=O stretch), 1311s (C–N stretch), 1155m (C–B stretch); δ_H (600 MHz, acetonitrile-d_3) 8.15 (1 H, d *J* 12.0, C*H*-Ar), 7.90 (1 H, d, *J* 6.0, C*H*-Ar), 7.79 (1 H, td, *J* 12.0 & 6.0, C*H*-Ar), 7.67 (1 H, td, *J* 12.0 & 6.0, C*H*-Ar), 2.56 (3 H, s, CH_3); δ_C (151 MHz; acetonitrile-d_3) 20.2 (CH_3), 126.7 – 135.8 (4 × *C*H-Ar & 2 × *C*-Ar), 146.9 (*γ*-*C*H), 164.0 (*C*=O); δ_B (193 MHz, acetonitrile-d_3) 29.8; LC-MS (retention time: 6.0 – 6.4 min) *m/z* (ESI) 204 (M^+ + H, 100%); HRMS (ESI) calcd. for $C_9H_{10}BN_3O_2$ $[M+H]^+$ *m/z* = 204.0939, found: 204.0941.

Benzo[*d*][1,2,3]-diazaborinin-1(*2H*)-ol (3)

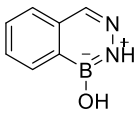

3

The diazaborine **3** was synthesised according to the general procedure, the clear reaction mixture was lyophilised and the residue was purified using RP-HPLC (retention time: 9.7 – 10.1 min) (5.0 – 50% TFA (0.1% *v/v*) in MeCN/ TFA (0.1% *v/v*) in H_2O over 40 min; 3.0 ml min^{-1}, 40 °C) to furnish the desired compound **3** as a white powder (38 mg; 31%); mp 232 – 239 °C (dec.); ν_{max}/cm^{-1} (ATR) 3323m (N–H stretch in diazaborine), 1558 – 1440s (C=C aromatic stretch), 1380s (B–O stretch), 1342s (B–N stretch); δ_H (600 MHz, acetonitrile-d_3) 8.09 (1 H, d, *J* 8.0, C*H*-Ar), 7.96 (1 H, s, *γ*-C*H*), 7.71 (2 H, m, 2 × C*H*-Ar), 7.60 (1 H, m, C*H*-Ar); δ_C (151 MHz; acetonitrile-d_3) 127.8 – 136.4 (4 × *C*H-Ar & 2 × *C*-Ar), 140.4 (*γ*-*C*H); δ_B (193 MHz, acetonitrile-d_3) 27.7; LC-MS (retention time: 4.5 min) *m/z* (ESI) 147 (M^+ + H, 100%); HRMS (ESI) calcd. for $C_7H_7BN_2O$ $[M+H]^+$ *m/z* = 147.0724, found: 147.0721.

8*H*-benzo[4,5][1,2,3]diazaborinino[3,2-*b*]benzo[4,5][1,2,3]diazaborinino[2,3-e][1,3,5,2,6]oxadiazadiborinin-8-one (4)

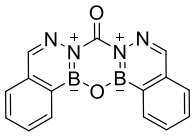

4

The diazaborine **4** was synthesised according to the general procedure, the clear reaction mixture was lyophilised and the residue was purified using RP-HPLC (retention time: 10.1 – 10.5 min) (5.0 – 50% TFA (0.1% *v/v*) in MeCN/ TFA (0.1% *v/v*) in H_2O over 40 min; 3.0 ml min^{-1}, 40 °C) to yield the desired compound **4** as a white powder (11 mg; 7.0%); mp 221 – 225 °C (dec.); ν_{max}/cm^{-1} (ATR) 2928w (C_{sp3}–H stretch), 1682s (C=O stretch), 1209m (C–B stretch); δ_H (600 MHz, methanol-d_4) 8.35 (2 H, s, γ-C*H*), 8.23 (2 H, d, *J* 7.5, 2 × C*H*-Ar), 7.83 – 7.75 (4 H, m, 4 × C*H*-Ar), 7.70 (2 H, t, *J* 7.5, 2 × C*H*-Ar); δ_C (151 MHz; methanol-d_4) 130.4 – 133.8 (8 × *C*H-Ar & 2 × *C*-Ar), 146.8 (γ-*C*H), 175.5 (*C*=O); δ_B (193 MHz, methanol-d_4) 16.2; LC-MS (retention time: 4.06 min) *m/z* (ESI) 301 (M^+ + H, 100%); HRMS (ESI) calcd. for $C_{15}H_{12}B_2N_4O_3$ $[M+H]^+$ *m/z* = 301.1063, found: 301.1060.

5,11-Dimethyl-8*H*-benzo[4,5][1,2,3]diazaborinino[3,2-*b*]benzo[4,5][1,2,3]diazaborinino[2,3-e][1,3,5,2,6]oxadiazadiborinin-8-one (5)

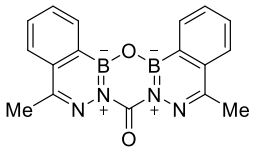

5

The diazaborine **5** was synthesised according to the general procedure, the clear reaction mixture was lyophilised and the residue was purified using RP-HPLC (retention time: 12.2 – 12.5 min) (5.0 – 50% TFA (0.1% *v/v*) in MeCN/ TFA (0.1% *v/v*) in H_2O over 40 min; 3.0 ml min^{-1}, 40 °C) to furnish the desired compound **5** as a white fluffy powder (3.0 mg; 2.0%); mp 244 – 258 °C (dec.); ν_{max}/cm^{-1} (ATR) 3399br (O–H stretch), 2923w (C_{sp3}–H stretch), 1683s (C=O stretch), 1210s (C–B stretch); δ_H (600 MHz, acetonitrile-d_3) 8.55 (2 H, d, *J* 8.0, 2 × C*H*-Ar), 8.08 (2 H, d, *J* 8.0, 2 × C*H*-Ar), 7.96 (2 H, dd, *J* 12.0 & 8.0, 2 × C*H*-Ar), 7.86 (2 H, dd, *J* 12.0 & 8.0, 2 × C*H*-Ar), 2.77 (6 H, s, 2 × CH_3); δ_B (193 MHz, acetonitrile-d_3) 28.3; LC-MS (retention time: 7.16 min) *m/z* (ESI) 329 (M^+ + H, 100%) 346 (M^+ + H_3O, 20); HRMS (ESI) calcd. for $C_{17}H_{14}B_2N_4O_2$ $[M+H]^+$ *m/z* = 329.1376, found: 329.1373.

1-Hydroxythieno[3,2-*d*][1,2,3]diazaborinine-2(1*H*)-carboxamide (6)

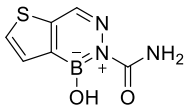

6

The diazaborine **6** was synthesised according to the general procedure, the clear reaction mixture was lyophilised and the residue was purified using RP-HPLC (retention time: 17.1 – 18.2 min) (5.0 – 50% TFA (0.1% *v/v*) in MeCN/ TFA (0.1% *v/v*) in H_2O over 40 min; 3.0 ml min^{-1}, 40 °C) to furnish the desired compound **6** as a pale-yellow powder (60 mg; 61%); mp 273 °C (dec.); ν_{max}/cm^{-1} (ATR) 3500 – 3200br (H-bonding O–H), 1698s (C=O stretch), 1425vs (B–O stretch), 1331s (B–N stretch), 1287m (C–B stretch); δ_H (600 MHz, acetonitrile-d_3) 8.20 (1 H, s, γ-C*H*), 7.80 (1 H, d, *J* 5.0, C*H*-Ar), 7.58 (1 H, d, *J* 5.0, C*H*-Ar); δ_C (151 MHz; acetonitrile-d_3) 127.3 – 135.3 (2 × *C*H-Ar & 2 × *C*-Ar), 140.0 (γ-*C*H), 164.0 (*C*=O); δ_B (193 MHz, acetonitrile-d_3) 28.6; LC-MS (retention time: 5.8 min) *m/z* (ESI) 196 (M^+ + H, 100%), 373 (2 × M^+ + H, 6.0); HRMS (ESI) calcd. for $C_6H_6BN_3O_2S$ $[M+H]^+$ *m/z* = 196.0347, found: 196.0346.

1-Hydroxy-4-methylthieno[3,2-*d*][1,2,3]diazaborinine-2(1*H*)-carboxamide (7)

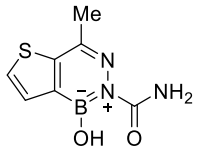

7

The diazaborine **7** was synthesised according to the general procedure, the clear reaction mixture was lyophilised and the residue was purified using RP-HPLC (retention time: 18.3 – 19.0 min) (5.0 – 50% TFA (0.1% *v/v*) in MeCN/ TFA (0.1% *v/v*) in H_2O over 40 min; 3.0 ml min^{-1}, 40 °C) to furnish the desired compound **7** as a white fluffy powder (75 mg; 72%); mp 278 °C (dec.); ν_{max}/cm^{-1} (ATR) 3448w (N–H asymmetric stretch), 3261br (N–H symmetric stretch), 1699s (C=O stretch), 1421s (B–O stretch), 1350s (B–N stretch), 1286vs (C–B stretch), 663vs (B–O wagging); δ_H (600 MHz, acetonitrile-d_3) 7.76 (1 H, d, *J* 6.0, C*H*-Ar), 7.57 (1 H, d, *J* 6.0, C*H*-Ar), 2.49 (3 H, s, CH_3); δ_C (151 MHz; acetonitrile-d_3) 20.9 (*C*H_3), 130.3 – 131.3 (2 × *C*H-Ar & 2 × *C*-Ar), 142.4 (*γ-C* and *C*=O); δ_B (193 MHz, acetonitrile-d_3) 28.4; LC-MS (retention time: 6.3 min) *m/z* (ESI) 210 (M^+ + H, 100%); HRMS (ESI) calcd. for $C_7H_8BN_3O_2S$ $[M+H]^+$ *m/z* = 210.0503, found: 210.0502.

1-Hydroxythieno[2,3-*d*][1,2,3]diazaborinine-2(1*H*)-carboxamide (8)

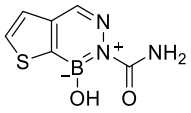

8

3-Formyl-2-thienylboronic acid (0.5 mmol) in acetonitrile (0.10 M) was added to a solution of semicarbazide hydrochloride in acetonitrile (0.1 M) and the resulting mixture was stirred at reflux (90 °C) overnight. Upon completion (LC-MS controlled) the solvent was removed *in vacuo* and the residue was washed with excess water, filtered and dried in a desiccator to furnish the desired compound **8** as pale brown needle-like crystals (42 mg; 43%); mp 314 °C (dec.); ν_{max}/cm^{-1} (ATR) 3445w (N–H asymmetric stretch), 3190br (N–H symmetric stretch), 1700m (C=O stretch), 1449m (B–O stretch), 1396m (B–N stretch), 1309s (C–B stretch), 672m (B–O wagging); δ_H (600 MHz, acetonitrile-d_3) 8.15 (1 H, s, γ-C*H*), 7.98 (1 H, d, *J* 5.0, C*H*-Ar), 7.52 (1 H, d, *J* 5.0, C*H*-Ar); δ_C (151 MHz; acetonitrile-d_3) 126.7 – 136.4 (2 × *C*H-Ar & 2 × *C*-Ar), 145.0 (γ-*C*), 163.8 (*C*=O); δ_B (193 MHz, acetonitrile-d_3) 28.8; LC-MS (retention time: 5.9 min) *m/z* (ESI) 196 (M^+ + H, 100%), 373 (2 × M^+ + H, 6.0); HRMS (ESI) calcd. for $C_6H_6BN_3O_2S$ $[M+H]^+$ *m/z* = 196.0347, found: 196.0347.

1-Hydroxybenzo[*d*][1,2,3]-diazaborinine-2(1*H*)-carbothioamide (9)

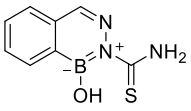

9

The diazaborine **9** was synthesised according to the general procedure, the needle-like crystals were collected, washed with cold water and purified using RP-HPLC (retention time: 10.2 – 10.5 min) (5.0 – 50% TFA (0.1% *v/v*) in MeCN/ TFA (0.1% *v/v*) in H_2O over 40 min; 3.0 ml min^{-1}, 40 °C) to furnish the desired compound **9** as a white fluffy powder (27 mg; 26%); mp 187 °C (dec.); ν_{max}/cm^{-1} (ATR) 3398m (N–H asymmetric stretch), 3263 (N–H symmetric stretch), 3040w (C_{sp3}–H stretch), 1586s (C=S stretch), 1297m (C–N stretch), 1255m (C–B stretch); δ_H (600 MHz, acetonitrile-d_3) 8.14 (1 H, d, *J* 2.0, γ-C*H*), 7.79 – 7.72 (1 H, m, C*H*-Ar), 7.58 (1 H, m, C*H*-Ar), 7.38 (2 H, m, 2 × C*H*-Ar); δ_C (151 MHz; acetonitrile-d_3) 128.6 – 136.6 (4 × *C*H-Ar & 2 × *C*-Ar), 142.4 and 145.9 (γ-*C*H), 178.8 (*C*=S); δ_B (193 MHz, acetonitrile-d_3) 29.9; LC-MS (retention time: 5.01 min) *m/z* (ESI) 206 (M^+ + H, 100%), 224 (M^+ + H_3O, 35), 393 (2 × M^+, 15); HRMS (ESI) calcd. for $C_8H_8BN_3OS$ $[M+H]^+$ *m/z* = 206.0554, found: 206.0553.

1-Hydroxy-4-methylbenzo[*d*][1,2,3]diazaborinine-2(1*H*)-carbothioamide (10)

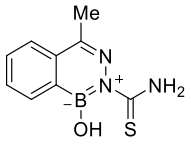

10

The diazaborine **10** was synthesised according to the general procedure, the precipitated powder was washed with cold water and purified using RP-HPLC (retention time: 16.3 – 16.6 min) (5.0 – 50% TFA (0.1% *v/v*) in MeCN/ TFA (0.1% *v/v*) in H_2O over 40 min; 3.0 ml min^{-1}, 40 °C) to furnish the desired compound **10** as a white powder (61 mg; 56%); mp 249 °C (dec.); ν_{max}/cm^{-1} (ATR) 3389m (N–H asymmetric stretch), 3251 (N–H symmetric stretch), 1586m (C=S stretch), 1408s (C_{sp2}=C_{sp2} stretch), 1303m (C–N stretch); δ_H (600 MHz, acetonitrile-d_3) 8.16 (1 H, m, C*H*-Ar), 7.89 (1 H, m, C*H*-Ar), 7.78 (1 H, m, C*H*-Ar), 7.68 (1 H, m, C*H*-Ar), 2.57 (3 H, s, CH_3); δ_C (151 MHz; acetonitrile-d_3) 20.2 (*C*H_3) 126.8 – 134.9 (4 × *C*H-Ar & 2 × *C*-Ar), 147.6 (*γ*-*C*), 186.7 (*C*=S); δ_B (193 MHz, acetonitrile-d_3) 30.0; LC-MS (retention time: 7.37 min) *m/z* (ESI) 220 (M^+ + H, 100%), 420 (2 × M^+ + H, 10); HRMS (ESI) calcd. for $C_9H_{10}BN_3OS$ $[M+H]^+$ *m/z* = 220.0710, found: 220.0710.

(2a*S*)-4a-Hydroxy-2,2a,4a,8b-tetrahydro-3*H*-4-oxa-1-thia-2a^{1}-aza-4aλ^{4}-borapentaleno[1,6-*ab*]inden-3-one (11)

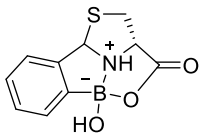

11

The heterocycle **11** was synthesised according to the general procedure, the clear reaction mixture was lyophilised and the residue was purified using RP-HPLC (retention time: 20.1 – 21.4 min) (5.0–50% TFA (0.1% *v/v*) in MeCN/ TFA (0.1% *v/v*) in H_2O over 40 min; 3.0 ml min^{-1}, 40 °C) to yield the desired compound **11** as a white fluffy powder (83 mg; 71%); mp 310 – 313 °C (dec.); $[\alpha]_D^{25}$ -19.6 (c 0.025 in acetonitrile); ν_{max}/cm^{-1} (ATR) 3060w (C_{sp3}–H stretch), 1730s (C=O stretch of ester), 1320m (C–N stretch), 1204m (C–B stretch); δ_H (600 MHz, acetonitrile-d_3) 7.43 (1 H, m, C*H*-Ar), 7.30 (2 H, m, 2 × C*H*-Ar), 7.18 (1 H, m, C*H*-Ar), 6.16 (1 H, s, *δ*-C*H*), 4.74 (1 H, d, *J* 6.0, *α*-C*H*), 3.57 (1 H, dd, *J* 12.0 & 6.0, *β*-C*H*), 3.44 (1 H, dd, *J* 12.0 & 6.0, *β*-C*H*); δ_C (151 MHz; acetonitrile-d_3) 37.9 (*β*-*C*H$_2$), 65.6 (*δ*-*C*H), 73.4 (*α*-*C*H), 123.1 – 143.2 (4 × *C*H-Ar & 2 × *C*-Ar), 174.1 (*C*=O); δ_B (193 MHz, acetonitrile-d_3) 11.4; LC-MS (retention time: 4.58 min) *m/z* (ESI) 236 (M^+ + H, 100%), 453 (2 × M^+ + H, 100); HRMS (ESI) calcd. for $C_{10}H_{10}BNO_3S$ $[M+H]^+$ *m/z* = 236.0547, found: 236.0545.

(2a*R*)-4a-Hydroxy-2,2a,4a,8b-tetrahydro-3*H*-4-oxa-1-thia-2a^1-aza-4aλ^4-borapentaleno[1,6-*ab*]inden-3-one (12)

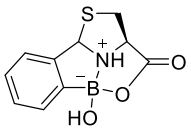

12

The heterocycle **12** was synthesised according to the general procedure, the clear reaction mixture was lyophilised and the residue was purified using RP-HPLC (retention time: 19.8 – 20.5 min) (5.0–50% TFA (0.1% *v/v*) in MeCN/ TFA (0.1% *v/v*) in H_2O over 40 min; 3.0 ml min^{-1}, 40 °C) to yield the desired compound **12** as a white fluffy powder (78 mg; 67%); mp 310 – 313 °C (dec.); $[\alpha]_D^{25}$ +5.8 (c 0.025 in acetonitrile); ν_{max}/cm^{-1} (ATR) 3060w (C_{sp3}–H stretch), 1730s (C=O stretch of ester), 1320m (C–N stretch), 1204m (C–B stretch); δ_H (600 MHz, acetonitrile-d_3) 7.43 (1 H, m, C*H*-Ar), 7.30 (2 H, m, 2 × C*H*-Ar), 7.18 (1 H, m, C*H*-Ar), 6.16 (1 H, s, *δ*-C*H*), 4.74 (1 H, d, *J* 6.0, *α*-C*H*), 3.57 (1 H, dd, *J* 12.0 & 6.0, *β*-CH_2), 3.44 (1 H, dd, *J* 12.0 & 6.0, *β*-CH_2); δ_C (151 MHz; acetonitrile-d_3) 37.9 (*β*-CH_2), 65.6 (*δ*-*C*H), 73.4 (*α*-*C*H), 123.1 – 143.2 (4 × *C*H-Ar & 2 × *C*-Ar), 174.1 (*C*=O); δ_B (193 MHz, acetonitrile-d_3) 11.4; LC-MS (retention time: 4.58 min) *m/z* (ESI) 236 (M^+ + H, 100%), 453 (2 × M^+ + H, 100); HRMS (ESI) calcd. for $C_{10}H_{10}BNO_3S$ $[M+H]^+$ *m/z* = 236.0547, found: 236.0545.

(2a*R*)-4a-Hydroxy-2,2-dimethyl-2,2a,4a,8b-tetrahydro-3*H*-4-oxa-1-thia-2a^{1}-aza-4aλ^{4}-borapentaleno[1,6-*ab*]inden-3-one (13)

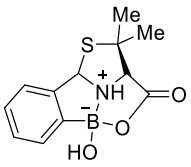

13

The heterocycle **13** was synthesised according to the general procedure, the clear reaction mixture was lyophilised and the residue was purified using RP-HPLC (retention time: 17.5 – 18.3 min) (5.0 – 50% TFA (0.1% *v/v*) in MeCN/ TFA (0.1% *v/v*) in H_2O over 40 min; 3.0 ml min^{-1}, 40 °C) to yield the desired compound **13** as a white fluffy powder (59 mg; 45%); mp 250 – 255 °C (dec.); $[\alpha]_D^{25}$ +21.3 (c 0.025 in acetonitrile); ν_{max}/cm^{-1} (ATR) 2935w (C_{sp3}–H stretch), 1713s (C=O stretch of ester), 1204s (C–N stretch), 1167vs (C–B stretch); δ_H (600 MHz, acetonitrile-d_3) 7.42 – 7.14 (4 H, m, 4 × C*H*-Ar), 6.25 (1 H, s, *δ*-C*H*), 4.29 (1 H, s, *α*-C*H*), 1.61 (3 H, s, CH_3), 1.41 (3 H, s, CH_3); δ_C (151 MHz; acetonitrile-d_3) 23.4 and 29.9 (2 × *C*H$_3$), 58.7 (*β*-*C*H$_3$), 71.2 (*δ*-*C*H), 72.1 (*α*-*C*H), 128.7 – 143.7 (4 × *C*H-Ar & 2 × *C*-Ar), 171.5 (*C*=O); δ_B (193 MHz, acetonitrile-d_3) 11.3; LC-MS (retention time: 5.4 min) *m/z* (ESI) 264 (M^+ + H, 100%), 509 (2 × M^+ + H, 100); HRMS (ESI) calcd. for $C_{12}H_{14}BNO_3S$ $[M+H]^+$ *m/z* = 264.0860, found: 264.0862.

(2a*S*)-4a-Hydroxy-2,2-dimethyl-2,2a,4a,8b-tetrahydro-3H-4-oxa-1-thia-2a^{1}-aza-4aλ^{4}-borapentaleno[1,6-*ab*]inden-3-one (14)

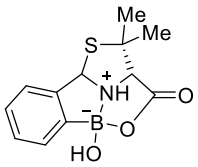

14

The heterocycle **14** was synthesised according to the general procedure, the clear reaction mixture was lyophilised and the residue was purified using RP-HPLC (retention time: 17.1 – 17.9 min) (5.0 – 50% TFA (0.1% *v/v*) in MeCN/ TFA (0.1% *v/v*) in H_2O over 40 min; 3.0 ml min^{-1}, 40 °C) to yield the desired compound **14** as a white fluffy powder (67 mg; 51%); mp 250 – 255 °C (dec.); $[\alpha]_D^{25}$ -16.4 (c 0.025 in acetonitrile); ν_{max}/cm^{-1} (ATR) 2935w (C_{sp3}–H stretch), 1713s (C=O stretch of ester), 1204s (C–N stretch), 1167vs (C–B stretch);); δ_H (600 MHz, acetonitrile-d_3) 7.42 – 7.14 (4 H, m, 4 × C*H*-Ar), 6.25 (1 H, s, *δ*-C*H*), 4.29 (1 H, s, *α*-C*H*), 1.61 (3 H, s, CH_3), 1.41 (3 H, s, CH_3); δ_C (151 MHz; acetonitrile-d_3) 23.4 and 29.9 (2 × *C*H$_3$), 58.7 (*β*-*C*H$_3$), 71.2 (*δ*-*C*H), 72.1 (*α*-*C*H), 128.7 – 143.7 (4 × *C*H-Ar & 2 × *C*-Ar), 171.5 (*C*=O); δ_B (193 MHz, acetonitrile-d_3) 11.3; LC-MS (retention time: 5.4 min) *m/z* (ESI) 264 (M^+ + H, 100%), 509 (2 × M^+ + H, 100); HRMS (ESI) calcd. for $C_{12}H_{14}BNO_3S$ $[M+H]^+$ *m/z* = 264.0860, found: 264.0862.

(2a*S*)-4a-Hydroxy-8b-methyl-2,2a,4a,8b-tetrahydro-3*H*-4-oxa-1-thia-2a^{1}-aza-4aλ^{4}-borapentaleno[1,6-*ab*]inden-3-one (15)

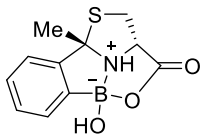

15

The heterocycle **15** was synthesised according to the general procedure, the clear reaction mixture was lyophilised and the residue was purified using RP-HPLC (retention time: 19.3 – 20.5 min) (5.0 – 50% TFA (0.1% *v/v*) in MeCN/ TFA (0.1% *v/v*) in H_2O over 40 min; 3.0 ml min^{-1}, 40 °C) to yield the desired compound **15** as a white fluffy powder (77 mg; 62%); mp 200 °C (dec.); $[\alpha]_D^{25}$ -14.4 (c 0.025 in acetonitrile); ν_{max}/cm^{-1} (ATR) 3416w (O-H stretch), 1715s (C=O stretch of ester), 1260m (C–N stretch), 1227m (C–B stretch); δ_H (600 MHz, acetonitrile-d_3) 7.41 (1 H, d, *J* 6.0, C*H*-Ar), 7.34 – 7.28 (2 H, m, 2 × C*H*-Ar), 7.23 (1 H, d, *J* 6.0, C*H*-Ar), 4.78 (1 H, dd, *J* 8.0 & 4.0, *α*-C*H*), 3.64 (1 H, dd, *J* 12.0 & 8.0, *β*-CH_2), 3.41 (1 H, dd, *J* 12.0 & 4.0, *β*-CH_2), 2.01 (3 H, s, CH_3); δ_C (151 MHz; acetonitrile-d_3) 29.1 (*C*H$_3$), 35.7 (*β*-*C*H$_2$) 66.8 (*δ*-*C*), 85.6 (*α*-*C*H), 122.0 – 147.9 (4 × *C*H-Ar & 2 × *C*-Ar), 174.0 (*C*=O); δ_B (193 MHz, acetonitrile-d_3) 11.1; LC-MS (retention time: 3.59 min) *m/z* (ESI) 250 (M^+ + H, 100%), 521 (2 × M^+ + Na, 20); HRMS (ESI) calcd. for $C_{11}H_{12}BNO_3S$ $[M+H]^+$ *m/z* = 250.0704, found: 250.0701.

(2a*R*)-4a-Hydroxy-8b-methyl-2,2a,4a,8b-tetrahydro-3*H*-4-oxa-1-thia-2a^{1}-aza-4aλ^{4}-borapentaleno[1,6-*ab*]inden-3-one (16)

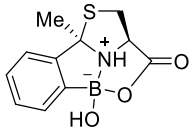

16

The heterocycle **16** was synthesised according to the general procedure, the clear reaction mixture was lyophilised and the residue was purified using RP-HPLC (retention time: 19.8 – 20.9 min) (5.0 – 50% TFA (0.1% *v/v*) in MeCN/ TFA (0.1% *v/v*) in H_2O over 40 min; 3.0 ml min^{-1}, 40 °C) to yield the desired compound **16** as a white fluffy powder (77 mg; 62%); mp 200 °C (dec.); $[\alpha]_D^{25}$ +2.3 (c 0.025 in acetonitrile); ν_{max}/cm^{-1} (ATR) 3416w (O-H stretch), 1715s (C=O stretch of ester), 1260m (C–N stretch), 1227m (C–B stretch); δ_H (600 MHz, acetonitrile-d_3) 7.41 (1 H, d, *J* 6.0, C*H*-Ar), 7.34 – 7.28 (2 H, m, 2 × C*H*-Ar), 7.23 (1 H, d, *J* 6.0, C*H*-Ar), 4.78 (1 H, dd, *J* 8.0 & 4.0, *α*-C*H*), 3.64 (1 H, dd, *J* 12.0 & 8.0, *β*-CH_2), 3.41 (1 H, dd, *J* 12.0 & 4.0, *β*-CH_2), 2.01 (3 H, s, CH_3); δ_C (151 MHz; acetonitrile-d_3) 29.1 (*C*H$_3$), 35.7 (*β*-*C*H$_2$) 66.8 (*δ*-*C*), 85.6 (*α*-*C*H), 122.0 – 147.9 (4 × *C*H-Ar & 2 × *C*-Ar), 174.0 (*C*=O); δ_B (193 MHz, acetonitrile-d_3) 11.1; LC-MS (retention time: 3.59 min) *m/z* (ESI) 250 (M^+ + H, 100%), 521 (2 × M^+ + Na, 20); HRMS (ESI) calcd. for $C_{11}H_{12}BNO_3S$ $[M+H]^+$ *m/z* = 250.0704, found: 250.0701.

(2a*S*)-4a-Hydroxy-2,2,8b-trimethyl-2,2a,4a,8b-tetrahydro-3*H*-4-oxa-1-thia-2a^1-aza-4aλ^4-borapentaleno[1,6-*ab*]inden-3-one (17)

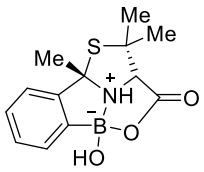

17

The heterocycle **17** was synthesised according to the general procedure, the clear reaction mixture was lyophilised and the residue was purified using RP-HPLC (retention time: 22.7 – 24.1 min) (5.0 – 50% TFA (0.1% *v/v*) in MeCN/ TFA (0.1% *v/v*) in H_2O over 40 min; 3.0 ml min^{-1}, 40 °C) to yield the desired compound **17** as a white powder (54 mg; 39%); mp 201 °C (dec.); $[\alpha]_D^{25}$ -4.5 (c 0.015 in acetonitrile); ν_{max}/cm^{-1} (ATR) 3040w (C_{sp3}–H stretch), 1723s (C=O stretch of ester), 1281m (C–N stretch), 1242m (C–B stretch); δ_H (600 MHz, acetonitrile-d_3) 7.38 – 7.28 (4 H, m, 4 × C*H*-Ar), 4.47 (1 H, s, *α*-C*H*), 1.94 (3 H, s, CH_3), 1.55 and 0.83 (6 H, s, 2 × CH_3); δ_C (151 MHz; acetonitrile-d_3) 26.5 (2 × *C*H$_3$), 29.9 (*C*H$_3$), 56.4 (*β*-*C*), 76.2 (*δ*-*C*), 83.5 (*α*-*C*H), 123.0 – 151.6 (4 × *C*H-Ar & 2 × *C*-Ar), 171.4 (*C*=O); δ_B (193 MHz, acetonitrile-d_3) 11.5; LC-MS (retention time: 4.47 min) *m/z* (ESI) 278 (M^+ + H, 100%), 537 (2 × M^+, 40), 577 (2 × M^+ + MeCN, 20); HRMS (ESI) calcd. for $C_{13}H_{16}BNO_3S$ $[M+H]^+$ *m/z* = 278.1017, found: 278.1014.

(2a*R*)-4a-Hydroxy-2,2,8b-trimethyl-2,2a,4a,8b-tetrahydro-3*H*-4-oxa-1-thia-2a^1-aza-4aλ^4-borapentaleno[1,6-*ab*]inden-3-one (18)

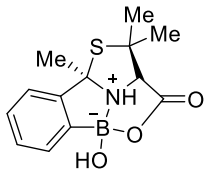

18

The heterocycle **18** was synthesised according to the general procedure, the clear reaction mixture was lyophilised and the residue was purified using RP-HPLC (retention time: 22.4 – 23.9 min) (5.0 – 50% TFA (0.1% *v/v*) in MeCN/ TFA (0.1% *v/v*) in H_2O over 40 min; 3.0 ml min^{-1}, 40 °C) to yield the desired compound **18** as a white powder (37 mg; 27%); mp 201 °C (dec.); $[\alpha]_D^{25}$ +8.3 (c 0.025 in MeCN); ν_{max}/cm^{-1} (ATR) 3040w (C_{sp3}–H stretch), 1723s (C=O stretch of ester), 1281m (C–N stretch), 1242m (C–B stretch); δ_H (600 MHz, acetonitrile-d_3) 7.38 – 7.28 (4 H, m, 4 × C*H*-Ar), 4.47 (1 H, *α*-C*H*), 1.94 (3 H, s, CH_3), 1.55 and 0.83 (6 H, s, 2 × CH_3); δ_C (151 MHz; acetonitrile-d_3) 26.5 (2 × *C*H$_3$), 29.9 (*C*H$_3$), 56.4 (*β*-*C*), 76.2 (*δ*-*C*), 83.5 (*α*-*C*H), 123.0 – 151.6 (4 × *C*H-Ar & 2 × *C*-Ar), 171.4 (*C*=O); δ_B (193 MHz, acetonitrile-d_3) 11.5; LC-MS (retention time: 4.47 min) *m/z* (ESI) 278 (M^+ + H, 100%), 537 (2 × M^+, 40), 577 (2 × M^+ + MeCN, 20); HRMS (ESI) calcd. for $C_{13}H_{16}BNO_3S$ $[M+H]^+$ *m/z* = 278.1017, found: 278.1014.

(*E*)-2-(Thiophen-3-ylmethylene)hydrazine-1-carboxamide (19)

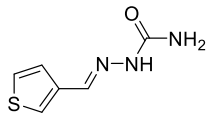

19

The carboxamide **19** was synthesised according to the general procedure, the precipitated powder was washed with cold water and lyophilised to furnish the desired compound **19** as an off-white powder (53 mg; 54%); mp 220 °C (dec.) (lit.[iii] 233 – 234 °C); ν_{max}/cm^{-1} (ATR) 3453w (N–H asymmetric stretch), 3106br (N–H symmetric stretch), 1684s (C=O stretch), 1598s (C_{sp2}–C_{sp2} aromatic stretch), 1170m (C–N stretch); δ_H (600 MHz, acetonitrile-d_3) 7.90 (1 H, s, γ-C*H*), 7.62 (1 H, m, C*H*-Ar), 7.50 (1 H, m, C*H*-Ar), 7.42 (1 H, m, C*H*-Ar); δ_C (151 MHz; acetonitrile-d_3) 125.3 – 127.6 (3 × *C*H-Ar & 1 × *C*-Ar), 138.0 (γ-*C*H), 138.7 (*C*=O); LC-MS (retention time: 5.1 min) *m/z* (ESI) 170 (M^+ + H, 100%); HRMS (ESI) calcd. for $C_6H_7N_3OS$ $[M+H]^+$ *m/z* = 170.0383, found: 170.0382.

[iii] E. Campaigne and W.M. LeSuer, *J. Am. Chem. Soc.*, 1948, **70**, 1555.

Propane-1-sulfonohydrazide (20)

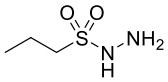

20

To a chilled solution of hydrazine monohydrate (4.9 ml, 0.10 mol) in dry THF (20 ml) was added 1-propanesulfonyl chloride (1.1 ml, 10 mmol) in dry THF (10 ml) at 5.0 °C dropwise. The thus obtained clear reaction mixture was stirred at 10 – 20 °C for 18 h. Upon completion (LC-MS controlled) the clear reaction mixture was extracted with EtOAc (5.0 × 50 ml), the combined organic extracts were washed with aqueous sodium hypochlorite 5% *w/w* (100 ml), dried over Na_2SO_4, filtered and the solvent was removed *in vacuo*. The crude product was purified by flash column chromatography to yield the desired compound **20** as a white solid (1.3 g; 94%); R_f 0.40 (10% MeOH in CH_2Cl_2); mp 44 – 45 °C (lit.[iv] 40 – 41 °C); ν_{max}/cm^{-1} (ATR) 3303m (N–H asymmetric stretch), 3243m (N–H symmetric stretch), 1619s (C=O stretch); δ_H (400 MHz, $CDCl_3$) 3.12 – 3.04 (2 H, m, *α*-C*H*$_2$), 1.91 – 1.80 (2 H, m, *β*-C*H*$_2$), 1.07 (3 H, t, *J* 7.5, *γ*-C*H*$_3$); δ_C (101 MHz, $CDCl_3$) 13.1 (*γ*-*C*H$_3$), 17.1, (*β*-*C*H$_2$), 51.2 (*α*-*C*H$_2$); LC-MS (retention time: 1.94 min) *m/z* (ESI) 139 (M^+ + H, 100%).

[iv] U.O. Ozdemir, F. Ilbiz, A.B. Gunduzalp, N. Ozbek, Z.K. Genç, F. Hamurcu and S. Tekin, *J. Mol. Struct.*, 2015, **1100**, 464.

6-Methylthieno[3,2-*d*][1,2,3]diazaborinin-1(2*H*)-ol (21)

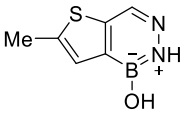

21

To a solution of bread thiophene (40 mg, 0.30 mmol) in dichloroethane (5.0 ml) was added the hydrazide **20** dropwise. Thereto was added BBr_3 (0.10 ml, 1.0 mmol) in dichloroethane (0.30 ml) followed by $AlCl_3$ (4.0 mg, 30 μmol) dissolved in dichloroethane (2.0 ml) under argon. The thus obtained yellow reaction mixture was stirred at reflux under argon for 20 min. The reaction mixture was cooled in an ice bath and poured into ice-water (3.0 ml), the organic phase was separated, washed with deionised water (2.0 × 0.50 ml) and extracted with 1.0 M aqueous sodium hydroxide (3.0 × 2.0 ml). The aqueous extracts were collected and conc. HCl added until acidic to Congo red. The acidified aqueous extracts were extracted with CH_2Cl_2 (2.0 × 5.0 ml), dried over Na_2SO_4 and the solvent was removed *in vacuo* to yield a yellow wax. The crude was purified by flash chromatography to furnish the desired compound **21** as a green wax (30 mg; 60%); R_f 0.40 (10% MeOH in CH_2Cl_2); δ_H (600 MHz, acetonitrile-d_3) 9.95 (1 H, s, C*H*=N), 8.01 (1 H, s, C=C*H*=*C*), 2.57 (3 H, d, *J* 1.0, C*H*$_3$); δ_C (151 MHz; acetonitrile-d_3) 29.6 (*C*H$_3$), 127.2 – 135.2 (1 × *C*H-Ar & 3 × *C*-Ar), 186.5 (*C*H=N); δ_B (193 MHz, acetonitrile-d_3) 26.3; LC-MS (retention time: 4.7 min) *m/z* (ESI) 167 (M^+ + H, 100%).

(*E*)-*N*′-((5-Methylthiophen-2-yl)methylene)propane-1-sulfonohydrazide (22)

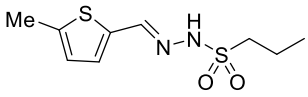

22

To a solution of bread thiophene (0.78 ml, 7.2 mmol) and the hydrazide **20** (1.0 g, 7.2 mmol) in EtOH (10 ml) was added glacial AcOH (6 drops), and the resulting brown reaction mixture was stirred at ambient temperature for 1.0 h. Upon completion (LC-MS controlled), the solvent was removed *in vacuo* and the crude was purified by flash column chromatography to furnish the desired compound **22** as a yellow solid (1.6 g; 94%); R_f 0.35 (7% MeOH in CH_2Cl_2); mp 107 – 108 °C (lit.[v] 109 – 110 °C); ν_{max}/cm^{-1} (ATR) 3186m (N–H stretch), 1148vs (S=O stretch), 945s (S–O stretch); δ_H (400 MHz, $CDCl_3$) 7.95 (1 H, s, *γ*-C*H*), 7.75 (1 H, s, *α*-NH), 7.06 (1 H, d, *J* 3.5, C*H*-Ar), 6.75 – 6.66 (1 H, m, C*H*-Ar), 3.33 – 3.15 (2 H, m, *α*-CH_2), 2.49 (3 H, d, *J* 1.0, CH_3), 1.97 – 1.79 (2 H, m, *β*-CH_2), 1.07 (3 H, t, *J* 7.5, *γ*-CH_3); δ_C (101 MHz, $CDCl_3$) 13.0 (*γ*-*C*CH_3), 15.7 (*β*-*C*CH_2), 17.0 (*C*H_3), 52.7 (*α*-*C*H_2), 125.8 and 131.1 (*C*H-Ar), 135.4 (*C*-Ar), 143.7 (*γ*-*C*H), 144.5 (*C*-Ar); LC-MS (retention time: 7.13 min) *m/z* (ESI) 247 (M^+ + H, 100%); HRMS (ESI) calcd. for $C_9H_{15}N_2O_2S_2$ $[M+H]^+$ *m/z* = 247.0570, found: 247.0571.

[v] M.A. Grassberger, *Liebigs Ann.*, 1985, **4**, 683.

6-Methyl-2-(propylsulfonyl)thieno[3,2-*d*][1,2,3]diazaborinin-1(2*H*)-ol (23)

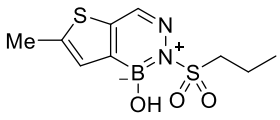

23

To a solution of $FeCl_3$ (60 mg, 0.37 mmol) in dry dichloroethane was added the hydrazone **22** (0.90 g, 3.7 mmol) in anhydrous dichloroethane (50 ml), and BBr_3 (1.1 ml, 11 mmol) in anhydrous dichloroethane (3.0 ml) simultaneously under argon with vigorous stirring at 70 °C for 15 min. The orange reaction mixture was cooled in an ice bath and poured into ice-water (30 ml). The subsequent reaction mixture was washed with deionised water (30 ml) and the organic phase was extracted with 1.0 M aqueous sodium hydroxide (3.0 × 30 ml). The aqueous extracts were combined and conc. HCl added until a cloudy mixture was obtained (pH ~ 2 – 3). The thus obtained colloidal was extracted with CH_2Cl_2 (4.0 × 100 ml), dried over Na_2SO_4 and the solvent was removed *in vacuo*. The green crude wax was purified by flash column chromatography to furnish the desired compound **23** as a white powder (0.72 g; 72%); R_f 0.30 (5.0% MeOH in CH_2Cl_2); mp 92 – 94 °C (dec.) (lit.[vi] 85 – 86 °C); ν_{max}/cm^{-1} (ATR) 3200 – 2800br (O–H hydrogen bonding), 1361m and 1136s (S=O stretch), 900vs (S–O stretch); δ_H (400 MHz, acetonitrile-d_3) 8.19 (1 H, s, γ-C*H*), 7.26 (1 H, t, *J* 1.0, C*H*-Ar), 3.48 – 3.42 (2 H, m, α-CH_2), 2.59 (3 H, d, *J* 1.0, CH_3), 1.71 (2 H, dq, *J* 15.0 & 7.5, β-CH_2), 0.95 (3 H, t, *J* 7.5, γ-CH_3); δ_C (101 MHz, acetonitrile-d_3) 12.4 (γ-*C*H_3), 15.1 (β-*C*H_2), 17.3 (*C*H_3), 53.8 (α-*C*H_2), 128.2 (*C*H-Ar), 136.8 (γ-*C*H), 148.2 (*C*-Ar); δ_B (193 MHz, acetonitrile-d_3) 27.2; LC-MS (retention time: 7.25 min) *m/z* (ESI) 273 (M^+ + H, 100%); HRMS (ESI) calcd. for $C_9H_{14}BN_2O_3S_2$ $[M+H]^+$ *m/z* = 273.0533, found: 273.0534.

[vi] Sandoz - DE2750878, *Chem. Abstr.*, 1978, **89**, 109937.

Methyl (*R*)-thiazolidine-4-carboxylate (24)

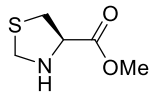

24

A: L-Cysteine methyl ester (2.6 g, 15 mmol) was dissolved in aqueous MeOH 40% *v/v* (50 ml). Sodium bicarbonate (1.3 g, 16 mmol) and formalin 39% *w/w* (1.1 ml, 16 mmol) was then added. The thus obtained clear reaction mixture was stirred at ambient temperature overnight. The pale yellow reaction mixture was extracted with CH_2Cl_2 (2.0 × 100 ml), the combined organic extracts were dried over Na_2SO_4, filtered and the solvent was removed *in vacuo*, the crude oil was purified by flash column chromatography to furnish the desired compound **24** as a pale green oil (2.1 g; 93%); R_f 0.35 (5% MeOH in CH_2Cl_2); $[\alpha]_D^{25}$ -14.6 (c 0.10 in MeOH) (lit.[vii] $[\alpha]_D^{21}$ -94.7 (MeOH)); ν_{max}/cm^{-1} (ATR) 3320w (N–H stretch), 2930w (C_{sp3}–H stretch), 1735s (C=O stretch in ester), 1220s (C–N stretch); δ_H (400 MHz, $CDCl_3$) 4.37 (1 H, d, *J* 9.5, *δ*-C*H*$_2$), 4.12 (1 H, d, *J* 9.5, *δ*-C*H*$_2$), 3.86 (1 H, t, *J* 7.5, *α*-C*H*), 3.78 (3 H, s, C*H*$_3$), 3.25 (1 H, dd, *J* 10.5 & 7.5, *β*-C*H*$_2$), 2.88 (1 H, dd, *J* 10.5 & 7.5, *β*-C*H*$_2$); δ_C (101 MHz, $CDCl_3$) 37.1 (*β*-*C*H$_2$), 52.7 (*C*H$_3$), 54.6 (*α*-*C*H), 65.3 (*δ*-*C*H$_2$), 171.9 (*C*=O); LC-MS (retention time: 1.47 min) *m/z* (ESI) 148 (M^+ + H, 100%).

B: To a solution of L-thiaproline (3.3 g, 25 mmol) in MeOH (50 ml) was added thionyl chloride (2.8 ml, 38 mmol) dropwise with vigorous stirring at 60 °C and the reaction mixture was refluxed for 3.0 h. Upon completion (TLC controlled – 5% MeOH in CH_2Cl_2) deionised water (25 ml) was added followed by saturated sodium bicarbonate (75 ml) and the reaction mixture was extracted with ether (4.0 × 100 ml), the combined organic extracts were dried over Na_2SO_4, filtered and the solvent was removed *in vacuo*, the crude oil was purified by flash column chromatography to furnish the desired compound **24** as a pale green oil (3.0 g; 83%); R_f 0.35 (5% MeOH in CH_2Cl_2); $[\alpha]_D^{25}$ -16.8° (c 0.10 in MeOH); ν_{max}/cm^{-1} (ATR)

[vii] S. Ratner and H.T. Clarke, *J. Am. Chem. Soc.*, 1937, **59**, 200.

3320w (N–H stretch), 2930w (C_{sp3}–H stretch), 1735s (C=O stretch in ester), 1220s (C–N stretch); δ_H (400 MHz, $CDCl_3$) 4.37 (1 H, d, *J* 9.5, *δ*-C*H*$_2$), 4.12 (1 H, d, *J* 9.5, *δ*-C*H*$_2$), 3.86 (1 H, t, *J* 7.5, *α*-C*H*), 3.78 (3 H, s, C*H*$_3$), 3.25 (1 H, dd, *J* 10.5, 7.5, *β*-C*H*$_2$), 2.88 (1 H, dd, *J* 10.5, 7.5, *β*-C*H*$_2$); δ_C (101 MHz, $CDCl_3$) 37.1 (*β*-*C*H$_2$), 52.7 (*C*H$_3$), 54.6 (*α*-*C*H), 65.3 (*δ*-*C*H$_2$), 171.9 (*C*=O); LC-MS (retention time: 1.47 min) *m/z* (ESI) 148 (M^+ + H, 100%).

(*S*)-Thiazolidine-4-carboxylic acid (25)

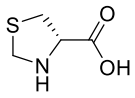

25

D-Cysteine hydrochloride (2.4 g, 15 mmol) was dissolved in aqueous MeOH 40% *v/v* (50 ml), thereto was added sodium bicarbonate (3.8 g, 45 mmol) and formalin 39% *w/w* (1.1 ml, 16 mmol). The thus obtained clear reaction mixture was stirred at ambient temperature overnight. Upon completion (LC-MS controlled) the clear reaction mixture was acidified using conc. HCl until it was acidic to Congo red and was concentrated *in vacuo*. The residue was purified using RP-HPLC (retention time: 10.5 – 12.3 min) (5.0 – 50% TFA (0.1% *v/v*) in MeCN/ TFA (0.1% *v/v*) in H_2O over 40 min; 3.0 ml min^{-1}, 40 °C) to furnish the desired compound **25** as a white fluffy powder (1.6 g; 80%); mp 190 – 192 °C (dec.) (lit.[viii] 202 – 204 °C); $[\alpha]_D^{25}$ +24.9 (c 0.10 in acetonitrile) (lit.[viii] $[\alpha]_D^{20}$ +141 (water)); ν_{max}/cm^{-1} (ATR) 3046w (C_{sp3}–H stretch), 1621vs (C=O stretch in carboxylic acid), 1286s (C–N stretch); δ_H (400 MHz, DMSO-*d*$_6$) 4.23 (1 H, d, *J* 9.0, *δ*-C*H*), 4.06 (1 H, d, *J* 9.0, *δ*-C*H*), 3.97 (1 H, t, *J* 7.0, *α*-C*H*), 3.13 (1 H, dd, *J* 10.0 & 7.0, *β*-C*H*), 2.88 (1 H, dd, *J* 10.0 & 7.0, *β*-C*H*); δ_C (101 MHz, DMSO-*d*$_6$) 36.0 (*β*-*C*H$_2$), 53.5 (*α*-*C*H), 65.0 (*δ*-*C*H$_2$), 172.3 (*C*=O); LC-MS (retention time: 1.37 min) *m/z* (ESI) 134 (M^+ + H, 100%).

[viii] S. Tadashi, S. Yujin, K. Masamitsu and K. Hidemoto, *Bull. Chem. Soc. Jpn.*, 1987, **60**, 3277.

Methyl (*S*)-thiazolidine-4-carboxylate (26)

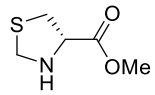

26

D-Cysteine methyl ester (3.5 g, 20 mmol) was dissolved in aqueous MeOH 40% *v/v* (100 ml), thereto was added sodium bicarbonate (1.9 g, 22 mmol) and formalin 39% *w/w* (1.4 ml, 18 mmol). The thus obtained clear reaction mixture was stirred at ambient temperature overnight. The pale yellow reaction mixture was extracted with CH_2Cl_2 (3.0 × 50 ml), the combined organic extracts were dried over Na_2SO_4, filtered and the solvent was removed *in vacuo*, the crude oil was purified by flash column chromatography to furnish the desired compound **26** as a pale green oil (2.5 g; 83%); R_f 0.35 (5.0% MeOH in CH_2Cl_2); $[\alpha]_D^{25}$ +25.7 (c 0.10 in MeOH); ν_{max}/cm^{-1} (ATR) 3320w (N–H stretch), 2930w (C_{sp3}–H stretch), 1735s (C=O stretch of ester), 1220s (C–N stretch); δ_H (400 MHz, $CDCl_3$) 4.37 (1 H, d, *J* 9.5, *δ*-C*H*), 4.12 (1 H, d, *J* 9.5, *δ*-C*H*), 3.86 (1 H, t, *J* 7.5, *α*-C*H*), 3.78 (3 H, s, CH_3), 3.25 (1 H, dd, *J* 10.5 & 7.5, *β*-C*H*), 2.88 (1 H, dd, *J* 10.5 & 7.5, *β*-C*H*); δ_C (101 MHz, $CDCl_3$) 37.1 (*β*-CH_2), 52.7 (CH_3), 54.6 (*α*-CH), 65.3 (*δ*-CH_2), 171.9 (*C*=O); LC-MS (retention time: 1.47 min) *m/z* (ESI) 148 (M^+ + H, 100%).

L-Cysteine (27)

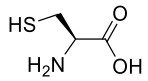

27

A: L-Thiaproline (13 mg, 0.1 mmol) and TCEP.HCl (43 mg, 0.2 mmol) were dissolved in deionised water (0.5 ml) and 1.0 M aqueous HCl (one drop) was added. The thus obtained clear reaction mixture was stirred at 40 °C for 2.0 days and purified using RP-HPLC (retention time: 20.1 – 20.2 min) (5.0 – 30% TFA (0.1% *v/v*) in MeCN/ TFA (0.1% *v/v*) in H_2O over 40 min; 3.0 ml min^{-1}, 40 °C) to furnish the desired compound **27** as a white fluffy powder (3.0 mg; 25%); δ_H (400 MHz, D_2O) 4.41 (1 H, t, *J* 7.0, *α*-C*H*), 4.07 (1 H, d, *J* 7.0, *β*-C*H*), 3.53 (1 H, d, *J* 7.0, *β*-C*H*); LC-MS (retention time: 1.33 min) *m/z* (ESI) 122 (M^+ + H, 100%).

B: L-Thiaproline (13 mg, 0.1 mmol) and $MeONH_3Cl$ (17 mg, 0.2 mmol) were dissolved in D_2O (0.5 ml) and the resulting clear reaction mixture was stirred at 40 °C for 16 days – the progress of the reaction was monitored using ^1H NMR and LC-MS; δ_H (400 MHz, D_2O) 4.41 (1 H, t, *J* 7.0, *α*-C*H*), 4.07 (1 H, d, *J* 7.0, *β*-C*H*), 3.53 (1 H, d, *J* 7.0, *β*-C*H*); δ_C (101 MHz, D_2O) 24.2 (*β*-CH_2), 55.0 (*α*-CH), 171.3 (*C*=O); LC-MS (retention time: 1.33 min) *m/z* (ESI) 122 (M^+ + H, 100%).

(*R*)-Thiazolidine-4-carbohydrazide (28)

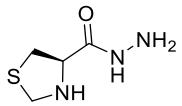

28

L-Thiaproline methyl ester (0.22 ml, 2.0 mmol) was dissolved in EtOH (2.0 ml) and thereto was added hydrazine monohydrate (0.44 ml, 18 mmol) in a sealed pressure vessel and stirred at 85 °C for 10 min. Upon completion (TLC controlled – 10% MeOH in CH_2Cl_2) aqueous sodium hypochlorite 5.0% *w/w* (10 ml) was added, thereafter the reaction mixture was concentrated and the remnant was purified by flash column chromatography to yield the desired compound **28** as a white solid (0.25 g; 83%); R_f 0.20 (10% MeOH in CH_2Cl_2); mp 110 – 111 °C (lit.[ix] 112 – 114 °C); $[\alpha]_D^{25}$ +37.0 (c 0.10 in MeOH); ν_{max}/cm^{-1} (ATR) 3273m (N–H stretch), 2930w (C_{sp3}–H stretch), 1644s (C=O stretch in hydrazide), 1208w (C–N stretch); δ_H (400 MHz, methanol-d_4) 4.20 – 4.09 (2 H, m, δ-CH_2), 3.91 (1 H, t, *J* 6.5, α-C*H*), 3.14 – 3.00 (2 H, m, β-CH_2); δ_C (101 MHz, methanol-d_4) 35.2 (β-*C*H_2), 52.8 (α-*C*H), 64.5 (δ-*C*H_2), 171.1 (*C*=O); LC-MS (retention time: 1.42 min) *m/z* (ESI) 148 (M^+ + H, 100%).

[ix] R. Nurdinov, É.É. Liepin'sh, I.B. Mazheika, I.Ya. Kalvin'sh, *Chem. Heterocycl. Compd.*, 1993, **29**, 1093.

(*R*)-*N*′-[(*R*)-Thiazolidine-4-carbonyl]thiazolidine-4-carbohydrazide (29)

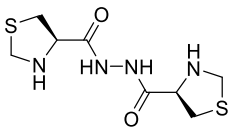

29

L-Thiaproline (0.52 g, 4.0 mmol) and K_2CO_3 (1.6 g, 12 mmol) were suspended in acetonitrile (20 ml) and thereto was added HATU (1.8 g, 5.0 mmol). The thus obtained pale green reaction mixture was vigorously stirred at ambient temperature for 15 min and the hydrazide **28** (0.57 g, 4.0 mmol) was added in one portion. The reaction mixture was further stirred at ambient temperature overnight. The solvent was removed *in vacuo* and the residue was purified by flash column chromatography to furnish the desired compound **29** as a yellow solid (0.61 g; 60%); R_f 0.40 (20% MeOH in CH_2Cl_2); mp 124 – 125 °C; ν_{max}/cm^{-1} (ATR) 3183w (N–H stretch), 2981w (C_{sp3}–H stretch), 1609s (C=O stretch in hydrazide), 1206w (C–N stretch); δ_H (400 MHz, methanol-d_4) 4.22 – 4.14 (4 H, m, 2 × δ-CH_2), 4.08 (2 H, dd, *J* 7.0 & 6.0, 2 × α-C*H*), 3.14 (4 H, dd, *J* 6.0, 4.0, 2 × β-CH_2); δ_C (101 MHz, methanol-d_4) 36.4 (β-*C*H_2), 54.3 (α-*C*H), 66.0 (δ-*C*H_2), 172.5 (*C*=O); LC-MS (retention time: 2.55 min) *m/z* (ESI) 130 (M^{2+} + 2 H, 100%); HRMS (ESI) calcd. for $C_8H_{15}N_4O_2S_2$ $[M+H]^+$ *m/z* = 263.0631, found: 263.0628.

(*R*)-*N*′-(L-Cysteinyl)-2-amino-3-mercaptopropanehydrazide (30)

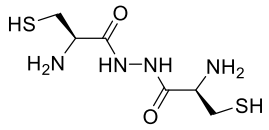

30

A: The hydrazide **29** (13 mg, 50 μmol) and TCEP.HCl (7.0 mg, 25 μmol) were intimately mixed and degassed under argon, thereto was added deionised water (0.50 ml) and stirred under argon at 85 °C for 24 h. The final reaction mixture was purified using RP-HPLC (retention time: 2.0 – 3.0 min) (1.0 – 2.0% TFA (0.1% *v/v*) in MeCN/ TFA (0.1% *v/v*) in H_2O over 10 min; 3.0 ml min^{-1}, 40 °C) to furnish the desired compound **30** as a white fluffy powder (3.5 mg; 30%); mp 210 – 212 °C (dec.); ν_{max}/cm^{-1} (ATR) 3368w (N–H asymmetric stretch), 3136m (N–H symmetric stretch), 2939m (C_{sp3}–H stretch), 1672s (C=O stretch in hydrazide), 1215m (C–N stretch); δ_H (400 MHz, D_2O) 4.27 (2 H, t, *J* 5.5, *α*-C*H*), 3.09 (2 H, d, *J* 5.5, *β*-CH_2); δ_C (101 MHz, D_2O) 24.8 (*β*-CH_2), 53.4 (*α*-*C*H), 167.3 (*C*=O); LC-MS (retention time: 1.56 min) *m/z* (ESI) 239 (M^+ + H, 100%); HRMS (ESI) calcd. for $C_6H_{15}N_4O_2S_2$ $[M+H]^+$ *m/z* = 239.0631, found: 239.0634.

B: The hydrazide **29** (100 mg, 0.4 mmol) and $MeONH_3Cl$ (160 mg, 2.0 mmol) were intimately mixed and degassed under argon, thereto was added deionised water (1.0 ml) and stirred under argon at 85 °C for 24 h. The final reaction mixture was purified using RP-HPLC (retention time: 2.0 – 3.0 min) (1.0 – 2.0% TFA (0.1% *v/v*) in MeCN/ TFA (0.1% *v/v*) in H_2O over 10 min; 3.0 ml min^{-1}, 40 °C) to furnish the desired compound **30** as a white fluffy powder (40 mg; 45%); mp 210 – 212 °C (dec.); ν_{max}/cm^{-1} (ATR) 3368w (N–H asymmetric stretch), 3136m (N–H symmetric stretch), 2939m (C_{sp3}–H stretch), 1672s (C=O stretch in hydrazide), 1215m (C–N stretch); δ_H (400 MHz, D_2O) 4.27 (2 H, t, *J* 5.5, *α*-C*H*), 3.09 (2 H, d, *J* 5.5, *β*-CH_2); δ_C (101 MHz, D_2O) 24.8 (*β*-CH_2), 53.4 (*α*-*C*H), 167.3 (*C*=O); LC-MS (retention time: 1.50 min) *m/z* (ESI) 239 (M^+ + H, 100%); HRMS (ESI) calcd. for $C_6H_{15}N_4O_2S_2$ $[M+H]^+$ *m/z* = 239.0631, found: 239.0634.

D,L-Homocysteine (31)

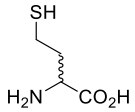

31

D,L-HCTL.HCl (3.1 g, 20 mmol) was dissolved in dry MeOH (40 ml), thereto was added methanolic solution of NaOMe 25% *w/w* (9.0 ml, 40 mmol) and stirred under argon at ambient temperature overnight. Upon completion (LC-MS controlled) the solvent was removed *in vacuo* and the remnant stirred in 1.0 M aqueous LiOH (20 ml) for 36 h. The thus obtained clear yellow solution was neutralised with glacial AcOH (4.0 ml) and the product was precipitated with acetone (200 ml). The crude was purified using RP-HPLC (retention time: 15.0 – 17.0 min) (1.0 – 5.0% TFA (0.1% *v/v*) in MeCN/ TFA (0.1% *v/v*) in H_2O over 50 min; 3.0 ml min^{-1}, 40 °C) to furnish the desired compound **31** as a white solid (2.6 g; 97%); δ_H (400 MHz, D_2O) 4.06 – 3.72 (1 H, m, *α*-C*H*), 7.59 – 7.48 (2 H, m, *γ*-C*H*$_2$), 2.08 – 1.98 (2 H, m, *β*-C*H*$_2$); δ_C (101 MHz, D_2O) 23.2 (*β*-*C*H_2), 34.6 (*γ*-*C*H_2), 53.5 (*α*-*C*H), 181.4 (*C*=O); LC-MS (retention time: 1.44 min) *m/z* (ESI) 136 (M^+ + H, 100%).

1,3-Thiazinane-4-carboxylic acid (32)

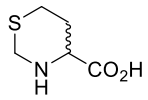

32

D,L-Homocysteine (3.0 g, 22 mmol) and sodium bicarbonate (1.7 g, 20 mmol) were suspended in aqueous MeOH 40% *v/v* (100 ml), the thus obtained cloudy mixture was stirred at ambient temperature for 15 min, followed by addition of formalin 39% *w/w* (1.6 ml, 18 mmol). The clear reaction mixture was stirred at ambient temperature for 2.5 h. Upon completion (LC-MS controlled) the clear reaction mixture was acidified using conc. HCl until it was acidic to Congo red and was concentrated *in vacuo*. The residue was purified using RP-HPLC (retention time: 10.5 – 12.3 min) (2.0 – 50% TFA (0.1% *v/v*) in MeCN/ TFA (0.1% *v/v*) in H_2O over 40 min; 3.0 ml min^{-1}, 40 °C) to furnish the desired compound **32** as a white fluffy powder (0.78 g; 24%); mp 210 – 212 °C (dec.) (lit.[x] 210 °C (dec.)); ν_{max}/cm^{-1} (ATR) 3390 – 2934w (O–H hydrogen bonding in carboxylic acid), 1581s (C=O stretch in carboxylic acid); δ_H (400 MHz, D_2O) 4.10 – 3.90 (2 H, m, *ε*-CH_2), 3.23 (1 H, dd, *J* 12.0 & 3.0, *α*-C*H*), 2.99 (1 H, ddd, *J* 13.5, 12.0 & 2.5, *γ*-C*H*), 2.77 (1 H, dtd, *J* 13.5, 3.5 & 2.0, *γ*-C*H*), 2.10 (1 H, dq, *J* 15.0 & 3.0, *β*-C*H*), 1.56 (1 H, dtd, *J* 15.0, 12.0 & 3.5, *β*-C*H*); δ_C (101 MHz, D_2O) 27.2 (*γ*-CH_2), 29.5 (*β*-CH_2), 46.8 (*ε*-CH_2), 60.6 (*α*-CH), 171.0 (*C*=O); LC-MS (retention time: 1.33 min) *m/z* (ESI) 148 (M^+ + H, 100%).

[x] J.H. Musser, K. Bailey and J.T. Suh, *Heterocycles*, 1985, **23**, 889.

Methyl-1,3-thiazinane-4-carboxylate (33)

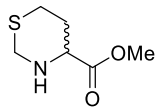

33

D,L-HCTL.HCl (3.1 g, 20 mmol) was dissolved in dry MeOH (40 ml), thereto was added a methanolic solution of NaOMe 25% *w/w* (9.0 ml, 40 mmol) and stirred under argon at ambient temperature in the dark for 22 h. The solvent was removed *in vacuo* and the residue was dissolved in 1.0 M LiOH (20 ml) and stirred under argon at ambient temperature for 6.0 h. Thereto was added deionised water (40 ml) and MeOH (40 ml) alongside glacial AcOH (~ 3.0 ml) so as to adjust the pH to 7.0, followed by formalin 39% *v/v* (1.6 ml) and the clear reaction mixture was stirred at ambient temperature under argon for 2.0 h. The solvent was removed *in vacuo* and the residue was suspended in MeOH (80 ml), thereto was added thionyl chloride (6.0 ml, 30 mmol) and the reaction mixture was stirred at 60 °C for 5.0 h. Thereafter the solvent was removed *in vacuo* and saturated sodium bicarbonate was added to adjust the pH to 7.0; the resulting cloudy mixture was extracted with EtOAc (4.0 × 50 ml), the combined organic extracts were dried over Na_2SO_4, filtered and the solvent was removed *in vacuo*, the crude oil was purified by flash column chromatography to furnish the desired compound **33** as an off-white solid (2.5 g; 78%); R_f 0.30 (5% MeOH in CH_2Cl_2); mp 48 – 49 °C; ν_{max}/cm^{-1} (ATR) 3323w (N–H stretch), 2910w (C_{sp3}–H stretch), 1731s (C=O stretch in ester), 1211vs (C–N stretch), 1123vs (C–O stretch), 737s (C–S stretch); δ_H (400 MHz, $CDCl_3$) 4.24 – 4.02 (2 H, m, ε-CH_2), 3.73 (3 H, s, CH_3), 3.54 (1 H, dd, *J* 11.5 & 3.0, α-C*H*), 3.05 (1 H, ddd, *J* 13.5, 11.5 & 3.0, γ-C*H*), 2.85 (1 H, dddd, *J* 13.5, 4.5, 3.5 & 2.0, γ-C*H*), 2.14 – 2.04 (1 H, m, β-C*H*), 1.67 (1 H, m, β-C*H*); δ_C (101 MHz, $CDCl_3$) 27.9 (γ -*C*H_2), 29.6 (β-*C*H_2), 49.0 (ε-CH_2), 52.1 (*C*H_3), 59.0 (α-*C*H), 172.8 (*C*=O); LC-MS (retention time: 1.54 min) *m/z* (ESI) 162 (M^+ + H, 100%); HRMS (ESI) calcd. for $C_6H_{12}NO_2S$ $[M+H]^+$ *m/z* = 162.0583, found: 162.0584.

1,3-Thiazinane-4-carbohydrazide (34)

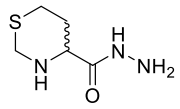

34

To a solution of the ester **33** (0.16 g, 1.0 mmol) in EtOH (2.0 ml) was added hydrazine monohydrate (0.1 ml, 2.0 mmol) in a sealed pressure vessel. The clear solution was stirred at 80 °C under argon for 4.0 h. Upon completion (TLC controlled – 20% MeOH in CH_2Cl_2) the solvent was removed *in vacuo* and the crude was purified by flash column chromatography to yield the desired compound **34** as a clear oil (55 mg; 34%); R_f 0.30 (20% MeOH in CH_2Cl_2); δ_H (400 MHz, acetonitrile-d_3) 4.08 – 3.92 (2 H, m, ε-CH_2), 3.30 (1 H, dd, *J* 11.0 & 3.0, α-C*H*), 2.98 (1 H, ddd, *J* 14.0, 12.0 & 3.0, γ-C*H*), 2.75 (1 H, dddd, *J* 13.5, 4.5, 3.5 & 2.5, γ-C*H*), 1.91 (1 H, m, β-C*H*), 1.62 (1 H, dddd, *J* 13.5, 12.0, 11.0 & 3.5, β-C*H*); δ_C (101 MHz, acetonitrile-d_3) 27.2 (γ-*C*H_2), 29.0 (β-*C*H_2), 48.3 (ε-CH_2), 58.2 (α-*C*H), 172.9 (*C*=O); LC-MS (retention time: 1.47 min) *m/z* (ESI) 162 (M^+ + H, 100%); HRMS (ESI) calcd. for $C_5H_{12}N_3OS$ $[M+H]^+$ *m/z* = 162.0696, found: 162.0694.

N′-(1,3-Thiazinane-4-carbonyl)-1,3-thiazinane-4-carbohydrazide (35)

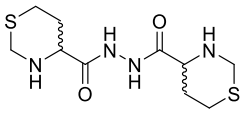

35

The thiazinane carboxylic acid **32** (40 mg, 0.25 mmol) and K_2CO_3 (0.10 g, 0.85 mmol) were suspended in acetonitrile (5.0 ml), thereto was added HATU (0.15 g, 0.40 mmol) and the resulting slurry was stirred at ambient temperature for 30 min, followed by addition of the thiazinane carbohydrazide **34** (50 mg, 0.25 mmol) and the resulting slurry was stirred at ambient temperature overnight. The solvent was removed *in vacuo* and the residue was purified by flash column chromatography to furnish the desired compound **35** as an off-white wax (40 mg; 56%); R_f 0.35 (20% MeOH in CH_2Cl_2); ν_{max}/cm^{-1} (ATR) 3233w (N–H stretch), 2952w (C_{sp3}–H stretch), 1589s (C=O stretch in hydrazide), 1221w (C–N stretch); δ_H (400 MHz, methanol-d_4) 4.17 – 4.00 (4 H, m, 2 × ε-CH_2), 3.48 (2 H, dd, *J* 10.5 & 3.0, 2 × α-C*H*), 2.99 (2 H, ddd, *J* 14.0, 11.0 & 3.0, 2 × γ-C*H*), 2.80 (2 H, dddd, *J* 13.5, 5.0, 3.5 & 1.5, 2 × γ-C*H*), 2.08 (2 H, ddt, *J* 13.5, 5.5 & 3.0, 2 × β-C*H*), 1.75 (2 H, dtd, *J* 14.0, 11.0 & 3.5, 2 × β-C*H*); δ_C (101 MHz, methanol-d_4) 28.1 (γ-*C*H_2), 30.1 (β-*C*H_2), 49.0 (ε-CH_2), 59.3 (α-*C*H), 173.3 (*C*=O); LC-MS (retention time: 1.63 min) *m/z* (ESI) 291 (M^+ + H, 100%); HRMS (ESI) calcd. for $C_{10}H_{19}N_4O_2S_2$ $[M+H]^+$ *m/z* = 291.0944, found: 291.0942.

2-Amino-*N′*-homocysteinyl-4-mercaptobutanehydrazide (36)

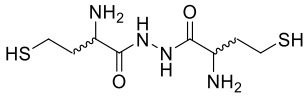

36

The carbohydrazide **35** (40 mg, 0.14 mmol) and $MeONH_3Cl$ (0.12 g, 1.4 mmol) were intimately mixed and degassed under argon, thereto was added D_2O (1.0 ml) and stirred under argon at 85 °C for 4.0 h. Upon completion (LC-MS controlled) the reaction mixture was purified using RP-HPLC (retention time: 10 – 11 min) (0.1 – 2.0% TFA (0.1% *v/v*) in MeCN/ TFA (0.1% *v/v*) in H_2O over 20 min; 4.0 ml min^{-1}, 40 °C) to furnish the desired compound **36** as a white fluffy powder (10 mg; 27%); mp 150 – 152 °C (dec.); ν_{max}/cm^{-1} (ATR) 3350w (N–H asymmetric stretch), 3287m (N–H symmetric stretch), 2912w (C_{sp3}–H stretch), 1655s (C=O stretch in carbohydrazide), 1241m (C–N stretch); δ_H (400 MHz, D_2O) 4.25 (2 H, dd, *J* 13.0 & 7.0, 2 × *α*-C*H*), 3.49 – 3.40 (4 H, m, 2 × *γ*-CH_2), 2.81 – 2.75 (2 H, m, 2 × *β*-C*H*), 2.22 (2 H, dt, *J* 13.0 & 7.0, 2 × *β*-C*H*); δ_C (101 MHz, D_2O) 27.9 (*γ*-CH_2), 29.0 (*β*-CH_2), 58.2 (*α*-CH), 205.9 (*C*=O); LC-MS (retention time: 1.63 min) *m/z* (ESI) 118 (M^+ + H, 100%); HRMS (ESI) calcd. for $C_8H_{19}N_4O_2S_2$ $[M+H]^+$ *m/z* = 267.0944, found: 267.0942.

(7a*R*,7'a*R*)-Tetrahydro-3*H*,3'*H*,5*H*,5'*H*,7*H*,7'*H*[6,6'-biimidazo[1,5-*c*]thiazole]-7,7'-dione (37)

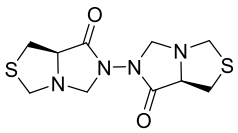

37

A: To a solution of dicysteinyl hydrazide **30** (10 mg, 50 µmol) in water (2.0 ml) was added cracked paraformaldehyde (10 equiv.) in D_2O (0.20 ml). The thus obtained clear mixture was stirred at ambient temperature for 48 h and purified using RP-HPLC (retention time: 16.1 – 16.5 min) (1.0 – 40% TFA (0.1% *v/v*) in MeCN/ TFA (0.1% *v/v*) in H_2O over 20 min; 4.0 ml min^{-1}, 40 °C) to furnish the desired compound **37** as a hygroscopic white fluffy powder (4.0 mg; 30%); ν_{max}/cm^{-1} (ATR) 2956w (C_{sp3}–H stretch), 1680s (C=O stretch in carbohydrazide), 1245m (C–N stretch); δ_H (600 MHz, acetonitrile-d_3) 4.52 (2 H, d, $^1J_{H\zeta\,H\zeta'}$ 5.4, 2 × ζ-C*H*), 4.21 (2 H, dd, $^1J_{H\zeta'\,H\zeta}$ 5.4 & $^4J_{H\zeta,H\alpha}$ 1.4, 2 × ζ'-C*H*), 4.16 (2 H, d, $^1J_{H\delta,H\delta'}$ 11.1, 2 × δ-C*H*), 4.09 (2 H, d, $^1J_{H\delta',H\delta}$ 11.1, 2 × δ'-C*H*), 4.01 (2 H, ddd, *J* 7.2, 3.6 & $^4J_{H\alpha\,H\zeta'}$ 1.4 Hz, 2 × α-C*H*), 3.18 (4 H, m, 2 × β-CH_2); δ_C (151 MHz, acetonitrile-d_3) 36.9 (β-CH_2), 62.3 (δ-CH_2), 67.2 (α-CH), 68.8 (ζ-CH_2), 171.7 (*C*=O); LC-MS (retention time: 4.2 min) *m/z* (ESI) 287 (M^+ + H, 100%); HRMS (ESI) calcd. for $C_{10}H_{14}N_4O_2S_2$ $[M+Na]^+$ *m/z* = 309.0450, found: 309.0452.

B: To a suspension of hydrazide **29** (25 mg, 0.10 mmol) in water (0.50 ml) was added cracked paraformaldehyde (5.0 equiv.) in D_2O (0.10 ml). The thus obtained cloudy mixture was stirred at ambient temperature for 6.0 days, and purified using RP-HPLC (retention time: 15.0 – 16.2 min) (1.0 – 40% TFA (0.1% *v/v*) in MeCN/ TFA (0.1% *v/v*) in H_2O over 20 min; 4.0 ml min^{-1}, 40 °C) to furnish the desired compound **37** as a white fluffy and hygroscopic powder (7.0 mg; 25%). This product was identical to that obtained from the preceding procedure as judged by ^1H and ^{13}C NMR, IR, LC-MS and HRMS.

(*E*)-(5-Nitrofuran-2-yl)methylene hydrazine (44)

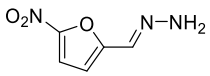

44

A: 5-Nitrofurfural (250 mg, 1.8 mmol) and anhydrous Na_2SO_4 (50 mg) were placed in a flame-dried reaction vessel, sealed and degassed under argon. Thereto was added anhydrous THF (1.0 ml) and stirred for 2.0 min, followed by addition of hydrazine monohydrate (0.10 ml, 2.0 mmol), and the thus obtained red mixture was stirred under argon at ambient temperature for 24 h. Upon completion – TLC controlled (5.0% methanol in CH_2Cl_2; R_f 0.20) – the dark red cloudy reaction mixture was diluted with deionised water (5.0 ml), and extracted with EtOAc (5.0 × 25 ml). The extracts were combined and dried over anhydrous Na_2SO_4, filtered and the solvent was removed *in vacuo* to afford crude hydrazide **44** (250 mg; 90%) as a red solid, which was further purified by flash column chromatography (EtOAc/cyclohexane, 1:5) to afford the desired product **44** (100 mg; 36%) as needle-like orange crystals; R_f 0.25 (80% EtOAc in cyclohexane); mp 153–154 °C (from acetonitrile) (lit.[xi] 164 °C *dec.*); δ_H (400 MHz, acetonitrile-d_3) 7.58 (1 H, s, CC*H*N unsaturated), 7.43 (1 H, d, *J* 3.9, C*H*-Ar), 6.66 (1 H, d, *J* 3.9, C*H*-Ar); δ_C (101 MHz, DMSO-d_6) 108.8 (*C*H-Ar), 116.1 (*C*H-Ar), 123.7 (*CC*HN unsaturated); LC-MS (retention time: 3.87 min) *m/z* (ESI) 156 (M^+ + H, 100%); HRMS (ESI) calcd. for $C_5H_5N_3O_3$ $[M+H]^+$ *m/z* 156.0404, found 156.0403.

B: 5-Nitrofurfural (2.5 g, 18 mmol) and anhydrous Na_2SO_4 (300 mg, 1.8 mmol) were intimately mixed and cooled in an ice-bath, thereto was added THF (10 ml), followed by hydrazine monohydrate (1.0 ml, 20 mmol). The thus obtained red mixture was stirred for 2.0 h, and then purified by flash column chromatography (EtOAc/cyclohexane, 1:5) to afford the desired product **44** (1.7 g, 62%) as an orange solid. This product was identical to that obtained from the preceding procedure as judged by ^1H and ^{13}C NMR, melting point, LC-MS and HRMS.

[xi] R. Hull, *GB816886 (A)*, Imp. Chem. Ind., Imp. Chem. House, Millbank, London, SW1, 1959.

5-Nitrofuran-2-yl methanamine (47)

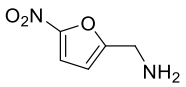

47

5-Nitrofurfural (250 mg, 1.8 mmol) and sodium triacetoxyborohydride (570 mg, 2.7 mmol) were degassed under argon and cooled in an ice-bath, 0.50 M ammoniacal 1,4-dioxane (4.0 ml, 2.0 mmol) was added therein, followed by glacial AcOH (5.0 drops). The thus obtained dark red mixture was stirred at ambient temperature for 2.0 h. The neutral slurry (pH ~ 7.5) was purified by flash column chromatography (methanol/CH_2Cl_2, 1:9) to afford the desired amine **47** (210 mg; 78%) as an orange oil; R_f 0.20 (80% EtOAc in cyclohexane); δ_H (400 MHz, acetonitrile-d_3) 7.36 (1 H, d, *J* 3.7, C*H*-Ar), 6.59 (1 H, d, *J* 3.7, C*H*-Ar), 4.56 (2 H, s, α-CH_2); δ_C (101 MHz, acetonitrile-d_3) 57.3 (α-*C*H_2), 111.4 (*C*H-Ar), 113.9 (*C*H-Ar), 160.0 (2 × *C*-Ar); LC-MS (retention time: 3.38 min) *m/z* (ESI) 144 (M^+ + H, 100%); HRMS (ESI) calcd. for $C_5H_6N_2O_3$ $[M+H]^+$ *m/z* 143.0451, found 143.0452.

Methyl (2-chlorophenyl)methanesulfonimidate (50)

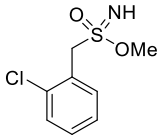

50

Sulfonimidate **50** was synthesised according to the previously published procedure[xii] with some modification which as follows:

To a solution of 2-chlorobenzyl mercaptan (130 µl, 1.0 mmol) in methanol (5.0 ml) was added simultaneously ammonium carbamate (625 mg, 8.0 mmol) alongside iodobenzene diacetate (2.6 g, 8.0 mmol), and the thus obtained cloudy reaction mixture which later turned clear yellow in colour was stirred at ambient temperature for 2.0 h. The reaction mixture was purified by flash column chromatography (methanol/CH_2Cl_2, 1:20) to give the desired sulfonimidate **50** (40 mg; 25%) as a pale yellow wax; R_f 0.30 (10% methanol in CH_2Cl_2); δ_H (400 MHz, methanol-d_4) 7.61 – 7.51 (1 H, m, *o*-C*H*-Ar), 7.50 – 7.41 (1 H, m, C*H*-Ar), 7.40 – 7.28 (2 H, m, 2 × C*H*-Ar), 4.83 – 4.47 (4 H, m, S=N*H* & O–CH_3), 3.94 – 3.68 (2 H, m, Ph–CH_2); δ_C (101 MHz, methanol-d_4) 56.0 (Ph–*C*H_2), 56.5 (O–*C*H_3), 128.1 (*C*H-Ar), 130.8 – 131.1 (2 × *C*H-Ar), 134.2 (*C*H-Ar), 134.3 – 136.2 (2 × *C*-Ar); LC-MS (retention time: 2.60 min) *m/z* (ESI) 221 (M^+ + H, 100%).

[xii] M. Zenzola, R. Doran, L. Degennaro, R. Luisi and J. A. Bull, *Angew. Chem. Int. Ed.*, 2016, **55**, 7203.

1,2-Bis(2-chlorobenzyl)disulfane (51)

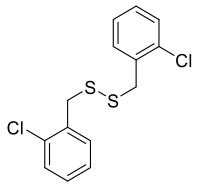

51

Disulfane **51** was synthesised according to the previously published procedure[xii] with some modification which as follows:

To a solution of 2-chlorobenzyl mercaptan (130 µl, 1.0 mmol) in methanol (5.0 ml) was added simultaneously ammonium carbamate (312 mg, 4.0 mmol) alongside iodobenzene diacetate (1.3 g, 4.0 mmol), and the thus obtained cloudy reaction mixture which rapidly turned clear yellow in colour was stirred at ambient temperature for 2.0 h. The reaction mixture was purified by flash column chromatography (EtOAc/cyclohexane, 1:9) to give the unwanted disulfane **51** (80 mg; 37%) as a yellow oil; R_f 0.20 (15% EtOAc in cyclohexane); δ_H (400 MHz, $CDCl_3$) 7.30 (2 H, m, 2 × C*H*=CCl-Ar), 7.23 – 7.11 (6 H, m, 6 × C*H*-Ar), 3.71 (4 H, s, 2 × Ph–CH_2); δ_C (101 MHz, $CDCl_3$) 41.3 (2 × Ph–*C*H_2), 126.9 – 131.7 (8 × *C*H-Ar), 134.3 & 135.1 (4 × *C*-Ar); LC-MS (retention time: 9.25 min) *m/z* (ESI) 359 (M^+ + formate, 18%), 358 (100), 231 (10).

Benzenesulfonimidic acid (53)

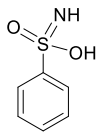

53

Sulfonimidic acid **53** was synthesised according to the previously published procedure[xii] with some modification which as follows:

To a solution of phenyl mercaptan (50 µl, 0.50 mmol) in methanol (2.0 ml) was added ammonium carbamate (160 mg, 4.0 mmol), followed by iodobenzene diacetate (650 mg, 4.0 mmol), and the thus obtained clear yellow reaction mixture was stirred at ambient temperature for 2.0 h. The reaction mixture was purified by flash column chromatography (EtOAc/cyclohexane, 1:2) to give the unexpected sulfonimidic acid **53** (10 mg; 12%) as a pale yellow wax; R_f 0.20 (30% EtOAc in cyclohexane); δ_H (400 MHz, $CDCl_3$) 8.02 – 7.81 (2 H, m, 2 × *o*-C*H*-Ar), 7.60 (1 H, m, *p*-C*H*-Ar), 7.56 – 7.50 (2 H, m, 2 × *m*-C*H*-Ar); δ_C (101 MHz, $CDCl_3$) 126.6 (2 × *o*-*C*H-Ar), 129.3 (2 × *m*-*C*H-Ar), 133.0 (*p*-*C*H-Ar); LC-MS (retention time: 3.52 min) *m/z* (ESI) 158 (M^+ + H, 61%), 141 (100), 105 (18).

(*E*)-1-(4-Bromophenyl)-*N*′-5-nitrofuran-2-ylmethylene methanesulfonohydrazide (54)

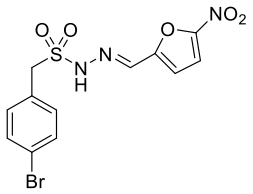

54

p-Bromobenzyl sulfonyl chloride (270 mg, 1.0 mmol) and hydrazone **44** (190 mg, 1.2 mmol) were intimately mixed and thereto was added THF (10 ml), followed by pyridine (1.6 ml, 20 mmol). The thus obtained slurry was stirred at ambient temperature for 5.0 h, and purified by flash column chromatography (EtOAc/cyclohexane, 1:3) to give the desired nitrofuranyl sulfonohydrazide **54** (170 mg; 44%) as a yellow wax; R_f 0.20 (40% EtOAc in cyclohexane); ν_{max}/cm^{-1} (ATR) 3342w (N–H asymmetric stretch), 3286m (N–H symmetric stretch), 3100w (C_{sp2}–H stretch), 2905w (C_{sp3}–H stretch), 1682 – 1660s (C=C & C=N stretches), 1389s (N–O asymmetric stretch), 1329m (N–O symmetric stretch), 1220vs (C–N asymmetric stretch), 1212w (C–N symmetric stretch), 1135s (SO_2 sulfone stretch), 1124s (C–O asymmetric stretch), 1072s (C–O symmetric stretch), 740vs (CH_2, rocking); δ_H (400 MHz, acetonitrile-d_3) 9.46 (1 H, s, SN*H*N), 7.76 (1 H, s, NHN=C*H*), 7.55 (2 H, m, 2 × *o*-C*H*-Ar), 7.48 (1 H, d, *J* 3.9, C^4*H*-Ar), 7.28 (2 H, m, 2 × *m*-C*H*-Ar), 6.98 (1 H, d, *J* 3.9, C^3*H*-Ar), 4.50 (2 H, s, Ph–CH_2); δ_C (101 MHz, acetonitrile-d_3) 57.4 (Ph–*C*H_2), 114.5 (*C*^{4}H-Ar), 115.8 (*C*^{3}H-Ar), 123.5 (*ipso*-*C*-Ar), 129.2 (*p*-*C*-Ar), 132.8 (2 × *o*-*C*H-Ar), 134.0 (2 × *m*-*C*H-Ar), 135.7 (NHN=*C*H), 152.8 (*C*-Ar furan); LC-MS (retention time: 7.06 min) *m/z* (ESI) 388 & 390 (1:1) (M^+ + H, 100%).

Ethyl 7-isopropyl-1*H*indole-2-carboxylate (56)

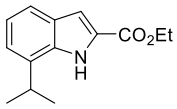

56

Oven-dried molecular sieves 4Å (10 g) were degassed under argon, thereto was added *o*-isopropylaniline (5.2 ml, 37 mmol) together with ethyl pyruvate (8.2 ml, 74 mmol) and toluene (24 ml); the thus obtained reaction mixture was stirred under argon at ambient temperature for 18 h. The resulting dark yellow reaction mixture was filtered through a pad of cotton wool, rinsed with EtOAc and concentrated *in vacuo*. Thereto was added $Cu(OAc)_2$ (10 g, 55 mmol) alongside $Pd(OAc)_2$ (0.83 g, 3.7 mmol), sealed and degassed under argon, DMSO (160 ml) was added therein and stirred under argon at 40 °C for 24 h. Upon completion – TLC controlled (25% EtOAc in cyclohexane; R_f 0.35) – the resulting green slurry was filtered through Celite® and rinsed with EtOAc (250 ml). Thereto was added 1.0 M HCl_{aq} (300 ml), the organic layer was separated and the aqueous was further extracted with EtOAc (250 ml). The extracts were combined, washed with brine (250 ml), dried over anhydrous Na_2SO_4 and the solvent was removed *in vacuo*. The thus obtained residue was purified by flash column chromatography (EtOAc/cyclohexane, 1:3) to give the desired carboxylate ethyl ester **56** (5.5 g; 64%) as a yellow solid; R_f 0.30 (25% EtOAc in cyclohexane); mp 90–94 °C (from EtOAc); ν_{max}/cm^{-1} (ATR) 3390 – 3270w (N–H asymmetric & symmetric stretches), 1762s (conj. C=O carboxyl ester stretch); δ_H (400 MHz, $CDCl_3$) 9.22 (1 H, s, N*H*-InC), 7.41 (1 H, dd, *J* 7.9 & 1.1, C^4*H*-Ar), 7.15 (1 H, d, *J* 2.1, C^3*H*-Ar), 7.09 – 6.97 (2 H, m, 2 × C*H*-Ar), 4.31 (2 H, q, *J* 7.1, *α*-CH_2), 3.20 (1 H, hept, *J* 6.9, C*H*-^{i}Pr), 1.29 (3 H, t, *J* 7.1, *β*-CH_3), 1.24 (6 H, d, *J* 6.9, CH(CH_3)$_2$); δ_C (101 MHz, $CDCl_3$) 14.5 (*β*-CH_3), 22.7 (CH(CH_3)$_2$), 29.0 (*C*H-^{i}Pr), 61.0 (*α*-CH_2), 109.3 (C^3H-Ar), 120.2 (C^4H-Ar), 120.9 (C^6H-Ar), 121.2 (C^5H-Ar), 127.2 – 135.7 (4 × *C*-Ar), 162.5 (*C*=O InC ester); LC-MS (retention time: 8.36 min) *m/z* (ESI) 232 (M^+ + H, 100%).

Ethyl 3-iodo-7-isopropyl-1*H*indole-2-carboxylate (57)

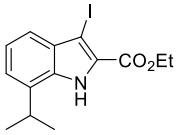

57

To a solution of InC ethyl ester **56** (1.5 g, 6.5 mmol) in CH_2Cl_2 (20 ml) was added NIS (1.5 g, 6.8 mmol) and the thus obtained reaction mixture was stirred at ambient temperature for 12 h. Saturated $NaHCO_{3aq}$ (20 ml) was added therein and extracted with CH_2Cl_2 (6.0 × 20 ml). The extracts were combined, washed with brine (50 ml), dried over anhydrous Na_2SO_4 and the solvent was removed *in vacuo* to give a yellow solid which was further purified by flash column chromatography (EtOAc/cyclohexane, 1:4) to give the desired iodo-InC ethyl ester **57** (2.2 g; 97%) as a coral pink solid; R_f 0.30 (20% EtOAc in cyclohexane); mp 102–105 °C (from EtOAc); ν_{max}/cm^{-1} (ATR) 3350 – 3210w (N–H asymmetric & symmetric stretches), 1720s (conj. C=O carboxyl ester stretch), 520m (C–I stretch); δ_H (400 MHz, $CDCl_3$) 9.20 (1 H, s, N*H*-InC), 7.32 (1 H, dd, *J* 7.8 & 1.3, C*H*-Ar), 7.23 – 7.00 (2 H, m, 2 × C*H*-Ar), 4.38 (2 H, q, *J* 7.1, *α*-CH_2), 3.19 (1 H, hept, *J* 6.9, C*H*-^{i}Pr), 1.39 (3 H, t, *J* 7.1, *β*-CH_3), 1.27 (6 H, d, *J* 6.9, CH(CH_3)$_2$); δ_C (101 MHz, $CDCl_3$) 14.5 (*β*-*C*H$_3$), 22.8 (CH(*C*H$_3$)$_2$), 28.8 (*C*H-^{i}Pr), 61.6 (*α*-*C*H$_2$), 121.2 – 122.3 (3 × *C*H-Ar), 127.1 – 134.7 (5 × *C*-Ar), 161.3 (*C*=O InC ester); LC-MS (retention time: 9.25 min) *m/z* (ESI) 358 (M^+ + H, 100%).

Ethyl 7-isopropyl-3-(4,4,5,5-tetramethyl-1,3,2-dioxaborolan-2-yl)-1*H*indole-2-carboxylate (58)

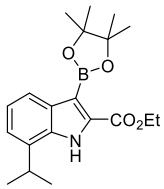

58

A pressure reaction vessel was charged with InC **57** (0.18 g, 0.50 mmol), bis(pinacolato)diboron (0.17 g, 0.70 mmol), BrettPhos Pd G3 (45 mg, 50 µmol), potassium acetate (0.20 g, 2.0 mmol), sealed and degassed under argon. Thereto was added degassed 1,4-dioxane (2.0 ml) and the thus obtained reaction mixture was irradiated in a microwave reactor at 105 °C for 10 min. The resulting tarry reaction mixture was filtered through Celite® and rinsed with EtOAc (25 ml). Thereto was added deionised water (25 ml), the organic layer was separated and the aqueous was further extracted with EtOAc (25 ml). The extracts were combined, washed with brine (25 ml), dried over anhydrous Na_2SO_4 and the solvent was removed *in vacuo* to give a brown solid, which was further purified by flash column chromatography (EtOAc/cyclohexane, 1:9) to give the desired boronate ester **58** (50 mg; 28%) as a green wax; R_f 0.30 (20% EtOAc in cyclohexane); ν_{max}/cm^{-1} (ATR) 3430 – 3310w (N–H asymmetric & symmetric stretches), 1790s (conj. C=O carboxyl ester stretch), 1391s (B–O stretch); δ_H (400 MHz, $CDCl_3$) 9.10 (1 H, s, N*H*-InC), 7.91 – 7.67 (1 H, m, C*H*-Ar), 7.22 – 7.08 (2 H, m, 2 × C*H*-Ar), 4.44 (2 H, q, *J* 7.1, *α*-CH_2), 3.25 (1 H, hept, *J* 6.9, C*H*-^{i}Pr), 1.49 – 1.32 (22 H, m); δ_C (101 MHz, $CDCl_3$) 14.6 (*β*-*C*H_3), 22.8 (2 × *C*H_3-^{i}Pr), 25.1 (4 × *C*H_3-pin), 29.4 (*C*H-^{i}Pr), 61.4 (*α*-*C*H_2), 83.7 (2 × *C*–O-pin), 121.0 – 121.6 (3 × *C*H-Ar), 131.8 – 135.3 (4 × *C*-Ar), 162.7 (*C*=O InC ester); δ_B (128 MHz, $CDCl_3$) 31.0; LC-MS (retention time: 9.51 min) *m/z* (ESI) 359 (M^+ + H, 100%).

Ethyl 3-bromo-7-isopropyl-1*H*indole-2-carboxylate (61)

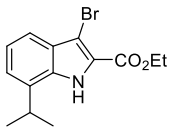

61

A solution of InC ethyl ester **56** (0.23 g, 1.0 mmol) in CH_2Cl_2 (3.0 ml) was cooled in an ice-bath, thereto was added NBS (0.20 g, 1.1 mmol) and the thus obtained orange reaction mixture was stirred for 1.0 h. Saturated $NaHCO_{3aq}$ (5.0 ml) was added therein and extracted with CH_2Cl_2 (6.0 × 20 ml). The extracts were combined, washed with brine (25 ml), dried over anhydrous Na_2SO_4 and the solvent was removed *in vacuo* to give a yellow wax, which was further purified by flash column chromatography (EtOAc/cyclohexane, 1:6) to give the desired mono bromo-InC ethyl ester **61** (0.20 g; 86%) in >90% purity as a yellow solid; R_f 0.20 (15% EtOAc in cyclohexane); mp 115–120 °C (from EtOAc); ν_{max}/cm^{-1} (ATR) 3310 – 3205w (N–H asymmetric & symmetric stretches), 1751s (conj. C=O carboxyl ester stretch), 680m (C–Br stretch); δ_H (400 MHz, $CDCl_3$) 9.34 (1 H, s, N*H*-InC), 7.57 (1 H, m, C*H*-Ar), 7.32 – 7.19 (2 H, m, 2 × C*H*-Ar), 4.52 (2 H, q, *J* 7.1, *α*-CH_2), 3.34 (1 H, hept, *J* 6.9, C*H*-^{i}Pr), 1.51 (3 H, t, *J* 7.1, *β*-CH_3), 1.40 (6 H, d, *J* 6.9, CH(CH_3)$_2$); δ_C (101 MHz, $CDCl_3$) 14.3 (*β*-*C*H$_3$), 22.7 (CH(*C*H$_3$)$_2$), 28.5 (*C*H-^{i}Pr), 61.4 (*α*-*C*H$_2$), 98.8 (C^3-Ar), 118.8 – 122.1 (3 × *C*H-Ar), 128.0 – 134.0 (4 × *C*-Ar), 161.5 (*C*=O InC ester); LC-MS (retention time: 9.10 min) *m/z* (ESI) 310 & 312 (1:1) (M^+ + H, 100%).

Ethyl (*E*)-7-isopropyl-3-[2-((5-nitrofuran-2-yl)methylene)hydrazineyl]-1*H*indole-2-carboxylate (60)

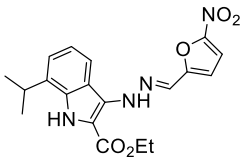

60

InC ethyl ester **61** (0.25 g, 0.81 mmol), hydrazone **44** (0.15 g, 0.97 mmol), Cs_2CO_3 (0.53 g, 1.6 mmol), BrettPhos Pd G3 (72 mg, 81 µmol) and BrettPhos (44 mg, 81 µmol) were intimately mixed, sealed and degassed under argon. Thereto was added anhydrous degassed THF (20 ml), and the thus obtained dark red reaction mixture was stirred under a partial flow of argon at 80 °C for 2.0 h. The resulting tarry reaction mixture was filtered through Celite® and rinsed with EtOAc (25 ml). Thereto was added deionised water (25 ml), the organic layer was separated and the aqueous was further extracted with EtOAc (5.0 × 25 ml). The extracts were combined, washed with brine (25 ml), dried over anhydrous Na_2SO_4 and the solvent was removed *in vacuo* to give an orange wax, which was further purified by flash column chromatography (methanol/CH_2Cl_2, 1:9) to give the desired NInC ethyl ester **60** (70 mg; 23%) as a dark red solid; R_f 0.30 (10% methanol in CH_2Cl_2); ν_{max}/cm^{-1} (ATR) 3435 – 3260w (N–H asymmetric & symmetric stretches), 1771s (conj. C=O carboxyl ester stretch), 1415s (N–O asymmetric stretch), 1350m (N–O symmetric stretch), 1260vs (C–N asymmetric stretch), 1234w (C–N symmetric stretch); δ_H (400 MHz, $CDCl_3$) 10.04 (1 H, s, N*H*-InC), 8.17 (1 H, d, *J* 9.0, CC*H*N unsaturated), 7.90 (1 H, s, N*H*-hydrazone), 7.51 (1 H, m, C*H*-Ar indole), 7.32 (1 H, d, *J* 3.8, C^4*H*-Ar furan), 7.24 – 7.00 (2 H, m, 2 × C*H*-Ar indole), 6.75 (1 H, d, *J* 3.8, C^3*H*-Ar furan), 4.37 (2 H, q, *J* 7.1, *α*-CH_2), 3.14 (1 H, hept, *J* 6.9, C*H*-^{i}Pr), 1.38 (3 H, t, *J* 7.1, *β*-CH_3), 1.32 (6 H, d, *J* 6.9, CH(CH_3)$_2$); δ_C (101 MHz, $CDCl_3$) 14.8 (*β*-CH_3), 22.8 (CH(CH_3)$_2$), 28.8 (*C*H-^{i}Pr), 61.0 (*α*-CH_2), 107.5 (C^3-Ar indole), 109.1 – 114.5 (2 × *C*H-Ar furan), 118.4 (*C*-Ar indole), 120.9 (C^4H-Ar indole), 121.8 (C*C*HN unsaturated), 123.2 – 125.0 (2 × *C*H-Ar indole), 131.9 – 134.8 (4 × *C*-Ar indole), 151.5 – 154.3 (2 × *C*-Ar furan), 162.4 (*C*=O InC ester); LC-MS (retention time: 8.76 min) *m/z* (ESI) 385 (M^+ + H, 100%).

Improved Method: InC ethyl ester **61** (0.20 g, 0.65 mmol), hydrazone **44** (0.12 g, 0.78 mmol), Cs_2CO_3 (0.65 g, 2.0 mmol), BrettPhos Pd G4 (64 mg, 70 µmol) and BrettPhos (38 mg, 70 µmol) were intimately mixed, sealed and degassed under argon. Thereto was added anhydrous degassed THF (15 ml), and the thus obtained dark red reaction mixture was stirred under a partial flow of argon at 80 °C for 2.0 h. The resulting tarry reaction mixture was filtered through Celite® and rinsed with EtOAc (25 ml). Thereto was added deionised water (25 ml), the organic layer was separated and the aqueous was further extracted with EtOAc (5.0 × 25 ml). The extracts were combined, washed with brine (25 ml), dried over anhydrous Na_2SO_4 and the solvent was removed *in vacuo* to give an orange wax, which was further purified by flash column chromatography (EtOAc/cyclohexane, 1:4) to give the desired NInC ethyl ester **60** (0.12 g; 48%) as a dark red solid; R_f 0.25 (30% EtOAc in cyclohexane). This product was identical to that obtained from the preceding procedure as judged by ^{1}H and ^{13}C NMR, IR and LC-MS.

3-Iodo-7-isopropyl-1*H*indole-2-carboxylic acid (64)

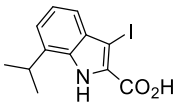

64

InC ethyl ester **57** (0.18 g, 0.50 mmol) and lithium hydroxide monohydrate (0.21 g, 2.5 mmol) were dissolved in THF (2.0 ml) and deionised water (1.0 ml). The thus obtained clear reaction mixture was stirred at ambient temperature for 24 h. Upon completion – TLC controlled (5.0% methanol in CH_2Cl_2; R_f 0.30) – the reaction mixture was washed with EtOAc (2.0 × 25 ml), the aqueous layer was collected and acidified with formic acid until acidic to Congo red; followed by extraction with EtOAc (5.0 × 25 ml). The extracts were combined and dried over anhydrous Na_2SO_4, filtered and the solvent was removed *in vacuo* to afford crude carboxylic acid **64** (0.16 g; 97%) as an orange wax, which was further purified by flash column chromatography (methanol/CH_2Cl_2, 1:18) to afford the desired product **64** (0.15 g; 91%) as a yellow solid; R_f 0.25 (5.0% methanol in CH_2Cl_2 + 1.0% formic acid); ν_{max}/cm^{-1} (ATR) 3410m (N–H stretch), 3321 – 2476br (O–H H-bonding stretch), 1685s (C=O carboxylic acid stretch), 550m (C–I stretch); δ_H (400 MHz, $CDCl_3$) 9.26 (1 H, s, N*H*-InC), 7.47 (1 H, dd, *J* 8.0 & 1.0, C*H*-Ar), 7.37 – 7.23 (2 H, m, 2 × C*H*-Ar), 3.33 (1 H, hept, *J* 6.9, C*H*-^{i}Pr), 1.44 (6 H, d, *J* 6.9, CH(CH_3)$_2$); δ_C (101 MHz, $CDCl_3$) 22.8 (CH(*C*H_3)$_2$), 29.1 (*C*H-^{i}Pr), 121.6 – 123.2 (3 × *C*H-Ar), 131.9 – 135.3 (5 × *C*-Ar), 166.1 (*C*=O carboxylic acid); LC-MS (retention time: 7.70 min) *m/z* (ESI) 330 (M^+ + H, 100%).

Heptyl 1*H*indole-2-carboxylate (66)

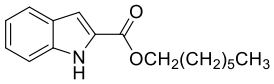

66

A pressure reaction vessel was charged with 1*H*-indole-2-carboxylic acid (0.16 g, 1.0 mmol) and dissolved in *n*-heptanol (1.5 ml, 10 mmol) at 80 °C, thereto was added thionyl chloride (0.10 ml, 1.5 mmol), sealed and stirred at 80 °C for 3.0 h. Upon completion – TLC controlled (10% EtOAc in cyclohexane; R_f 0.30) – the thus obtained reaction mixture was concentrated *in vacuo*, saturated $NaHCO_{3aq}$ (5.0 ml) was added and extracted with EtOAc (5.0 × 25 ml). The extracts were combined, washed with brine (2.0 × 20 ml), dried over anhydrous Na_2SO_4, filtered and the solvent was removed *in vacuo* to afford crude ester **66** (0.23 g; 89%) as a yellow wax, which was further purified by flash column chromatography (EtOAc/cyclohexane, 1:9) to afford the desired product **66** (0.19 g; 73%) as a white solid; R_f 0.25 (10% EtOAc in cyclohexane); ν_{max}/cm^{-1} (ATR) 3361 – 3290w (N–H asymmetric & symmetric stretches), 1751s (conj. C=O carboxyl ester stretch); δ_H (400 MHz, $CDCl_3$) 8.91 (1 H, s, N*H*-InC), 7.69 (1 H, ddd, *J* 8.1, 7.0 & 1.0, C^6*H*-Ar), 7.43 (1 H, dd, *J* 8.3 & 1.0, C^4*H*-Ar), 7.32 (1 H, ddd, *J* 8.3, 7.0 & 1.2, C^5*H*-Ar), 7.23 (1 H, dd, *J* 2.2 & 1.0 Hz, C^3*H*-Ar), 7.16 (1 H, dd, *J* 8.1 & 1.2, C^7*H*-Ar), 4.35 (2 H, t, *J* 6.7, *α*-CH_2), 1.85 – 1.72 (2 H, m, *β*-CH_2), 1.53 – 1.20 (8 H, m, *γ*-CH_2 –[…]–*ζ*- CH_2), 1.05 – 0.74 (3 H, m, *η*-CH_3); δ_C (101 MHz, $CDCl_3$) 14.2 (*η*-*C*H_3), 22.7 (*ζ*-*C*H_2), 25.1 (*ε*-*C*H_2), 28.9 (*δ*-*C*H_2), 29.1 (*γ*-*C*H_2), 31.9 (*β*-*C*H_2), 65.3 (*α*-*C*H_2), 108.7 (*C*^{3}H-Ar), 112.0 (*C*^{4}H-Ar), 120.9 (*C*^{7}H-Ar), 122.7 (*C*^{6}H-Ar), 125.5 (*C*^{5}H-Ar), 127.7 – 136.9 (2 × *C*-Ar), 162.2 (*C*=O InC ester); LC-MS (retention time: 9.51 min) *m/z* (ESI) 260 (M^+ + H, 100%).

Methyl 7-isopropyl-1*H*indole-2-carboxylate (67)

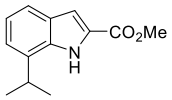

67

Oven-dried molecular sieves 4Å (35 g) were degassed under argon, thereto was added *o*-isopropylaniline (14.5 ml, 0.10 mol) together with methyl pyruvate (18 ml, 0.20 mol) and toluene (500 ml); the thus obtained reaction mixture was stirred under argon at ambient temperature for 18 h. The resulting dark yellow reaction mixture was filtered through a pad of cotton wool, rinsed with EtOAc and concentrated *in vacuo*. Thereto was added $Cu(OAc)_2$ (27 g, 0.15 mol) alongside $Pd(OAc)_2$ (2.3 g, 10 mmol), sealed and degassed under argon, DMSO (400 ml) was added therein and stirred under argon at 40 °C for 48 h. Upon completion – TLC controlled (25% EtOAc in cyclohexane; R_f 0.35) – the resulting green slurry was filtered through Celite® and rinsed with EtOAc (500 ml). Thereto was added 1.0 M HCl_{aq} (500 ml), the organic layer was separated and the aqueous was further extracted with EtOAc (250 ml). The extracts were combined, washed with brine (2.0 × 250 ml), dried over anhydrous Na_2SO_4 and the solvent was removed *in vacuo*. The thus obtained residue was further purified by recrystallisation from minimal amount of hot EtOAc to furnish the desired carboxylate methyl ester **67** (8.2 g; 40%) as light brown rock salt crystals; R_f 0.30 (25% EtOAc in cyclohexane); mp 98–99 °C (from EtOAc); ν_{max}/cm^{-1} (ATR) 3389 – 3273w (N–H asymmetric & symmetric stretches), 1759s (conj. C=O carboxyl ester stretch); δ_H (400 MHz, $CDCl_3$) 9.07 (1 H, s, N*H*-InC), 7.58 (1 H, d, *J* 7.9, C^4*H*-Ar), 7.29 (1 H, d, *J* 2.1, C^3*H*-Ar), 7.25 – 7.14 (2 H, m, 2 × C*H*-Ar), 4.00 (3 H, s, *α*-CH_3), 3.34 (1 H, hept, *J* 6.9, C*H*-^{i}Pr), 1.43 (6 H, d, *J* 6.9, CH(CH_3)$_2$); δ_C (101 MHz, $CDCl_3$) 22.8 (CH(*C*H_3)$_2$), 29.2 (*C*H-^{i}Pr), 52.1 (*α*-*C*H_3), 109.5 (*C*^{3}H-Ar), 120.3 (*C*^{4}H-Ar), 121.2 (*C*^{6}H-Ar), 121.3 (*C*^{5}H-Ar), 126.9 – 135.6 (4 × *C*-Ar), 162.8 (*C*=O InC ester); LC-MS (retention time: 8.59 min) *m/z* (ESI) 218 (M^+ + H, 100%).

Methyl 3-bromo-7-isopropyl-1*H*indole-2-carboxylate (68)

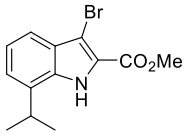

68

A solution of InC methyl ester **67** (2.2 g, 10 mmol) dissolved in CH_2Cl_2 (50 ml) was cooled in an ice-bath, thereto was added NBS (1.9 g, 11 mmol) and the thus obtained orange reaction mixture was stirred for 40 min. Saturated $NaHCO_{3aq}$ (20 ml) was added therein and extracted with CH_2Cl_2 (6.0 × 50 ml). The extracts were combined, washed with brine (2.0 × 50 ml), dried over anhydrous Na_2SO_4 and the solvent was removed *in vacuo* to give a yellow wax, which was further purified by flash column chromatography (EtOAc/cyclohexane, 1:6) to give the desired mono bromo-InC methyl ester **68** (2.7 g; 93%) in >80% purity as an orange solid; R_f 0.20 (10% EtOAc in cyclohexane); ν_{max}/cm^{-1} (ATR) 3295 – 3210w (N–H asymmetric & symmetric stretches), 1706s (conj. C=O carboxyl ester stretch), 650m (C–Br stretch); δ_H (400 MHz, $CDCl_3$) 8.89 (1 H, s, N*H*-InC), 7.45 (1 H, dd, *J* 7.8 & 1.1, C^4*H*-Ar), 7.19 – 7.11 (2 H, m, 2 × C*H*-Ar), 3.94 (3 H, s, *α*-CH_3), 3.20 (1 H, hept, *J* 6.9, C*H*-^{i}Pr), 1.32 (6 H, d, *J* 6.9, CH(CH_3)$_2$); δ_C (101 MHz, $CDCl_3$) 22.8 (CH(*C*H$_3$)$_2$), 28.9 (*C*H-^{i}Pr), 52.4 (*α*-*C*H$_3$), 99.0 (*C*^{3}-Ar), 119.1 (*C*^{4}H-Ar), 122.1 (*C*^{6}H-Ar), 122.5 (*C*^{5}H-Ar), 123.8 – 134.0 (4 × *C*-Ar), 161.7 (*C*=O InC ester); LC-MS (retention time: 9.25 min) *m/z* (ESI) 296 & 298 (1:1) (M^+ + H, 100%).

Methyl (*E*)-7-isopropyl-3-[2-((5-nitrofuran-2-yl)methylene)hydrazineyl]-1*H*indole-2-carboxylate (69)

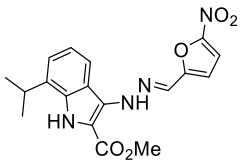

69

InC methyl ester **68** (0.30 g, 1.0 mmol), hydrazone **44** (0.18 g, 1.2 mmol), Cs_2CO_3 (1.0 g, 3.0 mmol), BrettPhos Pd G3 (90 mg, 0.10 mmol) and BrettPhos (54 mg, 0.1 mmol) were intimately mixed, sealed and degassed under argon. Thereto was added anhydrous degassed THF (10 ml), and the thus obtained dark red reaction mixture was stirred under a partial flow of argon at 80 °C for 4.0 h. Upon completion – TLC controlled (40% EtOAc in cyclohexane; R_f 0.20) – the resulting tarry reaction mixture was filtered through Celite® and rinsed with EtOAc (50 ml). Thereto was added deionised water (25 ml), the organic layer was separated and the aqueous was further extracted with EtOAc (5.0 × 25 ml). The extracts were combined, washed with brine (2.0 × 25 ml), dried over anhydrous Na_2SO_4 and the solvent was removed *in vacuo* to give a tarry wax, which was further purified by flash column chromatography (EtOAc/cyclohexane, 1:4) to give the desired NInC methyl ester **69** (80 mg; 22%) as a dark purple hygroscopic fine powder; R_f 0.15 (30% EtOAc in cyclohexane); ν_{max}/cm^{-1} (ATR) 3451 – 3259w (N–H asymmetric & symmetric stretches), 1786s (conj. C=O carboxyl ester stretch), 1427s (N–O asymmetric stretch), 1348m (N–O symmetric stretch), 1271vs (C–N asymmetric stretch), 1242w (C–N symmetric stretch); δ_H (400 MHz, $CDCl_3$) 10.09 (1 H, s, N*H*-InC), 8.27 (1 H, d, *J* 8.2, CC*H*N unsaturated), 7.96 (1 H, s, N*H*-hydrazone), 7.65 (1 H, m, C*H*-Ar indole), 7.42 (1 H, d, *J* 3.9, C^4*H*-Ar furan), 7.28 – 7.16 (2 H, m, 2 × C*H*-Ar indole), 6.87 (1 H, d, *J* 3.9, C^3*H*-Ar furan), 3.98 (3 H, s, *α*-CH_3), 3.22 (1 H, hept, *J* 6.9, C*H*-^{i}Pr), 1.39 (6 H, d, *J* 6.9, CH(CH_3)$_2$); δ_C (101 MHz, DMSO-d_6) 23.0 (CH(CH_3)$_2$), 26.7 (*C*H-^{i}Pr), 51.4 (*α*-CH_3), 108.1 (C^3-Ar indole), 110.7 – 116.1 (2 × *C*H-Ar furan), 117.9 (*C*-Ar indole), 119.9 (C^4H-Ar indole), 121.3 (C*C*HN unsaturated), 121.9 – 125.7 (2 × *C*H-Ar indole), 130.4 – 135.0 (4 × *C*-Ar indole), 151.0 – 154.6 (2 × *C*-Ar furan), 162.0 (*C*=O InC ester)); LC-MS (retention time: 8.83 min) *m/z* (ESI) 369 (M^+ + H, 100%).

(*E*)-7-Isopropyl-3-[2-((5-nitrofuran-2-yl)methylene]hydrazineyl)-1*H*indole-2-carboxylic acid (63)

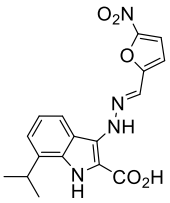

63

NInC methyl ester **69** (19 mg, 50 µmol) was degassed under a partial flow of argon, thereto was added CH_2Cl_2 (1.0 ml) and further degassed under a partial flow of argon, making sure no or only minimal loss of CH_2Cl_2. The thus obtained clear ruby in colour reaction mixture was sealed and cooled to -78 °C, followed by addition of BCl_3 0.10 M in CH_2Cl_2 (0.20 ml), and stirred under a partial flow of argon at -78 °C for 15 min.

The reaction mixture was warmed up to the ambient temperature with stirring under a partial flow of argon over 15 min, and thereto was added anhydrous methanol (0.25 ml), followed by further stirring under a partial flow of argon at ambient temperature for 15 min. The volatiles were removed *in vacuo* and even though residual starting material, namely, NInC methyl ester **69** was detected on the LC-MS, the desired product **63** was mostly decomposed.

Improved Method: NInC methyl ester **69** (19 mg, 50 µmol) was degassed under a partial flow of argon, thereto was added CH_2Cl_2 (3.0 ml) and further degassed under a partial flow of argon, making sure no or only minimal loss of CH_2Cl_2. The thus obtained clear ruby in colour reaction mixture was sealed and cooled to -78 °C, followed by addition of 1.0 M BCl_3 in CH_2Cl_2 (0.10 ml) and stirred under a partial flow of argon at -78 °C for 15 min. The thus obtained green reaction mixture was warmed up to the ambient temperature with stirring under a partial flow of argon over 5.0 min, and thereto was added anhydrous 0.10 M methanolic ammonia (0.25 ml), followed by further stirring under a partial flow of argon at ambient temperature for 5.0 min.

The volatiles were removed *in vacuo* and the residue was dissolved in deionised water (2.0 ml) at which point the pH value of the mixture was *ca.* 6.0 – 7.0. The clear mixture was purified using preparative RP-HPLC (retention time: 25.4 – 25.7 min) (30 – 95% MeCN in H_2O over 30 min; 15 ml min^{-1}, 40 °C) to furnish the desired NInC **63** as a brown solid (*ca.* < 1.0 mg); LC-MS (retention time: 7.39 min) *m/z* (ESI) 356 (M^+, 13%), 355 (100), 279 (14), 233 (50), 201 (11).

3-Hydrazineyl-7-isopropyl-1*H*-indole-2-carboxylic acid (70)

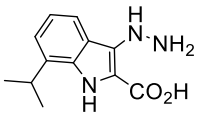

70

NInC methyl ester **69** (19 mg, 50 µmol) was degassed under a partial flow of argon, thereto was added CH_2Cl_2 (3.0 ml) and further degassed under a partial flow of argon, making sure no or only minimal loss of CH_2Cl_2. The thus obtained clear ruby in colour reaction mixture was sealed and cooled to -78 °C, followed by addition of BCl_3 0.10 M in CH_2Cl_2 (0.10 ml), and stirred under a partial flow of argon at -78 °C for 20 min. The reaction mixture was warmed up to the ambient temperature with stirring under a partial flow of argon over 15 min, and thereto was added anhydrous methanol (0.50 ml), followed by further stirring under a partial flow of argon at ambient temperature for 10 min.

The volatiles were removed *in vacuo* and the residue was dissolved in deionised water (2.0 ml), which was purified using preparative RP-HPLC (retention time: 25.0 – 25.1 min) (30 – 95% MeCN in H_2O over 30 min; 15 ml min^{-1}, 40 °C) to furnish hydrazide **70** (4.5 mg; 38%) as a brown solid; R_f 0.25 (80% CH_2Cl_2 in cyclohexane + 1.0% formic acid); ν_{max}/cm^{-1} (ATR) 3465 – 2289br (O–H H-bonding stretch & N–H asymmetric and symmetric stretches), 1679s (C=O carboxylic acid stretch); δ_H (400 MHz, acetonitrile-d_3) 8.54 (1 H, m, C*H*-Ar), 7.51 (1 H, dd, *J* 3.9 & 1.6, C*H*-Ar), 7.25 (1 H, m, C*H*-Ar), 1.92 (6 H, m, CH(CH_3)$_2$); LC-MS (retention time: 7.41 min) *m/z* (ESI) 234 (M^+ + H, 11%), 233 (100), 201 (15).

3-Bromo-7-isopropyl-1*H*-indole-2-carboxylic acid (71)

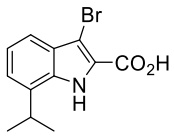

71

InC ethyl ester **61** (0.16 g, 0.50 mmol) and lithium hydroxide monohydrate (0.21 g, 2.5 mmol) were dissolved in THF (2.0 ml) and deionised water (1.0 ml). The thus obtained clear reaction mixture was stirred at ambient temperature for 4.0 h. The resulting reaction mixture was washed with EtOAc (2.0 × 25 ml), the aqueous layer was collected and acidified with formic acid until acidic to Congo red; followed by extraction with EtOAc (5.0 × 25 ml). The extracts were combined and dried over anhydrous Na_2SO_4, filtered and the solvent was removed *in vacuo* to afford crude carboxylic acid **71** (0.13 g; 91%) as an orange wax, which was further purified by flash column chromatography (methanol/CH_2Cl_2, 1:18) to afford the desired carboxylic acid **71** (0.11 g; 79%) as an off-white powder; R_f 0.25 (5.0% methanol in CH_2Cl_2 + 1.0% formic acid); ν_{max}/cm^{-1} (ATR) 33870m (N–H stretch), 3305 – 2481br (O–H H-bonding stretch), 1679s (C=O carboxylic acid stretch), 621m (C–Br stretch); δ_H (400 MHz, $CDCl_3$) 9.01 (1 H, s, N*H*-InC), 7.55 (1 H, dd, *J* 8.0 & 1.1, C^4*H*-Ar), 7.39 – 7.11 (2 H, m, 2 × C*H*-Ar), 3.29 (1 H, hept, *J* 6.9, C*H*-^{i}Pr), 1.41 (6 H, d, *J* 6.9, CH(CH_3)$_2$); δ_C (101 MHz, $CDCl_3$) 22.8 (CH(*C*H_3)$_2$), 29.0 (*C*H-^{i}Pr), 101.1 (*C*^{3}-Ar), 119.3 (*C*^{4}H-Ar), 122.4 (*C*^{6}H-Ar), 122.8 (*C*-Ar), 123.2 (*C*^{5}H-Ar), 128.2 – 134.6 (3 × *C*-Ar), 165.0 (*C*=O carboxylic acid); LC-MS (retention time: 7.58 min) *m/z* (ESI) 282 & 284 (1:1) (M^+ + H, 100%).

4-Methoxybenzyl 3-bromo-7-isopropyl-1-(4-methoxybenzyl)-1*H*indole-2-carboxylate (72)

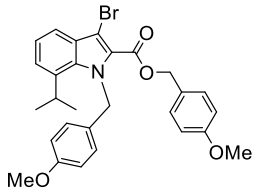

72

To a solution of carboxylic acid **71** (40 mg, 0.14 mmol) and PMB-Br (30 mg, 0.15 mmol) in anhydrous THF (2.0 ml) was added Et_3N (58 µl, 0.42 mmol) and stirred at ambient temperature for 6.0 h. Upon completion – TLC controlled (20% EtOAc in cyclohexane; R_f 0.30) – the volatiles were removed *in vacuo*, and the residue was dissolved in EtOAc (20 ml); thereto was added saturated $NaHCO_{3aq}$ (20 ml), the organic layer was separated and the aqueous was further extracted with EtOAc (5.0 × 25 ml). The extracts were combined, washed with brine (2.0 × 25 ml), dried over anhydrous Na_2SO_4 and the solvent was removed *in vacuo* to yield a viscous oil, which was further purified by flash column chromatography (EtOAc/cyclohexane, 1:5) to furnish di-PMB protected InC **72** (40 mg; 71%) as a colourless oil; R_f 0.25 (15% EtOAc in cyclohexane); ν_{max}/cm^{-1} (ATR) 2962m (C_{sp3}–H stretch), 1751s (C=O carboxyl ester stretch), 1145s (C–O stretch), 520m (C–Br stretch); δ_H (400 MHz, $CDCl_3$) 7.52 – 7.29 (3 H, m, 3 × C*H*-Ar indole), 7.26 – 7.07 (4 H, m, 4 × C*H*-Ar PMB), 6.87 – 6.76 (4 H, m, 4 × C*H*-Ar PMB), 5.30 (2 H, s, *α*-CH_2), 4.37 (1 H, s, N–C*H*), 3.76 – 3.67 (6 H, m, 2 × O–CH_3), 3.64 (1 H, s, N–C*H*), 3.14 (1 H, hept, *J* 7.0, C*H*-^{i}Pr), 1.27 (6 H, d, *J* 7.0, CH(CH_3)$_2$); LC-MS (retention time: 11.02 min) *m/z* (ESI) 554 & 556 (1:1) (M^+ + CH_3OH + H, 100%).

[2-(Trimethylsilyl)ethoxy]methyl 2-oxopropanoate (73)

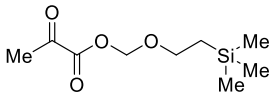

73

To a flame-dried reaction vessel charged with pyruvic acid (70 µl, 1.0 mmol) was added anhydrous THF (5.0 ml), degassed under a partial flow of argon, sealed and cooled in an ice-bath. Thereto was added SEM-Cl (0.18 ml, 1.0 mmol) and the clear mixture was stirred under a partial flow of argon at 0 °C for 15 min, followed by Et_3N (0.28 ml, 2.0 mmol). The thus obtained reaction mixture was stirred at 0 °C for 1.5 h. Upon completion – TLC controlled (10% EtOAc in cyclohexane; R_f 0.10) – the reaction mixture was warmed up to room temperature, the volatiles were removed *in vacuo*, and the residue was dissolved in chloroform (20 ml); thereto was added saturated NH_4Cl_{aq} (20 ml), the organic layer was separated and the aqueous was further extracted with chloroform (5.0 × 25 ml). The extracts were combined, washed with brine (2.0 × 25 ml), dried over anhydrous Na_2SO_4 and the solvent was removed *in vacuo* to furnish SEM-protected pyruvate **73** (0.20 g; 92%) as an orange oil, which was used in the subsequent steps without further purification; R_f 0.20 (20% EtOAc in cyclohexane); ν_{max}/cm^{-1} (ATR) 2988m (C_{sp3}–H stretch), 1748vs (C=O *α*-keto ester stretch), 1105s (C–O stretch), 842s ($SiMe_3$ stretch); δ_H (700 MHz, $CDCl_3$) 5.41 (2 H, s, *γ*-CH_2), 3.76 (2 H, m, *ε*-CH_2), 2.46 (3 H, s, *α*-CH_3), 0.95 (2 H, m, *ζ*-CH_2), -0.02 (9 H, s, Si(CH_3)$_3$); δ_C (193 MHz, $CDCl_3$) -1.4 (Si(*C*H_3)$_3$), 18.1 (*ζ*-*C*H_2), 26.7 (*α*-*C*H_3), 68.8 (*ε*-*C*H_2), 91.0 (*γ*-*C*H_2), 160.3 (*C*=O *α*-keto ester), 191.8 (CH_3–*C*=O ketone).

2-(4-Bromophenyl)-1,3-dioxolane (75)

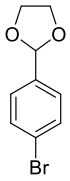

75

To a solution of 4-bromobenzaldehyde (0.19 g, 1.0 mmol) in anhydrous THF (1.0 ml) was added ethylene glycol (2.7 ml, 50 mmol) alongside TfOH (90 µl, 1.0 mmol) under a partial flow of argon at ambient temperature and stirred for 5.0 min. The thus obtained reaction mixture was sealed and stirred at 60 °C overnight. Upon completion – TLC controlled (20% EtOAc in cyclohexane; R_f 0.15) – the reaction mixture was suspended onto silica, the volatiles were removed *in vacuo*, and the residue was purified by flash column chromatography (EtOAc/cyclohexane, 1:3) to yield the desired acetal **75** (2.2 g; 85%) as a clear oil; R_f 0.25 (30% CH_2Cl_2 in cyclohexane); ν_{max}/cm^{-1} (ATR) 3106w (C_{sp2}–H stretch), 2988m (C_{sp3}–H stretch), 1679s (C=C stretches), 1136s (C–O asymmetric stretch), 1098s (C–O symmetric stretch), 568m (C–Br stretch); δ_H (400 MHz, $CDCl_3$) 7.47 – 7.39 (2 H, m, 2 × C*H*-Ar), 7.33 – 7.22 (2 H, m, 2 × C*H*-Ar), 5.69 (1 H, s, O–C*H*–O), 4.07 – 3.90 (4 H, m, 2 × O–CH_2); δ_C (101 MHz, $CDCl_3$) 61.5 (O–*C*H_2), 67.0 (O–*C*H–O), 131.4 – 132.0 (2 × *C*H-Ar); LC-MS (retention time: 7.72 min) *m/z* (ESI) 229 & 231 (1:1) (M^+ + H, 100%).

Ethyl 3-[4-(1,3-dioxolan-2-yl)phenyl]-7-isopropyl-1*H*-indole-2-carboxylate (76)

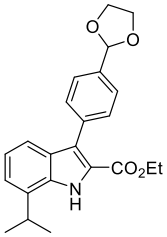

76

Boronate ester **58** (70 mg, 0.20 mmol) and acetal **75** (70 mg, 0.30 mmol) were dissolved in anhydrous CH_2Cl_2 (2.0 ml) and the volatiles were removed under a flow of argon and at a reduced pressure ~ 0.1 mbar. The thus obtained residue was intimately mixed with BrettPhos Pd G3 (20 mg, 20 µmol) and Cs_2CO_3 (0.33 g, 1.0 mmol); sealed and degassed under a partial flow of argon. Thereto was added THF (1.0 ml) and stirred at 70 °C overnight. Upon completion – LC-MS controlled (retention time: 9.77 min) *m/z* (ESI) 380 (M^+ + H, 100%) – the resulting reaction mixture was filtered through Celite® and rinsed with EtOAc (25 ml). Thereto was added deionised water (25 ml), the organic layer was separated and the aqueous was further extracted with EtOAc (5.0 × 25 ml). The extracts were combined, washed with brine (2.0 × 25 ml), dried over anhydrous Na_2SO_4 and the solvent was removed *in vacuo* to give a tarry wax, which was further purified by flash column chromatography (EtOAc/cyclohexane, 1:4) to give the desired InC ethyl ester **76** (50 mg; 66%) as a brown wax; R_f 0.25 (20% EtOAc in cyclohexane); ν_{max}/cm^{-1} (ATR) 3440 – 3215w (N–H asymmetric & symmetric stretches), 1762s (conj. C=O carboxyl ester stretch); δ_H (400 MHz, $CDCl_3$) 8.88 (1 H, s, N*H*-InC), 7.49 (4 H, s, 4 × C*H*-phenylic), 7.43 – 7.35 (1 H, m, C^4*H*-Ar indole), 7.24 – 6.94 (2 H, m, 2 × C*H*-Ar indole), 5.84 (1 H, s, O–C*H*–O), 4.22 (2 H, q, *J* 7.1, *α*-CH_2), 4.15 – 3.95 (4 H, m, 2 × O–CH_2), 3.45 – 3.00 (1 H, hept, *J* 6.9, C*H*-^{i}Pr), 1.35 (6 H, d, *J* 6.9, CH(CH_3)$_2$), 1.15 (3 H, t, *J* 7.1, *β*-CH_3); δ_C (101 MHz, $CDCl_3$) 14.2 (*β*-CH_3), 22.9 (CH(CH_3)$_2$), 29.2 (*C*H-^{i}Pr), 61.1 (*α*-CH_2), 65.5 (O–CH_2), 104.0 (O–*C*H–O), 119.4 – 121.6 (3 × *C*H-Ar indole), 126.0 – 130.8 (4 × *C*H-phenylic), 132.1 – 136.8 (4 × *C*-Ar), 162.4 (*C*=O InC ester) (LC-MS (retention time: 9.56 min) *m/z* (ESI) 380 (M^+ + H, 100%).

3-(4-Formylphenyl)-7-isopropyl-1*H*-indole-2-carboxylic acid (77)

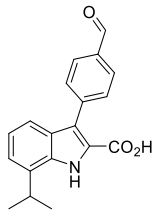

77

InC ethyl ester **76** (38 mg, 0.10 mmol) and lithium hydroxide monohydrate (60 mg, 0.65 mmol) were dissolved in THF (1.0 ml) and deionised water (0.50 ml). The thus obtained clear reaction mixture was stirred at ambient temperature for 4.0 h. Upon completion – TLC controlled (10% methanol in CH_2Cl_2 + 1.0% formic acid; R_f 0.45) – the volatiles were removed *in vacuo* until dryness and the residue was dissolved in 6.0 M HCl_{aq} (10 ml). The resulting clear mixture which was acidic to Congo red was stirred at ambient temperature for 1.0 h. Upon completion – TLC controlled (20% EtOAc in cyclohexane + 1.0% formic acid; R_f 0.10) thereto was added $NaHCO_{3aq}$ (10 ml) to adjust the pH to ~ 6.0 – 7.0 and the thus obtained cloudy reaction mixture was washed with EtOAc (2.0 × 25 ml), the aqueous layer was collected and acidified with formic acid until acidic to Congo red; followed by extraction with EtOAc (5.0 × 25 ml). The extracts were combined, washed with brine (2.0 × 50 ml), dried over anhydrous Na_2SO_4, filtered and the solvent was removed *in vacuo* to afford crude carboxylic acid **77** (60 mg; >100%) as a yellow solid, which was further purified by flash column chromatography (EtOAc/cyclohexane, 1:2) to afford the desired carboxylic acid **77** (20 mg; 70%) as a yellow smear; R_f 0.25 (30% EtOAc in cyclohexane + 1.0% formic acid); ν_{max}/cm^{-1} (ATR) 3361m (N–H stretch), 3355 – 2360br (O–H H-bonding stretch), 1685s (C=O carboxylic acid stretch); δ_H (600 MHz, acetonitrile-d_3) 10.03 (1 H, s, C*H*O), 7.96 (2 H, d, *J* 8.2, 2 × C*H*-Bn), 7.74 (2 H, d, *J* 8.2, 2 × C*H*-Bn), 7.36 (1 H, m, C*H*-Ar indole), 7.26 (1 H, m, C*H*-Ar indole), 7.12 (1 H, m, C*H*-Ar indole), 3.49 (1 H, hept, *J* 6.9, C*H*-^{i}Pr), 1.34 (6 H, d, *J* 6.9, CH(CH_3)$_2$); δ_C (151 MHz, acetonitrile-d_3) 23.2 (CH(*C*H_3)$_2$), 29.1 (*C*H-^{i}Pr), 119.1 – 122.7 (3 × *C*H-Ar indole), 123.2 – 128.3 (3 × *C*-Ar indole), 130.1 – 132.4 (4 × *C*H-Bn), 134.2 – 141.9 (4 × *C*-Ar), 163.7 (*C*=O carboxylic acid), 193.9 (*C*HO); LC-MS (retention time: 7.99 min) *m/z* (ESI) 308 (M^+ + H, 100%).

7-Isopropyl-3-[4-((*E*)-(((*E*)-(5-nitrofuran-2-yl)methylene)hydrazineylidene)methyl)phenyl]-1*H*indole-2-carboxylic acid (78)

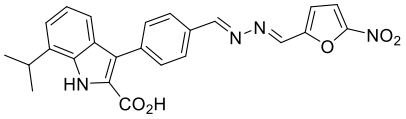

78

Carboxylic acid **77** (15 mg, 50 µmol) was dissolved in anhydrous THF (0.50 ml) and thereto was added anhydrous Na_2SO_4 (10 mg, 70 µmol) alongside anhydrous Et_3N (14 µl, 0.10 mmol) and stirred for 10 min, followed by addition of hydrazone **44** (13 mg, 80 µmol). The thus obtained dark green reaction mixture was sealed and stirred at ambient temperature overnight. Upon completion – TLC controlled (10% methanol in CH_2Cl_2 + 1.0% formic acid; R_f 0.50) – formic acid (~ 2.0 drops) was added thereto until the reaction mixture was acidic to Congo red, followed by addition of silica; the volatiles were removed *in vacuo* until dryness and the residue was purified by flash column chromatography (methanol/CH_2Cl_2, 1:9) to afford the desired NInC **78** (15 mg; 68%) as a yellow wax; R_f 0.30 (5.0% methanol in CH_2Cl_2 + 1.0% formic acid); ν_{max}/cm^{-1} (ATR) 3306m (N–H stretch), 3221 – 2189br (O–H H-bonding stretch), 1693s (C=O carboxylic acid stretch); δ_H (400 MHz, $CDCl_3$) 10.09 (1 H, s, N*H*-InC), 8.77 (1 H, s, CC*H*N unsaturated), 8.56 (1 H, s, CC*H*N unsaturated), 7.80 – 7.67 (4 H, m, 4 × C*H*-Bn), 7.58 – 7.28 (3 H, m, 3 × C*H*-Ar indole), 7.17 (2 H, m, 2 × C*H*-Ar furan), 3.36 – 3.27 (1 H, hept, *J* 6.9, C*H*-^{i}Pr), 1.45 (6 H, d, *J* 6.9, CH(CH_3)$_2$); LC-MS (retention time: 9.16 min) *m/z* (ESI) 445 (M^+ + H, 100%).

5-Nitro-*N′*-(5-nitrofuran-2-carbonyl)furan-2-carbohydrazide (80), (81) & (82)

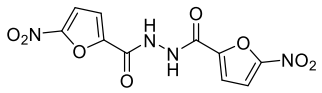

80

5-Nitro-2-furonyl chloride (0.18 g, 1.0 mmol) and anhydrous Na_2SO_4 (50 mg) were placed in a flame-dried reaction vessel, sealed and degassed under argon. Thereto was added anhydrous THF (10 ml) and stirred for 2.0 min, followed by addition of hydrazine monohydrate (49 µl, 1.0 mmol), and the thus obtained red mixture was stirred under argon at 70 °C overnight. Upon completion – TLC controlled (60% EtOAc in cyclohexane; R_f 0.25) – the dark red cloudy reaction mixture which was acidic to Congo red, was diluted with deionised water (5.0 ml), and washed with EtOAc (5.0 × 25 ml). Thereto was added saturated $NaHCO_{3aq}$ to adjust the pH to ~ 7.0 (*caution! effervescent)*, and the aqueous was extracted with EtOAc (6.0 × 25 ml). The extracts were combined and dried over anhydrous Na_2SO_4, filtered and the solvent was removed *in vacuo* to afford crude carbohydrazide **80** (250 mg; 81%) as a dark orange solid, which was further purified by flash column chromatography (EtOAc/cyclohexane, 2:1) to afford the desired product **80** (200 mg; 65%) as a coral pink solid; R_f 0.25 (80% EtOAc in cyclohexane); mp 180–185 °C *dec.* (from methanol); δ_H (400 MHz, DMSO-d_6) 7.74 (2 H, d, *J* 3.9, 2 × C*H*-Ar), 7.34 (2 H, d, *J* 3.9, 2 × C*H*-Ar); δ_C (101 MHz, DMSO-d_6) 113.8 – 114.9 (2 × *C*H-Ar), 149.9 – 151.3 (2 × *C*-Ar), 154.0 (*C*=O carbohydrazide); LC-MS (retention time: 5.08 min) *m/z* (ESI) 311 (M^+ + H, 100%), 172 (50), 141 (16).

Methyl 5-nitrofuran-2-carboxylate (83)

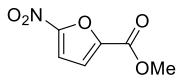

83

A pressure reaction vessel was charged with 5-nitro-2-furonyl chloride (0.36 g, 2.0 mmol) and dissolved in methanol (20 ml) at ambient temperature. The thus obtained clear reaction mixture was sealed and stirred at 70 °C overnight. The resulting reaction mixture was concentrated *in vacuo*, saturated $NaHCO_{3aq}$ (5.0 ml) was added and extracted with EtOAc (5.0 × 25 ml). The extracts were combined, washed with brine (2.0 × 20 ml), dried over anhydrous Na_2SO_4, filtered and the solvent was removed *in vacuo* to afford crude ester **83** (0.34 g; 99%) as a white solid, which was further purified by flash column chromatography (EtOAc/cyclohexane, 1:4) to afford the desired ester **83** (0.33 g; 95%) as a white fluff; R_f 0.20 (10% EtOAc in cyclohexane); δ_H (400 MHz, $CDCl_3$) 7.35 – 7.28 (2 H, m, 2 × C*H*-Ar), 3.97 (3 H, s, O–CH_3); δ_C (101 MHz, $CDCl_3$) 53.1 (O–*C*H_3), 111.6 – 119.0 (2 × *C*H-Ar), 120.2 – 144.9 (2 × *C*-Ar), 157.6 (*C*=O methyl ester); LC-MS (retention time: 5.90 min) *m/z* (ESI) 172 (M^+ + H, 100%).

5-Nitrofuran-2-carbohydrazide (79)

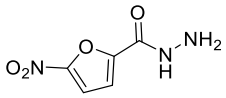

79

Ester **83** (0.34 g, 2.0 mmol) and anhydrous Na_2SO_4 (50 mg) were placed in a flame-dried reaction vessel, sealed and degassed under argon. Thereto was added anhydrous THF (2.0 ml) and stirred for 2.0 min, followed by addition of hydrazine monohydrate (0.11 ml, 2.2 mmol), and the thus obtained tarry mixture was stirred under argon at 0 °C overnight. Upon completion – TLC controlled (80% EtOAc in cyclohexane; R_f 0.25) – the resulting reaction mixture was diluted with deionised water (5.0 ml), and extracted with EtOAc (5.0 × 25 ml). The extracts were combined, washed with brine (2.0 × 50 ml), dried over anhydrous Na_2SO_4, filtered and the solvent was removed *in vacuo* to afford crude carbohydrazide **79** (0.31 g; 90%) as a dark green solid, which was further purified by flash column chromatography (EtOAc) to afford the desired carbohydrazide **79** (0.29 g; 85%) as a yellow powder; R_f 0.30 (EtOAc); δ_H (400 MHz, acetonitrile-d_3) 8.54 (1 H, s, CON*H*), 7.44 (1 H, d, *J* 3.9, C*H*-Ar), 7.18 (1 H, d, *J* 3.9, C*H*-Ar), 4.16 (2 H, s, NHNH_2); δ_C (101 MHz, acetonitrile-d_3) 113.6 – 116.2 (2 × *C*H-Ar), 148.6 (2 × *C*-Ar), 157.7 (*C*=O carbohydrazide); LC-MS (retention time: 3.07 min) *m/z* (ESI) 172 (M^+ + H, 100%), 155 (10); HRMS (ESI) calcd. for $C_5H_4N_3O_4$ [M−H]⁻ *m/z* 170.0207, found 170.0207.

Methyl 3-iodo-7-isopropyl-1*H*indole-2-carboxylate (84)

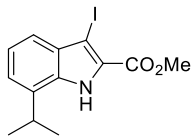

84

To a solution of InC methyl ester **67** (0.44 g, 2.0 mmol) in CH_2Cl_2 (10 ml) was added NIS (0.47 g, 2.1 mmol) and the thus obtained reaction mixture was stirred at ambient temperature for 12 h. Saturated $NaHCO_{3aq}$ (10 ml) was added therein and extracted with CH_2Cl_2 (6.0 × 20 ml). The extracts were combined, washed with brine (50 ml), dried over anhydrous Na_2SO_4 and the solvent was removed *in vacuo* to give a yellow wax which was further purified by flash column chromatography (EtOAc/cyclohexane, 1:9) to give the desired iodo-InC methyl ester **84** (0.55 g; 80%) as an off-pink solid; R_f 0.20 (10% EtOAc in cyclohexane); ν_{max}/cm^{-1} (ATR) 3323 – 3187w (N–H asymmetric & symmetric stretches), 17360s (conj. C=O carboxyl ester stretch), 532m (C–I stretch); δ_H (400 MHz, $CDCl_3$) 9.57 – 8.65 (1 H, m, N*H*-InC), 7.63 – 7.34 (1 H, m, C^4*H*-Ar), 7.26 – 7.07 (2 H, m, 2 × C*H*-Ar), 4.20 – 3.69 (3 H, m, *α*-C*H*$_3$), 3.30 (1 H, hept, *J* 6.9, C*H*-^{i}Pr), 1.40 (6 H, d, *J* 6.9, CH(C*H*$_3$)$_2$); δ_C (101 MHz, $CDCl_3$) 22.8 (CH(*C*H$_3$)$_2$), 28.9 – 29.2 (*C*H-^{i}Pr), 52.1 – 52.2 (*α*-*C*H$_3$), 109.5 – 120.3 (*C*^{4}H-Ar), 121.2 – 121.3 (*C*^{6}H-Ar), 122.2 – 122.4 (*C*^{5}H-Ar), 126.9 – 135.6 (4 × *C*-Ar), 161.7 – 162.8 (*C*=O InC ester); LC-MS (retention time: 9.37 min) *m/z* (ESI) 344 (M^+ + H, 100%).

Methyl 3-(3-fluoro-4-formylphenyl)-7-isopropyl-1*H*indole-2-carboxylate (85)

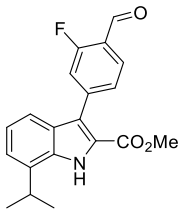

85

Iodo-InC methyl ester **84** (0.30 g, 1.0 mmol) and 3-fluoro-4-formylphenyl boronic acid (0.25 g, 1.5 mmol) were dissolved in anhydrous CH_2Cl_2 (2.0 ml) and the volatiles were removed under a flow of argon and at a reduced pressure ~ 0.1 mbar. The thus obtained residue was intimately mixed with Pd(dppf)Cl_2 (73 mg, 0.10 mmol) and potassium acetate (0.29 g, 3.0 mmol); sealed and degassed under a partial flow of argon. Thereto was added toluene (10 ml) and stirred at 80 °C for 2.0 h. Upon completion – LC-MS controlled (retention time: 9.51 min) *m/z* (ESI) 340 (M^+ + H, 100%) – the resulting reaction mixture was filtered through Celite® and rinsed with EtOAc (25 ml). Thereto was added deionised water (25 ml), the organic layer was separated and the aqueous was further extracted with EtOAc (5.0 × 25 ml). The extracts were combined, washed with brine (2.0 × 25 ml), dried over anhydrous Na_2SO_4 and the solvent was removed *in vacuo* to give a tarry wax, which was further purified by flash column chromatography (EtOAc/cyclohexane, 1:9) to give the desired InC methyl ester **85** (0.18 g; 53%) as an orange wax ; R_f 0.15 (10% EtOAc in cyclohexane); ν_{max}/cm^{-1} (ATR) 3371 – 3183w (N–H asymmetric & symmetric stretches), 1752s (conj. C=O carboxyl ester stretch); δ_H (400 MHz, $CDCl_3$) 10.36 (1 H, s, C*H*O), 8.97 (1 H, s, N*H*-InC), 7.88 (1 H, m, C*H*-Bn), 7.45 – 7.27 (3 H, m, 3 × C*H*-Ar indole), 7.21 (1 H, dd, *J* 7.2 & 1.0, C*H*-Bn), 7.11 (1 H, dd, *J* 8.1 & 1.2 Hz, C*H*-Bn), 3.79 (3 H, s, O–CH_3), 3.26 (1 H, hept, *J* 6.9, C*H*-^{i}Pr), 1.36 (6 H, d, *J* 6.9, CH(CH_3)$_2$); δ_C (101 MHz, $CDCl_3$) 22.8 (CH(*C*H_3)$_2$), 29.3 (*C*H-^{i}Pr), 52.2 (O–*C*H_3), 118.5 – 143.0 (*C*H-Ar & *C*-Ar), 162.1 (*C*=O InC ester), 187.2 (*C*HO); LC-MS (retention time: 9.37 min) *m/z* (ESI) 340 (M^+ + H, 100%).

3-(3-Fluoro-4-formylphenyl)-7-isopropyl-1*H*indole-2-carboxylic acid (86)

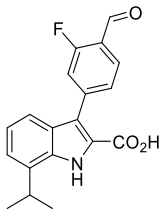

86

InC methyl ester **85** (0.17 g, 0.50 mmol) and lithium hydroxide monohydrate (0.23 g, 2.5 mmol) were dissolved in THF (1.5 ml) and deionised water (1.0 ml). The thus obtained clear reaction mixture was stirred at ambient temperature for 24 h. Upon completion – TLC controlled (10% methanol in CH_2Cl_2 + 1.0% formic acid; R_f 0.45) – the resulting slurry was washed with EtOAc (5.0 × 25 ml). Thereto was added formic acid to adjust the pH to ~ 5.0, followed by extraction with EtOAc (5.0 × 25 ml). The extracts were combined, washed with brine (2.0 × 50 ml), dried over anhydrous Na_2SO_4, filtered and the solvent was removed *in vacuo* to afford crude carboxylic acid **86** (0.12 g; 74%) as a tarry solid, which was further purified by flash column chromatography (EtOAc/cyclohexane, 1:4) to afford the desired carboxylic acid **86** (70 mg; 43%) as a pale-yellow wax; R_f 0.20 (30% EtOAc in cyclohexane + 1.0% formic acid); ν_{max}/cm^{-1} (ATR) 3371w (N–H stretch), 3320 – 2268br (O–H H-bonding stretch), 1679s (C=O carboxylic acid stretch); δ_H (400 MHz, acetonitrile-d_3) 10.29 (1 H, s, C*H*O), 7.90 (1 H, m, C*H*-Bn), 7.52 (1 H, dd, *J* 8.2 & 1.5, C*H*-Ar indole), 7.46 (1 H, dd, *J* 12.0 & 1.5 Hz, C*H*-Ar indole), 7.39 (1 H, dd, *J* 8.2 & 1.5 Hz, C*H*-Ar indole), 7.27 (1 H, d, *J* 7.2, C*H*-Bn), 7.17 – 7.11 (1 H, m, C*H*-Bn), 3.49 (1 H, hept, *J* 6.9, C*H*-^{i}Pr), 1.33 (6 H, d, *J* 6.9, CH(CH_3)$_2$); δ_C (101 MHz, acetonitrile-d_3) 23.2 (CH(*C*H_3)$_2$), 29.0 (*C*H-^{i}Pr), 118.7 – 135.4 (*C*H-Ar & *C*-Ar), 163.6 (*C*=O carboxylic acid), 188.8 (*C*HO); LC-MS (retention time: 8.31 min) *m/z* (ESI) 326 (M^+ + H, 80%), 223 (100).

(*E*)-3-(3-Fluoro-4-[(2-(5-nitrofuran-2-carbonyl)hydrazineylidene)methyl)phenyl]-7-isopropyl-1*H*indole-2-carboxylic acid (87)

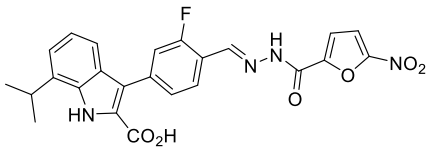

87

Carboxylic acid **86** (11 mg, 35 µmol) was dissolved in anhydrous THF (2.0 ml) and thereto was added anhydrous Na_2SO_4 (10 mg, 70 µmol) alongside anhydrous Et_3N (14 µl, 0.10 mmol) and stirred for 10 min, followed by addition of carbohydrazide **79** (10 mg, 60 µmol). The thus obtained reaction mixture was sealed and stirred under argon at ambient temperature overnight. Upon completion – TLC controlled (10% methanol in CH_2Cl_2; R_f 0.30) – formic acid (~ 2.0 drops) was added thereto until the reaction mixture was acidic to Congo red, followed by addition of silica; the volatiles were removed *in vacuo* until dryness and the residue was purified by flash column chromatography (methanol/CH_2Cl_2, 1:18) to afford the desired NInC **87** (5.0 mg; 30%) as an orange wax; R_f 0.25 (5.0% methanol in CH_2Cl_2); δ_H (400 MHz, methanol-d_4 + $CDCl_3$ 5.0% *v/v*) 8.74 (1 H, m, CC*H*N unsaturated), 8.19 (1 H, m, C*H*-Bn), 7.54 – 7.47 (2 H, d, *J* 3.8, 2 × C*H*-Bn), 7.45 – 7.31 (3 H, m, 3 × C*H*-Ar indole), 7.20 (1 H, d, *J* 7.2, C^4*H*-Ar furan), 7.09 (1 H, dd, *J* 8.1 & 7.2, C^3*H*-Ar furan), 3.49 (1 H, hept, *J* 6.8, C*H*-^{i}Pr), 1.38 (6 H, d, *J* 6.8, CH(CH_3)$_2$); LC-MS (retention time: 8.46 min) *m/z* (ESI) 479 (M^+ + H, 100%); HRMS (ESI) calcd. for $C_{24}H_{18}FN_4O_6$ $[M+H]^+$ *m/z* 479.1274, found 479.1278.

Ethyl 7-acetyl-1*H*indole-2-carboxylate (88)

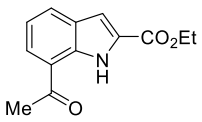

88

A flame-dried pressure vessel was charged with Ethyl 7-bromo-1-*H*-indole-2-carboxylate (0.13 g, 0.35 mmol), *n*-butoxyethylene (0.15 ml, 1.2 mmol), $Pd(OAc)_2$ (5.0 mg, 20 µmol) and DPPP (15 mg, 40 µmol), sealed and degassed under a partial flow of argon. Thereto was added anhydrous degassed ethanol (0.75 ml) alongside Et_3N (0.13 ml, 0.90 mmol), the thus obtained reaction mixture was irradiated in a microwave reactor at 110 °C for 2.0 h. Upon completion – TLC controlled (20% EtOAc in cyclohexane; R_f 0.30) – the resulting tarry reaction mixture was filtered through Celite® and rinsed with EtOAc (50 ml). The volatiles were removed *in vacuo* and the residue was suspended in 6.0 M HCl_{aq} (5.0 ml) and stirred for 15 min. Thereto was added deionised water (25 ml), followed by EtOAc (50 ml). The organic layer was separated and the aqueous was further extracted with EtOAc (5.0 × 25 ml). The extracts were combined, washed with brine (2.0 × 25 ml), dried over anhydrous Na_2SO_4 and the solvent was removed *in vacuo* to give a brown solid, which was further purified by flash column chromatography (EtOAc/cyclohexane, 1:4) to give the desired InC ethyl ester **88** (0.10 g; 90%) as a green wax; R_f 0.25 (20% EtOAc in cyclohexane); δ_H (400 MHz, $CDCl_3$) 10.74 (1 H, s, N*H*-InC), 7.85 (2 H, ddd, *J* 12.5, 7.7 & 0.9 Hz, 2 × C*H*-Ar), 7.21 – 7.13 (2 H, m, 2 × C*H*-Ar), 4.36 (2 H, q, *J* 7.1, *α*-CH_2), 2.64 (3 H, s, CH_3C=O), 1.35 (3 H, t, *J* 7.1, *β*-CH_3); δ_C (101 MHz, $CDCl_3$) 14.5 (*β*-*C*H_3), 26.6 (*C*H_3C=O), 61.3 (*α*-*C*H_2), 108.5 (*C*^{3}H-Ar), 120.1 (*C*^{4}H-Ar), 121.2 (*C*^{2}-Ar), 128.2 (*C*^{6}H-Ar), 129.0 (*C*^{7}-Ar), 129.1 (*C*^{5}H-Ar), 129.5 – 135.4 (2 × *C*-Ar), 161.5 (*C*=O InC ester), 199.9 (*C*=O ketone); LC-MS (retention time: 8.15 min) *m/z* (ESI) 232 (M^+ + H, 100%).

Ethyl 7-[(*E*)-1-(((*E*)-(5-nitrofuran-2-yl)methylene)hydrazineylidene)ethyl]-1*H*indole-2-carboxylate (89)

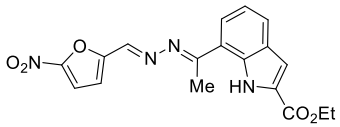

89

InC ethyl ester **88** (25 mg, 0.10 mmol) was dissolved in anhydrous THF (1.0 ml) and thereto was added anhydrous Na_2SO_4 (20 mg, 0.14 mmol) together with $ZnCl_2$ (2.0 mg, 10 µmol) and stirred for 15 min, followed by addition of hydrazone **44** (20 mg, 0.12 mmol). The thus obtained reaction mixture was sealed and stirred under argon at ambient temperature overnight. Upon completion – TLC controlled (30% EtOAc in cyclohexane; R_f 0.30). Thereto was added deionised water (25 ml) alongside EtOAc (25 ml), the organic layer was separated and the aqueous was further extracted with EtOAc (5.0 × 25 ml). The extracts were combined, washed with brine (2.0 × 25 ml), dried over anhydrous Na_2SO_4 and the solvent was removed *in vacuo* to give a brown wax, which was further purified by flash column chromatography (EtOAc/cyclohexane, 2:5) to afford the desired NInC ethyl ester **89** (13 mg; 40%) as a yellow wax; R_f 0.25 (20% EtOAc in cyclohexane); δ_H (400 MHz, $CDCl_3$) 11.22 (1 H, s, N*H*-InC), 8.49 (1 H, s, CC*H*N unsaturated), 7.85 (1 H, dd, *J* 8.0 & 7.6, C^5H-Ar indole), 7.79 (1 H, dd, *J* 7.6 & 1.0, C^6H-Ar indole), 7.44 (1 H, d, *J* 3.8, C^4H-Ar furan), 7.32 – 7.18 (2 H, m, 2 × C*H*-Ar indole), 7.14 (1 H, d, *J* 3.8, C^3H-Ar furan), 4.44 (2 H, q, *J* 7.1, α-CH_2), 2.72 (3 H, s, CH_3C=O), 1.44 (3 H, t, *J* 7.1, β-CH_3); δ_C (101 MHz, $CDCl_3$) 14.6 (β-CH_3), 14.8 (*C*H_3C=O), 61.2 (α-*C*H_2), 108.4 (C^3H-Ar indole), 113.1 – 114.9 (2 × *C*H-Ar furan), 120.5 (C^2-Ar indole), 120.5 (C^4H-Ar indole), 126.7 (2 × *C*H-Ar indole), 128.5 – 128.6 (2 × *C*-Ar indole), 134.6 (C^7-Ar indole), 146.2 (C*C*HN unsaturated) 152.1 (2 × *C*-Ar furan), 162.0 (*C*=O InC ester), 169.6 (N*C*CH_3 unsaturated); δ_C (101 MHz, $CDCl_3$); LC-MS (retention time: 9.75 min) *m/z* (ESI) 369 (M^+ + H, 100%).

7-Acetyl-1*H*indole-2-carboxylic acid (91)

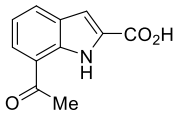

91

InC ethyl ester **89** (92 mg, 0.40 mmol) and lithium hydroxide monohydrate (42 mg, 1.0 mmol) were dissolved in THF (1.0 ml) and deionised water (0.50 ml). The thus obtained clear reaction mixture was stirred at ambient temperature overnight. Upon completion – TLC controlled (5.0% EtOAc in CH_2Cl_2 + 1.0% formic acid; R_f 0.20) – the resulting slurry was diluted with deionised water (2.0 ml) and washed with EtOAc (2.0 × 5.0 ml). Thereto was added formic acid to adjust the pH to ~ 5.0, followed by extraction with EtOAc (5.0 × 10 ml). The extracts were combined, washed with brine (2.0 × 10 ml), dried over anhydrous Na_2SO_4, filtered and the solvent was removed *in vacuo* to afford crude carboxylic acid **91** (81 mg; ≥99%) as a pale yellow solid, which was further purified by flash column chromatography (EtOAc/CH_2Cl_2, 1:18) to afford the desired carboxylic acid **91** (80 mg; 99%) as an off-white solid; R_f 0.25 (10% EtOAc in CH_2Cl_2 + 1.0% formic acid); ν_{max}/cm^{-1} (ATR) 3395w (N–H stretch), 3301 – 2187br (O–H H-bonding stretch), 1705s (C=O carbonyl stretch); δ_H (400 MHz, acetonitrile-d_3) 7.99 (2 H, ddd, *J* 14.8, 7.8 & 1.1, 2 × C*H*-Ar), 7.32 – 7.17 (2 H, m, 2 × C*H*-Ar), 2.65 (3 H, s, C*H*$_3$C=O); δ_C (101 MHz, acetonitrile-d_3) 26.9 (*C*H$_3$C=O), 109.4 (*C*^{3}H-Ar), 121.2 (*C*^{4}H-Ar), 121.8 (*C*^{2}-Ar), 129.7 (*C*-Ar), 129.9 (*C*^{6}H-Ar), 130.2 (*C*^{5}H-Ar), 130.3 (*C*-Ar), 135.8 (*C*^{7}-Ar), 163.9 (*C*=O carboxylic acid), 202.0 (*C*=O ketone); LC-MS (retention time: 6.05 min) *m/z* (ESI) 204 (M^+ + H, 80%), 223 (100).

7-[(*E*)-1-(((*E*)-(5-nitrofuran-2-yl)methylene)hydrazineylidene)ethyl]-1*H*indole-2-carboxylic acid (92)

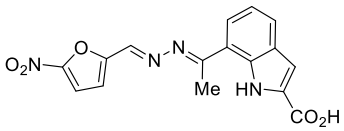

92

Carboxylic acid **91** (10 mg, 50 µmol) was dissolved in anhydrous THF (2.0 ml) and thereto was added anhydrous Na_2SO_4 (10 mg, 70 µmol) together with $FeCl_3$ (4.0 mg, 25 µmol) and stirred for 15 min, followed by addition of hydrazone **44** (16 mg, 0.10 mmol). The thus obtained reaction mixture was sealed and stirred under argon at ambient temperature overnight. Upon completion – TLC controlled (20% EtOAc in CH_2Cl_2 + 1.0% formic acid; R_f 0.25) – formic acid (~ 2.0 drops) was added thereto until the reaction mixture was acidic to Congo red, followed by addition of silica; the volatiles were removed *in vacuo* until dryness and the residue was purified by flash column chromatography (EtOAc/CH_2Cl_2, 1:18) to afford the desired NInC **92** (5.0 mg; 29%) as an orange wax; R_f 0.10 (5.0% methanol in CH_2Cl_2 + 0.50% formic acid); δ_H (400 MHz, acetonitrile-d_3) 11.15 (1 H, s, N*H*-InC), 8.49 (1 H, s, CC*H*N unsaturated), 7.88 (1 H, m, C*H*-Ar indole), 7.52 (1 H, d, *J* 3.9, C*H*-Ar furan), 7.32 – 7.23 (3 H, m, 3 × C*H*-Ar indole), 7.23 (1 H, d, *J* 3.9, C*H*-Ar furan), 2.68 (3 H, s, CH_3C=O); LC-MS (retention time: 8.03 min) *m/z* (ESI) 341 (M^+ + H, 100%).

(*E*)-[5-((2-carbamoylhydrazineylidene)methyl)furan-2-yl]boronic acid (93)

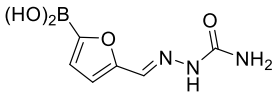

93

2-Formylfuranyl boronic acid (0.14 g, 1.0 mmol) was suspended in 0.10 M PBS buffer pH ~ 7.4 (0.50 ml), thereto was added semicarbazide (0.11 g, 1.0 mmol) dissolved in 0.10 M PBS buffer pH ~ 7.4 (0.50 ml) together with THF (0.25 ml) and ethanol (0.25 ml) and the thus obtained clear mixture was nutated at ambient temperature for 2.0 h. Upon completion – LC-MS controlled (retention time: 1.47 & 3.45 min) *m/z* (ESI) 198 (M^+ + H, 100%) – the gelatinous aggregates were collected at the pump, washed with cold deionised water and dried at the pump. The thus obtained off-white residue was suspended in deionised water (5.0 ml), vortexed for 15 min and centrifuged at 5.0 °C for 45 min. The solid was again suspended in deionised water (10 ml), vortexed for 15 min and centrifuged at 5.0 °C for 45 min. The thus obtained solid was suspended in water (5.0 ml) and stirred at 80 °C for 1.0 h. The clear reaction mixture was cooled to room temperature and lyophilised to afford the desired boronic acid **93** (0.18 g; 92%) as a fluffy beige powder; ν_{max}/cm^{-1} (ATR) 3366w (N–H stretch), 3291 – 2187br (O–H H-bonding stretch), 1667s (C=O semicarbazide stretch), 1218s (C–B stretch); δ_H (400 MHz, acetonitrile-d_3) 8.60 (1 H, s, NN*H*C), 7.70 (1 H, s, CC*H*=N), 7.06 (1 H, d, *J* 3.5, C^4*H*-Ar), 6.75 (1 H, dd, *J* 3.5 & 0.4, C^3*H*-Ar), 6.24 (2 H, s, CONH_2); δ_C (151 MHz, acetonitrile-d_3) 113.6 (*C*^{3}H-Ar), 124.2 (*C*^{4}H-Ar), 133.2 (C*C*H=N), 153.9 – 158.9 (2 × *C*-Ar); δ_B (193 MHz, acetonitrile-d_3) 24.8; LC-MS (retention time: 1.47 min) *m/z* (ESI) 198 (M^+ + H, 100%); HRMS (ESI) calcd. for $C_6H_8BN_3O_4$ $[M+H]^+$ *m/z* 198.0681, found 198.0683.